BEILSTEIN JOURNAL OF ORGANIC CHEMISTRY

Progress in metathesis chemistry

Edited by Karol Grela

Imprint

Beilstein Journal of Organic Chemistry
www.bjoc.org
ISSN 1860-5397
Email: journals-support@beilstein-institut.de

The *Beilstein Journal of Organic Chemistry* is published by the Beilstein-Institut zur Förderung der Chemischen Wissenschaften.

Beilstein-Institut zur Förderung der Chemischen Wissenschaften
Trakehner Straße 7–9
60487 Frankfurt am Main
Germany
www.beilstein-institut.de

Beilstein Journal
of Organic Chemistry

Progress in metathesis chemistry

Karol Grela[1,2]

Editorial

Open Access

Address:
[1]Faculty of Chemistry, University of Warsaw, Żwirki i Wigury Street 101, 02-089 Warsaw, Poland and [2]Institute of Organic Chemistry, Polish Academy of Sciences, Kasprzaka 44/52, 01-224 Warsaw, Poland

Email:
Karol Grela - klgrela@gmail.com

Beilstein J. Org. Chem. **2010,** *6,* 1089–1090.
doi:10.3762/bjoc.6.124

Received: 17 November 2010
Accepted: 18 November 2010
Published: 23 November 2010

Guest Editor: K. Grela

In contrast to the production of simple bulk chemicals and polymers, which started shortly after the discovery of the "olefin scrambling" reaction, it was not until much later that this transformation was "rediscovered" by the academic world. In the last decade of the 20th century, the so-called olefin metathesis reaction gained real significance in advanced organic synthesis [1]. The development of well-defined catalysts and an understanding of the reaction mechanism prompted an extraordinary scientific turnaround, revolutionizing retro-synthetic planning in total synthesis groups and in medicinal chemistry R&D laboratories around the world. The importance of "the development of the metathesis method in organic synthesis" has been fully recognized by the award of the Nobel Prize in Chemistry for 2005 jointly to Yves Chauvin, Robert H. Grubbs, and Richard R. Schrock [2].

Organic chemists are now provided with molybdenum and ruthenium complexes that present good application profiles for a range of metathesis reactions. Most of the ruthenium initiators can be handled in air and are compatible with functionalized substrates, such as unsaturated esters, amides, ketones, aldehydes and even alkenes bearing protic functions, e.g., hydroxy or carboxylic acid groups. While more sensitive towards air and moisture, molybdenum catalysts provide excellent results in stereoselective metathesis and are sometimes more active. Therefore these catalyst families can be used in a complementary fashion. Currently, olefin metathesis (and its sister reaction, alkyne metathesis) [3] is one of the most intensively studied transformations in synthetic organic chemistry, as witnessed by a veritable "explosion" in the number of published syntheses where metathesis is the key step. Despite its power and applicability, metathesis is still experiencing some growing pains outside academic laboratories and the industrial production of simple chemicals. It is surprising that while this transformation has been used in laboratory scale syntheses of thousands of natural and biologically active compounds, it has not yet entered commercial pharmaceutical manufacturing. This could be due to a variety of reasons, such as the still not perfect stability and sometimes low activity of existing catalysts, problems with removing/recycling of catalysts after the reaction, unfavorable patent situation and licensing strategies etc. [4]. Fortunately, the international community of chemists, fully aware of the above limitations, is working hard to develop new metathesis catalysts and strategies in order to solve some of the existing problems. The enormous progress which has been made over last few years provides an equally impressive lesson about the chemist's ability to innovate. The variety of metathesis catalysts now available on the market as well as the number of commercial players involved, are increasing. New applications of this methodology are being developed, including

sustainable production of valuable chemicals from renewable sources. The importance of these developments is now widely appreciated and more and more commercial applications will surely follow.

The papers collected in this Thematic Series nicely highlight many of the aspects mentioned above and will certainly help to update the "state of the art" knowledge in this fascinating field. In this Thematic Series contributions from many of the leading practitioners in the area, which cover a wide range of topics related to alkene and alkyne metathesis, are presented. It is therefore a pleasure to serve as Guest Editor for this Thematic Series in the *Beilstein Journal of Organic Chemistry*, on "Progress in metathesis chemistry". I would like to thank all authors for their excellent contributions. Enjoy reading them!

Karol Grela

Warsaw, November 2010

References

1. Grubbs, R. H., Ed. *Handbook of Metathesis;* Wiley-VCH: Weinheim, Germany, 2003; Vol. 1-3.
2. For more details, see http://nobelprize.org/chemistry/laureates/2005/chemadv05.pdf
3. Fürstner, A. *Angew. Chem., Int. Ed.* **2000,** *39,* 3012–3043. doi:10.1002/1521-3773(20000901)39:17<3012::AID-ANIE3012>3.0.CO;2-G
4. Thayer, A. M. *Chem. Eng. News* **2007,** *85,* 37–47. http://pubs.acs.org/cen/coverstory/85/8507cover2.html

License and Terms

The definitive version of this article is the electronic one which can be found at: doi:10.3762/bjoc.6.124

Beilstein Journal of Organic Chemistry

Halide exchanged Hoveyda-type complexes in olefin metathesis

Julia Wappel[1], César A. Urbina-Blanco[2], Mudassar Abbas[1], Jörg H. Albering[1], Robert Saf[1], Steven P. Nolan[2] and Christian Slugovc[*1]

Full Research Paper

Open Access

Address:
[1]Institute for Chemistry and Technology of Materials (ICTM), Graz University of Technology, Stremayrgasse 9, 8010 Graz, Austria and [2]EaStCHEM School of Chemistry, University of St Andrews, St Andrews KY16 9ST, United Kingdom

Email:
Julia Wappel - julia.wappel@tugraz.at;
Mudassar Abbas - mabbas@student.tugraz.at;
Steven P. Nolan - snolan@st-andrews.ac.uk;
Christian Slugovc* - slugovc@tugraz.at

* Corresponding author

Keywords:
cross metathesis; olefin metathesis; RCM; ROMP; ruthenium

Beilstein J. Org. Chem. **2010,** *6,* 1091–1098.
doi:10.3762/bjoc.6.125

Received: 18 August 2010
Accepted: 08 October 2010
Published: 23 November 2010

Guest Editor: K. Grela

Abstract

The aims of this contribution are to present a straightforward synthesis of 2nd generation Hoveyda-type olefin metathesis catalysts bearing bromo and iodo ligands, and to disclose the subtle influence of the different anionic co-ligands on the catalytic performance of the complexes in ring opening metathesis polymerisation, ring closing metathesis, enyne cycloisomerisation and cross metathesis reactions.

Introduction

Since the pioneering reports on the utilisation of *N*-heterocyclic carbenes (NHC) as co-ligands in ruthenium-based carbene complexes for olefin metathesis [1-3] in the late nineties of the last century, olefin metathesis has become a powerful carbon-carbon double-bond-forming tool presenting unique synthetic opportunities [4]. Developments in this area can be attributed to a steady and competitive research, focused on improving activity, selectivity and functional group tolerance of the catalysts by changing the leaving co-ligand [4,5], by using tailored carbene ligands [5-7], by introducing new NHC ligands [5,8,9], or by variation of the anionic co-ligands [5] (Figure 1).

Compared with other modifications, little attention has been paid to the exchange of anionic co-ligands. In most cases chloro

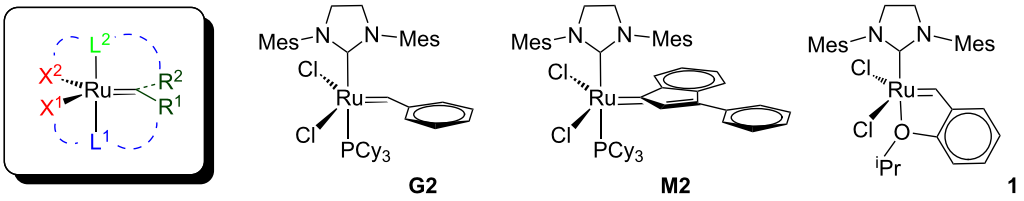

Figure 1: General layout for modifications of ruthenium-based olefin metathesis catalysts (red: anionic ligands; green: nondissociating ligand, e.g. NHC; blue: leaving group, e.g. phosphine or pyridine; olive: carbine substituents; and dashed lines symbolise possibilities of chelation). Three commercial and frequently used catalysts (**G2**: Grubbs 2nd generation catalyst; **M2**: Neolyst M2; and **1**: Hoveyda 2nd generation catalyst).

ligands have been exchanged for sulfonates or fluorocarboxylates [10], often with the aim to heterogenise the catalysts [11], but also phenolates [12,13] and pseudohalides [14] as well as halides other than chloride [15-19]. An early study dealing with the change of reactivity upon exchanging the chloride ligands in **G2** for bromides and iodides showed increasing initiation rates (phosphine dissociation is facilitated), but decreasing propagation rates with increasing steric bulk of the halides [15]. Iodide bearing catalysts have been successfully used in asymmetric olefin metathesis reactions, where they show, in most cases, better enantio- or diastereo-selectivity compared to their chloride counterparts, but at the price of lower activity [16-19]. As shown by Braddock et al., halides and more generally various anionic ligands are labile in solution, and these complexes undergo anionic ligand exchange even in nonprotic media at room temperature [20]. This particular result is an important consideration whenever charged substrates are transformed.

The lack of reactivity data for halide-exchanged complexes prompted us to investigate the catalytic activity of bromo and iodo analogues of Hoveyda 2nd generation catalyst (**1**) in ring closing metathesis (RCM), enyne metathesis and cross metathesis (CM). Moreover, the scope of these compounds in ring opening metathesis polymerisation (ROMP) [21] was also studied.

Results and Discussion

Synthesis and characterisation

Although complex **1** is commercially available, we prepared **1** from (H_2IMes)(PCy_3)Cl_2Ru(3-phenyl-indenylid-1-ene) (**M2**) as the ruthenium-containing starting material (Scheme 1). **M2** is a relatively more economic alternative to **G2**, bearing an indenylidene instead of a benzylidene ligand [22-24]. Adopting Hoveyda's protocol for obtaining **1** from **G2** [25] and using 1-isopropoxy-2-(prop-1-en-1-yl)benzene as the carbene precursor, **1** can be obtained in 78% yield. Complexes **2** and **3** were prepared by addition of excess potassium bromide (KBr) or potassium iodide (KI) to a suspension of **1** in methanol, following the procedures for similar transformations of different dichloro carbene complexes to their diiodo analogues [26]. In these cases THF [15,26] or acetone [27] rather than methanol were used as the solvents.

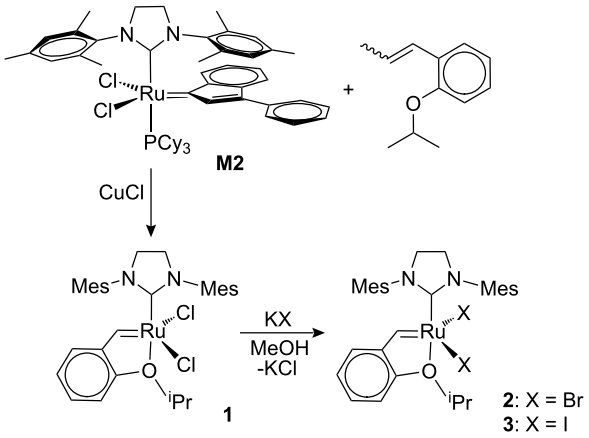

Scheme 1: Synthesis of **1**, **2** and **3**.

The halogen exchange reaction proved rapid at room temperature and reached an equilibrium comprising of three different species within less than 1 h. The compounds were identified as the starting material **1**, the desired product **2** (or **3**), and a "mixed halogen" compound bearing a chloride and a bromide or an iodide ligand, respectively (Figure 2). Upon removal of the inorganic salts and addition of a further portion of KBr or KI, the equilibrium can be directed towards the desired product. Typically, three successive additions of the potassium salt are necessary to obtain **2** or **3** in 90–92% yield and 95–98 % purity. Efforts to further shift the equilibrium towards **2** or **3** have so far proved unsuccessful. The impurity, which could not be separated by recrystallisation or column chromatography, was identified as the "mixed halogen" compound and as revealed by field desorption mass spectrometry (FD-MS) measurements. FD-MS was found to be a suitable technique for the characteri-

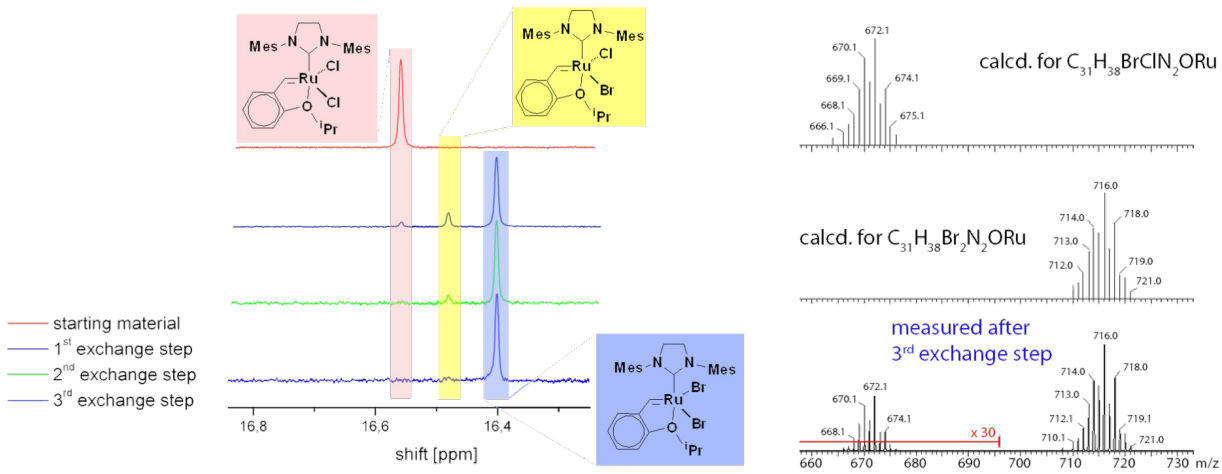

Figure 2: Details of the ^{1}H NMR spectra acquired during the synthesis of **2** and the FD-MS spectrum of **2** isolated after the 3rd exchange step.

sation of this type of complex. Selecting appropriate acquisition parameters – the emitter current was slowly increased until desorption/ionisation started, in this way only molecular ions M^+ were observed (Figure 2).

Quantification was carried out by integration of the corresponding ^{1}H NMR signals. ^{1}H NMR spectra allowed convenient monitoring of the halide exchange by observing the carbene region at the very low field region of the spectra. The starting complex **1** exhibits a carbene peak at 16.56 ppm. Exchange of both chloride ligands for bromide shifts the carbene peak upfield to 16.40 ppm and the mixed chloro-bromo complex appears at 16.48 ppm. In the case of **3**, the carbene proton exhibits a singlet at 15.66 ppm and the chloro-iodo species displays the corresponding peak at 16.10 ppm. All other features of the ^{1}H NMR spectrum of **2** are similar to those of **1** indicating slightly hindered rotation of the *N*-heterocyclic carbene ligand and a *trans*-disposition of the two halide ligands. In contrast, the rotation of the NHC ligand around the Ru–NHC bond in **3** is hindered as shown by a magnetic non-equivalency of the signals corresponding to the two mesityl moieties. The same behaviour was observed in the corresponding ^{13}C NMR spectra (Supporting Information File 1).

X-Ray

Compound **3** crystallises in the monoclinic space group $P2_1/c$, and the overall geometrical arrangement is isostructural to the parent Hoveyda complex **1** (Figure 3). The ruthenium atom is pentacoordinated; the ligands form a slightly distorted square pyramid. The two iodides are, as expected, as supported by NMR data, *trans*-oriented in the basal plane of the square pyramid. The other positions in the basal plane are occupied by C11 (of the NHC ligand) and the atom O1. The strong ruthenium–carbon bond to the carbene was found in the apical position of the square pyramidal coordination around the metal center. Selected bond lengths and angles are provided in Table 1. The overall geometry around the transition metal centre and most of the bond lengths in **3** are analogous to their related values in complex **1**. This is surprising since the Ru–I bond lengths are considerably longer compared to the Ru–Cl bonds in **1**. The bond angles vary slightly due to the significantly larger ionic radius of the iodide ligands [28], which lead to a slight distortion of the complex compared to the chloride-bearing compound.

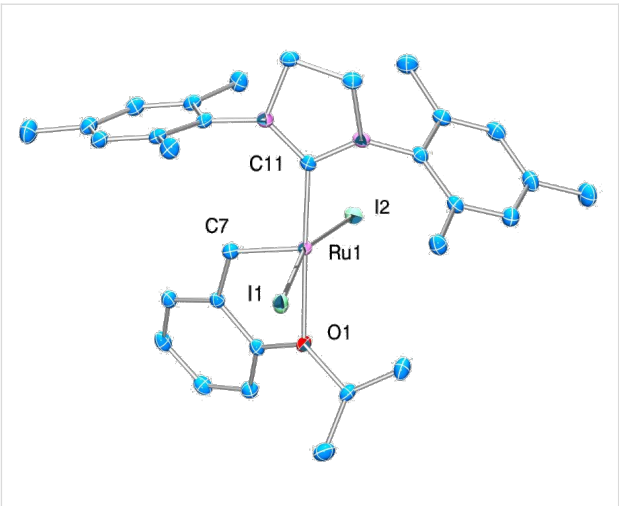

Figure 3: ORTEP drawing of **3**. Thermal ellipsoids are drawn at 50% probability level. Hydrogen atoms are omitted for clarity.

Table 1: Comparison of bond lengths and angles in **1** and **3**.

Bond	Bond length in 3 [Å]	Bond length in 1 [Å][a]
Ru–C11	1.982	1.981
Ru–C7	1.834	1.834
Ru–O	2.282	2.261
Ru–X1	2.677	2.340
Ru–X2	2.663	2.328
Angle	**Bond angle in 3 [°]**	**Bond angle in 1 [°][a]**
C7–Ru–C11	102.94 (7)	101.5 (14)
C7–Ru–O	78.82 (6)	79.3 (17)
C11–Ru–O	178.13 (5)	176.2 (14)
C7–Ru–X2	96.07 (5)	100.2 (15)
C11–Ru–X2	96.08 (4)	96.6 (12)
O–Ru–X2	84.35 (3)	86.9 (9)
C7–Ru–X1	96.70 (5)	100.1 (15)
C11–Ru–X1	90.78 (4)	90.9 (12)
O–Ru–X1	88.35 (3)	85.3 (9)
X2–Ru–X1	163.78 (6)	156.5 (5)

[a]Taken from Ref. [25]

Although the overall structure is quite similar to **1**, some parameters concerning the ruthenium environment are worth discussing in more detail. As expected the main difference appears in the ruthenium halide bond lengths (in case of **3** about 0.3 Å longer) and in the I–Ru–I angle (enlarged by some 7°). Both, the longer bond distance and the enlarged angle, are caused by the larger ionic radii of the iodides. The fact that the Ru–C and Ru–O distances are not significantly affected by the larger ionic radius of the halide ligands can be easily understood by considering the structural flexibility of the coordination polyhedron around the ruthenium atom. The X1–Ru–X2 angle has a relatively high degree of freedom as the opposed position to the apical Ru–C bond is not occupied, and thus the halide ions can avoid close contact with other ligands – which would distort the complex severely – by shifting their positions towards (chloride) or away from (iodide) the empty coordination position, depending on the Ru–X distances.

Catalytic testing of the compounds

ROMP

Initiators **1**–**3** were benchmarked in the ROMP of dimethyl bicyclo[2.2.1]hept-5-ene-2,3-dicarboxylate (**4**). The conversion of the monomer was monitored using arrayed ^{1}H NMR spectroscopy (Figure 4). Initiator **1** yields complete conversion of **4** at 20 °C in about 10 min (half-life $t_{½} \approx 2$ min), while the dibromo derivative **2** requires about 35 min ($t_{½} \approx 7$ min) for complete consumption of the monomer. Complex **3** is almost unable to initiate ROMP of **4** at room temperature.

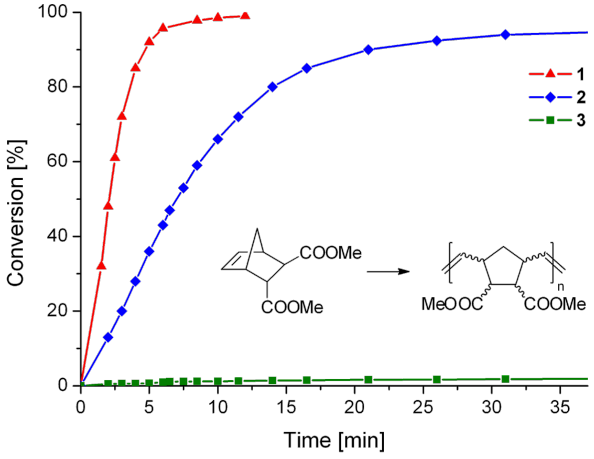

Figure 4: Polymerisation of **4** as a function of time, initiated by **1**, **2** or **3**, monitored by ^{1}H NMR spectroscopy; Reaction conditions: **4**:initiator = 50:1; [**4**] = 0.1 mol/L; solvent: $CDCl_3$; 20 °C.

Additional polymerisation tests were carried out using standard conditions [29], and, in addition to **4**, two further monomers, namely 5,6-bis(methoxymethyl)bicyclo[2.2.1]hept-2-ene (**5**) and (*Z*)-cyclooct-5-ene-1,2-diyl diacetate (**6**), were used. Polymers made of **4** and **5** are not prone to backbiting, i.e., no secondary metathesis reaction affects the double bonds of the formed polymer. Therefore the average number molecular weight (M_n) can be used to establish an indirect, qualitative comparison of the ratio of initiation rate to propagation rate (k_i/k_p) of a given initiator and monomer combination [30]. Polymers made with **M2** and **M31** were used for further comparison. **M2** ($k_i/k_p \approx 1$–0.01) is a typical initiator, producing in most cases polymers with high M_n values and high polydispersity indices (PDI) (Table 2, Entry 1 and 7), while polymers prepared with **M31** ($k_i/k_p \approx 10$–1000) are typically characterised by low M_n values and low PDIs [24] (Table 2, Entry 2 and 8).

Polymerisations initiated with the dichloro derivative **1** yield polymers with relatively low M_n and fairly narrow molecular weight distributions (Table 2, Entry 3 and 9), meaning that k_i is higher than k_p although both values are of the same order of magnitude. In the case of monomer **4**, k_i/k_p increases upon changing from the chloro to the bromo ligands as can be deduced from the lower M_n value of the resulting polymer (68500 g/mol in case of **2** and 106000 g/mol in case of **1** as the initiator). As can be seen in Figure 4, the polymerisation with initiator **2** is distinctly slower than for the one initiated with **1**, meaning that k_p for a polymerisation system consisting of **1** and **4** is distinctly higher than k_p for **2** and **4**. Diiodo-bearing initiator **3** failed in the polymerisation of **4** at room temperature, but gave 75% conversion upon heating in toluene at 80 °C for 19 h, meaning that k_p is very low in this system. In summary,

Table 2: Polymerisation results[a].

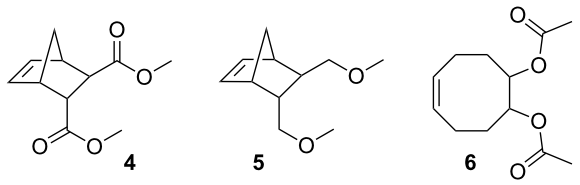

4 **5** **6**

Entry	Monomer	Initiator	Time [min]	Conversion [%]	Yield [%]	M_n[b] [kg/mol]	PDI[b]
1[c]	**4**	**M2**	300	100	89	654	2.7
2[c]	**4**	**M31**	80	100	72	45.5	1.08
3	**4**	**1**	80	100	85	106	1.2
4	**4**	**2**	80	100	79	68.5	1.3
5	**4**	**3**	1080	3	—	—	—
6[d]	**4**	**3**	1140	75	47	53.1	2.3
7[c]	**5**	**M2**	360	100	87	967	2.3
8[c]	**5**	**M31**	90	100	74	64.7	1.09
9	**5**	**1**	80	100	87	65.7	1.2
10	**5**	**2**	80	100	77	75.3	1.5
11	**5**	**3**	1080	78	44	82.8	8.8
12[d]	**5**	**3**	135	90	67	73.3	2.3
13	**6**	**1**	75	95	54	130[e]	5.2
14	**6**	**2**	240	92	60	220[e]	1.9
15	**6**	**3**	2880	58	37	190[e]	2.8

[a]Reaction conditions: Monomer:Initiator = 300:1; [monomer] = 0.2 mol/L; solvent: CH_2Cl_2; 20 °C.; [b]determined by GPC, solvent THF, relative to polystyrene standards; [c]values taken from Ref. [30]; [d]solvent: toluene, temperature: 80 °C; [e]additionally a second peak with a M_n of about 1000 g/mol was observed.

the following qualitative trends for the polymerisation of **4** with initiators **1**, **2** and **3** could be established: the propagation rate constant decreases with increasing steric demand of the halo ligands (i.e., k_p(**1**) > k_p(**2**) >> k_p(**3**)) and the ratio of initiation rate to propagation rate increases on going from **1** to **2** (i.e., k_i/k_p(**1**) < k_i/k_p(**2**) ≈ k_i/k_p(**3**) > 1) but remains of the same order of magnitude.

By studying the polymerisation of monomer **5** with **1**, **2** and **3**, a slightly different picture emerged. While the trend for k_p is the same as in the case of monomer **4**, k_i/k_p decreases with increasing steric bulk of the halo ligands i.e., k_i/k_p(**1**) > k_i/k_p(**2**) > k_i/k_p(**3**), meaning that the decrease of k_i within the series is more pronounced than the decrease of k_p.

At this stage a comment on the presence of the small amounts of mixed halogen complexes (Br–Cl–Ru and Cl–I–Ru both < 5%) is necessary. These species might be responsible for the somewhat higher PDIs of the polymers prepared with **2** compared to those prepared with **1**. Still it can be ruled out that the mixed halogen species is the only active initiator (otherwise the low M_n values observed for the polymers would not be explicable). Accordingly, the activity of the corresponding mixed halogen species is similar to the activity of **2** or **3**, respectively.

In contrast to monomers **4** and **5**, monomer **6** gives polymers which can be degraded by secondary metathesis reactions [31]. Complex **1** polymerises 300 equiv of **6** in 75 min at room temperature with a conversion of 95% (54% isolated yield). The M_n of this polymer was 130600 g/mol. Initiator **2** requires 4 h to achieve a conversion higher than 90% (60% yield) and the corresponding M_n is 220000 g/mol. Finally, **3** gave only 58% conversion after a reaction time of 48 h (M_n = 190000 g/mol). From these data, it is evident that k_p decreases within the series **1**, **2** and **3**, and that k_i/k_p in the case of **6** is considerably smaller when compared to the monomers discussed above.

In all cases, **poly6** degraded over time (Figure 5), i.e., the overall M_n decreases after a certain point and broad multimodal molecular weight distributions are observed. In the case of **1** and **2**, the rate of degradation is relatively low when compared to the rate of polymerisation, allowing for the preparation of high molecular weight **poly6** combined with high conversion in short reaction times. In contrast, in the case of **3**, degradation is an important issue and **poly6** of high molecular weight, formed

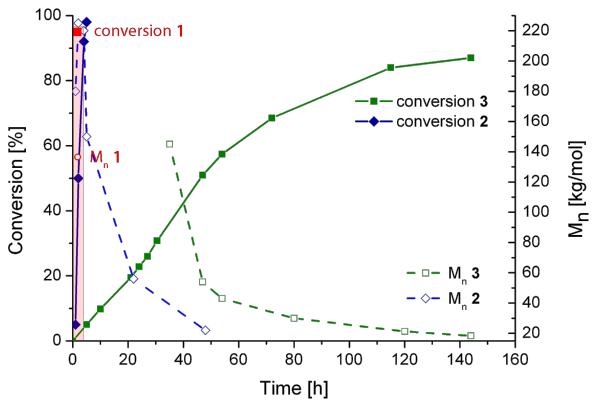

Figure 5: Polymerisations of **6** as a function of time, initiated by **1**–**3**, monitored by ^{1}H NMR spectroscopy (solid lines) and GPC (dashed lines); reaction conditions: **6**:initiator = 300:1; [**6**] = 0.2 mol/L; solvent: CH_2Cl_2; 20 °C. The red circle symbolises the number molecular weight of **poly6** initiated by **1** (the red square symbolises the conversion after 1 h reaction time); reaction conditions for the polymerisation with **3** is 6:3 = 100:1; [**1**] = 0.05 mol/L; solvent: CH_2Cl_2; 20 °C).

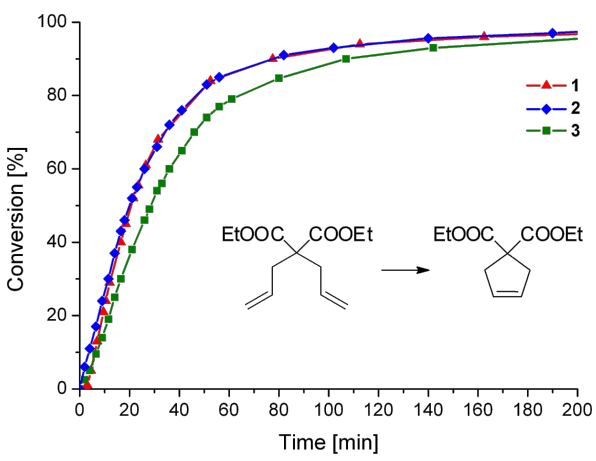

Figure 6: The RCM reaction of **7** as a function of time, catalysed by **1**, **2** or **3**, monitored by ^{1}H NMR spectroscopy; Reaction conditions: **7**:catalyst = 100:1; [**7**] = 0.1 mol/L; solvent: $CDCl_3$; 20 °C.

at the early stages of the polymerisation, is substantially degraded long before the remaining monomer is completely consumed.

RCM, enyne cycloisomerisation and cross metathesis

Catalytic activities of **1**, **2** and **3** were then evaluated in RCM of diethyl diallylmalonate (**7**). The reaction progress is shown in Figure 6 (for details see Table 3). While **1** and **2** perform equally, **3** is the slowest catalyst for this transformation. Nevertheless, the performance of **3** is, when taking the results from the benchmarking in ROMP into account, remarkable. Complex **3** is a fairly good catalyst for this easy transformation and outperforms **M2** [32].

With these results at our disposal, we concentrated on further elucidating the catalytic potential of **3** in RCM, enyne cycloisomerisation and cross metathesis (CM).

Benchmark substrates were selected according to protocols for testing of metathesis catalysts [33]. Substrates with low steric hindrance (Table 3, Entry 1 and 3) were transformed with satisfying results. Even the formation of tetra-substituted olefin bonds (Table 3, Entry 2 and 4) was feasible, although yields fell short in comparison to those obtained with catalyst **1**. In cross metathesis, **3** was not particularly active in coupling terminal mono-substituted olefins with methyl acrylate and failed in the CM of di-substituted terminal olefins (Table 3, Entry 5 and 6) under the reaction conditions used. An interesting example is the cross metathesis of erucic acid with *tert*-butyl acrylate (Table 3, Entry 7). In this case, very similar results were obtained with **1** and **3**. Still a difference exists as only **1** produced small amounts of the homodimer of the acrylate. Finally, the homo-dimerisation of an acrylate was our last test reaction. Diiodo-complex **3** catalyses the dimerisation of 2-hydroxyethyl acrylate, but compared to **1,** catalyst **3** is considerably slower (Table 3, Entry 8).

Conclusion

The results presented indicate a slight activity change in various olefin metathesis reactions when changing the anionic co-ligands from chlorides to iodides. In general, the catalysts are good for RCM and enyne metathesis of moderately hindered substrates; however, they exhibit low activity towards catalyzing transformations of sterically hindered substances. The parent dichloro derivative **1** is the most active catalyst in every transformation studied. The diiodo derivative **3** is a slightly inferior catalyst in RCM, enyne metathesis and CM, but **3** is reluctant or even ineffective to initiate ROMP of norbornene derivatives. Another example of selectivity was observed during the cross metathesis of an internal olefin with an electron deficient alkene, where in the case of **3** no side reaction (i.e., homodimerisation of the electron-deficient olefin) occurred. Thus **3** might prove in the future an interesting catalyst for special applications demanding selectivity.

The current results might be of particular importance whenever the transformation of charged substrates is of interest. In light of the easy exchange of anionic co-ligands in ruthenium-based olefin metathesis catalysts, anionic counterions should preferably be chlorides or bromides but not iodides. The latter might cause a decrease of the reaction rate or might even impede the desired transformation.

Table 3: Results of the catalytic testing.

Entry	Substrate	Product	cat	Reaction conditions	Conv. [%]
1	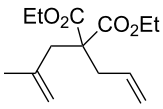	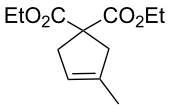	**3** **1**	1 mol %; CH_2Cl_2; 20 °C; 24 h	93 >99
2	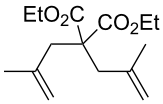	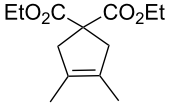	**3** **1**	5 mol %; toluene; 80 °C; 5 h	33 35
3	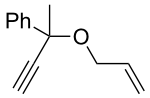	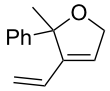	**3** **1**	1 mol %; CH_2Cl_2; 20 °C; 20 h	>99 >99
4	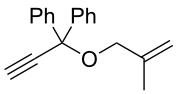	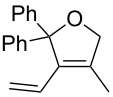	**3** **1**	5 mol %; toluene; 80 °C; 5 h	15 41
5	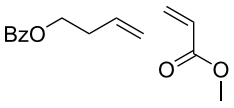 1:2	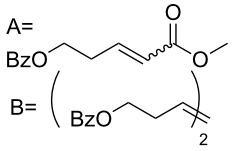	**3** **1**	1 mol %; CH_2Cl_2; 20 °C; 24 h	A = 30; B = 52 A = 69; B = 9
6	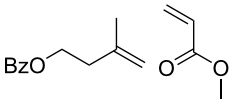 1:2	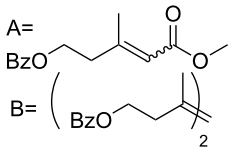	**3** **1**	5 mol %; toluene; 80 °C; 5 h	0 0
7	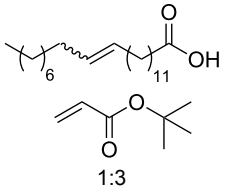 1:3	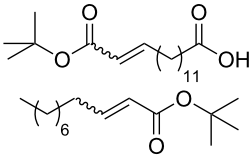	**3** **1** **3** **1**	2.5 mol %; CH_2Cl_2; 40 °C; 22 h 0.5 mol %; CH_2Cl_2; 40 °C; 17 h	>99 >99[a] 75 81[b]
8	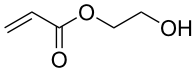	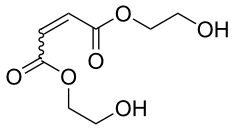	**3** **1**	2.5 mol %; CH_2Cl_2; 40 °C; 48 h 2.5 mol %; CH_2Cl_2; 40 °C; 2 h	>99 >99

[a]4% homodimer of acrylate; [b]1% homodimer of acrylate.

Supporting Information

Supporting information contains full experimental and spectral data for complexes **1**–**3** and the test reactions.

Supporting Information File 1

[http://www.beilstein-journals.org/bjoc/content/supplementary/1860-5397-6-125-S1.pdf]

Acknowledgements

Financial support by the European Community (CP-FP 211468-2 EUMET) is gratefully acknowledged. The Higher Education Commission of Pakistan is gratefully thanked for financial support of M. A. as is Umicore AG for the generous gift of materials. SPN is a Royal Society-Wolfson Research Merit holder.

References

1. Weskamp, T.; Schattenmann, W. C.; Spiegler, M.; Herrmann, W. A. *Angew. Chem., Int. Ed.* **1998,** *37,* 2490–2493. doi:10.1002/(SICI)1521-3773(19981002)37:18<2490::AID-ANIE2490>3.0.CO;2-X

2. Huang, J.; Stevens, E. D.; Petersen, J. L.; Nolan, S. P. *J. Am. Chem. Soc.* **1999,** *121,* 2674–2678. doi:10.1021/ja9831352
3. Scholl, M.; Ding, S.; Lee, C. W.; Grubbs, R. H. *Org. Lett.* **1999,** *1,* 953–956. doi:10.1021/ol990909q
4. Grubbs, E. H., Ed. *Handbook of Metathesis;* Wiley-VCH: Weinheim, 2003.
5. Vougioukalakis, G. C.; Grubbs, R. H. *Chem. Rev.* **2010,** *110,* 1746–1787. doi:10.1021/cr9002424
6. Szadkowska, A.; Grela, K. *Curr. Org. Chem.* **2008,** *12,* 1631–1647. doi:10.2174/138527208786786264
7. Szadkowska, A.; Gstrein, X.; Burtscher, D.; Jarzembska, K.; Wozniak, K.; Slugovc, C.; Grela, K. *Organometallics* **2010,** *29,* 117–124. doi:10.1021/om900857w
8. Samojłowicz, C.; Bieniek, M.; Grela, K. *Chem. Rev.* **2009,** *109,* 3708–3742. doi:10.1021/cr800524f
9. Díez-González, S.; Marion, N.; Nolan, S. P. *Chem. Rev.* **2009,** *109,* 3612–3676. doi:10.1021/cr900074m
   For the use of NHCs in late transition metal catalysis.
10. Krause, J. O.; Nuyken, O.; Wurst, K.; Buchmeiser, M. R. *Chem.–Eur. J.* **2004,** *10,* 777–784. doi:10.1002/chem.200305031
11. Halbach, T. S.; Mix, S.; Fisher, D.; Maechling, S.; Krause, J. O.; Sievers, C.; Blechert, S.; Nuyken, O.; Buchmeiser, M. R. *J. Org. Chem.* **2005,** *70,* 4687–4694. doi:10.1021/jo0477594
12. Conrad, J. C.; Amoroso, D.; Czechura, P.; Yap, G. P. A.; Fogg, D. E. *Organometallics* **2003,** *22,* 3634–3636. doi:10.1021/om030494j
13. Monfette, S.; Camm, K. D.; Gorelsky, S. I.; Fogg, D. E. *Organometallics* **2009,** *28,* 944–946. doi:10.1021/om900006f
14. Buchmeiser, M. R.; Kumar, S.; Ahmad, I. *Abstracts of Papers*. 240th ACS National Meeting, Boston, MA, United States, Aug 22–26, 2010; INOR-61.
15. Sanford, M. S.; Love, J. A.; Grubbs, R. H. *J. Am. Chem. Soc.* **2001,** *123,* 6543–6554. doi:10.1021/ja010624k
16. Seiders, T. J.; Ward, D. W.; Grubbs, R. H. *Org. Lett.* **2001,** *3,* 3225–3228. doi:10.1021/ol0165692
17. Gillingham, D. G.; Kataoka, O.; Garber, S. B.; Hoveyda, A. H. *J. Am. Chem. Soc.* **2004,** *126,* 12288–12290. doi:10.1021/ja0458672
18. van Veldhuizen, J. J.; Campbell, J. E.; Giudici, R. E.; Hoveyda, A. H. *J. Am. Chem. Soc.* **2005,** *127,* 6877–6882. doi:10.1021/ja050179j
19. Funk, T. W.; Berlin, J. M.; Grubbs, R. H. *J. Am. Chem. Soc.* **2006,** *128,* 1840–1846. doi:10.1021/ja055994d
20. Tanaka, K.; Böhm, V. P. W.; Chadwick, D.; Roeper, M.; Braddock, D. C. *Organometallics* **2006,** *25,* 5696–5698. doi:10.1021/om060913n
21. Leitgeb, A.; Wappel, J.; Slugovc, C. *Polymer* **2010,** *51,* 2927–2946. doi:10.1016/j.polymer.2010.05.002
22. Jafarpour, L.; Schanz, H. J.; Stevens, E. D.; Nolan, S. P. *Organometallics* **1999,** *18,* 5416–5419. doi:10.1021/om990587u
23. Fürstner, A.; Grabowski, J.; Lehmann, C. W. *J. Org. Chem.* **1999,** *64,* 8275–8280. doi:10.1021/jo991021i
24. Burtscher, D.; Lexer, C.; Mereiter, K.; Winde, R.; Karch, R.; Slugovc, C. *J. Polym. Sci., Part A: Polym. Chem.* **2008,** *46,* 4630–4635. doi:10.1002/pola.22763
25. Garber, S. B.; Kingsbury, J. S.; Gray, B. L.; Hoveyda, A. H. *J. Am. Chem. Soc.* **2000,** *122,* 8168–8179. doi:10.1021/ja001179g
26. Sanford, M. S.; Love, J. A.; Grubbs, R. H. *Organometallics* **2001,** *20,* 5314–5318. doi:10.1021/om010599r
27. Gatard, S.; Kahlal, S.; Méry, D.; Nlate, S.; Cloutet, E.; Saillard, J.-Y.; Astruc, D. *Organometallics* **2004,** *23,* 1313–1324. doi:10.1021/om030608r
28. The ionic radii of chloride and iodide are 167 pm and 206 pm; the covalent radii of chlorine and iodine are 99 pm and 133 pm.
29. Demel, S.; Schoefberger, W.; Slugovc, C.; Stelzer, F. *J. Mol. Catal. A: Chem.* **2003,** *200,* 11–19. doi:10.1016/S1381-1169(03)00048-7
30. Broggi, J.; Urbina-Blanco, C. A.; Clavier, H.; Leitgeb, A.; Slugovc, C.; Slawin, A. M. Z.; Nolan, S. P. *Chem.–Eur. J.* **2010,** *16,* 9215–9225. doi:10.1002/chem.201000659
31. Alb, A. M.; Enohnyaket, P.; Craymer, J. F.; Eren, T.; Coughlin, E. B.; Reed, W. F. *Macromolecules* **2007,** *40,* 444–451. doi:10.1021/ma062241i
32. Bieniek, M.; Michrowska, A.; Usanov, D. L.; Grela, K. *Chem.–Eur. J.* **2008,** *14,* 806–818. doi:10.1002/chem.200701340
33. Ritter, T.; Hejl, A.; Wenzel, A. G.; Funk, T. W.; Grubbs, R. H. *Organometallics* **2006,** *25,* 5740–5745. doi:10.1021/om060520o

License and Terms

Beilstein Journal of Organic Chemistry

Cross-metathesis of allylcarboranes with *O*-allylcyclodextrins

Ivan Šnajdr[1], Zbyněk Janoušek[2], Jindřich Jindřich[1] and Martin Kotora[*1]

Letter

Open Access

Address:
[1]Department of Organic and Nuclear Chemistry, Faculty of Science, Charles University in Prague, Hlavova 8, 128 43 Praha 2, Czech Republic and [2]Institute of Inorganic Chemistry of the Academy of Science, v.v.i., Husinec-Řež 1001, 250 68 Řež, Czech Republic

Email:
Martin Kotora* - kotora@natur.cuni.cz

* Corresponding author

Keywords:
carborane; catalysis; cross-metathesis; cyclodextrin; ruthenium

Beilstein J. Org. Chem. **2010,** *6,* 1099–1105.
doi:10.3762/bjoc.6.126

Received: 08 September 2010
Accepted: 14 October 2010
Published: 23 November 2010

Guest Editor: K. Grela

Abstract

Cross-metathesis between allylcarboranes and *O*-allylcyclodextrins was catalyzed by Hoveyda–Grubbs 2nd generation catalyst in toluene. The corresponding carboranyl-cyclodextrin conjugates were isolated in 15–25% yields.

Introduction

Cross-metathesis of two different alkenes constitutes an efficient and powerful tool for synthesis of various unsymmetrically substituted alkenes. This procedure has found enormous application in organic synthesis of various types of molecules such as natural and biologically active compounds [1]. One of the key aspects of this methodology, which is responsible for a high cross-metathesis selectivity, is a proper choice of a suitable ruthenium catalyst [2,3]. Efficacy of the cross-metathesis procedure has prompted also us to investigate hitherto unexplored combinations of two different alkenes. Recently, we have shown that metathesis of various terminal alkenes with perfluoroalkylpropenes constitutes a simple and efficient approach for the synthesis of wide array of perfluoroalkylated compounds [4]. This methodology was then applied for the synthesis of perfluoroalkylated analogs of brassinosteroids [5], 17α-perfluoroalkylestradiols [6], perfluoroalkylcyclodextrins [7], and perfluoroalkylcarboranes [8]. Successful execution of these reactions prompted us to study also cross-metathesis of allylcarboranes with *O*-allylcyclodextrins as a route to carborane-cyclodextrin conjugates. Herein, we report our preliminary results.

Results and Discussion

Although studies on the inclusion of carboranes into cyclodextrins have previously been reported [9-13], a synthesis of cyclodextrin-carborane conjugates connected by a linker has not been, to the best of our knowledge, described. Since carboranes are of potential interest for various applications in medicine (e.g. boron neutron capture therapy for cancer, radionuclide diagnostics and therapy, and related fields [14-17], whilst some

carboranes possess antiviral activity [18,19]), consequently, there is considerable interest in the synthesis of water soluble carborane derivatives. One strategy to access such compounds is based on the synthesis of carborane conjugates bearing a water-soluble moiety. With this in mind, we envisioned that this concept could be realized by the synthesis of carborane-cyclodextrin conjugates by the means of cross-metathesis between readily available allycarboranes and *O*-allylcyclodextrins (Figure 1).

The preparation of the starting allylcarboranes, i.e., 1-allyl-1,2-$C_2B_{10}H_{11}$ **1a** [20], 8,8'-allyl-S-$(C_2B_9H_{11})_2$Co **1b** [21], and 8,8'-allyl-S_2-$(C_2B_9H_{11})_2$Co **1c** [21], was carried out according to the previously reported procedures [8]. *O*-Allylcyclodextrins **2** were prepared by allylation of β-cyclodextrins under various reaction conditions (2^I-*O*-allyl-β-cyclodextrin for **2a** [22], 3^I-*O*-allyl-β-cyclodextrin for **2b** [23], and 6^I-*O*-allyl-β-cyclodextrin for **2c**) followed by peracetylation [7,24].

At the outset cross-metathesis of allylcarborane **1a** with 2^I-*O*-allylcyclodextrin **2a** and various ruthenium-carbene complexes (10 mol %) in dichloromethane was carried out to assess the most suitable catalyst (for cross-metatheses involving carboranes, see: [25,26]). However, when the reaction was carried out in the presence of any of the following catalysts, Grubbs 1st, Grubbs 2nd, or Hoveyda–Grubbs 1st generation, no cross-metathesis products were obtained. Only catalysis by Hoveyda–Grubbs 2nd generation catalyst gave the desired product **3** in 14% yield. The suitability of Hoveyda–Grubbs 2nd generation catalyst for cross-metathesis reactions was consistent with the previously observed results [5-8]. Further tuning of the reaction conditions showed that the best yields were obtained by carrying out the reaction in toluene at 120 °C for 16 h (Scheme 1). Interestingly, when the reactions were carried out in CH_2Cl_2 (40 °C) the yields of the corresponding products were lower by 5–10%.

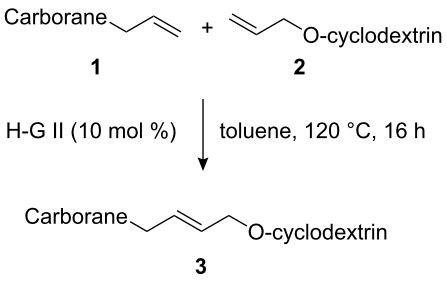

Scheme 1: Cross-metathesis of allylcarboranes **1** and *O*-allylcyclodextrins **2**.

Cross-metatheses of various allylcarboranes **1** and *O*-allylcyclodextrins **2** were then carried out. In general, the reactions proceeded to give the expected products without any problems (Table 1). Thus, the cross-metathesis of **1a** with **2a, 2b,** and **2c** furnished the corresponding carboranylcyclodextrins **3aa**, **3ab**, and **3ac** in 24, 17, and 15% isolated yields, respectively. In an analogous manner the cross-metathesis reactions of **1b** with **2a** and **2c** gave the carboranylcyclodextrins **3ba** and **3bc** in 20 and 19% yields, respectively. Finally, the reactions of the cyclodextrin derivatives **2a**–**2c** with **1c** afforded the corresponding carboranylcyclodextrins **3ca**, **3cb**, and **3cc** in 18, 19 and 20% isolated yields, respectively. It is also of note to mention here

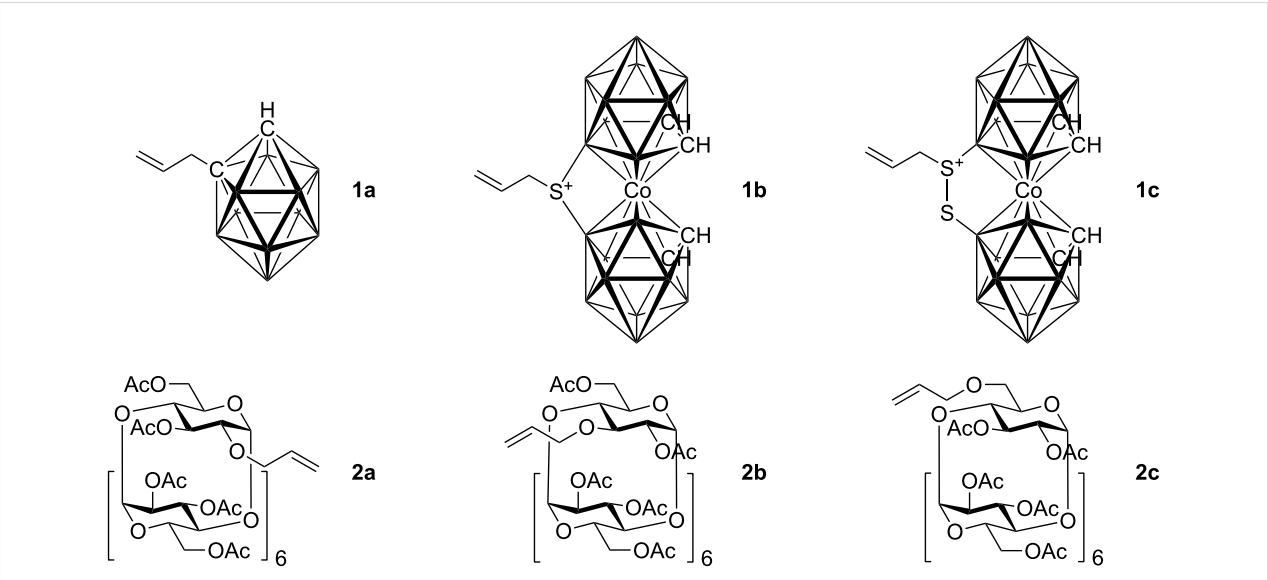

Figure 1: Starting allylcarboranes **1a**–**1c** and *O*-allylcyclodextrins **2a**–**2c**.

Table 1: The prepared carborane-cyclodextrin conjugates **3**.

Reactants		Product	Yield (%)[a]
1a	**2a**	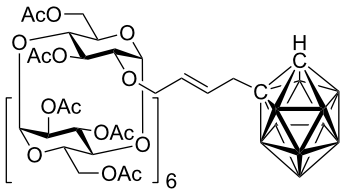	**3aa** 24
	2b	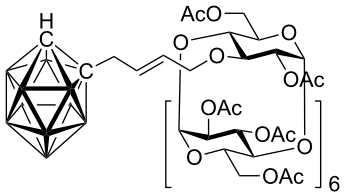	**3ab** 17
	2c	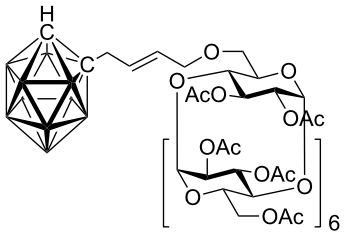	**3ac** 15
1b	**2a**	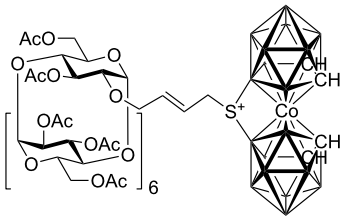	**3ba** 20
	2c	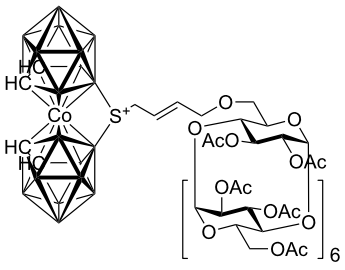	**3bc** 19
1c	**2a**	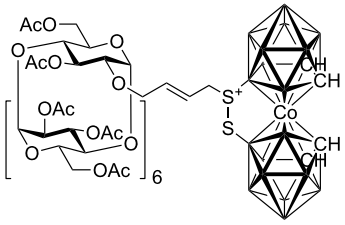	**3ca** 18
2b		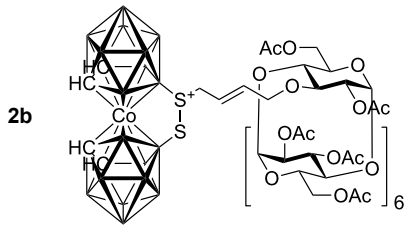	**3cb** 19
2c		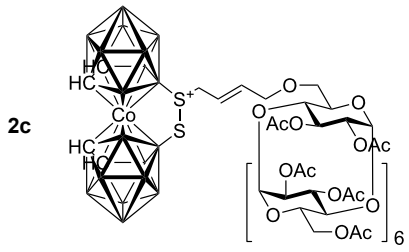	**3cc** 20

[a]Isolated yields.

the impressive *E*-selectivity of the cross-metathesis reactions, which has also been observed in other metathetical reactions with alkenylcyclodextrins derivatives [27] and can be explained by several factors [28]. Firstly, by a chelation of the intermediate Ru-carbene complex to the oxygen atoms of the cyclodextrin which results in a conformationally rigid intermediate and secondly, by a steric effect of the bulky carborane moiety. Although it may appear that the isolated yields are not high, conversions were in the range of ~50%. Isolation and purification of the products was a tedious task and the isolated yields we obtained represent the amounts of analytically pure compounds. It has been reported that low yields and conversions could be explained by isomerization of terminal to internal double bonds in both reactants (e.g., isomerization of allyl ethers to vinyl ethers [29-31] and allylcarboranes to propenylcarboranes [25]) and thus decreasing the reactant activity. However, NMR analysis of compounds isolated from the reaction mixtures revealed only the presence of the starting material and products, thus the low conversions could be attributed to deactivation of the catalysts by other routes. A similar effect has been also been observed in other cross-metathesis of various *O*-alkenylcyclodextrins which required the use of large amounts of catalyst [32,33]. Attempts to carry out the reaction with free (unprotected) *O*-allylcyclodextrins in dichloromethane or toluene has not so far resulted in the formation of any of the expected products, presumably because of their insolubility in the aforementioned solvents. To overcome the problem of the solubility of free *O*-allylcyclodextrins, the reaction was carried out in water in the presence of surfactant (SDS – sodium dodecyl sulfate), however, cross-metathesis did not occur.

Conclusion

The results described above clearly indicate that the cross-metathesis of allylcarboranes and *O*-allylcyclodextrins catalyzed by Hoveyda–Grubbs 2nd generation catalyst provides

a simple and straightforward method for the synthesis of cyclodextrin-carborane conjugates. The high boron content and the presence of a water soluble moiety (after removal of the protecting groups) suggest that the compounds may have potential for use in medical applications.

Experimental

General procedure for metathesis of allylcyclodextrins with allylcarboranes. The Hoveyda–Grubbs 2nd generation catalyst (3.13 mg, 0.005 mmol) was added under an argon atmosphere to a mixture of an allylcyclodextrin (0.07 mmol) and an allylcarborane (0.05 mmol) in toluene (5 mL). The resulting solution was stirred at 110 °C overnight. Removal of the solvent under reduced pressure gave a brown residue that was purified by column chromatography (85/15 MeOH/H_2O) on C_{18}-reversed phase.

Per-*O*-acetyl-2^I-*O*-[4-(1,2-dicarbadodecaboran-1-yl)-but-2-en-1-yl]-β-cyclodextrin (3aa). The compound was prepared from **2a** (0.15 g, 0.07 mmol) and **1a** (15 mg, 0.05 mmol). Column chromatography gave the title compound, 0.041 g (24%), as a white powder: m. p. 188–190 °C; IR (KBr) $\tilde{\nu}$ = 2591, 1747, 1371, 1236, 1044 cm^{-1}; ^{1}H NMR (300 MHz, $CDCl_3$): δ = 6.08–6.02 (m, 1 H, H-2'), 5.66–5.58 (m, 1 H, H-3'), 5.46–5.15 (m, 7 H, 7 × H-3), 5.13–4.92 (m, 7 H, 7 × H-1), 4.86–4.70 (m, 6 H, 6 × H-2), 4.61–4.43 (m, 6 H, 6 × H-6), 4.39–3.82 (m, 17 H, 8 × H-6, 7 × H-5, 2 × H-1'), 3.78–3.53 (m, 9 H, 7 × H-4, 2 × H-4'), 3.34 (d, *J* = 7.0 Hz, 1 H, H-2^I), 2.97 (s, 1 H, C_{carb}-H), 2.11–1.97 (m, 60 H, 20 × CH_3); ^{13}C NMR (100 MHz, $CDCl_3$): *δ* = 171.15–169.71 (20 × C=O), 132.28 (C-2'), 126.69 (C-3'), 98.35–97.06 (7 × C-1), 78.05–76.42 (7 × C-4), 74.19 (C-1'), 72.29–69.66 (7 × C-2, 7 × C-3, 7 × C-5), 63.10–62.85 (7 × C-6), 60.34 (2 × C_{carb}), 40.54 (C-4'), 21.56-21.02 (20 × CH_3); ^{11}B NMR (128 MHz, $CDCl_3$): *δ* = −3.29 (s, 1 B, B-9), −6.45 (s, 1 B, B-12), −10.14 (s, 2 B, B-8, B-10), −12.21 (s, 2 B, B-4, B-5), −13.47 (s, 4 B, B-3, B-6, B-7, B-11); MS (EI, *m/z* (rel.%)) 1108.7 (80), 1010.5 (19), 799.0 (12), 516.9 (14), 456.8 (25), 374.0 (29), 242.3 (100), 228.6 (56), 168.9 (41); HR-MS (ESI) calcd. for $C_{88}H_{126}O_{55}B_{10}$: 1108.3925, found 1108.3954 ($C_{88}H_{126}O_{55}{}^{10}B_2B_8Na_2$).

Per-*O*-acetyl-3^I-*O*-[4-(1,2-dicarbadodecaboran-1-yl)-but-2-en-1-yl]-β-cyclodextrin (3ab). The compound was prepared from **2b** (0.15 g, 0.07 mmol) and **1a** (15 mg, 0.05 mmol). Column chromatography gave the title compound, 0.029 g (17%), as a white powder: m. p. 198–201 °C; IR (KBr): $\tilde{\nu}$ = 2593, 1747, 1369, 1237, 1043 cm^{-1}; ^{1}H NMR (400 MHz, $CDCl_3$): δ = 5.91–5.70 (m, 1 H, H-2'), 5.60–5.50 (m, 1 H, H-3'), 5.49–5.28 (m, 6 H, H-3), 5.24–5.05 (m, 7 H, H-1), 4.89–4.66 (m, 8 H, 7 × H-4, 1 × H-1'), 4.66–3.64 (m, 31 H, 14 × H-6, 1 × H1', 2 × H-4', 7 × H-5, 7 × H-4), 3.23–3.13 (m, 1 H, H-3^I), 2.84 (bs, 1 H, C_{carb}-H), 2.20–1.95 (m, 60 H, 20 × CH_3); ^{13}C NMR (100 MHz, $CDCl_3$): *δ* = 170.76–170.04 (20 × C=O), 133.74 (C-2'), 126.51 (C-3'), 97.41–96.70 (7 × C-1), 77.68–75.86 (7 × C-4), 72.42–69.46 (7 × C-2, 7 × C-3, 7 × C-5), 62.91–62.18 (7 × C-6), 60.57 (2 × C_{carb}), 40.31(C-4'), 21.14–20.87 (20 × CH_3); ^{11}B NMR (128 MHz, $CDCl_3$): *δ* = −3.32 (s, 1 B, B-9), −6.47 (s, 1 B, B-12), −10.12 (s, 2 B, B-8, B-10), −12.02 (s, 2 B, B-4, B-5), −13.99 (s, 4 B, B-3, B-6, B-7, B-11); MS (EI, *m/z* (rel.%)): 1108.6 (100), 917.4 (19), 802.8 (20), 690.9 (18), 469.4 (42), 413.2 (65), 370.1 (96), 301.1 (75); HR-MS (ESI) calcd. for $C_{88}H_{126}O_{55}B_{10}$ 1108.3925, found 1108.3957 ($C_{88}H_{126}O_{55}{}^{10}B_2B_8Na_2$).

Per-*O*-acetyl-6^I-*O*-[4-(1,2-dicarbadodecaboran-1-yl)-but-2-en-1-yl]-β-cyclodextrin (3ac). The compound was prepared from **2c** (0.15 g, 0.07 mmol) and **1a** (15 mg, 0.05 mmol). Column chromatography gave the title compound,0.026 g (15%), as a white powder: m. p. 194–197 °C; IR (KBr): $\tilde{\nu}$ = 2917, 2848, 1747, 1370, 1235, 1044 cm^{-1}; ^{1}H NMR (400 MHz, $CDCl_3$): δ = 5.91–5.82 (m, 1 H, H-2'), 5.75–5.65 (m, 1 H, H-3'), 5.42–5.00 (m, 14 H, 7 × H-3, 7 × H-1), 4.91–4.68 (m, 7 H, 7 × H-2), 4.64–4.42 (m, 5 H, 5 × H-6), 4.40–3.94 (m, 17 H, 2 × H-1', 5 × H-5, 8 × H-6, 2 × H-4'), 3.90–3.82 (m, 2 H, 2 × H-5), 3.80–3.56 (m, 8 H, 1 × H-6^I, 7 × H-4), 2.96 (bs, 1 H, C_{carb}-H), 2.17–1.97 (m, 60 H, 20 × CH_3); ^{13}C NMR (100 MHz, $CDCl_3$): *δ* = 171.10–169.81 (20 × C=O), 134.05 (C-2'), 126.31 (C-3'), 97.45–96.64 (7 × C-1), 77.69–76.30 (7 × C-4), 71.94–69.79 (7 × C-2, 7 × C-3, 7 × C-5, C-1'), 68.12 (C-6^I), 63.02–62.71 (6 × C-6), 60.18 (2 × C_{carb}), 40.08 (C-4'), 21.87–21.16 (20 × CH_3); ^{11}B NMR (128 MHz, $CDCl_3$): *δ* = −3.27 (s, 1 B, B-9), −6.69 (s, 1 B, B-12), −10.12 (s, 2 B, B-8, B-10), −12.04 (s, 2 B, B-4, B-5), −13.94 (s, 4 B, B-3, B-6, B-7, B-11); MS (EI, *m/z* (rel.%)): 1108.5 (52), 1010.1 (62), 928.6 (51), 909.0 (60), 667.1 (31), 351.3 (57), 307.3 (100); HR-MS (ESI) calcd. for $C_{88}H_{126}O_{55}B_{10}$: 1108.3925, found 1108.3955 ($C_{88}H_{126}O_{55}{}^{10}B_2B_8Na_2$).

Per-*O*-acetyl-2^I-*O*-{4-{8,8'-μ-(sulfido)-[3,3'-commo-cobalt(III)-bis-(1,2-dicarbaundecaborate)]-8-yl}but-2-en-1-yl}-β-cyclodextrin (3ba). The compound was prepared from **2a** (0.15 g, 0.07 mmol) and **1b** (20 mg, 0.05 mmol). Column chromatography gave the title compound, 0.023 g (18%), as an orange powder: m. p. 207–209 °C; IR (KBr): $\tilde{\nu}$ = 2575, 1746, 1371, 1236, 1044 cm^{-1}. ^{1}H NMR (600 MHz, $CDCl_3$): δ = 5.75 (dt, *J* = 20.4, 5.4 Hz, 1 H, H-2'), 5.65–5.58 (m, 1 H, H-3'), 5.43–5.13 (m, 7 H, 7 × H-3), 5.12–4.91 (m, 6 H, 6 × H-1), 4.86 (d, *J* = 3.6 Hz, 1 H, H-1^I), 4.98–4.62 (m, 6 H, 6 × H-2), 4.56–4.38 (m, 6 H, 6 × H-6), 4.30–3.87 (m, 17 H, 8 × H-6, 7 × H-5, 2 × H-1'), 3.72–3.50 (m, 9 H, 7 × H-4, 2 × H-4'), 3.46–3.34 (m, 4 H, C_{carb}-H), 3.24 (dd, *J* = 3.0, 9.6 Hz, 1 H, H-2^I), 2.09–1.97 (m, 60 H, 20 × CH_3); ^{13}C NMR (150 MHz,

$CDCl_3$): δ = 170.81–169.37 (20 × C=O), 134.55 (C-2'), 122.80 (C-3'), 98.16–96.58 (7 × C-1), 78.05–76.17 (7 × C-4), 71.03–69.54 (7 × C-2, 7 × C-3, 7 × C-5, C-1'), 62.85–62.41 (7 × C-6), 49.33–48.66 (4 × C_{carb}), 42.02 (C-4'), 20.99–20.22 (20 × CH_3); ^{11}B NMR (128 MHz, $CDCl_3$): δ = 1.26 (bs, 2 B, B-8, B-8'), −4.70 (bs, 2 B, B-10, B-10'), −(6.00–11.72) (m, 12 B, B-4, B-4', B-5, B-5', B-7, B-7', B-9, B-9', B-11, B-11', B-12, B-12'), −14.68 (bs, 2 B, B-6, B-6'); MS (EI, *m/z* (rel.%)): 1214.4 (100), 1010.3 (10), 413.3 (68), 391.3 (10), 307.2 (52); HR-MS (ESI) calcd. for $C_{90}H_{135}O_{55}{}^{10}B_3B_{15}CoNa_2S$: 1213.9194, found 1213.9233.

Per-*O*-acetyl-6^{I}-*O*-{4-{8,8'-μ-(sulfido)-[3,3'-commo-cobalt(III)-bis-(1,2-dicarbaundecaborate)]-8-yl}but-2-en-1-yl}-β-cyclodextrin (3bc). The compound was prepared from **2c** (0.15 g, 0.07 mmol) and **1b** (20 mg, 0.05 mmol). Column chromatography gave the title compound, 0.028 g (22%), as an orange powder: m. p. 188–191 °C; IR (KBr): $\tilde{\nu}$ = 2955, 2575, 1747, 1370, 1237, 1046 cm^{-1}; ^{1}H NMR (600 MHz, $CDCl_3$): δ = 5.90 (dt, *J* = 15.1, 5.1 Hz, 1 H, H-2'), 5.78–5.68 (m, 1 H, H-3'), 5.40–5.19 (m, 7 H, 7 × H-3), 5.17–5.02 (m, 7 H, 7 × H-1), 4.86–4.69 (m, 7 H, 7 × H-2), 4.63–4.42 (m, 5 H, 5 × H-6), 4.36–3.96 (m, 17 H, 2 × H-1', 2 × H-4', 5 × H-5, 8 × H-6), 3.90–3.85 (m, 2 H, 2 × H-5), 3.78–3.65 (m, 10 H, 1 × H-6^{I}, 7 × H-4, 2 × C_{carb}-H), 3.48 (bs, 1 H, C_{carb}-H), 3.42 (bs, 1 H, C_{carb}-H), 2.16–1.98 (m, 60 H, 20 × CH_3); ^{13}C NMR (100 MHz, $CDCl_3$): δ = 171.10–169.80 (20 × C=O), 134.85 (C-2'), 122.80 (C-3'), 97.46–96.77 (7 × C-1), 77.69–76.21 (7 × C-4), 72.02–69.63 (7 × C-2, 7 × C-3, 7 × C-5, C-1'), 68.28 (C-6^{I}), 62.99–62.77 (6 × C-6), 49.93–49.27 (4 × C_{carb}), 42.71 (C-4'), 21.15–20.58 (20 × CH_3); ^{11}B NMR (128 MHz, $CDCl_3$): δ = 1.39 (bs, 2 B, B-8, B-8'), −4.58 (bs, 2 B, B-10, B-10'), −(5.84–11.21) (m, 12 B, B-4, B-4', B-5, B-5', B-7, B-7', B-9, B-9', B-11, B-11', B-12, B-12'), −14.92 (bs, 2 B, B-6, B-6'); MS (EI, *m/z* (rel.%)): 1214.1 (100), 1010.3 (10), 414.3 (52), 360.3 (10), 307.2 (96); HR-MS (ESI) calcd. for $C_{90}H_{135}O_{55}{}^{10}B_3B_{15}CoNa_2S$: 1213.9194, found 1213.9234.

Per-*O*-acetyl-2^{I}-*O*-{4-{8,8'-μ-(disulfido)-[3,3'-commo-cobalt(III)-bis-(1,2-dicarbaundecaborate)]-8-yl}but-2-en-1-yl}-β-cyclodextrin (3ca). The compound was prepared from **2a** (0.15 g, 0.07 mmol) and **1c** (20 mg, 0.05 mmol). Column chromatography gave the title compound, 0.026 g (20%), as a red powder: m. p. 188–191 °C; IR (KBr): $\tilde{\nu}$ = 2581, 1746, 1371, 1236, 1043 cm^{-1}; ^{1}H NMR (600 MHz, $CDCl_3$): δ = 6.04–5.95 (m, 1 H, H-2'), 5.72–5.63 (m, 1 H, H-3'), 5.34–5.16 (m, 7 H, 7 × H-3), 5.10–4.97 (m, 6 H, 6 × H-1), 4.96 (t, *J* = 3.6 Hz, 1 H, H-1^{I}), 4.84–4.76 (m, 6 H, 6 × H-2), 4.58–4.47 (m, 7 H, 7 × H-6), 4.37–4.00 (m, 18 H, 2 × H-1', 2 × H-4', 7 × H-5, 7 × H-6), 3.74–3.55 (m, 8 H, 6 × H-4, 2 × C_{carb}-H), 3.51–3.45 (m, 1 H, C_{carb}-H), 3.37–3.31 (m, 2 H, 1 × H-2^{I}, 1 × C_{carb}-H), 2.12–1.95 (m, 60 H, 20 × CH_3); ^{13}C NMR (150 MHz, $CDCl_3$): δ = 171.11–169.56 (20 × C=O), 138.15 (C-2'), 121.0 (C-3'), 98.27–96.81 (7 × C-1), 77.97–76.38 (7 × C-4), 72.24–69.43 (7 × C-2, 7 × C-3, 7 × C-5, C-1'), 63.06–62.62 (7 × C-6), 51.99 (C_{carb}), 50.92 (C_{carb}), 50.85 (C_{carb}), 49.36–49.08 (C-4', C_{carb}), 21.24–21.01 (20 × CH_3); ^{11}B NMR (128 MHz, $CDCl_3$): δ = 21.13 (bs, 2 B, B-8, B-8'), 0.56 (bs, 2 B, B-10, B-10'), −(1.91–10.86) (m, 12 B, B-4, B-4', B-5, B-5', B-7, B-7', B-9, B-9', B-11, B-11', B-12, B-12'), −15.30 (bs, 2 B, B-6, B-6'); MS (EI, *m/z* (rel.%)): 2436.4 (60), 2037.3 (10), 1272.7 (10), 1230.2 (100), 1030.6 (16), 1010.1 (10), 307.1 (61); HR-MS (ESI) calcd. for $C_{90}H_{135}O_{55}{}^{10}B_6B_{12}CoNa_2S_2$: 1228.4109, found 1228.4128.

Per-*O*-acetyl-3^{I}-*O*-{4-{8,8'-μ-(disulfido)-[3,3'-commo-cobalt(III)-bis-(1,2-dicarbaundecaborate)]-8-yl}but-2-en-1-yl}-β-cyclodextrin (3cb). The compound was prepared from **2b** (0.15 g, 0.07 mmol) and **1c** (20 mg, 0.05 mmol). Column chromatography gave the title compound, 0.029 g (25%), as a red powder: m. p. 201–203 °C; IR (KBr): $\tilde{\nu}$ = 2955, 2582, 1747, 1368, 1236, 1042 cm^{-1}; ^{1}H NMR (600 MHz, $CDCl_3$): δ = 6.15–6.06 (m, 1 H, H-2'), 5.74–5.65 (m, 1 H, H-3'), 5.50–5.22 (m, 7 H, 7 × H-3), 5.15–4.99 (m, 6 H, 6 × H-1), 4.85–4.61 (m, 8 H, 7 × H-4, 1 × H-1'), 4.60–3.85 (m, 25 H, 14 × H-6, 2 × H1', 2 × H-4', 7 × H-5), 3.84–3.49 (m, 9 H, 7 × H-4, 2 × C_{carb}-H), 3.37 (bs, 1 H, C_{carb}-H), 3.34 (bs, 1 H, C_{carb}-H), 2.12–1.93 (m, 60 H, 20 × CH_3); ^{13}C NMR (150 MHz, $CDCl_3$): δ = 170.86–169.86 (20 × C=O), 139.90 (C-2'), 119.35 (C-3'), 97.80–96.37 (7 × C-1), 77.89–75.67 (7 × C-4), 73.50 (C-1'), 72.23–69.05 (7 × C-2, 7 × C-3, 7 × C-5), 62.94–62.28 (7xC-6), 51.82 (C_{carb}), 51.07 (C_{carb}), 50.83 (C_{carb}), 49.63–49.42 (C-4', C_{carb}), 21.09–21.00 (20 × CH_3); ^{11}B NMR (128 MHz, $CDCl_3$): δ = 20.96 (bs, 2 B, B-8, B-8'), 0.54 (bs, 2 B, B-10, B-10'), −(1.99–10.87) (m, 12 B, B-4, B-4', B-5, B-5', B-7, B-7', B-9, B-9', B-11, B-11', B-12, B-12'), −15.42 (bs, 2 B, B-6, B-6'); MS (EI, *m/z* (rel.%)): 2438.8 (41), 2250.9 (10), 2037.7 (15), 1229.9 (50), 1030.8 (33), 307.2 (100); HR-MS (ESI) calcd. for $C_{90}H_{135}O_{55}{}^{10}B_6B_{12}CoNa_2S_2$: 1228.4109, found 1228.4127.

Per-*O*-acetyl-6^{I}-*O*-{4-{8,8'-μ-(disulfido)-[3,3'-commo-cobalt(III)-bis-(1,2-dicarbaundecaborate)]-8-yl}but-2-en-1-yl}-β-cyclodextrin (3cc). The compound was prepared from **2c** (0.15 g, 0.07 mmol) and **1c** (20 mg, 0.05 mmol). Column chromatography gave the title compound, 0.022 g (19%), as a red powder: m. p. 198–200 °C; IR (KBr): $\tilde{\nu}$ = 2578, 1747, 1370, 1236, 1045 cm^{-1}; ^{1}H NMR (600 MHz, $CDCl_3$): δ = 6.07 (dt, *J* = 15.0, 5.0 Hz, 1 H, H-2'), 5.77–5.70 (m, 1 H, H-3'), 5.40–5.21 (m, 7 H, 7 × H-3), 5.16–5.05 (m, 7 H, 7 × H-1), 4.86–4.69 (m, 7 H, 7 × H-2), 4.63–4.52 (m, 4 H, 4 × H-6), 4.46 (dd, *J* = 10.8, 3.5 Hz, 1 H, 1 × H-6), 4.41–4.03 (m, 17 H, 2 × H-1', 2 × H-4', 5 × H-5, 8 × H-6), 3.93–3.89 (m, 2 H, 2 × H-5), 3.87 (m, 2 H, 2

× H-4), 3.75–3.62 (m, 8 H, 1 × H-6^{I}, 5 × H-4, 2 × C_{carb}-H), 3.49 (bs, 1 H, C_{carb}-H), 3.34 (bs, 1 H, C_{carb}-H), 2.16–2.00 (m, 60 H, 20 × CH_3); ^{13}C NMR (150 MHz, $CDCl_3$): δ = 171.13–169.51 (20 × C=O), 137.95 (C-2'), 120.88 (C-3'), 97.38–96.55 (7 × C-1), 77.82–76.21 (7 × C-4), 71.86–68.37 (7 × C-2, 7 × C-3, 7 × C-5, C-1'), 68.37 (C-6^{I}), 62.93–62.65 (6 × C-6), 52.23 (C_{carb}), 51.68 (C_{carb}), 50.99 (C_{carb}), 49.64–49.21 (C-4', C_{carb}), 21.07–20.98 (20 × CH_3); ^{11}B NMR (128 MHz, $CDCl_3$) δ 21.66 (bs, 2 B, B-8, B-8'), 0.18 (s, 1 B, B-10 or B-10'), −1.02 (s, 1 B, B-10 or B-10'), −(1.93-10.95) (m, 12 B, B-4, B-4', B-5, B-5', B-7, B-7', B-9, B-9', B-11, B-11', B-12, B-12'), −15.63 (s, 2 B, B-6, B-6'); MS (EI, *m/z* (rel.%)): 2437.8 (23), 2085.6 (11), 1229.9 (20), 1010.1 (15), 528.1 (10), 307.2 (100); HR-MS (ESI) calcd. for $C_{90}H_{135}O_{55}{}^{10}B_6B_{12}CoNa_2S_2$: 1228.4109, found 1228.4119.

Supporting Information

Supporting Information File 1

Experimental details and characterisation data of peracetylated cyclodextrins **2a**, **2b** and **2c**.
[http://www.beilstein-journals.org/bjoc/content/supplementary/1860-5397-6-126-S1.pdf]

Acknowledgements

This work was supported by the Ministry of Education, Youth, and Sports (project No. MSM0021620857) and the Academy of Sciences of the Czech Republic (project No. KAN 200200651).

References

1. Connon, S. J.; Blechert, S. *Angew. Chem., Int. Ed.* **2003,** *42,* 1900–1923. doi:10.1002/anie.200200556
2. Bieniek, M.; Michrowska, A.; Usanov, D. L.; Grela, K. *Chem.–Eur. J.* **2008,** *14,* 806–818. doi:10.1002/chem.200701340
3. Vougioukalakis, G. C.; Grubbs, R. H. *Chem. Rev.* **2010,** *110,* 1746–1787. doi:10.1021/cr9002424
4. Eignerová, B.; Dračínský, M.; Kotora, M. *Eur. J. Org. Chem.* **2008,** 4493–4499. doi:10.1002/ejoc.200800230
5. Eignerová, B.; Slavíková, B.; Buděšínský, M.; Dračínský, M.; Klepetářová, B.; Šťastná, E.; Kotora, M. *J. Med. Chem.* **2009,** *52,* 5753–5757. doi:10.1021/jm900495f
6. Eignerová, B.; Sedlák, D.; Dračínský, M.; Bartůněk, P.; Kotora, M. *J. Med. Chem.* **2010,** *53,* 6947–6953. doi:10.1021/jm100563h
7. Řezanka, M.; Eignerová, B.; Jindřich, J.; Kotora, M. *Eur. J. Org. Chem.* **2010,** 6256–6262. doi:10.1002/ejoc.201000807
8. Eignerová, B.; Janoušek, Z.; Dračínský, M.; Kotora, M. *Synlett* **2010,** 885–887.
9. Grüner, B.; Holub, J.; Plešek, J.; Vaněk, T.; Votavová, H. *J. Chromatogr., A* **1998,** *793,* 249–256. doi:10.1016/S0021-9673(97)00904-7
10. Frixa, C.; Scobie, M.; Black, S. J.; Thompson, A. S.; Threadgill, M. D. *Chem. Commun.* **2002,** 2876–2877. doi:10.1039/b209339a
11. Ohta, K.; Konno, S.; Endo, Y. *Tetrahedron Lett.* **2008,** *49,* 6525–6528. doi:10.1016/j.tetlet.2008.08.107
12. Ohta, K.; Konno, S.; Endo, Y. *Chem. Pharm. Bull.* **2009,** *57,* 307–310. doi:10.1248/cpb.57.307
13. Uchman, M.; Jurkiewicz, P.; Cígler, P.; Grüner, B.; Hof, M.; Procházka, K.; Matějíček, P. *Langmuir* **2010,** *26,* 6268–6275. doi:10.1021/la904047k
14. Plešek, J. *Chem. Rev.* **1992,** *92,* 269–278. doi:10.1021/cr00010a005
15. Soloway, A. H.; Tjarks, W.; Barnum, B. A.; Rong, F.-G.; Barth, R. F.; Codogni, I. M.; Wilson, J. G. *Chem. Rev.* **1998,** *98,* 1515–1562. doi:10.1021/cr941195u
16. Hawthorne, M. F.; Maderna, A. *Chem. Rev.* **1999,** *99,* 3421–3434. doi:10.1021/cr980442h
17. Sivaev, I. B.; Bregadze, V. V. *Eur. J. Inorg. Chem.* **2009,** 1433–1450. doi:10.1002/ejic.200900003
18. Cígler, P.; Kožíšek, M.; Řezáčová, P.; Brynda, J.; Otwinowski, Z.; Pokorná, J.; Plešek, J.; Grüner, B.; Dolečková-Marešová, L.; Máša, M.; Sedláček, J.; Bodem, J.; Kräusslich, H.-G.; Král, V.; Konvalinka, J. *Proc. Natl. Acad. Sci. U. S. A.* **2005,** *102,* 15394–15399. doi:10.1073/pnas.0507577102
19. Řezáčová, P.; Pokorná, J.; Brynda, J.; Kožíšek, M.; Cígler, P.; Lepšík, M.; Fanfrlík, J.; Řezáč, J.; Šašková, K. G.; Sieglová, I.; Plešek, J.; Šícha, V.; Grüner, B.; Oberwinkler, H.; Sedláček, J.; Kräusslich, H.-G.; Hobza, P.; Král, V.; Konvalinka, J. *J. Med. Chem.* **2009,** *52,* 7132–7141. doi:10.1021/jm9011388
20. Plešek, J.; Štíbr, B.; Drdácká, E.; Plzák, Z.; Heřmánek, S. *Chem. Ind.* **1982,** 778–779.
21. Janoušek, Z.; Plešek, J.; Heřmánek, S.; Baše, K.; Todd, L. J.; Wright, W. F. *Collect. Czech. Chem. Commun.* **1981,** *46,* 2818–2833.
22. Jindrich, J.; Pitha, J.; Lindberg, B.; Seffers, P.; Harata, K. *Carbohydr. Res.* **1995,** *266,* 75–80. doi:10.1016/0008-6215(94)00251-A
23. Masurier, N.; Estour, F.; Lefèvre, B.; Brasme, B.; Masson, P.; Lafont, O. *Carbohydr. Res.* **2006,** *341,* 935–940. doi:10.1016/j.carres.2006.02.012
24. Jindřich, J.; Tišlerová, I. *J. Org. Chem.* **2005,** *70,* 9054–9055. doi:10.1021/jo051339c
25. Wei, X.; Carroll, P. J.; Sneddon, L. G. *Organometallics* **2006,** *25,* 609–621. doi:10.1021/om050851l
26. Simon, Y. C.; Ohm, C.; Zimny, M. J.; Coughlin, E. B. *Macromolecules* **2007,** *40,* 5628–5630. doi:10.1021/ma0709093
27. Ghera, B. B.; Fache, F.; Parrot-Lopez, H. *Tetrahedron* **2006,** *62,* 4807–4813. doi:10.1016/j.tet.2006.03.010
28. Connon, S. J.; Blechert, S. *Angew. Chem., Int. Ed.* **2003,** *42,* 1900–1923. doi:10.1002/anie.200200556
29. Schmidt, B. *Eur. J. Org. Chem.* **2003,** 816–819. doi:10.1002/ejoc.200390124
30. Hong, S. H.; Sanders, D. P.; Lee, C. W.; Grubbs, R. H. *J. Am. Chem. Soc.* **2005,** *127,* 17160–17161. doi:10.1021/ja052939w
31. Finnegan, D.; Seigal, B. A.; Snapper, M. L. *Org. Lett.* **2006,** *8,* 2603–2606. doi:10.1021/ol060918g
32. Chiu, S.-H.; Myles, D. C.; Garrell, R. L.; Stoddart, J. F. *J. Org. Chem.* **2000,** *62,* 2792–2796. doi:10.1021/jo9910381
33. Aime, S.; Gianolio, E.; Palmisano, G.; Robaldo, B.; Barge, A.; Boffa, L.; Cravotto, G. *Org. Biomol. Chem.* **2006,** *4,* 1124–1130. doi:10.1039/b517068k

Beilstein Journal of Organic Chemistry

Light-induced olefin metathesis

Yuval Vidavsky and N. Gabriel Lemcoff*

Review

Open Access

Address:
Chemistry Department, Ben-Gurion University of the Negev, Beer-Sheva 84105, Israel

Email:
N. Gabriel Lemcoff* - lemcoff@bgu.ac.il

* Corresponding author

Keywords:
catalysis; light activation; olefin metathesis; photoactivation; photoinitiation; photoisomerisation; RCM; ROMP; ruthenium; tungsten

Beilstein J. Org. Chem. **2010,** *6,* 1106–1119.
doi:10.3762/bjoc.6.127

Received: 29 August 2010
Accepted: 14 October 2010
Published: 23 November 2010

Guest Editor: K. Grela

Abstract

Light activation is a most desirable property for catalysis control. Among the many catalytic processes that may be activated by light, olefin metathesis stands out as both academically motivating and practically useful. Starting from early tungsten heterogeneous photoinitiated metathesis, up to modern ruthenium methods based on complex photoisomerisation or indirect photoactivation, this survey of the relevant literature summarises past and present developments in the use of light to expedite olefin ring-closing, ring-opening polymerisation and cross-metathesis reactions.

Introduction

The metal catalysed olefin metathesis reaction [1-8] has undoubtedly become one of the most widely used methodologies for the formation of carbon–carbon bonds. Its ubiquitous use in polymer chemistry [9-13] and natural product [14-17] and fine chemical synthesis [3,18-20], ultimately led to the 2005 Nobel Prize award to Yves Chauvin, Richard Schrock and Robert Grubbs [21] for the development of this reaction. Since, olefin metathesis has seen much progress, such as the use of new ligands for aqueous applications [22-26], asymmetric synthesis [27-30] and latent catalysis [31]. Among the methods used to activate latent olefin metathesis catalysts we find, chemical methods [32] and physical methods; such as the use of thermal energy [33], mechanochemical energy [34] and, perhaps more conveniently, the use of light [35]. In this review we summarise the early beginnings of light induced olefin metathesis by the use of ill defined tungsten complexes, up to the most recent developments in light induced ruthenium based isomerisation and activation.

Review

Early tungsten catalysed photometathesis

The first examples for photoinitiated metathesis were published independently by Dubois and McNelis in 1975 using simple tungsten hexacarbonyl as the metal initiator in carbon tetra-

chloride solvent [36,37]. This straightforward, cocatalyst free technique encouraged many research groups to investigate and develop this system.

Dubois demonstrated the photoinduced metathesis (335 nm) of *trans*-2-pentene to 2-butene and 3-hexene in 50% conversion; while McNelis used a 254 nm Rayonet reactor for the metathesis of hept-3-ene, pent-2-ene, and *E,E*-deca-2,8-diene (Scheme 1).

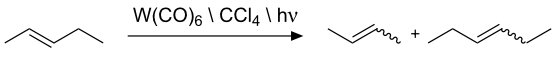

Scheme 1: Light activated metathesis of *trans*-2-pentene.

In the Dubois paper, when either light or carbon tetrachloride was excluded, no reaction could be observed. Furthermore, this research led to the proposal of the controversial mechanism shown in Scheme 2, which includes the generation of phosgene and the proposed active species, chloropentacarbonyl tungsten (**2**).

Alternatively, McNelis proposed that the active species was actually dichlorotetracarbonyl tungsten and demonstrated that phosgene was not generated by illumination of **1** when oxygen was excluded [38].

Following these first communications, Krausz, Garnier and Dubois published a series of papers investigating the photo-induced olefin metathesis with complex **1** [39-42]. Their main conclusions were:

a: $W(CO)_5$ and CO are created by photolysis of $W(CO)_6$. The reactivity of $W(CO)_5$ was found to be solvent dependent.

b: The intensity of irradiation, and the concentrations of both olefin and catalyst had a significant effect on reaction yields.

c: The $RCH{=}CCl_2$ produced in the reaction was a result of a reaction between a tungsten dichlorocarbene species and the double bond.

Research on the photo-activation of $W(CO)_6$ was further expanded by Harfouch et al. [43,44], Matsuda et al. [45], Szymańska-Buzar and Ziółkowski [46,47] and Zümreoglu [48], and was first reviewed in 1988 by Szymańska-Buzar [49]. The main conclusions from this wave of research dealt with the mechanistic role of the halide additives, as well as diverse reaction conditions, such as the use of other metals (i.e., Cr and Mo) that usually led to addition type reactions instead of metathesis.

In later work, Mol et al. [50] determined the heterogeneous character of the active catalytic species obtained on irradiation of **1** in CCl_4, supporting the previous proposal by Harfouch and coworkers. In another example of heterogeneous light induced metathesis, Shelimov and Kazansky [51] also found that silica supported molybdenum trioxide (MoO_3/SiO_2) could be activated by UV irradiation under an alkane atmosphere in the metathesis of propene and 1-hexene.

More recently, Sundararajan et al. [52-54], and Higashimura et al. [55] applied $W(CO)_6/CX_4/h\nu$ methodologies for the polymerisation of alkyne derivatives, especially phenylacetylene. These works were based on earlier observations by Katz et al. [56,57] and Geoffrey et al. [58] that acetylenes irradiated in the presence of tungsten complexes form metal carbenes that can produce polymeric species.

Well-defined tungsten catalysed photometathesis

The first example of well-defined early transition metal complexes for photocatalysed ROMP (PROMP) **3** and **4** (Figure 1) was published by van der Schaaf, Hafner, and Mühlebach [59].

Complexes **3** and **4** displayed reasonable thermal stability in solution (no decomposition was observed after 1 d at 80 °C), but were moisture sensitive and had to be handled under an inert atmosphere. Complex **3** slowly polymerised dicyclopentadiene (DCPD) in the dark at 60 °C, in contrast, when exposed to light even at room temperature, polymerisation was rapid and complete after 15 min. Enhanced behaviour was observed with complex **4**, which boasted true latency [60] and did not show

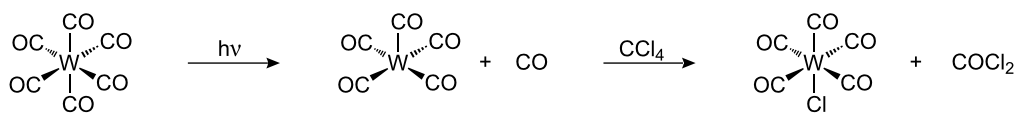

1 **2**

Scheme 2: Light induced generation of metathesis active species **2**.

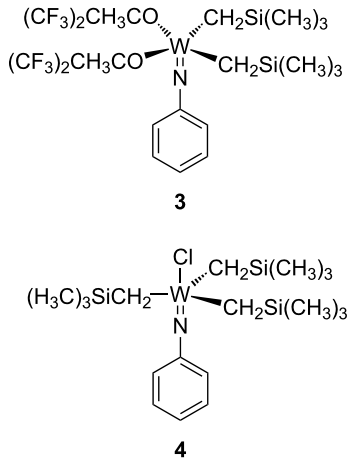

Figure 1: Well-defined tungsten photoactive catalysts.

any polymerisation of DCPD at 80 °C. Whilst a solution of **4** and DCPD can stand for days with no apparent polymerisation, irradiation with UV light led to fast polymerisation.

Ruthenium catalysed photometathesis

The first example for PROMP using ruthenium initiators was disclosed by Mühlebach et al. in 1995 [61]. Three main types of ruthenium-based precatalysts: η^6-arene sandwich complexes, half-sandwich complexes and nitrile complexes (Figure 2) were shown to promote the polymerisation of strained cyclic alkenes (Figure 3) when irradiated by UV light.

Advantageously, the systems showed none to moderate activity for normal ROMP, and were not sensitive to oxygen and humidity compared to the tungsten initiators described above. Notably, heating the sandwich catalysts for more than 24 h at 50 °C in the presence of the monomers did not induce polymerisation, on the other hand, the nitrile complexes displayed low

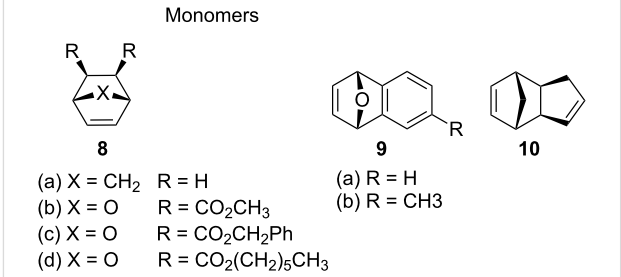

Figure 3: Cyclic strained alkenes for PROMP.

activity even at room temperature. UV irradiation at 364 nm significantly enhanced the activity of all these complexes. The activity of the compounds, including comparisons with thermally active catalysts, are summarised in Table 1.

Overall, the polymers obtained from norbornene and oxanorbornene derivatives had high molecular weights (M_w > 150 kDa) and also high monomodal polydispersities (M_w/M_n > 2.3). Polymerisation was also found to occur if the monomer was added after irradiation of the complex. In addition, the initial rate of polymerisation was found to be linearly dependent on the irradiation time. Conversely, irradiation above 420 nm did not initiate polymerisation for most of the complexes investigated.

As in most systems of this type, activation of the precatalyst is dependent on the photochemically induced cleavage of a metal–ligand bond which leads to the active species. The mechanism for initiation of the sandwich compounds was proposed to proceed through gradual photodissociation of the arene ligand, followed by solvation of the photochemically excited molecule (Scheme 3).

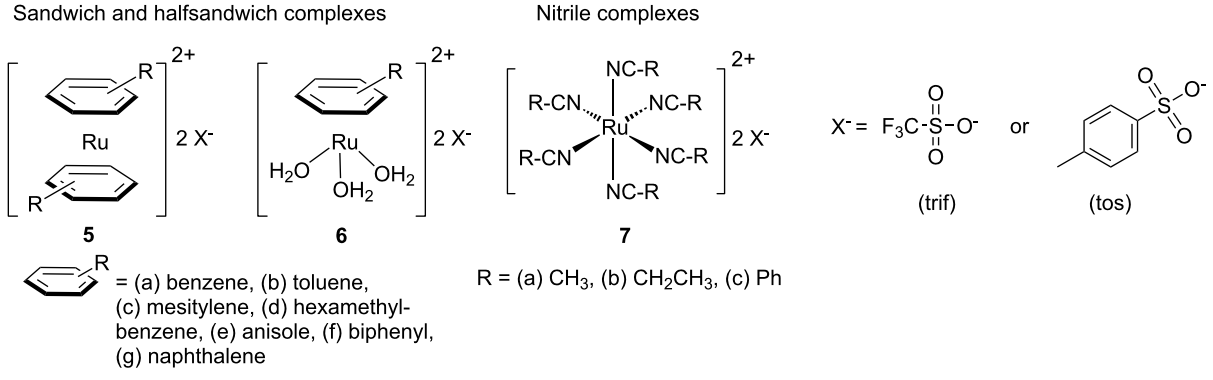

Figure 2: The first ruthenium based complexes for PROMP.

Table 1: Activation of ruthenium complexes with and without irradiation[a].

Entry	Compound	Catalytic activity	
		Thermal	hν[b]
1	$[Ru(H_2O)_6](tos)_2$	Very high	
2	$[Ru(H_2O)_6](trif)_2$	Very high	
Half-sandwich complexes			
3	$[(C_6H_6)Ru(H_2O)_3](tos)_2$	Medium	High
4	$[(toluene)Ru(H_2O)_3](tos)_2$	Weak	Medium
5	$[(hexamethylbenzene)Ru(H_2O)_3](tos)_2$	Very weak	Very weak
6	$[(C_6H_6)Ru(acetonitrile)_3](tos)_2$	Medium	
Sandwich complexes			
7	$[(C_6H_6)_2Ru](tos)_2$	None	High
8	$[(C_6H_6)Ru(toluene)](tos)_2$	None	Medium
9	$[(C_6H_6)Ru(mesitylene)](tos)_2$	None	Weak
10	$[(C_6H_6)Ru(hexamethylbenzene)](tos)_2$	None	Weak
11	$[(mesitylene)Ru(hexamethylbenzene)](BF_4)_2$	None	Weak
12	$[(hexamethylbenzene)_2Ru](tos)_2$	None	Very weak
13	$[(C_6H_6)Ru(anisole)](tos)_2$	Weak	High
14	$[(C_6H_6)Ru(biphenyl)](tos)_2$	None	Very high
15	$[(C_6H_6)Ru(naphthalene)](tos)_2$	Medium	Very high
16	$[(C_6H_6)Ru(chrysene)](tos)_2$	Medium	Very high
17	$[(C_6H_6)Ru(tetramethylthiophene)](tos)_2$	None	Very high
18	$[(C_6H_6)Ru(triphos)](tos)_2$	None	None
19	$[(C_6H_6)Ru(1,2,4\text{-}C_6H_3Me_3)](BF_4)_2$	None	Weak
20	$[(C_6H_6)Ru(1R,2S\text{-trans—}C_{12}H_{16}O)](BF_4)_2$	None	Weak
21	$[(C_6H_6)Ru(1S,2R\text{-trans—}C_{12}H_{16}O)](BF_4)_2$	None	weak
Nitrile complexes			
22	$[Ru(acetonitrile)_6](tos)_2$	Weak	High
23	$[Ru(acetonitrile)_6](trif)_2$	Weak	High
24	$[Ru(propionitrile)_6](tos)_2$	Weak	High
25	$[Ru(propionitrile)_6](trif)_2$	Weak	High
26	$[Ru(benzonitrile)_6](tos)_2$	Weak	Medium
27	$[Ru(benzonitrile)_6](trif)_2$	Weak	Medium

[a]monomers: **8a** or **8b**, concentration 50–200 mg/mL; catalyst, 1 wt %; [b]irradiation with a Hg lamp for 15 min prior to the addition of monomer.

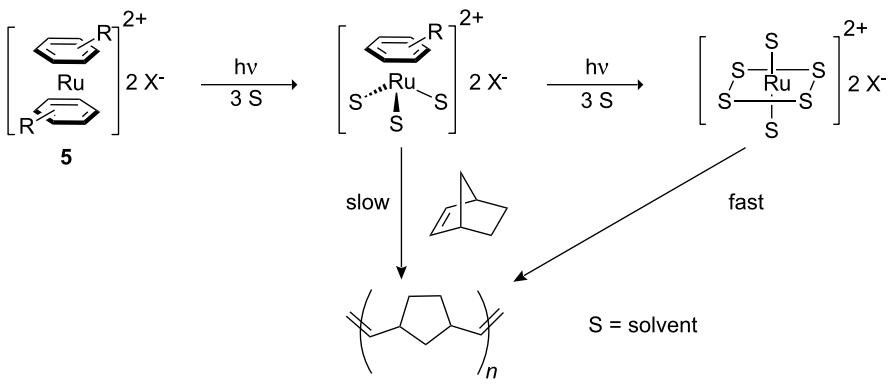

Scheme 3: Proposed mechanism for photoactivation of sandwich complexes.

Both the intermediate half-sandwich species $[(\eta^6\text{-arene})Ru(solvent)_3]^{2+}$ and the fully solvated complex $[Ru(solvent)_6]^{2+}$ are thermally active ROMP catalysts for strained bicyclic olefins, the latter being the more active. Thus, Mühlebach concluded that PROMP results mainly from the phototransformation of the sandwich complex to the fully solvated complex. The nitrile complexes are proposed to be activated by a similar mechanism where several species of the type $[Ru(RCN)_{6-x}(H_2O)_x]$ are responsible for the polymerisation initiation.

Disadvantages of these catalysts are the overall moderate activities achieved and that they are only soluble in polar solvents, due to their cationic character. On the other hand, the complexes are readily available and the use of aqueous solvents as the reaction media can also be envisaged as an attractive feature.

Mühlebach, Hafner and van der Schaaf [62] carried on the development of ruthenium and osmium photoactivated catalysts (Figure 4) by adding a bulky phosphane ligand to the complex. Thus, a more active and soluble neutral species with the anionic ligands bound to the metal could be obtained. The same concept of arene displacement by UV radiation was used for the release of a *p*-cymene ligand to produce a more reactive catalytic species.

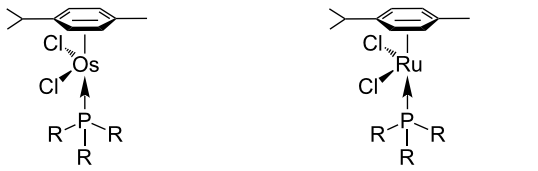

11 **12**

R = (a) *n*-butyl, (b) isopropyl, (c) cyclohexyl, (d) phenyl, (e) methyl, (f) *m*-tolyl

R = (a) *n*-butyl, (b) cyclohexyl, (c) *m*-tolyl

Figure 4: Ruthenium and osmium complexes with *p*-cymene and phosphane ligands for PROMP.

Osmium precatalysts **11a**–**f** did not polymerise norbornene under standard conditions. However, 5 min irradiation of a toluene solution of the complex with a 200 W Hg lamp led to active catalysts. The more active catalysts were those possessing more sterically hindered phosphane ligands. Thus, complexes with larger cone angles θ, such as **11b** (θ = 160°) and **11c** (θ = 170°) showed strong metathetic activity for PROMP of norbornene and dicylopentadiene in toluene solution or even in aqueous dispersions; by contrast, complexes **11a**,**d**,**e**,**f** (θ = 130°, 145°, 120°, 150°) showed slow no reaction even after UV irradiation. The ruthenium complexes **12** showed much higher reactivity in the polymerisation of norbornene, albeit none of these complexes was completely thermally latent for this reaction. The remarkable tolerance of **12b** to impurities and water, was highlighted by the fact that polymerisation can take place in water dispersions containing fillers such as SiO_2, $AI(OH)_3$, or $CaCO_3$ up to a loading of 70 wt %. The electrical and mechanical properties of PDCPD were preserved, making this system highly interesting for novel applications. The work of Mühlebach, Hafner and van der Schaaf on photoinduced ring-opening metathesis polymerisation was reviewed in 1997 [63].

The interest in photoactivated olefin metathesis motivated Fürstner [64] to use complex **12b** for photoinduced ring closing metathesis (RCM) by using regular neon light or strong daylight as a photon source instead of the UV lamps used thus far. Indeed, **12b** catalysed the ring-closing metathesis reaction of diallyl tosylamide in 90% yield when illuminated by neon light. Alternatively, the commercially available dimer complex **13** (Figure 5) mixed with PCy_3 could be irradiated to produce similar results.

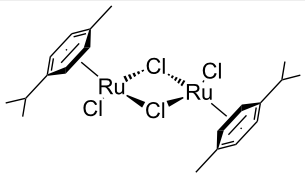

13

Figure 5: Commercially available photoactive ruthenium precatalyst.

Some of the photoinduced RCM products obtained by neon light irradiation of dimer **13** are highlighted in Figure 6. Perhaps the main benefit of this procedure lies in its simplicity since it only requires commercially available metal complexes and commonly used lighting equipment.

An additional expansion to photopromoted RCM was described in 1998 by Dixneuf et al. [65], who used the cationic allenylidene ruthenium complex **14** (Scheme 4) for the ene-yne RCM of propargylic allyl ethers into 3-vinyl-2,5-dihydrofurans.

The best conditions reported for this reaction were the irradiation of a toluene solution of **14** and substrate with an Hg lamp at 300 nm for 30 min at room temperature, followed by heating at 80 °C until completion of the reaction. The reaction time, compared to the non-irradiated control experiment, was reduced six fold. The various dihydrofuran rings obtained by this method are shown in Figure 7 along with their respective yields and the required reaction times.

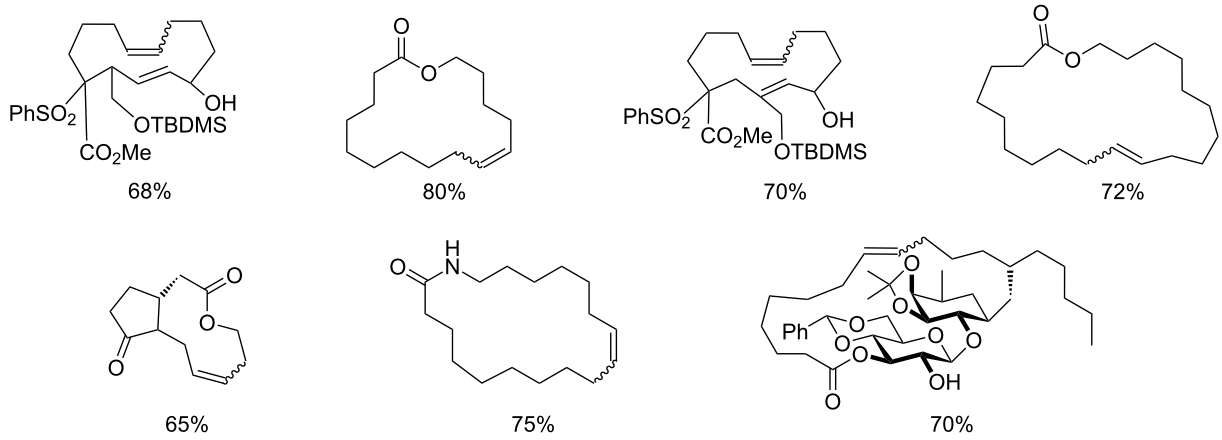

Figure 6: Some of the rings produced by photo-RCM.

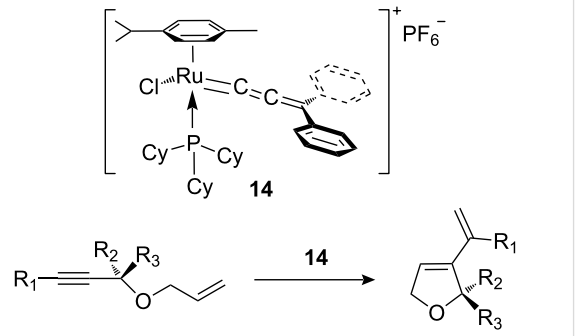

Scheme 4: Photopromoted ene-yne RCM by cationic allenylidene ruthenium complex **14**.

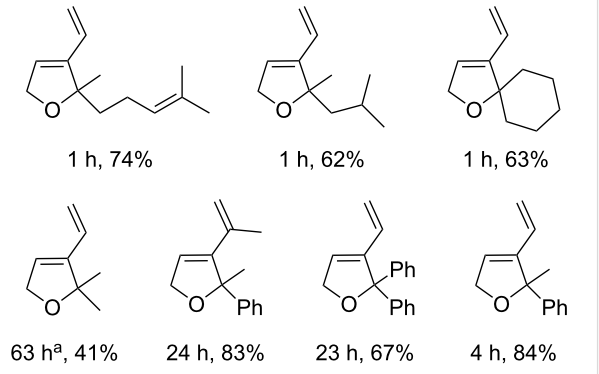

Figure 7: Dihydrofurans synthesised by photopromoted ene-yne RCM.

In line with the development of ruthenium benzylidene initiators [66,67], the phosphane ligand was replaced by an *N*-heterocyclic carbene (NHCs) in the photoactivated precatalysts. Accordingly, Noels et al. [68,69] synthesised a range of NHC substituted ruthenium cymene complexes (Figure 8) either by replacing the phosphane ligand in complex **12** by NHC ligands or via direct synthesis from **13**. Complexes **15** and **16** were tested as photoactivated ROMP catalysts. In all cases cyclooctene was used as a standard cyclic olefin monomer for the polymerisation studies.

Illuminating **15** or **16** with intense visible light, or even with regular laboratory lighting, revealed a dramatic improvement in their ROMP activity. Results of PROMP by complex **16g** (Mes ligand) and cyclooctene are summarised in Table 2. The large difference in polymer molecular weight between the dark and light reactions was not explained, even though it is slightly counterintuitive.

In order to improve the understanding of the photoactivation mechanism, complex **16g** was irradiated by visible light both in the presence and absence of cyclooctene. NMR and UV spectra confirmed the release of *p*-cymene from the complex in the photochemical process; however, the active species and overall mechanism were not elucidated. Both saturated and unsaturated NHC ligands afforded similar results. However, blocking both *ortho* positions on the aromatic groups of the NHCs was crucial for the performance of the catalyst.

The ruthenium photoactivated catalytic systems described so far possessed noticeable ROMP activity at temperatures higher than room temperature even without being exposed to light; especially with the more reactive monomers such as norbornene and dicyclopentadiene. Buchmeiser argued that in order to integrate light activated precatalyst in practical applications, latency must be significant also at higher temperatures. Therefore, Buchmeiser et al. concentrated efforts towards the design of 'true' latent photoactivated ruthenium precatalysts for

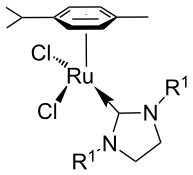

15

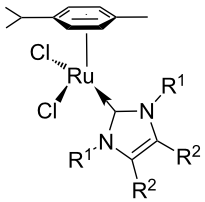

16

(a) R^1 = Dipp (e) R^1 = dmph
(b) R^1 = Mes (f) R^1 = biph
(c) R^1 = Ph (g) R^1 = 2-tolyl
(d) R^1 = Naph (h) R^1 = xylyl

(a) $R^1 = R^2$ = Me
(b) R^1 = ^{i}Pr, R^2 = H
(c) R^1 = ^{i}Pr, R^2 = Me
(d) R^1 = Cy, R^2 = H
(e) R^1 = Cy, R^2 = Me

(f) R^1 = Dipp, R^2 = H
(g) R^1 = Mes, R^2 = H
(h) R^1 = Mes, R^2 = Me
(i) R^1 = Mes, R^2 = Cl
(j) R^1 = Ph, R^2 = H

(k) R^1 = Naph, R^2 = H
(l) R^1 = dmph, R^2 = H
(m) R^1 = biph, R^2 = H
(n) R^1 = 2-tolyl, R^2 = H
(o) R^1 = xylyl, R^2 = H

Cy = cyclohexyl
Dipp = 2,6-diisopropylphenyl
Mes = 2,4,6-trimethylphenyl
dmph = 3,5-dimethylphenyl
biph = 4-biphenyl
2-tolyl = 2-methylphenyl
xylyl = 2,6-dimethylphenyl

Figure 8: Ruthenium complexes with *p*-cymene and NHC ligands.

Table 2: Effect of light on the ROMP of cyclooctene using **16g** as catalyst.

Lighting conditions	Monomer conversion (%)	Isolated yield (%)	M_n (×10^3 g)
Darkness	20	20	21
Normal[a]	93	84	625
Neon tube[b]	99	93	553
Light bulb[c]	>99	91	537

[a]normal lighting, a combination of daylight and fluorescent light; bordinary 40 W 'cold white' fluorescent tube, 10 cm away from the standard Pyrex reaction flask; [c]250 W incandescent light bulb, 10 cm away from the standard Pyrex reaction flask.

ROMP [70]. These precatalysts, similar to Noels' complexes, included NHCs, and in some cases the *p*-cymene ligand was exchanged for phenylisonitrile and in others the chloride ligands were replaced by trifluroacetate. These transformations were expected to generate more stable, inert, precatalysts that would require external triggers to initiate the dissociation of the neutral ligand to produce the active species.

Complexes **17**–**20** (Scheme 5) initiated ROMP of norborn-5-ene-2-ylmethanol **21** only at temperatures over 40 °C or by illumination at 172 nm. However, the reaction conditions required the removal of oxygen from the system, an encumbrance in practical applications. In addition, more reactive monomers, such as 2-norbornene, were thermally polymerised by the complexes even at room temperature.

In 2008 Buchmeiser introduced the improved cationic latent phototriggered precatalysts **22** and **23** (Figure 9) [71]. These cationic species were inactive at higher temperatures (T < 45 °C) and did not thermally initiate the polymerisation of several ROMP monomers, including the highly reactive dicyclopentadiene **25** (DCPD) (Figure 10).

Irradiation at 308 nm of complex **22** or **23** in chloroform in the presence of the monomers resulted in polymerisations with 5–99% conversion yields (Table 3). On changing the light source to a 254 nm Hg lamp improved the yields to 70–99% (Table 3).

The proposed mechanism for the photoactivation of precatalysts **22** and **23** is displayed in Scheme 6.

Three additional new complexes for PROMP were recently published by Buchmeiser et al. [72] Although the complexes

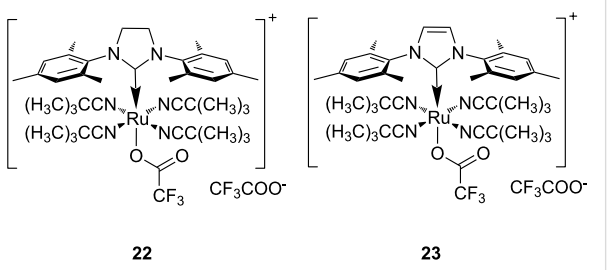

22 23

Figure 9: Photoactivated cationic ROMP precatalysts.

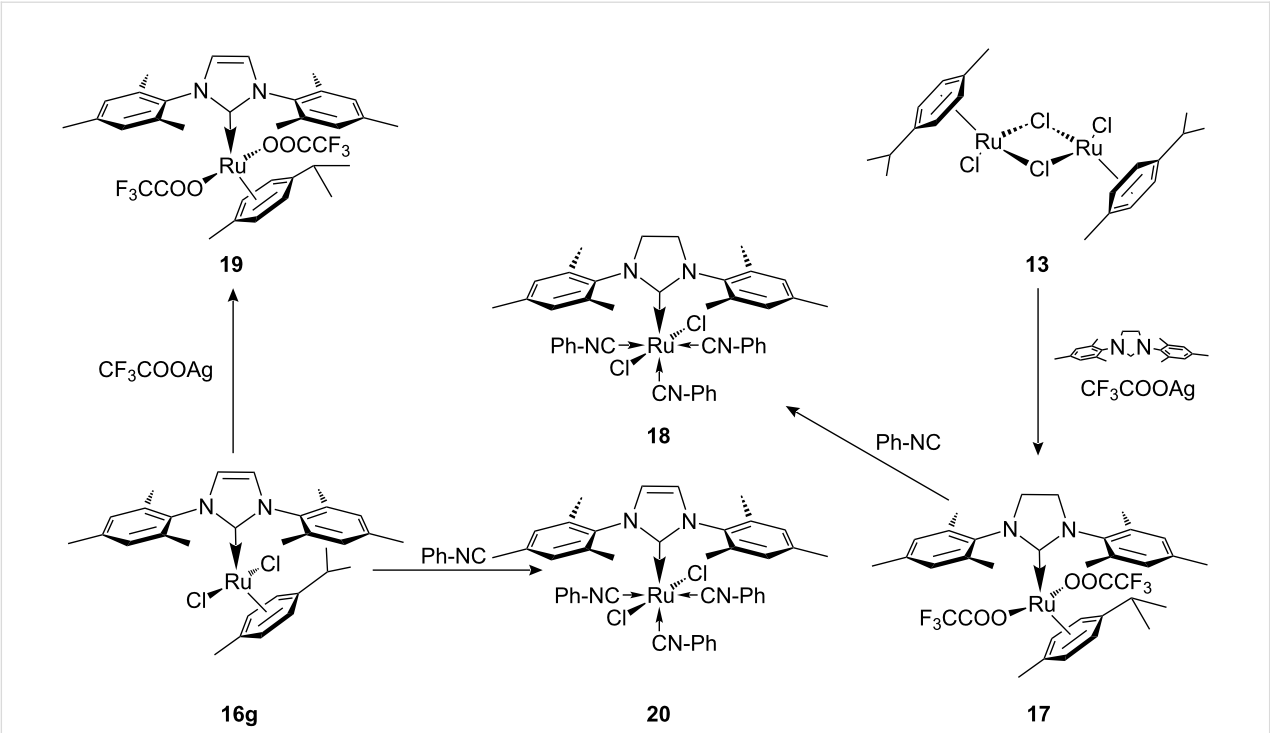

Scheme 5: Ruthenium NHC complexes for PROMP containing *p*-cymene and trifluroacetate (**17**, **19**) or phenylisonitrile ligands (**18**, **20**).

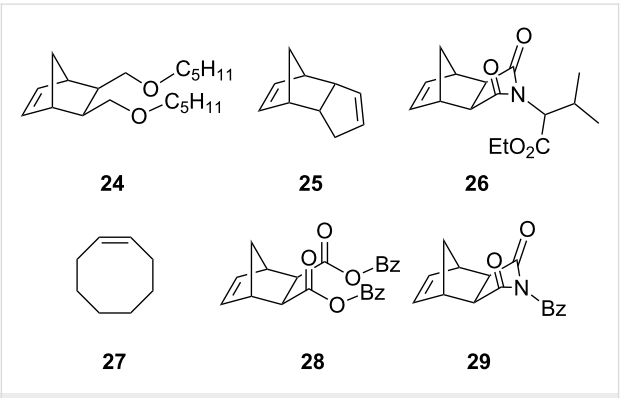

Figure 10: Different monomers for PROMP.

30–**32** (Figure 11) are not true latent precatalysts, only minor polymerisation occurred in the absence light (<5% at room temperature after 24 h). However, when the monomer–complex mixture was irradiated with a 254 nm UV source, polymerisation occurred with more than 60% conversion within 1 h in most cases.

A desirable enhancement in phototriggered catalysis is the generation of photoswitchable systems. Thus, a specific reaction may be turned on by one type of stimulus (heat, light), and turned off by another. We have recently developed latent sulfur chelated Hoveyda–Grubbs type complexes (Figure 12), as thermo-switchable catalysts for RCM and ROMP [73-77].

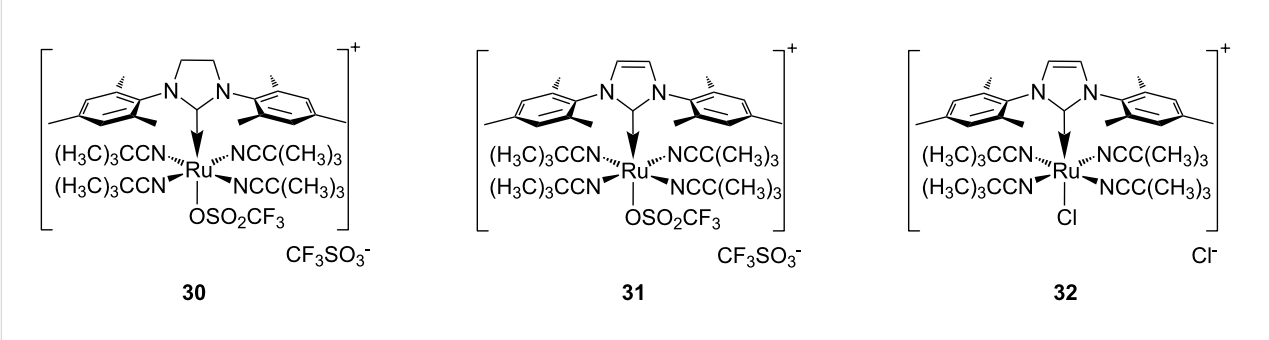

Figure 11: Light-induced cationic catalysts for ROMP.

Table 3: Polymerisation results for monomers **24**–**29** by **22** and **23**[a].

Catalyst	Monomer	Yield[b]		M_n[d]
		308 nm	254 nm	
22	**24**	40[c]	95[c]	4.8×10^5
22	**25**	82	99	—
22	**26**	69	85	2.1×10^5
22	**27**	90	92	8.8×10^5
22	**28**	<5[c]	90	2.6×10^5
22	**29**	33[c]	99[c]	4.0×10^5
23	**24**	41[c]	92[c]	—
23	**25**	>99	99	—
23	**26**	61	67	4.4×10^5
23	**27**	91	90	8.8×10^5
23	**28**	<5[c]	86	4.5×10^5
23	**29**	21[c]	>99[c]	4.9×10^4

[a]polymerisations were carried out in 5 mL $CDCl_3$, monomer:initiator 200:1, 30 °C, 1 h; [b]yield of isolated polymer; [c]yield determined by ^1H NMR; [d]molecular weights measured for the polymers obtained with 254 nm irradiation.

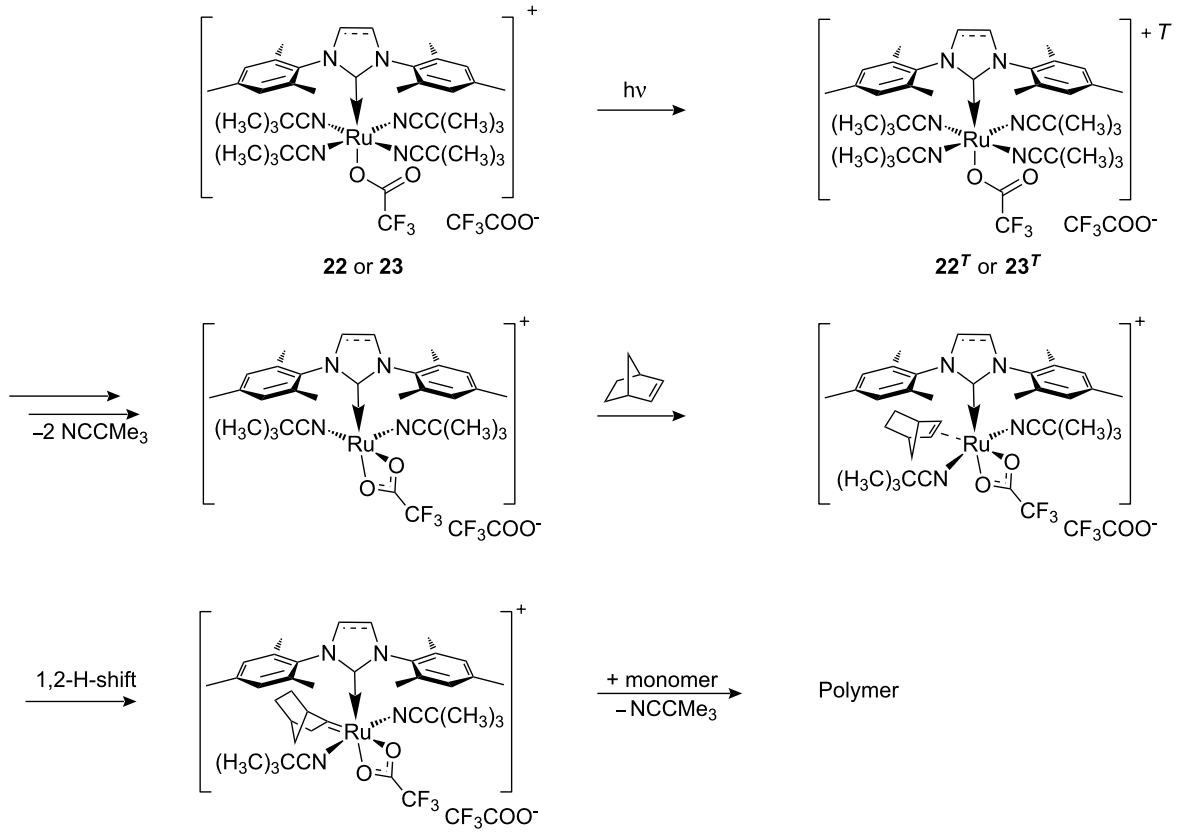

Scheme 6: Proposed mechanism for photoinitiated polymerisation by **22** and **23**.

The thermal latency of the sulfur chelated complexes make them ideal candidates for photoswitchable applications; especially in light of the well documented photodissociation of ruthenium sulfur ligands.

Therefore, complexes **33a, e, f, g** were irradiated at 365 nm in the presence of RCM and ROMP substrates [78]. A summary of the results is presented in Table 4 and Table 5.

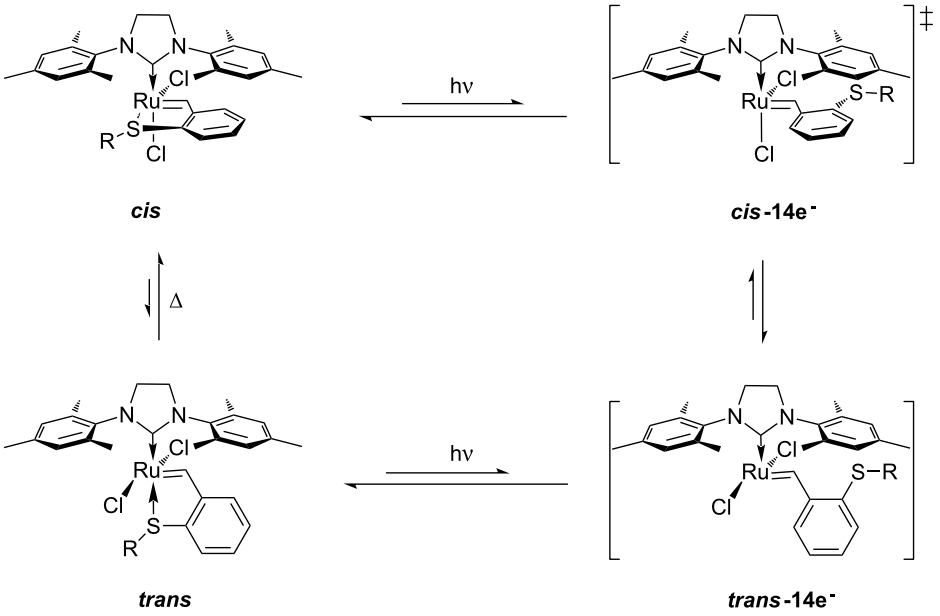

Scheme 7: Proposed mechanism for the photoactivation of sulfur-chelated ruthenium benzylidene.

Table 4: Photo RCM of different substrates[a].

Catalyst	Substrate	Product	Yield[b]
33e	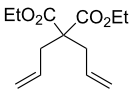	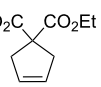	86%
33f			77%
33e	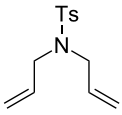		85%
33f			78%
33e	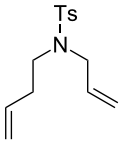	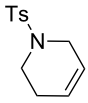	>99%
33f			97%
33e	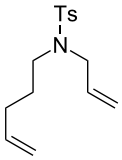	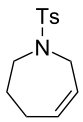	>99%
33f			94%
33e	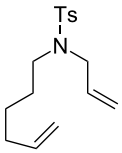	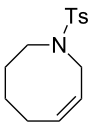	65%[c]
33f			54%[c]

[a]5 mol% catalyst, 0.1 M substrate in CH_2Cl_2 at 28 °C; 365 nm UV irradiation for 5 h; [b]yields were determined by GC-MS after 24 h; no reaction observed without UV irradiation; [c]includes isomerisation products.

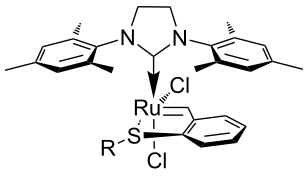

33

R = (a) ^{i}Pr, (b) Me, (c) *t*-Bu, (d) Et, (e) Ph, (f) b-Naph, (g) 1-Pyr

Figure 12: Sulfur chelated ruthenium benzylidene pre-catalysts for olefin metathesis.

Table 5: PROMP with sulfur chelated complexes[a].

Monomer	Catalyst	Conversion[b]	PDI[c]	M_n[c]
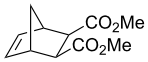	**33e**	40%	1.5	2.5×10^5
	33f	66%	1.5	2.5×10^5
	**33e**	96%	1.3	1.1×10^5
	33f	>99%	1.2	1.3×10^5
	**33e**	86%	1.4	5.0×10^4
	33f	84%	1.5	7.0×10^4

[a]monomer concentration 0.5 M in CH_2Cl_2; [monomer]/[cat] = 300; [b]conversions were determined by GC-MS after 24 h with mesitylene as internal standard; [c]M_n and PDI values were determined by GPC.

The discovery that light irradiation induces photoisomerisation of the *cis*-dichloro complexes led to the proposed mechanism shown in Scheme 7. Thus, photoactivation of sulfur-chelated ruthenium benzylidene complexes was found to depend on the generation of the active *trans*-dichloro isomer via 14-electron intermediates.

The design of a photoswitchable system was based on the fact that the latent isomer (*cis*-dichloro) was thermodynamically more stable than its active counterpart (*trans*-dichloro). Thus, illumination with UV light generates an active isomer, but a short heating period regenerates the inactive isomer. The switchable nature of the system was demonstrated by 15 min irradiation of a tetrachloroethane solution of diethyldiallyl malonate with 5 mol % of catalyst **33e** (activation), followed by 5 min heating at 80 °C (deactivation). Thus, whilst heating may be initially perceived as counterintuitive, it may be used to regenerate the latent species instead of activating it.

Indirect metathesis photoactivation

An alternative approach for photoinitiated metathesis is indirect activation.

Grubbs et al. [79] demonstrated the use of photoacid generators (PAG) **34** and **35** (Figure 13) for the sub-300 nm UV activation of metathesis precatalysts **36** and **37** (Scheme 8). Thus, an acid sensitive olefin metathesis catalyst can be photoactivated by using a PAG in a tandem approach. Clearly, all other acids must be excluded from the reaction mixtures for the procedure to be effective.

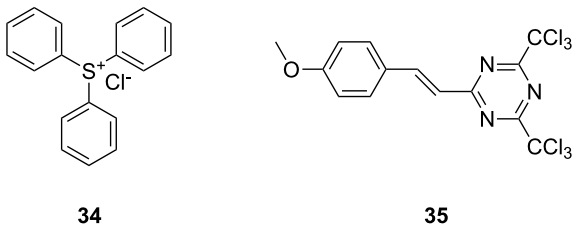

34 **35**

Figure 13: Photoacid generators for photoinduced metathesis.

Acid sensitive complexes **36** and **37** were synthesised starting from the Grubbs type catalysts **38** and **39** and thallium hexamethylacetylacetonate (Scheme 8). Several RCM substrates were closed as shown in Table 6 by the PAG induced metathesis. Complexes **36** or **37** and PAG **34** also polymerised typical ROMP monomers in excellent conversion (Table 7).

A dramatic loss of activity was observed when the chloride anion of PAG **31** was replaced by the non-nucleophilic nonaflate ion, implying that the chloride plays a crucial role in the photoactivation of this system. A cunning trapping experiment using the isopropoxy aromatic derivative **40** (Scheme 9) provided a better understanding of the activation mechanism and led to the proposal of the well-known 14-electron complex **41** as the actual active species.

Another excellent example for nondirect activation of metathesis is the light-triggerable liquid-filled solid microcapsules (MCs) presented by Fréchet et al. in 2009 [80]. A solution of **39** in toluene inside macrocapsules (Figure 14) can stand for weeks in neat DCPD without any appreciable reaction. However, near-IR laser bursting of the MCs causes gelling due to polymerisation within min.

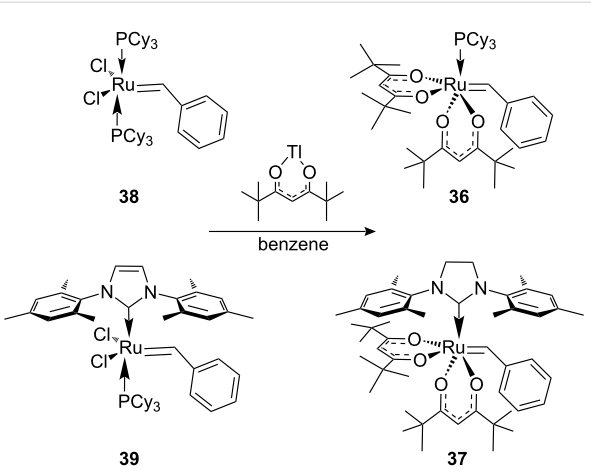

Scheme 8: Synthesis of precatalysts **36** and **37**.

Table 6: RCM by PAG and precatalysts **36** and **37**[a].

Catalyst	Substrate	Product	Yield
36	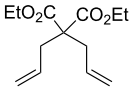	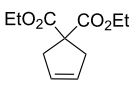	77%
37			83%
36	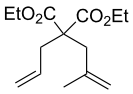	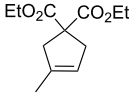	42%
37			88%
36	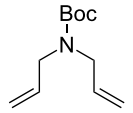		70%
37			93%
36	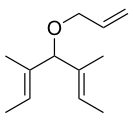	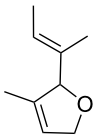	23%
37			62%

[a]5 mol % of **33/34**, 10 mol % of **31** and substrate in a quartz NMR tube in CD_2Cl_2 (0.1 M); [b]isolated after column chromatography.

Table 7: ROMP by PAG and precatalysts **36** and **37**[a].

Monomer	Cat.	Conversion[b]	PDI	M_n[c]
	**36**	>95%	1.38	1.39×10^4
	37	>95%	1.26	0.85×10^4
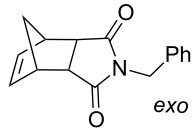	**36**	>95%	1.33	5.75×10^4
	37	>95%	1.25	12.7×10^4
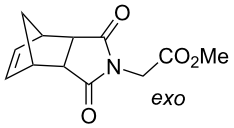	**36**	>95%	1.44	5.99×10^4
	37	>95%	1.29	18.7×10^4
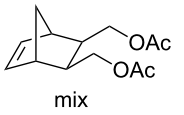	**36**	>95%	—[d]	—[d]
	37	>95%	—[d]	—[d]

[a]**36, 37** (5 mol %), **34** (10 mol %) and monomer (0.1 M) in a quartz NMR tube with CD_2Cl_2; [b]determined by ^1H NMR spectroscopy; [c]measured by MALLS-GPC; [d]insolubility precluded GPC analysis.

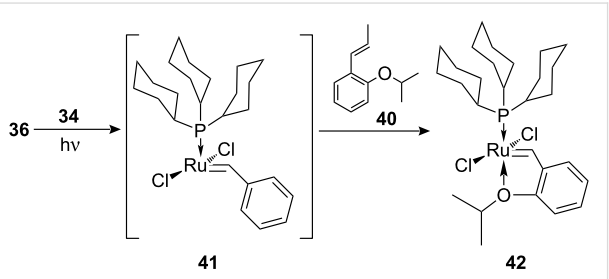

Scheme 9: Trapping of proposed intermediate **41**.

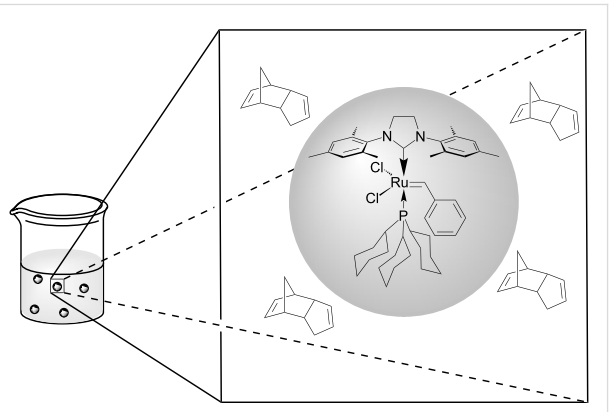

Figure 14: Encapsulated **39**, isolated from the monomer.

Conclusion

Initially, the field of photoinduced olefin metathesis was mainly based on $W(CO)_6$ chemistry. However, slowly over time functional group tolerant ruthenium applications emerged and these now dominate the field. Either by indirect or direct methods, the activation of ruthenium olefin metathesis catalysts may lead the way to novel applications in the areas of photolithography [81,82], roll-to-roll coating [69], 3D-printing, and self-healing [83] procedures in polymers. The use of photoswitchable catalysts may also have important safety advantages for industrial processes. As frequently seen in the successful field of olefin metathesis, the use of light to activate and direct these reactions certainly has a bright future ahead.

References

1. Hoveyda, A. H.; Zhugralin, A. R. *Nature* **2007,** *450,* 243–250. doi:10.1038/nature06351
2. Malcolmson, S. J.; Meek, S. J.; Sattely, E. S.; Schrock, R. R.; Hoveyda, A. H. *Nature* **2008,** *456,* 933–937. doi:10.1038/nature07594
3. Fürstner, A. *Angew. Chem., Int. Ed.* **2000,** *39,* 3012–3043. doi:10.1002/1521-3773(20000901)39:17<3012::AID-ANIE3012>3.0.CO;2-G
4. Schrock, R. R.; Czekelius, C. *Adv. Synth. Catal.* **2007,** *349,* 55–77. doi:10.1002/adsc.200600459
5. Diesendruck, C. E.; Tzur, E.; Lemcoff, N. G. *Eur. J. Inorg. Chem.* **2009,** *28,* 4185–4203. doi:10.1002/ejic.200900526
6. Bieniek, M.; Michrowska, A.; Usanov, D. L.; Grela, K. *Chem.–Eur. J.* **2008,** *14,* 806–818. doi:10.1002/chem.200701340
7. Trnka, T. M.; Grubbs, R. H. *Acc. Chem. Res.* **2001,** *34,* 18–29. doi:10.1021/ar000114f
8. Lozano-Vila, A. M.; Monsaert, S.; Bajek, A.; Verpoort, F. *Chem. Rev.* **2010,** *110,* 4865–4909. doi:10.1021/cr900346r
9. Leitgeb, A.; Wappel, J.; Slugovc, C. *Polymer* **2010,** *51,* 2927–2946. doi:10.1016/j.polymer.2010.05.002
10. Bielawski, C. W.; Grubbs, R. H. *Prog. Polym. Sci.* **2007,** *32,* 1–29. doi:10.1016/j.progpolymsci.2006.08.006

11. Grubbs, R. H., Ed. *Handbook of Metathesis;* Wiley-VCH: Weinheim, Germany, 2003; Vol. 3.
12. Mol, J. C. *J. Mol. Catal. A* **2004,** *213,* 39–45. doi:10.1016/j.molcata.2003.10.049
13. Baughman, T. W.; Wagener, K. B. *Adv. Polym. Sci.* **2005,** *176,* 1–42.
14. Hoveyda, A. H.; Malcolmson, S. J.; Meek, S. J.; Zhugralin, A. R. *Angew. Chem., Int. Ed.* **2010,** *49,* 34–44. doi:10.1002/anie.200904491
15. Reymond, S.; Ferrié, L.; Guérinot, A.; Capdevielle, P.; Cossy, J. *Pure Appl. Chem.* **2008,** *80,* 1683–1691. doi:10.1351/pac200880081683
16. Mori, M. *Adv. Synth. Catal.* **2007,** *349,* 121–135. doi:10.1002/adsc.200600484
17. Nicolaou, K. C.; Bulger, P. G.; Sarlah, D. *Angew. Chem., Int. Ed.* **2005,** *44,* 4490–4527. doi:10.1002/anie.200500369
18. Connon, S. J.; Blechert, S. *Angew. Chem., Int. Ed.* **2003,** *42,* 1900–1923. doi:10.1002/anie.200200556
19. Pozgan, F.; Dixneuf, P. H. Recent applications of alkene metathesis for fine chemical and supramolecular system synthesis.. In *Metathesis Chemistry: From Nanostructure Design to Synthesis of Advanced Materials;* Imamoglu, Y.; Dragutan, V., Eds.; NATO Science Series II: Mathematics, Physics and Chemistry, Vol. 243; Springer: Dordrecht, The Netherlands, 2007; pp 195–222.
20. Mele, G.; Li, J.; Vasapollo, G. *Chim. Oggi* **2008,** *26,* 72–74.
21. The Nobel Prize in Chemistry **2005**, 5 Oct 2005, http://nobelprize.org.
22. Connon, S. J.; Blechert, S. *Bioorg. Med. Chem. Lett.* **2002,** *12,* 1873–1876. doi:10.1016/S0960-894X(02)00260-3
23. Gulajski, L.; Michrowska, A.; Bujok, R.; Grela, K. *J. Mol. Catal. A* **2006,** *254,* 118–123. doi:10.1016/j.molcata.2005.12.049
24. Jordan, J. P.; Grubbs, R. H. *Angew. Chem., Int. Ed.* **2007,** *46,* 5152–5155. doi:10.1002/anie.200701258
25. Michrowska, A.; Gulajski, L.; Kaczmarska, Z.; Mennecke, K.; Kirschning, A.; Grela, K. *Green Chem.* **2006,** *8,* 685–688. doi:10.1039/b605138c
26. Burtscher, D.; Grela, K. *Angew. Chem., Int. Ed.* **2009,** *48,* 442–454. doi:10.1002/anie.200801451
27. Giudici, R. E.; Hoveyda, A. H. *J. Am. Chem. Soc.* **2007,** *129,* 3824–3825. doi:10.1021/ja070187v
28. Keitz, B. K.; Grubbs, R. H. *Organometallics* **2010,** *29,* 403–408. doi:10.1021/om900864r
29. Stenne, B.; Timperio, J.; Savoie, J.; Dudding, T.; Collins, S. K. *Org. Lett.* **2010,** *12,* 2032–2035. doi:10.1021/ol100511d
30. Schmidt, B.; Staude, L. *J. Org. Chem.* **2009,** *74,* 9237–9240. doi:10.1021/jo9018649
31. Szadkowska, A.; Grela, K. *Curr. Org. Chem.* **2008,** *12,* 1631–1647. doi:10.2174/138527208786786264
32. Monsaert, S.; Ledoux, N.; Drozdzak, R.; Verpoort, F. *J. Polym. Sci., Part A: Polym. Chem.* **2010,** *48,* 302–310. doi:10.1002/pola.23784
33. Gstrein, X.; Burtscher, D.; Szadkowska, A.; Brabasiewicz, M.; Stelzer, F.; Grela, K.; Slugovc, C. *J. Polym. Sci., Part A: Polym. Chem.* **2007,** *45,* 3494–3500. doi:10.1002/pola.22083
34. Piermattei, A.; Karthikeyan, S.; Sijbesma, R. P. *Nat. Chem.* **2009,** *1,* 133–137. doi:10.1038/nchem.167
35. Stoll, R. S.; Hecht, S. *Angew. Chem., Int. Ed.* **2010,** *49,* 5054–5075.
36. Krausz, P.; Garnier, F.; Dubois, J.-E. *J. Am. Chem. Soc.* **1975,** *97,* 437–438. doi:10.1021/ja00835a044
37. Agapiou, A.; McNelis, E. *J. Chem. Soc., Chem. Commun.* **1975,** *6,* 187a. doi:10.1039/C3975000187A
38. Agapiou, A.; McNelis, E. *J. Organomet. Chem.* **1975,** *99,* C47–48. doi:10.1016/S0022-328X(00)86301-9
39. Krausz, P.; Garnier, F.; Dubois, J.-E. *J. Organomet. Chem.* **1976,** *108,* 197–202. doi:10.1016/S0022-328X(00)82140-3
40. Krausz, P.; Garnier, F.; Dubois, J.-E. *J. Organomet. Chem.* **1978,** *146,* 125–134. doi:10.1016/S0022-328X(00)91439-6
41. Garnier, F.; Krausz, P.; Dubois, J.-E. *J. Organomet. Chem.* **1979,** *170,* 195–201. doi:10.1016/S0022-328X(00)81083-9
42. Garnier, F.; Krausz, P.; Rudler, H. *J. Organomet. Chem.* **1980,** *186,* 77–83. doi:10.1016/S0022-328X(00)93819-1
43. Tanielian, C.; Kieffer, R.; Harfouch, A. *Tetrahedron Lett.* **1977,** *18,* 4589–4592. doi:10.1016/S0040-4039(01)83576-0
44. Tanielian, C.; Kieffer, R.; Harfouch, A. *J. Mol. Catal.* **1981,** *10,* 269–284. doi:10.1016/0304-5102(81)85049-3
45. Nagasowa, M.; Kikukawa, K.; Takagi, M.; Matsuda, T. *Bull. Chem. Soc. Jpn.* **1978,** *51,* 1291–1293.
46. Borowczak, D.; Szymańska-Buzar, T.; Ziłkowski, J. J. *J. Mol. Catal.* **1984,** *27,* 355–365. doi:10.1016/0304-5102(84)85094-4
47. Szymańska-Buzar, T.; Ziłkowski, J. J. *J. Mol. Catal.* **1987,** *43,* 161–170. doi:10.1016/0304-5102(87)87003-7
48. Imamoglu, Y.; Zümreoglu, B.; Amass, A. J. *J. Mol. Catal.* **1986,** *36,* 107–114. doi:10.1016/0304-5102(86)85106-9
49. Szymańska-Buzar, T. *J. Mol. Catal.* **1988,** *48,* 43–57. doi:10.1016/0304-5102(88)85127-7
50. Schilder, P. G. M.; Stufkens, D. J.; Oskam, A.; Mol, J. C. *J. Organomet. Chem.* **1992,** *426,* 351–359. doi:10.1016/0022-328X(92)83068-S
51. Subbotina, I. R.; Shelimov, B. N.; Kazansky, V. B. *Kinet. Catal.* **1997,** *38,* 678–684.
52. Gita, B.; Sundararajan, G. *Tetrahedron Lett.* **1993,** *34,* 6123–6126. doi:10.1016/S0040-4039(00)61746-X
53. Gita, B.; Sundararajan, G. *J. Mol. Catal. A* **1997,** *79,* 79–84. doi:10.1016/S1381-1169(96)00085-4
54. Bhukta, G.; Manivannan, R.; Sundarajan, G. *J. Organomet. Chem.* **2000,** *601,* 16–21. doi:10.1016/S0022-328X(00)00015-2
55. Tamura, K.; Masuda, T.; Higashimura, T. *Polym. Bull.* **1994,** *32,* 289–296. doi:10.1007/BF00308539
56. Katz, T. J.; Ho, T. H.; Shih, N. Y.; Ying, Y. C.; Stuart, V. I. W. *J. Am. Chem. Soc.* **1984,** *106,* 2659–2668. doi:10.1021/ja00321a029
57. Katz, T. J.; Lee, S. J. *J. Am. Chem. Soc.* **1980,** *102,* 422–424. doi:10.1021/ja00521a094
58. Foley, H. C.; Strubinger, L. M.; Targos, T. S.; Geoffrey, G. L. *J. Am. Chem. Soc.* **1983,** *105,* 3064–3073. doi:10.1021/ja00348a020
59. Hafner, A.; Mühlebach, A.; van der Schaaf, P. *Angew. Chem., Int. Ed.* **1996,** *35,* 1845–1847. doi:10.1002/anie.199618451
60. The term ‘latency’ may lead to some controversy. We define a catalyst as latent when no appreciable reaction is observed for a given time period (i.e., 24 h) without an external stimulus (i.e., UV light) and noticeable product formation may be measured after the external stimulus is applied. See also reference [78].
61. Karlen, T.; Ludi, A.; Mühlebach, A.; Bernhard, P.; Pharisa, C. *J. Polym. Sci., Part A: Polym. Chem.* **1995,** *33,* 1665–1674. doi:10.1002/pola.1995.080331013
62. Hafner, A.; Mühlebach, A.; van der Schaaf, P. *Angew. Chem., Int. Ed.* **1997,** *36,* 2121–2124. doi:10.1002/anie.199721211
63. Hafner, A.; van der Schaaf, P.; Mühlebach, A.; Bernhard, P.; Schaedeli, U.; Karlen, T.; Ludi, A. *Prog. Org. Coat.* **1997,** *32,* 89–96. doi:10.1016/S0300-9440(97)00064-7
64. Fürstner, A.; Ackermann, L. *Chem. Commun.* **1999,** 95–96. doi:10.1039/A808810A
65. Picquet, M.; Bruneau, C.; Dixneuf, P. H. *Chem. Commun.* **1998,** *20,* 2249–2250. doi:10.1039/A806005C

66. Huang, J.; Stevens, E. D.; Nolan, S. P.; Petersen, J. L. *J. Am. Chem. Soc.* **1999,** *121,* 2674–2678. doi:10.1021/ja9831352
67. Scholl, M.; Ding, S.; Lee, C. W.; Grubbs, R. H. *Org. Lett.* **1999,** *1,* 953–956. doi:10.1021/ol990909q
68. Delaude, L.; Demonceau, A.; Noels, A. F. *Chem. Commun.* **2001,** 986–987. doi:10.1039/B101699G
69. Delaude, L.; Szypa, M.; Demonceau, A.; Noels, A. F. *Adv. Synth. Catal.* **2002,** *344,* 749–756. doi:10.1002/1615-4169(200208)344:6/7<749::AID-ADSC749>3.0.CO;2-T
70. Zhang, Y.; Wang, D.; Lönnecke, P.; Scherzer, T.; Buchmeiser, M. R. *Macromol. Symp.* **2006,** *236,* 30–37. doi:10.1002/masy.200690064
71. Wang, D.; Wurst, K.; Knolle, W.; Decker, U.; Prager, L.; Naumov, S.; Buchmeiser, M. R. *Angew. Chem., Int. Ed.* **2008,** *47,* 3267–3270. doi:10.1002/anie.200705220
72. Wang, D.; Decker, U.; Kühnel, C.; Buchmeiser, M. R. *Polym. Prepr.* **2010,** *51,* 384–385.
73. Ben-Asuly, A.; Tzur, E.; Diesendruck, C. E.; Sigalov, M.; Goldberg, I.; Lemcoff, N. G. *Organometallics* **2008,** *27,* 811–813. doi:10.1021/om701180z
74. Kost, T.; Sigalov, M.; Goldberg, I.; Ben-Asuly, A.; Lemcoff, N. G. *J. Organomet. Chem.* **2008,** *693,* 2200–2203. doi:10.1016/j.jorganchem.2008.03.028
75. Diesendruck, C. E.; Vidavsky, Y.; Ben-Asuly, A.; Lemcoff, N. G. *J. Polym. Sci., Part A: Polym. Chem.* **2009,** *47,* 4209–4213. doi:10.1002/pola.23476
76. Diesendruck, C. E.; Iliashevsky, O.; Ben-Asuly, A.; Goldberg, I.; Lemcoff, N. G. *Macromol. Symp.* **2010,** *293,* 33–38. doi:10.1002/masy.200900036
77. Tzur, E.; Szadkowska, A.; Ben-Asuly, A.; Makal, A.; Goldberg, I.; Wozniak, K.; Grela, K.; Lemcoff, N. G. *Chem.–Eur. J.* **2010,** *16,* 8726–8737. doi:10.1002/chem.200903457
78. Ben-Asuly, A.; Aharoni, A.; Diesendruck, C. E.; Vidavsky, Y.; Goldberg, I.; Straub, B. F.; Lemcoff, N. G. *Organometallics* **2009,** *28,* 4652–4655. doi:10.1021/om9004302
79. Keitz, B. K.; Grubbs, R. H. *J. Am. Chem. Soc.* **2009,** *131,* 2038–2039. doi:10.1021/ja807187u
80. Pastine, S. J.; Okawa, D.; Zettl, A.; Fréchet, J. M. J. *J. Am. Chem. Soc.* **2009,** *131,* 13586–13587. doi:10.1021/ja905378v
81. Ito, H.; Willson, C. G. Applications of Photoinitiators to the Design of Resists for Semiconductor Manufacturing. In *Polymers in Electronics;* Davidson, T., Ed.; ACS Symposium Series, Vol. 242; ACS Publications: Washington, U. S. A., 1984; pp 11–23. doi:10.1021/bk-1984-0242.ch002
82. Harris, R. F.; Ricci, M. J.; Farrer, R. A.; Praino, J.; Miller, S. J.; Saleh, B. E. A.; Teich, M. C.; Fourkas, J. T. *Adv. Mater.* **2005,** *17,* 39–42. doi:10.1002/adma.200400311
83. Toohey, K. S.; Sottos, N. R.; Lewis, J. A.; Moore, J. S.; White, S. R. *Nat. Mater.* **2007,** *6,* 581–585. doi:10.1038/nmat1934

License and Terms

Beilstein Journal of Organic Chemistry

Backbone tuning in indenylidene–ruthenium complexes bearing an unsaturated *N*-heterocyclic carbene

César A. Urbina-Blanco[1], Xavier Bantreil[1], Hervé Clavier[1,2], Alexandra M. Z. Slawin[1] and Steven P. Nolan[*1]

Full Research Paper

Open Access

Address:
[1]EaStCHEM School of Chemistry, University of St Andrews, St Andrews KY16 9ST, United Kingdom and [2]present address: Institut des Sciences Moléculaires de Marseille Université Aix-Marseille, UMR CNRS 6263, France

Email:
César A. Urbina-Blanco - caub@st-andrews.ac.uk; Steven P. Nolan* - snolan@st-andrews.ac.uk

* Corresponding author

Keywords:
N-heterocyclic carbene; olefin metathesis; percent buried volume; ruthenium–indenylidene; Tolman electronic parameter

Beilstein J. Org. Chem. **2010,** *6,* 1120–1126.
doi:10.3762/bjoc.6.128

Received: 17 September 2010
Accepted: 03 November 2010
Published: 23 November 2010

Guest Editor: K. Grela

Abstract

The steric and electronic influence of backbone substitution in IMes-based (IMes = 1,3-bis(2,4,6-trimethylphenyl)imidazol-2-ylidene) *N*-heterocyclic carbenes (NHC) was probed by synthesizing the [RhCl(CO)$_2$(NHC)] series of complexes to quantify experimentally the Tolman electronic parameter (electronic) and the percent buried volume (%V_{bur}, steric) parameters. The corresponding ruthenium–indenylidene complexes were also synthesized and tested in benchmark metathesis transformations to establish possible correlations between reactivity and NHC electronic and steric parameters.

Introduction

The use of *N*-heterocyclic carbenes (NHC) as spectator ligands in ruthenium-mediated olefin metathesis represents one of the most important breakthroughs in this field [1-8]. Mixed complexes bearing both a phosphane and a NHC ligand, so-called 2nd generation catalysts, typically display better thermal stability and activities compared to 1st generation catalysts [9,10]. Key to the success and research activity involving 2nd generation catalysts has been the wide selection of NHCs available [11,12]. These highly basic ligands have now been featured in a number of catalysts that display excellent activity in olefin metathesis. NHCs have become the ligand *par excellence* in olefin metathesis (Figure 1) [7,8].

In order to improve catalytic activity, the possibility of fine-tuning of NHC steric and electronic properties has been exploited. Bulkier and more electron-donating NHCs allow faster initiation with usually a concurrent increase in reaction rate when the olefin substrate is of low steric hindrance [13-17].

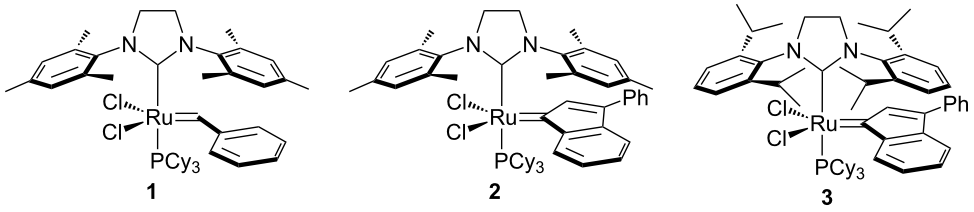

Figure 1: Representative olefin metathesis catalysts.

Less sterically demanding NHCs are typically used for the synthesis of highly encumbered olefins [18]. Recent studies have shown that backbone substitution in saturated NHCs greatly improves catalyst stability by restricting rotation around the *N*–C_{aryl} bond (Figure 2); this presumably slows catalyst decomposition via an observed C–H activation route [19].

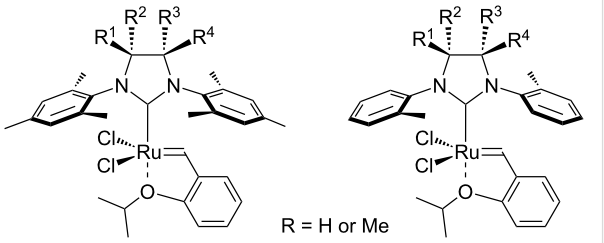

Figure 2: Highly active olefin metathesis catalysts bearing NHC with backbone substitution.

These results encouraged us to explore the electronic influence of backbone substitution in unsaturated NHCs with ruthenium–indenylidene complexes. Indenylidene catalysts are rapidly becoming quite popular [20,21], due to the availability of ruthenium precursors [22] and their straightforward synthesis. The higher steric hindrance and improved electronic donor ability of the indenylidene moiety also contribute to the observed increased stability compared to benzylidene congeners. This family of complexes displayed interesting stability even when forcing reaction conditions are required [13,23-25].

Herein, we present the synthesis and characterization of three new ruthenium–indenylidene catalysts and their performance in benchmark metathesis transformations. In order to quantify the Tolman electronic parameter associated with IMes-type (IMes = 1,3-bis(2,4,6-trimethylphenyl)imidazol-2-ylidene) ligands possessing variable backbone substitution patterns, the corresponding series of [RhCl(CO)$_2$(NHC)] complexes was synthesized. X-ray diffraction studies permit the determination of the percent buried volume (%V_{bur}) of these NHCs ligands and quantify their respective steric parameter.

Results and Discussion

Evaluation of the ligand electronic and steric properties

Previous studies have shown that the electronic parameter of NHC (and other) ligands can be quantified employing the stretching frequency of CO (ν_{CO}) in various transition metal–carbonyl complexes [26-32]. This method was initially developed by Tolman [33], using the average infrared frequency of CO in [Ni(CO)$_3$L] complexes. This electronic parameter has become known as the Tolman electronic parameter (TEP) and has been used to quantify the electron donor ability of phosphanes, and more recently, has been used to study the electronic properties of NHCs [34].

However, the high toxicity of [Ni(CO)$_4$] encouraged the search for analogous systems using different metals to determine the TEP. One of the most popular and suitable alternatives to nickel is a rhodium carbonyl system, since it is easily synthesised and handled [34]. In this work, a series of [RhCl(CO)$_2$(NHC)] complexes were synthesized in order to evaluate the electronic donor ability of the NHCs.

The free carbenes were prepared according to literature procedures. Free IMes (**4b**) [35] and IMesMe (**4a**) [36] were synthesized from the corresponding tetrafluoroborate salts; free IMesBr (**4c**) [37] and IMesCl (**4d**) [38] were synthesized in situ prior to complex synthesis by reacting free IMes with CBr_4 and CCl_4, respectively (Scheme 1).

The complexes **5a**–**d** were prepared by reacting [Rh(CO)$_2$Cl]$_2$ with the corresponding free carbene in THF (Scheme 2). After stirring for 4 h at room temperature, removal of the solvents and washing of the residue with pentane, the corresponding complexes were obtained as yellow microcrystalline solids, in good yields (71–80%).

Infrared spectra were recorded in DCM for **5a**–**d** and the carbonyl stretching frequencies (ν_{COav}) were used to provide the TEP (Table 1). As expected, the backbone substitution pattern has a profound effect on the electronic donor capacity of the

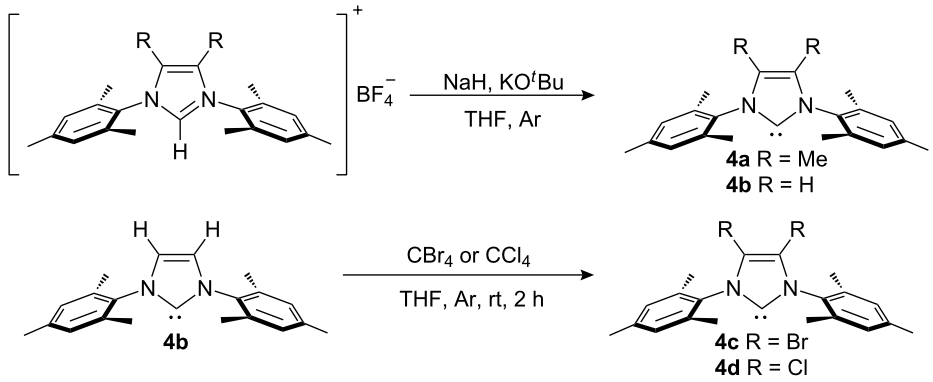

Scheme 1: Synthesis of the free NHCs.

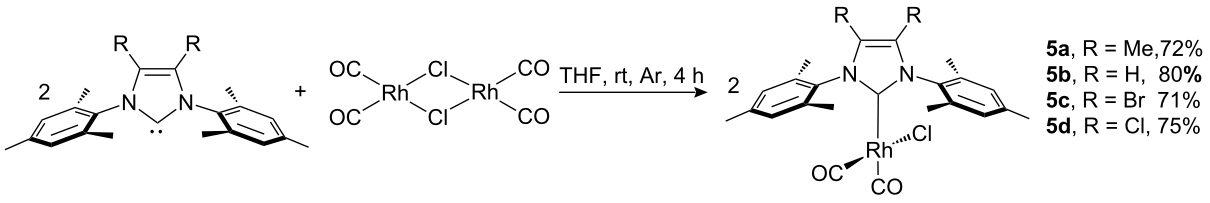

Scheme 2: Synthesis of [RhCl(CO)$_2$(NHC)] complexes.

NHC, and a linear correlation between the electronegativity of the backbone substituent (measured as the Hammett parameter, σ_p) and the average carbonyl stretching frequency (ν_{COav}) in [RhCl(CO)$_2$(NHC)] complexes is observed ($R^2 = 0.98$).

The electron donating nature of the NHC decreases along the series: IMesMe > IMes > IMesBr > IMesCl. As an internal check of the data, it is worth noting that the calculated TEP for IMes (2050.3 cm^{-1}) agrees well with the experimentally obtained value in the nickel system (2051.5 cm^{-1}) [34].

Given their steric and geometric variability, evaluating the steric parameters of NHCs poses a more challenging task. One of the more recent methodologies defines a percent buried volume (%V_{bur}), which quantifies the volume of a sphere centred around the metal (with a specific radius distance) occupied by the ligand. The more sterically demanding ligands will correspond to larger %V_{bur} values [36,39].

Analysis of the crystal structures of **5a**–**d**, in conjunction with the aforementioned computational tool, allow us to conclude that a hydrogen–methyl or hydrogen–halogen exchange in the backbone creates small steric variation in the NHC evidenced by the very close values obtained for the %V_{bur} [40]. However, the %V_{bur} for the ligands correlates very well with the size of the substituent: IMesCl ≈ IMesBr > IMes ≈ IMesMe.

Synthesis of ruthenium–indenylidene catalysts and their performance in olefin metathesis

The ruthenium–indenylidene complexes were synthesized in order to establish how strongly the electronic and steric parameters of the NHC influence catalytic activity in olefin metathesis. As reported for **6b** [41], precatalysts **6a**, **6c** and **6d** were synthesized by exchange between PCy_3 and the corresponding free carbene in [$RuCl_2(PCy_3)_2$(Ind)] (Scheme 3). The new complexes proved challenging to purify by recrystallization,

Table 1: Electronic and steric parameters of NHCs in [RhCl(CO)$_2$(NHC)] complexes.

Complex	ν_{COav} (cm^{-1})	TEP[a] (cm^{-1})	σ_p	%V_{bur}
[RhCl(CO)$_2$(IMesMe)]	2034.8	2048.0	−0.170	31.7 ± 0.1[b]
[RhCl(CO)$_2$(IMes)]	2037.6	2050.3	0.000	31.8 ± 0.5[b]
[RhCl(CO)$_2$(IMesBr)]	2041.3	2053.3	0.227	32.6
[RhCl(CO)$_2$(IMesCl)]	2042.5	2054.2	0.232	32.7

[a]TEP calculated using equation TEP = 0.8001 ν_{COav} + 420.0 cm^{-1}. [b]Average of the independent structures.

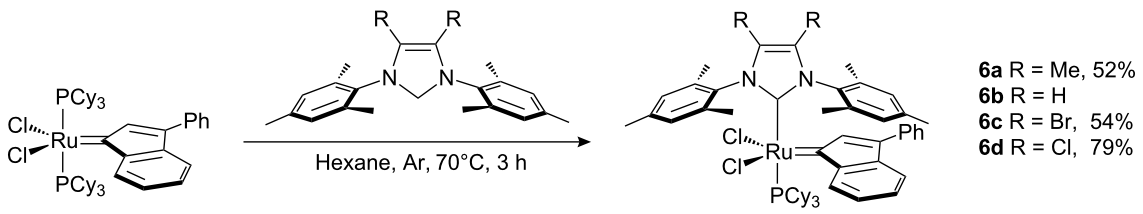

Scheme 3: Synthesis of $[RuCl_2(NHC)(PCy_3)(Ind)]$ complexes.

however flash column chromatography on silica gel afforded highly pure compounds in moderate yields (52–79%). The use of this purification technique also attests to the robustness of the novel complexes.

Complexes **6a**, **6c** and **6d** are stable in the solid state under aerobic conditions and exhibit remarkable stability in solution under inert atmosphere. ^{1}H NMR analysis of their solutions showed little decomposition even after 24 h in dichloromethane-d_2 at 40 °C. Traces of degradation could be observed after 1 h in toluene at 80 °C with complete decomposition after 24 h.

Complexes **6a**–**d** were then tested in benchmark metathesis transformations with substrates featuring different steric properties (Table 2). The catalysts were found to perform very

Table 2: Catalytic evaluation of **6a–d** in benchmark metathesis transformations.[a]

Substrate	Product	Catalyst	Loading (mol %)	*T* (°C)	Time (h)	Conv[b] (%) (yield (%))
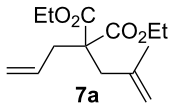 **7a**	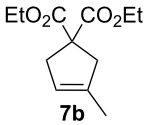 **7b**	**6a** **6b** **6c** **6d**	1	rt[c]	24	22 49 9 3
		6d		80	2	<99 (95)
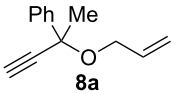 **8a**	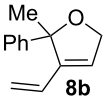 **8b**	**6a** **6b** **6c** **6d**	1	rt[c]	24	33 39 65 33
		6d		80	2	<99 (97)
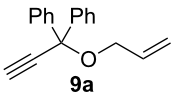 **9a**	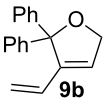 **9b**	**6d**	1	80	2	<99 (98)
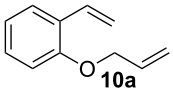 **10a**	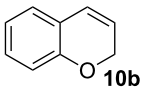 **10b**	**6d**	1	80	2	<99 (85)
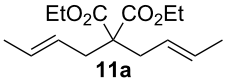 **11a**	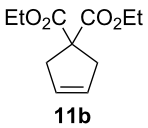 **11b**	**6d**	1	80	2	<99 (96)
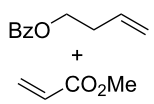	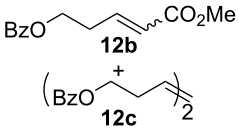 **12b** + **12c**	**6d**	1	80	5	**b**: 69 (55) E/Z > 20:1 **c**: 9

Table 2: Catalytic evaluation of **6a–d** in benchmark metathesis transformations.[a] (continued)

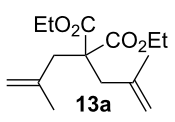 **13a**	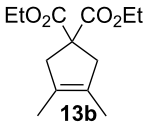 **13b**	**6a** **6b** **6c** **6d**	5	80	5	62 37 69 78 (72)
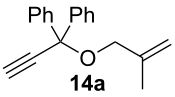 **14a**	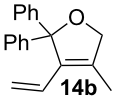 **14b**	**6a** **6b** **6c** **6d**	5	80	2	31 36 18 43
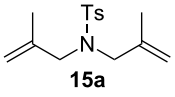 **15a**	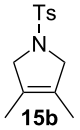 **15b**	**6a** **6b** **6c** **6d**	2	80	3	58 86 98 98 (95)
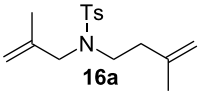 **16a**	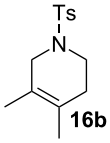 **16b**	**6a** **6b** **6c** **6d**	2	80	3	90 97 99 99 (99)

[a]Reaction conditions: substrate (0.5 mmol), toluene (0.1 M), N_2, 80 °C. [b]Conversions determined by ^{1}H NMR. [c]DCM (0.1 M).

modestly in the synthesis of poorly hindered substrates **7b** and **8b** at room temperature, but their performance improves significantly upon thermal activation. Thus, **6d** achieves full conversion within 2 h at 80 °C. Similar results were achieved with substrates **9a**–**12a.** Interestingly transformations at room temperature exhibit no correlation between the electronic properties of the carbene and the catalytic outcome. However, more challenging substrates that effect the formation of tetrasubstituted double bonds do present a trend. Even if catalysts performed similarly, the highest conversions were constantly reached with the catalyst bearing the least electron-donating carbene, namely IMesCl (**6d**). These results can be rationalized in terms of the mechanism of the reaction. Although a more electron-donating NHC should better stabilize the 14-electron active species and allow better catalytic activity, the faster initiation is also related to faster catalyst decomposition; at 80 °C, this deactivation contributes considerably to the catalytic outcome. In conclusion, we suggest that **6d** represents the most advantageous catalyst owing to its improved stability, which is attributed to reduced initiation from poorer electron-donating ability of the NHC ligand.

Conclusion

The effects of modulating the nature of substituents on the backbone (C4 and C5) positions of the IMes ligand have permitted a quantification of the electronic and steric parameters associated with these synthetic variations. Using a rhodium carbonyl system, the electronic variations brought about by substituents on the NHC lead to the following ligand electronic donor scale: IMesMe > IMes > IMesBr > IMesCl. The size of the substituent also affects the steric hindrance of the ligands, and the percent buried volume of the NHCs decreases in the following order: IMesCl ≈ IMesBr > IMes ≈ IMesMe. A modest trend between the electronic properties of the carbene and the catalytic outcome was found in the synthesis of tetrasubstituted olefin. This was attributed to improved stability of the catalyst derived from lower electron-donating properties of the NHC.

Supporting Information

Detailed experimental procedures for the synthesis of complexes **5a**–**d**, **6a**, **6c** and **6d**, and procedures for the catalysis are available in the supporting information. The CIF files of crystal structures **5a**–**d** have been deposited with the CCDC, No. 793640–793643, respectively. Copies of the data can be obtained free of charge on applications to CCDC, 12 Union Road, Cambridge CB2 1EZ, UK, fax: +44 1223 336 033; http://www.ccdc.cam.ac.uk; e-mail: deposit@ccdc.cam.ac.uk.

Supporting Information File 1

Supporting Information.
[http://www.beilstein-journals.org/bjoc/content/supplementary/1860-5397-6-128-S1.pdf]

Acknowledgements

We are grateful to the EC for funding through the seventh framework program (CP-FP 211468-2-EUMET). SPN is a Royal Society-Wolfson Research Merit Award holder.

References

1. Fürstner, A. *Angew. Chem., Int. Ed.* **2000,** *39,* 3012–3043. doi:10.1002/1521-3773(20000901)39:17<3012::AID-ANIE3012>3.0.CO;2-G
2. Huang, J.; Stevens, E. D.; Petersen, J. L.; Nolan, S. P. *J. Am. Chem. Soc.* **1999,** *121,* 2674–2678. doi:10.1021/ja9831352
3. Trnka, T. M.; Grubbs, R. H. *Acc. Chem. Res.* **2001,** *34,* 18–29. doi:10.1021/ar000114f
4. Grubbs, R. H. *Handbook of Metathesis;* Wiley-VCH: Weinheim, 2003. doi:10.1002/9783527619481
5. Astruc, D. *New J. Chem.* **2005,** *29,* 42–56. doi:10.1039/b412198h
6. Deshmukh, P. H.; Blechert, S. *Dalton Trans.* **2007,** 2479–2491. doi:10.1039/b703164p
7. Samojłowicz, C.; Bieniek, M.; Grela, K. *Chem. Rev.* **2009,** *109,* 3708–3742. doi:10.1021/cr800524f
8. Vougioukalakis, G. C.; Grubbs, R. H. *Chem. Rev.* **2009,** *110,* 1746–1787. doi:10.1021/cr9002424
9. Weskamp, T.; Schattenmann, W. C.; Spiegler, M.; Herrmann, W. A. *Angew. Chem., Int. Ed.* **1998,** *37,* 2490–2493. doi:10.1002/(SICI)1521-3773(19981002)37:18<2490::AID-ANIE2490>3.0.CO;2-X
10. Huang, J.; Schanz, H.-J.; Stevens, E. D.; Nolan, S. P. *Organometallics* **1999,** *18,* 5375–5380. doi:10.1021/om990788y
11. Dröge, T.; Glorius, F. *Angew. Chem., Int. Ed.* **2010,** *49,* 6940–6952. doi:10.1002/anie.201001865
12. Díez-González, S.; Marion, N.; Nolan, S. P. *Chem. Rev.* **2009,** *109,* 3612–3676. doi:10.1021/cr900074m
13. Clavier, H.; Nolan, S. P. *Chem.–Eur. J.* **2007,** *13,* 8029–8036. doi:10.1002/chem.200700256
14. Clavier, H.; Urbina-Blanco, C. S. A.; Nolan, S. P. *Organometallics* **2009,** *28,* 2848–2854. doi:10.1021/om900071t
15. Jafarpour, L.; Stevens, E. D.; Nolan, S. P. *J. Organomet. Chem.* **2000,** *606,* 49–54. doi:10.1016/S0022-328X(00)00260-6
16. Fürstner, A.; Ackermann, L.; Gabor, B.; Goddard, R.; Lehmann, C. W.; Mynott, R.; Stelzer, F.; Thiel, O. R. *Chem.–Eur. J.* **2001,** *7,* 3236–3253. doi:10.1002/1521-3765(20010803)7:15<3236::AID-CHEM3236>3.0.CO;2-S
17. Luan, X. J.; Mariz, R.; Gatti, M.; Costabile, C.; Poater, A.; Cavallo, L.; Linden, A.; Dorta, R. *J. Am. Chem. Soc.* **2008,** *130,* 6848–6858. doi:10.1021/ja800861p
18. Chung, C. K.; Grubbs, R. H. *Org. Lett.* **2008,** *10,* 2693–2696. doi:10.1021/ol800824h
19. Kuhn, K. M.; Bourg, J.-B.; Chung, C. K.; Virgil, S. C.; Grubbs, R. H. *J. Am. Chem. Soc.* **2009,** *131,* 5313–5320. doi:10.1021/ja900067c
20. Leitgeb, A.; Burtscher, D.; Bauer, T.; Slugovc, C. *Chim. Oggi* **2009,** *27* (3), 30.
21. Burtscher, D.; Lexer, C.; Mereiter, K.; Winde, R.; Karch, R.; Slugovc, C. *J. Polym. Sci., Part A: Polym. Chem.* **2008,** *46,* 4630–4635. doi:10.1002/pola.22763
22. Complexes **3** and other indenylidene–Ru complexes are commercially available from Evonik Degussa, Strem and Umicore.
23. Clavier, H.; Petersen, J. L.; Nolan, S. P. *J. Organomet. Chem.* **2006,** *691,* 5444–5447. doi:10.1016/j.jorganchem.2006.08.007
24. Bieniek, M.; Michrowska, A.; Usanov, D. L.; Grela, K. *Chem.–Eur. J.* **2008,** *14,* 806–818. doi:10.1002/chem.200701340
25. Boeda, F.; Clavier, H.; Nolan, S. P. *Chem. Commun.* **2008,** 2726–2740. doi:10.1039/b718287b
26. Hahn, F. E.; Paas, M.; Le Van, D.; Frohlich, R. *Chem.–Eur. J.* **2005,** *11,* 5080–5085. doi:10.1002/chem.200500306
27. Kelly, R. A.; Clavier, H.; Giudice, S.; Scott, N. M.; Stevens, E. D.; Bordner, J.; Samardjiev, I.; Hoff, C. D.; Cavallo, L.; Nolan, S. P. *Organometallics* **2008,** *27,* 202–210. doi:10.1021/om701001g
28. Chianese, A. R.; Li, X. W.; Janzen, M. C.; Faller, J. W.; Crabtree, R. H. *Organometallics* **2003,** *22,* 1663–1667. doi:10.1021/om021029+
29. Mercs, L.; Labat, G.; Neels, A.; Ehlers, A.; Albrecht, M. *Organometallics* **2006,** *25,* 5648–5656. doi:10.1021/om060637c
30. César, V.; Lugan, N.; Lavigne, G. *J. Am. Chem. Soc.* **2008,** *130,* 11286–11287. doi:10.1021/ja804296t
31. Nonnenmacher, M.; Kunz, D.; Rominger, F.; Oeser, T. *J. Organomet. Chem.* **2005,** *690,* 5647–5653. doi:10.1016/j.jorganchem.2005.07.033
32. Wolf, S.; Plenio, H. *J. Organomet. Chem.* **2009,** *694,* 1487–1492. doi:10.1016/j.jorganchem.2008.12.047
33. Tolman, C. A. *Chem. Rev.* **1977,** *77,* 313–348. doi:10.1021/cr60307a002
34. Dorta, R.; Stevens, E. D.; Scott, N. M.; Costabile, C.; Cavallo, L.; Hoff, C. D.; Nolan, S. P. *J. Am. Chem. Soc.* **2005,** *127,* 2485–2495. doi:10.1021/ja0438821
35. Viciu, M. S.; Navarro, O.; Germaneau, R. F.; Kelly, R. A.; Sommer, W.; Marion, N.; Stevens, E. D.; Cavallo, L.; Nolan, S. P. *Organometallics* **2004,** *23,* 1629–1635. doi:10.1021/om034319e
36. Clavier, H.; Correa, A.; Cavallo, L.; Escudero-Adan, E. C.; Benet-Buchholz, J.; Slawin, A. M. Z.; Nolan, S. P. *Eur. J. Inorg. Chem.* **2009,** 1767–1773. doi:10.1002/ejic.200801235
37. Cole, M. L.; Jones, C.; Junk, P. C. *New J. Chem.* **2002,** *26,* 1296–1303. doi:10.1039/b204422f
38. Arduengo, A. J.; Krafczyk, R.; Schmutzler, R.; Craig, H. A.; Goerlich, J. R.; Marshall, W. J.; Unverzagt, M. *Tetrahedron* **1999,** *55,* 14523–14534. doi:10.1016/S0040-4020(99)00927-8
39. Clavier, H.; Nolan, S. P. *Chem. Commun.* **2010,** *46,* 841–861. doi:10.1039/b922984a
40. Calculated using http://www.molnac.unisa.it/OMtools/sambvca.php (accessed Sept 15, 2010) using the default parameters (Sphere radius 3.5 Å, Distance from the center of the sphere 2.10 Å, Mesh spacing 0.05).
41. Jafarpour, L.; Schanz, H.-J.; Stevens, E. D.; Nolan, S. P. *Organometallics* **1999,** *18,* 5416–5419. doi:10.1021/om990587u

Beilstein Journal of Organic Chemistry

About the activity and selectivity of less well-known metathesis catalysts during ADMET polymerizations

Hatice Mutlu[1,2], Lucas Montero de Espinosa[1,3], Oğuz Türünç[1,2] and Michael A. R. Meier[*1,§]

Full Research Paper

Open Access

Address:
[1]University of Potsdam, Institute of Chemistry, Karl-Liebknecht-Str. 24-25, 14476 Golm, Germany, [2]University of Applied Sciences Emden/Leer, Constantiaplatz 4, 26723 Emden, Germany and [3]Max-Planck-Institute of Colloids and Interfaces, Department of Colloid Chemistry, Potsdam, Germany

Email:
Michael A. R. Meier[*] - michael.meier@uni-potsdam.de

* Corresponding author
§ Internet: http://www.meier-michael.com

Keywords:
ADMET; metathesis; olefin isomerization; renewable raw materials; ruthenium–indenylidene catalysts

Beilstein J. Org. Chem. **2010,** *6,* 1149–1158.
doi:10.3762/bjoc.6.131

Received: 17 August 2010
Accepted: 28 October 2010
Published: 03 December 2010

Guest Editor: K. Grela

Abstract

We report on the catalytic activity of commercially available Ru-indenylidene and "boomerang" complexes **C1**, **C2** and **C3** in acyclic diene metathesis (ADMET) polymerization of a fully renewable α,ω-diene. A high activity of these catalysts was observed for the synthesis of the desired renewable polyesters with molecular weights of up to 17000 Da, which is considerably higher than molecular weights obtained using the same monomer with previously studied catalysts. Moreover, olefin isomerization side reactions that occur during the ADMET polymerizations were studied in detail. The isomerization reactions were investigated by degradation of the prepared polyesters via transesterification with methanol, yielding diesters. These diesters, representing the repeat units of the polyesters, were then quantified by GC-MS.

Introduction

Among the large number of organic and organometallic reactions allowing the formation of carbon–carbon bonds, olefin metathesis has found its place in organic synthesis as well as polymer science as a very versatile tool that allows transformations that were previously not (or hardly) possible [1-6]. This academic and industrial success is also closely associated with the development and commercialization of efficient catalysts.

In the past few years, researchers realized that olefin isomerization is an important side reaction of Ru-catalyzed metathesis reactions. First reports on olefin isomerization claimed that this undesired side reaction was observed on substrates containing allylic oxygen or nitrogen functional groups in combination with first generation catalysts [7-11]. Later it was demonstrated that the degradation product of Grubbs 1st generation catalyst

was capable of catalyzing olefin isomerization [12]. Double bond isomerization was also observed with 2nd generation catalysts on a broad variety of substrates competitively and sometimes prior to olefin metathesis [13-17]. In a number of other publications this problem was addressed and further discussions on the possible mechanism of the two proposed pathways, the π-allyl metal hydride and the metal hydride addition-elimination mechanisms, were reported [8,11,13-18]. In most cases isomerization was attributed to the presence of a Ru-hydride species [13,14]. The cause of formation of such Ru-hydride species was long a subject of discussion. Grubbs reported that certain ruthenium carbene complexes can thermally decompose to Ru-hydride species [19]. Moreover, mechanistic investigation of the thermal decomposition of the Grubbs second generation catalyst carried out by Grubbs and co-workers clearly showed that prolonged heating of the catalyst results in the formation of a binuclear ruthenium hydride complex [20]. The observation that this binuclear product was capable of efficiently isomerizing terminal olefins is a clear indication that metal hydride species are indeed the source of the isomerization. It was reported that a proper selection of solvents and additives can eliminate isomerization with Ru-based metathesis catalysts in RCM [16]. The addition of $POCy_3$ or oxygen inhibits isomerization, whereas the use of more coordinating solvents favors it. Additional research in this area reported that other types of additives, such as acetic acid [21], chlorocatecholborane [22], boron-based Lewis acid (such as: Cy_2BCl) [23], or $PhOP(O)(OH)_2$ [24] can reduce the isomerization activity of the catalyst. Furthermore, Johnson and coworkers reported that during a RCM to make a 9-membered ring, chlorinated solvents, such as 1,2-dichloroethane, inhibited olefin isomerization [25]. Grubbs and collaborators showed that catalytic amounts (10 mol %) of 1,4-benzoquinone (**BQ**) can prevent the isomerization of a number of allylic ethers and long chain aliphatic alkenes during RCM and cross metathesis [21]. In the context of ADMET, isomerization of a terminal to an internal olefin, followed by a productive metathesis step with a terminal olefin, would liberate an α-olefin, such as propene or 1-butene, as opposed to the ethylene liberated from a conventional ADMET reaction of two terminal olefins (Figure 1) [26]. Release of these higher condensate molecules would decrease the mass yield of the polymer, and if olefin isomerization occurs in a similar timescale as metathesis, this would result in polymers with ill-defined repeat units, which would also affect the physical properties of the polymer. Noteworthy, under ADMET conditions, the first-generation Ru-catalyst was found not to isomerize olefins [27].

In model studies carried out with simple olefins, Wagener and co-workers demonstrated that, while Grubbs 1st generation and Schrock's molybdenum alkylidene catalysts did not produce

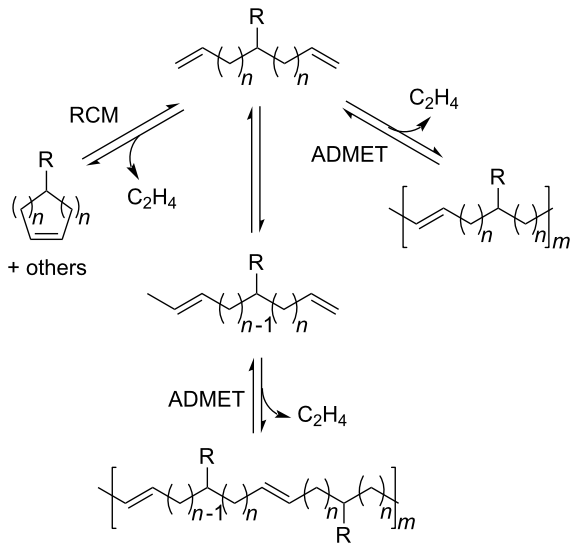

Figure 1: Olefin isomerization during ADMET polymerization.

appreciable double bond isomerization, Grubbs 2nd generation catalyst presented significant isomerization activity, which was greatly reduced at temperatures below 30 ºC [17,28]. These studies were further complemented and confirmed by MALDI analysis of an amino acid polymer synthesized with Grubbs 2nd generation catalyst [29].

Recently, a detailed study of temperature, catalyst, and polymerization condition dependent isomerization side reactions that occur during ADMET polymerizations was reported by Meier and Fokou [27]. The study clearly showed that high temperatures, such as 100 °C, increased the amount of isomerization for Grubbs 2nd generation catalyst. In order to better understand the behavior of several second generation metathesis catalysts under ADMET conditions, their isomerization tendencies were subsequently studied [30]. The investigated catalysts showed high degrees of isomerization at 80 °C. The addition of **BQ** provided the best results in terms of reducing the isomerization reactions when added prior to the catalyst, indicating that catalyst decomposition begins as soon as the catalyst is added to the reaction mixture at high reaction temperatures. The effects of nitrogen purging and higher temperatures in the presence of **BQ** were also investigated and revealed that with nitrogen purging the degree of isomerization remained similar or even decreased.

Among the numerous metathesis initiators available, we focused this study on the application of the less investigated indenylidene Ru-based catalysts: (1,3-bis(2,4,6-trimethylphenyl)-2-imidazolidinylidene) dichloro-(3-phenyl-1*H*-inden-1-ylidene)(tricyclohexylphosphine) ruthenium(II) (**C1**), (1,3-

bis(2,4,6-trimethylphenyl)-2-imidazolidinylidene)dichloro-(3-phenyl-1*H*-inden-1-ylidene)(pyridyl) ruthenium(II) (**C2**) and the newly developed "boomerang" complex (1,3-bis(2,4,6-trimethylphenyl)-2-imidazolidinylidene)dichloro(2-(1-methylacetoxy)phenyl)methylene ruthenium(II) (**C3**) [31] (Figure 2).

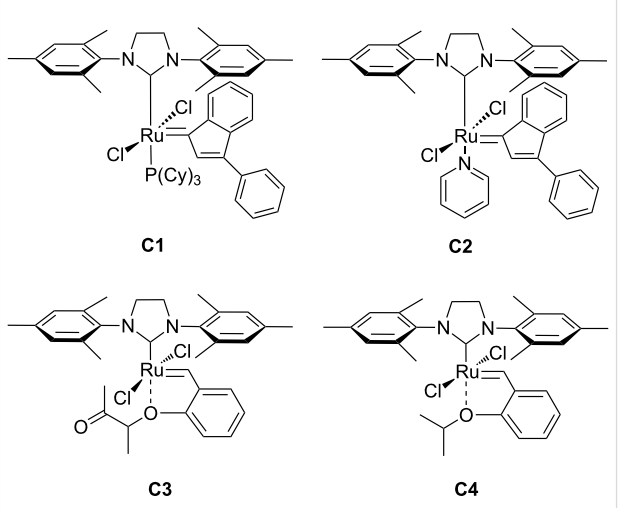

Figure 2: Ru–indenylidene metathesis catalysts **C1** and **C2**, "boomerang" complexes **C3,** and Hoveyda–Grubbs 2nd generation catalyst **C4** were studied for their efficiency and isomerization tendency in ADMET polymerizations.

These indenylidene Ru-complexes provide an attractive alternative to the Ru–benzylidene compounds. It was shown that all indenylidene Ru-catalysts were more robust under the demanding reaction conditions (temperature and functional group tolerance) compared to their Ru–benzylidene counterparts [32-40]. In addition, good catalytic activities in RCM of linear dienes [32,34,35] and ROMP of cycloolefins [36-40] were reported. RCM studies with diethyl diallylmalonate and diallyl tosylamine as substrates showed an appreciable catalytic activity and selectivity for the 2nd generation 16-electron Ru–indenylidene complex (**C1**) [41]. High temperatures allow for better ligand dissociation, and hence for a higher initiation rate of **C1** in RCM [33,35]. Moreover, good activities were obtained in the self-metathesis reaction of undecylenic aldehyde, a renewable building block derived from castor oil cracking [42]. Research performed by Monsaert et al. illustrated that **C2** enables high conversions in ROMP of 1,5-cyclooctadiene, and conversions of up to 80% in the RCM of diethyl diallylmalonate in short reaction times (5–10 min), thus being superior to the benzylidene analogue [35].

Recently, a useful and practical guide to application of olefin metathesis catalysts was published by Grela and co-workers [43]. They examined the effectiveness of Ru–indenylidene complexes in standard olefin metathesis reactions and compared their activities to those of Grubbs and Hoveyda–Grubbs type catalysts. In contrast to Grubbs and Hoveyda–Grubbs catalysts, **C1** was found to be practically inactive toward the RCM of diethyl diallylmalonate at room temperature with catalyst loadings as low as 0.05 mol %. However, conversions dramatically increased when the reaction temperature was increased to 70 °C. In addition, application of **C1** to challenging substrates, such as diethyl di(methallyl)malonate in fluorinated aromatic hydrocarbon solvents, resulted in a remarkable enhancement of catalytic activity. Moreover, this approach was successfully extended to the RCM of natural products and the cross-metathesis formation of trisubstituted alkenes [44].

Thus, we decided to study the catalytic activity of **C1**, **C2** and **C3** in ADMET polymerizations. Furthermore, to gain insight into isomerization activities of the catalysts, detailed isomerization studies were also performed using a procedure already described in the literature [30]. The catalyst loading (0.5 mol %) was kept constant throughout the entire screening process and temperatures varied from 60 °C to 120 °C during the investigation.

Results and Discussion

To date, only one example of ADMET polymerization with an in situ generated Ru–indenylidene catalyst has been reported [38]. The related arene Ru–indenylidene complex (Figure 3) was generated in situ from [RuCl(*p*-cymene)(=C=C=CPh_2)-(PCy_3)][CF_3SO_3], as the catalyst precursor and $HOSO_2CF_3$, and applied in the ADMET of 1,9-decadiene to yield a polymer with 94% conversion in 12 h at 0 °C.

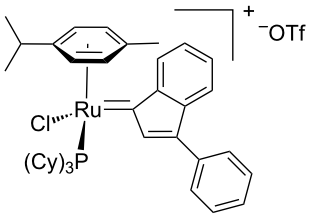

Figure 3: Representative scheme for the in situ generated Ru–indenylidene [38].

In this contribution, we report for the first time on the performance of two well-defined, stable Ru–indenylidene catalysts **C1** and **C2**, and the "boomerang complex" **C3** (Figure 2) during ADMET polymerizations. The ADMET monomer was synthesized by a procedure adapted from the literature using 1,3-propanediol, which can be prepared from glycerol, and 10-undecenoic acid [45], a commercial derivative of castor oil (Figure 4). A set of ADMET polymerizations was used to evaluate the performance of complexes **C1**, **C2** and **C3** at four

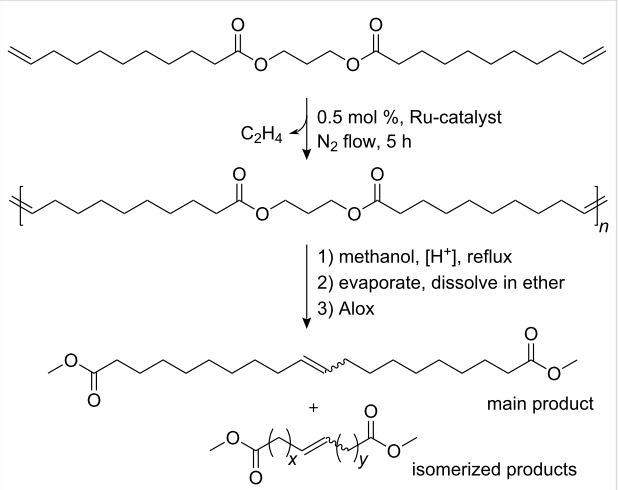

Figure 4: Synthesis of the studied α,ω-diene, its ADMET polymerization, and the strategy to evaluate isomerization side reactions.

different temperatures (60, 80, 100 and 120 °C), under bulk conditions, after 5 h reaction time, and constant catalyst loading (200:1 = monomer **1**: catalyst). This provided a broad data set to screen the catalytic systems tested (Table 1 and Table 2). The activity of these catalysts was compared to the Hoveyda–Grubbs 2nd generation catalyst (**C4**), which was previously examined in ADMET polymerizations of the same monomer [30]. In all cases, continuous nitrogen purging was applied throughout the polymerizations and polymerizations were run in duplicate to obtain a reliable set of data.

Moreover, the resulting ADMET polymers were transesterified with methanol to yield α,ω-diesters, which were subsequently analyzed by GC-MS (Figure 4). For the polymerizations in which isomerization does not occur, the GC-MS would only show a single peak corresponding to the unsaturated C-20 repeating unit of the studied polymers (compare Figure 4). However, most ruthenium-based metathesis catalysts are known to promote olefin isomerization. As a result, the corresponding transesterified polymer yields a mixture of diesters with different chain lengths, since double bond isomerisation and olefin metathesis occur concurrently. The molecular weight of the isomerized diesters thus varies by multiples of 14 g/mol (one methylene group).

The analytical data of the polymers synthesized is summarized in Table 1 and Table 2 and selected GPC traces are depicted in Figure 5. Except for the cases in which only oligomers were obtained, monomer conversion was quantitative as determined by the total disappearance of the monomer signal in the GPC traces of the reaction mixtures. The runs at 60 °C showed that, among **C1**, **C2** and **C3** (compare entries 1, 3 and 5 in Table 1, respectively; and Figure 4), **C1** led to the highest molecular weight of around 10 kDa, with a moderate isomerization degree of 36.3% (Table 1, entry 1). Interestingly at this temperature, **C2** showed a considerably lower degree of isomerization of 9.91%; however only oligomers (M_n 1700 Da) were obtained. Another goal of this research was to suppress the isomerization side reaction and thus to synthesize well-defined polyesters. Benzoquinones are very effective additives for the prevention of the olefin isomerization [21]. Thus, we performed the same set of experiments in the presence of **BQ**, and observed that the degree of isomerization was significantly reduced for **C1,** from 36.3% to 0.7%**.** However, this decrease in the degree of isomer-

Table 1: Overview of polymerization and the isomerization results of the corresponding polymers obtained at 60 and 80 °C after 5 h reaction time.

Entry	Polymer	Cat % [0.5 mol %]	Temp °C	Conditions[a]	Iso %[b]	M_n (Da)[c]	PDI
1	**P1**	**C1**	60		36.3	10500	2.00
2	**P2**	**C1**	60	**BQ** [1%]	0.70	8300	2.05
3	**P3**	**C2**	60		9.91	1700	1.16
4	**P4**	**C2**	60	**BQ** [1%]	NI[d]	2200	1.36
5	**P5**	**C3**	60		69.6	8000	1.60
6	**P6**	**C3**	60	**BQ** [1%]	63.9	4200	1.76
7	**P7**	**C1**	80		63.9	14000	1.92
8	**P8**	**C1**	80	**BQ** [1%]	74.2	14000	2.09
9	**P9**	**C2**	80		41.9	14200	1.90
10	**P10**	**C2**	80	**BQ** [1%]	28.6	9200	1.90
11	**P11**	**C3**	80		91.4	11850	1.80
12	**P12**	**C3**	80	**BQ** [1%]	59.2	11300	1.93

[a]Additional conditions applied during polymerization: **BQ**: amount of benzoquinone in % with respect to monomer; [b]% amount of isomerized diesters observed with GC-MS after transesterification of the respective polymer; [c]GPC was performed in THF, containing BHT, with PMMA calibration; [d]NI: no isomerization.

Table 2: Overview of polymerization and the isomerization results of the corresponding polymers obtained at 100 and 120 °C after 5 h reaction time.

Entry	Polymer	Cat % [0.5 mol %]	Temp °C	Conditions[a]	Iso %[b]	M_n (Da)[c]	PDI
13	**P13**	**C1**	100		79.3	10000	1.79
14	**P14**	**C1**	100	**BQ** [1%]	81.6	11300	1.74
15	**P15**	**C2**	100		53.6	9000	1.85
16	**P16**	**C2**	100	**BQ** [1%]	0.80	4500	1.60
17	**P17**	**C3**	100		55.2	6700	1.72
18	**P18**	**C3**	100	**BQ** [1%]	37.2	10150	1.92
19	**P19**	**C1**	120		89.4	16700	1.80
20	**P20**	**C1**	120	**BQ** [1%]	73.0	11000	1.83
21	**P21**	**C2**	120		83.7	13000	1.66
22	**P22**	**C2**	120	**BQ** [1%]	16.0	8500	1.78
23	**P23**	**C3**	120		87.4	12200	1.73
24	**P24**	**C3**	120	**BQ** [1%]	73.8	14850	1.73
25	**P25**	**C4**	120		80.5	10400	1.93
26	**P26**	**C4**	120	**BQ** [1%]	66.5	12000	1.67

[a]Additional conditions applied during polymerization: **BQ**: amount of benzoquinone in % respective to monomer; [b]% amount of isomerized diesters observed with GC-MS after transesterification of the respective polymer [c]GPC was performed in THF, containing BHT, with PMMA calibration..

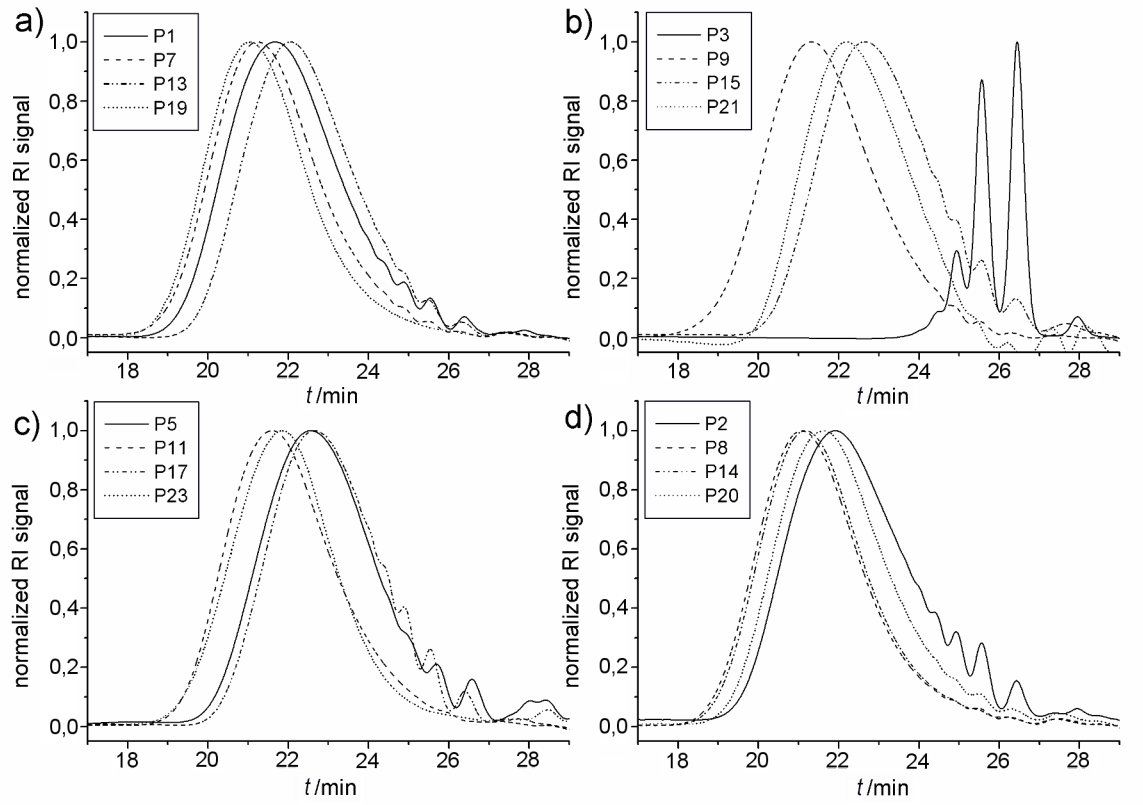

Figure 5: GPC traces of the polymerizations performed at 60, 80, 100 and 120 ºC in presence of a) 0.5 mol % **C1**, b) 0.5 mol % **C2**, c) 0.5 mol % **C3**, and d) 0.5 mol % **C1** with 1 mol % **BQ**.

ization was accompanied with reduced molecular weights for all studied catalysts. In the worst case of **C2**, the molecular weight was reduced by a factor of 3 (compare entries 3 and 4 in Table 1).

When the polymerization temperature was increased to 80 °C, higher molecular weight polymers were obtained with all the studied catalysts. For instance, **C2** produced a polymer with more than double the molecular weight when increasing the reaction temperature from 60 to 80 °C. Furthermore, the increase of the temperature led to an increase in the amount of isomerization for all of the catalysts. Concerning the isomerization inhibition effect of **BQ** on the catalyst, the effect was significant (factor of 1.5) for **C2** and **C3**, whereas **BQ** was ineffective in the presence of **C1**. In case of **C3**, the molecular weights of the corresponding polymers synthesized with and without **BQ** were similar, with a lower degree of isomerization for **P12**, as expected. Surprisingly, **C1** showed a higher degree of isomerization in the presence of **BQ** at 80 °C.

In an attempt to further increase the molecular weights of the obtained polyesters, all catalysts were also investigated at 100 °C (Table 2). Surprisingly, this further increase of the polymerization temperature led to lower molecular weights for all the studied catalysts. Quite interestingly, at that temperature the most significant inhibition effect of **BQ** on the degree of isomerization was observed for **C2** (compare entries 15 and 16 in Table 2), however, only oligomers were produced. Similarly as for the results at 80 °C, when we used **C1** and **BQ**, we observed an increase of the degree of isomerization along with similar M_n values (Table 2, entries 13 and 14). On the other hand, **C3** showed the same tendency as at 80 °C. The obtained polymers were less isomerized and had quite high molecular weights. The latter results with **C3** are in good agreement with the results previously obtained for the structurally similar **C4** [30].

Furthermore, the catalysts **C1**, **C2,** and **C3,** together with **C4** for comparison, were investigated at 120 °C (Table 2, entries 19, 21, 23, and 25). All complexes provided comparatively high molecular weights, following the order **C1** (~17000 Da) > **C2** (13000 Da) > **C3** (12200 Da) > **C4** (10500 Da). Regardless of the catalyst, all the polymers at that temperature possessed high isomerization values. Subsequently, we tried to reduce the amount of isomerization by performing the same set of reactions in the presence of **BQ** (Table 2, entries 20, 22, 24 and 26). The degree of isomerization was slightly reduced when using **C1** (Figure 6a), and the most prominent effect of **BQ** was observed again for **C2** (Figure 6b); however, this time the polymerization in the presence of **BQ** resulted in polymer with M_n of 8.5 kDa, compared to the results at lower temperatures. Interestingly, the polymerization with **C3** in the presence of **BQ** followed the same tendency as at 100 °C and resulted in higher molecular weight polymers in comparison to the polymerization without **BQ**, whereas the isomerization remained high (Table 2, entries 23 and 24).

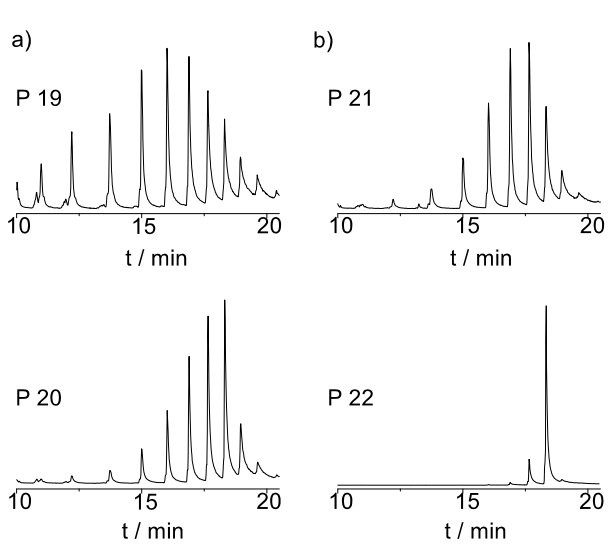

Figure 6: GC-MS study of the acid-catalyzed degradation products of polymers **P19**, **P20**, **P21**, and **P22**.

In a previous work, we reported that Hoveyda–Grubbs 2nd generation catalyst (**C4**) yields polymers with molecular weights M_n of 8000 Da at 80 °C, and 8800 Da at 100 ºC. The isomerization degrees were found to be 24% and 20%, respectively [30]. Herein we have demonstrated that **C4** can be used at a higher temperature (120 °C), in the presence of **BQ** (1 mol %), and with a low amount of catalyst (0.5 mol %), to yield a polymer with M_n of 12000 Da. However, at 120 °C the amount of isomerization was high with and without **BQ** (entries 25 and 26, Table 2). These results, along with the results discussed in our previous work, clearly show that **C4** can be used in a quite broad temperature range. Interestingly, **BQ** has a more pronounced effect in terms of isomerization inhibition, when compared to the structurally similar **C3** over the whole temperature range studied.

In summary, the tendency found for the activity of these catalysts as a function of the temperature was not linear. A clear increase in the activities was observed on increasing the temperature from 60 ºC to 80 ºC, however, when the temperature was increased to 100 ºC a general activity decrease was observed for all the catalysts, and finally the activity increased again when performing the reactions at 120 ºC. As the temperature is increased the activity of the catalyst increases, however, its degradation might also be accelerated. At 100 ºC, the deg-

radation of the catalyst could be predominant, thus resulting in lower molecular weights. On the other hand, when the temperature is raised to 120 ºC, the catalysts degradation could be compensated by an extremely fast initiation and short-term propagation promoted by the high temperature, giving as a result high molecular weight polymers before degradation of the catalysts occurs. This argumentation is speculative, but in order to provide some data to support this idea, the progress of the polymerization was examined at different times for **C1** at 80, 100 and 120 ºC. Samples were taken at 5, 15, 30, and 120 minutes for each temperature and analyzed by GPC (Figure 7). As predicted from the arguments above, the propagation observed for the polymerization at 80 ºC was slower than that at 100 ºC at short times, however, the polymerization stalled at 100 ºC, possibly due to catalyst degradation, yielding lower molecular weights. Furthermore, the propagation in the initial steps for the polymerization at 120 ºC was found to be the fastest, leading to high molecular weight species in short times before catalyst degradation became predominant.

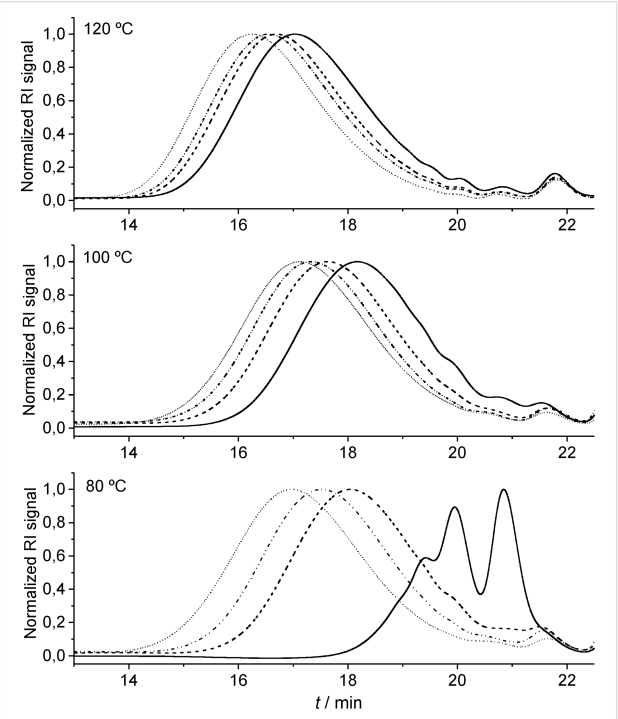

Figure 7: GPC traces of polymerizations performed with **C1** at 80, 100, and 120 ºC. Samples taken at 5 min (——), 15 min (–), 30 min (– • •), and 120 min (-).

Olefin isomerization occurring during ADMET polymerization leads to macromolecules with ill-defined structures. Depending on the degree of isomerization, the physical properties of the polymers are correspondingly affected. A different insight into the effect of the isomerization ratio on the thermal properties of the polymers can be achieved by differential scanning calorimetry (DSC) analysis of the synthesized polymers. The thermal behavior of two polymers with similar M_n, synthesized at same temperature with and without **BQ**, was studied by DSC (Figure 8). Polymer **P12** (Table 1, entry 12), possessing a lower degree of isomerization, exhibited a quite sharp T_m peak at 47 °C. On the other hand, the DSC trace of polymer **P11** (Table 1, entry 11), with higher isomerization degree, presented multiple peak melting transitions at lower temperatures resulting from its ill-defined repeat unit structure. These results show that, even if the addition of **BQ** does not completely avoid isomerization in most of the presented examples, polymers with a higher structural regularity can be obtained by with **BQ**.

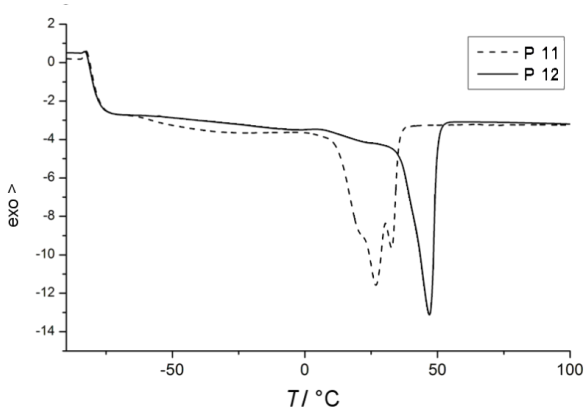

Figure 8: DSC traces of ADMET polymers **P11** and **P12** (Table 1, entries 11 and 12, respectively).

Conclusion

The indenylidene Ru-complexes provided an attractive alternative to the benzylidene compounds and allowed polyesters of up to 17000 Da via ADMET polymerization to be prepared, even at elevated temperatures with enhanced activity. Unfortunately, the attempt to synthesize regular polymer architectures by the addition of **BQ** to supress the isomerization reaction, was rather unsuccessful. Nevertheless, the results presented should be regarded as a first experimental data set on these catalysts and further improvement, building on these results, can be expected in the future.

Experimental

Materials

10-undecenoic acid (Sigma–Aldrich, 98%), 1,3-propanediol (Sigma–Aldrich, 99.6%), *p*-toluenesulfonic acid monohydrate (Sigma–Aldrich, 98.5%), ethyl vinyl ether (Sigma–Aldrich, 99%), sulfuric acid (Fluka, 95–97%), *p*-benzoquinone (Fluka, 98%), (1,3-bis(2,4,6-trimethylphenyl)-2-imidazolidinylidene) dichloro-(3-phenyl-1*H*-inden-1-ylidene)(tricyclohexylphosphine) ruthenium(II) (Umicore, **C1**), (1,3-bis(2,4,6-trimethyl-

phenyl)-2-imidazolidinylidene)dichloro-(3-phenyl-1*H*-inden-1-ylidene) (pyridyl) ruthenium(II) (Umicore, **C2**), (1,3-bis(2,4,6-trimethylphenyl)-2-imidazolidinylidene)dichloro(2-(1-methylacetoxy)phenyl]methylene ruthenium(II) (Umicore, **C3**), (1,3-bis(2,4,6-trimethylphenyl)-2-imidazolidinylidene)dichloro(*o*-isopropoxyphenylmethylene) ruthenium(II) (Hoveyda–Grubbs catalyst 2nd generation, **C4**, Sigma–Aldrich).

General Methods

Thin layer chromatography (TLC) was performed on silica gel TLC-cards (layer thickness 0.20 mm, Fluka). Compounds were visualized by permanganate reagent. For column chromatography silica gel 60 (0.035–0.070 mm, Fluka) was used.

^{1}H NMR spectra were recorded in $CDCl_3$ on Bruker AVANCE DPX spectrometers operating at 300 and 500 MHz. Chemical shifts (δ) are reported in parts per million relative to the internal standard tetramethylsilane (TMS, δ = 0.00 ppm). For the analysis of the polymers the relaxation time was set to 5 seconds.

Mass spectra (ESI) were recorded on a VARIAN 500-MS ion trap mass spectrometer with the TurboDDS^{TM} option installed. Samples were introduced by direct infusion with a syringe pump. Nitrogen served both as the nebulizer gas and the drying gas. Helium was used as cooling gas for the ion trap and collision gas for MS^n. Nitrogen was generated by a nitrogen generator Nitrox from Dominick Hunter.

GC-MS (EI) chromatograms were recorded with a Varian 431-GC instrument with a capillary column FactorFourTM VF-5ms (30 m × 0.25 mm × 0.25 μm) and a Varian 210-MS detector. Scans were performed from 40 to 650 m/z at a rate of 1.0 scans × s^{-1}. The oven temperature was programmed as follows: initial temperature 95 °C, hold for 1 min, ramp at 15 °C × min^{-1} to 200 °C, hold for 2 min, ramp at 15 °C × min^{-1} to 325 °C, hold for 5 min. The injector transfer line temperature was set to 250 °C. Measurements were performed in the split–split mode (split ratio 50:1) with helium as carrier gas (flow rate 1.0 ml × min^{-1}).

Polymer molecular weights were determined with an SEC System LC-20 A from Shimadzu equipped with a SIL-20A auto sampler, three PSS SDV columns (5 μm, 300 mm × 7.5 mm, 100 Å, 1000 Å, 10000 Å), and a RID-10A refractive index detector in THF (flow rate 1 mL × min^{-1}) at 50 °C. All determinations of molar mass were performed relative to PMMA standards (Polymer Standards Service, M_p 1100–981.000 Da).

Differential scanning calorimetry (DSC) experiments were carried out under a nitrogen atmosphere at a heating rate of 10 °C × min^{-1} with a DSC821e (Mettler Toledo) calorimeter up to a temperature of 150 °C with a sample mass of approximately 4 mg. The melting temperature, T_m, was recorded as the peak of the endotherm on the second heating scan unless annealing was used as a pretreatment.

Synthesis of 1,3-propylene diundec-10-enoate (1)

10-Undecenoic acid (50.00 g, 0.27 mol), 1,3-propanediol (8.4 g, 0.11 mol) and *p*-toluensulfonic acid (3 g, 0.0157 mol) were placed in a round-bottomed flask provided with a magnetic stirrer and a Dean-Stark apparatus. Toluene (200 mL) was added and the resulting reaction mixture heated to reflux. Water was collected as the reaction proceeded and once the reaction was completed, the reaction mixture was allowed to cool. Toluene was removed under reduced pressure and the residue was filtered through a short pad of basic aluminium oxide with hexane as eluent. After removing the hexane, the crude product was dissolved in diethyl ether (200 mL) and washed two times with water (200 mL). The organic fraction was dried over anhydrous $MgSO_4$ and the solvent removed under reduced pressure. The desired product was isolated in 87% yield (39 g).

^{1}H NMR ($CDCl_3$): δ = 5.85–5.76 (m, 2H, 2x-C*H*=CH_2), 5.00–4.91 (m, 4H, 2xCH=CH_2), 4.15 (t, 4H, J=6.1 Hz, 2xCH_2OCO-), 2.30 (t, 4H, *J* = 7.3 Hz, CH_2COO-), 2.00 (m, 4H, 2xCH_2-CH=CH2), 1.99–1.94 (m, 2H, *J* = 6.1 Hz, CH_2CH$_2$OCO-), 1.64–1.58 (m, 4H, 2xCH_2CH$_2$COO-), 1.38–1.34 (m, 4H, 2xCH_2) 1.29–1.24 (br.s, 16H, 2x[4CH_2]) ppm. ^{13}C NMR (CDCl3): δ = 173.6 (s, -*C*OO-), 139.0 (s, -*C*H=CH_2), 114.1 (s, -CH=*C*H$_2$), 60.7 (s, *C*H$_2$OCO-), 34.1 (s, *C*H$_2$), 33.7 (s, *C*H$_2$), 29.2 (s, *C*H$_2$), 29.1 (s, *C*H$_2$), 29.0 (s, *C*H$_2$), 28.8 (s, *C*H$_2$), 24.8 (s, CH$_2$) ppm. MS (EI): *m/z* = 408 $[M]^+$, calc. 408.3239.

ADMET polymerization (P1-P26)

To 1 g (2.45 mmol) of 1,3-propylene diundec-10-enoate in a tube equipped with a screw, 0.5 mol % of the corresponding ruthenium catalyst, (**C1**: 11.6 mg (0.0122 mmol), **C2**: 9.1 mg (0.0122 mmol), **C3**: 8 mg (0.0122 mmol) and **C4**: 7.7 mg) was added at the desired reaction temperature (60–120 °C). In some cases, 1 mol % of **BQ** was added to the reaction mixture 10 min before the addition of the catalyst. Reactions were carried out in parallel using a carousel reaction station from Radleys. Stirring was continued at the selected temperature under a continuous flow of nitrogen for 5 h. After 5 h reaction time, the reaction mixture was dissolved in 1 mL of THF and polymerization halted by the addition of 1 mL of ethyl vinyl ether. The mixture was then stirred for 30 min at room temperature. The crude product was purified by precipitation into cold methanol. Final polymer molecular weights were determined after precipitation with the above mentioned GPC system.

Transesterification of the obtained polymers (P1-P26) and GC-MS analysis

The respective polymer (30 mg), excess methanol (4 mL) and concentrated sulfuric acid (5 drops) were added to a carousel reaction tube, stirred magnetically, and refluxed at 85 °C for 5 h. At the end of the reaction, the excess of methanol was removed under reduced pressure. The residue was then dissolved in diethyl ether and filtered through a small column of basic aluminium oxide. Subsequently, GC-MS samples were prepared by taking 500 µL of this solution and diluting it with methanol (500 µL). The percentage of olefin isomerization was calculated based on peak areas of the isomerized diesters.

Acknowledgements

This work was partially financially supported by the German Federal Ministry of Food, Agriculture and Consumer Protection (represented by the Fachagentur Nachwachsende Rohstoffe). LME is grateful for a Max Planck postdoctoral fellowship. The authors are grateful to Prof. Beuermann for providing access to DSC equipment and to Umicore for their generous donation of catalysts.

References

1. Schuster, M.; Blechert, S. *Angew. Chem., Int. Ed.* **1997,** *36,* 2036–2056. doi:10.1002/anie.199720361
2. Fürstner, A. *Angew. Chem., Int. Ed.* **2000,** *39,* 3012–3043. doi:10.1002/1521-3773(20000901)39:17<3012::AID-ANIE3012>3.0.CO;2-G
3. Trnka, T. M.; Grubbs, R. H. *Acc. Chem. Res.* **2001,** *34,* 18–29. doi:10.1021/ar000114f
4. Connon, S.; Blechert, S. *Angew. Chem.* **2003,** *115,* 1944–1968. doi:10.1002/ange.200200556
5. Grubbs, R. H. *Tetrahedron* **2004,** *60,* 7117–7140. doi:10.1016/j.tet.2004.05.124
6. Rybak, A.; Fokou, P. A.; Meier, M. A. R. *Eur. J. Lipid Sci. Technol.* **2008,** *110,* 797–804. doi:10.1002/ejlt.200800027
7. Miller, S. J.; Blackwell, H. E.; Grubbs, R. H. *J. Am. Chem. Soc.* **1996,** *118,* 9606–9614. doi:10.1021/ja961626l
8. Maynard, H. D.; Grubbs, R. H. *Tetrahedron Lett.* **1999,** *40,* 4137–4140. doi:10.1016/S0040-4039(99)00726-1
9. Bourgeois, D.; Pancrazi, A.; Ricard, L.; Prunet, J. *Angew. Chem., Int. Ed.* **2000,** *112,* 742–744. doi:10.1002/(SICI)1521-3773(20000218)39:4<725::AID-ANIE725>3.0.CO;2-I
10. Edwards, S. D.; Lewis, T.; Taylor, R. J. K. *Tetrahedron Lett.* **1999,** *40,* 4267–4270. doi:10.1016/S0040-4039(99)00703-0
11. Schmidt, B.; Wildemann, H. *J. Org. Chem.* **2000,** *65,* 5817–5822. doi:10.1021/jo005534x
12. Dinger, M. B.; Mol, J. C. *Adv. Synth. Catal.* **2002,** *344,* 671–677. doi:10.1002/1615-4169(200208)344:6/7<671::AID-ADSC671>3.0.CO;2-G
13. Fürstner, A.; Thiel, O. R.; Ackermann, L.; Schanz, H.-J.; Nolan, S. P. *J. Org. Chem.* **2000,** *65,* 2204–2207. doi:10.1021/jo9918504
14. Sutton, A. E.; Seigal, B. A.; Finnegan, D. F.; Snapper, M. L. *J. Am. Chem. Soc.* **2002,** *124,* 13390–13391. doi:10.1021/ja028044q
15. Sworen, J. C.; Pawlow, J. H.; Case, W.; Lever, J.; Wagener, K. B. *J. Mol. Catal.* **2002,** *194,* 69–78. doi:10.1016/S1381-1169(02)00524-1
16. Bourgeois, D.; Pancrazi, A.; Nolan, S. P.; Prunet, J. *J. Organomet. Chem.* **2002,** *643,* 247–252. doi:10.1016/S0022-328X(01)01269-4
17. Lehman, S. E., Jr.; Schwendeman, J. E.; O'Donnell, P. M.; Wagener, K. B. *Inorg. Chim. Acta* **2002,** *345,* 190–198. doi:10.1016/S0020-1693(02)01307-5
18. Schmidt, B. *Eur. J. Org. Chem.* **2004,** 1865–1880. doi:10.1002/ejoc.200300714
19. Louie, J.; Grubbs, R. H. *Organometallics* **2002,** *21,* 2153–2164. doi:10.1021/om011037a
20. Hong, S. H.; Day, M. W.; Grubbs, R. H. *J. Am. Chem. Soc.* **2004,** *126,* 7414–7415. doi:10.1021/ja0488380
21. Hong, S. H.; Sanders, D. P.; Lee, C. W.; Grubbs, R. H. *J. Am. Chem. Soc.* **2005,** *127,* 17160–17161. doi:10.1021/ja052939w
22. Moïse, J.; Arseniyadis, S.; Cossy, J. *Org. Lett.* **2007,** *9,* 1695–1698. doi:10.1021/ol0703940
23. Vedrenne, E.; Dupont, H.; Oualef, S.; Elkaïm, L.; Grimaud, L. *Synlett* **2005,** *4,* 670–672. doi:10.1055/s-2005-862375
24. Formentin, P.; Gimeno, N.; Steinke, J. H. G.; Vilar, R. *J. Org. Chem.* **2005,** *70,* 8235–8238. doi:10.1021/jo051120y
25. Campbell, J. M.; Johnson, S. *J. Am. Chem. Soc.* **2009,** *131,* 10370–10371. doi:10.1021/ja904136q
26. Mutlu, H.; Montero de Espinosa, L.; Meier, M. A. R. *Chem. Soc. Rev.* **2011,** in press. doi:10.1039/b924852h
27. Fokou, P. A.; Meier, M. A. R. *J. Am. Chem. Soc.* **2009,** *131,* 1664–1665. doi:10.1021/ja808679w
28. Courchay, F. C.; Sworen, J. C.; Wagener, K. B. *Macromolecules* **2003,** *36,* 8231–8239. doi:10.1021/ma0302964
29. Petkovska, V. I.; Hopkins, T. E.; Powell, D. H.; Wagener, K. B. *Macromolecules* **2005,** *38,* 5878–5885. doi:10.1021/ma050480k
30. Fokou, P. A.; Meier, M. A. R. *Macromol. Rapid Commun.* **2010,** *31,* 368–373. doi:10.1002/marc.200900678
31. Arlt, D.; Bieniek, M.; Karch, R. Novel Metathesis Catalysts. PCT/EP2007/007972, Sept 13, 2007.
32. Jafarpour, L.; Schanz, H.-J.; Stevens, E. D.; Nolan, S. P. *Organometallics* **1999,** *18,* 5416–5419. doi:10.1021/om990587u
33. Broggi, J.; Urbina-Blanco, C. A.; Clavier, H.; Leitgeb, A.; Slugovc, C.; Slawin, A. M. Z.; Nolan, S. P. *Chem.–Eur. J.* **2010,** *16,* 9215–9225. doi:10.1002/chem.201000659
34. Clavier, H.; Petersen, J. L.; Nolan, S. P. *J. Organomet. Chem.* **2006,** *691,* 5444–5447. doi:10.1016/j.jorganchem.2006.08.007
35. Monsaert, S.; Drozdzak, R.; Dragutan, V.; Dragutan, I.; Verpoort, F. *Eur. J. Inorg. Chem.* **2008,** 432–440. doi:10.1002/ejic.200700879
36. de Fremont, P.; Clavier, H.; Montembault, V.; Fontaine, L.; Nolan, S. P. *J. Mol. Catal. A: Chem.* **2008,** *283,* 108–113. doi:10.1016/j.molcata.2007.11.038
37. Opstal, T.; Verpoort, F. *Angew. Chem., Int. Ed.* **2003,** *42,* 2876–2879. doi:10.1002/anie.200250840
38. Castarlenas, P.; Dixneuf, P. H. *Angew. Chem., Int. Ed.* **2003,** *42,* 4524–4527. doi:10.1002/anie.200352108
39. Adekunle, O.; Tanner, S.; Binder, W. H. *Beilstein J. Org. Chem.* **2010,** *6,* No. 59. doi:10.3762/bjoc.6.59
40. Burtscher, D.; Lexer, C.; Mereiter, K.; Winde, R.; Karch, R.; Slugovc, C. *J. Polym. Sci., Part A: Polym. Chem.* **2008,** *46,* 4630–4635. doi:10.1002/pola.22763
41. Clavier, H.; Nolan, S. P. *Chem.–Eur. J.* **2007,** *13,* 8029–8036. doi:10.1002/chem.200700256

42. Miao, X.; Fischmeister, C.; Bruneau, C.; Dixneuf, P. H. *ChemSusChem* **2009,** *2,* 542–545. doi:10.1002/cssc.200900028
43. Bieniek, M.; Michrowska, A.; Usanov, D. L.; Grela, K. *Chem.–Eur. J.* **2008,** *14,* 806–818. doi:10.1002/chem.200701340
44. Samojlowicz, C.; Bieniek, M.; Zarecki, A.; Kadyrov, R.; Grela, K. *Chem. Commun.* **2008,** 6282–6284. doi:10.1039/b816567j
45. Mutlu, H.; Meier, M. A. R. *Eur. J. Lipid Sci. Technol.* **2010,** *112,* 10–30. doi:10.1002/ejlt.200900138

License and Terms

Beilstein Journal of Organic Chemistry

New library of aminosulfonyl-tagged Hoveyda–Grubbs type complexes: Synthesis, kinetic studies and activity in olefin metathesis transformations

Etienne Borré[1,2], Frederic Caijo[1,3], Christophe Crévisy*[1,2] and Marc Mauduit*[1,2]

Full Research Paper

Open Access

Address:
[1]École Nationale Supérieure de Chimie de Rennes, CNRS, UMR 6226, Av. du Général Leclerc, CS 50837 35708 Rennes cedex 7, France, [2]Université Européenne de Bretagne, 35000 Rennes, France and [3]Omega cat system Sàrl - École Nationale Supérieure de Chimie de Rennes, Av. du Général Leclerc, CS 50837 35708 Rennes cedex 7, France

Email:
Etienne Borré - etienne.borre@ensc-rennes.fr; Frederic Caijo - f.caijo@omcat-system.com; Christophe Crévisy* - christophe.crevisy@ensc-rennes.fr; Marc Mauduit* - marc.mauduit@ensc-rennes.fr

* Corresponding author

Keywords:
cross-metathesis; kinetic studies; olefin metathesis; RCM; ruthenium

Beilstein J. Org. Chem. **2010,** *6,* 1159–1166.
doi:10.3762/bjoc.6.132

Received: 13 September 2010
Accepted: 09 November 2010
Published: 06 December 2010

Guest Editor: K. Grela

Abstract

Seven novel Hoveyda–Grubbs precatalysts bearing an aminosulfonyl function are reported. Kinetic studies indicate an activity enhancement compared to Hoveyda's precatalyst. A selection of these catalysts was investigated with various substrates in ring-closing metathesis of dienes or enynes and cross metathesis. The results demonstrate that these catalysts show a good tolerance to various chemical functions.

Introduction

In the last decades, olefin metathesis has become a powerful tool in organic chemistry. Since the discovery of the well-defined ruthenium precatalyst ($Cl_2(PPh_3)_2Ru$=CHPh) [1], which is tolerant to many functional groups, several synthetic routes (from petrochemical to fine chemical products) have been facilitated [2-4]. However, many research groups have focused their research on the development of more efficient precatalysts (Figure 1). In 1999, Grubbs (**1a**) [5] and Nolan (**1b**) [6] reported ruthenium species bearing one *N*-heterocyclic carbene (NHC) moiety. Despite the stability enhancement of the active species (due to NHC), these catalysts still required a high catalytic loading (up to 20 mol % in some cases [7]). Later, Hoveyda synthesized a recyclable phosphine-free precatalyst (**2a**) [8] based on a release/return concept of the benzylidene ether fragment. Electronic or steric modifications made by Blechert (**2b**) [9,10], Grela (**2c**) [11,12] or Zhan (**2d**) [13] have allowed a decrease of precatalyst loading (down to 1 mol %).

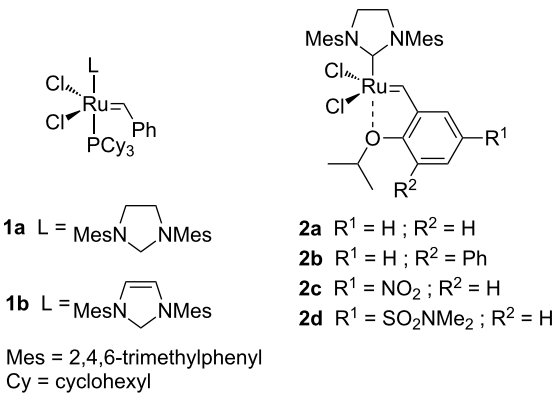

Figure 1: Ruthenium precatalysts for olefin metathesis.

Nevertheless, despite all these recent developments, the problem of the ruthenium contamination in products has still not yet been resolved. Indeed, high concetrations of metal impurities are often present in the final products, limiting industrial applications. Several attempts have been made to reduce the Ru-contamination to <10 ppm, as required by regulatory bodies, for example, by the use of Ru-scavengers, biphasic extraction, silica gel chromatography etc. [14]. Nevertheless, some difficulties remain, for instance: Lower yields are observed when successive silica gel chromatography is performed and some scavengers are very toxic ($PbOAc_2$, DMSO…) [15]. Another strategy aims to control the catalyst activity in order to improve recyclability. Recently, various aminocarbonyl-containing "boomerang" precatalysts **3** were synthesized in our laboratory (Figure 2) [16-18]. The results

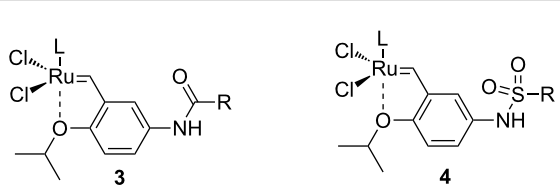

Figure 2: Structure of precatalyst **3** and **4**.

obtained with these catalysts enabled us not only to combine the enhancement of activity with a better stability (1 month in dichloromethane solution) but also to combine it with excellent recyclability (up to 60% at 0.3 mol %). Extremely low levels of Ru-contamination in the final products were determined by ICP-MS analyses (below 6 ppm) after silica gel chromatography. Additionally, a recent study in the synthesis of natural products involving a library of precatalysts **3** [7] shows that the structure of the catalyst must be carefully designed and adapted for a specific transformation.

Owing to this substrate dependency, we focused our attention on the development of a new library of catalysts bearing an aminosulfonyl function **4** (Figure 2).

Results and Discussion

To synthesize the catalysts, the required aminosulfonyl function had to be introduced into the styrenylether fragment. The ligands (**6a**–**f**) were synthesized in one step from the previously reported aniline **5** [19,20] and either trifluoromethanesulfonic anhydride or various chlorosulfonyl derivatives (Scheme 1).

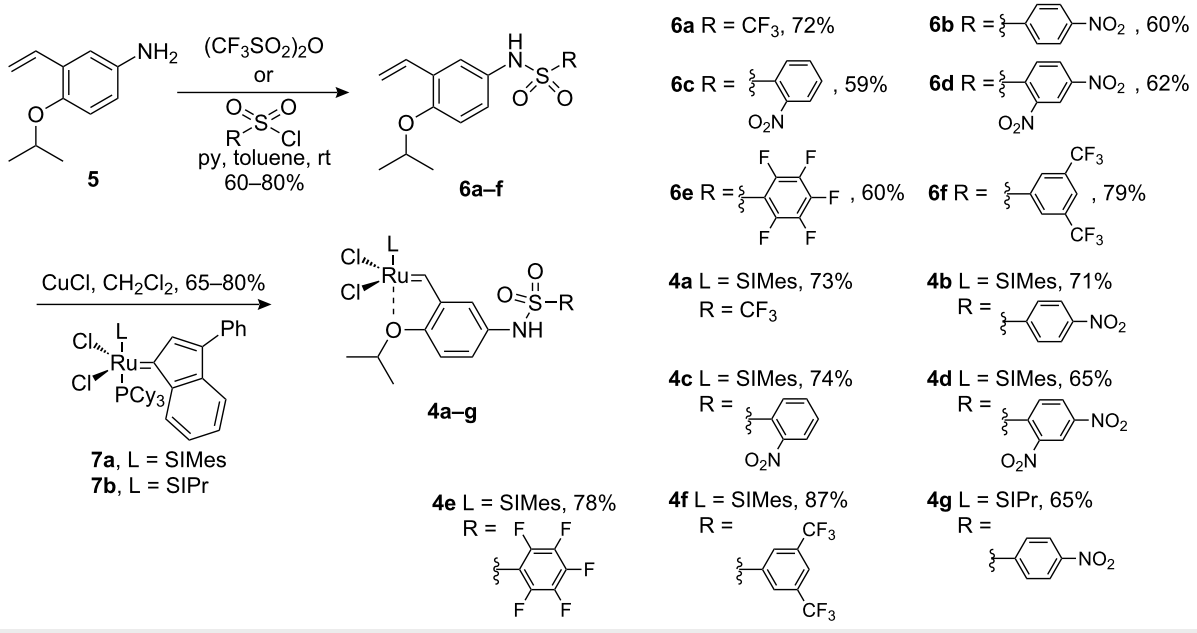

Scheme 1: Synthesis of catalysts **4a**–**g**.

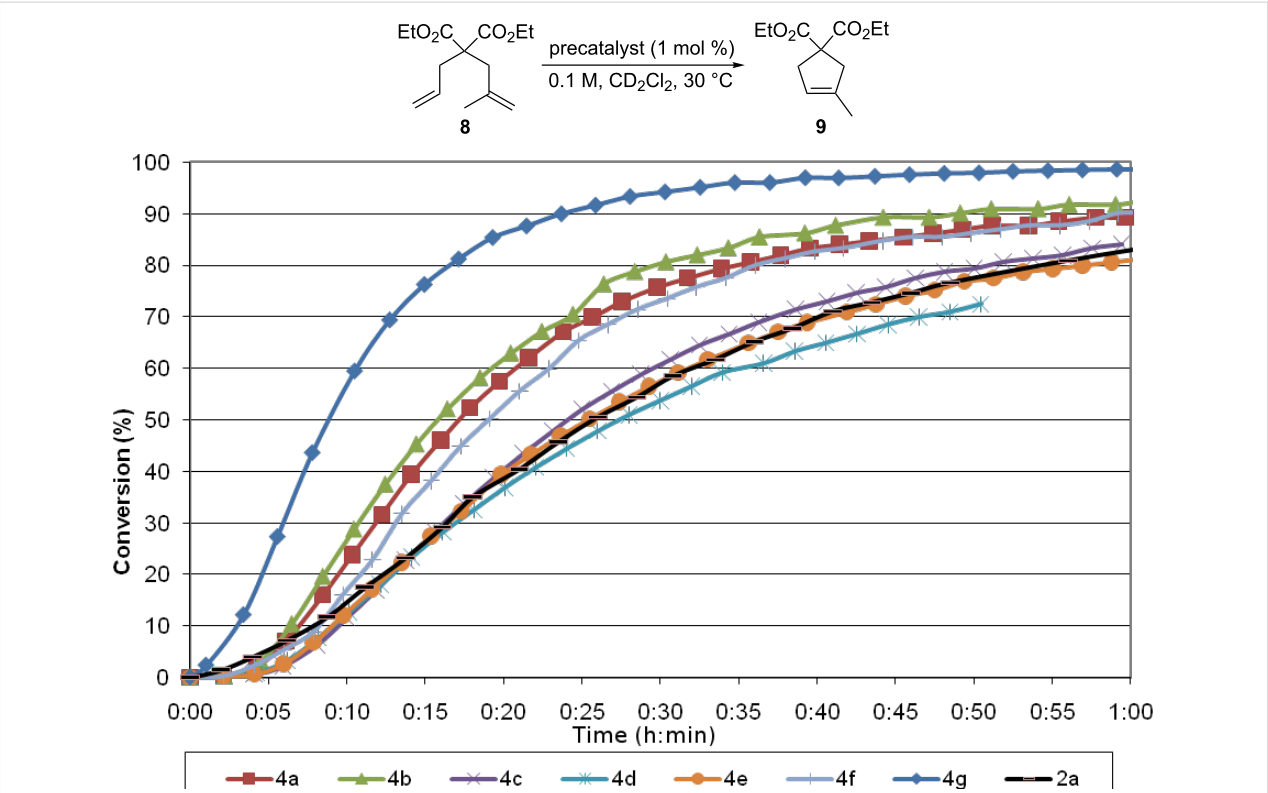

Figure 3: Kinetic studies of RCM of **8** (0.1 M) with precatalysts **4a–g** (1 mol %) in CD_2Cl_2 at 30 °C.

Ligands **6a–f** were isolated in moderate to good yields (60–80%). Their reaction with Ru-indenylidene complex **7a** [21] or **7b** [22] in the presence of CuCl afforded the expected precatalysts **4a–g** in good yields.

Then, the reactivity profile of each catalyst was investigated using ^{1}H NMR monitored kinetic studies. Comparison between catalysts was done at the initiation step. Moreover, conversions were compared over a reaction time of one hour. The 2-allyl-2-methallylmalonate **8** is usually used as benchmark substrate for ring-closing metathesis, inasmuch it shows significant differences between an activated or a non-activated precatalyst. The reactions were performed at low loading of precatalyst (1 mol %) and 30 °C (Figure 3).

The graphs presented in Figure 3 show three different types of behavior. The catalysts **4c**, **4d** and **4e** are not activated compared to Hoveyda's complex **2a**. They can be classified as Hoveyda-like complexes. Complexes **4a**, **4b** and **4f** can be considered to be activated catalysts, while catalyst **4g** bearing a more sterically demanding NHC (SIPr) ligand shows a faster initiation compared to its SIMes analogue catalyst **4b**. Additionally, **4g** gave the best conversion over a reaction time of one hour.

In order to investigate potential substrate dependency, the activity of the five SIMes-catalysts **4a–e** was evaluated in three different cross-metathesis (CM) reactions involving methyl acrylate, methyl vinyl ketone (MVK) and acrylonitrile as electro-deficient alkenes and the two electron-rich olefins **S1** and **S2** (Table 1).

In the reaction of methyl acrylate and **S1**, complexes **4c** and **4d** proved to be the most efficient catalysts (entries 1–5) while no clear-cut difference in reactivity was observed when MVK and **S2** were used (entries 6–10). The CM of **S1** and acrylonitrile, which is known to be a demanding substrate, was more problematic since low conversions were observed after 24 h of reaction at 2 mol % catalyst loading (entries 11–15). Unexpectedly, complex **4c** was half as efficient as the other analogues (entry 13). So, the nature of the electron-withdrawing group (EWG) appears to have a rather weak influence on the behaviour of the catalysts in these cases.

Finally, the reactivity profiles of **4a** and **4g** were compared in various metathesis reactions in order to evaluate the influence of the NHC ligand. The last point of our study was the comparison between catalysts in RCM of dienes or enynes and in one CM reaction (Table 2).

Table 1: Scope of **4a–e** for CM transformations[a].

Entry	Substrates	Product	Time	Catalyst	Conversion (%)[b,c]
1 2 3 4 5	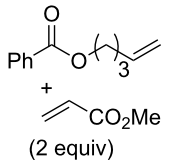 **S1** (2 equiv)	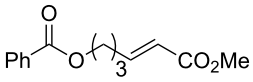 **P1a**	0.5 h	**4a** **4b** **4c** **4d** **4e**	69 50 71 73 62
6 7 8 9 10	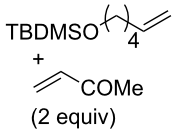 **S2** (2 equiv)	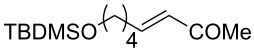 **P2**	0.5 h	**4a** **4b** **4c** **4d** **4e**	81 88 86 83 80
11 12 13 14 15	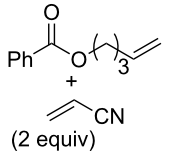 **S1** (2 equiv)	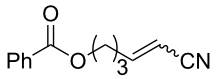 **P2b**	24 h	**4a**[d] **4b**[d] **4c**[d] **4d**[d] **4e**[d]	39 (*E*/*Z* 1/4) 42 (*E*/*Z* 1/4) 24 (*E*/*Z* 1/4) 47 (*E*/*Z* 1/4) 49 (*E*/*Z* 1/4)

[a]Reaction conditions: 1 mol % of catalyst, CH_2Cl_2, 0.1 M, rt. [b]Determined by ^1H NMR, [c]*E*/*Z* ratio 20/1, [d]2 mol % of catalyst, CH_2Cl_2, 0.1 M, 40 °C.

Both catalysts **4b** and **4g** proved to be efficient in all reactions, except in the formation of tetrasubstituted olefin **P6** (entries 7–8). Nevertheless, in almost all cases, either the conversion was higher and/or the reaction duration shorter when SIPr-based complex **4g** was used showing its highest efficiency. This confirms the reactivity profile found in the kinetic study. The outstanding reactivity of **4g** in the CM of **S1** and acrylonitrile must be highlighted since a very good conversion was obtained (entry 14, 84%) [23]. This demonstrates the beneficial combination between the SIPr unit and the electronic activation of the benzylidene fragment.

Conclusion

A new library of Hoveyda type catalysts bearing aminosulfonyl functions has been synthesized. Their activity profiles have been investigated through kinetic studies and through evaluation of a group of substrates. Most of these have shown high activities, nevertheless the SIPr-based complex **4g** proved to be

Table 2: Comparison of **4b** and **4g** in metathesis reactions[a].

Entry	Substrate	Product	Catalyst	Time	Conversion (%)[b]
1 2	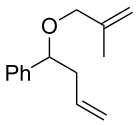 **S3**	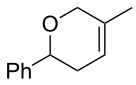 **P3**	**4b** **4g**	5 h 2 h	62 100
3 4	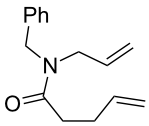 **S4**	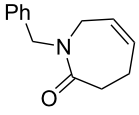 **P4**	**4b** **4g**	1.75 h 1 h	100 100
5 6	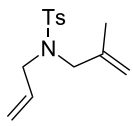 **S5**	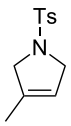 **P5**	**4b** **4g**	4.5 h 2 h	96 100
7 8	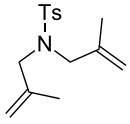 **S6**	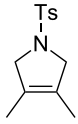 **P6**	**4b** **4g**	24 h 24 h	18[c] 3[c]

Table 2: Comparison of **4b** and **4g** in metathesis reactions[a]. (continued)

9 10	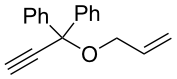 **S7**	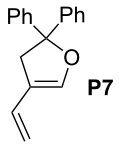 **P7**	**4b** **4g**	0.75 h 0.5 h	100 100
11 12	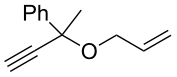 **S8**	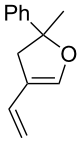 **P8**	**4b** **4g**	0.5 h 0.5 h	100 100
13 14	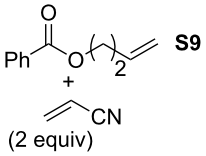 **S9** (2 equiv)	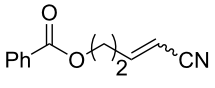 **P9**	**4b** **4g**	24 h 24 h	48[c] (*E*/*Z* 1/4) 84[c] (*E*/*Z* 1/4)

[a]Reaction conditions: 1 mol % of catalyst, CH_2Cl_2, 0.1 M, rt. [b]Determined by ^1H NMR, [c]2 mol % of catalyst, CH_2Cl_2, 0.1 M, 40 °C.

the most efficient, notably in the case where acrylonitrile was involved in the CM.

Experimental

Synthesis of 1,1,1-trifluoro-*N*-(4-isopropoxy-3-vinylphenyl)-methanesulfonamide (**6a**):To a solution of aniline **5** (40 mg, 0.23 mmol) in dry DCM (3 mL), 2,6-lutidine (54 µL, 0.46 mmol, 2 equiv) was added at 0 °C. Then, trifluoromethanesulfonic anhydride (41 µL, 0.25 mmol, 1.1 equiv) was added dropwise and the mixture was allowed to warm to rt during 12 h. After removal of the solvent under vacuum, the crude product was purified by flash chromatography on silica gel (DCM) to give the expected product as a brown oil (42 mg, 72%). ^1H NMR (400 MHz, $CDCl_3$, δ): 1.35 (d, *J* = 6.1 Hz, 6H, 2 CH_3), 4.54 (sept, *J* = 6.1 Hz, 1H, CH), 5.30 (dd, *J* = 11.2 Hz and 1.2 Hz, 1H, CH), 5.73 (dd, *J* = 17.7 Hz and 1.2 Hz, 1H, CH), 6.85 (d, *J* = 8.9 Hz, 1H, CH), 6.97 (dd, *J* = 17.7 Hz and 11.2 Hz, 1H, CH), 7.13 (dd, *J* = 8.9 Hz and 2.8 Hz, 1H, CH), 7.36 (d, *J* = 2.8 Hz, 1H, CH). ^{13}C NMR (100 MHz, $CDCl_3$, δ): 22.0 (2C), 71.2, 114.4, 115.6, 119.8 (q, *J* = 322.8 Hz), 121.4, 125.6, 125.8, 128.9, 130.8, 154.8. ^{19}F NMR (376 MHz, $CDCl_3$, δ): −74,1 (s, 3F).

Synthesis of *N*-(4-isopropoxy-3-vinylphenyl)-4-nitrobenzenesulfonamide (**6b**): To a solution of aniline **5** (40 mg, 0.23 mmol) in dry toluene (4 mL), were added successively pyridine (37 µL, 0.46 mmol, 2 equiv) and a solution of *p*-nitrobenzenesulfonyl chloride (50 mg, 0.23 mmol, 1 equiv) in 1 mL of toluene. The mixture was stirred at rt overnight. After removal of the solvent under vacuum, the crude product was purified by chromatography (cyclohexane/ethyl acetate, 8:2) to give **6b** as a pale yellow amorphous solid (49 mg, 60%). ^1H NMR (400 MHz, $CDCl_3$, δ): 1.25 (d, *J* = 6.0 Hz, 6H, 2 CH_3), 4.4 (sept, *J* = 6.0 Hz, 1H, CH), 5.15 (dd, *J* = 11.2 Hz and 1.3 Hz, 1H, CH), 5.52 (dd, *J* = 17.8 Hz and 1.3 Hz, 1H, CH), 6.67 (d, *J* = 8.7 Hz, 1H, CH), 6.83 (dd, *J* = 8.7 Hz and 2.8 Hz, 1H, CH), 6.84 (dd, *J* = 17.8 Hz and 11.2 Hz, 1H, CH), 7.07 (d, *J* = 2,8 Hz, 1H, CH), 7.82 (d, *J* = 9.0 Hz, 2H, CH), 8.19 (d, *J* = 9,0 Hz, 2H, CH). ^{13}C NMR (100 MHz, $CDCl_3$, δ): 22.0 (2C), 71.1, 114.5, 115.3, 122.6, 124.1 (2C), 124.5, 127.5, 128.6 (2C), 128.8, 130.9, 144.7, 150.1, 154.0.

Synthesis of *N*-(4-isopropoxy-3-vinylphenyl)-2-nitrobenzenesulfonamide (**6c**): Following the procedure described for **6b** using *o*-nitrobenzenesulfonyl chloride, **6c** was obtained as a pale yellow amorphous solid (46 mg, 57%). ^1H NMR (400 MHz, $CDCl_3$, δ): 1.31 (d, *J* = 6.1 Hz, 6H, 2 CH_3), 4.47 (sept., *J* = 6.1 Hz, 1H, CH), 5.21 (dd, *J* = 11.2 Hz and 1.3 Hz, 1H, CH), 5.59 (dd, *J* = 17.8 Hz and 1.3 Hz, 1H, CH), 6.75 (d, *J* = 8.8 Hz, 1H, CH), 6.91 (dd, *J* = 17.8 Hz and 11.2 Hz, 1H, CH), 7.01 (dd, *J* = 8.8 Hz and 2.7 Hz, 1H, CH), 7.11 (s, 1H, NH), 7.22 (d, *J* = 2.7 Hz, 1H, CH), 7.56 (td, *J* = 7.7 Hz and 1.3 Hz, 1H, CH), 7.69 (td, *J* = 7.5 Hz and 1.4 Hz, 1H, CH), 7.77 (dd, *J* = 7.8 Hz and 1.4 Hz, 1H, CH), 7.85 (dd, *J* = 7.9 Hz and 1.3 Hz, 1H, CH). ^{13}C NMR (100 MHz, $CDCl_3$, δ): 22.0 (2C), 71.1, 114.4, 115.2, 122.8, 124.9, 125.1, 127.8, 128.6, 130.9, 131.9, 132.2, 134.4, 133.8, 148.2, 154.0.

N-(4-isopropoxy-3-vinylphenyl)-2,4-dinitrobenzenesulfonamide (**6d**): Following the procedure described for **6b** using 2,4-dinitrobenzenesulfonyl chloride, **6d** was obtained as a yellow oil (57 mg, 62%). ^1H NMR (400 MHz, $CDCl_3$, δ): 1.31 (d, *J* = 6.1 Hz, 6H, 2 CH_3), 4.48 (sept., *J* = 6.1 Hz, 1H, CH), 5.24 (dd, *J* = 11.2 Hz and 1.3 Hz, 1H, CH), 5.63 (dd, *J* = 17.8

Hz and 1.3 Hz, 1H, CH), 6.75 (d, J = 8.9 Hz, 1H, CH), 6.91 (dd, J = 17.8 Hz and 11.2 Hz, 1H, CH), 6.99 (dd, J = 8.9 Hz and 2.7 Hz, 1H, CH), 7.24 (d, J = 2.7 Hz, 1H, CH), 8.00 (d, J = 8.6 Hz, 1H, CH), 8.37 (dd, J = 8.6 Hz and 2.2 Hz, 1H, CH), 8.65 (d, J = 2.2 Hz, 1H, CH). ^{13}C NMR (100 MHz, $CDCl_3$, δ): 22.0 (2C), 71.2, 114.2, 115.6, 116.4, 119.0, 122.5, 127.7, 129.2, 129.9, 131.3, 134.7, 140.5, 144.0, 146.3, 152.1.

N-(4-isopropoxy-3-vinylphenyl)-2,3,4,5,6-pentafluorobenzenesulfonamide (**6e**): Following the procedure described for **6b** using 2,3,4,5,6-pentafluorobenzenesulfonyl chloride, **6e** was obtained as a red oil (65 mg, 71%). ^{1}H NMR (400 MHz, $CDCl_3$, δ): 1.32 (d, J = 6.1 Hz, 6H, 2 CH_3), 4.49 (sept, J = 6.1 Hz, 1H, CH), 5.27 (dd, J = 11.2 Hz and 1.1 Hz, 1H, CH), 5.67 (dd, J = 17.8 Hz and 1.1 Hz, 1H, CH), 6.79 (d, J = 8.8 Hz, 1H, CH), 6.93 (dd, J = 17.8 Hz and 11.2 Hz, 1H, CH), 7.04 (dd, J = 8.8 Hz and 2.7 Hz, 1H, CH), 7.19 (s, 1H, NH), 7.25 (d, J = 2.7 Hz, 1H, CH). ^{13}C NMR (100 MHz, $CDCl_3$, δ): 22.0 (2C), 71.2, 114.7, 115.5, 121.1, 123.1, 126.9, 127.5–131.2 (dm, J = 245 Hz), 129.0, 130.8,135.3-138.3 (dm, J = 256 Hz), 142.2–145.1 (dm, J = 259 Hz), 154.1. ^{19}F NMR (376 MHz, $CDCl_3$, δ): −158 (2F), −144.7 (1F), −136 (2F).

N-(4-isopropoxy-3-vinylphenyl)-3,5-bis(trifluoromethyl)-benzenesulfonamide (**6f**): Following the procedure described for **6b** using 3,5-bis(trifluoromethyl)benzenesulfonyl chloride, **6f** was obtained as a brown solid (81 mg, 79%). ^{1}H NMR (400 MHz, $CDCl_3$, δ): 1.32 (d, J = 6.1 Hz, 6H), 4.48 (sept., J = 6.1 Hz, 1H), 5.22 (dd, J = 1.2 and 11.2 Hz, 1H), 5.57 (dd, J = 1.2 and 17.8 Hz, 1H), 6.78 (d, J = 8.84 Hz, 1H), 6.92 (m, 2H), 7.02 (s, 1H), 7.12 (d, J = 2.7 Hz, 1H), 8.03 (s, 1H), 8.14 (s, 2H). ^{13}C NMR (100 MHz, $CDCl_3$, δ): 21.9 (2C), 71.3, 114.8, 115.2, 122.4 (q, 270 Hz, 2C), 123.0, 124.9, 126.3 (q, J = 3.7 Hz, 2C), 127.2, 127.6 (2C), 129.1, 130.7, 132.7 (q, 34.0 Hz, 2C), 141.5, 154.3. ^{19}F NMR (376 MHz, $CDCl_3$, δ): −63.1.

General procedure for catalyst formation: To a solution of catalyst **7** and copper chloride (1.1 equiv) in dry DCM (1 mL for 0.02 mmol of Ru-indenylidene complex) was added a solution of **6a**–**f** (1 equiv) in DCM (1 mL for 0.05 mmol of ligand). The resulting mixture was stirred at 35 °C for 5 h. Volatiles were removed under reduced pressure, acetone was added to the residue, and the solution was filtered trough a pad of Celite. The filtrate was concentrated and purified by chromatography on silica gel (pentane/acetone, 75/25) to yield the expected complexes **4a**–**i**.

(1,3-dimesitylimidazolidin-2-ylidene)(2-isopropoxy-5-(trifluoromethylsulfonamido)benzylidene)ruthenium(II) chloride (**4a**): Following the general procedure using the ligand **6a**, complex **4a** was isolated as a green powder (62 mg, 73%). ^{1}H (400 MHz, $CDCl_3$, δ): 1.13 (d, J = 6.1 Hz, 6H, 2 CH_3), 2.34 (s, 18H, 6 CH), 4.08 (s, 4H, 2 CH_2), 4.72 (sept, J = 6.1 Hz, 1H, CH), 6.54 (d, J = 8.7 Hz, 1H, CH), 6.61 (d, J = 2.2 Hz, 1H, CH), 6.98 (s, 4H, CH), 7.08 (dd, J = 8.7 and 2.2 Hz, 1H, CH), 16.21 (s, 1H, CH). ^{19}F (376 MHz, $CDCl_3$, δ): -75.72 (s, 3F)

(1,3-dimesitylimidazolidin-2-ylidene)(2-isopropoxy-5-(4-nitrophenylsulfonamido)benzylidene)ruthenium(II) chloride (**4b**): Following the general procedure using the ligand **6b**, complex **4b** was isolated as a green powder (55 mg, 71%). ^{1}H NMR (400 MHz, $CDCl_3$, δ): 1.21 (d, J = 6.1 Hz, 6H, 2 CH_3), 2.42 (s, 18H, 6 CH), 4.19 (s, 4H, 2CH_2), 4.84 (sept, J = 6.1 Hz, 1H, CH), 6.57 (d, J = 7.3 Hz, 1H, CH), 6.71 (bs, 1H, NH), 6.95 (d, J = 7.1 Hz, 1H, CH), 7.08 (s, 4H, 4 CH), 7.33 (s, 1H, CH), 7.91 (d, J = 7.1 Hz, 2H, 2 CH), 8.27 (d, J = 7.3 Hz, 2H, 2 CH), 16.34 (s, 1H, CH).

(1,3-dimesitylimidazolidin-2-ylidene)(2-isopropoxy-5-(2-nitrophenylsulfonamido)benzylidene)ruthenium(II) chloride (**4c**): Following the general procedure using the ligand **6c**, complex **4c** was isolated as a green powder (78 mg, 74%). ^{1}H NMR (400 MHz, $CDCl_3$, δ): 1.09 (d, J = 6.1 Hz, 6H, 2 CH_3), 2.30 (s, 18H, 6 CH_3), 4.07 (s, 4H, 2 CH_2), 4.71 (sept., J = 6.1 Hz, 1H, CH), 6.64 (d, J = 8.8 Hz, 1H, CH), 6.66 (d, J = 2.6 Hz, 1H, CH), 6.95 (s, 4H, 4 CH), 7.15 (s, 1H, CH), 7.33 (dd, J = 8.8 and 2.6 Hz, 1H, CH), 7.51 (dt, J = 7.7 and 1.2 Hz, 1H, CH), 7.64 (dt, J = 7.8 and 1.4 Hz, 1H, CH), 7.70 (dd, J = 7.8 and 1.3 Hz, 1H, CH), 7.79 (dd, J = 8.0 and 1.1 Hz, 1H, CH), 16.14 (s, 1H, CH).

(1,3-dimesitylimidazolidin-2-ylidene)(5-(2,4-dinitrophenylsulfonamido)-2-isopropoxybenzylidene)ruthenium(II) chloride (**4d**): Following the general procedure using the ligand **6d**, complex **4d** was isolated as a green powder (55 mg, 65%). ^{1}H NMR (400 MHz, $CDCl_3$, δ): 1.09 (d, J = 6.1 Hz, 6H, 2 CH_3), 2.31 (s, 18H, 6 CH_3), 4.07 (s, 4H, 2 CH_2), 4.70 (sept., J = 6.1 Hz, 1H, CH), 6.64 (d, J = 8.7 Hz, 1H, CH), 6.73 (d, J = 2.4 Hz, 1H, CH), 6.96 (s, 4H, 4 CH), 7.33 (dd, J = 8.6 and 2.4 Hz, 1H, CH), 7.98 (d, J = 8.6 Hz, 1H, CH), 8.28 (dd, J = 8.6 and 2.2 Hz, 1H, CH), 8.56 (d, J = 2.2 Hz, 1H, CH), 16.17 (s, 1H, CH).

(1,3-dimesitylimidazolidin-2-ylidene)(2-isopropoxy-5-(perfluorophenylsulfonamido)benzylidene)ruthenium(II) chloride (**4e**): Following the general procedure using the ligand **6e**, complex **4e** was isolated as a green powder (69 mg, 78%). ^{1}H NMR (400 MHz, $CDCl_3$, δ): 1.09 (d, J = 6.1 Hz, 6H, 2 CH_3), 2.33 (s, 18H, 6 CH_3), 4.08 (s, 4H, 2 CH_2), 4.72 (sept., J = 6.1 Hz, 1H, CH), 6.61 (d, J = 8.8 Hz, 1H, CH), 6.67 (d, J = 2.5 Hz, 1H, CH), 6.98 (s, 4H, 4 CH), 7.24 (dd, J = 8.8 and 2.5 Hz, 1H, CH), 16.20 (s, 1H, CH). ^{19}F NMR (376 MHz, $CDCl_3$, δ): −159.1 (2F), −145.6 (1F), −137.2 (2F).

(5-(3,5-bis(trifluoromethyl)phenylsulfonamido)-2-isopropoxybenzylidene)(1,3-dimesitylimidazolidin-2-ylidene)ruthenium(II) chloride (**4f**): Following the general procedure using the ligand **6f**, complex **4f** was isolated as a green powder (96 mg, 87%). ^{1}H NMR (400 MHz, $CDCl_3$, δ): 1.08 (d, *J* = 6.1 Hz, 6H, 2 CH_3), 2.31 (s, 18H, 6 CH_3), 4.06 (s, 4H, 2 CH_2), 4.69 (sept., *J* = 6.1 Hz, 1H, CH), 6.48 (d, *J* = 2.6 Hz, 1H, CH), 6.61 (d, *J* = 8.7 Hz, 2H, CH), 6.95 (s, 4H, 4 CH), 7.26 (dd, *J* = 8.7 and 2.6 Hz, 1H, CH), 7.47 (t, *J* = 7.8 Hz, 1H, CH), 7.60 (t, *J* = 7.7 Hz, 1H, CH), 7.82 (dd, *J* = 13.2 and 7.8 Hz, 2H, 2 CH), 16.13 (s, 1H, CH). ^{19}F NMR (376 MHz, $CDCl_3$, δ): −58.1 (3F).

(1,3-bis(2,6-diisopropylphenyl)imidazolidin-2-ylidene)(2-isopropoxy-5-(4-nitrophenylsulfonamido)benzylidene)ruthenium(II) chloride (**4g**): Following the general procedure using the ligand **6g**, complex **4g** was isolated as a green powder (88 mg, 65%). ^{1}H NMR (400 MHz, $CDCl_3$, δ): 1.11 (bd, *J* = 5.3 Hz, 12H, 4 CH_3), 1.17 (d, *J* = 6.9 Hz, 12H, 4 CH_3), 1.19 (d, *J* = 6.1 Hz, 6H, 2 CH_3), 3.45 (sept., *J* = 6.7 Hz, 4H, CH), 4.11 (s, 4H, CH_2), 4.78 (sept., *J* = 6.1 Hz, 1H, CH), 6.27 (d, *J* = 8.6 Hz, 1H, CH), 6.50 (m, 2H, 2 CH), 7.15 (bs, 1H, NH), 7.29 (d, *J* = 7.8 Hz,4H, CH), 7.46 (m, 2H, CH), 7.73 (m, 2H, 2 CH), 8.13 (m, 2H, 2 CH), 16.16 (s, 1H, CH).

General Procedure for the kinetic reaction: A NMR tube equipped with a septum was filled with diethylallylmethallyl malonate (**8**) (25 mg, 0.1 mmol) and CD_2Cl_2 (900 µL) under an argon atmosphere. The sample was equilibrated at 30 °C in the NMR probe. The sample was locked and shimmed before the catalyst addition (100 µL, 1 µmol, 0.01 M solution of catalyst). The reaction progress was monitored by the periodical acquisition of data over 1 h and the conversions were calculated from the integration of allylic protons signals of substrates and products.

General Procedure for Cross-Metathesis Reactions: A Schlenk tube under an argon atmosphere was filled with the activated substrate (0.1 mmol), the unactivated substrate (0.2 mmol, 2 equiv) and CH_2Cl_2 (1 mL). Then, the precatalyst solution (0.01 M, 100 µL, 1 µmol) was added. After the required time, the solvent was removed. The conversion was determined by ^{1}H NMR.

General Procedure for RCM Reactions: A Schlenk tube under an argon atmosphere was filled with the olefin substrate (0.1 mmol) and CH_2Cl_2 (1 mL). Then, the precatalyst (1 µmol) was added. After the required time, the solvent was removed. The conversion was determined by ^{1}H NMR.

Supporting Information

Supporting Information File 1

The Supporting Information contains the ^{1}H NMR spectrum of **P8**, the calculation of the substrate/dimer ratio (Table 2, entry 1) and the calculation of product/substrate/dimer ratio (Table 2, entry 14).
[http://www.beilstein-journals.org/bjoc/content/supplementary/1860-5397-6-132-S1.pdf]

Acknowledgements

We thank the European Community for its financial support (CP-FP 211468-2 EUMET). Financial support by the CNRS, the ENSCR, the region-Bretagne (Feder Program) and OSEO are also gratefully acknowledged.

References

1. Schwab, P.; France, M. B.; Ziller, J. W.; Grubbs, R. H. *Angew. Chem., Int. Ed. Engl.* **1995,** *34,* 2039–2041. doi:10.1002/anie.199520391
2. Bourcet, E.; Virollaud, M.-A.; Fache, F.; Piva, O. *Tetrahedron Lett.* **2008,** *49,* 6816–6818. doi:10.1016/j.tetlet.2008.09.077
3. Nicolaou, K. C.; Bulger, P. G.; Sarlah, D. *Angew. Chem., Int. Ed.* **2005,** *44,* 4490–4527. doi:10.1002/anie.200500369
4. Compain, P. *Adv. Synth. Catal.* **2007,** *349,* 1829–1846. doi:10.1002/adsc.200700161
5. Scholl, M.; Ding, S.; Lee, C. W.; Grubbs, R. H. *Org. Lett.* **1999,** *1,* 953–956. doi:10.1021/ol990909q
6. Huang, J.; Stevens, E. D.; Nolan, S. P.; Petersen, J. L. *J. Am. Chem. Soc.* **1999,** *121,* 2674–2678. doi:10.1021/ja9831352
7. Mohapatra, D. K.; Somaiah, R.; Rao, M. M.; Caijo, F.; Mauduit, M.; Yadav, J. S. *Synlett* **2010,** 1223–1226. doi:10.1055/s-0029-1219807
8. Garber, S. B.; Kingsbury, J. S.; Gray, B. L.; Hoveyda, A. H. *J. Am. Chem. Soc.* **2000,** *122,* 8168–8179. doi:10.1021/ja001179g
9. Wakamatsu, H.; Blechert, S. *Angew. Chem., Int. Ed.* **2002,** *41,* 794–796. doi:10.1002/1521-3773(20020301)41:5<794::AID-ANIE794>3.0.CO;2-B
10. Wakamatsu, H.; Blechert, S. *Angew. Chem., Int. Ed.* **2002,** *41,* 2403–2405. doi:10.1002/1521-3773(20020703)41:13<2403::AID-ANIE2403>3.0.CO;2-F
11. Grela, K.; Harutyunyan, S.; Michrowska, A. *Angew. Chem., Int. Ed.* **2002,** *41,* 4038–4040. doi:10.1002/1521-3773(20021104)41:21<4038::AID-ANIE4038>3.0.CO;2-0
12. Michrowska, A.; Bujok, R.; Harutyunyan, S.; Sashuk, V.; Dolgonos, G.; Grela, K. *J. Am. Chem. Soc.* **2004,** *126,* 9318–9325. doi:10.1021/ja048794v
13. Zhan, Z.-Y. J. WO Patent 2007003135, 2007.
14. Clavier, H.; Grela, K.; Kirschning, A.; Mauduit, M.; Nolan, S. P. *Angew. Chem., Int. Ed.* **2007,** *46,* 6786–6801. doi:10.1002/anie.200605099
15. Galan, B. R.; Kalbarczyk, K. P.; Szczepankiewicz, S.; Keister, J. B.; Diver, S. T. *Org. Lett.* **2007,** *9,* 1203–1206. doi:10.1021/ol0631399

16. Mauduit, M.; Laurent, I.; Clavier, H. WO Patent 2008065187, 2008.
17. Rix, D.; Caijo, F.; Laurent, I.; Boeda, F.; Clavier, H.; Nolan, S. P.; Mauduit, M. *J. Org. Chem.* **2008,** *73,* 4225–4228. doi:10.1021/jo800203d
18. Clavier, H.; Caijo, F.; Borré, E.; Rix, D.; Boeda, F.; Nolan, S. P.; Mauduit, M. *Eur. J. Org. Chem.* **2009,** 4254–4265. doi:10.1002/ejoc.200900407
19. Rix, D.; Clavier, H.; Coutard, Y.; Gulajski, L.; Grela, K.; Mauduit, M. *J. Organomet. Chem.* **2006,** *691,* 5397–5405. doi:10.1016/j.jorganchem.2006.07.042
20. Rix, D.; Caïjo, F.; Laurent, I.; Gulajski, L.; Grela, K.; Mauduit, M. *Chem. Commun.* **2007,** 3771–3773. doi:10.1039/b705451c
21. Jafarpour, L.; Schanz, H.-J.; Stevens, E. D.; Nolan, S. P. *Organometallics* **1999,** *18,* 5416–5419. doi:10.1021/om990587u
22. Clavier, H.; Urbina-Blanco, C. A.; Nolan, S. P. *Organometallics* **2009,** *28,* 2848–2854. doi:10.1021/om900071t
23. Bruneau, C.; Fischmeister, C.; Miao, X.; Malacea, R.; Dixneuf, P. H. *Eur. J. Lipid Sci. Technol.* **2010,** *112,* 3–9. doi:10.1002/ejlt.200900105

License and Terms

Beilstein Journal of Organic Chemistry

Tandem catalysis of ring-closing metathesis/ atom transfer radical reactions with homobimetallic ruthenium–arene complexes

Yannick Borguet[1], Xavier Sauvage[1], Guillermo Zaragoza[2], Albert Demonceau[1] and Lionel Delaude[*1]

Full Research Paper

Open Access

Address:
[1]Laboratory of Macromolecular Chemistry and Organic Catalysis, Institut de Chimie (B6a), Université de Liège, Sart-Tilman par 4000 Liège, Belgium and [2]Unidade de Raios X, Edificio CACTUS, Universidade de Santiago de Compostela, Campus Vida, 15782 Santiago de Compostela, Spain

Email:
Lionel Delaude[*] - l.delaude@ulg.ac.be

* Corresponding author

Keywords:
Grubbs catalyst; indenylidene ligands; Kharasch reaction; microwave heating; olefin metathesis

Beilstein J. Org. Chem. **2010,** *6,* 1167–1173.
doi:10.3762/bjoc.6.133

Received: 23 September 2010
Accepted: 09 November 2010
Published: 08 December 2010

Guest Editor: K. Grela

Abstract

The tandem catalysis of ring-closing metathesis/atom transfer radical reactions was investigated with the homobimetallic ruthenium–indenylidene complex [(*p*-cymene)Ru(μ-Cl)$_3$RuCl(3-phenyl-1-indenylidene)(PCy$_3$)] (**1**) to generate active species in situ. The two catalytic processes were first carried out independently in a case study before the whole sequence was optimized and applied to the synthesis of several polyhalogenated bicyclic γ-lactams and lactones from α,ω-diene substrates bearing trihaloacetamide or trichloroacetate functionalities. The individual steps were carefully monitored by ^{1}H and ^{31}P NMR spectroscopies in order to understand the intimate details of the catalytic cycles. Polyhalogenated substrates and the ethylene released upon metathesis induced the clean transformation of catalyst precursor **1** into the Ru(II)–Ru(III) mixed-valence compound [(*p*-cymene)Ru(μ-Cl)$_3$RuCl$_2$(PCy$_3$)], which was found to be an efficient promoter for atom transfer radical reactions under the adopted experimental conditions.

Introduction

During the course of our investigations on homobimetallic ruthenium–arene complexes, we found that the indenylidene compound [(*p*-cymene)Ru(μ-Cl)$_3$RuCl(3-phenyl-1-indenylidene)(PCy$_3$)] (**1**) was a very efficient promoter for the ring-closing metathesis (RCM) of diethyl 2,2-diallylmalonate [1]. Contrastingly, this catalyst precursor was almost inactive in the self-metathesis of styrene, as stilbene formation leveled off after a few minutes without going past the 10% threshold. We attributed this negative result to a rapid degradation of the active species via a bimolecular pathway leading to the ethylene com-

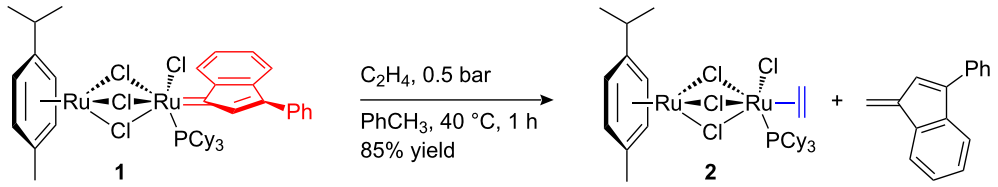

Scheme 1: Reaction of homobimetallic ruthenium–indenylidene complex **1** with ethylene.

plex [(*p*-cymene)Ru(μ-Cl)$_3$RuCl(η^2-C_2H_4)(PCy_3)] (**2**). Support in favor of this hypothesis came from the observation that complex **1** reacted quantitatively with ethylene at 40 °C to afford product **2** [1], which is completely devoid of metathetical activity (Scheme 1) [2]. Moreover, early work from Grubbs and co-workers had shown that bimetallic ruthenium–methylidene or ethylidene complexes decomposed rapidly to afford an unidentified ruthenium–ethylene species [3]. We were able to isolate and characterize this product, which turned out to be complex **2** [1]. The synthesis of this compound was first reported in 2005 by Severin et al. who successfully used it as a catalyst for atom transfer radical addition (ATRA) and cyclization (ATRC) reactions [4,5]. In 2007, we further extended its application field to the related process of atom transfer radical polymerization (ATRP) [2].

Because the transformation of complex **1** into compound **2** occurs seamlessly in the presence of ethylene, which is a byproduct of many metathesis reactions, we reasoned that it could serve to trigger a change in mechanism, thereby allowing us to perform two consecutive catalytic cycles in a single procedure (Scheme 2). This process, known as assisted tandem catalysis [6], presents significant advantages over multistep synthesis for increasing molecular complexity, particularly in terms of time- and cost-savings, atom economy, environmental friendliness, or applicability to diversity-oriented high-throughput synthesis [7-10]. The monometallic ruthenium–benzylidene complex [$RuCl_2$(=CHPh)(PCy_3)$_2$] (**3**) and its second- or even third-generation analogues developed by Grubbs and co-workers are prominent examples of catalyst precursors that were applied to olefin metathesis in tandem with ATRA [11], ATRC [11-14], ATRP [15-18], cyclopropanation [19], dihydroxylation [20], hydrogenation [21-23], hydrovinylation [24], isomerization [25-28], oxidation [29], or Wittig reactions [30], to name just a few [31].

In this contribution, we investigate the tandem catalysis of RCM/ATRC reactions with homobimetallic ruthenium–indenylidene complex **1** to generate active species in situ. The two catalytic processes were first carried out independently in a case study before the whole sequence was optimized and applied to the synthesis of several polyhalogenated bicyclic γ-lactams and lactones.

Results and Discussion

2,2,2-Trichloro-*N*-(octa-1,7-dien-3-yl)acetamide (**4**) was chosen as a model substrate to begin our investigations (Scheme 3). The RCM of this functionalized α,ω-diene was carried out in toluene-d_8 (0.2 M) at 30 °C in the presence of 5 mol % of catalyst precursor **1** and monitored by ^{1}H NMR spectroscopy. Under these conditions, ring closure took place readily and a full conversion of the substrate into its cyclohexene derivative **5** was achieved within 20 minutes. At this temperature, the second step of ATRC did not occur. Previous work had shown that a significant thermal activation was required to perform the radical cyclization of this cyclohexenyl trichloroacetamide, presumably due to the unfavorable disposition of the trichloromethyl unit and the endocyclic double bond in the most stable rotamer of the amido group [11]. Hence, this preliminary experiment allowed us to determine the nature of the catalytic

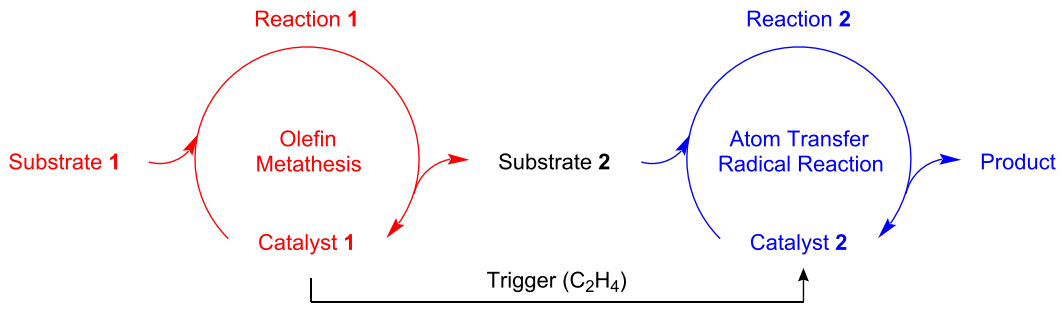

Scheme 2: Schematic illustration of tandem assisted catalysis with complexes **1** and **2**.

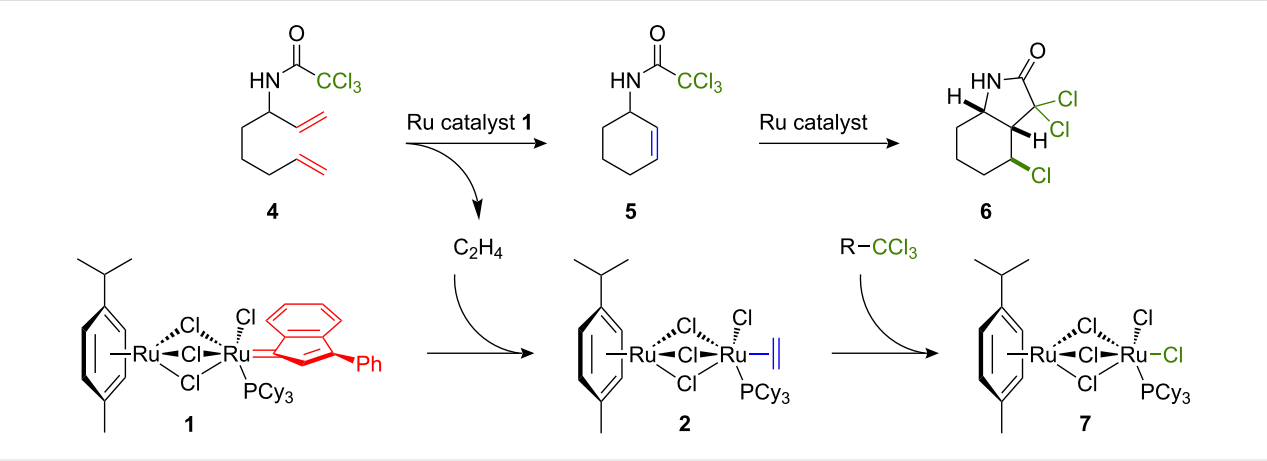

Scheme 3: Tandem RCM/ATRC of 2,2,2-trichloro-*N*-(octa-1,7-dien-3-yl)acetamide (**4**) catalyzed by complex **1**.

species present in the reaction mixture after the metathesis step. No meaningful information could be obtained by ^{31}P NMR spectroscopy even when acquisition was prolonged overnight to compensate for the low catalyst concentration in the sample. Visual inspection of the NMR tube revealed, however, the formation of a phosphorus-containing precipitate. Suitable crystals for X-ray diffraction analysis were obtained by repeating the RCM experiment on a larger scale in toluene at room temperature. Their structure was solved and assigned to the paramagnetic complex [(*p*-cymene)Ru(μ-Cl)$_3$RuCl$_2$(PCy$_3$)] (**7**). This mixed valence Ru(II)–Ru(III) compound had already been isolated and fully characterized by Severin and co-workers when they investigated the reaction of ethylene complex **2** with carbon tetrachloride in toluene [4]. Yet, differences between the molecular structures obtained by the Swiss team and our group indicate that complex **7** can adopt various crystalline structures (see Supporting Information File 2 for more details on crystal structures and Supporting Information File 3 for X-ray crystal data).

The clean transformation of catalyst precursor **1** into compound **7** induced by polyhalogenated substrates is in line with the general mechanism postulated for ruthenium-catalyzed atom transfer radical reactions, as it involves a reversible oxidation of the metal center [32,33]. Under the experimental conditions adopted for our study, conversion of indenylidene precursor **1** into labile ethylene complex **2** probably occurred rapidly upon release of ethylene in the reaction mixture by the RCM of substrate **4** (Scheme 3). The low concentration of compound **2** in solution prevented, however, its instantaneous detection by NMR spectroscopy. When a longer acquisition time was applied, only oxidized product **7** was obtained. It should be noted that when the Grubbs first-generation catalyst **3** was allowed to react with substrate **4** for 2 h in toluene-d_8 at room temperature, the RCM product **5** was also formed quantitatively. In this case, however, ^{31}P NMR analysis of the reaction mixture revealed the presence of at least five different ruthenium–phosphine species in solution. Unless all these species are able to promote the ATRC reaction, the catalytic switch required to complete the tandem process should therefore be far less efficient with monometallic benzylidene complex **3** than with bimetallic indenylidene precursor **1**.

Next, we investigated separately the ATRC of 2,2,2-trichloro-*N*-(cyclohex-2-en-1-yl)acetamide (**5**) with different catalyst precursors. The starting material employed in these experiments was prepared by trichloroacetylation of 2-cyclohexenol with CCl$_3$COCl in the presence of Et$_3$N [34]. This procedure guaranteed the absence of any residual metal catalyst coming from the RCM reaction. A solution of 2-cyclohexenyl trichloroacetamide **5** in toluene was heated for 2 h at 160 °C in the presence of various ruthenium initiators (1 mol %). Conversion into racemic product **6** was then determined by GC analysis of the reaction mixture (Scheme 3 and Table 1). Previous work from the group of Itoh et al. had already established that the ruthenium-catalyzed cyclization of *N*-allyl trichloroacetamides proceeded diastereoselectively, and a mechanism accounting for

Table 1: ATRC of 2,2,2-trichloro-*N*-(cyclohex-2-en-1-yl)acetamide (**5**) catalyzed by various ruthenium complexes.[a]

Entry	Ru cat.	Conversion (%)[b]
1	–	0
2	**1**	94
3	**2**	98
4	**3**	55
5	**7**	97

[a]Experimental conditions: substrate (0.2 mmol), catalyst (2 μmol), toluene (1 mL) in a sealed tube under Ar for 2 h at 160 °C.
[b]Determined by GC with *n*-dodecane as internal standard.

the formation of a *cis*-fused bicyclic system was proposed [35]. Nuclear Overhauser effects also indicated that the angular H-3a and the CHCl H-4 protons were *trans* to each other.

Because radical reactions may occur spontaneously at high temperature, we first carried out a blank test in the absence of an initiator (Table 1, entry 1). This experiment confirmed the necessity of mediating the transformation of **5** into **6** with a transition metal complex. Unlike the Grubbs benzylidene catalyst **3**, bimetallic compound **1** was an efficient catalyst precursor for this reaction (Table 1, entries 2 and 4). Opstal and Verpoort had already established that monometallic ruthenium–indenylidene complexes were able to promote the ATRA and ATRP of vinyl monomers [36,37]. In a tandem RCM/ATRC process, it is, however, very unlikely for the indenylidene species to remain unaltered in solution after the metathesis step. Indeed, during the course of our investigations on the RCM of various α,ω-dienes catalyzed by complex **1**, ^{31}P NMR monitoring of the reaction media always showed a rapid disappearance of the signal originating from this precatalyst, and its replacement by a new singlet at ca. 40.5 ppm due to the ethylene complex **2**. As expected, this compound was highly suitable for catalyzing the ATRC of **5** (Table 1, entry 3). To our great satisfaction, oxidation product **7** was equally active under the experimental conditions adopted for this cyclization and did not require any co-catalyst (Table 1, entry 5). This result contrasts with previous observations from Severin and co-workers, who found that the presence of a radical initiator or a reducing agent (typically Mg) was mandatory to activate complex **7** for ATRA and ATRC reactions at room temperature [5]. At 160 °C, a reduction of the mixed Ru(II)–Ru(III) compound probably takes place under the sole influence of radicals generated via thermal dissociation of the substrate.

In order to complete the full sequence of RCM and ATRC reactions, we carried out a third series of catalytic tests based on literature procedures developed for this type of tandem catalysis [11,13,14]. These experiments were conducted on a preparative microscale in sealed tubes under inert atmosphere. Substrate **4** and complex **1** were dissolved in toluene. A color change from red to orange occurred within a few minutes, which indicated the formation of metathetically active species. Stirring was prolonged for 2 h at 25 °C. The vessel was then heated in an oil bath to trigger the ruthenium-catalyzed cyclization of intermediate **5** into 3,3,4-trichlorohexahydro-1*H*-indol-2(3*H*)-one (**6**) (Scheme 3). This final product was isolated by column chromatography. Its identity and purity were confirmed by ^{1}H and ^{13}C NMR analyses. Table 2 summarizes the results of these experiments.

When a 5 mol % catalyst loading was employed and the ATRC reaction was allowed to proceed for 2 h at 160 °C, bicyclic lactam **6** was isolated in 71% yield (Table 2, entry 1). We were pleased to note that homobimetallic complex **1** slightly outperformed the Grubbs first-generation catalyst **3**, which led to a 61% yield under identical conditions (Table 2, entry 2). We tried to further optimize the catalytic process by reducing the reaction temperature and the catalyst loading. Performing the second step at 110 °C completely inhibited the cyclization as evidenced by GC analysis, which revealed a complete conversion of substrate **4** into intermediate **5**, but did not show any sign of product **6** formation (Table 2, entry 3). On the other hand, it was possible to accomplish the dual catalysis at 160 °C with only 1 mol % of catalyst precursor **1** (Table 2, entry 4). The slight increase in isolated yield compared to run #1 should not be over interpreted. It probably reflects the systematic errors in the weighing of the reagents and in the chromatographic purification of the product formed. A control experiment carried out with $[RuCl_2(=CHPh)(PCy_3)_2]$ **3** confirmed the superiority of the bimetallic system under these conditions (Table 2, entry 5). Attempts to further decrease the molar ratio of complex **1** remained unsuccessful (see Table 2, entry 6 for a representative example). Finally, we were able to significantly shorten and simplify the whole process through the use of a monomodal

Table 2: Tandem RCM/ATRC of 2,2,2-trichloro-*N*-(octa-1,7-dien-3-yl)acetamide (**4**).

Entry	Catalyst precursor	Exp. conditions for RCM	Exp. conditions for ATRC[a]	Isolated yield of product 6 (%)
1	**1** (5 mol %)	25 °C, 2 h	Δ, 160 °C, 2 h	71
2	**3** (5 mol %)	25 °C, 2 h	Δ, 160 °C, 2 h	61
3	**1** (5 mol %)	40 °C, 2 h	Δ, 110 °C, 2 h	0[b]
4	**1** (1 mol %)	25 °C, 30 min	Δ, 160 °C, 2 h	76
5	**3** (1 mol %)	25 °C, 2 h	Δ, 160 °C, 2 h	20
6	**1** (0.5 mol %)	–	Δ, 160 °C, 2 h	0[b]
7	**1** (1 mol %)	–	μw, 160 °C, 40 min	73

[a]Δ: conductive heating in an oil bath, μw: microwave heating in a monomodal reactor.
[b]Only RCM product **5** was present.

microwave reactor (Table 2, entry 7). Such a device is becoming increasingly popular in organic synthesis and has already been used as a convenient heating source for numerous ruthenium-catalyzed reactions [38].

Because thermal degradation of the catalyst is likely to occur at the high temperature required to promote the ATRC of 2-cyclohexenyl trichloroacetamide **5**, we searched for alternative substrates that would allow us to perform the tandem reaction under less drastic conditions. We were guided in this endeavor by Snapper et al. who had shown that adding a benzyl or tosyl group to the amide functionality of compound **5** facilitated its radical cyclization mediated by complex **3**. Replacing the trichloroacetamide moiety with the corresponding tribromoacetamide unit was also found to enhance the Kharasch reactivity [11]. Thus, we synthesized four additional *N*-protected octadienyl trichloro- or tribromoacetamide substrates and we followed their transformation under the influence of bimetallic catalyst precursor **1** (see Supporting Information File 1 for details). As expected, *N*-benzyl trichloroacetamide **8** underwent the RCM/ATRC sequence at a lower temperature than its parent **4** (110 °C vs 160 °C), although the reaction time had to be extended in order to achieve a full conversion into bicyclic lactam **9** (Table 3, entry 1). The reaction of *N*-tosyl trichloroacetamide **10** proceeded faster, but followed a different course, as demonstrated by the isolation of a diastereomeric mixture of unsaturated bicyclic lactams **11** (Table 3, entry 2). The two products were separated by column chromatography. 2D NMR spectroscopy and mass spectrometry analyses confirmed that dehydrochlorination had occurred during the catalytic process. Further work is underway to rationalize this change of reaction path and to address all its stereochemical implications.

With the *N*-benzyl tribromoacetamide **12**, the RCM step proceeded swiftly at 25 °C, but ATRC did not occur at this temperature, in sharp contrast with previous results obtained by

Table 3: Reactions of various octadienyl trichloro- or tribromoacetamide substrates catalyzed by complex **1**.[a]

Entry	Substrate	Product(s)	Conditions	Isolated yield (%)
1	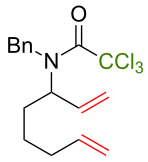 **8**	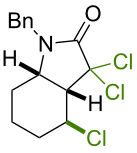 **9**	μw, 110 °C, 4 h	89%
2	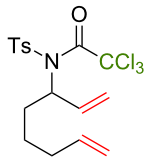 **10**	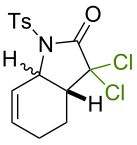 **11**	μw, 110 °C, 2 h	73%[b]
3	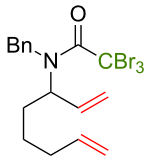 **12**	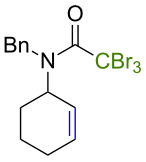 **13**	25 °C, 2.5 h	89%
4	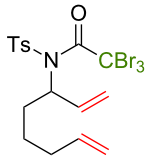 **14**	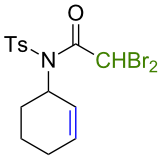 **15**	25 °C, 2.5 h	96%

[a]Experimental conditions: substrate (0.3 mmol), catalyst (3 μmol), and toluene (1.5 mL) stirred in a pressure vessel under Ar in a monomodal microwave reactor (μw, 110 °C) or in a thermostated oil bath (25 °C).
[b]Diastereomeric ratio: 44:56.

Snapper et al. with catalyst precursor **3** [11]. Work-up afforded only cyclohexenyl tribromoacetamide **13** in high yield (Table 3, entry 3). Attempts to promote the cyclization of this compound at higher temperatures led to a complex mixture of uncharacterized products. A final experiment carried out with the *N*-tosyl tribromoacetamide **14** afforded quantitatively the cyclohexenyl dibromoacetamide **15** (Table 3, entry 4). We suspected that the high Kharasch reactivity of the starting material or the intermediate RCM product caused a radical transfer to the solvent. However, performing the reaction in benzene or dichloromethane instead of toluene led to similar outcomes. Adding a larger amount of complex **1** (5 mol %) to substrates **12** and **14** did not seem to improve the ATRC step.

To complement the data acquired with trihaloacetamide starting materials, we also investigated the transformation of hepta-1,6-dien-3-yl 2,2,2-trichloroacetate **16** in the presence of ruthenium–indenylidene catalyst precursor **1** (5 mol %). A preliminary experiment was carried out in toluene-d_8 and monitored by ^{1}H NMR spectroscopy. The RCM of the α,ω-diene occurred readily at 25 °C and a quantitative conversion into cyclopentene derivative **17** was achieved within 1 h (Scheme 4). The temperature was then raised to 60 °C in an attempt to initiate an ATRC reaction. Under these conditions, ^{1}H NMR analysis unambiguously revealed the formation of cyclopentadiene instead of the expected bicyclic lactone. The decomposition of cyclopentenyl trichloroacetate **17** into cyclopentadiene and trichloroacetic acid was already observed by Quayle et al. under similar conditions [13,14]. These authors successfully trapped the diene via a Diels–Alder reaction with maleic anhydride. They also reported that a heterobimetallic catalytic system derived from the Grubbs second-generation complex [$RuCl_2$(=CHPh)(SIMes)(PCy_3)], CuCl, and dHbipy (SIMes is 1,3-dimesitylimidazolin-2-ylidene, dHbipy is 4,4'-di-*n*-heptyl-2,2'-bipyridine) was able to promote the ATRA of trichloroacetic acid onto cyclopentadiene followed by a lactonization into 3,3-dichloro-3,3a,4,6a-tetrahydro-2*H*-cyclopenta[*b*]furan-2-one (**18**). These results prompted us to examine the cascade RCM/decomposition/ATRA/lactonization of substrate **16** into dichloro compound **18** with homobimetallic complex **1** under mild thermolysis conditions. Thus, the substrate and the catalyst precursor (5 mol %) were dissolved in toluene and heated for 1 h at 80 °C under microwave irradiation. Under these conditions, product **18** was isolated in 52% yield after chromatographic purification. ^{1}H NMR data matched those reported for a sample known to possess a *cis* stereochemistry for its bridgehead hydrogens [39].

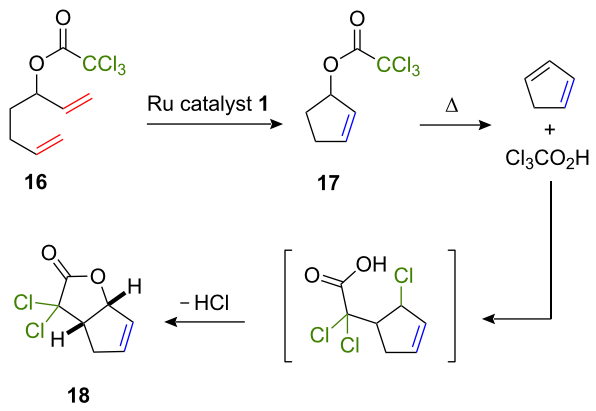

Scheme 4: Ruthenium catalyzed transformation of substrate **16**.

Conclusion

In this study, we have demonstrated that homobimetallic ruthenium–indenylidene complex **1** is a suitable catalyst precursor for the tandem RCM/ATRC of polyhalogenated α,ω-dienes **4** and **8** into the corresponding bicyclic γ-lactam derivatives. A more complex cascade sequence involving RCM and ATRA reactions afforded γ-lactone **18** starting from acyclic unsaturated ester **16**. The individual steps were carefully monitored by ^{1}H and ^{31}P NMR spectroscopies in order to understand the intimate details of the catalytic cycles. The RCM of model substrate **4** into cyclohexenyl trichloroacetamide **5** was accompanied by a clean transformation of complex **1** into mixed-valence bimetallic scaffold **7**. This well-defined compound was an efficient promoter for the ATRC of intermediate **5** into the final product **6**.

Supporting Information

Full experimental procedures and spectral data for the new compounds, detailed crystallographic analysis of [(*p*-cymene)Ru(μ-Cl)$_3$$RuCl_2$($PCy_3$)] (**7**), and a cif file with crystallographic data for complex **7**.

Supporting Information File 1

Experimental procedures and spectral data.
[http://www.beilstein-journals.org/bjoc/content/supplementary/1860-5397-6-133-S1.pdf]

Supporting Information File 2

Detailed crystallographic analysis of complex **7**.
[http://www.beilstein-journals.org/bjoc/content/supplementary/1860-5397-6-133-S2.pdf]

Supporting Information File 3

X-ray crystal data for complex **7**.
[http://www.beilstein-journals.org/bjoc/content/supplementary/1860-5397-6-133-S3.cif]

References

1. Sauvage, X.; Borguet, Y.; Zaragoza, G.; Demonceau, A.; Delaude, L. *Adv. Synth. Catal.* **2009,** *351,* 441–455. doi:10.1002/adsc.200800664
2. Sauvage, X.; Borguet, Y.; Noels, A. F.; Delaude, L.; Demonceau, A. *Adv. Synth. Catal.* **2007,** *349,* 255–265. doi:10.1002/adsc.200600515
3. Dias, E. L.; Grubbs, R. H. *Organometallics* **1998,** *17,* 2758–2767. doi:10.1021/om9708788
4. Quebatte, L.; Solari, E.; Scopelliti, R.; Severin, K. *Organometallics* **2005,** *24,* 1404–1406. doi:10.1021/om050027x
5. Wolf, J.; Thommes, K.; Briel, O.; Scopelliti, R.; Severin, K. *Organometallics* **2008,** *27,* 4464–4474. doi:10.1021/om8004096
6. Fogg, D. E.; dos Santos, E. N. *Coord. Chem. Rev.* **2004,** *248,* 2365–2379. doi:10.1016/j.ccr.2004.05.012
7. Ajamian, A.; Gleason, J. L. *Angew. Chem., Int. Ed.* **2004,** *43,* 3754–3760. doi:10.1002/anie.200301727
8. Lee, J. M.; Na, Y.; Han, H.; Chang, S. *Chem. Soc. Rev.* **2004,** *33,* 302–312. doi:10.1039/b309033g
9. Wasilke, J.-C.; Obrey, S. J.; Baker, R. T.; Bazan, G. C. *Chem. Rev.* **2005,** *105,* 1001–1020. doi:10.1021/cr020018n
10. Shindoh, N.; Takemoto, Y.; Takasu, K. *Chem.–Eur. J.* **2009,** *15,* 12168–12179. doi:10.1002/chem.200901486
11. Seigal, B. A.; Fajardo, C.; Snapper, M. L. *J. Am. Chem. Soc.* **2005,** *127,* 16329–16332. doi:10.1021/ja055806j
12. Schmidt, B.; Pohler, M. *J. Organomet. Chem.* **2005,** *690,* 5552–5555. doi:10.1016/j.jorganchem.2005.06.042
13. Edlin, C. D.; Faulkner, J.; Quayle, P. *Tetrahedron Lett.* **2006,** *47,* 1145–1151. doi:10.1016/j.tetlet.2005.12.018
14. Edlin, C. D.; Faulkner, J.; Fengas, D.; Helliwell, M.; Knight, C. K.; House, D.; Parker, J.; Preece, I.; Quayle, P.; Raftery, J.; Richards, S. N. *J. Organomet. Chem.* **2006,** *691,* 5375–5382. doi:10.1016/j.jorganchem.2006.08.017
15. Bielawski, C. W.; Louie, J.; Grubbs, R. H. *J. Am. Chem. Soc.* **2000,** *122,* 12872–12873. doi:10.1021/ja001698j
16. Charvet, R.; Novak, B. M. *Macromolecules* **2004,** *37,* 8808–8811. doi:10.1021/ma049244k
17. Cheng, C.; Khoshdel, E.; Wooley, K. L. *Nano Lett.* **2006,** *6,* 1741–1746. doi:10.1021/nl0611900
18. Airaud, C.; Héroguez, V.; Gnagnou, Y. *Macromolecules* **2008,** *41,* 3015–3022. doi:10.1021/ma702682s
19. Kim, B. G.; Snapper, M. L. *J. Am. Chem. Soc.* **2006,** *128,* 52–53. doi:10.1021/ja055993l
20. Beligny, S.; Eibauer, S.; Maechling, S.; Blechert, S. *Angew. Chem., Int. Ed.* **2006,** *45,* 1900–1903. doi:10.1002/anie.200503552
21. Drouin, S. D.; Zamanian, F.; Fogg, D. E. *Organometallics* **2001,** *20,* 5495–5497. doi:10.1021/om010747d
22. Fogg, D. E.; Amoroso, D.; Drouin, S. D.; Snelgrove, J.; Conrad, J.; Zamanian, F. *J. Mol. Catal. A: Chem.* **2002,** *190,* 177–184. doi:10.1016/S1381-1169(02)00242-X
23. Schmidt, B.; Pohler, M. *Org. Biomol. Chem.* **2003,** *1,* 2512–2517. doi:10.1039/b303441k
24. Gavenonis, J.; Arroyo, R. V.; Snapper, M. L. *Chem. Commun.* **2010,** *46,* 5692–5694. doi:10.1039/c0cc00008f
25. Sutton, A. E.; Seigal, B. A.; Finnegan, D. F.; Snapper, M. L. *J. Am. Chem. Soc.* **2002,** *124,* 13390–13391. doi:10.1021/ja028044q
26. Schmidt, B. *Chem. Commun.* **2004,** 742–743. doi:10.1039/b400229f
27. Finnegan, D.; Seigal, B. A.; Snapper, M. L. *Org. Lett.* **2006,** *8,* 2603–2606. doi:10.1021/ol060918g
28. Fustero, S.; Sánchez-Roselló, M.; Jiménez, D.; Sanz-Cervera, J. F.; del Pozo, C.; Aceña, J. L. *J. Org. Chem.* **2006,** *71,* 2706–2714. doi:10.1021/jo0525635
29. Scholte, A. A.; An, M. H.; Snapper, M. L. *Org. Lett.* **2006,** *8,* 4759–4762. doi:10.1021/ol061837n
30. Murelli, R. P.; Snapper, M. L. *Org. Lett.* **2007,** *9,* 1749–1752. doi:10.1021/ol070445t
31. Alcaide, B.; Almendros, P.; Luna, A. *Chem. Rev.* **2009,** *109,* 3817–3858. doi:10.1021/cr9001512
32. Delaude, L.; Demonceau, A.; Noels, A. F. Ruthenium-promoted radical processes toward fine chemistry. In *Ruthenium Catalysts and Fine Chemistry;* Bruneau, C.; Dixneuf, P. H., Eds.; Topics in Organometallic Chemistry, Vol. 11; Springer: Berlin, 2004; pp 155–171. doi:10.1007/b94645
33. Severin, K. *Curr. Org. Chem.* **2006,** *10,* 217–224. doi:10.2174/138527206775192915
34. Overman, L. E. *J. Am. Chem. Soc.* **1976,** *98,* 2901–2910. doi:10.1021/ja00426a038
35. Nagashima, H.; Wakamatsu, H.; Ozaki, N.; Ishii, T.; Watanabe, M.; Tajima, T.; Itoh, K. *J. Org. Chem.* **1992,** *57,* 1682–1689. doi:10.1021/jo00032a016
36. Opstal, T.; Verpoort, F. *New J. Chem.* **2003,** *27,* 257–262. doi:10.1039/b210040a
37. Opstal, T.; Verpoort, F. *Angew. Chem., Int. Ed.* **2003,** *42,* 2876–2879. doi:10.1002/anie.200250840
38. Nicks, F.; Borguet, Y.; Delfosse, S.; Bicchielli, D.; Delaude, L.; Sauvage, X.; Demonceau, A. *Aust. J. Chem.* **2009,** *62,* 184–207. doi:10.1071/CH08510
39. Fleming, I.; Au-Yeung, B.-W. *Tetrahedron* **1981,** *37,* 13–24. doi:10.1016/0040-4020(81)85036-3

License and Terms

Beilstein Journal of Organic Chemistry

The catalytic performance of Ru–NHC alkylidene complexes: PCy_3 versus pyridine as the dissociating ligand

Stefan Krehl, Diana Geißler, Sylvia Hauke, Oliver Kunz, Lucia Staude and Bernd Schmidt*

Full Research Paper

Open Access

Address:
Universität Potsdam, Institut für Chemie, Organische Synthesechemie, Karl-Liebknecht-Straße 24–25, D-14476 Golm, Germany

Email:
Bernd Schmidt* - bernd.schmidt@uni-potsdam.de

* Corresponding author

Keywords:
homogeneous catalysis; *N*-heterocyclic carbenes; olefin metathesis; pyridine ligand; Ruthenium carbene complexes

Beilstein J. Org. Chem. **2010,** *6,* 1188–1198.
doi:10.3762/bjoc.6.136

Received: 10 September 2010
Accepted: 09 November 2010
Published: 15 December 2010

Guest Editor: K. Grela

Abstract

The catalytic performance of NHC-ligated Ru-indenylidene or benzylidene complexes bearing a tricyclohexylphosphine or a pyridine ligand in ring closing metathesis (RCM), cross metathesis, and ring closing enyne metathesis (RCEYM) reactions is compared. While the PCy_3 complexes perform significantly better in RCM and RCEYM reactions than the pyridine complex, all catalysts show similar activity in cross metathesis reactions.

Introduction

Over the past two decades, the olefin metathesis reaction became one of the most important C–C-bond forming reactions in organic synthesis [1]. The elucidation of the crucial role of metal carbenes by Chauvin [2] and the development of stable and defined precatalysts for homogeneously catalyzed reactions by Schrock [3] and Grubbs [4] paved the way for this development. Since then, molybdenum- [5] and ruthenium-based [6] catalysts have experienced extensive further developments and improvements. Due to their robustness towards air and moisture, and their comparatively low sensitivity towards functional groups, Ru-carbene complexes have attracted a particularly high degree of attention and "numerous variations on a theme by Grubbs", as so accurately phrased by Fürstner [7], have been published. In the early stages of catalyst evolution improved methods for the introduction of the alkylidene ligand were the main focus. Thus, the original version of first generation Grubbs' catalyst (**A**) [8], in which the alkylidene moiety originates from 2,2-diphenylcyclopropene, was soon

replaced by the second version **B** [9], since the benzylidene ligand is more conveniently available from phenyldiazomethane. The obvious disadvantages of handling non-stabilized diazo compounds stimulated investigations into the use of propargylic alcohols as alkylidene precursors [10], which resulted in the synthesis of a first generation analogue **C** with an indenylidene ligand [11,12]. A landmark in the evolution of Ru-metathesis catalysts was the introduction of alkylidene complexes bearing *N*-heterocyclic carbenes (NHC) [13-15], in particular complex **D**, which became known as second generation Grubbs' catalyst [16], and the Umicore M2 catalyst **E** [17,18]. The ligation of strongly σ-donating NHC's leads to an improvement of catalytic activity, which sometimes equals the activity of Mo-based catalysts while maintaining the general robustness and tolerance towards several functional groups [19]. A third major topic in catalyst development has been the variation of the dissociating "placeholder"-ligand. In this respect, the introduction and further improvement of hemilabile benzylidene ligands by Hoveyda [20], Grela[21] and Blechert [22,23] have been important achievements. These phosphine-free catalysts of the general type **F** sometimes show higher activities due to enhanced catalyst lifetimes and have often been applied in cross metathesis reactions [24]. An alternative approach to phosphine-free Ru-metathesis catalysts uses pyridines as placeholders. Originally, complex **G** was synthesized as a precursor for mixed NHC-phosphine complexes other than **D** [25-28] or, very recently, for the synthesis of Ru-alkylidenes with two different NHC ligands [29]. Comparatively little information is available concerning the catalytic activity of these pyridine-NHC complexes. They were found to initiate ring opening metathesis polymerization reactions very rapidly [30,31] and show a certain preference for cross metathesis [32-35]. If the pyridine ring is attached to the alkylidene ligand [36], a latent catalyst results which might be a particularly useful property for metathesis polymerization reactions [37]. More recently, Ru-indenylidene complexes bearing one or two pyridine ligands were also synthesized [38,39], with the commercially available Umicore M31 catalyst **H** being a particularly interesting example. This catalyst is available from the M2 complex by ligand substitution [18] and shows high activity in living ROMP [40], whereas the reactivity in some RCM and CM reactions appears to be diminished [18,41].

During our research directed at the development of novel metathesis-non metathesis reaction sequences [42] catalyzed by a single site catalyst and initiated by organometallic transformations in situ, we became interested in the use of phosphine-free catalyst **H**. Unfortunately, only limited data is available concerning the catalytic efficiency of this catalyst in small molecule metathesis, in particular in comparison to the established phosphine containing catalysts **D** and **E** (Figure 1).

In this contribution, representative ring closing olefin, ring closing enyne and cross metathesis reactions of indenylidene complexes **E** and **H** and benzylidene complex **D** are compared.

Results and Discussion

Effects of solvent and catalyst loading

As a test reaction, we initially investigated the ring closing metathesis of allyl ether **1** to dihydropyran **2** (Scheme 1). To this end, conversion to the desired product in the presence of 5 mol % of catalyst **H** was determined after a reaction time of one hour at a slightly elevated temperature in seven different solvents, under otherwise identical conditions.

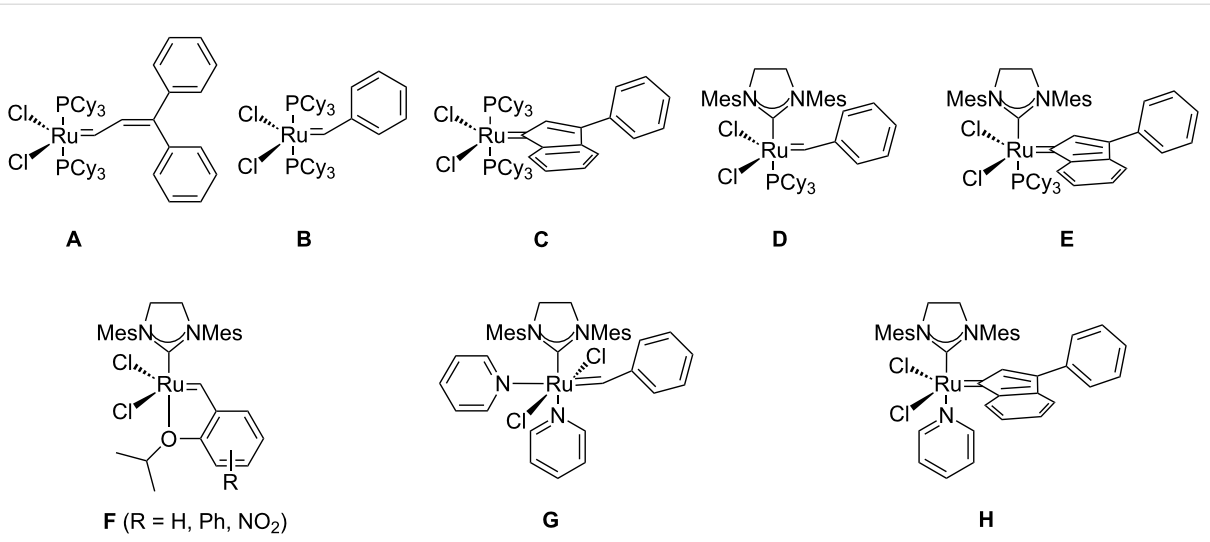

Figure 1: Ru-based metathesis catalysts.

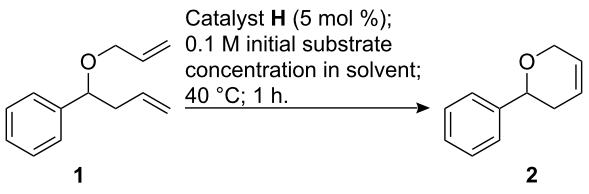

Scheme 1: RCM of an allyl ether catalyzed by catalyst **H**.

The results are summarized in Figure 2. Benzene, toluene, dichloromethane and 1,2-dichloroethane are commonly used solvents in Ru-catalyzed RCM reactions. However, for catalyst **H** only in dichloromethane was high conversion to the desired RCM product observed. In hexafluorobenzene, which has recently been shown to give highly impressive results, even in difficult metathesis reactions catalyzed by **D**, **E**, or **F** [43,44], the rate of conversion to dihydropyran **2** is quite similar to benzene or dichloroethane. Polar and, in particular, protic solvents would normally be considered inappropriate for metathesis reactions, because catalyst inhibition or degradation to Ru-hydrides might occur [45-47]. Nevertheless, such solvents have previously been investigated and useful results were obtained for esters [48] and – even more surprising – for acetic acid [49]. Therefore, we used ethyl acetate and acetic acid for our test reaction. While ethyl acetate gave a conversion of 75%, which is better than most of the classical solvents, nearly quantitative conversion to the RCM product was observed in acetic acid. Presumably, the pyridine ligand is protonated under these conditions which would result in a higher amount of the catalytically active 14-electron species. This interpretation is corroborated by the kinetic data obtained by Adjiman, Taylor et al. in their original investigation on solvent effects [49].

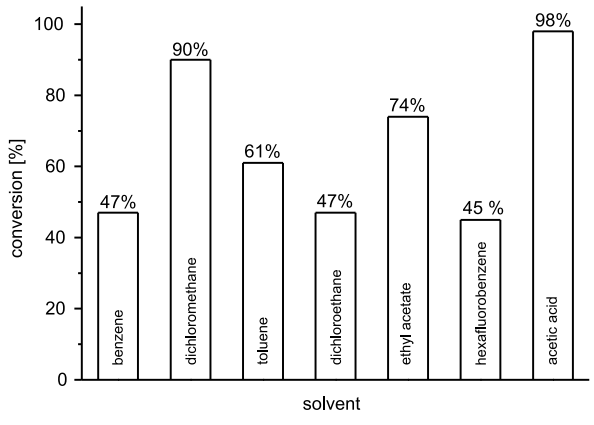

Figure 2: Solvent screening for the RCM of **1** catalyzed by **H** (standardized conditions as denoted in Scheme 1).

Next, we were interested to see how the performance of pyridine containing catalyst **H** compares with the more established phosphine complexes **D** and **E**. The test reaction depicted in Scheme 1 was therefore repeated in toluene and in acetic acid with a significantly lower catalyst loading, because we assumed that the highly active catalysts **D** and **E** would otherwise lead to full conversion in extremely short time (Figure 3).

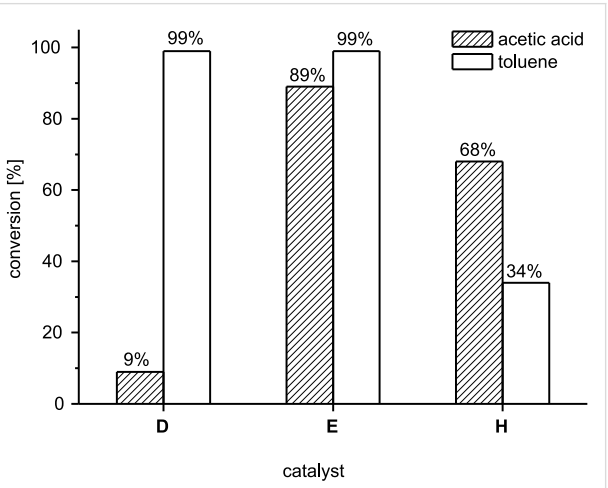

Figure 3: Comparison of catalysts **D**, **E** and **H** in toluene and acetic acid (standardized conditions as denoted in Scheme 1).

Thus, with 1.0 mol % of catalyst under conditions identical to those given in Scheme 1, a quantitative conversion to the dihydropyran **2** was observed for both catalysts **D** and **E** in toluene. In accord with the results summarized in Figure 2, catalyst **H** gave only 34% conversion in this solvent after one hour, suggesting that initiation was rather slow. In acetic acid, the analogous phosphine containing indenylidene catalyst **E** displayed a slightly reduced conversion of 89%, which might be attributed to slow catalyst deactivation, whereas pyridine complex **H** showed significantly enhanced activity in acetic acid, with a conversion of 68% after one hour. This result suggests that by switching from toluene to acetic acid the balance of catalyst deactivation and enhanced initiation is shifted to the deactivation side for phosphine catalyst **E**, and to the enhanced initiation side for pyridine catalyst **H**. The most remarkable result from this set of experiments, however, is a collapse of conversion if benzylidene catalyst **D** is used in acetic acid. With **D**, a reproducible conversion of only 9% to the dihydropyran **2** was observed, compared to 89% conversion with the analogous indenylidene complex **E**. This result seems to contradict the observations by Adjiman, Taylor et al. who reported preparatively useful conversions and yields for second generation Grubbs' catalyst **D** in acetic acid [49], however, their studies were conducted at ambient temperature and for different substrates, while our experiments were conducted at 40 °C. It is

possible that our result suggests a higher robustness of indenylidene catalyst **E** compared to benzylidene catalyst **D**, at least under these rather unusual conditions.

To further evaluate the catalytic performance of pyridine catalyst **H** in acetic acid, we next wanted to determine the minimum amount of catalyst required to obtain a preparatively useful (>90%) rate of conversion. Consequently, it was demonstrated that, instead of using the conditions noted in Scheme 1, a catalyst loading of 2 mol % was sufficient to achieve a 92% conversion within one hour (Figure 4).

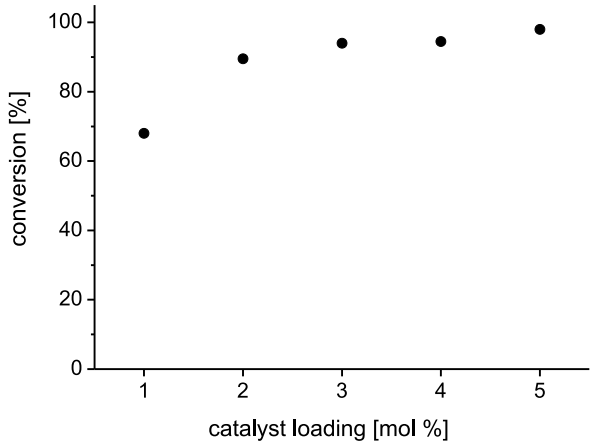

Figure 4: Conversion vs catalyst loading for the RCM of **1** in acetic acid (standardized conditions as denoted in Scheme 1).

Ring closing metathesis of acrylates

Having established the beneficial effect of acetic acid for the ring closing metathesis reaction of allyl ether **1** catalyzed by **H**, we were interested to see if a similar effect exists for other substrates. Therefore, acrylate **3a** was subjected to the conditions of a ring closing metathesis reaction (Scheme 2 and Table 1). Not unexpectedly [50], significantly reduced initial substrate concentrations were required for useful rates of conversion to the desired α,β-unsaturated lactone **4a**. It transpired, that preparatively useful yields could only be obtained with the phosphine containing catalysts **D** and **E** in toluene (Table 1, entries 1 and 2), whereas pyridine complex **H** gave a conversion of approximately 65% and an isolated yield of 41% of lactone **4a** in this solvent (Table 1, entry 3). In contrast to the ring closing metathesis of allyl ether **1**, the rate of conversion decreased significantly when catalyst **H** was used in acetic acid (Table 1, entry 4). Notably, the ^{1}H NMR-spectra of the crude reaction mixtures did not indicate the presence of any decomposition products, thus, even the comparatively labile acrylate **3** appears to be quite stable in acetic acid at elevated temperatures for several hours.

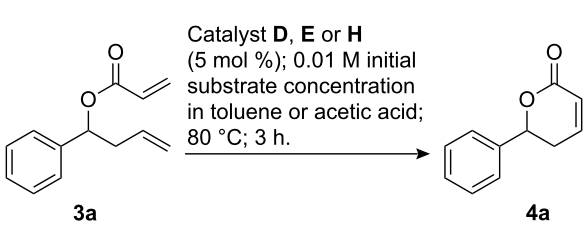

Scheme 2: Catalyst screening for RCM of acrylate **3a**.

Table 1: RCM of acrylate **3a**.

Entry	Solvent	Catalyst[a]	Ratio **4a**:**3a**[b]	Yield of **4a**
1	toluene	**D**	>15:1	80%
2	toluene	**E**	>15:1	92%
3	toluene	**H**	10:5	41%
4	acetic acid	**H**	10:17	—[c]

[a]A catalyst loading of 5 mol % was used in all experiments. [b]Ratio of product to starting material was determined from the ^{1}H NMR-spectrum of the crude reaction mixture after three hours at 80 °C. [c]Yield was not determined due to low conversion.

Because acetic acid did not lead to the expected improvement in acrylate metathesis reactions, only toluene was tested as a solvent in further experiments (Figure 5 and Table 2). Toluene was preferred over dichloromethane, because reactions are more conveniently conducted at elevated temperatures in this solvent.

The acrylates **3** investigated in ring closing metathesis reactions with catalysts **D**, **E** and **H** are listed in Figure 5, together with the resulting unsaturated lactones **4**. Results for the ring closing metathesis of acrylates **3a**–**g** are summarized in Table 2. Lactones **4b**–**f** [50] are accessible in preparatively useful yields with catalyst loadings of 2.5 mol % to 5.0 mol % if catalysts **D** and **E** are used. Conversions observed with catalyst **H** under otherwise identical conditions are significantly lower and yields exceed 50% only in few cases such as **4b**, **4e** and **4f**. A particularly difficult substrate for olefin metathesis reactions is acrylate **3g**, which has recently been used by us as an intermediate in the synthesis of the natural product (–)-cleistenolide [51]. Acrylate **3g** requires very high dilution, the addition of phenol as a rate accelerating additive [52], a rather high catalyst loading of 10 mol % and an even higher reaction temperature. Under these conditions, the best product to substrate ratio and the best isolated yield was obtained with the indenylidene complex **E** (Table 2, entry 6).

Ring closing enyne metathesis

Imahori et al. have recently discovered that allylic hydroxy groups significantly enhance the rate of ring closing enyne metathesis reactions [53,54]. In these cases, addition of an

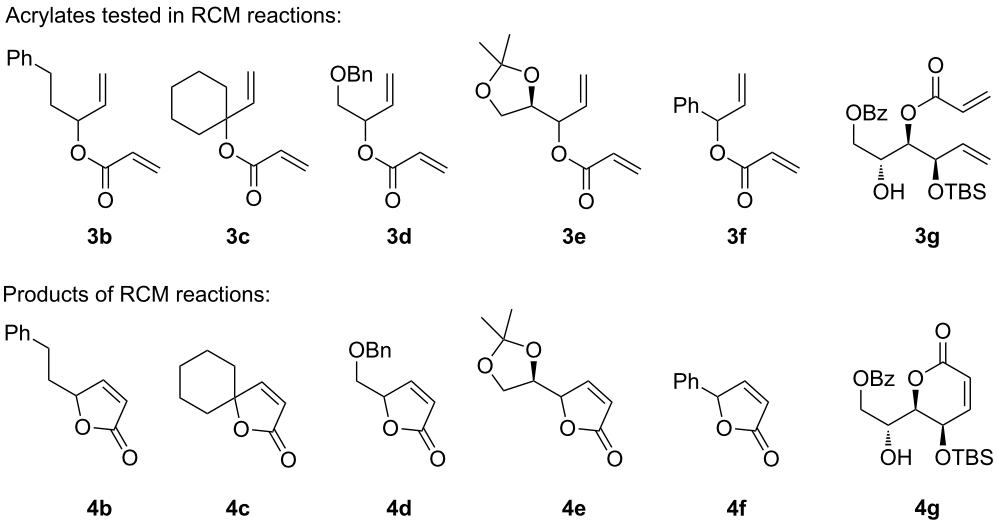

Figure 5: Acrylates **3** and their RCM products **4**.

Table 2: RCM reactions of acrylates to unsaturated lactones.[a]

Entry	3	4	*c*/mol·L^{-1}	Catalyst loading	Ratio[b] **4**:**3** (isolated yields) for		
					D	**E**	**H**
1	**3b**	**4b**	0.02	2.5 mol %	> 20:1 (86%)	>20:1 (90%)	1.8:1 (52%)
2	**3c**	**4c**	0.02	2.5 mol %	>20:1 (75%)	>20:1 (85%)	2.1:1 (43%)
3	**3d**	**4d**	0.02	2.5 mol %	7.1:1 (79%)	3.3:1 (41%)	0.6:1 (27%)
4	**3e**	**4e**	0.01	5.0 mol %	>10:1 (59%)	>20:1 (71%)	1.8:1 (56%)
5	**3f**	**4f**	0.02	2.5 mol %	>20:1 (80%)	>20:1 (53%)	4.5:1 (65%)
6[c]	**3g**	**4g**	0.002	10.0 mol %	1.1:1 (36%)	2.6:1 (58%)	0.3:1 (14%)

[a]Reactions were run in toluene at 80 °C for 1 h, unless otherwise stated. [b]The substrate to product ratio was determined from the ^{1}H NMR-spectra of the crude reaction mixtures. [c]Reaction was run in toluene at 110 °C for 3 h in the presence of 0.5 equiv of phenol.

ethylene atmosphere [55] which is normally considered to be mandatory for good results, is not required. We have recently investigated the highly selective enyne metathesis of substrates such as **5a**,**b** to dihydropyrans **6a**,**b** in the presence of first generation catalysts **B** and **C** [56]. Notably, no dihydrofurans or other isomers were observed. Sometimes, the selectivity decreases when the more reactive second generation catalysts are used [57,58], and we were therefore interested to test NHC-ligated catalysts in this transformation (Scheme 3).

The results for ring closing enyne metathesis reactions with indenylidene catalysts **E** and **H** are summarized in Table 3. Enyne **5a** reacted to afford the expected dihydropyran **6a** with high conversion and high selectivity in toluene at 80 °C and at

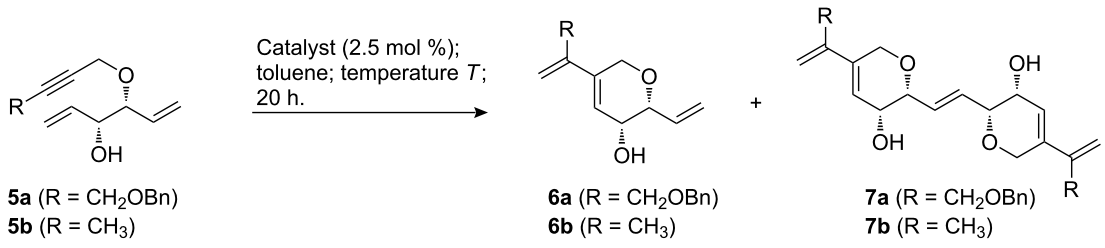

Scheme 3: Ring closing enyne metathesis reactions.

Table 3: Ring closing enyne metathesis reactions catalyzed with **E** and **H**.

Entry	5	–R	Catalyst[a]	*T*	Conversion[b]	Ratio of 6:7[b]	Product (Yield)
1	**5a**	$–CH_2OBn$	**E**	80 °C	95%	>20:1	**6a** (50%)
2	**5a**	$–CH_2OBn$	**E**	110 °C	95%	>20:1	**6a** (44%)
3	**5a**	$–CH_2OBn$	**H**	80 °C	50%	>20:1	**6a** (29%) **5a** (21%)
4	**5a**	$–CH_2OBn$	**H**	110 °C	80%	>20:1	**6a** (34%)
5	**5b**	$–CH_3$	**E**	80 °C	100%	10:10.7	n. d.
6	**5b**	$–CH_3$	**E**	110 °C	100%	10:10.3	n. d.
7	**5b**	$–CH_3$	**H**	80 °C	100%	10:10.2	n. d.
8	**5b**	$–CH_3$	**H**	110 °C	100%	10:9.6	**6b** (24%) **7b** (45%)

[a]2.5 mol % of catalyst, toluene as a solvent and an initial substrate concentration of 0.1 mol/L were used in all experiments. [b]Rates of conversion and monomer/dimer ratios were determined from the ^{1}H NMR-spectra of the crude reaction mixtures, which showed only signals of starting materials **5**, dihydropyrans **6** and dimers **7**.

110 °C in the presence of phosphine complex **E** (Table 3, entries 1 and 2). The dimerization product **7a** was not detected, and although the ^{1}H NMR spectra of the crude reaction mixtures showed only signals of **6a** and trace amounts of the starting material **5a**, the isolated yields are mediocre which can be attributed to a significant loss of material during purification. Significantly lower conversions of 50% and 80% were observed with the pyridine complex **H** at 80 °C or 110 °C, respectively. Again, ^{1}H NMR-spectra of the crude reaction mixtures showed only signals for **6a** and the starting material **5a** and not even trace amounts of a dimerization product **7a** (Table 3, entries 3 and 4) were detected. Different results were found for the methyl substituted enyne precursor **5b**. Remarkably, with both catalysts and both reaction temperatures apparently identical conversions and product distributions were observed: In all cases (Table 3, entries 5–8) the starting material was fully consumed and the ^{1}H NMR-spectra of the crude reaction mixtures revealed only the presence of dihydropyran **6b** and its dimer **7b** in roughly a 1:1 ratio. This ratio is reflected nicely in the isolated yields, which were determined for one example (Table 3, entry 8). From these results, it can be concluded that benzyloxy-substituted enyne **5a** is significantly less reactive in enyne metathesis reactions which becomes more obvious if the pyridine complex **H** is used as a catalyst. For other examples, we have previously observed that benzyl ether moieties in close proximity to a C–C-multiple bond retard or inhibit metathesis reactions [50]. Presumably, partial catalyst deactivation by coordination of the benzyloxy group to the metal plays a role, and this might also explain why no dimerization product **7a** was observed, whereas **7b**, the self-metathesis product of **6b**, was isolated in significant quantities, which might suggest a remarkable residual activity of the catalysts after completion of the enyne metathesis.

The results discussed above for the less reactive enyne **5a** suggest that pyridine complex **H** is less active than **E** in enyne metathesis reactions, however, the results for the apparently more reactive substrate **5b** may indicate that the gap in catalytic activity between **E** and **H** is much smaller for ring closing enyne reactions than for ring closing acrylate metathesis reactions. However, the remarkably high amount of homodimerization product **7b** points to considerable activity of **H** in cross metathesis reactions, a peculiarity which has previously been noted for the bis(pyridine) complex **G** [33-35].

Cross metathesis reactions

Allylic alcohol **8** [59] was chosen to test the catalysts investigated in this study for cross metathesis activity, because allylic alcohols are known to undergo undesired “redox isomerization” in the presence of Ru metathesis catalysts in some cases with the formation of ethyl ketones [47,60]. Therefore, **8** can be considered as a rather challenging substrate. As partners in the cross metathesis reactions, three acrylates **9a**–**c** were chosen. In addition, homodimerization of **8** to diol **11** was also investigated (Scheme 4).

The results are summarized in Table 4. With methyl acrylate **9a** in dichloromethane at 40 °C, only the benzylidene catalyst **D** showed a satisfactory rate of conversion (Table 4, entry 1). A significantly lower conversion was observed under these conditions for pyridine complex **H** (Table 4, entry 3), however, the isolated yields were similar in both cases. Surprisingly, with catalyst **E** conversion was incomplete and a considerable amount of dimer **11** was formed (Table 4, entry 2). Compound **11** is an inseparable mixture of diastereomers, because **10a** was used as a racemate. Raising the temperature to 80 °C in toluene solved the problems of incomplete conversion and competing

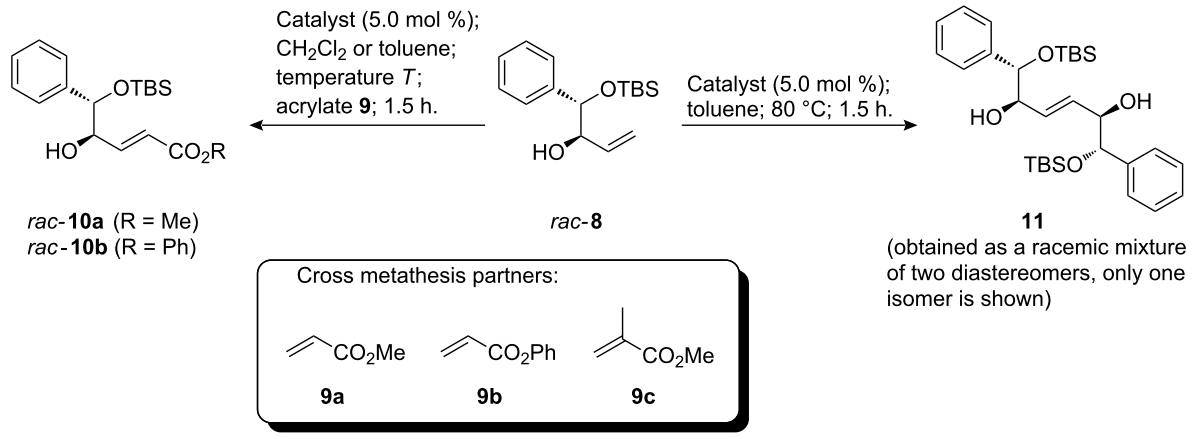

Scheme 4: Cross metathesis reactions with allylic alcohol **8**.

dimerization for all three catalysts (Table 4, entries 4–6) and *rac*-**10a** was isolated in comparable yields of between 83% and 86%. Phenyl acrylate (**9b**) is a less reactive cross metathesis partner, and all three catalysts led to incomplete conversion (Table 4, entries 7–9). The best result in this series was achieved with catalyst **H**, which gave a 2:1 ratio of product **10b** and starting material **8**, and an isolated yield of 60% (Table 4, entry 9). Methyl methacrylate (**9c**) did not react in cross metathesis reactions with **8** using either **D** or **H**. Instead, dimerization to compound **11** occurred. We [50] and others [61] have recently observed a considerable reduction of isomerization side reactions if acrylates are present during a metathesis reaction. Therefore, **8** was subjected to olefin metathesis conditions in the absence of acrylates to check if any isomerization occurred, or if dimer **11** was the preferred or sole product. With all three catalysts similar results were obtained: The starting material was rapidly and almost completely consumed, and the two diastereomers of **11** were the only detectable products in the reaction mixture (Table 4, entries 12–14).

These results demonstrate that the novel catalyst **H**, albeit significantly less active than **D** or **E** in the ring closing metathesis of acrylates, appears to be competitive in cross metathesis reactions.

Table 4: Cross metathesis reactions catalyzed by **D**, **E**, and **H**.

Entry	Acrylate	Solvent	*T*	Catalyst[a]	Ratio of **10**:**8**:**11**[b]	Product (Yield)[c]
1	**9a**	CH_2Cl_2	40 °C	**D**	16:1:0	*rac*-**10a** (72%)
2	**9a**	CH_2Cl_2	40 °C	**E**	1.4:1.3:1	n. d.
3	**9a**	CH_2Cl_2	40 °C	**H**	3.7:1:0	*rac*-**10a** (65%)
4	**9a**	toluene	80 °C	**D**	1:0:0	*rac*-**10a** (84%)
5	**9a**	toluene	80 °C	**E**	1:0:0	*rac*-**10a** (83%)
6	**9a**	toluene	80 °C	**H**	1:0:0	*rac*-**10a** (86%)
7	**9b**	toluene	80 °C	**D**	1.2:1:0	*rac*-**10b** (53%)
8	**9b**	toluene	80 °C	**E**	1:1:0	*rac*-**10b** (47%)
9	**9b**	toluene	80 °C	**H**	2:1:0	*rac*-**10b** (60%)
10	**9c**	toluene	80 °C	**D**	0:0:1	**11** (n. d.)
11	**9c**	toluene	80 °C	**H**	0:0:1	**11** (n. d.)
12	—	toluene	80 °C	**D**	—:1:30	**11** (68%)
13	—	toluene	80 °C	**E**	—:1:9	**11** (n. d.)
14	—	toluene	80 °C	**H**	—:1:16	**11** (n. d.)

[a]A catalyst loading of 5.0 mol % was used in all experiments. [b]Ratios were determined from the ^{1}H NMR-spectra of crude reaction mixtures. [c]All cross metathesis products were obtained as single *E*-isomers.

Conclusion

In conclusion, we have evaluated and compared the catalytic performance of two indenylidene NHC-metathesis catalysts and the well established second generation Grubbs catalyst in various small molecule metathesis reactions. The activity of the mixed NHC-phosphine catalysts **D** and **E** appears to be similar in most applications. Some results hint at a somewhat faster reaction with benzylidene complex **D**, while **E** apparently performs slightly better in "slow" metathesis reactions, presumably since it is more robust. The novel pyridine complex **H** was also tested in several olefin metathesis reactions. While this catalyst gives rather unsatisfactory results in the ring closing metathesis of acrylates, its performance in ring closing enyne metathesis reactions is only slightly lower than the phosphine complexes **D** and **E**. However, the activity of **H** in cross metathesis reactions is similar to **D** and **E**. Furthermore, initial studies concerning the use of unconventional solvents revealed that **H** might be quite active, at least for some applications, in acetic acid.

Experimental

All experiments were conducted in dry reaction vessels under an atmosphere of dry argon. Solvents were purified by standard procedures. All yields and conversions reported herein are average values of at least two experiments. ^{1}H NMR spectra were obtained at 300 MHz in $CDCl_3$ with $CHCl_3$ (δ = 7.26 ppm) as the internal standard. Coupling constants (*J*) are given in Hz. ^{13}C NMR spectra were recorded at 75 MHz in $CDCl_3$ with $CDCl_3$ (δ = 77.0 ppm) as the internal standard. IR spectra were recorded as films on NaCl or KBr plates or as KBr discs. Wavenumbers (ν) are given in cm^{-1}. Mass spectra were obtained at 70 eV. Whenever known compounds were used as starting materials, reagents or catalysts, they were either purchased or were synthesized following literature procedures: **1** [62], **3a** [63], **3b**–**3e** [50], **3g** [51], **5a**,**b** [56]. Catalyst **D** was purchased from Aldrich and used without further purification. Catalysts **E** and **H** were donated by Umicore, Hanau, Germany, and also used without further purification. The following products have previously been synthesized via olefin metathesis reactions under different conditions: **2** [62], **4a** [63], **4b**–**4e** [50], **4f** [64], **4g** [51], **6a**,**b** [56].

General procedure for the RCM of 1: variation of solvent, catalyst and catalyst loading

Allyl ether **1** (94.0 mg, 0.5 mmol) was dissolved in the appropriate dry and degassed solvent (5.0 mL). Catalyst **D** (4.2 mg for 1.0 mol %), **E** (4.7 mg for 1.0 mol %) or **H** (3.7 mg for 1.0 mol %, 7.4 mg for 2.0 mol %, 11.2 mg for 3.0 mol %, 15.0 mg for 4.0 mol % or 18.8 mg for 5.0 mol %) was then added. Immediately after addition of the catalyst, the reaction vessel was immersed in an oil bath preheated to 40 °C (electronic temperature control) for a period of time between 60 and 62 min. After this time, the reaction vessel was allowed to cool to ambient temperature, the solvent was removed by evaporation, and the residue immediately subjected to NMR spectroscopy. The ratio of dihydropyran **2** to allyl ether **1** was determined by integration of characteristic, baseline separated signals. Each experiment was repeated at least two times. The reported rates of conversion are average values.

Ring closing metathesis of acrylates

General procedure for the synthesis of furanones 4b–4f by RCM: To a solution of the appropriate acrylate **3** (1.0 mmol) in dry and degassed toluene (50 mL for 0.02 $mol \cdot L^{-1}$ or 100 mL for 0.01 $mol \cdot L^{-1}$), was added either catalyst **D** (21.2 mg for 2.5 mol % or 42.4 mg for 5.0 mol %), **E** (23.7 mg for 2.5 mol % or 47.4 mg for 5.0 mol %) or **H** (18.7 mg for 2.5 mol % or 37.4 mg for 5.0 mol %). The solution was heated to 80 °C for 90 min. The solvent was then removed by evaporation and the residue purified by flash column chromatography on silica to give the corresponding lactones **4**. The ratio of lactone **4** to acrylate **3** was determined by integration of characteristic, baseline separated signals in the ^{1}H NMR-spectrum of the crude reaction mixture. Representative example: **5-phenylfuran-2(5*H*)-one (4f)**. This compound was obtained as a colourless oil from **3f** (189 mg, 1.0 mmol) following the general procedure. Yield of **4f** using catalyst **D**: 128 mg (0.80 mmol, 80%). Yield of **4f** using catalyst **E**: 85 mg (0.53 mmol, 53%). Yield of **4f** using catalyst **H**: 104 mg (0.65 mmol, 65%). ^{1}H NMR (300 MHz, $CDCl_3$) δ 7.53 (dd, *J* = 5.7, 1.7, 1H), 7.45–7.35 (3H), 7.30–7.23 (2H), 6.23 (dd, *J* = 5.7, 2.1, 1H), 6.01 (t (br), *J* = 1.9, 1H); ^{13}C NMR (75 MHz, $CDCl_3$) δ 173.0 (0), 155.8 (1), 134.4 (0), 129.3 (1), 129.0 (1), 126.5 (1), 121.0 (1), 84.3 (1); HRMS (ESI) calcd for $C_{10}H_8O_2Na$ $[M+Na]^+$: 183.0422, found: 183.0439.

Procedure for the synthesis of 6-phenyl-5,6-dihydropyran-2-one (4a): The acrylate **3a** (201 mg, 1.0 mmol) was dissolved in dry and degassed toluene (100 mL). After adding the catalyst (**D**: 42.4 mg **B**: 47.4 mg **H**: 37.4 mg, 0.05 mmol, 5 mol %) the solution was stirred for 3 h at 80 °C. After cooling the solution to ambient temperature, all volatiles were evaporated. The residue was purified by chromatography on silica (hexane/MTBE 2:1). Yield of **4a** using catalyst **D**: 139 mg (0.80 mmol, 80%). Yield of **4a** using catalyst **E**: 160 mg (0.92 mmol, 92%). Yield of **4a** using catalyst **H**: 170 mg (0.41 mmol, 41%). The ratios of lactone **4a** to acrylate **3a** were determined by integration of characteristic, baseline separated signals in the ^{1}H NMR-spectrum of the crude reaction mixture. mp 58–59 °C; ^{1}H NMR (300 MHz, $CDCl_3$) δ 7.43–7.33 (5H), 6.97 (ddd, *J* = 9.7, 5.7, 2.6, 1H), 6.13 (ddd, *J* = 9.7, 1.1, 1.1, 1H), 5.45 (dd, *J* = 11.2, 4.8, 1H), 2.70–2.57 (2H); ^{13}C NMR (75 MHz, $CDCl_3$) δ 164.0

(0), 144.8 (1), 138.4 (0), 128.6 (1), 128.6 (1), 126.0 (1), 121.7 (1), 79.2 (1), 31.6 (2); IR (neat) ν 3064 (w), 2904 (w), 1716 (s), 1381 (m), 1242 (s), 1059 (m), 1020 (m), 909 (m); EIMS (%) *m/z* 174 (M^+, 6), 77 (13), 68 (100), 39 (63); HRMS (EI) calcd. for $C_{11}H_{10}O_2$ [M^+]: 174.0675, found 174.0689; Anal. calcd for $C_{11}H_{10}O_2$: C, 75.8, H, 5.8; found: C, 75.6, H, 5.8.

Procedure for the synthesis of (*R*)-2-((2*R*,3*R*)-3-(*tert*-butyldimethylsilyloxy)-6-oxo-3,6-dihydro-2*H*-pyran-2-yl)-2-hydroxyethyl benzoate (4g): The acrylate **3g** (330 mg, 0.78 mmol) and phenol (37 mg, 0.39 mmol) were dissolved in dry and degassed toluene (390 mL). After adding the catalyst (**D**: 66.1 mg **B**: 73.9 mg **H**: 58.3 mg, 0.078 mmol, 10 mol %), the solution was stirred for 3 h at 80 °C. The solution was cooled to ambient temperature and all volatiles were evaporated. The residue was purified by chromatography on silica. Yield of **4g** using catalyst **D**: 110 mg (0.28 mmol, 36%). Yield of **4g** using catalyst **E**: 177 mg (0.45 mmol, 58%). Yield of **4g** using catalyst **H**: 43 mg (0.11 mmol, 14%). The ratios of lactone **4g** to acrylate **3g** were determined by integration of characteristic, baseline separated signals in the ^{1}H NMR-spectrum of the crude reaction mixture. All analytical data were identical to those reported previously in the literature [51].

Ring closing enyne metathesis reactions

General procedure: To a solution of the corresponding precursor **5** (2.0 mmol) in toluene (40 mL), was added catalyst **E** (47.4 mg, 2.5 mol %) or **H** (37.4 mg, 2.5 mol %). The solution was heated to the appropriate temperature (80 °C or 110 °C) for 20 h, then cooled to ambient temperature and the solvent evaporated. The crude product was analyzed by ^{1}H and ^{13}C NMR spectroscopy. Analytically pure samples were obtained by column chromatography on silica. Representative example: **Ring closing enyne metathesis of 5b.** Following the general procedure, **5b** (330 mg, 2.0 mmol) was treated with catalyst **H** (37.4 mg, 2.5 mol %) at 80 °C. After column chromatography, **6b** (80 mg, 0.48 mmol, 24%) and **7b (**274 mg, 0.90 mmol, 45%) were isolated. The rate of conversion and the ratios of **6b** to **7b** were determined by integration of characteristic, baseline separated signals in the ^{1}H NMR-spectrum of the crude reaction mixture. All analytical data of **6b** were identical to those reported previously in the literature.[56] Analytical data for **(2*R*,2'*R*,3*R*,3'*R*,*E*)-2,2'-(ethene-1,2-diyl)bis(5-(prop-1-en-2-yl)-3,6-dihydro-2*H*-pyran-3-ol (7b):** $[\alpha]_D^{25}$: –390.0 (*c* 0.13, CH_2Cl_2); ^{1}H NMR (300 MHz, CDCl) δ 6.05 (d, *J* = 5.4, 2H); 5.96 (d, *J* = 1.7, 2H); 4.93 (s, 1H); 4.83 (s, 2H); 4.49 (d, *J* = 15.6, 2H); 4.25 (d, *J* = 15.5, 2H); 4.04 (s, 2H); 3.99 (d, *J* = 5.5, 1H); 3.32 (s, 2H); 1.87 (s, 6H); ^{13}C NMR (75 MHz, $CDCl_3$) δ 139.5 (0), 138.5 (0); 129.1 (2), 122.8 (1); 112.3, (2); 77.3 (1), 66.2 (2); 64.2 (1); 20.1 (3); IR ν 3297 (s); 3087 (m); 2945 (m); 2828 (m); 1606 (m); 1371 (w); 1124 (s); 1103 (m); 1055 (m), 882 (s), 827 (s); HRMS (EI) calcd for $C_{18}H_{24}O_4$ [M^+]: 304.1675, found: 304.1683; Anal. calcd for $C_{18}H_{24}O_4$: C, 71.0, H, 8.0, found: C, 70.8, H, 7.7.

Cross-metathesis reactions

General procedure: A solution of the allylic alcohol *rac*-**8** (139 mg, 0.5 mmol) and the corresponding acrylate **9** (5 mmol) in dry and degassed toluene (1.0 mL for 0.5 mol·L^{-1}, 5.0 mL for 0.1 mol·L^{-1}) was warmed to approximately 45 °C. Then the catalyst (0.025 mmol, 5 mol %, **D**: 42.4 mg **E**: 47.4 mg **H**: 18.7 mg) was added to the solution and stirred for 90 min at 80 °C. After cooling to ambient temperature all volatiles were evaporated and the residue purified by chromatography on silica. The rates of conversion and the ratios of **10** to **8** to **11** were determined by integration of characteristic, baseline separated signals in the ^{1}H NMR-spectrum of the crude reaction mixture.

(4*RS*,5*SR*,*E*)-methyl 5-(*tert*-butyldimethylsilyloxy)-4-hydroxy-5-phenylpent-2-enoate (*rac*-10a). Obtained as colourless oil from *rac*-**8** (139 mg, 0.5 mmol) and methyl acrylate (**9a**) following the general procedure. Yield of *rac*-**10a** using catalyst **D**: 141 mg (0.42 mmol, 84%). Yield of *rac*-**10a** using catalyst **E**: 139 mg (0.41 mmol, 83%). Yield of *rac*-**10a** using catalyst **H**: 145 mg (0.43 mmol, 86%). ^{1}H NMR (300 MHz, $CDCl_3$) δ 7.37–7.25 (5 H), 6.73 (dd, *J* = 15.7, 4.1, 1 H), 6.07 (dd, *J* = 15.7, 1.9, 1 H), 4.47 (d, *J* = 6.8, 1 H), 4.29 (dddd, *J* = 6.6, 4.1, 3.6, 2.0, 1 H), 3.70 (s, 3 H), 2.90 (d, *J* = 3.9, 1 H), 0.89 (s, 9 H), 0.03 (s, 3 H), −0.18 (s, 3 H); ^{13}C NMR (75 MHz, $CDCl_3$) δ 166.7 (0), 145.8 (1), 140.2 (0), 128.4 (1), 128.2 (1), 126.9 (1), 121.6 (1), 78.4 (1), 75.8 (1), 51.5 (3), 25.7 (3), 18.1 (0), −4.6 (3), −5.1 (3); IR ν 3492 (w), 2952 (w), 2857 (w), 1724 (m), 1253 (m), 1068 (m), 835 (s), 777 (s); HRMS (ESI) calcd for $C_{18}H_{28}O_4NaSi$ [M+Na]$^+$: 359.1655, found: 359.1652; EIMS (%) *m/z* = 337 (M^+, 1), 221 (100), 187 (11), 173 (6), 145 (9), 115 (11), 91 (6), 73 (15); Anal. calcld $C_{18}H_{28}O_4$:C, 64.3, H: 8.4; found: C: 64.2, H: 8.4.

(4*RS*,5*SR*,*E*)-phenyl 5-(*tert*-butyldimethylsilyloxy)-4-hydroxy-5-phenylpent-2-enoate (*rac*-10b). Obtained as colourless solid from *rac*-**8** (139 mg, 0.5 mmol) and phenyl acrylate (**9b**) following the general procedure. Yield of *rac*-**10b** using catalyst **D**: 105 mg (0.27 mmol, 53%). Yield of *rac*-**10a** using catalyst **E**: 94 mg (0.30 mmol, 47%). Yield of *rac*-**10a** using catalyst **H**: 119 mg (0.43 mmol, 60%). mp 82–84 °C; ^{1}H NMR (300 MHz, $CDCl_3$) δ 7.41–7.18 (8 H), 7.12–7.06 (2 H), 6.93 (dd, *J* = 15.6, 4.0, 1 H), 6.30 (dd, *J* = 15.6, 1.8, 1 H), 4.55 (d, *J* = 6.6, 1 H), 4.37 (dddd, *J* = 6.1, 4.2, 4.0, 1.9, 1 H), 2.96 (d, *J* = 4.0, 1 H), 0.91 (s, 9 H), 0.06 (s, 3 H), −0.16 (s, 3 H); ^{13}C NMR (75 MHz, $CDCl_3$) δ 164.6 (0), 150.7 (0), 147.9 (1), 140.2 (0), 129.3 (1), 128.5 (1), 128.3 (1), 126.9 (1), 125.7 (1), 121.5 (1), 121.3 (1), 78.4 (1), 76.0 (1), 25.8 (3), 18.2 (0), −4.5 (3),

−5.1 (3); IR ν 3545 (w), 2929 (w), 2857 (w), 1739 (s), 1493 (m), 1194 (s), 836 (s), 778 (s); HRMS (ESI) calcd for $C_{23}H_{30}O_4NaSi$ $[M+Na]^+$: 421.1811, found: 421.1800; EIMS (%) *m/z* = 341 (2), 332 (2), 292 (1), 249 (3), 247 (4), 221 (100), 75 (21) 73 (47); Anal. calcd C, 69.3, H, 7.6; found C, 69.4, H, 7.5.

Dimerization of *rac*-8 (Compound 11). The catalyst (5 mol %, 0.029 mmol, **D**: 24.2 mg, **E**: 27.0 mg, **H**: 21.3 mg) was added to a solution of alcohol *rac*-**8** (150 mg, 0.57 mmol) in dry and degassed toluene (1.13 mL, 0.5 M). The reaction mixture was stirred for 90 min at 80 °C. After cooling to room temperature all volatiles were evaporated. The crude product **11** was purified by chromatography on silica. Compound **11** was isolated as a partially separable mixture of diastereomers (combined yield for catalyst **D**: 107 mg, 0.39 mmol, 68%). The rates of conversion were determined by integration of characteristic, baseline separated signals in the ^{1}H NMR-spectrum of the crude reaction mixture. Analytical data for diastereomer **11a**: ^{1}H NMR (300 MHz, $CDCl_3$) δ 7.30–7.24 (3H), 7.11–7.06 (2H), 5.44 (dd, *J* = 2.6, 0.9, 1H), 4.20 (d, *J* = 7.5, 1H), 4.00 (dm, *J* = 7.4, 1 H), 2.83 (d, *J* = 2.4, 1H), 0.87 (s, 9H), 0.01 (s, 3H), −0.22 (s, 3H); ^{13}C NMR (75 MHz, $CDCl_3$) δ 141.0 (0), 129.9 (1), 128.0 (1), 127.7 (1), 127.3 (1), 79.5 (1), 76.7 (1), 25.8 (3), 18.1 (0), −4.5 (3), −5.1 (3); HRMS (ESI) calcd for $C_{30}H_{48}O_4Si_2Na$ $[M+Na]^+$: 551.2989, found: 551.3010; EIMS (%) *m/z* = 283 (4), 189 (4), 157 (56), 129 (16), 103 (22), 99 (100). Analytical data for diastereomer **11b**: ^{1}H NMR (300 MHz, $CDCl_3$) δ 7.33–7.17 (5H), 5.52 (dd, *J* = 2.6, 0.9, 1H), 4.38 (d, *J* = 6.6, 1 H), 4.03 (ddm, *J* = 6.0, 3.0, 1H), 2.74 (d, *J* = 3.4, 1H), 0.89 (s, 9H), 0.03 (s, 3H), −0.19 (s, 3H); ^{13}C NMR (75 MHz, $CDCl_3$) δ 141.0 (0), 130.3 (1), 128.0 (1), 127.7 (1), 127.1 (1), 79.0 (1), 76.4 (1), 25.8 (3), 18.1 (0), −4.6 (3), −5.1 (3).

Supporting Information

Supporting Information File 1

Experimental procedures and characterization data for starting materials which have previously not been described in the literature; representative illustrations for determination of conversions; copies of spectra for new compounds.
[http://www.beilstein-journals.org/bjoc/content/supplementary/1860-5397-6-136-S1.pdf]

Acknowledgements

We thank Umicore, Hanau (Germany) for a generous donation of various Umicore M olefin metathesis catalysts, including Umicore M2 and Umicore M31 used in this study.

References

1. Grubbs, R. H., Ed. *Handbook of metathesis;* Wiley-VCH: Weinheim, 2003.
2. Hérisson, J.-L.; Chauvin, Y. *Makromol. Chem.* **1971,** *141,* 161–176. doi:10.1002/macp.1971.021410112
3. Schrock, R. R.; Murdzek, J. S.; Bazan, G. C.; Robbins, J.; DiMare, M.; O'Regan, M. *J. Am. Chem. Soc.* **1990,** *112,* 3875–3886. doi:10.1021/ja00166a023
4. Fu, G. C.; Nguyen, S. T.; Grubbs, R. H. *J. Am. Chem. Soc.* **1993,** *115,* 9856–9857. doi:10.1021/ja00074a085
5. Hoveyda, A. H.; Schrock, R. R. *Chem.–Eur. J.* **2001,** *7,* 945–950. doi:10.1002/1521-3765(20010302)7:5<945::AID-CHEM945>3.0.CO;2-3
6. Dragutan, V.; Dragutan, I.; Delaude, L.; Demonceau, A. *Coord. Chem. Rev.* **2007,** *251,* 765–794. doi:10.1016/j.ccr.2006.09.002
7. Fürstner, A. *Angew. Chem., Int. Ed.* **2000,** *39,* 3013–3043.
8. Nguyen, S. T.; Johnson, L. K.; Grubbs, R. H.; Ziller, J. W. *J. Am. Chem. Soc.* **1992,** *114,* 3974–3975. doi:10.1021/ja00036a053
9. Schwab, P.; Grubbs, R. H.; Ziller, J. W. *J. Am. Chem. Soc.* **1996,** *118,* 100–110. doi:10.1021/ja952676d
10. Bruneau, C.; Dixneuf, P. H. *Acc. Chem. Res.* **1999,** *32,* 311–323. doi:10.1021/ar980016i
11. Harlow, K. J.; Hill, A. F.; Wilton-Ely, J. D. E. T. *J. Chem. Soc., Dalton Trans.* **1999,** 285–291.
12. Fürstner, A.; Liebl, M.; Hill, A. F.; Wilton-Ely, J. D. E. T. *Chem. Commun.* **1999,** 601–602. doi:10.1039/a900187e
13. Weskamp, T.; Kohl, F. J.; Herrmann, W. A. *J. Organomet. Chem.* **1999,** *582,* 362–365. doi:10.1016/S0022-328X(99)00163-1
14. Weskamp, T.; Schattenmann, W. C.; Spiegler, M.; Herrmann, W. A. *Angew. Chem., Int. Ed.* **1998,** *37,* 2490–2493. doi:10.1002/(SICI)1521-3773(19981002)37:18<2490::AID-ANIE2490>3.0.CO;2-X
15. Huang, J.; Stevens, E. D.; Nolan, S. P.; Petersen, J. L. *J. Am. Chem. Soc.* **1999,** *121,* 2674–2678. doi:10.1021/ja9831352
16. Scholl, M.; Ding, S.; Lee, C. W.; Grubbs, R. H. *Org. Lett.* **1999,** *1,* 953–956. doi:10.1021/ol990909q
17. Jafarpour, L.; Schanz, H.-J.; Stevens, E. D.; Nolan, S. P. *Organometallics* **1999,** *18,* 5416–5419. doi:10.1021/om990587u
18. Monsaert, S.; Drozdzak, R.; Dragutan, V.; Dragutan, I.; Verpoort, F. *Eur. J. Inorg. Chem.* **2008,** 432–440. doi:10.1002/ejic.200700879
19. Schmidt, B.; Hermanns, J. *Top. Organomet. Chem.* **2004,** *13,* 223–267.
20. Garber, S. B.; Kingsbury, J. S.; Gray, B. L.; Hoveyda, A. H. *J. Am. Chem. Soc.* **2000,** *122,* 8168–8179. doi:10.1021/ja001179g
21. Michrowska, A.; Bujok, R.; Harutyunyan, S.; Sashuk, V.; Dolgonos, G.; Grela, K. *J. Am. Chem. Soc.* **2004,** *126,* 9318–9325. doi:10.1021/ja048794v
22. Gessler, S.; Randl, S.; Blechert, S. *Tetrahedron Lett.* **2000,** *41,* 9973–9976. doi:10.1016/S0040-4039(00)01808-6
23. Wakamatsu, H.; Blechert, S. *Angew. Chem., Int. Ed.* **2002,** *41,* 2403–2405. doi:10.1002/1521-3773(20020703)41:13<2403::AID-ANIE2403>3.0.CO;2-F
24. Connon, S. J.; Blechert, S. *Angew. Chem., Int. Ed.* **2003,** *42,* 1900–1923. doi:10.1002/anie.200200556
25. Sanford, M. S.; Love, J. A.; Grubbs, R. H. *Organometallics* **2001,** *20,* 5314–5318. doi:10.1021/om010599r
26. Love, J. A.; Sanford, M. S.; Day, M. W.; Grubbs, R. H. *J. Am. Chem. Soc.* **2003,** *125,* 10103–10109. doi:10.1021/ja027472t
27. Zhang, W.-Z.; He, R.; Zhang, R. *Eur. J. Inorg. Chem.* **2007,** 5345–5352. doi:10.1002/ejic.200700631

28. Williams, J. E.; Harner, M. J.; Sponsler, M. B. *Organometallics* **2005,** *24,* 2013–2015. doi:10.1021/om050040h
29. Bantreil, X.; Randall, R. A. M.; Slawin, A. M. Z.; Nolan, S. P. *Organometallics* **2010,** *29,* 3007–3011. doi:10.1021/om100310f
30. Choi, T.-L.; Grubbs, R. H. *Angew. Chem., Int. Ed.* **2003,** *42,* 1743–1746. doi:10.1002/anie.200250632
31. P'Pool, S. J.; Schanz, H.-J. *J. Am. Chem. Soc.* **2007,** *129,* 14200–14212. doi:10.1021/ja071938w
32. Kang, B.; Kim, D.; Do, Y.; Chang, S. *Org. Lett.* **2003,** *5,* 3041–3043. doi:10.1021/ol035014z
33. Love, J. A.; Morgan, J. P.; Trnka, T. M.; Grubbs, R. H. *Angew. Chem., Int. Ed.* **2002,** *41,* 4035–4037. doi:10.1002/1521-3773(20021104)41:21<4035::AID-ANIE4035>3.0.CO;2-I
34. Bai, C.-X.; Zhang, W.-Z.; He, R.; Lu, X.-B.; Zhang, Z.-Q. *Tetrahedron Lett.* **2005,** *46,* 7225–7228. doi:10.1016/j.tetlet.2005.08.062
35. Bai, C.-X.; Lu, X.-B.; He, R.; Zhang, W.-Z.; Feng, X.-J. *Org. Biomol. Chem.* **2005,** *3,* 4139–4142. doi:10.1039/b510776h
36. Ung, T.; Hejl, A.; Grubbs, R. H.; Schrodi, Y. *Organometallics* **2004,** *23,* 5399–5401. doi:10.1021/om0493210
37. Monsaert, S.; Vila, A. L.; Drozdzak, R.; van der Voort, P.; Verpoort, F. *Chem. Soc. Rev.* **2009,** *38,* 3360–3372. doi:10.1039/b902345n
38. Clavier, H.; Petersen, J. L.; Nolan, S. P. *J. Organomet. Chem.* **2006,** *691,* 5444–5447. doi:10.1016/j.jorganchem.2006.08.007
39. Boeda, F.; Clavier, H.; Nolan, S. P. *Chem. Commun.* **2008,** 2726–2740. doi:10.1039/b718287b
40. Burtscher, D.; Lexer, C.; Mereiter, K.; Winde, R.; Karch, R.; Slugovc, C. *J. Polym. Sci., Part A: Polym. Chem.* **2008,** *46,* 4630–4635. doi:10.1002/pola.22763
41. Monsaert, S.; De Canck, E.; Drozdzak, R.; van der Voort, P.; Verpoort, F.; Martins, J. C.; Hendrickx, P. M. S. *Eur. J. Org. Chem.* **2009,** 655–665. doi:10.1002/ejoc.200800973
42. Schmidt, B. *Pure Appl. Chem.* **2006,** *78,* 469–476. doi:10.1351/pac200678020469
43. Samojłowicz, C.; Bieniek, M.; Zarecki, A.; Kadyrov, R.; Grela, K. *Chem. Commun.* **2008,** 6282–6284. doi:10.1039/b816567j
44. Rost, D.; Porta, M.; Gessler, S.; Blechert, S. *Tetrahedron Lett.* **2008,** *49,* 5968–5971. doi:10.1016/j.tetlet.2008.07.161
45. Dinger, M. B.; Mol, J. C. *Organometallics* **2003,** *22,* 1089–1095. doi:10.1021/om0208218
46. Dinger, M. B.; Mol, J. C. *Eur. J. Inorg. Chem.* **2003,** 2827–2833. doi:10.1002/ejic.200200702
47. Schmidt, B. *Eur. J. Org. Chem.* **2004,** 1865–1880. doi:10.1002/ejoc.200300714
48. Miao, X.; Fischmeister, C.; Bruneau, C.; Dixneuf, P. H. *ChemSusChem* **2008,** *1,* 813–816. doi:10.1002/cssc.200800074
49. Adjiman, C. S.; Clarke, A. J.; Cooper, G.; Taylor, P. C. *Chem. Commun.* **2008,** 2806–2808. doi:10.1039/b802921k
50. Schmidt, B.; Geißler, D. *ChemCatChem* **2010,** *2,* 423–429. doi:10.1002/cctc.200900282
51. Schmidt, B.; Kunz, O.; Biernat, A. *J. Org. Chem.* **2010,** *75,* 2389–2394. doi:10.1021/jo1002642
52. Forman, G. S.; McConnell, A. E.; Tooze, R. P.; van Rensburg, W. J.; Meyer, W. H.; Kirk, M. M.; Dwyer, C. L.; Serfontein, D. W. *Organometallics* **2005,** *24,* 4528–4542. doi:10.1021/om0503848
53. Imahori, T.; Ojima, H.; Tateyama, H.; Mihara, Y.; Takahata, H. *Tetrahedron Lett.* **2008,** *49,* 265–268. doi:10.1016/j.tetlet.2007.11.098
54. Imahori, T.; Ojima, H.; Yoshimura, Y.; Takahata, H. *Chem.–Eur. J.* **2008,** *14,* 10762–10771. doi:10.1002/chem.200801439
55. Mori, M.; Sakakibara, N.; Kinoshita, A. *J. Org. Chem.* **1998,** *63,* 6082–6083. doi:10.1021/jo980896e
56. Schmidt, B.; Staude, L. *J. Org. Chem.* **2009,** *74,* 9237–9240. doi:10.1021/jo9018649
57. Schmidt, B.; Nave, S. *Chem. Commun.* **2006,** 2489–2491. doi:10.1039/b604359c
58. Schmidt, B.; Nave, S. *Adv. Synth. Catal.* **2007,** *349,* 215–230. doi:10.1002/adsc.200600473
59. Lombardo, M.; Licciulli, S.; Trombini, C. *Tetrahedron: Asymmetry* **2004,** *15,* 289–292. doi:10.1016/j.tetasy.2003.10.026
60. Gurjar, M. K.; Yakambram, P. *Tetrahedron Lett.* **2001,** *42,* 3633–3636. doi:10.1016/S0040-4039(01)00449-X
61. Djigoué, G. B.; Meier, M. A. R. *Appl. Catal., A* **2009,** *368,* 158–162. doi:10.1016/j.apcata.2009.08.025
62. Schmidt, B. *J. Chem. Soc., Perkin Trans. 1* **1999,** 2627–2638. doi:10.1039/a902961c
63. Sawant, K. B.; Jennings, M. P. *J. Org. Chem.* **2006,** *71,* 7911–7914. doi:10.1021/jo061296f
64. Ghosh, A. K.; Cappiello, J.; Shin, D. *Tetrahedron Lett.* **1998,** *39,* 4651–4654. doi:10.1016/S0040-4039(98)00887-9

License and Terms

Beilstein Journal of Organic Chemistry

ROMP-Derived cyclooctene-based monolithic polymeric materials reinforced with inorganic nanoparticles for applications in tissue engineering

Franziska Weichelt[1], Solvig Lenz[2], Stefanie Tiede[2], Ingrid Reinhardt[1], Bernhard Frerich[*2,§] and Michael R. Buchmeiser[*3,4,¶]

Full Research Paper

Open Access

Address:
[1]Leibniz-Institut für Oberflächenmodifizierung e. V. (IOM), Permoserstrasse 15, D-04318 Leipzig, Germany, [2]Klinik und Poliklinik für Mund-, Kiefer- und Plastische Gesichtschirurgie, Universität Rostock, Schillingallee 35, D-18057 Rostock, Germany, [3]Institut für Polymerchemie, Lehrstuhl für Makromolekulare Stoffe und Faserchemie, Universität Stuttgart, Pfaffenwaldring 55, D-70569 Stuttgart, Germany and [4]Institut für Textilchemie und Chemiefasern, Körschtalstrasse 26, D-73770 Denkendorf, Germany

Email:
Bernhard Frerich[*] - bernhard.frerich@med.uni-rostock.de;
Michael R. Buchmeiser[*] - michael.buchmeiser@ipoc.uni-stuttgart.de

* Corresponding author
§ Tel.: +49 (0) 381 494 6550; Fax: +49 (0) 381 494 6698
¶ Tel: +49 (0) 711 685 64075; Fax: +49 (0) 711 685 64050

Keywords:
hybrid materials; monoliths; nanoparticles; ring-opening metathesis polymerization (ROMP); tissue engineering

Beilstein J. Org. Chem. **2010,** *6,* 1199–1205.
doi:10.3762/bjoc.6.137

Received: 20 August 2010
Accepted: 12 November 2010
Published: 17 December 2010

Guest Editor: K. Grela

Abstract

Porous monolithic inorganic/polymeric hybrid materials have been prepared via ring-opening metathesis copolymerization starting from a highly polar monomer, i.e., *cis*-5-cyclooctene-*trans*-1,2-diol and a 7-oxanorborn-2-ene-derived cross-linker in the presence of porogenic solvents and two types of inorganic nanoparticles (i.e., $CaCO_3$ and calcium hydroxyapatite, respectively) using the third-generation Grubbs initiator $RuCl_2(Py)_2(IMesH_2)(CHPh)$. The physico-chemical properties of the monolithic materials, such as pore size distribution and microhardness were studied with regard to the nanoparticle type and content. Moreover, the reinforced monoliths were tested for the possible use as scaffold materials in tissue engineering, by carrying out cell cultivation experiments with human adipose tissue-derived stromal cells.

Introduction

Tissue engineering (TE), a sub-area of regenerative medicine, brings together diverse technologies and interdisciplinary fields such as biology, engineering, material and life sciences, polymer and inorganic chemistry [1-3]. Its general task is the development of functional substitutes for the replacement or restoration of tissue or organ function with scaffolds containing specific populations of living cells [4,5]. After the cultivation of cells on such biological substitutes, they are subsequently applied to living organisms, where they ideally should restore, maintain or improve tissue function or whole organs [2,3]. A challenging task in this context is the development of suitable scaffold materials, which can act as matrices for the delivery of the cells to defect sites, with desired properties such as adequate pore size and pore structure, biocompatibility, biodegradability or mechanical strength.

Due to their unitary porous structure and the ease of synthesis via polymerization or consolidation processes, monolithic materials were introduced into the field of TE some years ago [6,7]. Several studies have shown that the properties of the scaffold material, such as mechanical properties, porosity or surface structure, strongly affect the differentiation of mesenchymal stem cells (i.e., the formation of osseous, muscle or neural cells) and especially for the differentiation into osteoblasts, stiff materials are required [7-12]. Bone is a natural composite material, being composed of an inorganic compound (calcium hydroxyapatite) incorporated into an organic matrix (collagen) and thus resulting in a material, which possesses high stiffness and fracture toughness [13,14].

Ring-opening metathesis polymerization (ROMP) derived norborn-2-ene (NBE)-based monolithic materials have previously been successfully tested for both osseous and adipose cell growth [6]. However, it has also been reported that the mechanical properties, such as hardness, of such scaffold materials were quite low. Harder materials with a specific surface structure and porosity, however, would allow for the differentiation of mesenchymal stem cells into osteoblasts, and thus the development of scaffold materials for bone regeneration. Ideal biomaterials for bone TE should be non-immunogeneic, biodegradable, highly osteoinductive and provide mechanical support when needed [15]. As an alternative to poly(NBE)-based monoliths, we investigated the preparation of monolithic structures from a highly polar cyclooctene derivative. So far, ROMP-derived monolithic materials have successfully been applied to separation science as well as heterogeneous catalysis [16-18]. Generally, cyclooctene-derived monoliths differ from their NBE-based counterparts in that they are less prone to oxidation and display higher elastic moduli. With the aim to synthesize organic-inorganic monolithic hybrid materials for application as scaffold materials in TE with specific properties, e.g., high mechanical strength and biocompatibility, we report here ROMP-derived cyclooctene-based monoliths reinforced with two of the most frequently used inorganic materials in nature, i.e., calcite and calcium hydroxyapatite [19], respectively.

Results and Discussion

Synthesis of $CaCO_3$ and HAp

Nanosized calcium carbonate (**$CaCO_3$**) and calcium hydroxyapatite (**HAp**) were prepared by precipitation reactions in aqueous solution from $CaCl_2{\cdot}2H_2O$ and anhydrous Na_2CO_3, and from $CaCl_2{\cdot}H_2O$, H_3PO_4 and NH_4OH, respectively. For **$CaCO_3$**, scanning electron microscopic (SEM) images of the powders showed agglomerates of nanoparticles (~50–100 nm) and a rhombohedral calcite crystal structure was detected both by X-ray diffraction (XRD) and Raman measurements. Nanosized platelets with a thickness <20 nm were formed in the synthesis of **HAp** and exhibited a calcium phosphate hydroxide crystal structure again from XRD and Raman measurements (Figure 1).

Preparation and characterization of monolithic materials

Monolithic hybrid materials were then prepared via ROMP from *cis*-5-cyclooctene-*trans*-1,2-diol (**COE**), a 7-oxanorborn-2-ene-derived cross-linker (**CL**) and up to 12 wt % of the inorganic compounds in the presence of a microporogen (toluene) and a macroporogen (2-propanol) under phase separation conditions using the third-generation Grubbs initiator $RuCl_2(Py)_2(IMesH_2)(CHPh)$ ($IMesH_2$ = 1,3-dimesitylimidazolin-2-ylidene, Py = pyridine) (Scheme 1, Table 1).

Table 1: Compositions of *cis*-5-cyclooctene-*trans*-1,2-diol (**COE**)-based monoliths.

CL[a]	COE[a]	Toluene[a]	2-Propanol[a]	Nanoparticles[a]
22.5	22.5	9	46	—
26	26	9	33	6 ($CaCO_3$)
24	24	9	31	12 ($CaCO_3$)
26	26	9	33	6 (HAp)
24	24	9	31	12 (HAp)

[a]in [wt %]; 0.07 wt % of initiator were used throughout.

cis-5-Cyclooctene-*trans*-1,2-diol was chosen as a highly polar monomer, which should together with the 7-oxanorborn-2-ene-based cross-linker form a polar polymeric matrix that facilitates the incorporation and homogeneous distribution of the polar nanoparticles. The cross-linker itself has already been reported

to be biocompatible [7]. SEM images of the nanoparticle-reinforced monolithic materials revealed an increase of the pore sizes with increasing nanoparticle content. An increase of the pore size from 10–30 µm (for monoliths without any inorganic component) up to 25–70 µm was observed with the addition of 12 wt % **$CaCO_3$**, while pores up to 130–450 µm were formed using 12 wt % nano-sized **HAp** (Figure 1). Thus, as reported previously [20], the inorganic nanoparticles serve as macroporogens in the phase-separation-triggered synthesis of the monolithic matrix. The adjustment of the pore size by variation

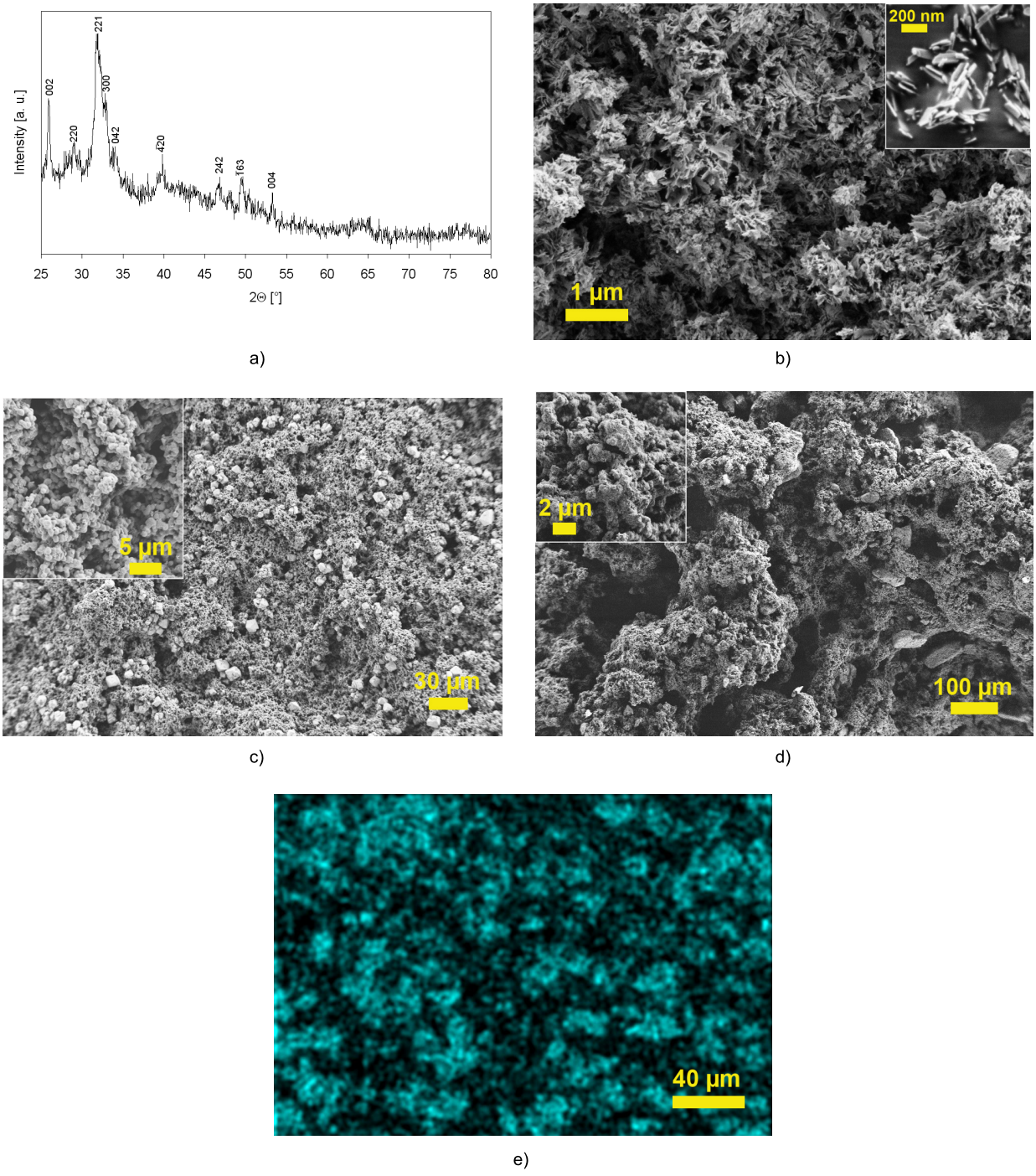

Figure 1: Nanoscale **HAp**: calcium phosphate hydroxide ($Ca_5(PO_4)_3OH$) as evidenced by XRD measurements (a), SEM picture of the nanoparticles (b), structures of **COE**-derived monoliths containing 12 wt % **$CaCO_3$** (c) and 12 wt % **HAp** (d), and EDX-measurements of a monolith containing 12 wt % **$CaCO_3$** (Ca-mapping) (e).

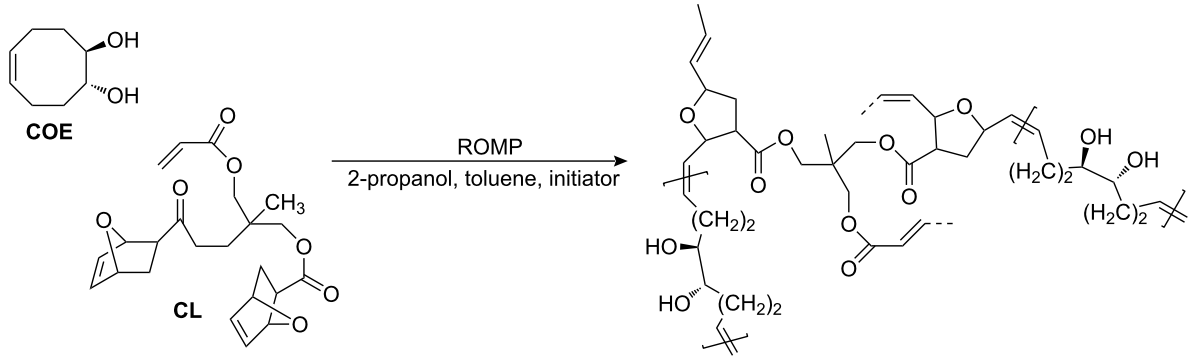

Scheme 1: ROMP-based synthesis of *cis*-5-cyclooctene-*trans*-1,2-diol based polymeric monolithic scaffolds.

of the nanoparticle content and type is advantageous and may allow for an alleviated cell attachment as well as ingrowth of living cells on the scaffold materials. Due to the OH groups present at its surface, **HAp** is more polar than **$CaCO_3$** and thus affects the pore formation process more strongly, resulting in even larger pore size. Energy dispersive X-ray mapping (EDX) revealed a homogeneous and non-aggregated distribution of **$CaCO_3$** in the polymeric matrix (Figure 1). In contrast, agglomerates of **HAp** up to 100 µm in size were found for **HAp**-based monoliths and also the distribution of the inorganic compound was less homogeneous, supporting the explanation of polar interactions between organic components and **HAp** in the polymerization mixture. Nitrogen adsorption measurements of the monolithic powders confirmed their highly porous structure, showing specific surface areas of between 2 m^2/g (unfilled and **$CaCO_3$**-reinforced monoliths) and 43 m^2/g (**HAp**-reinforced monoliths). The microhardness of the monolithic materials was determined with a Vickers hardness measurement device. In comparison to the microhardness of unfilled **COE**-based monoliths (5.8 N/mm^2), a more than 2-fold increase of the microhardness was observed with the addition of 6 wt % **$CaCO_3$** (16.3 N/mm^2) and **HAp** (12.4 N/mm^2), which decreased with the addition of 12 wt % **$CaCO_3$** (4.5 N/mm^2) and **HAp** (8.1 N/mm^2), respectively. The decrease of the microhardness with increasing nanoparticle content is attributed to the increase of pore size and porosity as explained above. Thus, with the addition of inorganic components, the microhardness of **COE**-based monoliths could efficiently be increased, however, the content of nanoparticles must not be too high, otherwise the effect of the larger pore size and porosity becomes dominant and the microhardness decreases. A decrease of the compressibility, i.e., an increase in the compressive force-compression (CF-C) ratio of 56% was observed for reinforcement with the addition of 12 wt % **$CaCO_3$** (1.08 MPa for reinforced monolith vs 0.62 MPa for unmodified monolith). Thus, **$CaCO_3$**-reinforced monoliths were more resistant to the pressure applied. In contrast, a strong reduction of the CF-C ratio (0.03 MPa) was observed on reinforcement with 12 wt % **HAp**, verifying a high

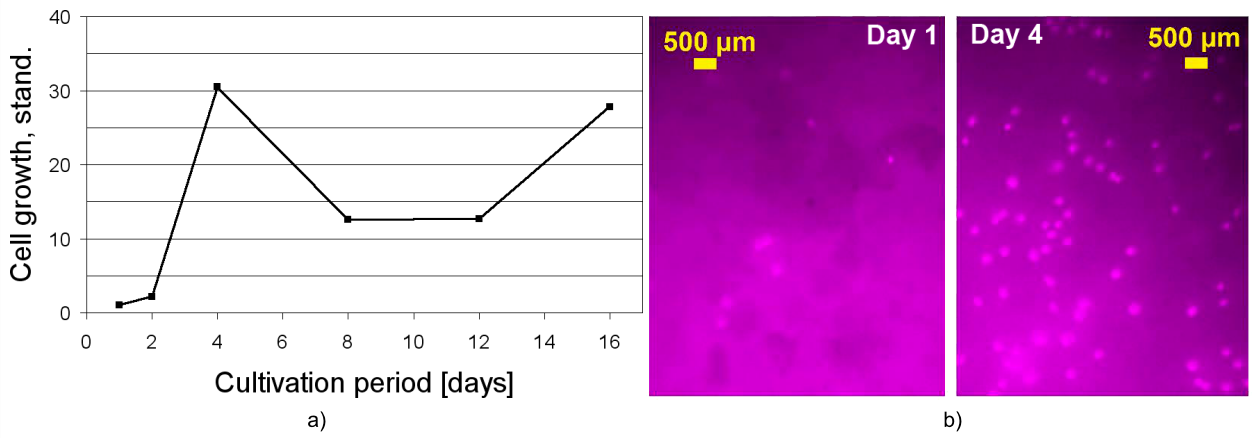

Figure 2: (a) Cell growth of human adipose tissue-derived stromal cells. Each data point is the average of 12 data points. (b) Fluorescence microscopy images of living cells after one and four days of cultivation; cells (human adipose tissue-derived stem cells) grown on a **COE**-based scaffold reinforced with 12 wt % **$CaCO_3$**.

compressibility of the **HAp**-based monoliths at simultaneously high microhardness.

Cell cultivation experiments

After careful washing and drying, the monolithic materials were cut into discs ~1–2 mm in height and ~10 mm in diameter and subsequently sterilized via γ-irradiation. Thereafter, these monolith scaffolds were seeded with human adipose tissue-derived stromal cells (hATSCs). Proliferation of the cells was monitored up to the 16th day (Figure 2).

After placing the sterilized discs into 24-well plates, the culture medium was added and the samples were seeded with hATSCs with a density of 20,000 cells/cm^2. Since only a part of the cells settled on the monolithic material, with the other part remaining in the surrounding culture medium, the cell number counted after the first day of cultivation was set as starting value for the proliferation curve. The determined cell numbers of the following days of cultivation were then divided by the starting value, in order to be able to compare the cell growth on different monolithic compositions. As it can be seen, a continuous increase of the cell number was observed up to the fourth day of proliferation, resulting in an increase of the cell number by a factor of 30 (709 cells/cm^2 after day 1 vs 21,615 cells/cm^2 after day 4). After the fourth day of proliferation the seeded scaffolds were transferred into 6-well plates, which probably affected the cell growth, and explains the decrease of the cell number between the fourth and eighth day of cultivation. Thereafter, proliferation continued with an increase of the cell number after the eighth day of cultivation. These data indicate a good biocompatibility of the monolithic hybrid support as well as sufficient cell adhesion on the monolithic material.

Conclusion

COE-based monolithic scaffolds have been prepared via ROMP in the presence of two different types of inorganic nanoparticles. It was shown that variation of both the nanoparticle type and content affected the pore size of the monoliths, i.e., the pore size was the larger, the higher the content of the inorganic component. In addition, the mechanical properties of the monolithic structures could be modified with the addition of inorganic components (calcium carbonate and calcium hydroxyapatite, respectively). Preliminary cell cultivation experiments showed that the prepared monolithic hybrid materials can be cultivated with human adipose tissue-derived stromal cells. Current work focuses on the biodegradability of the novel scaffolds under physiological conditions.

Experimental

IR spectra were recorded on a Bruker Vector 22 using ATR technology. Raman spectra were recorded on a Bruker RFS 100. Scanning electron microscopic (SEM) images were obtained on a Zeiss Ultra 55 field-emission (FEG) SEM device (Carl Zeiss SMT, Germany) at 0.6 keV for **$CaCO_3$** and **HAp** powders and 1.0 keV for the monoliths. Powder X-ray diffraction (XRD) was performed on a Philips X'Pert wide-angle diffractometer with slit optics, Cu K_α radiation (λ = 154 nm) and Ni K_β filter. The powder was applied to the specimen holder using double faced-adhesive tape and the upper site was covered with a thin layer of the powder. Measurements were carried out at a voltage of 40 kV and a current of 30 mA in the 2Θ-range of 20–80° with a step size of 0.05 and 1.00 seconds per step. The microhardness was measured on a Fischerscope H 100 (Helmut Fischer GmbH + Co. KG, Germany). A load of 100 mN was applied on the sample for 20 s. For the determination of the Martens hardness, a Vickers diamond indenter was used. Ten measurements were made to get an average for the sample. A Sonics Vibra-Cell Ultrasonic Processor (Sonics & Materials, Inc., Newtown, USA) was used for sonication. The compressibility of the monoliths was tested at a Z 1120 zwicki (Zwick/Roell, Germany). The diameter of the specimens was dependent on monomer and nanoparticle content (~0.8–1.3 cm), the average height was 4 mm. The traverse was applied with a test rate of 1 mm/min. Due to problems in sample preparation, a perfect sample geometry was difficult to adjust. Hence, it could not be completely excluded that stresses during the compressibility measurements were exclusively induced by the applied pressure of the traverse, but could also arise due to inhomogeneities (porosity, microcracks) within the monoliths. Therefore, the compressibility here was defined as the compressive force-compression ratio (CF-C ratio) applied to the cross-sectional area.

$CaCl_2{\cdot}2H_2O$ (99%) and NH_4OH (aqueous 26 wt % solution) were obtained from Riedel-de Haën. Anhydrous Na_2CO_3 (99%), anhydrous Na_2SO_4 (99%), $NaHCO_3$ (99+%), ethyl vinyl ether (99%, stabilized), 1,1,1-tris(hydroxymethyl)ethane (97%) and 2-propanol (99.5%) were obtained from Acros Organics (Germany). NaOH (≥98%), CH_3OH (99.8%) and H_3PO_4 (85%) were obtained from Fluka (Germany). $CHCl_3$ (99.8%), dimethyl sulfoxide (DMSO, 99.9%), tetrahydrofuran (THF, 99.0%) and CH_2Cl_2 (≥99.8%) were obtained from Merck. Norborn-2-ene (99%) was obtained from Aldrich (Germany). Diethyl ether (99.9%), toluene (technical) and H_2SO_4 (95%) were obtained from BDH Prolabo (VWR, Germany). The cross-linker (**CL**) [6,7], *cis*-5-cyclooctene-*trans*-1,2-diol (**COE**) [21] and calcium carbonate (**$CaCO_3$**) [22] were prepared according to literature procedures.

HAp: $CaCl_2{\cdot}2H_2O$ (13.26 g; 90.2 mmol) was dissolved in 900 mL of water. H_3PO_4 (85 wt % in water; 6.22 g; 53.9 mmol) was added and the solution heated to 90 °C. NH_4OH (26 wt % in

water) was added to give a pH of 9 and a white precipitate formed. The dispersion was cooled to room temperature, the precipitate collected by centrifugation and thoroughly washed with water. Finally, the powder was dried at 100 °C overnight. Yield: 6.41 g (71%). FT-IR (ATR mode) [20,23]: 3566 (w), 3221 (w), 1635 (w), 1402 (w, $\nu_{(CO3)2-}$), 1086 (m, $\nu_{(PO4)3-}$), 1014 (s, $\nu_{(PO4)3-}$), 960 (m, $\nu_{(PO4)3-}$), 866 (w) cm^{-1}. Raman [24]: 429 (w, $\nu_{(PO4)3-}$), 587 (w, $\nu_{(PO4)3-}$), 961 (s, $\nu_{(PO4)3-}$), 1044 (w, $\nu_{(PO4)3-}$), 1073 (w, $\nu_{(PO4)3-}$) cm^{-1}. XRD: Calcium phosphate hydroxide ($Ca_5(PO_4)_3OH$, monoclinic; ref. card: 76-0694).

Synthesis of monolithic scaffold materials [6,7]

Two solutions, A and B, were prepared and chilled to 0 °C. Solution A consisted of *cis*-5-cyclooctene-*trans*-1,2-diol, the CL, the macroporogen (2-propanol) and the inorganic filler (**$CaCO_3$** and **HAp**, respectively; 0–12 wt %). Solution B was obtained by dissolving $RuCl_2(Py)_2(IMesH_2)(CHPh)$ ($IMesH_2$ = 1,3-dimesitylimidazolin-2-ylidene, Py = pyridine; 0.07 wt %) in the microporogen (toluene, 9 wt %). Solutions A and B were mixed and stirred for a few seconds. The polymerization mixture was poured into 1 × 5 cm plastic devices. Polymer formation occurred within 12 hours in air. The monoliths were extensively washed with a mixture of $CHCl_3$, DMSO and ethyl vinyl ether (2:40:28 wt %). Finally, they were washed with MeOH, dried in vacuo and cut into 1 × 1.5 cm pieces. A summary of the compositions is given in Table 1.

Cultivation of adipose tissue-derived stromal cells

The harvesting and cultivation of human adipose tissue-derived stromal cells (hATSCs) has been previously described [25,26]. Briefly, small pieces of subcutaneous adipose tissue (<0.5 cm^3) from the lateral thigh region were collected during elective surgery in the Department of Oral and Maxillofacial Surgery of the University of Rostock. The adipose tissue was minced with sterile scissors and subjected to collagenase digestion (collagenase type II, Boehringer, Mannheim, Germany). The suspension was centrifuged (300 g, 10 min) and plated in tissue culture flasks (Greiner, Frickenhausen, Germany). Cells were cultured in a 5% humidified CO_2 atmosphere at 37 °C. Culture medium ("standard medium": Iscove's MDM / HAM F12 1:1, supplemented with 10% neonatal calf serum (NCS), all from Life Technology, Paisley, Scotland) was changed every second day. The stem cell character of these cells has been previously demonstrated by successful osteogenic, adipogenic and smooth muscle differentiation [6,7,20,27]. The cells were split in a 1:4 ratio and amplified up to the third passage.

Sterilization of the samples was accomplished with γ-irradiation with the aid of a ^{60}Co-γ-source at the Leibniz-Institute of Surface Modification (IOM, Leipzig, Germany) on a rotating table at a dose rate of 0.79 kGy/h. The dose rate was determined by Fricke-dosimetry. The reliability of the dose determination was checked against IAEA-alanine dosimeters resulting in an overall accuracy of the dose measurements of ±5%. The total dose applied was 24 kGy.

Cell proliferation assay

Tests were made in 24-well-plates and 6-well-plates with a well diameter of 2 and 3.5 cm, respectively. Sterile discs of the monolithic test material (1–2 mm in height) were placed into the wells and covered with standard cell culture medium. After incubation in a humidified atmosphere at 37 °C for two days, the medium was removed and the discs were seeded. Cultures of third passage hATSC of three individuals were pooled for the experiment and seeded onto the discs at a density of 20,000 cells per cm^2. After 1, 2, 4, 8, 12 and 16 days of culture, the discs were harvested and fixed in 4 wt % formaldehyde in PBS (phophate buffered saline, Serva, Heidelberg, Germany) for 20 minutes. Discs were incubated in 4',6-diamidino-2-phenylindole (DAPI, Sigma-Aldrich, Steinheim, Germany) solution and examined under a fluorescent microscope (Axiovert 25, Zeiss, Jena, Germany). In every specimen, cells were counted in six fields and averaged.

Supporting Information

Supporting Information File 1

IR and Raman spectra of HAp and $CaCO_3$.
[http://www.beilstein-journals.org/bjoc/content/supplementary/1860-5397-6-137-S1.pdf]

Acknowledgements

This work was supported by the *Graduate School of Excellence "BuildMoNa", University of Leipzig, Germany*. We wish to thank A. Prager for recording of the SEM and EDX pictures, Dr. M. Lorenz and Dr. W. Fritzsche for support during XRD measurements and Dr. W. Knolle for sterilization of the samples.

References

1. Puppi, D.; Chiellini, F.; Piras, A. M.; Chiellini, E. *Prog. Polym. Sci.* **2010,** *35,* 403–440. doi:10.1016/j.progpolymsci.2010.01.006
2. Marler, J. J.; Upton, J.; Langer, R.; Vacanti, J. P. *Adv. Drug Delivery Rev.* **1998,** *33,* 165–182. doi:10.1016/S0169-409X(98)00025-8
3. Nerem, R. M. *Ann. Biomed. Eng.* **1991,** *19,* 529–545. doi:10.1007/BF02367396
4. Langer, R.; Vacanti, J. P. *Science* **1993,** *260,* 920–926. doi:10.1126/science.8493529

5. Cortesini, R. *Transplant Immunol.* **2005,** *15,* 81–89. doi:10.1016/j.trim.2005.09.013
6. Buchmeiser, M. R. *J. Polym. Sci., Part A: Polym. Chem.* **2009,** *47,* 2219–2227. doi:10.1002/pola.23328
7. Löber, A.; Verch, A.; Schlemmer, B.; Höfer, S.; Frerich, B.; Buchmeiser, M. R. *Angew. Chem.* **2008,** *120,* 9278–9281. doi:10.1002/ange.200801872
   Angew. Chem., Int. Ed. **2008,** *47,* 9138–9141. doi:10.1002/anie.200801872.
8. Engler, A. J.; Sen, S.; Sweeney, H. L.; Discher, D. E. *Cell* **2006,** *126,* 677–689. doi:10.1016/j.cell.2006.06.044
9. Benoit, D. S. W.; Schwartz, M. P.; Durney, A. R.; Anseth, A. S. *Nat. Mater.* **2008,** *7,* 816–823. doi:10.1038/nmat2269
10. Lenhert, S.; Meier, M.-B.; Meyer, U.; Chi, L.; Wiesmann, H. P. *Biomaterials* **2005,** *26,* 563–570. doi:10.1016/j.biomaterials.2004.02.068
11. Liao, H.; Andersson, A.-S.; Sutherland, D.; Petronis, S.; Kasemo, B.; Thomsen, P. *Biomaterials* **2003,** *24,* 649–654. doi:10.1016/S0142-9612(02)00379-4
12. Gray, C. *Tissue Eng.* **1998,** *4,* 315–323. doi:10.1089/ten.1998.4.315
13. Weiner, S.; Wagner, H. D. *Annu. Rev. Mater. Sci.* **1998,** *28,* 271–298. doi:10.1146/annurev.matsci.28.1.271
14. Dorozhkin, S. V.; Epple, M. *Angew. Chem., Int. Ed.* **2002,** *41,* 3130–3146. doi:10.1002/1521-3773(20020902)41:17<3130::AID-ANIE3130>3.0.CO;2-1
15. Du, C.; Cui, F. Z.; Zhu, X. D.; de Groot, K. *J. Biomed. Mater. Res.* **1999,** *44,* 407–415. doi:10.1002/(SICI)1097-4636(19990315)44:4<407::AID-JBM6>3.0.CO;2-T
16. Bandari, R.; Knolle, W.; Buchmeiser, M. R. *J. Chromatogr., A* **2008,** *1191,* 268–273. doi:10.1016/j.chroma.2007.11.016
17. Schlemmer, B.; Gatschelhofer, C.; Pieber, T. R.; Sinner, F. M.; Buchmeiser, M. R. *J. Chromatogr., A* **2006,** *1132,* 124–131. doi:10.1016/j.chroma.2006.07.058
18. Buchmeiser, M. R. *Bioorg. Med. Chem. Lett.* **2002,** *12,* 1837–1840. doi:10.1016/S0960-894X(02)00275-5
19. Krenkova, J.; Lacher, N. A.; Svec, F. *Anal. Chem.* **2010,** *82,* 8335–8341. doi:10.1021/ac1018815
20. Weichelt, F.; Frerich, B.; Lenz, S.; Tiede, S.; Buchmeiser, M. R. *Macromol. Rapid Commun.* **2010,** *31,* 1540–1545. doi:10.1002/marc.201000317
21. Bandari, R.; Prager-Duschke, A.; Kühnel, C.; Decker, U.; Schlemmer, B.; Buchmeiser, M. R. *Macromolecules* **2006,** *39,* 5222–5229. doi:10.1021/ma0609883
22. Wang, A.; Liu, D.; Yin, H.; Wu, H.; Wada, Y.; Ren, M.; Jiang, T.; Cheng, X.; Xu, Y. *Mater. Sci. Eng., C* **2007,** *27,* 865–869. doi:10.1016/j.msec.2006.10.001
23. Okada, M.; Furuzono, T. J. *Nanopart. Res.* **2007,** *9,* 807–815. doi:10.1007/s11051-006-9126-1
24. Silva, C. C.; Sombra, A. S. B. *J. Phys. Chem. Solids* **2004,** *65,* 1031–1033. doi:10.1016/j.jpcs.2003.10.071
25. Frerich, B.; Kurtz-Hoffmann, J.; Lindemann, N.; Müller, S. *Mund Kiefer GesichtsChir.* **2000,** *4* (Suppl. 2), S490–S495.
26. Frerich, B.; Lindemann, N.; Kurtz-Hoffmann, J.; Oertel, K. *Int. J. Oral Maxillofac. Surg.* **2001,** *30,* 414–420. doi:10.1054/ijom.2001.0130
27. Weinzierl, K.; Hemprich, A.; Frerich, B. J. *Cranio-Maxillofac. Surg.* **2006,** *34,* 466–471. doi:10.1016/j.jcms.2006.07.860

License and Terms

Beilstein Journal of Organic Chemistry

The allylic chalcogen effect in olefin metathesis

Yuya A. Lin and Benjamin G. Davis*

Review

Open Access

Address:
Department of Chemistry, University of Oxford, Chemistry Research Laboratory, 12 Mansfield Road, Oxford OX1 3TA, United Kingdom

Email:
Benjamin G. Davis* - ben.davis@chem.ox.ac.uk

* Corresponding author

Keywords:
allyl substituent effect; allyl sulfides; aqueous chemistry; olefin metathesis; protein modifications

Beilstein J. Org. Chem. **2010,** *6,* 1219–1228.
doi:10.3762/bjoc.6.140

Received: 13 September 2010
Accepted: 09 November 2010
Published: 23 December 2010

Guest Editor: K. Grela

Abstract

Olefin metathesis has emerged as a powerful tool in organic synthesis. The activating effect of an allylic hydroxy group in metathesis has been known for more than 10 years, and many organic chemists have taken advantage of this positive influence for efficient synthesis of natural products. Recently, the discovery of the rate enhancement by allyl sulfides in aqueous cross-metathesis has allowed the first examples of such a reaction on proteins. This led to a new benchmark in substrate complexity for cross-metathesis and expanded the potential of olefin metathesis for other applications in chemical biology. The enhanced reactivity of allyl sulfide, along with earlier reports of a similar effect by allylic hydroxy groups, suggests that allyl chalcogens generally play an important role in modulating the rate of olefin metathesis. In this review, we discuss the effect of allylic chalcogens in olefin metathesis and highlight its most recent applications in synthetic chemistry and protein modifications.

Review

Olefin metathesis is one of the most useful chemical transformations for forming carbon–carbon bonds in organic synthesis (Scheme 1) [1-4]. The broad utility of olefin metathesis is largely due to the exquisite selectivity and the high functional group compatibility of ruthenium-based metathesis catalysts. Catalysts such as **1**–**4** were found to tolerate many functional groups also found in biomolecules, including amides, alcohols, and carboxylic acids. In some cases, metathesis is even compatible with amine and sulfur containing building blocks. Together with its high stability in various media and excellent chemoselectivity, olefin metathesis has been used on peptide substrates for various applications in chemical biology [5-8]. The development of water-soluble metathesis catalysts [9-13] and other advances in aqueous metathesis such as the use of organic co-solvents [14,15], reviewed in detail recently [16], has enabled more recent examples of the reaction on protein substrates [17,18].

The outcome of olefin metathesis is sensitive to multiple factors, such as the nature of the catalyst, steric crowding around the alkene and the directing effects of nearby heteroatoms. These factors are of great importance, especially when optimizing reaction conditions for delicate natural product synthesis or protein modification. Interestingly, the activating effect of allylic heteroatoms, such as oxygen and sulfur in olefin substrates, has been observed in many examples and was found to play an important role for effective olefin metathesis in synthesis. These reports suggest that allylic chalcogens can modulate the rate of olefin metathesis, and their effects appear to be a general phenomenon in metathesis chemistry.

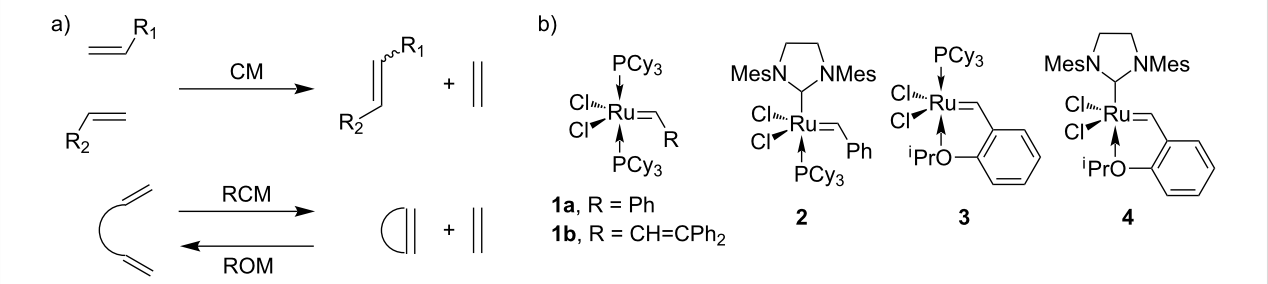

Scheme 1: a) Variation of olefin metathesis: CM = cross-metathesis; RCM = ring-closing metathesis; ROM = ring-opening metathesis. b) Conventional ruthenium-based metathesis catalysts.

In this review, we collect these reports and discuss the activating effect of allylic chalcogens, such as oxygen, sulfur and selenium, as well as their relative reactivity in olefin metathesis. The applications of the allylic chalcogen effect in protein modifications via olefin metathesis and the associated principles of cross-metathesis (CM) partner selection for reliable and efficient reaction on proteins are also highlighted.

The effect of allylic hydroxy groups in olefin metathesis

The activating effect of allylic hydroxy groups in ring-closing metathesis (RCM) was first identified by Hoye and Zhao in 1999 [19]. In this work, the influence of both the steric and electronic character of allylic substituent of linalool and related analogues in RCM was assessed. The free hydroxy group on linalool greatly enhanced RCM relative to the corresponding methyl ether or unsubstituted analogues (Figure 1). This activating effect was marked and initially surprising given that *tert*-butylethylene, containing a fully substituted allylic center, was reported to be almost inert to reaction with catalyst **1** [20].

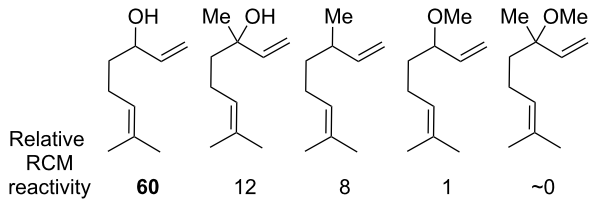

Figure 1: Allylic hydroxy activation in RCM [19].

A number of possible explanations for the rate acceleration due to allylic hydroxy groups in olefin metathesis have been proposed [19]. For example: The preassociation of the alcohol takes place at the ruthenium center through the rapid and reversible exchange of the alkoxy a for chloride ligand to give a complex such as **5**, or the exchange of the alcohol for a phosphine ligand exchange to generate **6**. The anionic complex **7** could also promote the reaction (Figure 2). Hydrogen bonding between the allylic hydroxy group on the substrate and the chloride ligand on the catalyst could also be another reason that favors subsequent metathesis events. Since the formation of **5** is unlikely under the reaction conditions reported by Hoye and Zhao [19], and species **6** and **7** would prevent metathesis proceeding further, the most plausible explanation for the positive effect of allylic hydroxy in olefin metathesis, bearing in mind that allyl ethers do not show such an effect, is through hydrogen-bonding to the catalyst.

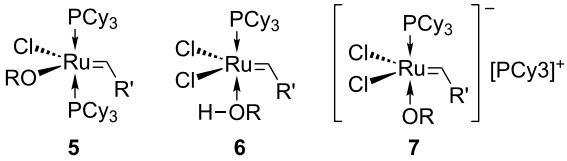

Figure 2: Possible complexes generated through preassociation of allylic alcohol with ruthenium.

Following Hoye and Zhao's observations, several organic chemists have further studied the effect of allylic alcohols and ethers in metathesis, and some have taken advantage of this activating effect for efficient and selective construction of complex molecules over the past 10 years. Here we outline a few pertinent and illustrative examples.

Schmidt prepared enantiomerically pure dihydropyrans and dihydrofurans bearing an unsaturated olefin tether based on a ring size-selectivity RCM reaction of a triene [21]. In this study, it was found that trienes containing a bulky hydroxy protecting group at the allylic position cyclized selectively to dihydrofurans, whereas the free alcohol yielded 6-membered rings with very high selection (Scheme 2).

This useful selectivity was attributed to the directing effect of the allylic hydroxy group. When the allylic alcohol was protected with a bulky group, the catalyst reacted preferentially at the less hindered allyl ether (pathway A where R′ = H). The formation of the 4,6-bicyclic intermediate is apparently disfa-

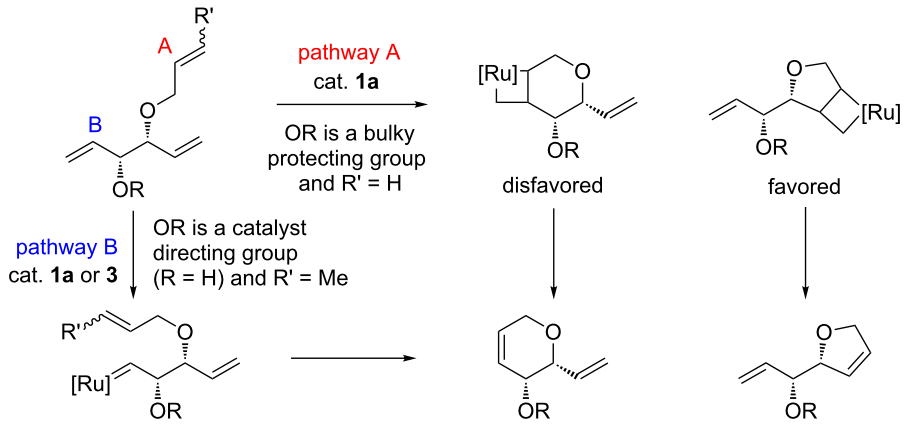

Scheme 2: The influence of different OR groups on ring size-selectivity [21].

vored with catalyst **1a** leading to largely the formation of the dihydrofuran product. It should be noted that when a more reactive second-generation catalyst (**2**) is used the selectivity for the dihydrofuran product is reduced. This selectivity was also found to be highly dependent on the size of protecting group. Significant decrease in ring-size selectivity was observed when smaller protecting groups, such as a methyl group, were used. Furthermore, when no protecting group was used (i.e., R = R′ = H, Scheme 2) the RCM reaction was unselective and resulted in a 1:1 mixture of 5- and 6-membered ring products. The selectivity for dihydropyran formation was therefore tuned by substitution at the terminal position of the allyl ether (e. g., R′ = Me), which directed the catalyst to react via pathway B. The authors were able to obtain significantly improved conversions and yields while maintaining high selectivity for dihydropyran by using, instead of **1a**, the Hoveyda–Grubbs first generation catalyst (**3**), where the catalytically active species is stabilized by a hemilabile benzylidene ligand. The activating effect of the allylic hydroxy group in RCM is further supported by the dramatic decrease in conversion when the free OH group was protected (i.e., R ≠ H, R′ = Me) in pathway B.

Pertinent examples have also emerged during target syntheses. In the synthesis of palmerolide A analogues by Nicolaou and co-workers, compounds **8a** and **9a** were found to undergo smooth macrocyclization via RCM, whereas **10a**, lacking the allylic hydroxy group, failed to form the desired macrocycle under the same conditions (Scheme 3) [22]. When **10a** was

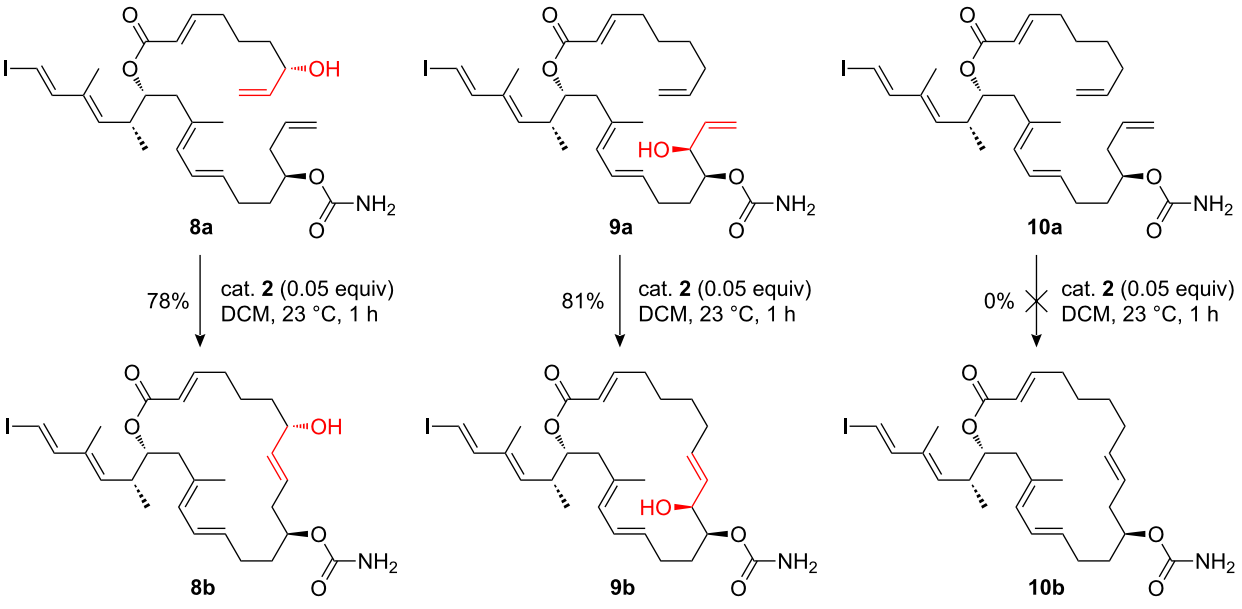

Scheme 3: Synthesis of palmerolide A precursors by Nicolaou et al. illustrates enhancement by an allylic hydroxy group in an RCM strategy [22].

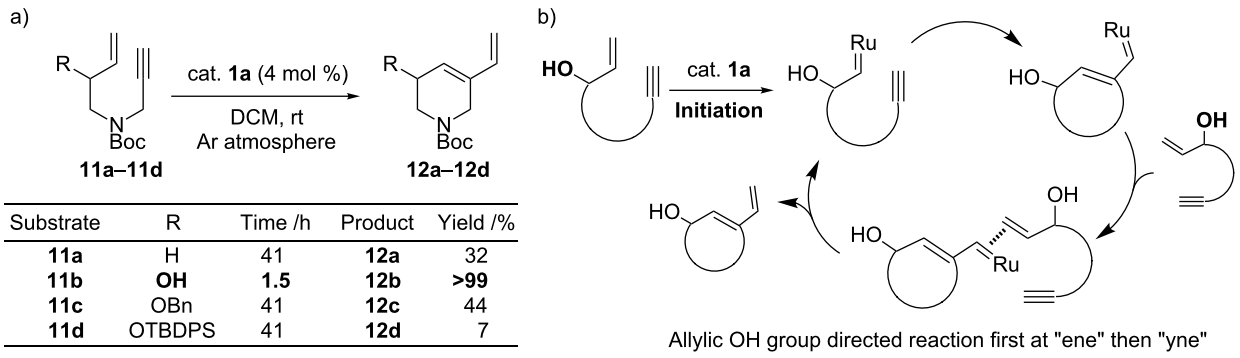

Substrate	R	Time /h	Product	Yield /%
11a	H	41	**12a**	32
11b	**OH**	**1.5**	**12b**	**>99**
11c	OBn	41	**12c**	44
11d	OTBDPS	41	**12d**	7

Scheme 4: a) Acceleration of ring-closing enyne metathesis by the allylic hydroxy group [23]. b) Proposed mode of action by the allylic hydroxy group in this reaction.

treated under more stringent conditions, decomposition and/or polymerization occurred. These observations suggest that the presence of an allylic hydroxy group in the molecule was crucial for enhancing the reactivity under the mild RCM conditions required by the potentially labile natural product scaffold.

Enhancement effects by an allylic hydroxy group have also been found in ring-closing enyne metathesis. Studies by Takahata et al. revealed that the ring-closing enyne metathesis of terminal alkynes containing an allylic hydroxy group proceeded smoothly without the ethylene atmosphere that is generally required to drive such reactions (Scheme 4a) [23]. Compound **11b** containing the allylic hydroxy group cyclized to the desired diene product **12b** with quantitative yield in 1.5 hours, whereas **11a**, without the allylic hydroxy group, required 41 hours to afford **12a** with a yield of only 32%. With the substituted allyl ethers **11c** and **11d**, reduction in yield was observed with increasing bulk of the protecting group (44% and 7%, respectively). Taking advantage of the allylic hydroxyl substituent effect, the authors synthesized (+)-isofagomine with the efficient ring-closing enyne metathesis of the acyclic starting material as the key cyclization step. Associated mechanistic studies suggested that the reaction proceeded via an "ene-then-yne" pathway, further suggesting that rate acceleration is likely due to the directing effect of the allylic hydroxy group on substrates (Scheme 4b).

As discussed earlier, the most likely explanation for the observed rate accelerations by the allylic hydroxy groups is hydrogen-bonding. Hoveyda and co-workers recently utilized hydrogen-bonding between the allylic hydroxy group and the ruthenium catalyst for stereoselective ring-opening cross-metathesis (ROCM) (Scheme 5) [24]. The activating effect from the allylic hydroxy group in metathesis is prominent in this example. The ROCM of cyclopropene **13** with enantiomerically enriched allylic alcohol **14a** is complete in 5 minutes (>98% conversion) with a high diastereomeric ratio (dr) (96:4) and *E*:*Z* selectivity (10:1) favoring the *S*,*R*-diasteromer. In contrast, the reaction of methyl ether **14b** and the methyl analogue **14c** is far less effective (51% and 56% conversion, respectively, in 18 hours) with lower and opposite stereoselectivity in favor of the *R*,*R*-diastereomers (Scheme 5a). The

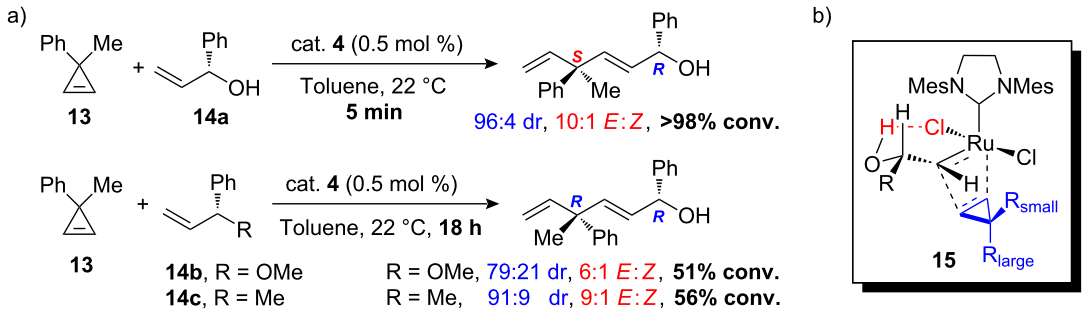

Scheme 5: a) Effect of the hydroxy group on the rate and steroselectivity of ROCM [24]. b) Proposed H-bonded ruthenium complex for stereoselective ROCM.

observed stereoselectivity can be explained by intramolecular hydrogen-bonding between the hydroxy group and the chloride ligand that results in a favored alkylidene intermediate complex with the substituted group of the stereogenic center situated away from the bulky mesityl groups. On coordination of the cyclopropene to the catalyst, the formation of a metallacyclobutane such as **15** with the larger R group pointing away from the main bulk of the catalyst is preferred (Scheme 5b). This intermediate then collapses to give the product with the observed stereoselectivity.

Sasaki and co-workers have also exploited both allylic and homoallylic hydroxy as directing groups in olefin metathesis for selective formation of key fragments in two recent examples of natural product syntheses. In the synthesis of aspergillide A, a key fragment **19** was synthesized by the CM reaction between diene **16** and methyl acrylate with very high yield [25]. Remarkably, none of the possible RCM products of the diene were detected. This observed chemoselectivity was ascribed to hydrogen-bonding of the allylic hydroxy to the chloride ligand of the catalyst resulting in an intermediate alkylidene **17** which has a conformation unfavorable for RCM. The open chain intermediate **17** favors CM, while RCM of **16**, must proceed via unfavorable higher energy conformations such as **18a**, generated by breaking hydrogen-bonding in **17**, and/or highly strained intermediate **18b**, if the reaction was to occur (Scheme 6). Similar directing effects of homoallylic alcohol in olefin metathesis have also been utilized in the concise synthesis of (+)-neopeltolide by the same group [26].

It should be noted that all of the illustrated examples regarding allyl hydroxy activation in olefin metathesis are predominantly secondary allyl alcohol substrates. The lack of primary allyl alcohol examples can be explained by the fact that, in general, these dehydrogenate at elevated temperature in the presence of ruthenium based metathesis catalysts. These in turn form ruthenium hydride species, which are effective catalysts for isomerization of alkene substrates [27,28].

The effect of other allylic chalcogens in olefin metathesis

Allyl sulfides are privileged substrates in olefin metathesis

While there are many examples of allylic alcohols and ethers in metathesis, examples with allyl sulfide substrates were until recently noticeably few. This is unsurprising since sulfur-containing molecules are often detrimental in many transition-metal-catalyzed transformations. Indeed, there have been several cases of olefin metatheses in which sulfides were problematic [29-32]. In our exploratory work in aqueous metathesis, cross-metathesis of unsaturated amino acids with allyl alcohol mediated by catalyst **4** was investigated. Unexpectedly, *S*-allylcysteine derivative **21a** was the only substrate that afforded a synthetically useful amount of CM product, whereas the reaction of the all carbon analogue homoallylglycine (**20**) and sulfide derivatives, *S*-butenyl and *S*-pentenyl cysteine (**21b** and **21c**, respectively), failed to work under identical conditions in aqueous media (Scheme 7a) [17]. In order to compare the relative CM reactivity between other allylic heteroatom derivatives,

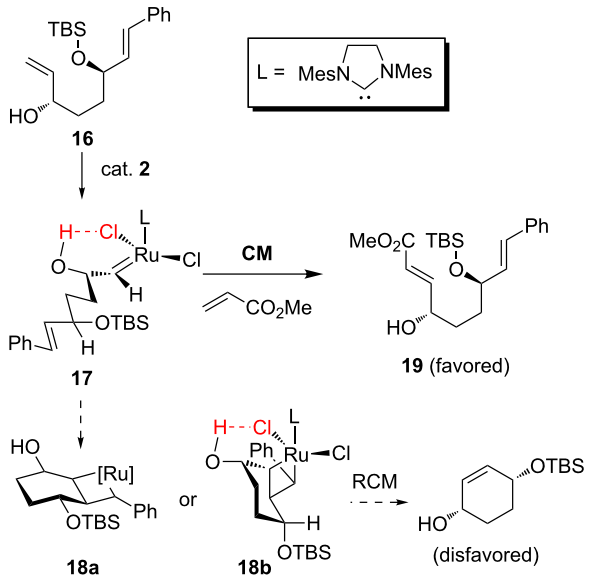

Scheme 6: Plausible explanation for chemoselective CM of diene **16** [25].

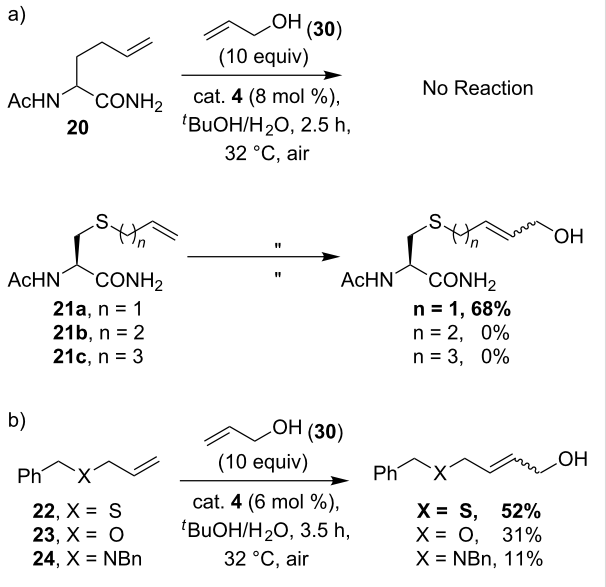

Scheme 7: a) Efficient cross-metathesis of *S*-allylcysteine [17]. b) Comparison of relative reactivity between allylic heteroatom derivatives.

further studies were carried out on the CM of allyl benzyl ether (**23**) and allyl dibenzylamine (**24**), but the allyl sulfide analogue **22** remained the most reactive substrate in aqueous media (Scheme 7b) [17].

We considered these observation in the light of the early work by Fürstner in the synthesis of macrocycles by RCM [33], in which a "carbonyl-relayed" mechanism was proposed as the explanation for favorable macrocyclization by RCM over oligomerization (Scheme 8a). Here, the coordination by the carbonyl oxygen to ruthenium brings the tethered alkene closer in proximity to the alkylidene allowing effective cyclization (Scheme 8b). In a similar manner, the rate enhancement caused by allyl sulfide could be explained with a sulfur relayed mechanism (Scheme 9a), where sulfur pre-coordination to the ruthenium center increases the effective concentration between the alkylidene and the alkene substrate. For the allyl sulfides this can occur without detrimental chelation, which is thought to be the case for butenyl and pentenyl sulfides (Scheme 9b). Grela and Lemcoff have synthesized the thio-derivatives of the Hoveyda-type catalyst and found that they initiate at much higher reaction temperature [34]. Their finding is in agreement with our observations of butenyl sulfides **21b**, which resulted in no productive CM at room temperature. This is presumably due to the formation of 5-membered stable chelates such as those depicted in Scheme 9b.

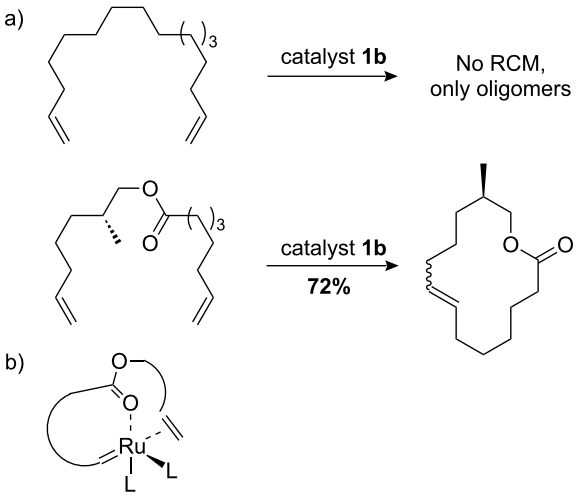

Scheme 8: a) Macrocycle synthesis by carbonyl-relayed RCM. b) Putative complex in carbonyl-relayed RCM [33].

In the few examples where allyl sulfides had previously been used in olefin metathesis [32,35,36], the prior focus of attention had been the tolerance of the catalyst for sulfur; the enhanced reactivity relative to other alkenes was apparently unnoticed. Our results showed that allyl sulfides are not simply tolerated as they can *enhance* the rate of olefin metathesis in a similar yet more effective way compared to allyl alcohols and ethers. This is likely due to the soft nature of sulfur as a Lewis base making it a better ligand for ruthenium than the oxygen atom in Hoveyda–Grubbs second-generation catalyst **4**. It is currently unclear whether a similar effect would be observed for phosphine-containing metathesis catalysts such as **1a** and **2**. As Hoye and others have realized, the presence of an allyl alcohol can also potentially accelerate catalyst decomposition [19,27,28]. The use of allyl sulfides in these systems is not exceptional, especially when aqueous solvents are used. However, the reaction with allyl sulfides proved to be sufficiently high in turnover frequency that it outcompetes catalyst decomposition, a likely key aspect of its success in water.

In recent work by Loh and co-workers, an allyl sulfide derivative was utilized in synthesis precisely for its enhanced metathesis reactivity [37]. Adopting the reaction conditions previously optimized by our group, compound **25** was efficiently function-

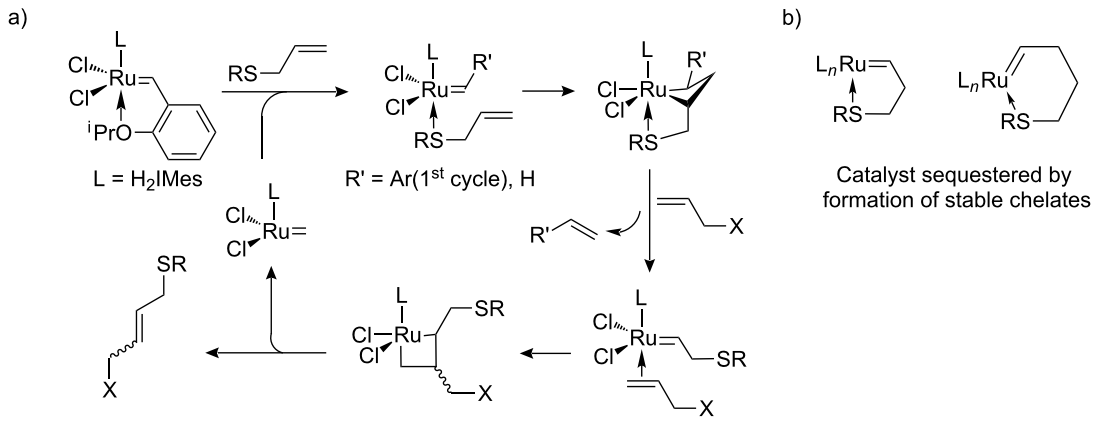

Scheme 9: a) Sulfur assisted cross-metathesis [17]. b) Putative unproductive chelates for larger ring sizes generated from butenyl or pentenyl sulfides.

alized with an allyl sulfide derived fluorescent probe **26** via CM in aqueous media to demonstrate the utility of functionalization of peptides and proteins by the Mukaiyama aldol reaction (Scheme 10).

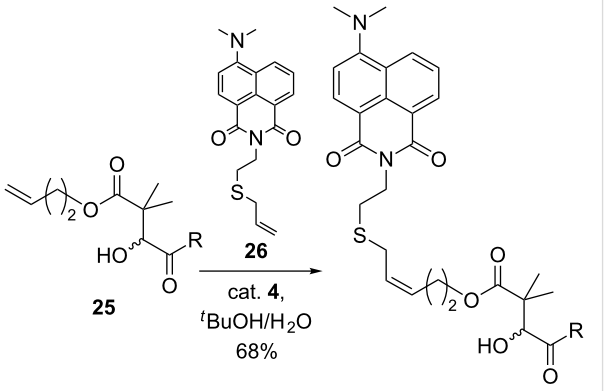

Scheme 10: Functionalization of Mukaiyama aldol product by CM in aqueous media [37].

Allyl selenides are superior metathesis substrates to allyl sulfides in aqueous cross-metathesis

Based on our results on allyl sulfides, alongside reports on the activating effect of allylic alcohols and ethers, the positive influence of allyl chalcogens on the rate of olefin metathesis is obvious. We naturally extended our investigation to allyl selenides, the next element in the group, expecting it to have a similar influence as oxygen and sulfur in metathesis. *Se*-allylselenocysteine derivative **28a** was tested along with the allyl sulfide analogue **27a** in model aqueous CM with allyl alcohol under identical reaction conditions. The allyl selenide **28a** was found to be more effective than the allyl sulfide case in CM, with respective yields of 72% and 56% (Scheme 11a). The CM reaction with a more complex and biochemically relevant carbohydrate substrate **29** was also examined. Indeed, the allyl selenide was overall more reactive than allyl sulfide with combined CM yields of 73% (CM and self-metathesis) and 45% (CM only, no self-metathesis observed), respectively (Scheme 11b) [38].

This further improvement in reactivity may be attributed to the increased softness of selenium which makes the coordination to ruthenium even more favorable than the sulfur in allyl sulfides. While, as a single example, Kotetsu and co-workers have synthesized selenium-containing bicyclic β-lactams via RCM of an allyl selenide derivative, enhanced reactivity was unnoticed [39]. With a better understanding of the allylic chalcogen effect, olefin metathesis has been further exploited in protein modifications. This is discussed next.

Applications in protein modifications

For the potential use of olefin metathesis in bioconjugation, the genetic incorporation of alkene containing amino acid residues has been well documented [18,40-44]. However, the reaction had been unsuccessful until the recent realization of the effect of allyl chalcogens, allyl sulfides especially, in enhancing the rate of aqueous metathesis [17].

Ai et al. have recently reported an example of RCM on a protein with genetically encoded alkene residues [18]. *O*-Crotylserine containing substituted allyl ether was chosen as the residue for incorporation for two reasons: The beneficial effect of allyl heteroatoms in metathesis, and the more water-stable propagating catalytic species generated from the substituted alkene compared with the methylidene that results from terminal olefins [45]. Indeed, the RCM on the double *O*-crotylserine mutant proceeded with near-complete conversion after 5 hours (Scheme 12).

Our group utilized the enhanced reactivity of allyl sulfides in aqueous cross-metathesis for application to protein modifications [17]. Very recently, with an aim to develop olefin meta-

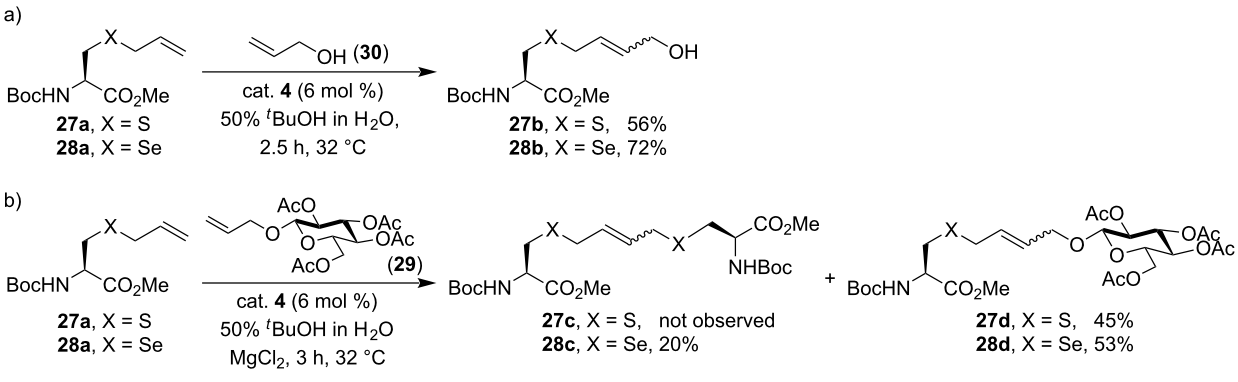

Scheme 11: Comparison of reactivity between allyl sulfides and allyl selenides in aqueous cross-metathesis [38].

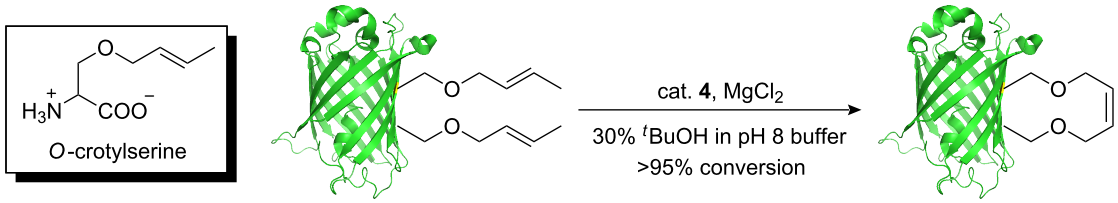

Scheme 12: Ring-closing metathesis on a protein [18].

thesis as a more general method for bioconjugation, we have considered various key factors including steric, electronic and allyl linker selection in substrates that contribute to successful CM on proteins (Scheme 13) [38].

These studies suggest that an unhindered allyl sulfide or selenide protein tag is a requirement for most effective CM. Allyl and hexenyl ethers were found to be the most compatible CM partners for allyl sulfide or selenide containing proteins. The more challenging alkene substrates, such as the ones containing electron-deficient *N*-acetylamine, GlcNAc and ethanolamine (compounds **34**, **36** and **41**), required the more reactive allyl selenide protein tag for the CM to proceed efficiently. Reactive allyl sulfides such as **39** were unsuitable as CM partners for the protein substrate since they led predominantly to self-metathesis. The allyl amine derivative **38** was unreactive in metathesis with proteins possibly due to an electron-deficient or sterically-demanding nature. Taking these factors into consideration, effective functionalization of proteins by CM (>95% conversion) was achieved with 9 different substrates including biochemically important molecules such as GlcNAc, mannose and *N*-acetylamine, which could serve as effective mimics of post-translational protein modifications (glycosylation, lysine acetylation).

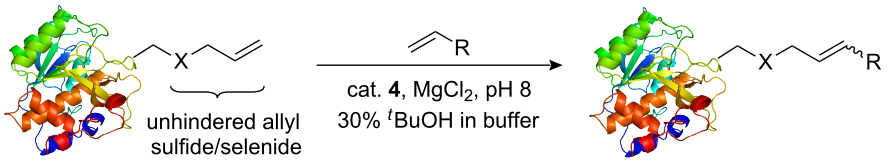

Range of cross-metathesis partners screened[a]

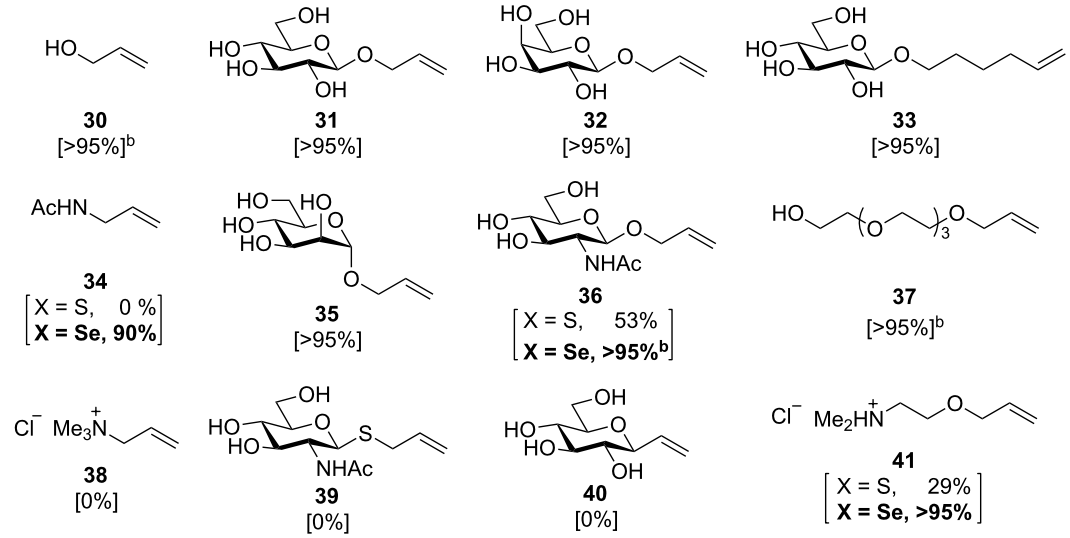

[a]numbers stated in brackets are the corresponding conversions of CM with protein; the conversion and conditions are the same for X = S and X = Se, unless stated otherwise.
[b]Shorter reaction time is required for X = Se. See reference [38] for more detailed information.

Scheme 13: Expanded substrate scope of cross-metathesis on proteins [38].

Conclusion

Since the early work by Hoye on secondary allylic alcohols [19] and later the studies on allyl sulfides by our group [17], the allyl chalcogen effect has affected the way chemists use metathesis in synthesis and chemical biology. Complex molecules and metathesis partners can be joined efficiently with the aid of the natural affinity of ruthenium for allyl chalcogens. In this review, we have highlighted various applications of olefin metathesis in synthesis and protein modifications where the positive influence of allyl chalcogens is utilized. These reports, now collected here, suggest that the directing effect of allyl chalcogens is indeed a general phenomenon in metathesis chemistry, and allow a better understanding of the metathesis reaction itself. We hope to see this concept being further exploited in bioconjugation and synthetic chemistry.

Acknowledgements

We gratefully acknowledge the EPSRC for financial support. BGD is a Royal Society Wolfson Research Merit Award recipient.

References

1. Fürstner, A. *Angew. Chem., Int. Ed.* **2000,** *39,* 3012–3043. doi:10.1002/1521-3773(20000901)39:17<3012::AID-ANIE3012>3.0.CO;2-G
2. Connon, S. J.; Blechert, S. *Angew. Chem., Int. Ed.* **2003,** *42,* 1900–1923. doi:10.1002/anie.200200556
3. Grubbs, R. H., Ed. *Handbook of Metathesis: Catalyst Development;* Wiley-VCH: Weinheim, Germany, 2003. doi:10.1002/9783527619481
4. Nicolaou, K. C.; Bulger, P. G.; Sarlah, D. *Angew. Chem., Int. Ed.* **2005,** *44,* 4490–4527. doi:10.1002/anie.200500369
5. Binder, J. B.; Raines, R. T. *Curr. Opin. Chem. Biol.* **2008,** *12,* 767–773. doi:10.1016/j.cbpa.2008.09.022
6. Brik, A. *Adv. Synth. Catal.* **2008,** *350,* 1661–1675. doi:10.1002/adsc.200800149
7. Henchey, L. K.; Jochim, A. L.; Arora, P. S. *Curr. Opin. Chem. Biol.* **2008,** *12,* 692–697. doi:10.1016/j.cbpa.2008.08.019
8. Lin, Y. A.; Chalker, J. M.; Davis, B. G. *ChemBioChem* **2009,** *10,* 959–969. doi:10.1002/cbic.200900002
9. Hong, S. H.; Grubbs, R. H. *J. Am. Chem. Soc.* **2006,** *128,* 3508–3509. doi:10.1021/ja058451c
10. Michrowska, A.; Gułajski, Ł.; Kaczmarska, Z.; Mennecke, K.; Kirschning, A.; Grela, K. *Green Chem.* **2006,** *8,* 685–688. doi:10.1039/b605138c
11. Binder, J. B.; Guzei, I. A.; Raines, R. T. *Adv. Synth. Catal.* **2007,** *349,* 395–404. doi:10.1002/adsc.200600264
12. Jordan, J. P.; Grubbs, R. H. *Angew. Chem., Int. Ed.* **2007,** *46,* 5152–5155. doi:10.1002/anie.200701258
13. Gułajski, Ł.; Michrowska, A.; Narożnik, J.; Kaczmarska, Z.; Rupnicki, L.; Grela, K. *ChemSusChem* **2008,** *1,* 103–109. doi:10.1002/cssc.200700111
14. Connon, S. J.; Rivard, M.; Zaja, M.; Blechert, S. *Adv. Synth. Catal.* **2003,** *345,* 572–575. doi:10.1002/adsc.200202201
15. Binder, J. B.; Blank, J. J.; Raines, R. T. *Org. Lett.* **2007,** *9,* 4885–4888. doi:10.1021/ol7022505
16. Burtscher, D.; Grela, K. *Angew. Chem., Int. Ed.* **2009,** *48,* 442–454. doi:10.1002/anie.200801451
17. Lin, Y. A.; Chalker, J. M.; Floyd, N.; Bernardes, G. J. L.; Davis, B. G. *J. Am. Chem. Soc.* **2008,** *130,* 9642–9643. doi:10.1021/ja8026168
18. Ai, H.-W.; Shen, W.; Brustad, E.; Schultz, P. G. *Angew. Chem., Int. Ed.* **2010,** *49,* 935–937. doi:10.1002/anie.200905590
19. Hoye, T. R.; Zhao, H. *Org. Lett.* **1999,** *1,* 1123–1125. doi:10.1021/ol990947+
20. Ulman, M.; Grubbs, R. H. *Organometallics* **1998,** *17,* 2484–2489. doi:10.1021/om9710172
21. Schmidt, B.; Nave, S. *Adv. Synth. Catal.* **2007,** *349,* 215–230. doi:10.1002/adsc.200600473
22. Nicolaou, K. C.; Leung, G. Y. C.; Dethe, D. H.; Guduru, R.; Sun, Y.-P.; Lim, C. S.; Chen, D. Y. K. *J. Am. Chem. Soc.* **2008,** *130,* 10019–10023. doi:10.1021/ja802803e
23. Imahori, T.; Ojima, H.; Yoshimura, Y.; Takahata, H. *Chem.–Eur. J.* **2008,** *14,* 10762–10771. doi:10.1002/chem.200801439
24. Hoveyda, A. H.; Lombardi, P. J.; O'Brien, R. V.; Zhugralin, A. R. *J. Am. Chem. Soc.* **2009,** *131,* 8378–8379. doi:10.1021/ja9030903
25. Fuwa, H.; Yamaguchi, H.; Sasaki, M. *Org. Lett.* **2010,** *12,* 1848–1851. doi:10.1021/ol100463a
26. Fuwa, H.; Saito, A.; Sasaki, M. *Angew. Chem., Int. Ed.* **2010,** *49,* 3041–3044. doi:10.1002/anie.201000624
27. Dinger, M. B.; Mol, J. C. *Organometallics* **2003,** *22,* 1089–1095. doi:10.1021/om0208218
28. Werner, H.; Grünwald, C.; Stüer, W.; Wolf, J. *Organometallics* **2003,** *22,* 1558–1560. doi:10.1021/om0210006
29. Armstrong, S. K.; Christie, B. A. *Tetrahedron Lett.* **1996,** *37,* 9373–9376. doi:10.1016/S0040-4039(97)82967-X
30. Mascareñas, J. L.; Rumbo, A.; Castedo, L. *J. Org. Chem.* **1997,** *62,* 8620–8621. doi:10.1021/jo9716439
31. Shon, Y.-S.; Lee, T. R. *Tetrahedron Lett.* **1997,** *38,* 1283–1286. doi:10.1016/S0040-4039(97)00072-5
32. Fürstner, A.; Seidel, G.; Kindler, N. *Tetrahedron* **1999,** *55,* 8215–8230. doi:10.1016/S0040-4020(99)00302-6
33. Fürstner, A.; Langemann, K. *Synthesis* **1997,** 792–803. doi:10.1055/s-1997-4472
34. Tzur, E.; Szadkowska, A.; Ben-Asuly, A.; Makal, A.; Goldberg, I.; Woźniak, K.; Grela, K.; Lemcoff, N. G. *Chem.–Eur. J.* **2010,** *16,* 8726–8737. doi:10.1002/chem.200903457
35. Spagnol, G.; Heck, M.-P.; Nolan, S. P.; Mioskowski, C. *Org. Lett.* **2002,** *4,* 1767–1770. doi:10.1021/ol025834w
36. Toste, F. D.; Chatterjee, A. K.; Grubbs, R. H. *Pure Appl. Chem.* **2002,** *74,* 7–10. doi:10.1351/pac200274010007
37. Alam, J.; Keller, T. H.; Loh, T.-P. *J. Am. Chem. Soc.* **2010,** *132,* 9546–9548. doi:10.1021/ja102733a
38. Lin, Y. A.; Chalker, J. M.; Davis, B. G. *J. Am. Chem. Soc.* **2010,** *132,* 16805–16811. doi:10.1021/ja104994d
39. Garud, D. R.; Garud, D. D.; Koketsu, M. *Org. Biomol. Chem.* **2009,** *7,* 2591–2598. doi:10.1039/b902698c
40. Noren, C. J.; Anthony-Cahill, S. J.; Griffith, M. C.; Schultz, P. G. *Science* **1989,** *244,* 182–188. doi:10.1126/science.2649980
41. van Hest, J. C. M.; Tirrell, D. A. *FEBS Lett.* **1998,** *428,* 68–70. doi:10.1016/S0014-5793(98)00489-X
42. van Hest, J. C. M.; Kiick, K. L.; Tirrell, D. A. *J. Am. Chem. Soc.* **2000,** *122,* 1282–1288. doi:10.1021/ja992749j
43. Link, A. J.; Mock, M. L.; Tirrell, D. A. *Curr. Opin. Biotechnol.* **2003,** *14,* 603–609. doi:10.1016/j.copbio.2003.10.011
44. Xie, J.; Schultz, P. G. *Nat. Rev. Mol. Cell Biol.* **2006,** *7,* 775–782. doi:10.1038/nrm2005

45. Lynn, D. M.; Mohr, B.; Grubbs, R. H.; Henling, L. M.; Day, M. W. *J. Am. Chem. Soc.* **2000,** *122,* 6601–6609. doi:10.1021/ja0003167

License and Terms

Beilstein Journal of Organic Chemistry

The cross-metathesis of methyl oleate with *cis*-2-butene-1,4-diyl diacetate and the influence of protecting groups

Arno Behr* and Jessica Pérez Gomes

Full Research Paper

Open Access

Address:
Chair of Technical Chemistry A, Department of Biochemical and Chemical Engineering, Technische Universität Dortmund, Emil-Figge-Str. 66, D-44227 Dortmund, Germany

Email:
Arno Behr* - behr@bci.tu-dortmund.de

* Corresponding author

Keywords:
cross-metathesis; methyl oleate; monomer; polyester; renewable resources

Beilstein J. Org. Chem. **2011,** *7,* 1–8.
doi:10.3762/bjoc.7.1

Received: 30 September 2010
Accepted: 01 December 2010
Published: 03 January 2011

Guest Editor: K. Grela

Abstract

Background: *α*,*ω*-Difunctional substrates are useful intermediates for polymer synthesis. An attractive, sustainable and selective (but as yet unused) method in the chemical industry is the oleochemical cross-metathesis with preferably symmetric functionalised substrates. The current study explores the cross-metathesis of methyl oleate (**1**) with *cis*-2-butene-1,4-diyl diacetate (**2**) starting from renewable resources and quite inexpensive base chemicals.

Results: This cross-metathesis reaction was carried out with several phosphine and *N*-heterocyclic carbene ruthenium catalysts. The reaction conditions were optimised for high conversions in combination with high cross-metathesis selectivity. The influence of protecting groups present in the substrates on the necessary catalyst loading was also investigated.

Conclusions: The value-added methyl 11-acetoxyundec-9-enoate (**3**) and undec-2-enyl acetate (**4**) are accessed with nearly quantitative oleochemical conversions and high cross-metathesis selectivity under mild reaction conditions. These two cross-metathesis products can be potentially used as functional monomers for diverse sustainable polymers.

Introduction

In the last decade, olefin metathesis has become a routine and competent synthetic method for the formation of carbon–carbon double bonds [1-5]. Among investigations of ring opening metathesis polymerisation [6] and ring closing metathesis [7], the olefin cross-metathesis has demonstrated its great importance in providing access to alkenes bearing a wide range of functional groups [8-11]. Especially, the olefin cross-metathesis with oleochemicals offers a versatile synthetic approach to

prepare value-added substrates starting from renewable raw materials. Due to the cross-metathesis reactions of fatty acid derivatives that yield diverse types of *α,ω*-difunctional monomers, which can be processed into polymers (polyamides, polyesters, polyolefins, etc.), partial or even complete substitution of the steadily decreasing petrochemicals by materials from renewable resources is warranted [12-14]. So far, cross-metathesis reactions of these raw materials with different cross-metathesis reaction partners (allyl alcohol [15,16], allyl chloride [16], acrylonitrile [17], fumaronitrile [18], acrolein [19], methyl acrylate [20] and diethyl maleate [21]) yielding *α,ω*-difunctional substrates have been investigated.

In this article, the ruthenium catalysed cross-metathesis of methyl oleate (**1**) with *cis*-2-butene-1,4-diyl diacetate (**2**) (Scheme 1) will be described. This synthetic approach gives rise to another group of *α,ω*-difunctional substrates: The metathetical conversion studied yields methyl 11-acetoxyundec-9-enoate (**3**) and undec-2-enyl acetate (**4**). The resulting protected *α*-hydroxy-*ω*-carboxylic acid derivatives have potential applications in the preparation of a variety of polymers [22] or lactones [14]. Moreover, undec-2-enyl acetate (**4**) could be processed into polyallylic alcohols under appropriate reaction conditions [22]. In contrast to many other oleochemical cross-metathesis reactions, both the resulting products can be used in polymer chemistry. This oleochemical cross-metathesis reaction described here was studied under different reaction conditions with the aim of optimising oleochemical conversions in combination with high cross-metathesis selectivities. Additionally, several phosphine and *N*-heterocyclic carbene ruthenium catalysts were studied. The optimised reaction conditions were subsequently investigated in the cross-metathesis reaction of oleic acid (**7**) with the unprotected *cis*-2-butene-1,4-diol (**8**). By avoiding the use of protecting groups the processing steps to the polymeric end products would be decisively shortened.

Moreover, the advantage of this cross-metathesis reaction is the use of the relatively inexpensive substrates **1** and **2**. The acylated substrate **2** can be directly synthesised by the catalytic reaction of 1,3-butadiene with acetic acid on a large scale. The classical preparative method for 1,4-butanediol is the copper catalysed reaction of acetylene with formaldehyde and subsequent hydrogenation of the intermediate [23].

Currently, the symmetric acylated substrate **2** is one of the most frequently used cross-metathesis substrates in classical metathesis research. For instance, the cross-metathesis of **2** with allyl benzene or terminal aliphatic alkenes has often been used in the development of new metathesis catalysts [24-27]. In oleochemical metathesis research only the tungsten catalysed cross-metathesis of methyl 10-undecenoate with **2** has been described [28]. The highest yield of the resulting cross-metathesis product was 51% after 2 h at 125 °C. With Grubbs 1st generation catalyst **[Ru]-1**, the reaction temperature could be lowered to 45 °C. Quantitative conversions of methyl 10-undecenoate were obtained with a catalyst loading of 5 mol % **[Ru]-1** [8].

Results and Discussion

Scheme 1 outlines the reaction investigated, i.e., the ruthenium catalysed cross-metathesis of methyl oleate (**1**) with *cis*-2-butene-1,4-diyl diacetate (**2**). The self-metathesis of methyl oleate (**1**), which yields octadec-9-ene (**5**) and dimethyl octadec-9-enedioate (**6**), is the only concurrent metathesis reaction which had to be suppressed (Scheme 1). The desired cross-

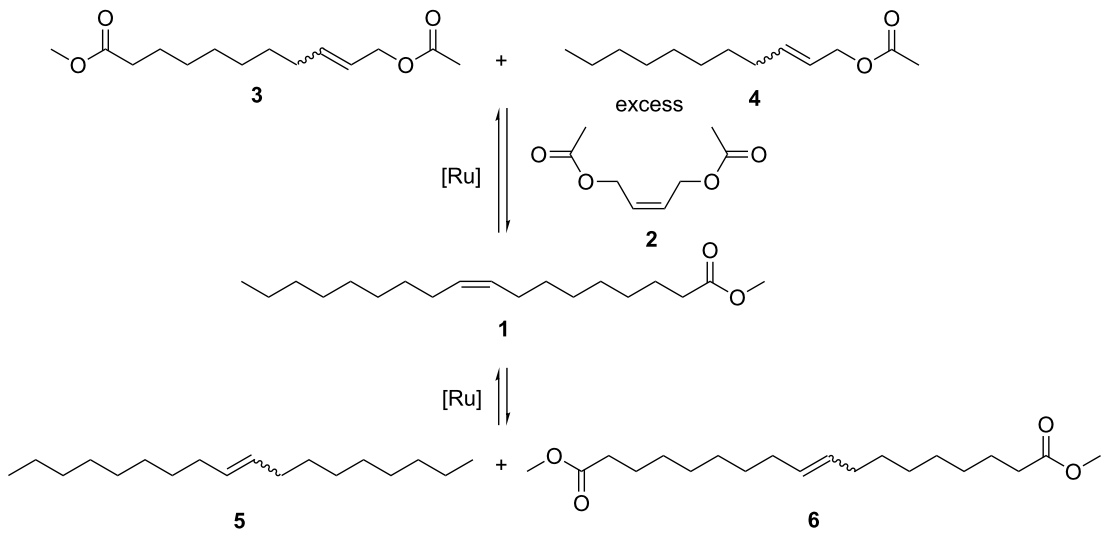

Scheme 1: Cross-metathesis of methyl oleate (**1**) with *cis*-2-butene-1,4-diyl diacetate (**2**) and the self-metathesis of **1**.

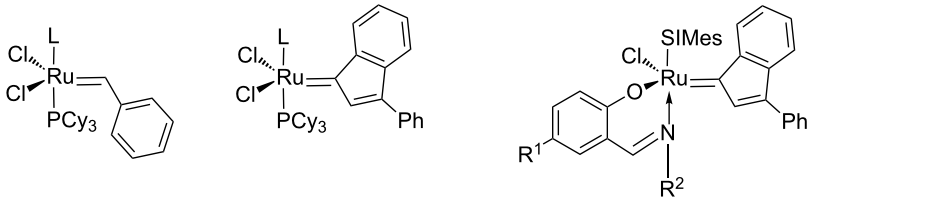

[Ru]-1 L = PCy_3
[Ru]-2 L = SIMes

[Ru]-3 L = PCy_3
[Ru]-4 L = SIMes

[Ru]-5 R^1 = H; R^2 = 1,5-Me-3-Br-C_6H_2
[Ru]-6 R^1 = NO_2; R^2 = 1,5-Me-3-Br-C_6H_2
[Ru]-7 R^1 = H; R^2 = 1,5-^{i}Pr-C_6H_3
[Ru]-8 R^1 = NO_2; R^2 = 1,5-^{i}Pr-C_6H_3

Figure 1: The ruthenium metathesis catalysts used. (SIMes: 1,3-bis-(2,4,6-trimethylphenyl)-4,5-dihydroimidazol-2-ylidene).

metathesis products are the *α*,*ω*-diester methyl 11-acetoxyundec -9-enoate (**3**) and undec-2-enyl acetate (**4**). Both are thus derived from a renewable precursor and are interesting substrates for the synthesis of different types of polymers. Substrate **2** can be considered as an important cross-metathesis partner for the metathetical conversion of methyl oleate **1** in terms of its short chain length. Thus, the chain length of the cross-metathesis products is appropriate for certain polymer applications. Therefore, in contrast to polymers prepared from short-chain monomers, these polymers have a higher flexibility and higher stability against hydrolysis [22]. Due to the *cis*-configuration of **2**, the metathesis reactivity is quite high, although this is slightly reduced by the two electron-withdrawing functional groups at the *β*-positions of the double bond. During our investigations of oleochemical cross-metathesis with diethyl maleate, it was found that the *trans*-isomer is less reactive than its *cis*-isomer [21]. The *trans*-isomer is not able to form the metallacyclobutane complex to give the desired metathesis products [28]. In the case of *trans*-2-butene-1,4-diyl diacetate (**2**), the generation of this intermediate cyclic complex is also hindered. In addition, its symmetry only leads to the two desired products.

The catalytic activity of the ruthenium complexes **[Ru]-1** to **[Ru]-8** (Figure 1) using a catalyst loading of 1.0 mol % was evaluated in the cross-metathesis of methyl oleate (**1**) with *cis*-2-butene-1,4-diyl diacetate (**2**). The reactions were performed with a fivefold excess of **2** in toluene at 50 °C for 5 h to shift the reaction equilibrium towards the cross-metathesis products **3** and **4**.

The differences in metathesis activity of these investigated metathesis initiators are presented in Table 1. Both conversions of **1** and yields of the cross-metathesis products **3** and **4** were determined by gas chromatography with internal standard.

As summarised in Table 1, the lowest conversions of **1** (about 15%) and yields of each of the desired cross-metathesis prod-

Table 1: Results of metathesis catalyst activities in the cross-metathesis of methyl oleate (**1**) with **2**.[a]

entry	catalyst	conversion **1** [%][b]	yield **3** [%][b]	yield **4** [%][b]	yield **5** [%][b]	yield **6** [%][b]
1	**[Ru]-1**	14	3	4	6	5
2	**[Ru]-2**	48	29	28	10	10
3	**[Ru]-3**	15	4	4	6	6
4	**[Ru]-4**	42	24	26	9	10
5	**[Ru]-5**[c]	34	15	14	10	11
6	**[Ru]-6**[c]	35	16	15	9	10
7	**[Ru]-7**[c]	90	59	58	16	15
8	**[Ru]-8**[c]	84	53	52	16	16

[a]reaction conditions: 1.0 mol % cat., *m*(**1**) = 0.17 mmol, 0.85 mmol **2**, toluene, 5 h, 50 °C, 900 rpm; [b]determined by gas chromatography with internal standard; [c]addition of 100 equiv of $PhSiCl_3$ according to **[Ru]-5**–**[Ru]-8**.

ucts **3** and **4** (about 5%) were achieved using the ruthenium phosphine complexes **[Ru]-1** and **[Ru]-3** (Table 1, entries 1 and 3). Only slight differences in activity were observed between the benzylidene catalyst **[Ru]-1** and its indenylidene counterpart **[Ru]-3**. The self-metathesis of methyl oleate (**1**) mentioned above could not be suppressed. Other side-reactions were not observed. No double-bound isomerisation took place. Promising results were obtained with catalysts bearing *N*-heterocyclic carbene ligands (Table 1, entries 2 and 4–8) [29]. Up to 48% of methyl oleate (**1**) was converted and the yields of the cross-metathesis products **3** and **4** of ca. 28% were achievable with ruthenium catalysts **[Ru]-2** and **[Ru]-4** (Table 1, entries 2 and 4). Here, the self-metathesis reaction of **1** is a side-reaction. The yields of **5** and **6** were nearly halved using the second generation ruthenium catalysts **[Ru]-2** and **[Ru]-4**. The cross-metathesis selectivity increased considerable. The difunctionalised co-substrate **2** was also converted to a greater extent. Accordingly, these metathesis catalysts illustrate once more their higher metathesis activity and their higher tolerance towards functional groups [2].

Comparable or higher conversions of **1** and cross-metathesis yields of **3** and **4** (Table 1, entries 5–8) were obtained with ruthenium complexes **[Ru]-5**–**[Ru]-8**. Due to their bidentate Schiff base ligands, they must be chemically activated by the addition of 100 equiv of phenyltrichlorosilane [30,31]. Within this catalyst family it can be concluded that with higher steric hindrance of the Schiff base ligands higher conversions and yields were achievable (Table 1, entries 7 and 8). Schiff base ligands with a nitro substituent did not lead to a significant increase or loss of metathesis activity. Consequently, in the oleochemical cross-metathesis reaction **[Ru]-7** and **[Ru]-8** were the most active catalysts due to their space-filling isopropyl substituted Schiff base ligands [31]. The cross-metathesis yields amounted to 59% and methyl oleate (**1**) was converted up to 90%. Moreover, the self-metathesis of methyl oleate (**1**) was reasonably well suppressed and could be considered as a side-reaction; the yield of the self-metathesis products **5** and **6** amounted to 16%. Furthermore, the cross-metathesis selectivity using the ruthenium catalysts **[Ru]-7** and **[Ru]-8** is decisively higher compared to the other catalysts used.

From the results in Table 2 an increase of conversion of methyl oleate **1** (from 15 to 94%) and of yield of each of the cross-metathesis products **3** and **4** (from 2 to 66%) were obtained with a catalyst loading of **[Ru]-7** in a range of 0.1 and 1.5 mol %. Cross-metathesis selectivity was increased by 60% to 67%. With a catalyst loading of 1.5 mol % of **[Ru]-7**, a nearly quantitative conversion of unsaturated fatty ester **1** was achievable (Table 2, entry 4). Moreover, the undesired self-metathesis products from **1** were obtained in lower amounts (ca. 14% of each self-metathesis product **5** and **6**). From the results, it can be concluded that a catalyst loading of above 1.0 mol % of the ruthenium catalyst **[Ru]-7** was necessary for efficient conversion of *cis*-2-butene-1,4-diyl diacetate (**2**). Further increasing the quantity of **[Ru]-7** led neither to an essentially higher oleochemical conversion nor to higher cross-metathesis yields (Table 2, entry 5). The yields of self-metathesis products also remained constant (about 15%).

The ratio of the two cross-metathesis reaction partners **1** and **2** has also a great influence on conversion (Table 3). Besides, it is also advantageous to reduce the excess of protected diol **2** in terms of green chemistry and industrial implementation.

Independent of the excess of **2** used, the conversion of methyl oleate (**1**) was quite high (<96%). The cross-metathesis yields reached its maximum at 77% using an eightfold excess of **2** (Table 3, entry 4). The yields could be increased by 32% to 77%. This indicates that the self-metathesis reaction was more and more suppressed; the yields of **5** and **6** were decreased by 15% to 10%. Further investigations were performed with an eightfold excess of **2**, because an additional excess of **2** did not have a positive effect on conversions and yields (Table 3, entry 5). Too high an excess of **2** hindered the conversion of methyl oleate (**1**).

Table 2: Results of catalytic investigations of cross-metathesis of **1** with **2** with various **[Ru]-7** loadings.[a]

entry	**[Ru]-7** loading [mol %][b]	conversion **2** [%][b]	yield **3** [%][b]	yield **4** [%][b]	yield **5** [%][b]	yield **6** [%][b]
1	0.1	15	1	2	7	7
2	0.5	32	6	6	12	13
3	1.0	90	59	58	15	16
4	1.5	94	66	65	15	14
5	2.0	96	64	63	15	15

[a]reaction conditions: **[Ru]-7**, *m*(**1**) = 0.17 mmol, 0.85 mmol **2**, *n*($PhSiCl_3$)/*n*(**[Ru]-7**) = 100/1, toluene, 5 h, 50 °C, 900 rpm; [b]determined by gas chromatography with internal standard.

Table 3: Results of catalytic investigations of cross-metathesis of **1** with various amounts of **2**.[a]

entry	equiv of **2**	conversion **2** [%][b]	yield **3** [%][b]	yield **4** [%][b]	yield **5** [%][b]	yield **6** [%][b]
1	2	96	45	45	25	26
2	4	92	54	54	19	18
3	5	94	66	65	13	14
4	8	96	76	78	10	9
5	10	96	77	79	10	10

[a]reaction conditions: 1.5 mol % **[Ru]-7**, *m*(**1**) = 0.17 mmol, *n*($PhSiCl_3$)/*n*(**[Ru]-7**) = 100/1, toluene, 5 h, 50 °C, 900 rpm; [b]determined by gas chromatography with internal standard.

The reactions were stopped after fixed reaction times in an attempt to shorten the necessary reaction time (Table 4). After 1 h, 94% of methyl oleate (**1**) was already converted (Table 4, entry 1). The highest yields of each cross-metathesis product **3** and **4** were just obtained after 5 h (Table 4, entry 3). With longer reaction times, conversions and yields remained constant. The reaction equilibrium was shifted towards the desired cross-metathesis products **3** and **4**, whereas the self-metathesis reaction of **1** was more and more suppressed and the yields of **5** and **6** amounted to around 10%.

Table 4: Results of variation of the reaction time of cross-metathesis of **1** with **2**.[a]

entry	time [h]	conversion **2** [%][b]	yield **3** [%][b]	yield **4** [%][b]	yield **5** [%][b]	yield **6** [%][b]
1	1	94	58	61	18	17
2	3	94	67	71	13	14
3	5	96	78	82	9	8
4	7	93	73	78	10	10
5	9	93	70	71	11	10

[a]reaction conditions: 1.5 mol % **[Ru]-7**, *m*(**1**) = 0.17 mmol, 1.36 mmol **2**, *n*($PhSiCl_3$)/*n*(**[Ru]-7**) = 100/1, toluene, 50 °C, 900 rpm; [b]determined by gas chromatography with internal standard.

Moreover, the conversion of methyl oleate (**1**) appears to be temperature-independent (Table 5); conversions were always higher than 92%. The unsaturated methyl oleate (**1**) underwent a rapid self-metathesis at low reaction temperatures (Table 5, entry 1). In contrast, the cross-metathesis became more predominant at higher reaction temperatures. This suggests that thermal activation of the *cis*-2-butene-1,4-diyl diacetate (**2**) is required. On increasing the reaction temperature from 30 to 50 °C an increase in the yields of the cross-metathesis products (up to 77%) was observed. At the same time the self-metathesis reaction of **1** was hindered and only 10% of each of the self-metathesis products **5** and **6** was produced.

Finally, it was desirable to avoid the use of protecting groups. Thus, the optimised reaction conditions for the cross-metathesis of methyl oleate (**1**) with *cis*-2-butene-1,4-diyl diacetate (**2**) were applied to the cross-metathesis reaction of the corresponding fatty acid **7** with the diol **8**. The oleic acid (**7**) was reacted with both *cis*-2-butene-1,4-diyl diacetate (**2**) and the diol **8** (Table 6).

Whilst the conversion of methyl oleate (**1**) with the protected diol **2** was nearly quantitative using 1.5 mol % of the ruthenium complex **[Ru]-7** at 50 °C within 5 h (Table 6, entry 1), comparative results in the cross-metathesis of oleic acid (**7**) with **2** were only achieved with the use of 3.0 mol % of the same ruthenium catalyst. Under otherwise similar reactions conditions, 75% of oleic acid was converted (Table 6, entry 2). The cross-metathesis yield amounted to 55%. In the complete absence of protecting groups, a catalyst loading of 4.0 mol % was necessary to produce similar results (Table 6, entry 3). With regard to technical implementation, it seems to be more

Table 5: Results of variation of the reaction temperature of cross-metathesis of **1** with **2**.[a]

entry	temperature [°C]	conversion **2** [%][b]	yield **3** [%][b]	yield **4** [%][b]	yield **5** [%][b]	yield **6** [%][b]
1	30	92	44	45	24	23
2	40	94	55	53	20	19
3	50	96	76	78	10	9

[a]reaction conditions: 1.5 mol % **[Ru]-7**, *m*(**1**) = 0.17 mmol, 1.36 mmol **2**, *n*($PhSiCl_3$)/*n*(**[Ru]-7**) = 100/1, toluene, 5 h, 900 rpm; [b]determined by gas chromatography with internal standard.

Table 6: Influence of the protecting groups on the ruthenium catalysed cross-metathesis.[a]

entry	cross-metathesis		c(**[Ru]-7**) [mol %]	X(**1** or **7**) [%]	Y(*α,ω*-product) [%]
	substrate	co-substrate			
1	**1**	**2**	1.5	96	78
2	**7**	**2**	3.0	75	55
3	**7**	**8**	4.0	76	53

[a]reaction conditions: **[Ru]-7**, *m*(**1** or **7**) = 0.17 mmol, *n*(**1** bzw. **7**)/*n*(**2** bzw. **8**) = 1/8, *n*($PhSiCl_3$)/*n*(**[Ru]-7**) = 100/1, toluene, 5 h, 50 °C, 900 rpm.

economical to use the protected substrates, since the catalyst loading of the expensive ruthenium complexes is considerably higher.

Conclusion

In conclusion, the cross-metathesis of methyl oleate (**1**) with *cis*-2-butene-1,4-diyl diacetate (**2**) was feasible with the relatively low catalyst loading of the Schiff base ruthenium catalyst **[Ru]-7** to yield two value-added and sustainable intermediates in one step. Methyl 11-acetoxyundec-9-enoate (**3**) and undec-2-enyl acetate (**4**) are both very interesting substrates for polymer synthesis. They could be prepared under mild reaction conditions within 5 h. Moreover, this is an advantageous contribution towards the synthesis of sustainable monomer units because a new *α,ω*-difunctional substrate class starting from a renewable compound and an inexpensive base chemical was prepared.

Various metathesis catalysts were investigated, disclosing that the Schiff base ruthenium indenylidene catalyst **[Ru]-7** bearing a *N*-heterocyclic carbene ligand, which is an already industrial implemented metathesis catalyst, led to high conversions and yields of the desired cross-metathesis products. Interestingly, this cross-metathesis could be performed without protecting groups, but the catalyst loading had to be adjusted to get similar oleochemical conversions and cross-metathesis yields.

Experimental

Materials

Sunflower oil with a high oleic content (91.4% oleic acid) was obtained from Emery Oleochemicals. *cis*-2-Butene-1,4-diol (**8**) (97%), solvents and reagents were purchased from Sigma-Aldrich. Benzylidene ruthenium catalysts **[Ru]-1** and **[Ru]-2** were obtained from Sigma-Aldrich and the remaining indenylidene ruthenium catalysts **[Ru]-3**–**[Ru]-8** were provided by *Umicore* AG & Co. KG and were used as received.

All reactions were performed under an inert atmosphere of argon using standard Schlenk line techniques. Methyl oleate (**1**) was prepared by transesterifcation of high oleic sunflower oil with methanol using hypostoichiometric amounts of sodium methoxide (30% in methanol). *cis*-2-Butene-1,4-diyl diacetate (**2**) was prepared by the pyridine catalysed acylation of the diol **8** with acetic anhydride according to [32].

Analytical equipment and methods

Analytical thin-layer chromatography (TLC) was performed on silica gel TLC-cards (layer thickness 0.20 µm, VWR International). Substrates were visualised with *p*-anisaldehyde reagent. Flash chromatography was conducted on silica gel 60 (40–60 µm, Acros Organics). Nuclear magnetic resonance (NMR) spectra were recorded in deuterated chloroform on a Bruker AVANCE DRX spectrometer operating at 400 MHz at 298 K. Chemical shifts (δ) are indicated in parts per million relative to tetramethylsilane as internal standard (TMS, δ = 0.0 ppm). Gas chromatographic (GC) analyses were performed on a Hewlett-Packard HP 6890 apparatus equipped with a HP5 capillary column (coating: 5% diphenyl-95%-dimethyl-polysiloxane; length 30 m, diameter 0.25 mm, thickness 0.25 µm) and flame ionisation detection (FID) connected to an autosampler. The oven temperature program was as follows: initial temperature 130 °C, hold for 6 min, increase by 25 °C/min to 320 °C, hold for 4 min. Measurements were performed in split–split mode (split ratio 70:1) using nitrogen as the carrier gas (linear velocity of 30.0 cm/s at 300 °C). Conversions and yields were determined with *n*-pentadecane as internal standard and isopropyl alcohol as solvent.

GC–mass spectroscopy (MS) chromatograms were recorded using a Hewlett-Packard HP 6890 instrument with the same capillary column as specified above and a HP 5973 mass detector set (70 eV). The oven temperature program, the split–split mode and the specifications of the carrier gas were similar to those in the GC-FID method.

Cross-metathesis of methyl oleate (**1**) and *cis*-2-butene-1,4-diyl diacetate (**2**)

A flame-dried Schlenk tube was charged with 0.050 g (0.17 mmol) methyl oleate (**1**) and 2–10 equiv *cis*-2-butene-1,4-diyl diacetate (**2**). The mixture was diluted to 1.250 g with toluene.

The solid metathesis catalysts **[Ru]-1**–**[Ru]-8** were added in the range of 0.1–2.0 mol % to the reaction mixture. In the case of Schiff base ruthenium catalysts **[Ru]-5**–**[Ru]-8**, 100 equiv of phenyltrichlorosilane (relative to the catalyst) were also added. The reaction mixture was stirred magnetically at the appropriate temperature (20–50 °C) for the appropriate time (1–9 h). After completion of the reaction, the mixture was cooled to ambient temperature. Conversion and yield analyses were performed by gas chromatography. The metathesis products were isolated after removing toluene in vacuo by flash chromatography on silica gel with cyclohexane/ethyl acetate (from 10/1 to 1/2) as eluent, and subsequently characterised by NMR spectroscopy.

Characterisation of the substrates

Methyl oleate (**1**)

^{1}H NMR (400 MHz; $CDCl_3$): δ (ppm) = 0.88 (t, 3H, J = 8.0 Hz, -C$\underline{H}_3$), 1.28 (m, 20H, -C$\underline{H}_2$-), 1.61 (m, 2H, -C(O)-CH$_2$-C$\underline{H}_2$-), 2.00 (m, 4H, -C$\underline{H}_2$-CH=), 2.30 (t, 2H, J = 8.0 Hz, -C(O)-C$\underline{H}_2$-), 3.66 (s, 3H, -C$\underline{H}_3$), 5.34 (m, 2H, -C$\underline{H}$=C$\underline{H}$-). ^{13}C NMR (100 MHz; $CDCl_3$): δ (ppm) = 14.0, 22.6, 24.9, 27.0, 27.1, 28.9, 29.0, 29.1, 29.2, 29.4, 29.6, 29.7, 31.8, 34.0, 51.3, 129.6, 129.9, 174.2. MS (EI, 70 eV): *m/z* (%) = 296 (4) [M^+], 264 (28), 246 (2), 235 (3), 222 (17), 207 (3), 194 (3), 180 (16), 166 (8), 152 (10), 137 (14), 123 (24), 110 (29), 97 (54), 83 (55), 74 (65), 69 (68), 55 (100), 41 (76), 29 (29).

cis-2-Butene-1,4-diyl diacetate (**2**)

^{1}H NMR (400 MHz; $CDCl_3$): δ (ppm) = 1.96 (s, 6H, -C(O)-C$\underline{H}_3$), 4.57 (d, 4H, J = 4.0 Hz, -O-C$\underline{H}_2$-), 5.64 (m, 2H, -C$\underline{H}$=). ^{13}C-NMR (100 MHz; $CDCl_3$): δ (ppm) = 20.6, 59.7, 127.8, 170.3. MS (EI, 70 eV): *m/z* (%) = 172 (14) [M^+], 113 (7), 99 (1), 82 (2), 70 (46), 61 (4), 53 (2), 43 (100), 39 (6), 27 (6).

Methyl 11-acetoxyundec-9-enoate (**3**)

^{1}H NMR (400 MHz; $CDCl_3$): δ (ppm) = 1.61 (m, 8H, -C$\underline{H}_2$-), 1.66 (m, 2H, -C(O)-CH$_2$-C$\underline{H}_2$-), 2.05 (s, 3H, -C(O)-C$\underline{H}_3$), 2.07 (m, 2H, =CH-C$\underline{H}_2$-), 2.30 (m, 2H, -C(O)-C$\underline{H}_2$-), 3.66 (s, 3H, -O-C$\underline{H}_3$), 4.67 (d, 2H, J = 8.0 Hz, -O-C$\underline{H}_2$-CH=), 5.87 (m, 2H, -CH=). ^{13}C NMR (100 MHz; $CDCl_3$): δ (ppm) = 21.0, 24.9, 28.7, 29.0, 29.3, 29.7, 32.2, 51.4, 65.3, 129.7, 130,9, 170.9, 174.2. MS (EI, 70 eV): *m/z* (%) = 256 (2) [M^+], 213 (3), 196 (3), 182 (23), 164 (31), 154 (8), 135 (14), 122 (14), 107 (8), 98 (15), 81 (29), 67 (24), 55 (34), 43 (100), 29 (9).

Undec-2-enyl acetate (**4**)

^{1}H NMR (400 MHz; $CDCl_3$): δ (ppm) = 0.88 (t, J = 8.0 Hz, 3H, -C$\underline{H}_3$), 1.29 (m, 12H, -C$\underline{H}_2$-), 2.56 (m, 5H, -C$\underline{H}_2$-CH=, -C$\underline{H}_3$), 4.50 (d, J = 8.0 Hz, 2H, -O-C$\underline{H}_2$-CH=), 5.66 (m, 2H, =C$\underline{H}$-). ^{13}C NMR (100 MHz; $CDCl_3$): δ (ppm) = 11.4, 21.0, 22.7, 29.2, 29.2, 29.3, 29.4, 31.9, 32.2, 65.3, 129.8, 136.8, 179.3. MS (EI, 70 eV): *m/z* (%) = 212 (4) [M^+], 170 (5), 152 (3), 141 (4), 124 (12), 110 (8), 96 (19), 82 (26), 67 (25), 54 (31), 43 (100), 39 (11), 29 (14).

9-Octadecene (**5**)

^{1}H NMR (500 MHz; $CDCl_3$): δ (ppm) = 0.89 (m, 6H, -C$\underline{H}_3$), 1.28 (s, 24H, -C$\underline{H}_2$-), 2.00 (m, 4H, =CH-C$\underline{H}_2$-), 5.37 (m, 2H; =C$\underline{H}$-). ^{13}C NMR (125 MHz; $CDCl_3$): δ (ppm) = 13.1, 25.9, 26.2, 28.2, 28.5, 28.8, 31.0, 33.4, 129.4. MS (EI, 70 eV): *m/z* (%) = 252 (5) [M^+], 154 (1), 139 (2), 125 (10), 111 (29), 97 (59), 91 (1), 83 (68), 79 (7), 69 (79), 65 (4).

Dimethyl octadec-9-enedioate (**6**)

^{1}H NMR (500 MHz; $CDCl_3$): δ (ppm) = 1.27 (m 16H, -C$\underline{H}_2$-), 1.59 (m, 4H, -C(O)-CH$_2$-C$\underline{H}_2$-), 1.93 (m, 4H, =CH-C$\underline{H}_2$-), 2.26 (m, 4H, -C(O)-C$\underline{H}_2$-), 3.63 (s, 6H, -O-C$\underline{H}_3$), 5.34 (m, 2H, =C$\underline{H}$-). ^{13}C NMR (125 MHz; $CDCl_3$): δ (ppm) = 24.9, 28.9, 29.4, 29.5, 29.6, 32.5, 34.0, 51.3, 130.2, 174.2. MS (EI, 70 eV): *m/z* (%) = 340 (1) [M^+], 308 (7), 290 (3), 276 (16), 265 (1), 207 (1), 165 (7), 151 (11), 133 (12), 121 (13), 109 (18), 95 (38), 81 (59), 74 (44), 67 (58), 55 (100).

Acknowledgements

This work was financially supported by the German Federal Ministry of Food, Agriculture and Consumer Protection (represented by the Fachagentur Nachwachsende Rohstoffe) and Emery Oleochemicals GmbH. The authors thank Dr. Alfred Westfechtel for helpful discussions. Furthermore, the authors would like to thank Umicore AG & Co. KG for the donation of several ruthenium metathesis catalysts.

References

1. Trnka, T. M.; Grubbs, R. H. *Acc. Chem. Res.* **2001,** *34,* 18–29. doi:10.1021/ar000114f
2. Grubbs, R. H., Ed. *Handbook of Metathesis;* Wiley-VCH: Weinheim, Germany, 2003.
3. Fürstner, A. *Angew. Chem., Int. Ed.* **2000,** *39,* 3012–3043. doi:10.1002/1521-3773(20000901)39:17<3012::AID-ANIE3012>3.0.CO;2-G
4. Desmuskh, P. H.; Blechert, S. *Dalton Trans.* **2007,** 2479–2491.
5. Hoveyda, A. H.; Zhugralin, A. R. *Nature* **2007,** *450,* 243–251. doi:10.1038/nature06351
6. Ivin, K. J.; Mol, J. C. *Olefin Metathesis and Metathesis Polymerisation,* 2nd ed.; Academic: San Diego, USA, 1997.
7. Grubbs, R. H.; Chang, S. *Tetrahedron* **1998,** *54,* 4413–4450. doi:10.1016/S0040-4020(97)10427-6
8. Blackwell, H. E.; OLeary, D. J.; Chatterjee, A. K.; Washenfelder, R. A.; Bussmann, D. A.; Grubbs, R. H. *J. Am. Chem. Soc.* **2000,** *122,* 58–71. doi:10.1021/ja993063u
9. Troste, F. D.; Chatterjee, A. K.; Grubbs, R. H. *Pure Appl. Chem.* **2002,** *74,* 7–10. doi:10.1351/pac200274010007
10. Stewart, I. C.; Douglas, C. J.; Grubbs, R. H. *Org. Lett.* **2008,** *10,* 441–444. doi:10.1021/ol702624n

11. Patel, J.; Mujcinovic, S.; Jackson, W. R.; Robinson, A. J.; Serelis, A. K.; Such, C. *Green Chem.* **2006,** *8,* 450–454.
12. Jenck, J. F.; Agterberg, F.; Droescher, M. J. *Green Chem.* **2004,** *6,* 544–556. doi:10.1039/b406854h
13. Behr, A.; Westfechtel, A.; Pérez Gomes, J. *Chem. Eng. Technol.* **2008,** *31,* 700–714. doi:10.1002/ceat.200800035
14. Behr, A.; Pérez Gomes, J. *Eur. J. Lipid Sci. Technol.* **2010,** *112,* 31–50. doi:10.1002/ejlt.200900091
15. Meier, M. A. R.; Rybak, A.; Geisker, D. Hydroxy- and aldehyde functional compounds. WO 2010/083934, Dec 30, 2009.
16. Meier, M. A. R.; Rybak, A.; Geisker, D.; Hannen, P.; Roos, M. Method for producing aldehyde functional compounds. WO 2010/084053, Jan 12, 2010.
17. Jacobs, T.; Rybak, A.; Meier, M. A. R. *Appl. Catal.* **2009,** *353,* 32–35. doi:10.1016/j.apcata.2008.10.026
18. Malacea, R.; Fischmeister, C.; Bruneau, C.; Dubois, J.-L.; Couturier, J.-L.; Dixneuf, P. H. *Green Chem.* **2009,** *11,* 152–155. doi:10.1039/b816917a
19. Miao, X.; Fischmeister, C.; Bruneau, C.; Dixneuf, P. H. *ChemSusChem* **2009,** *2,* 542–545. doi:10.1002/cssc.200900028
20. Rybak, A.; Meier, M. A. R. *Green Chem.* **2007,** *9,* 1356–1361. doi:10.1039/b712293d
21. Behr, A.; Pérez Gomes, J.; Bayrak, Z. *Eur. J. Lipid Sci. Technol.* **2010,** in press. doi:10.1002/ejlt.2010000299
22. Elias, H.-G. *Makromoleküle II. Technologie. Rohstoffe - Industrielle Synthesen - Polymere - Anwendungen;* Wiley-VCH: Weinheim, Germany, 1999.
23. Baerns, M.; Behr, A.; Brehm, A.; Gmehling, J.; Hofmann, H.; Onken, U.; Renken, A. *Technische Chemie;* Wiley-VCH: Weinheim, Germany, 2006.
24. Ritter, T.; Hejl, A.; Wenzel, A. G.; Funk, T. W.; Grubbs, R. H. *Organometallics* **2006,** *25,* 5740–5745. doi:10.1021/om060520o
25. Lozano Vila, A. M.; Monsaert, S.; Droszdzak, R.; Wolowiec, S.; Verpoort, F. *Adv. Synth. Catal.* **2009,** *351,* 2689–2701. doi:10.1002/adsc.200900477
26. Gułajski, L.; Michrowska, A.; Narożnik, J.; Kaczmarska, Z.; Rupnicki, L.; Grela, K. *ChemSusChem* **2008,** *1,* 103–109. doi:10.1002/cssc.200700111
27. Kniese, M.; Meier, M. A. R. *Green Chem.* **2010,** *9,* 169–173. doi:10.1039/b921126h
28. Churi, R. Y.; Subrahmanyam, V. V. R. J. *J. Oil Technol. Assoc. India (Hyderabad, India)* **1993,** *25,* 93–95.
29. Clavier, H.; Nolan, S. P. *Chem.–Eur. J.* **2007,** *13,* 8029–8036. doi:10.1002/chem.200700256
30. Allaert, B.; Dieltiens, N.; Ledoux, N.; Vercaemst, C.; van der Voort, P.; Stevens, C. V.; Linden, A.; Verpoort, F. *J. Mol. Catal. A: Chem.* **2006,** *260,* 221–226. doi:10.1016/j.molcata.2006.07.006
31. Ledoux, N.; Drozdzak, R.; Allaert, B.; Linden, A.; van der Voort, P.; Verpoort, F. *Dalton Trans.* **2007,** 5201–5210. doi:10.1039/b709994k
32. Zawisza, A. M.; Bouquillon, S.; Muzart, J. *Eur. J. Org. Chem.* **2007,** *23,* 3901–3904. doi:10.1002/ejoc.200700246

License and Terms

Beilstein Journal of Organic Chemistry

Stereoselectivity of supported alkene metathesis catalysts: a goal and a tool to characterize active sites

Christophe Copéret[1,2]

Review

Open Access

Address:
[1]Université de Lyon, Institut de Chimie de Lyon, Laboratoire C2P2 UMR 5265 (CNRS – CPE – UCBL) CPE Lyon, 43 Bd du 11 Novembre 1918, F-69616 Villeurbanne Cedex, France and [2]Department of Chemistry, ETH Zürich, Wolfgang-Pauli-Str. 10, CH-8093 Zürich, Switzerland

Email:
Christophe Copéret - ccoperet@inorg.chem.ethz.ch

Keywords:
active sites; metathesis; stereoselectivity; supported catalysts

Beilstein J. Org. Chem. **2011,** *7,* 13–21.
doi:10.3762/bjoc.7.3

Received: 23 August 2010
Accepted: 09 November 2010
Published: 05 January 2011

Guest Editor: K. Grela

Abstract

Stereoselectivity in alkene metathesis is a challenge and can be used as a tool to study active sites under working conditions. This review describes the stereochemical relevance and problems in alkene metathesis (kinetic vs. thermodynamic issues), the use of (*E*/*Z*) ratio at low conversions as a tool to characterize active sites of heterogeneous catalysts and finally to propose strategies to improve catalysts based on the current state of the art.

Introduction

Achieving high selectivity and, in particular, stereoselectivity are still important goals in organic synthesis, and several catalytic reactions such as alkene oxidation [1,2], hydrogenation [3], polymerisation [4], especially when using homogeneous catalysts, have reached a very high level of chemo-, diastereo- and enantioselectivy. In contrast, while alkene metathesis has been regarded as a powerful tool to introduce new C–C bonds into an organic skeleton and to generate alkenes [5-7], controlling the stereochemical outcome of this reaction [8-13] still remains a challenge despite several breakthroughs with homogeneous catalysts [14-18]; one of the most important and difficult targets is the control of the configuration of the double bond, the *E*- and *Z*-selectivity. Most often, high selectivity is only obtained for specific substrates, where thermodynamics favour one isomer, often that with an *E*-configured double bond (styrenyl systems or alkenes with electron withdrawing substituents) [19-21].

Here the discussion will focus on the stereoselectivity of alkene metathesis in order to delineate the current state of the art in the case of heterogeneous catalysts and show how it can be used to characterize active sites as well as to put forward possible strategies to approach the problem.

Review

Stereoselectivity in alkene metathesis: a challenge and a tool

Alkene metathesis is a reaction where the alkylidene fragments of alkenes are exchanged (transalkylidenation, Scheme 1a). The mechanism involves at least four steps: alkene coordination,

[2 + 2]-cycloaddition generating metallacyclobutanes and the corresponding reverse steps, i.e., cycloreversion and alkene dissociation (Scheme 1b). The approach of an alkene of a given configuration towards a metal–alkylidene intermediate in a given configuration will generate a metallacyclobutane from which a new alkylidene and alkene with specific configurations will be formed. Note that additional steps are possible such as: i) formation of the active alkylidene species or ii) interconversion of metallacyclobutane isomers (TBP vs SBP), however, these typically do not affect the stereochemical outcome of the overall reaction (Scheme 1c and Scheme 1d).

Overall the (*E*/*Z*) ratio of the resulting alkene products can provide information about the whole metathesis process and the structure of the active sites (vide infra) [22,23]. However, because alkene metathesis (for most acyclic alkenes) has a free energy close to 0 and is reversible, the (*E*/*Z*) ratio readily evolves towards a thermodynamic value [(*E*/*Z*) ≥ 3 for di-substituted alkenes] via metathesis, and all the valuable *kinetic stereochemical information* is easily lost, and consequently special care has to be taken in order to obtain useful information from (*E*/*Z*) ratios, i.e., they should be measured at low conversions or contact times.

As an example, let us analyse the metathesis of a dissymmetric *Z*-alkene, ***Z*-Alk$_{R1R2}$** ($R^1 = R^2$; $R^3 = R^4 = H$), into **Alk$_{R1R1}$** and ***Z*-Alk$_{R2R2}$**. First, such a reaction will lead to the formation of two alkylidene intermediates, M=CHR^1 and M=CHR^2, and for each intermediate, the alkene can approach in four possible ways: *syn*/head-to-head, *syn*/head-to-tail, *anti*/head-to-head and *anti*/head-to-tail (Scheme 2).

Of these eight possible pathways, four are productive leading to the (*Z*)- or the (*E*)-alkene products (**Alk$_{R1R1}$** and **Alk$_{R2R2}$**), two are degenerate leaving the reactant untouched (***Z*-Alk$_{R1R2}$** → ***Z*-Alk$_{R1R2}$**), and two yield the alkene reactant with the opposite stereochemistry (***Z*-Alk$_{R1R2}$** → ***E*-Alk$_{R1R2}$**); the latter corresponding to an isomerisation. As the products **Alk$_{R1R1}$** and **Alk$_{R2R2}$** build up in the reaction mixture, they will undergo the same processes, including isomerisation, until the overall thermodynamic equilibrium is reached, typically leading to the formation of the *E*-products for di-substituted alkenes, in particular when one of the substituent is an electron withdrawing group. Any kinetic information will be obtained only at low conversions, where isomerisation is minimal. This can be performed by looking at the (*E*/*Z*) ratio of products at low conversions, but the best approach is to study the evolution of the (*E*/*Z*) ratio of the reactant $(E/Z)_{t\text{-reactant}}$ vs products $(E/Z)_{t\text{-product}}$ as a function of time/conversion and to plot the (*E*/*Z*) ratio of products as a function of the (*E*/*Z*) ratio of the reactants; the latter approach leads to, in most cases, a straight line, any deviation indicating the approach to thermodynamic equilibrium or a change of the active site structure (a full kinetic treatment of this has been provided by Bilhou et al.) [24]. The intercept at x = 0 gives the intrinsic stereoselectivity of the catalyst, $(E/Z)_0$, and corresponds to a snapshot of the catalyst at

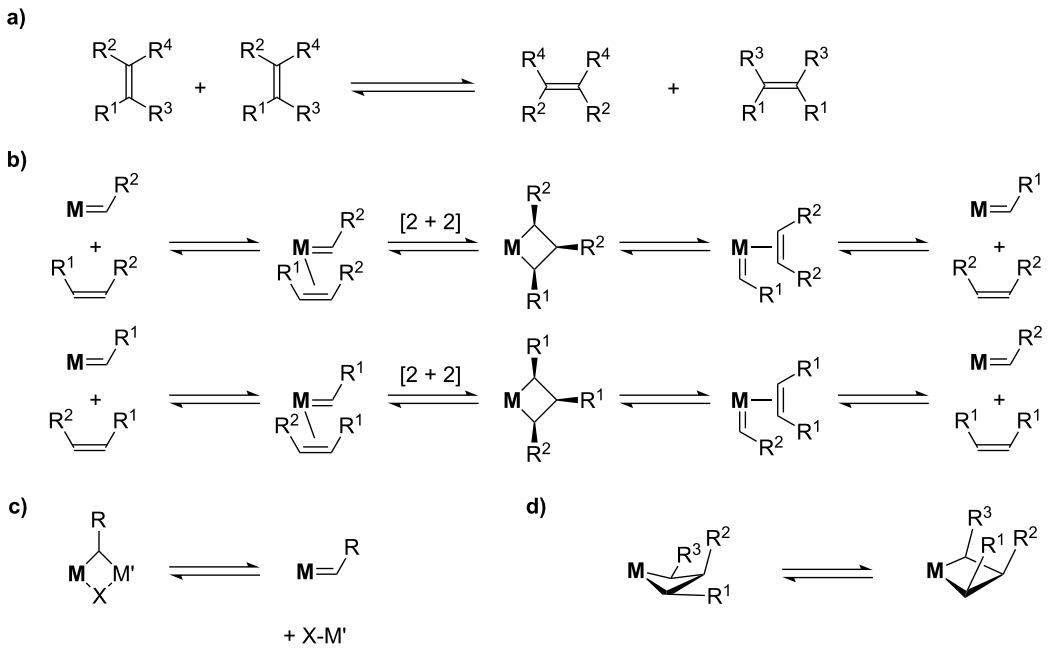

Scheme 1: Alkene metathesis mechanism.

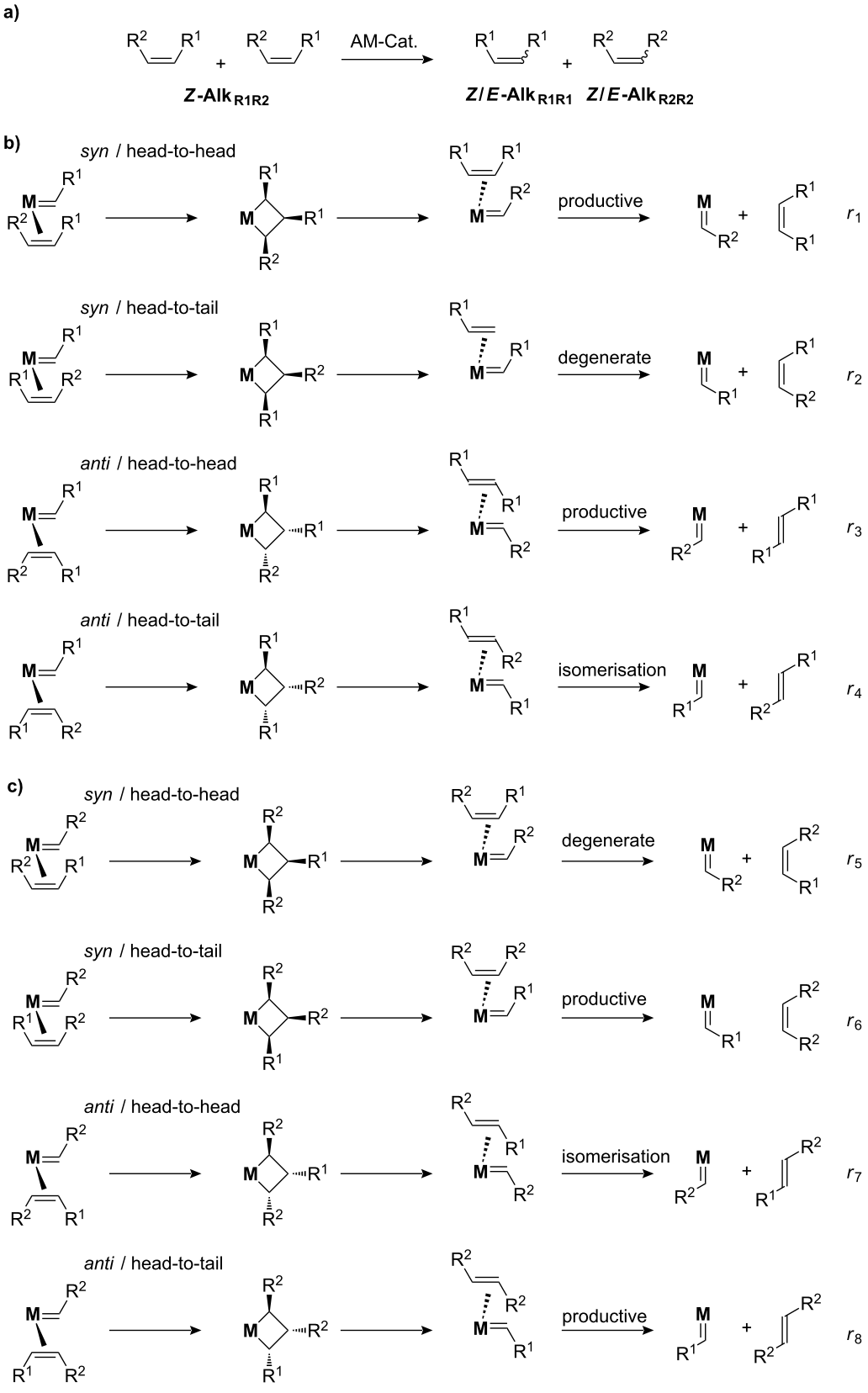

Scheme 2: Metathesis possibilities.

work. From a purely statistical standpoint (Scheme 2), one would expect to observe: i) a one-to-one (*E*/*Z*) kinetic ratio for each alkene products, $(E/Z)_0 = 1$, and ii) the formation of the opposite isomer of the alkene reactant for every two metathesis products transformed. If the catalyst show any selectivity, $(E/Z)_0$ of products will deviate from one. The same analysis can be performed for (*E*)- and terminal ($R^2 = R^3 = R^4 = H$) alkenes; for the former it is best to study the (*Z*/*E*) ratio rather than the (*E*/*Z*) ratio as a function of time.

Overall, this shows that it is not possible to avoid isomerisation in metathesis and achieving high stereoselectivity is thus difficult, because isomerisation of the starting material will occur as the reaction proceeds at a rate two times lower than metathesis, and self-metathesis of both isomers (of both the starting material and products) will then compete as the product concentration increases. This clearly illustrates the challenge in obtaining high stereoselectivity at high conversions; further underlining the need for highly stereoselective as well as stereospecific catalysts.

Finally, it also shows that monitoring the stereoselectivity at low conversions $(E/Z)_0$ can be very helpful in obtaining molecular information about the structure of the active sites and also how it evolves with time. Stereochemical analysis is therefore a powerful tool that will be exploited thereafter to obtain more information about supported catalysts.

Stereoselectivity of heterogeneous alkene metathesis catalysts: a snapshot of the structures of active sites

Well-defined silica supported catalysts

Metathesis of propene in flow reactors can easily allow the kinetic stereoselectivity of a catalyst at low contact times (high space velocity) to be obtained. For instance, [(≡SiO)(*t*-BuCH$_2$)Re(=CH*t*-Bu)(≡C*t*-Bu)] displays a $(E/Z)_0$ of 2, which is very close the thermodynamic equilibrium value of 3, even at low conversions and contact times [25-27]. Switching to Mo- and W-based catalysts that have variety of ligands ([(≡SiO)(X)M(=CHR')(=NR)], Table 1), in particular with different groups for X and on the imido ligands, the selectivity varies with $(E/Z)_0$ ranging from 1.6 to 0.5. In particular, with the bulky X = NPh$_2$ and small imido ligands (*N*-adamantyl), *Z*-selectivity is achieved, albeit never exceeding 67% [$(E/Z) = 0.5$]. While low, it shows that it should be possible to control the stereoselectivity by using the right combination of ligands. Note also that these low selectivities are in sharp contrast with the recent results of the groups of Hoveyda and Schrock, who showed that with very bulky aryloxide ligands in place of the siloxy, such systems achieved high levels of stereoselectivity (up to > 95% selectivity at high conversions) [15-18]. This demonstrates that the siloxy ligands on a silica surface should not been viewed as such a large ligand.

Stereoselectivity has been studied in greater details with the Re-based silica supported catalysts [26]. Using ethyl oleate as a representative *Z*-alkene, this catalyst is *Z*-selective with $(E/Z)_0$ values (*Z*-selectivities) ranging between 0.05 (> 95%, diastereoselectivity excess (de) > 90%) and 0.8 (55%, de = 10%), depending on the solvent (THF > toluene > heptane, Table 2); the best compromise between activity and selectivity being achieved in toluene. This *Z*-selectivity can be interpreted as a way to minimize interactions between the surface with all alkyl ligands of the alkene and the alkylidene ligand (Scheme 2).

Table 2: Initial rates (TOF) and selectivity at low conversions $(E/Z)_0$ in the metathesis of methyl oleate (0.12 M) with [(≡SiO)(*t*-BuCH$_2$)Re(=CH*t*-Bu)(≡C*t*-Bu)] (1 mol %).

Solvent	TOF/min^{-1}	$(E/Z)_0$
THF	<0.120	0.05–0.2
Toluene	4.8	0.2–0.4
Heptane	6.6	0.6–0.9

Table 1: Stereoselectivity of well-defined silica supported catalysts of general formula [(≡SiO)(X)M(=CHR')(=NR)] with M = Mo or W: (*E*/*Z*)-ratio at low conversions in propene metathesis.

Mo (W) X-ligand	Reference	Effect of the substituent on the imido ligand (=NR)			
		2,6-di-*i*-Pr-C$_6$H$_3$	Ad	2,6-di-Me-C$_6$H$_3$	*o*-CF$_3$-C$_6$H$_4$
CH$_2$*t*-Bu	[28]	0.8 (1.3) [29]	—	—	—
NPh$_2$	[30]	1.5	0.5	0.6	0.8
Pyr	[30]	0.8	0.6	—	—
2,5-di-Me-Pyr	[31]	1.1 (0.8) [32]	1.3	—	0.8
O*t*-Bu	[33]	0.7	—	—	—
OR$_{F6}$	[34]	1.3	—	—	—
OAr	[34]	0.8	—	—	—

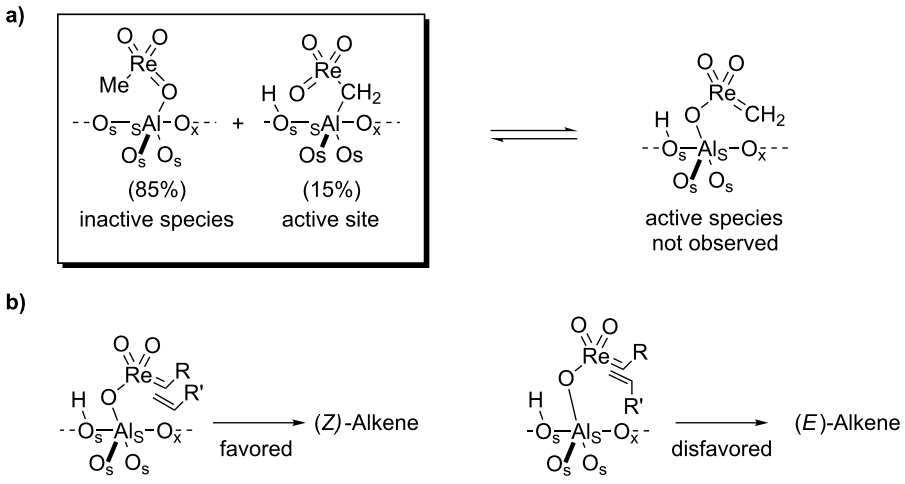

Scheme 3: Metathesis with Re-based alumina supported catalysts.

Re-based alumina supported systems

With Re-based alumina supported catalysts, the (*E*/*Z*) ratio in 2-butenes in the metathesis of propene is always close to the actual thermodynamic value (ca. 2 vs 3) even for conversions as low as 2% (vs ca. 30% thermodynamic plateau).

For $MeReO_3/Al_2O_3$, where the active sites is $[Al_SCH_2ReO_3]$ (Scheme 3a) [35,36], decreasing the conversion to well below 0.1% allows the measurement of a kinetic (*E*/*Z*) ratio of 0.4 thus showing that this catalyst is slightly *Z*-selective (70%), probably because the favoured pathway minimizes interaction of the substituents with the surface (Scheme 3b) [36]. Importantly, the evolution of the (*E*/*Z*) ratio in 2-butenes as a function of propene conversion shows hyperbolic behaviour (Figure 1a). This is reminiscent of Langmuir–Hinshelwood kinetics (or Michaelis–Menten kinetics if it were an enzyme), and in fact, when far from equilibrium, it is possible to express the rate of isomerisation of (*Z*)- into (*E*)-2-butenes via metathesis (r_{isom}) according to Equation 1, where k_{isom} is the rate constant of metathesis and $\Theta_{Z\text{-}C4}$ the surface coverage in (*Z*)-2-butene (*Z*-C4). Surface coverage describes the concentration of a gas at the surface as a function of the partial pressures of all components (P_i) and their equilibrium constant (λ_i). For (*Z*)-2-butenes, it can be expressed according to Equation 2, which explains the hyperbolic relationship obtained for the evolution of selectivity vs conversion.

$$r_{isom} = k \times \Theta_{Z\text{-}C4} \quad (1)$$

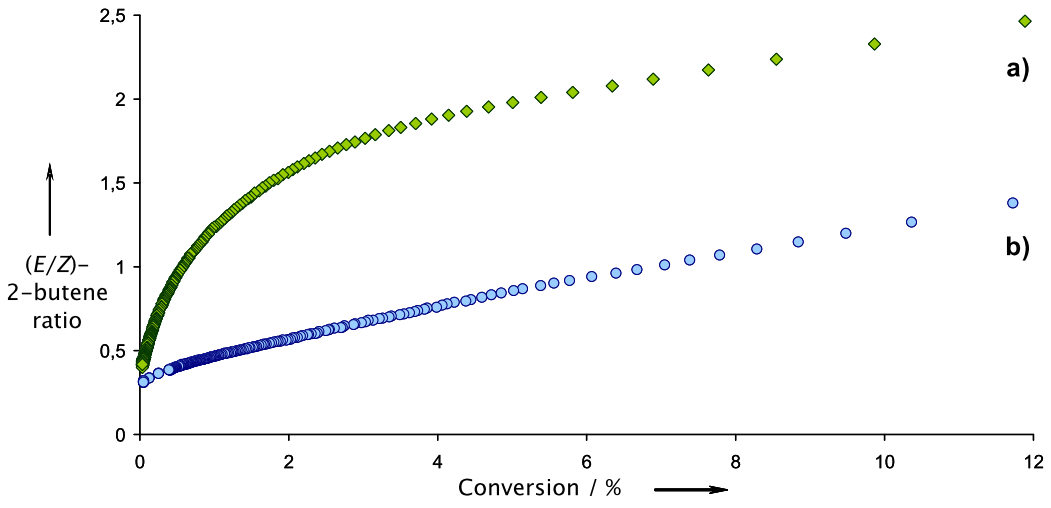

Figure 1: (*E*/*Z*) ratio as a function of conversion. a) $MeReO_3$ supported on alumina and b) $MeReO_3$ supported on alumina modified by trimethylsilyl functionalities.

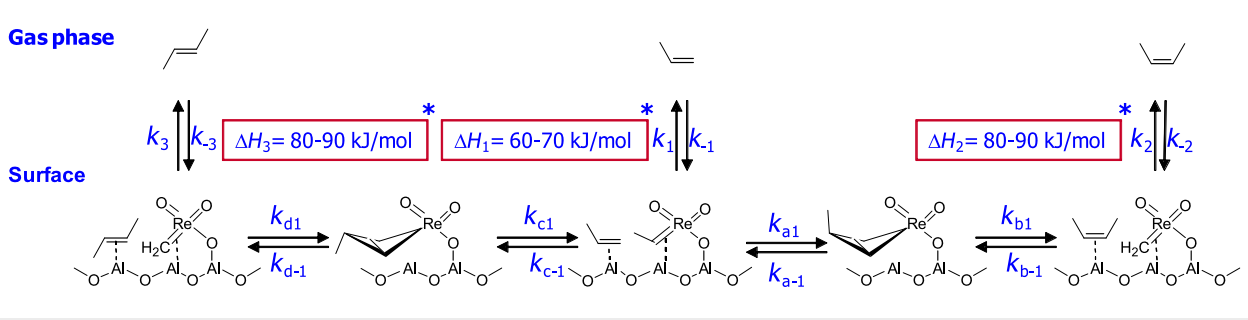

Scheme 4: Alkene selectivity of metathesis reactions.

$$\Theta_{Z\text{-}C4} = \frac{\lambda_{Z\text{-}C4} \times P_{Z\text{-}C4}}{1 + \sum_i \lambda_i P_i} \quad (2)$$

$$\Theta_{Z\text{-}C4} \approx \lambda_{Z\text{-}C4} \times P_{Z\text{-}C4} \quad (3)$$

From this equation, it is clear that what drives the selectivity (or the non-selectivity) is that 2-butenes have a better surface coverage than propene (the reactant) because of their lower vapour pressure and higher affinity for the surface (greater ΔH of adsorption) [37,38], and therefore reacts faster than propene (Scheme 4). In other words, isomerisation is faster than productive metathesis, so that the thermodynamic ratio of 2-butenes is almost reached even at relatively low conversions. This equation also indicates that modification of adsorption properties of the support should, in principle, modify the selectivity of the catalysts.

The introduction of hydrophobic groups ($OSiMe_3$) prior to chemisorption of $MeReO_3$ on alumina leads to a completely different behaviour in terms of selectivity (Figure 1b) [39]. Here, the selectivity nearly evolves linearly with respect to conversion, due to a lower surface coverage of alkenes on this modified support ($\lambda_i P_i << 1$, because of the loss of acidity and, as a result, interaction between alkenes and the alumina surface) so that the rate of isomerisation is now proportional to conversion (Equation 3) allowing higher *Z*-selectivities at higher conversions.

It is also noteworthy that the selectivity at low conversions with this modified catalyst is the same as the previous one, indicating that the structure of the active sites is probably similar in both cases. It is also worth noting that a similar value was also obtained for Re_2O_7/Al_2O_3 [40,41], which infers similar structural features for the active sites [42].

Finally, this shows that modifying the surface adsorption properties can favour the formation of primary products by slowing down secondary processes such as isomerisation, but that improving the selectivity requires tuning the structure of the active sites to favour one isomer over the other (modification of the first coordination sphere).

Hybrid materials containing Ru–NHC units

New strategies to develop supported homogeneous catalysts involves the preparation of hybrid organic–inorganic materials [43], where surface functionalities such as typical organic ligands are perfectly distributed within the pore networks of a mesoporous silica. For other approaches used to prepare supported homogeneous catalysts, see the reviews [44-46]. Selective grafting of organometallic complexes onto these pendant ligands can then be performed. Using this technology, several materials containing N-heterocyclic metal units (M–NHC) have been prepared, including a system containing a Ru–NHC unit (Scheme 5), which displayed unprecedented activity in the metathesis of ethyl oleate with turnover numbers in excess of 15,000 [47].

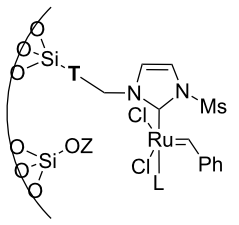

M-Ru-Bn: Z = $SiMe_3$, **T** = C_6H_4
M-Ru-Pr: Z = $SiMe_3$, **T** = $(CH_2)_2$

Scheme 5: Hybrid organic–inorganic catalyst containing a Ru–NHC unit.

Identity of the active sites for these systems could be obtained from stereochemical studies, i.e., the measurement of $(E/Z)_0$. Indeed, comprehensive studies of various Ru–NHC homogeneous catalysts showed that the so-called G-I catalysts (no NHC and PCy_3 coordinated to the metal centre) displayed selectivities at low conversions with $(E/Z)_0$ significantly different from G-II catalysts (one NHC ligand): 2.7–3.2 vs 1.5–2.1, respectively (or 3.5–3.6 vs 2.0–2.7, if one looks at $(E/Z)_0$ obtained by

extrapolating (E/Z) ratio to 0 from values obtained under steady state conditions; Table 3). These data show that one can know if active species is based on NHC–Ru as opposed to a Cy_3P–Ru. Moreover, the change of values between selectivities at low conversions and extrapolated data (values in parentheses) can be interpreted as an indication of a change of structure of active sites during the catalytic run. When applying this study to materials (**M-Ru-Pr** and **M-Ru-Bn**, Scheme 5 and Table 3), a $(E/Z)_0$ of 2.0–2.2 was found irrespective of whether the Ru–NHC containing materials had a propyl or a benzyl pendant group, in clear agreement with the presence of Ru–NHC active sites. This once again demonstrates the power of this method to probe active site structures.

Table 3: Stereoselectivity of Ru–NHC catalysts. Comparison of molecular complexes and materials containing Ru–NHC units.

Catalysts	$(E/Z)_0$ 9-Octadecene	$(E/Z)_0$ Diester[a]
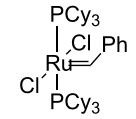	2.7 (3.6)	3.0 (3.4)
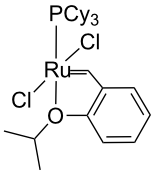	3.2 (3.5)	3.2 (3.5)
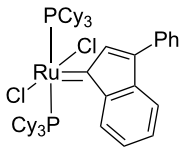	3.2 (3.5)	2.7 (3.4)
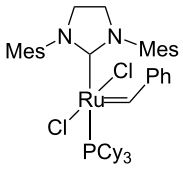	1.5 (2.5)	1.7 (2.7)
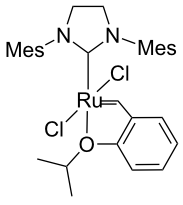	1.6 (2.3)	2.0 (2.5)
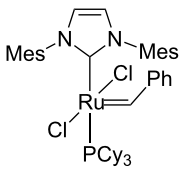	1.7 (2.6)	2.0 (2.6)
M-Ru-Pr	—	2.0 (2.0)
M-Ru-Bn	—	2.2 (2.2)

[a]The values in parentheses correspond to extrapolated (E/Z) ratio from the extrapolated value at the steady state.

Conclusion

Overall, obtaining selectivities at low conversions $(E/Z)_0$ can help to probe the structure of surface species at a molecular level, and should probably be used more often as a probe to understand the structure and the modification of structures of catalysts under working conditions, whether homogeneous or heterogeneous. Ru-based heterogeneous catalysts are *E*-selective (60–70%) when transforming (*Z*)-alkenes such as ethyl oleate, as their homogeneous equivalents. In contrast, the Re-based silica supported catalyst, in a d^0 configuration, is slightly *Z*-selective (70–95%) under the same reaction conditions.

For the conversion of propene, it is clear that silica supported catalysts are not selective with $(E/Z)_0$ ratio ranging from 0.5 to 2 and that the change of selectivity results from the structure of the ligands (first coordination sphere). Importantly, this low selectivity indicates that a surface siloxy group is not large enough to provide any control of selectivity in contrast to the bulky phenoxy ligands used for highly selective homogeneous catalysts [14-18]. In the case of catalysts supported on alumina, the support plays a major role because it controls the rate of adsorption/desorption of reactants and products. This precludes high selectivity being reached as secondary isomerisation processes via metathesis are favoured.

Overall, the current data show that developing selective heterogeneous catalysts will require developing more tuneable surfaces in particular through the control of the first coordination sphere of the metal centre. This has already been achieved for enantioselective heterogeneous catalysts [48], but remains to be realised for *Z*- or *E*-selective catalysts. Promising routes include the incorporation in a controlled manner of perfectly designed organic functionalities in organic or inorganic matrices [47,48].

Acknowledgements

CC acknowledges the co-authors involved in metathesis project, whose names are listed in the references. CC is also grateful to funding agencies and companies, in particular CNRS, ANR and BASF for financial supports.

References

1. Kolb, H. C.; VanNieuwenhze, M. S.; Sharpless, K. B. *Chem. Rev.* **1994,** *94,* 2483–2547. doi:10.1021/cr00032a009

2. Sharpless, K. B. *Angew. Chem., Int. Ed.* **2002,** *41,* 2024–2032. doi:10.1002/1521-3773(20020617)41:12<2024::AID-ANIE2024>3.0.CO;2-O
3. Noyori, R. *Angew. Chem., Int. Ed.* **2002,** *41,* 2008–2022. doi:10.1002/1521-3773(20020617)41:12<2008::AID-ANIE2008>3.0.CO;2-4
4. Resconi, L.; Cavallo, L.; Fait, A.; Piemontesi, F. *Chem. Rev.* **2000,** *100,* 1253–1345. doi:10.1021/cr9804691
5. Schrock, R. R. *Angew. Chem., Int. Ed.* **2006,** *45,* 3748–3759. doi:10.1002/anie.200600085
6. Grubbs, R. H. *Angew. Chem., Int. Ed.* **2006,** *45,* 3760–3765. doi:10.1002/anie.200600680
7. Chauvin, Y. *Angew. Chem., Int. Ed.* **2006,** *45,* 3741–3747. doi:10.1002/anie.200601234
8. Alexander, J. B.; La, D. S.; Cefalo, D. R.; Hoveyda, A. H.; Schrock, R. R. *J. Am. Chem. Soc.* **1998,** *120,* 4041–4042. doi:10.1021/ja974353i
9. Hoveyda, A. H.; Schrock, R. R. *Chem.–Eur. J.* **2001,** *7,* 945–950. doi:10.1002/1521-3765(20010302)7:5<945::AID-CHEM945>3.0.CO;2-3
10. Weatherhead, G. S.; Cortez, G. A.; Schrock, R. R.; Hoveyda, A. H. *Proc. Natl. Acad. Sci. U. S. A.* **2004,** *101,* 5805–5809. doi:10.1073/pnas.0307589101
11. Funk, T. W.; Berlin, J. M.; Grubbs, R. H. *J. Am. Chem. Soc.* **2006,** *128,* 1840–1846. doi:10.1021/ja055994d
12. Berlin, J. M.; Goldberg, S. D.; Grubbs, R. H. *Angew. Chem., Int. Ed.* **2006,** *45,* 7591–7595. doi:10.1002/anie.200602469
13. Cortez, G. A.; Baxter, C. A.; Schrock, R. R.; Hoveyda, A. H. *Org. Lett.* **2007,** *9,* 2871–2874. doi:10.1021/ol071008h
14. Lefebvre, F.; Leconte, M.; Pagano, S.; Mutch, A.; Basset, J.-M. *Polyhedron* **1995,** *14,* 3209–3226. doi:10.1016/0277-5387(95)85007-4
15. Jiang, A. J.; Zhao, Y.; Schrock, R. R.; Hoveyda, A. H. *J. Am. Chem. Soc.* **2009,** *131,* 16630–16631. doi:10.1021/ja908098t
16. Ibrahem, I.; Yu, M.; Schrock, R. R.; Hoveyda, A. H. *J. Am. Chem. Soc.* **2009,** *131,* 3844–3845. doi:10.1021/ja900097n
17. Flook, M. M.; Jiang, A. J.; Schrock, R. R.; Muller, P.; Hoveyda, A. H. *J. Am. Chem. Soc.* **2009,** *131,* 7962–7963. doi:10.1021/ja902738u
18. Hoveyda, A. H.; Malcolmson, S. J.; Meek, S. J.; Zhugralin, A. R. *Angew. Chem., Int. Ed.* **2010,** *49,* 34–44. doi:10.1002/anie.200904491
19. Ferre-Filmon, K.; Delaude, L.; Demonceau, A.; Noels, A. F. *Eur. J. Org. Chem.* **2005,** 3319–3325. doi:10.1002/ejoc.200500068
20. Pawluc, P.; Hreczycho, G.; Suchecki, A.; Kubicki, M.; Marciniec, B. *Tetrahedron* **2009,** *65,* 5497–5502. doi:10.1016/j.tet.2009.01.113
21. Sinha, A. K.; Kumar, V.; Sharma, A.; Sharma, A.; Kumar, R. *Tetrahedron* **2007,** *63,* 11070–11077. doi:10.1016/j.tet.2007.08.034
22. Basset, J. M.; Bilhou, J. L.; Mutin, R.; Theolier, A. *J. Am. Chem. Soc.* **1975,** *97,* 7376–7377. doi:10.1021/ja00858a029
23. Bilhou, J. L.; Basset, J. M.; Mutin, R.; Graydon, W. F. *J. Chem. Soc., Chem. Commun.* **1976,** 970–971. doi:10.1039/C39760000970
24. Bilhou, J. L.; Basset, J. M.; Mutin, R.; Graydon, W. F. *J. Am. Chem. Soc.* **1977,** *99,* 4083–4090. doi:10.1021/ja00454a029
25. Chabanas, M.; Baudouin, A.; Copéret, C.; Basset, J. M. *J. Am. Chem. Soc.* **2001,** *123,* 2062–2063. doi:10.1021/ja000900f
26. Chabanas, M.; Copéret, C.; Basset, J.-M. *Chem.–Eur. J.* **2003,** *9,* 971–975. doi:10.1002/chem.200390119
27. Leduc, A.-M.; Salameh, A.; Soulivong, D.; Chabanas, M.; Basset, J.-M.; Coperet, C.; Solans-Monfort, X.; Clot, E.; Eisenstein, O.; Boehm, V. P. W.; Roeper, M. *J. Am. Chem. Soc.* **2008,** *130,* 6288–6297. doi:10.1021/ja800189a
28. Blanc, F.; Copéret, C.; Thivolle-Cazat, J.; Basset, J.-M.; Lesage, A.; Emsley, L.; Sinha, A.; Schrock, R. R. *Angew. Chem., Int. Ed.* **2006,** *45,* 1216–1220. doi:10.1002/anie.200503205
29. Rhers, B.; Salameh, A.; Baudouin, A.; Quadrelli, E. A.; Taoufik, M.; Copéret, C.; Lefebvre, F.; Basset, J.-M.; Solans-Monfort, X.; Eisenstein, O.; Lukens, W. W.; Lopez, L. P. H.; Sinha, A.; Schrock, R. R. *Organometallics* **2006,** *25,* 3554–3557. doi:10.1021/om060279d
30. Blanc, F.; Thivolle-Cazat, J.; Basset, J.-M.; Copéret, C.; Hock, A. S.; Tonzetich, Z. J.; Schrock, R. R. *J. Am. Chem. Soc.* **2007,** *129,* 1044–1045. doi:10.1021/ja068249p
31. Blanc, F.; Berthoud, R.; Salameh, A.; Basset, J.-M.; Copéret, C.; Singh, R.; Schrock, R. R. *J. Am. Chem. Soc.* **2007,** *129,* 8434–8435. doi:10.1021/ja073095e
32. Blanc, F.; Berthoud, R.; Coperet, C.; Lesage, A.; Emsley, L.; Singh, R.; Kreickmann, T.; Schrock, R. R. *Proc. Natl. Acad. Sci. U. S. A.* **2008,** *105,* 12123–12127. doi:10.1073/pnas.0802147105
33. Blanc, F.; Rendon, N.; Berthoud, R.; Basset, J.-M.; Coperet, C.; Tonzetich, Z. J.; Schrock, R. R. *Dalton Trans.* **2008,** 3156–3158. doi:10.1039/b805686m
34. Rendon, N.; Berthoud, R.; Blanc, F.; Gajan, D.; Maishal, T.; Basset, J. M.; Coperet, C.; Lesage, A.; Emsley, L.; Marinescu, S. C.; Singh, R.; Schrock, R. R. *Chem.–Eur. J.* **2009,** *15,* 5083–5089. doi:10.1002/chem.200802465
35. Salameh, A.; Joubert, J.; Baudouin, A.; Lukens, W.; Delbecq, F.; Sautet, P.; Basset, J. M.; Copéret, C. *Angew. Chem., Int. Ed.* **2007,** *46,* 3870–3873. doi:10.1002/anie.200700211
36. Salameh, A.; Baudouin, A.; Soulivong, D.; Boehm, V.; Roeper, M.; Basset, J.-M.; Copéret, C. *J. Catal.* **2008,** *253,* 180–190. doi:10.1016/j.jcat.2007.10.007
37. Grinev, V. E.; Khalif, V. A.; Aptekar, E. L.; Krylov, O. V. *Izv. Akad. Nauk SSSR, Ser. Khim.* **1981,** 1648–1651.
38. Grinev, V. E.; Madden, M.; Khalif, V. A.; Aptekar, E. L.; Aldag, A. W., Jr.; Krylov, O. V. *Kinet. Catal.* **1983,** *24,* 753–755.
39. Salameh, A.; Baudouin, A.; Basset, J.-M.; Coperet, C. *Angew. Chem., Int. Ed.* **2008,** *47,* 2117–2120. doi:10.1002/anie.200704876
40. Salameh, A.; Copéret, C.; Basset, J.-M.; Bohm, V. P. W.; Roper, M. *Adv. Synth. Catal.* **2007,** *349,* 238–242. doi:10.1002/adsc.200600440
41. Mol, J. C. *Catal. Today* **1999,** *51,* 289–299. doi:10.1016/S0920-5861(99)00051-6
42. Salameh, A. Compréhension moléculaire du catalyseur de métathèse des oléfines ReO/AlO site actif, initiation et désactivation par chimie organométallique de surface. Ph.D. Thesis, Université Claude Bernard, Lyon 1, France, 2006.
43. Maishal, T. K.; Alauzun, J.; Basset, J.-M.; Copéret, C.; Corriu, R. J. P.; Jeanneau, E.; Mehdi, A.; Reyé, C.; Veyre, L.; Thieuleux, C. *Angew. Chem., Int. Ed.* **2008,** *47,* 8654–8656. doi:10.1002/anie.200802956
44. Copéret, C.; Basset, J. M. *Adv. Synth. Catal.* **2007,** *349,* 78–92. doi:10.1002/adsc.200600443
45. Clavier, H.; Grela, K.; Kirschning, A.; Mauduit, M.; Nolan, S. P. *Angew. Chem., Int. Ed.* **2007,** *46,* 6786–6801. doi:10.1002/anie.200605099
46. Buchmeiser, M. R. *Chem. Rev.* **2009,** *109,* 303–321. doi:10.1021/cr800207n
47. Karame, I.; Boualleg, M.; Camus, J. M.; Maishal, T. K.; Alauzun, J.; Basset, J. M.; Coperet, C.; Corriu, R. J. P.; Jeanneau, E.; Mehdi, A.; Reye, C.; Veyre, L.; Thieuleux, C. *Chem.–Eur. J.* **2009,** *15,* 11820–11823. doi:10.1002/chem.200901752

48. Hultzsch, K. C.; Jernelius, J. A.; Hoveyda, A. H.; Schrock, R. R. *Angew. Chem., Int. Ed.* **2002,** *41,* 589–593. doi:10.1002/1521-3773(20020215)41:4<589::AID-ANIE589>3.0.CO;2-V

License and Terms

Beilstein Journal of Organic Chemistry

Hoveyda–Grubbs type metathesis catalyst immobilized on mesoporous molecular sieves MCM-41 and SBA-15

Hynek Balcar*, Tushar Shinde, Naděžda Žilková and Zdeněk Bastl

Full Research Paper

Open Access

Address:
J. Heyrovský Institute of Physical Chemistry of AS CR, v.v.i, Dolejškova 3, 182 23 Prague 8, Czech Republic

Email:
Hynek Balcar* - balcar@jh-inst.cas.cz

* Corresponding author

Keywords:
alkene metathesis; catalyst immobilization; hybrid catalysts; mesoporous molecular sieves; Ru–alkylidene complexes

Beilstein J. Org. Chem. **2011,** *7,* 22–28.
doi:10.3762/bjoc.7.4

Received: 31 August 2010
Accepted: 16 November 2010
Published: 06 January 2011

Guest Editor: K. Grela

Abstract

A commercially available Hoveyda–Grubbs type catalyst (RC303 Zhannan Pharma) was immobilized on mesoporous molecular sieves MCM-41 and on SBA-15 by direct interaction with the sieve wall surface. The immobilized catalysts exhibited high activity and nearly 100% selectivity in several types of alkene metathesis reactions. Ru leaching was found to depend on the substrate and solvent used (the lowest leaching was found for ring-closing metathesis of 1,7-octadiene in cyclohexane – 0.04% of catalyst Ru content). Results of XPS, UV–vis and NMR spectroscopy showed that at least 76% of the Ru content was bound to the support surface non-covalently and could be removed from the catalyst by washing with THF.

Introduction

Ru–alkylidene complexes (Grubbs and Hoveyda–Grubbs catalysts, **1** and **2**, respectively, Figure 1) belong to the most active and frequently used metathesis catalysts. These catalysts are important tools in organic synthesis due to their high tolerance of heteroatoms in substrate molecules. Immobilization of these complexes on solid supports has attracted attention, because it opens the possibility for easy catalyst–product separation and catalyst reuse. The production of products free from catalyst residues is especially important in the synthesis of drugs and some other fine chemicals. Several strategies have been developed for the immobilization of Grubbs and Hoveyda–Grubbs catalysts on solid supports [1-6]. Generally, the complex can be attached to the supports: (a) by exchanging halide ligands X [7-11], (b) by exchanging phosphine and NHC ligands L [12,13], and (c) through the alkylidene ligand [14-19]. For these purposes, special ligand molecules with tags suitable

for the reaction with the support surface (linkers) are used. This usually requires a sophisticated synthetic procedure. Moreover, the changes in the Ru coordination sphere may lead to the decrease in catalyst activity (e.g., the exchange of chloro ligands for carboxylates [10,11]).

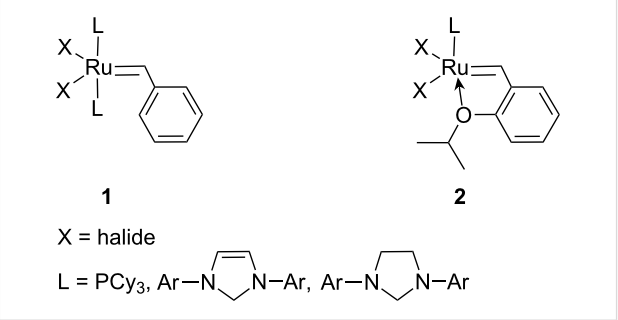

Figure 1: Grubbs **1** and Hoveyda–Grubbs **2** catalysts.

Recently, a convenient method for the immobilization of Hoveyda–Grubbs catalysts was reported [20]. A second generation Hoveyda–Grubbs catalyst was immobilized on silica without any linkers by simply placing the Ru complex in contact with silica in a suspension. Heterogeneous catalysts (loading from 0.05 to 0.6 wt % Ru) were prepared, which were active in ring-opening metathesis polymerization (ROMP) of cyclooctene, ring-closing metathesis (RCM) of diallylsilanes and several types of cross-metathesis reactions. High stability of catalysts, reusability and low Ru leaching were also reported. However, the mode of attachment of the Ru species on the silica surface was unclear.

The aims of this paper are the following: to report the immobilization of the Hoveyda–Grubbs type catalyst **3** (Figure 2, Zhan catalyst-1B) on mesoporous molecular sieves SBA-15 and MCM-41 as supports with this simple immobilization method; to describe the activity and stability of heterogeneous catalysts prepared; and to clarify the nature of the bond between the Ru complex and the support surface. Mesoporous molecular sieves are advanced siliceous materials [21], with high surface area, high pore volume and narrow distribution of pore size. Because of these unique qualities, they often find applications as supports of modern catalysts, including those used for metathesis reactions [22].

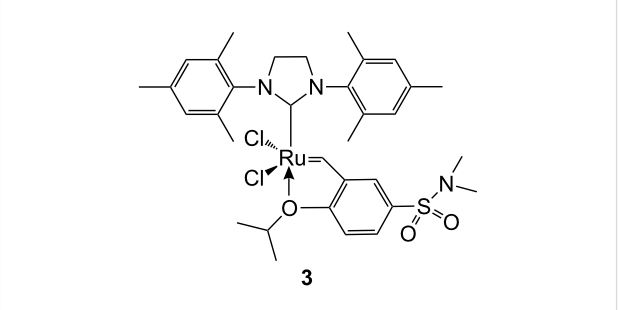

Figure 2: Zhan catalyst-1B.

Results and Discussion

Catalyst activity

Mixing a toluene solution of **3** with dried MCM-41 and SBA-15, respectively, for 30 min at room temperature led to green solids, which after isolation and drying afforded heterogeneous catalysts **3**/MCM-41 and **3**/SBA-15. The immobilization proceeded almost quantitatively: 97% and 94% of the Ru complex was transferred from the solution onto the MCM-41 and SBA-15 surface, respectively. The established catalyst loading was 0.98 wt % and 0.93 wt %, for **3**/MCM-41 and **3**/SBA-15, respectively.

The catalytic activity was tested in the RCM of 1,7-octadiene (Scheme 1, entry 1) and diethyl diallylmalonate (DEDAM) (Scheme 1, entry 2), in the metathesis of methyl oleate (Scheme 1, entry 3) and methyl 10-undecenoate (Scheme 1, entry 4), and in the ROMP of cyclooctene (Scheme 1, entry 5).

Figure 3 shows conversion curves for the RCM of DEDAM in dichloromethane, benzene, and cyclohexane, and the RCM of 1,7-octadiene in cyclohexane. For the RCM of DEDAM, **3** (as a homogeneous catalyst) and **3**/SBA-15 were used. The reaction proceeded very rapidly in all solvents used (TOF at 10 min was approximately 2500 h^{-1}). No decrease in the reaction rate was observed as a result of the immobilization of complex **3**. For the RCM of 1,7-octadiene, **3**/SBA-15 and **3**/MCM-41 in cyclohexane were used. The reaction profile was the same for both catalysts and the reaction rate was significantly lower compared to the RCM of DEDAM. The selectivity was near 100% in all cases (no side products were observed by GC).

The Ru leaching (in % of starting content of Ru in catalyst) for the reactions shown in Figure 3 is given in Table 1. It was observed that leaching was dependent on both the solvent and substrate used in the reaction – the highest leaching was found for the RCM of DEDAM in CH_2Cl_2 whilst negligible leaching was observed for the RCM of 1,7-octadiene in cyclohexane.

Filtration experiments carried out with **3**/SBA-15 (Figure 4) showed that the catalytic activity was completely bound to the solid phase for the RCM of 1,7-octadiene in cyclohexane. At 5 min after starting the reaction, about ½ of the volume of the liquid phase was separated by filtration and transferred into a new reactor, kept under identical reaction conditions. No increase in conversion was observed in this reactor. For the RCM of DEDAM in benzene, however, a considerable increase

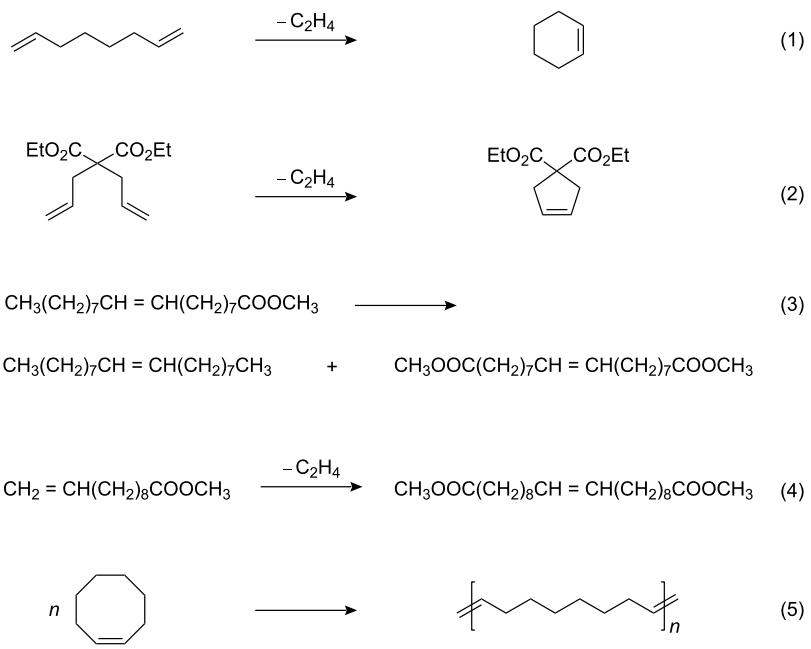

Scheme 1: Metathesis reactions studied.

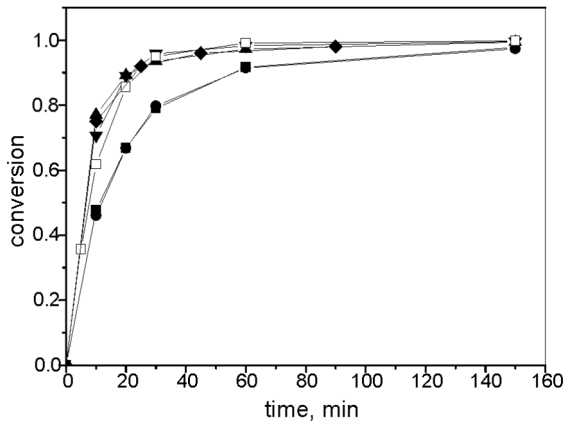

Figure 3: Conversion curves for the RCM of DEDAM with **3** in CH_2Cl_2 (open squares), **3**/SBA-15 in CH_2Cl_2 (inverted filled triangle), **3**/SBA-15 in benzene (filled diamond), **3**/SBA-15 in cyclohexane (filled triangle), and for the RCM of 1,7-octadiene with **3**/SBA-15 (filled squares) and **3**/MCM-41 (filled circles) in cyclohexane (T = 30 °C, molar ratio substrate/Ru = 600, $c^0_{substrate}$ = 0.2 mol/L).

Table 1: Ru leaching for **3**/SBA-15.

Reaction	Solvent	Ru leaching	Maximal Ru content in product[a]
(1)	cyclohexane	0.04%	0.6 ppm
(2)	benzene	4%	28 ppm
(2)	cyclohexane	9%	66 ppm
(2)	dichloromethane	14%	100 ppm

molar ratio substrate/Ru = 600, $c^0_{substrate}$ = 0.2 mmol/mL, T = 30 °C
[a]calculated as the amount of Ru per weight unit of substrate

of substrate conversion in liquid phase after its separation from solid catalyst indicated that the Ru species released from the solid catalyst were capable of initiating catalytic reactions.

Figure 5 shows the activity of **3**/MCM-41 and **3**/SBA-15 in the metathesis of methyl oleate and methyl 10-undecenoate. The reaction proceeded more slowly than in the case of the RCM of DEDAM (TOF at 30 min = 260 h^{-1} for methyl oleate and 35 h^{-1} for methyl 10-undecenoate, both with **3**/MCM-41). The metathesis of methyl oleate reached the equilibrium after 2 h. In the case of methyl 10-undecenoate, the reaction rate was lower than for methyl oleate (because of probable non-productive metathesis [23]) and the final conversion was about 65% (due to the evolution of ethylene into the gas phase). There was no significant difference observed in the conversion curves for reactions with **3**/MCM-41 and **3**/SBA-15. Selectivity near 100% was achieved in all cases.

The ROMP reactions were carried out for cyclooctene with both **3**/MCM-41 and **3**/SBA-15 (cyclooctene/Ru molar ratio = 500, $c^0_{cyclooctene}$ = 0.6 mol/L, T = 30 °C). High molecular weight polymers (M_w = 250 000, M_n = 110 000) were obtained in high yields (70% and 64% for **3**/MCM-41 and **3**/SBA-15, respectively) after 3 h.

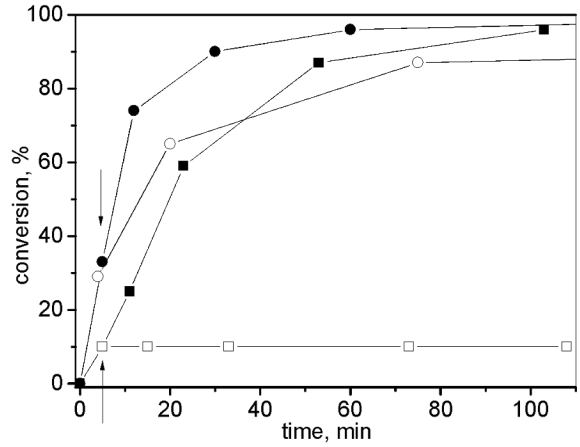

Figure 4: Filtration experiments with **3**/SBA-15. RCM of DEDAM in benzene (circles), 1,7-octadiene in cyclohexane (squares), liquid phase in contact with solid catalyst (filled symbols), liquid phase after filtration (open symbols), arrows indicate time of filtration. Substrate/Ru molar ratio 600, T = 30 °C, c^0_{DEDAM} = 0.22 mol/L, $c^0_{1,7\text{-octadiene}}$ = 0.16 mol/L.

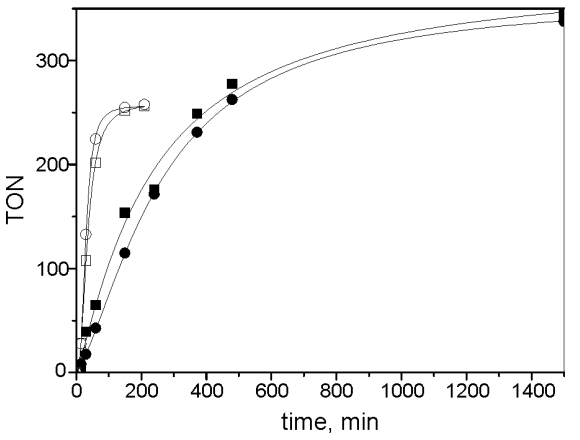

Figure 5: Metathesis of methyl oleate (open symbols) and methyl 10-undecenoate (filled symbols) with **3**/MCM-41 (circles) and **3**/SBA-15 (squares). Molar ratio substrate /Ru = 500, T = 30 °C, $c^0_{substrate}$ = 0.15 mol/L.

The catalysts **3**/MCM-41 and **3**/SBA-15 exhibited some features similar to those of Hoveyda–Grubbs catalyst immobilized on silica [20]: (a) Filtration experiments proved complete catalyst heterogeneity only for nonpolar solvents (cyclohexane and hexane, respectively); (b) catalyst leaching in these solvents was extremely low, ensuring more than one order of magnitude lower Ru concentration in products compared to the upper limit permissible in pharmaceutical production (10 ppm [3]); and (c) similar catalyst activity was observed. Although the slightly different reaction conditions applied in [20] do not allow an exact comparison, the initial TOF values achieved in [20] are of the same order as the TOF values obtained in our work. However, in the case of the ROMP of cyclooctene, catalysts **3**/MCM-41 and **3**/SBA-15 led to high molecular weight polymers, whereas in [20] the formation of polymer was not referred.

Interaction between the Ru complex and the support

For Hoveyda–Grubbs catalyst immobilized on silica, the authors in [20] proposed a direct chemical interaction between the Ru species and the silanol groups of the surface, instead of a weak physisorption. In order to shed light on the mode of complex attachment to the sieve surface, UV–vis and XPS spectra were measured. In Figure 6, the UV–vis spectra of **3**/SBA-15 and **3** in CH_2Cl_2 are compared. The bands at λ = 375 nm and at λ = 600 nm (2 orders of magnitude lower ε, not visible in Figure 6) in the spectrum of **3** reflect the d–d transition of the Ru(II) atoms [24]. Supported catalyst **3**/SBA-15 exhibits the same spectrum suggesting no changes in the coordination sphere of Ru atoms occurred during immobilization of **3** on the sieve.

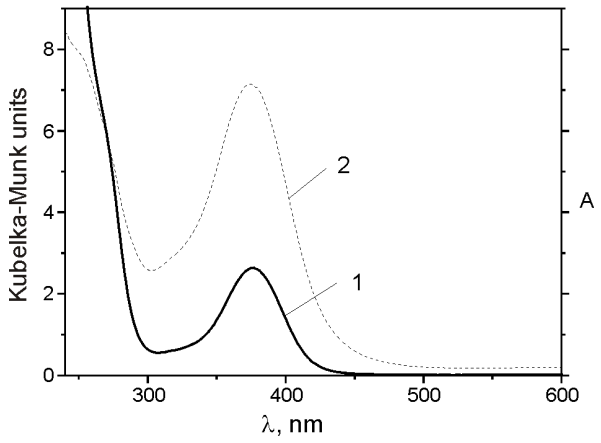

Figure 6: UV–vis spectra of **3**/SBA-15 (curve 2) and of **3** (curve 1) in dichloromethane (c = 0.001 mol/L, l = 0.2 cm).

Assuming non-covalent interactions between the Ru species and the support surface, we attempted to wash out the Ru species from **3**/SBA-15 with THF-d_8 and characterise the eluate by NMR spectroscopy. About 100 mg of **3**/SBA-15 was mixed with 1.5 mL of THF-d_8 and stirred for 2 h at room temperature. The dark green supernatant was then transferred into a NMR tube and the solid phase was washed with THF and dried in vacuo. According to the elemental analysis, 76% of the Ru was removed. In the supernatant, the presence of compound **3** was demonstrated by comparing ^{1}H and ^{13}C NMR spectra of the supernatant and corresponding spectra of a fresh solution of **3** in

THF-d_8. The catalytic activity of the solid phase was then tested in the RCM of DEDAM in cyclohexane (molar ratio DEDAM/Ru = 600, T = 30 °C, c^0_{DEDAM} = 0.2 mol/L). After 1 h, 55% conversion of DEDAM was achieved and 62% after 6 h. Only the RCM products were observed. This indicates that the remaining Ru species after washing was catalytically active; however, these species were rapidly deactivated.

Figure 7 shows high-resolution spectra of the Ru 3d–C 1s photoelectrons of neat compound **3**, catalyst **3**/SBA-15 and the same catalyst after leaching in THF. The measured binding energy of the Ru $3d_{5/2}$ electrons (281.2 ± 0.2 eV) was identical for all these samples and was in accord with the value 280.95 eV reported in literature [25] for a similar compound. This result indicates that the structure of the Ru complex is not substantially changed by the immobilization on the support surface. This conclusion is corroborated by the results of quantitative analysis. For this catalyst, the atomic concentration ratios Ru/Si = 3.5 × 10^{-3} and Cl/Ru = 2.0 were obtained from integrated intensities of Ru 3d, Si 2p and Cl 2p photoemission lines. For the sample leached by THF, the ratio Ru/Si = 9 × 10^{-4}, which is in accord with the amount of Ru removed from the support by leaching as determined from elemental analysis.

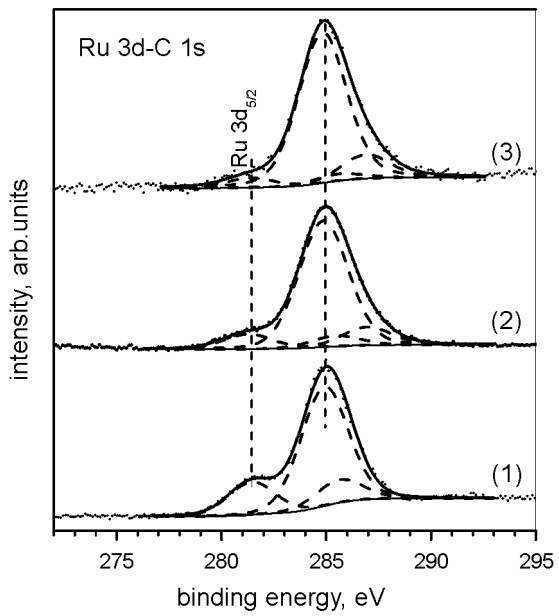

Figure 7: Spectra of the Ru 3d–C 1s photoelectrons for neat compound **3** (1), catalyst sample **3**/SBA-15 (2) and catalyst sample **3**/SBA-15 after leaching in THF (3).

The results obtained suggest that the Ru species in **3**/SBA-15 were attached to the sieves by a non-covalent interaction (probably via physical adsorption). The small residual Ru content, which was not possible to remove from **3**/SBA-15 with THF at room temperature, might be due to **3** more firmly attached to the surface (e.g., adsorbed at special sites on the surface, or embedded into micropores, etc.). Because of the low concentration of these species, we have not been able to investigate their bonding to the surface in greater detail.

Conclusion

The Hoveyda–Grubbs type catalyst **3** was immobilized on mesoporous molecular sieves MCM-41 and SBA-15 by mixing a suspension of **3** and sieves in toluene at room temperature. The immobilization proceeded quickly and almost quantitatively. Heterogeneous catalysts prepared in this way exhibited high activity and 100% selectivity in the RCM of 1,7-octadiene and diethyl diallylmalonate, in the metathesis of methyl oleate and methyl 10-undecenoate, and in the ROMP of cyclooctene. Ru leaching was found to depend on the polarity of substrate and solvent used. The lowest leaching was found for the RCM of 1,7-octadiene in cyclohexane – 0.04% of catalyst Ru content. On the other hand, for the RCM of diethyl diallylmalonate in dichloromethane, leaching reached 14% of initial Ru content in the catalysts.

Results from UV–vis and XPS studies suggested that **3** was attached to the sieve surface by non-covalent interactions. Approximately 76% of the Ru content could be recovered from the sieve as **3** (as shown by NMR) by washing with THF at room temperature (indicating physical adsorption of **3** on the sieve). The residual Ru species on the sieve exhibited catalytic activity in RCM but were rapidly deactivated.

The advantage of these catalysts is their simple preparation, avoiding support modification with special linker molecules. In nonpolar systems, they can function as true efficient heterogeneous catalysts. In the case of polar systems, the possibility of Ru leaching to a significant extent should be taken into account.

Experimental

Materials

Toluene was dried overnight over anhydrous Na_2SO_4, then distilled with Na and stored over molecular sieves 4 Å. Benzene (Lach-Ner, Czech Republic) was dried over anhydrous Na_2SO_4, distilled with P_2O_5 and then with NaH in vacuo. Dichloromethane (Lach-Ner) was dried overnight over anhydrous $CaCl_2$, then distilled with P_2O_5 and stored over molecular sieves 4 Å. Cyclohexane was distilled with P_2O_5, then dried with CaH_2 and stored over molecular sieves 4 Å. Diethyl diallylmalonate (Sigma-Aldrich, purity 98%), cyclooctene (Janssen Chimica, purity 95%), 1,7-octadiene (Fluka, purity ≥ 97.0%), methyl oleate (Research Institute of Inorganic Chemistry, a.s., Czech Republic, purity 94%: methyl palmitate, methyl stearate and

methyl linolate as the main impurities) were used as received. Methyl 10-undecenoate was prepared from 10-undecenoic acid [26]. The Ru complex **3** was purchased from Zannan Pharma. Ltd., China.

The synthesis of siliceous MCM-41 and SBA-15 was performed according to the procedure described in [27]. Their textural characteristics were determined for MCM-41 and SBA-15, respectively, from nitrogen adsorption isotherms: surface area S_{BET} = 972 and 934 m²/g, average pore diameter d = 3.8 and 6.9 nm and volume of pores V = 1.14 and 0.96 cm³/g. The particle size (by SEM) ranged from 1 to 3 μm for all supports used.

Techniques

UV–vis spectra of catalysts were recorded with a Perkin-Elmer Lambda 950 spectrometer. A Spectralon integration sphere was applied to collect diffuse reflectance spectra of powder samples. Spectralon served also as a reference. Catalyst samples were placed in a quartz cuvette under an Ar atmosphere. ^{1}H (300 MHz) and ^{13}C (75 MHz) NMR spectra were recorded on a Varian Mercury 300 spectrometer in THF-d_8 at 25 °C.

The photoelectron spectra of the samples were measured with an ESCA 310 (Scienta, Sweden) spectrometer equipped with a hemispherical electron analyzer operated in a fixed transmission mode. Monochromatic Al Kα radiation was used for the electron excitation. The samples were spread on aluminium plates and the spectra were recorded at room temperature. The Si 2p, O 1s, Cl 2p, C 1s and Ru 3d photoelectrons were measured. Sample charging was corrected using the C 1s peak at 284.8 eV as internal standard. For the overlapping C 1s and Ru 3d lines, the contributions of individual components were determined by curve fitting. The spectra were curve-fitted after subtraction of the Shirley background [28] using a Gaussian–Lorentzian line shape. The decomposition of the Ru 3d and C 1s profiles was made subject to the constraints of the constant Ru 3d doublet separation (4.17 eV) and the constant Ru $3d_{5/2}$/Ru $3d_{3/2}$ intensity ratio equal to the ratio of the corresponding partial photoionization cross sections (1.45) [29]. Quantification of the elemental concentrations was accomplished by correcting photoelectron peak intensities for their cross sections, analyzer transmission function and assuming a homogeneous sample.

A high-resolution gas chromatograph Agilent 6890 with DB-5 column (length: 50 m, inner diameter: 320 μm, stationary phase thickness: 1 μm) was used for reaction product analysis. Nonane was used as an internal standard when required. The Ru content was determined by ICP-MS (by Institute of Analytical Chemistry, ICT, Prague).

Catalyst preparation

About 1 g of support was transferred into a Schlenk tube and dried for 3 h at 300 °C in vacuo. After drying, the Schlenk tube was filled with argon. Then 10–20 mL of toluene and a calculated amount of **3** was added with stirring at room temperature. After stirring for 30 min, the solid phase turned green and the supernatant became colorless. Then, the supernatant was removed by filtration and the solid catalyst was washed two times with 10 mL toluene. Finally, the catalyst was dried in vacuo at room temperature.

Catalytic experiments

Catalytic experiments were performed in Schlenk tubes under an Ar atmosphere in CH_2Cl_2 or cyclohexane. In a typical experiment, 1,7-octadiene (225 mg, 2.05 mmol) was added to **3**/SBA-15 (34 mg, 3.4 μmol of Ru) in cyclohexane (10 mL) at 30 °C with stirring. Samples of the reaction mixture (100 μL) were taken at given intervals, quenched with ethyl vinyl ether and analyzed by GC. In the ROMP experiments, the reaction conditions were similar to those for the RCM of 1,7-octadiene, with an initial concentration of cyclooctene of 0.6 mol/L. After 3 h, the reaction mixture was terminated with ethyl vinyl ether, the solid catalyst was separated by centrifugation and the polymer isolated by precipitation in methanol (containing 2,6-di-*tert*-butyl-*p*-cresol as an antioxidant). The polymer yield was determined gravimetrically. The molecular weight was determined by SEC and the values related to the polystyrene standards.

Acknowledgements

The authors thank M. Lamač (J. Heyrovský Institute) for recording NMR spectra and J. Sedláček (Department of Physical and Macromolecular Chemistry, Charles University in Prague) for determination of polymer molecular weights by SEC. Financial support from the Grant Agency of the Academy of Science of the Czech Republic (project IAA400400805), and the Academy of Sciences of the Czech Republic (project KAN100400701) is gratefully acknowledged.

References

1. Buchmeiser, M. R. *Catal. Today* **2005,** *105,* 612–617. doi:10.1016/j.cattod.2005.06.005
2. Dragutan, I.; Dragutan, V. *Platinum Met. Rev.* **2008,** *52,* 71–82. doi:10.1595/147106708X297477
3. Clavier, H.; Grela, K.; Kirschning, A.; Mauduit, M.; Nolan, S. P. *Angew. Chem., Int. Ed.* **2007,** *46,* 6786–6801. doi:10.1002/anie.200605099
4. Copéret, C.; Basset, J.-M. *Adv. Synth. Catal.* **2007,** *349,* 78–92. doi:10.1002/adsc.200600443
5. Buchmeiser, M. R. *Chem. Rev.* **2009,** *109,* 303–321. doi:10.1021/cr800207n

6. Burtscher, D.; Grela, K. *Angew. Chem., Int. Ed.* **2009,** *48,* 442–454. doi:10.1002/anie.200801451
7. Nieczypor, P.; Buchowicz, W.; Meester, W. J. N.; Rutjes, F. P. J. T.; Mol, J. C. *Tetrahedron Lett.* **2001,** *42,* 7103–7105. doi:10.1016/S0040-4039(01)01460-5
8. Halbach, T. S.; Mix, S.; Fischer, D.; Maechling, S.; Krause, J. O.; Sievers, C.; Blechert, S.; Nuyken, O.; Buchmeiser, M. R. *J. Org. Chem.* **2005,** *70,* 4687–4694. doi:10.1021/jo0477594
9. Krause, J. O.; Nuyken, O.; Wurst, K.; Buchmeiser, M. R. *Chem.–Eur. J.* **2004,** *10,* 777–784. doi:10.1002/chem.200305031
10. Vehlow, K.; Maechling, S.; Köhler, K.; Blechert, S. *J. Organomet. Chem.* **2006,** *691,* 5267–5277. doi:10.1016/j.jorganchem.2006.08.019
11. Bek, D.; Žilková, N.; Dědeček, J.; Sedláček, J.; Balcar, H. *Top. Catal.* **2010,** *53,* 200–209. doi:10.1007/s11244-009-9418-7
12. Melis, K.; De Vos, D.; Jacobs, P.; Verpoort, F. *J. Mol. Catal. A: Chem.* **2001,** *169,* 47–56. doi:10.1016/S1381-1169(00)00563-X
13. Mayr, M.; Buchmeiser, M. R.; Wurst, K. *Adv. Synth. Catal.* **2002,** *344,* 712–719. doi:10.1002/1615-4169(200208)344:6/7<712::AID-ADSC712>3.0.CO;2-W
14. Kingsbury, J. S.; Garber, S. B.; Giftos, J. M.; Gray, B. L.; Okamoto, M. M.; Farrer, R. A.; Fourkas, J. T.; Hoveyda, A. H. *Angew. Chem., Int. Ed.* **2001,** *40,* 4251–4256. doi:10.1002/1521-3773(20011119)40:22<4251::AID-ANIE4251>3.0.CO;2-L
15. Fischer, D.; Blechert, S. *Adv. Synth. Catal.* **2005,** *347,* 1329–1332. doi:10.1002/adsc.200505106
16. Zarka, M. T.; Nuyken, O.; Weberskirch, R. *Macromol. Rapid Commun.* **2004,** *25,* 858–862. doi:10.1002/marc.200300297
17. Yao, Q.; Motta, A. R. *Tetrahedron Lett.* **2004,** *45,* 2447–2451. doi:10.1016/j.tetlet.2004.01.036
18. Elias, X.; Pleixats, R.; Man, M. W. C. *Tetrahedron* **2008,** *64,* 6770–6781. doi:10.1016/j.tet.2008.04.113
19. Lim, J.; Lee, S. S.; Ying, J. Y. *Chem. Commun.* **2010,** *46,* 806–808. doi:10.1039/b917986k
20. Van Berlo, B.; Houthoofd, K.; Sels, B. F.; Jacobs, P. A. *Adv. Synth. Catal.* **2008,** *350,* 1949–1953. doi:10.1002/adsc.200800211
21. Beck, J. S.; Vartuli, J. C.; Roth, W. J.; Leonowicz, M. E.; Kresge, C. T.; Schmitt, K. D.; Chu, C. T.-W.; Olson, D. H.; Sheppard, E. W.; McCullen, S. B.; Higgins, J. B.; Schlenker, J. L. *J. Am. Chem. Soc.* **1992,** *114,* 10834–10843. doi:10.1021/ja00053a020
22. Martín-Aranda, R. M.; Čejka, J. *Top. Catal.* **2010,** *53,* 141–153. doi:10.1007/s11244-009-9419-6
23. Stewart, I. C.; Keitz, B. K.; Kuhn, K. M.; Thomas, R. M.; Grubbs, R. H. *J. Am. Chem. Soc.* **2010,** *132,* 8534–8535. doi:10.1021/ja1029045
24. Lever, A. B. P. *Inorganic electronic spectroscopy;* Elsevier: Amsterdam, 1984; p 468.
25. Jarzembska, K.; Seal, S.; Wozniak, K.; Szadkowska, A.; Bieniek, M.; Grela, K. *ChemCatChem* **2009,** *1,* 144–151. doi:10.1002/cctc.200900052
26. Balcar, H.; Dosedlová, A.; Hanuš, V.; Petrusová, L.; Matyska, B. *Collect. Czech. Chem. Commun.* **1984,** *49,* 1736–1745.
27. Topka, P.; Balcar, H.; Rathouský, J.; Žilková, N.; Verpoort, F.; Čejka, J. *Microporous Mesoporous Mater.* **2006,** *96,* 44–54. doi:10.1016/j.micromeso.2006.06.016
28. Shirley, D. A. *Phys. Rev. B* **1972,** *5,* 4709–4714. doi:10.1103/PhysRevB.5.4709
29. Scofield, J. H. *J. Electron Spectrosc. Relat. Phenom.* **1976,** *8,* 129–137. doi:10.1016/0368-2048(76)80015-1

License and Terms

Beilstein Journal of Organic Chemistry

The intriguing modeling of *cis–trans* selectivity in ruthenium-catalyzed olefin metathesis

Naeimeh Bahri-Laleh[1,2], Raffaele Credendino[1] and Luigi Cavallo[*1]

Letter

Open Access

Address:
[1]MoLNaC - Modeling Lab for Nanostructures and Catalysis (http://www.molnac.unisa.it), Dipartimento di Chimica, Università di Salerno, Via Ponte don Melillo, I-84084 Fisciano (SA), Italy and [2]Polymerization Engineering Department, Iran Polymer and Petrochemical Institute (IPPI), P.O. Box 14965/115, Tehran, Iran

Email:
Luigi Cavallo[*] - lcavallo@unisa.it

* Corresponding author

Keywords:
cis–trans selectivity; cross metathesis; DFT calculations; olefin metathesis; Ru-catalyst

Beilstein J. Org. Chem. **2011,** *7,* 40–45.
doi:10.3762/bjoc.7.7

Received: 22 August 2010
Accepted: 06 December 2010
Published: 11 January 2011

Guest Editor: K. Grela

Abstract

In this study we have investigated computationally the origin of the *cis–trans* selectivity in the Ru-catalyzed cross metathesis (CM) of a prototype monosubstituted olefin, i.e., propene. Our calculations suggest that the origin of the preferential formation of *trans*-olefins is in the product release step, which prevents the initially formed *cis*-olefin from escaping the metal, and returns it to the reaction pool until the *trans*-olefin is formed.

Introduction

Olefin metathesis is among the most versatile tools when C=C double bonds must be manipulated. For this reaction Ru-based catalysts of various generations are particularly attractive due to their high tolerance for other functional groups [1-4]. Among the most useful possibilities is cross metathesis (CM), see Scheme 1, since it opens the door to the formation of functionalized and/or higher olefins from simpler unsaturated building blocks. Such a wide potential explains why CM applications span from the production of raw materials [5,6] to advanced and challenging organic synthesis [7-10]. On the other hand, the general scope of CM has made a challenging task the comprehension of the working mechanism and the development of rules to control this powerful synthetic tool [11-18]. Among the problems connected with the CM of reactive monosubstituted olefins are the minimization of homodimers and a control over the *cis–trans* selectivity, see Scheme 1. While minimization of homodimers can be achieved with proper handling of the reaction protocol [15], controlling the *cis–trans* selectivity is much more complicated, and is usually biased towards the formation of the *trans*-isomer.

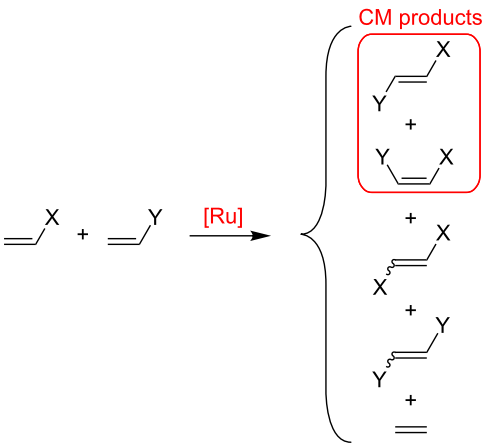

Scheme 1: Possible products resulting from the CM of terminal olefins.

For this reason, we decided to investigate computationally the *cis*–*trans* selectivity in the CM of the simplest terminal olefin, i.e., propene, to yield either *cis*- and *trans*-2-butene with the well characterized 2nd generation Ru-catalyst based on the SIMes *N*-heterocyclic carbene ligand, see Scheme 2. Although it is well known that the steric hindrance of the olefin substituent has a remarkable role on both reactivity and products distribution, propene can still be considered as a prototype of terminal olefins, and can provide insights into the energetics of the basic CM reaction. Steric or electronic effects that would arise from more complex olefins would add to the prototype energy profile investigated here. Finally, for the sake of brevity, we will focus only on the productive CM of propene with the Ru–propylidene bond, while degenerate propene metathesis with the Ru–propylidene moiety, or propene reactivity with the Ru–methylidene moiety, which would be the other Ru–alkylidene bonds present in the reaction mixture after complete activation of the starting precatalyst, are not considered.

Results and Discussion

The free energy profile in CH_2Cl_2 for the formation of both *cis*- and *trans*-2-butene from the starting 14e Ru–propylidene species is shown in Figure 1. Coordination of propene to the Ru center of **14e1**, leading to the coordination intermediate **Co1**, is favored by 3.4 kcal·mol^{-1}. In this intermediate the C=C double bond of the coordinated propene molecule is roughly perpendicular to the Ru–propylidene bond. From intermediate **Co1**, two transition states corresponding to productive metathesis, **TS1-*cis*** and **TS1-*trans***, can be reached via rather low energy barriers (3.1 and 2.5 kcal·mol^{-1} for **TS1-*cis*** and **TS1-*trans***, respectively). The two transition states differ in the relative orientation of the Me groups of the propene group and of the propylidene

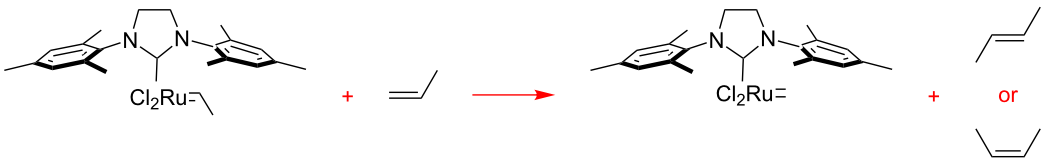

Scheme 2: Representation of the reactions investigated.

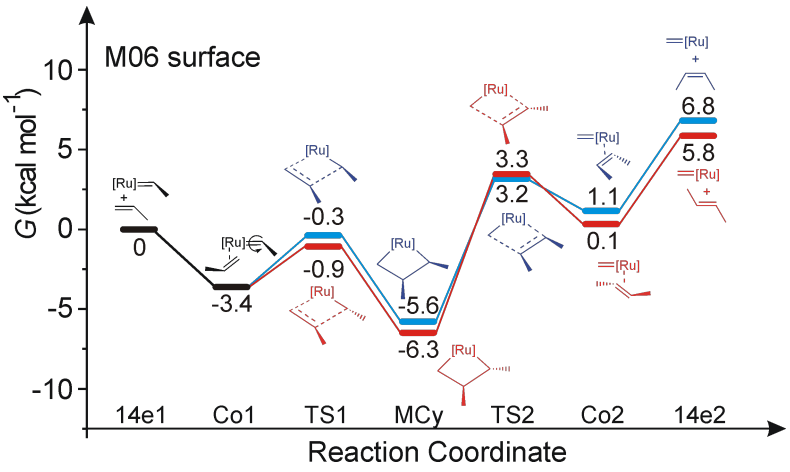

Figure 1: Reaction profile for the formation of *cis*- and *trans*-2-butene.

moiety, *syn* in **TS1-*cis***, and *anti* in **TS1-*trans***, with **TS1-*trans*** favored by 0.6 kcal/mol The experimentally proved free and fast rotation around the Ru–alkylidene bond allows both **TS1-*cis*** and **TS1-*trans*** to be reached from **Co1** [19,20]. The two transition states collapse into the corresponding **MCy-*cis*** and **MCy-*trans*** metallacycles, at 5.6 and 6.3 kcal·mol^{-1} below the starting **14e1** intermediate, respectively. The two metallacycles are the most stable structures along the reaction pathway. Release of *cis*- and *trans*-butene requires the breaking of the **MCy-*cis*** and **MCy-*trans*** metallacycles through the transition states **TS2-*cis*** and **TS2-*trans***, respectively, with formation of the two coordination intermediates **Co2-*cis*** and **Co2-*trans***, from which *cis*- and *trans*-butene are released. In this case, breaking the metallacycles is energetically quite expensive, around 9–10 kcal·mol^{-1}, and transition states **TS2-*cis*** and **TS2-*trans***, in agreement with other computational studies, are higher in energy than the transition states for metallacycle formation **TS1-*cis*** and **TS1-*trans*** [21]. The **Co2-*cis*** and **Co2-*trans*** coordination intermediates are slightly more stable than the corresponding **TS2-*cis*** and **TS2-*trans*** transition states, which means that the energy barrier for the backward reaction that would return the **Co2-*cis*** and **Co2-*trans*** coordination intermediates back into the corresponding metallacycle is rather low (2.1 and 3.2 kcal·mol^{-1} for **Co2-*cis*** and **Co2-*trans***, respectively).

This scenario indicates a rather surprising and unexpected result. First, *cis* versus *trans* selectivity is not determined at metallacycle formation, since both the *cis* and *trans* TS1 transition states are roughly 3–4 kcal·mol^{-1} lower in energy that the TS2 transition states. Second, neither is selectivity determined at metallacycle breaking. In fact, the **TS2-*cis*** and **TS2-*trans*** transition states, within the accuracy of this type of calculation, are of the same energy. On the other hand, and in line with expectations, the **MCy-*trans*** metallacycle is more stable than the **MCy-*cis*** metallacycle by roughly 1 kcal·mol^{-1}, and the **Co2-*trans*** coordination intermediate is similarly more stable than the **Co2-*cis*** coordination intermediate. Finally, our computational approach also reproduces well the experimental higher stability, by 1.0 kcal·mol^{-1}, of *trans*-2-butene relative to *cis*-2-butene in the gas-phase [22].

To test whether the relative stability of the four transition states could depend on the chosen HMGGA M06 functional [23], we localized the transition states for metallacycle formation and breaking with the popular GGA BP86 [24-26] and HGGA B3LYP [27-29] functionals, as well as with the more recent MGGA M06L functional [30]. All these tests are summarized in Table 1. First, in all the cases **TS1-*cis*** is somewhat higher in energy than **TS1-*trans*** but, more importantly, both the TS1 metallacycle forming transition states are 3–5 kcal·mol^{-1} lower in energy than the TS2 metallacycle breaking transition states. Considering that all the functionals we considered indicate that the metallacycle forming transition state is not rate (selectivity) determining, we will not discuss this point any further.

Table 1: Energy difference, in kcal·mol^{-1}, between the *cis* and *trans* transition states **TS1** and **TS2** of Figure 1, calculated with different computational approaches. In all cases **TS1-*trans*** is taken as reference at 0 kcal·mol^{-1}.

Functional	Transition State	$\Delta E^{\neq}_{cis-trans}$ gas-phase	$\Delta G^{\neq}_{cis-trans}$ gas-phase	$\Delta G^{\neq}_{cis-trans}$ CH_2Cl_2
BP86	**TS1-*trans***	0.0	0.0	0.0
	TS1-*cis*	0.2	1.2	1.4
	TS2-*trans*	4.5	4.1	4.1
	TS2-*cis*	4.1	3.8	3.8
B3LYP	**TS1-*trans***	0.0	0.0	0.0
	TS1-*cis*	0.5	0.1	0.3
	TS2-*trans*	4.2	3.3	3.2
	TS2-*cis*	3.7	2.1	2.0
M06L	**TS1-*trans***	0.0	0.0	0.0
	TS1-*cis*	0.1	2.3	2.2
	TS2-*trans*	6.0	6.5	5.6
	TS2-*cis*	4.6	5.7	5.4
M06	**TS1-*trans***	0.0	0.0	0.0
	TS1-*cis*	0.6	0.6	0.5
	TS2-*trans*	4.9	4.6	4.2
	TS2-*cis*	4.3	4.6	4.1

Focusing on the metallacycle breaking transition state, the values in Table 1 indicate that the difference between the **TS2-*cis*** and **TS2-*trans*** transition states is somewhat dependent on the computational approach used. Indeed, the BP86, B3LYP and M06L results suggest that the **TS2-*cis*** transition state is somewhat preferred over the **TS2-*trans*** transition state, thus suggesting a small preference for the formation of *cis*-olefins. The M06 functional, instead, indicates that these two transition states are practically of the same energy. Further, the values given in Table 1 indicate that in terms of gas-phase potential energy the **TS2-*cis*** is reasonably favored over **TS2-*trans*** also with the M06 functional. It is the inclusion of the vibrational/entropic part that makes the M06 *cis*- and *trans* transition states of similar energy, (compare the $\Delta E^{\neq}_{cis-trans}$ and $\Delta G^{\neq}_{cis-trans}$ values in the gas-phase in Table 1). Inclusion of solvent effects does not change the gas-phase trends (compare the $\Delta G^{\neq}_{cis-trans}$ in gas-phase and the $\Delta G^{\neq}_{cis-trans}$ in CH_2Cl_2 values in Table 1). In conclusion, if any preference exists at the level of the metallacycle breaking step, the consensus emerging from the comparison of various functionals is that the *cis* transition state is favored. The fact that the *cis* transition state is of lower or similar energy to the *trans* transition state, despite of the higher stability of the forming *trans* C=C skeleton, indicates that the SIMes ligand is more suitable to host a *cis* forming C=C bond rather than a *trans* C=C bond.

Based on these calculations, the conclusion emerging from the energy profiles of Figure 1 and the values given in Table 1 is that, in the framework of a dissociative mechanism, the key step determining the experimentally observed preferential formation of *trans*-olefins is product release with formation of the methylidene Ru 14e intermediate **14e2** and a free *cis*- or *trans*-2-butene molecule from **Co2-*cis*** and **Co2-*trans*** (in this regard it must be noted that an associative mechanism has been proposed to be operative for ethylene degenerate metathesis at low temperature [31,32], and for the activation step in Hoveyda/Grela type catalysts [33]). Product release is endoergonic due to the coordination energy of 2-butene that amounts to roughly 6 kcal·mol^{-1} both for the *cis*- and *trans*-isomers, and is clearly higher in energy than both TS2 transition states that would revert the just formed 2-butenes into the most stable metallacycle. For this reason, the energy profile of Figure 1 suggests that the most likely event from **Co2-*cis*** and **Co2-*trans*** is not product release, but rather their transformation into **MCy2-*cis*** and **MCy2-*trans***. The escape from **Co2-*cis*** and **Co2-*trans*** is controlled by the free energy difference between **14e2** and transition states **TS2-*cis*** and **TS2-*trans***, which amounts to 3.6 and 2.5 kcal·mol^{-1} for the *cis* and *trans* pathways, respectively. These numbers indicate that release of *trans*-2-butene is favored by the higher stability of the *trans*-olefin relative to the *cis*-isomer.

Of course, considering the high reactivity of both *trans*- and *cis*-butene towards metathesis, it is clear that secondary metathesis of the produced butenes, whose energetic can be still derived from Figure 1, will result in a statistical distribution of the products according to their thermodynamic stability [15,18]. Thus, a high *trans*/*cis*-butene ratio would be reached, even if a lower *trans*/*cis* ratio was initially produced. This conclusion is in qualitative agreement with CM experiments using terminal olefins, which resulted in a *trans/cis* ratio of around 2–4 at low conversions, that increased to 9–10 at higher conversions [18]. Finally, it is clear that the steric and electronic properties of more complex olefins can have a strong impact on the energy profile of Figure 1, which however, remains the base energy profile to be modified. We are currently working in this direction.

Conclusion

In this study we have investigated computationally the origin of the *cis–trans* selectivity in the CM of the prototype monosubstituted olefin, i.e., propene. Our calculations suggest that the origin of the preferential formation of *trans*-olefins is not the energy difference at the transition states corresponding to either metallacycle formation of breaking. Actually, focusing on the transition state higher in energy (the one corresponding to metallacycle breaking), we found that the transition state leading to the formation of *cis*-butene is of similar energy, or even favored, relative to that leading to the formation of *trans*-butene. Thus, CM of propene (and by consequence of simple linear 1-olefins) should kinetically lead first to the formation of *cis*-olefins, followed by gradual conversion to the more stable *trans*-isomer. Our calculations suggest that the key step to rationalize the preferential formation of *trans*-olefins, even at low conversion, is in the product release step, since *trans*-olefins have a higher tendency to be released from the catalyst at the end of the CM reaction. Conversely, the initially formed *cis*-olefins have a minor tendency to be released from the catalyst, and thus they have a higher chance to return to the reaction pool until the *trans*-olefin is formed.

Experimental

Computational Details

The DFT calculations of the full energy profile of Figure 1 were performed at the HMGGA level with the Gaussian09 package [34], using the M06 functional of Truhlar [23]. Free energies in CH_2Cl_2 were deduced from the gas-phase free energies plus the solvation energy term estimated in single point calculations on the gas-phase optimized structures, based on the polarizable continuum solvation model PCM using CH_2Cl_2 as the solvent [35]. In case of olefin coordination, we assumed a $-T\Delta S$ contribution of 10 kcal·mol^{-1}, since the gas-phase rotational/translational entropy of coordination from classical statistical thermo-

dynamics is generally considered to overestimate the coordination entropy in solution. The $-T\Delta S$ contribution of 10 kcal·mol^{-1} is the experimental coordination entropy of C_2H_4 to a Pd-complex [36]. The test calculations in Table 1 were performed with the GGA BP86 functional of Becke and Perdew [24-26], with the HGGA B3LYP functional of Becke, Lee, Parr, and Yang [27-29], and with the MGGA M06L functional of Truhlar [30]. In all cases the electronic configuration of the molecular systems was described with the standard split-valence basis set with a polarization function of Ahlrichs and co-workers for H, C, N, O and Cl (SVP keyword in Gaussian03) [37]. For Ru we used the small-core, quasi-relativistic Stuttgart/Dresden effective core potential, with an associated (8s7p6d)/[6s5p3d] valence basis set (SDD keywords in Gaussian03) [38]. Characterization of the located stationary points as minima or transition state was performed by frequency calculations.

Acknowledgements

We thank M. Barbasiewicz, Warsaw University, for useful discussions. The research leading to these results received funding from the European Community's Seventh Framework Programme (FP7/2007-2013) under grant agreement n° CP-FP 211468-2 EUMET. LC thanks the HPC team of Enea (http://www.enea.it) for use of the ENEA-GRID and the HPC facilities CRESCO (http://www.cresco.enea.it) in Portici, Italy.

References

1. Grubbs, R. H. *Handbook of Olefin Metathesis;* Wiley-VCH: Weinheim, Germany, 2003.
2. Connon, S. J.; Blechert, S. *Angew. Chem., Int. Ed.* **2003,** *42,* 1900–1923. doi:10.1002/anie.200200556
3. Samojłowicz, C.; Bieniek, M.; Grela, K. *Chem. Rev.* **2009,** *109,* 3708–3742. doi:10.1021/cr800524f
4. Vougioukalakis, G. C.; Grubbs, R. H. *Chem. Rev.* **2010,** *110,* 1746–1787. doi:10.1021/cr9002424
5. Malacea, R.; Fischmeister, C.; Bruneau, C.; Dubois, J.-L.; Couturier, J.-L.; Dixneuf, P. H. *Green Chem.* **2009,** *11,* 152–155. doi:10.1039/b816917a
6. Rybak, A.; Meier, M. A. R. *Green Chem.* **2007,** *9,* 1356–1361. doi:10.1039/b712293d
7. Demchuk, O. M.; Pietrusiewicz, K. M.; Michrowska, A.; Grela, K. *Org. Lett.* **2003,** *5,* 3217–3220. doi:10.1021/ol035011m
8. Cantrill, S. J.; Grubbs, R. H.; Lanari, D.; Leung, K. C. F.; Nelson, A.; Poulin-Kerstien, K. G.; Smidt, S. P.; Stoddart, J. F.; Tirrell, D. A. *Org. Lett.* **2005,** *7,* 4213–4216. doi:10.1021/ol051599g
9. Chatterjee, A. K.; Sanders, D. P.; Grubbs, R. H. *Org. Lett.* **2002,** *4,* 1939–1942. doi:10.1021/ol0259793
10. Boeda, F.; Bantreil, X.; Clavier, H.; Nolan, S. P. *Adv. Synth. Catal.* **2008,** *350,* 2959–2966. doi:10.1002/adsc.200800495
11. Berlin, J. M.; Goldberg, S. D.; Grubbs, R. H. *Angew. Chem., Int. Ed.* **2006,** *45,* 7591–7595. doi:10.1002/anie.200602469
12. Stewart, I. C.; Douglas, C. J.; Grubbs, R. H. *Org. Lett.* **2008,** *10,* 441–444. doi:10.1021/ol702624n
13. Funk, T. W.; Efskind, J.; Grubbs, R. H. *Org. Lett.* **2005,** *7,* 187–190. doi:10.1021/ol047929z
14. Chatterjee, A. K.; Grubbs, R. H. *Org. Lett.* **1999,** *1,* 1751–1753. doi:10.1021/ol991023p
15. Chatterjee, A. K.; Choi, T.-L.; Sanders, D. P.; Grubbs, R. H. *J. Am. Chem. Soc.* **2003,** *125,* 11360–11370. doi:10.1021/ja0214882
16. Choi, T.-L.; Chatterjee, A. K.; Grubbs, R. H. *Angew. Chem., Int. Ed.* **2001,** *40,* 1277–1279. doi:10.1002/1521-3773(20010401)40:7<1277::AID-ANIE1277>3.0.CO;2-E
17. Smith, A. B., III; Adams, C. M.; Kozmin, S. A. *J. Am. Chem. Soc.* **2001,** *123,* 990–991. doi:10.1021/ja003745d
18. Anderson, D. R.; Ung, T.; Mkrtumyan, G.; Bertrand, G.; Grubbs, R. H.; Schrodi, Y. *Organometallics* **2008,** *27,* 563–566. doi:10.1021/om7008028
19. Aagaard, O. M.; Meier, R. J.; Buda, F. *J. Am. Chem. Soc.* **1998,** *120,* 7174–7182. doi:10.1021/ja974131k
20. van der Eide, E. F.; Piers, W. E. *Nat. Chem.* **2010,** *2,* 571–576. doi:10.1038/nchem.653
21. Rowley, C. N.; van der Eide, E. F.; Piers, W. E.; Woo, T. K. *Organometallics* **2008,** *27,* 6043–6045. doi:10.1021/om8008519
22. Lide, D. R. *Handbook of Chemistry and Physics,* 84th ed.; CRC Press Inc.: London, 2004.
23. Zhao, Y.; Truhlar, D. G. *Theor. Chem. Acc.* **2008,** *120,* 215–241. doi:10.1007/s00214-007-0310-x
24. Becke, A. D. *Phys. Rev. A* **1988,** *38,* 3098–3100. doi:10.1103/PhysRevA.38.3098
25. Perdew, J. P. *Phys. Rev. B* **1986,** *33,* 8822–8824. doi:10.1103/PhysRevB.33.8822
26. Perdew, J. P. *Phys. Rev. B* **1986,** *34,* 7406. doi:10.1103/PhysRevB.34.7406
27. Becke, A. D. *J. Chem. Phys.* **1993,** *98,* 5648–5652. doi:10.1063/1.464913
28. Lee, C.; Yang, W.; Parr, R. G. *Phys. Rev. B* **1988,** *37,* 785–789. doi:10.1103/PhysRevB.37.785
29. Stephens, P. J.; Devlin, F. J.; Chabalowski, C. F.; Frisch, M. J. *J. Phys. Chem.* **1994,** *98,* 11623–11627. doi:10.1021/j100096a001
30. Zhao, Y.; Truhlar, D. G. *J. Chem. Phys.* **2006,** *125,* 194101. doi:10.1063/1.2370993
31. Romero, P. E.; Piers, W. E. *J. Am. Chem. Soc.* **2007,** *129,* 1698–1704. doi:10.1021/ja0675245
32. Webster, C. E. *J. Am. Chem. Soc.* **2007,** *129,* 7490–7491. doi:10.1021/ja071588d
33. Vorfalt, T.; Wannowius, K.-J.; Plenio, H. *Angew. Chem., Int. Ed.* **2010,** *49,* 5533–5536. doi:10.1002/anie.201000581
34. *Gaussian 03,* B. 1; Gaussian, Inc.: Pittsburg PA, 2003.
35. Tomasi, J.; Persico, M. *Chem. Rev.* **1994,** *94,* 2027–2094. doi:10.1021/cr00031a013
36. Rix, F. C.; Brookhart, M. *J. Am. Chem. Soc.* **1995,** *117,* 1137–1138. doi:10.1021/ja00108a034
37. Schäfer, A.; Horn, H.; Ahlrichs, R. *J. Chem. Phys.* **1992,** *97,* 2571–2577. doi:10.1063/1.463096
38. Küchle, W.; Dolg, M.; Stoll, H.; Preuss, H. *J. Chem. Phys.* **1994,** *100,* 7535–7542. doi:10.1063/1.466847

Beilstein Journal of Organic Chemistry

Recent advances in the development of alkyne metathesis catalysts

Xian Wu and Matthias Tamm*

Review

Open Access

Address:
Institut für Anorganische und Analytische Chemie, Technische Universität Braunschweig, Hagenring 30, 38106 Braunschweig, Germany

Email:
Xian Wu - wuxn03@hotmail.com;
Matthias Tamm* - m.tamm@tu-bs.de

* Corresponding author

Keywords:
alkynes; homogeneous catalysis; metathesis; molybdenum; tungsten

Beilstein J. Org. Chem. **2011,** *7,* 82–93.
doi:10.3762/bjoc.7.12

Received: 13 September 2010
Accepted: 08 December 2010
Published: 18 January 2011

Guest Editor: K. Grela

Abstract

The number of well-defined molybdenum and tungsten alkylidyne complexes that are able to catalyze alkyne metathesis reactions efficiently has been significantly expanded in recent years.The latest developments in this field featuring highly active imidazolin-2-iminato- and silanolate–alkylidyne complexes are outlined in this review.

Review

Introduction

C–C bond formation is one of the most important types of reaction in organic synthesis. Transformations employing organometallic compounds as catalysts have achieved a significant role because of their advantages such as simplicity (fewer reaction steps) and efficiency (higher yields) in comparison with traditional synthetic strategies. Nowadays, a plethora of methods is known, which can be used for the formation of C–C single and double bonds, whereas simple ways to create C–C triple bonds are less common, despite the importance and ubiquity of C–C triple bonds in research areas such as natural product synthesis and advanced material science [1].

Alkyne metathesis, which deals with the breaking and making of C–C triple bonds, has only relatively recently become part of the tool box of organic and polymer chemists for the preparation of their target molecules [2-11]. Catalyzed by organotransition metal complexes, this reaction type creates new C–C triple bonds very simply via the Katz mechanism (Scheme 1) [12], based on which a series of different reaction types such as alkyne cross metathesis (ACM), ring-closing alkyne metathesis (RCAM), ring-opening alkyne metathesis polymerization (ROAMP) and acyclic diyne metathesis polymerization (ADIMET) are known (Scheme 2).

In contrast to olefin metathesis, the number of catalysts for alkyne metathesis is far more limited. The first catalyst for alkyne metathesis was a heterogeneous system based on WO_3/silica, which was first reported by Pennella, Banks and Bailey in 1968 [13], while the first homogeneous system, which consisted of $[Mo(CO)_6]$ and resorcinol [14], was discovered by

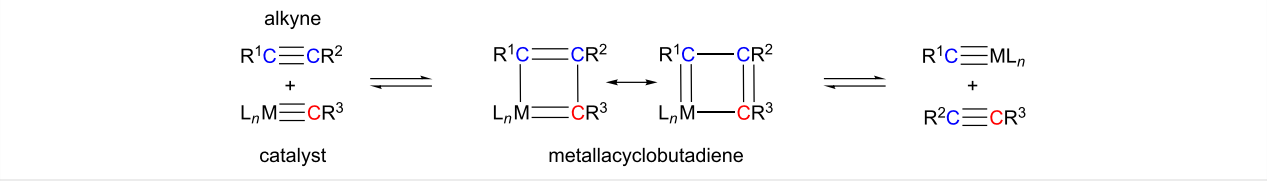

Scheme 1: Alkyne metathesis based on the Katz mechanism.

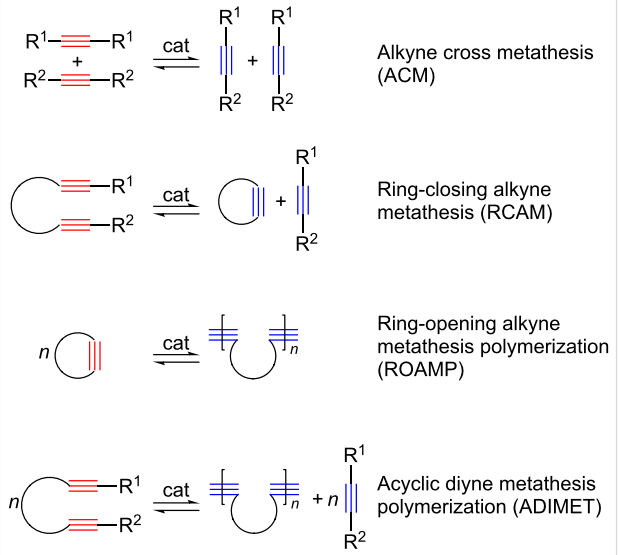

Scheme 2: Reaction patterns of alkyne metathesis.

Mortreux and Blanchard in 1974. Since then, great efforts have been made to develop highly efficient alkyne metathesis catalysts and this has led to three major systems which have dominated this area, i.e., the Mortreux system, the Schrock system and the Cummins–Fürstner–Moore system. Only recently, two novel systems, which exhibit highly promising catalytic performance in alkyne metathesis, were successfully introduced: 1. A modified Schrock system containing imidazolin-2-iminato ligands that was developed by our group; 2. silanolate-supported complexes such as molybdenum nitride and alkylidyne complexes with Ph_3SiO ligands developed by Fürstner and tungsten alkylidyne complexes with $(t\text{-BuO})_3SiO$ ligands introduced by us. Since there are already several reviews available that cover research progress up to 2006 [2-11], this article will focus on the two novel catalyst systems, which were established over the last four years (2007–10), commencing with a brief introduction to the established systems that have already been widely used by synthetic chemists.

Traditional catalyst systems

Mortreux system

First reported in 1974, the Mortreux system consists of two components: $[Mo(CO)_6]$ and phenol or derivatives thereof [14-19]. During the last decades, this system was intensively studied and its performance was significantly improved. However, some drawbacks including the requirement of high reaction temperatures and low functional group tolerance greatly limit its applicability. Moreover, the catalytic mechanism and the active species involved remain unknown, preventing a further rational catalyst design. Nevertheless, because of the commercial availability and high stability of the pre-catalysts as well as the simplicity of operation, this classical system is still widely used by chemists [20-28].

Schrock system

Schrock-type catalysts are high oxidation state molybdenum or tungsten alkylidyne complexes which form metallacyclobutadienes (the key intermediate in the Katz mechanism) upon treatment with internal alkynes. Among these, the tungsten neopentylidyne complex $[Me_3C{\equiv}CW(OCMe_3)_3]$ is the most widely used species and is reliably synthesized in several steps from commercially available WCl_6. Accordingly, numerous applications of this catalyst have been reported, which usually requires elevated reaction temperatures and relatively high catalyst loadings [29-35].

Cummins–Fürstner–Moore system

Cummins introduced triamido molybdenum(III) complexes of the type $[Mo\{NR(Ar)\}_3]$ in the mid 1990s, which are able to cleave the N–N triple bond in the dinitrogen molecule [36-38]. Based on this discovery, Fürstner developed a catalyst system that is formed upon treatment of $[Mo\{N(t\text{-Bu})Ar\}_3]$ with dichloromethane to give the methylidyne complex $[HC{\equiv}Mo\{N(t\text{-Bu})Ar\}_3]$ and the chloro complex $[ClMo\{N(t\text{-Bu})Ar\}_3]$ [39]. Although the detailed reaction mechanism has not been fully uncovered, the latter complex is, somewhat counterintuitively, considered to be the active species. Similarly, Moore was able to isolate molybdenum alkylidyne complexes such as $[EtC{\equiv}Mo\{N(t\text{-Bu})Ar\}_3]$, which are able to catalyze alkyne metathesis reactions efficiently, albeit only after treatment with phenol derivatives or by capture on silica [40-46]. The reaction with phenolic compounds presumably leads to partial or complete cleavage of the Mo–N bonds to produce catalytically active phenolate complexes. In agreement with this assumption, Cummins was able to report the synthesis of well-defined molybdenum benzylidyne complexes from the molybdaziridine $[Mo(H)(\eta^2\text{-}Me_2CNAr)\{N(i\text{-Pr}\}Ar)]$ and could

demonstrate that these systems are efficient initiators for alkyne metathesis even at ambient temperature and low catalyst loadings [47]. Scheme 3 shows some typical examples of the three traditional catalyst systems.

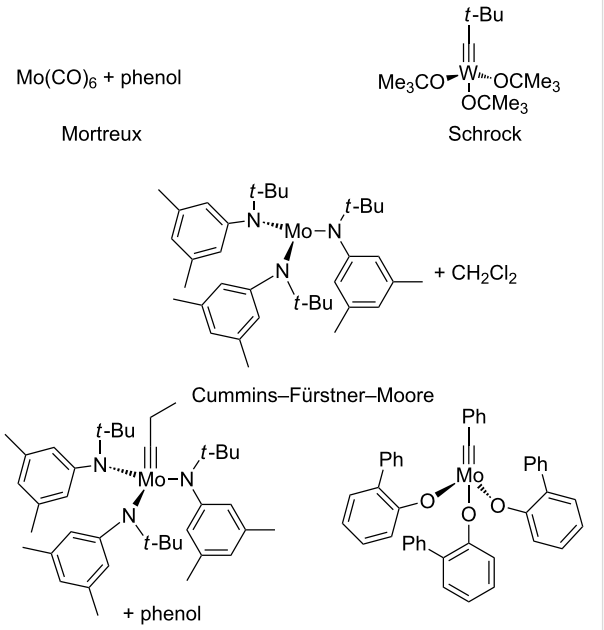

Scheme 3: Typical examples from traditional catalyst systems.

Novel catalyst systems

Imidazolin-2-iminato tungsten and molybdenum alkylidyne complexes

Imidazolin-2-iminato ligands, which are isolobal to phosphoraneimides (R_3PN^-) and cyclopentadienides ($C_5R_5^-$) [48-52], can be described by the resonance structures shown in Scheme 4, indicating that the ability of the imidazolium ring to stabilize a positive charge affords highly basic ligands with a strong electron-donating capacity towards early transition metals or metals in a higher oxidation state [53-55]. In recent years, our group has significantly expanded the use of these 2σ,4π-electron donor ligands in organometallic chemistry and homogeneous catalysis [56-67]. Their synthesis starts from *N*-heterocyclic carbenes **1** which react with trimethylsilyl azide to afford 2-trimethylsilyliminoimidazolines **2**. After treatment with methanol, the corresponding imidazolin-2-imines **3** can be conveniently isolated [60]. Deprotonation by alkyl lithium reagents leads to imidazolin-2-iminato lithium compounds **4**, which serve as ligand transfer reagents during the catalyst preparation (Scheme 4).

The idea to use imidazolin-2-iminato ligands for the modification of Schrock-type alkylidyne complexes is based on the consideration that they can be regarded as monoanionic analogues of dinegative imido ligands, which are present in some of the most active olefin metathesis catalysts, i. e., Schrock–Hoveyda-type tungsten and molybdenum imido-alkylidene complexes [10]. We presumed that substitution of the imido ligands by imidazolin-2-iminato ligands and concurrent conversion of the metal–carbon double bond into a triple bond would afford metal alkylidyne species with a well-preserved structural and electronic integrity, and therefore with potentially undiminished catalytic activity (Scheme 4). Thus, the resulting new complexes should then be highly active alkyne metathesis catalysts.

In order to verify this design strategy, high oxidation state tungsten and molybdenum alkylidyne complexes bearing imidazolin-2-iminato ligands (**5** and **6**) were synthesized by two different routes. The low-oxidation-state route (on the right-hand side in Scheme 5) starting from metal hexacarbonyl has advantages such as higher atom economy, easier operation and suitability for both tungsten and molybdenum [68-70] in com-

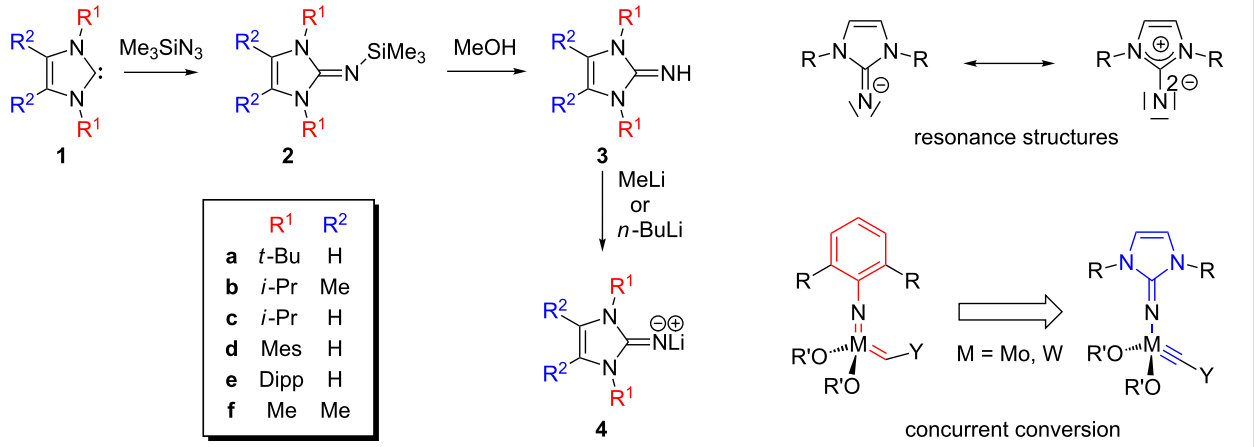

Scheme 4: Ligand synthesis and catalyst design.

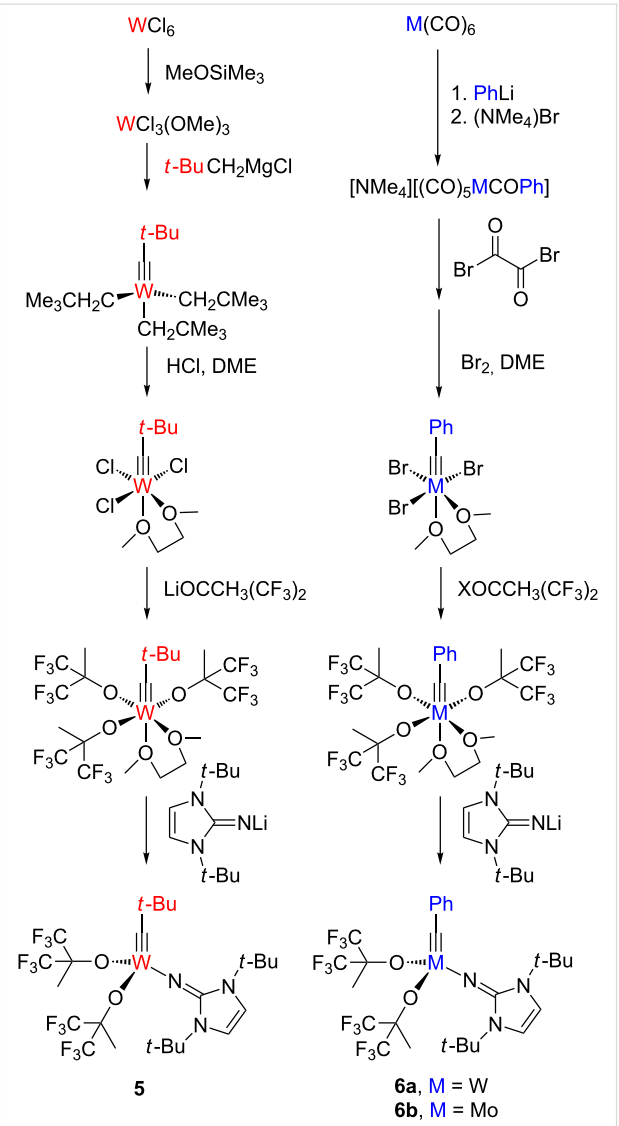

Scheme 5: Catalysts synthesis using high- and low-oxidation-state routes (for **6a**, X = Li or K; for **6b**, X = K).

parison with the high-oxidation-state route (on the left- hand side in Scheme 5) starting from tungsten hexachloride [71-73]. The use of partially fluorinated alkoxides such as hexafluoro-*tert*-butoxide, $OCCH_3(CF_3)_2$, proved to be essential for creating active catalysts [74], indicating that successful catalyst design in this system relies on establishing a push-pull situation in a similar fashion present in Schrock–Hoveyda olefin metathesis catalysts (Scheme 4) [10] and also in an isolobal rhenium(VII) imido-alkylidyne complex [Re(NAr)(C*t*-Bu)(OR^F)] (Ar = 2,6-diisopropylphenyl, $R^F = CCH_3(CF_3)_2$), which is able to metathesize aliphatic alkynes [75]. In contrast, however, anionic molybdenum imido-alkylidyne complexes such as $[Mo(NAr)(Ct\text{-}Bu)(OR^F)]^-$ do not promote alkyne metathesis, since the more electron-rich nature of the alkylidyne anion may disfavor alkyne binding [76].

The catalysts **5** and **6** were proved to catalyze various alkyne metathesis reactions including ACM, RCAM and ROAMP. In addition, the isolation and structural characterization of a metallacyclobutadiene complex from the reaction of **5** with an excess of 3-hexyne confirmed that the [2 + 2]-cycloaddition (Katz) mechanism is operative [73,74]. The prototype **5** of our new catalyst system was used for the ACM of 1-phenylpropyne (**7**) and was shown to be significantly more active than the classic Schrock alkylidyne complex $[Me_3CC{\equiv}W(Ot\text{-}Bu)_3]$ at both ambient and elevated temperatures [73,74]. Its performance was also compared with those of two other catalysts **9** and **10** bearing $Im^{Dipp}N$ and N(*t*-Bu)Ar ligands, respectively (Table 1, Figure 1). The results show that **5** is significantly more active than **9** and **10**, whereas **10** is more active than **9**. This is supported by DFT calculations for the metathesis of 2-butyne as the model reaction, which reveal that the activation barrier for the three catalysts follows the order **9** > **10** > **5**.

Table 1: ACM of **7** using **5**, **9** and **10** as catalysts.

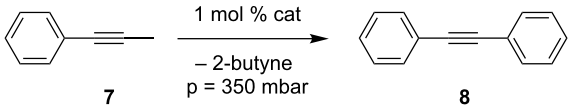

cat	temp (°C)	*t* (min)	solvent	yield (%)
5	ambient	50	hexane	100
5	80	40	toluene	100
9	ambient	50	hexane	2
9	80	40	toluene	6
10	ambient	50	hexane	28
10	80	40	toluene	89

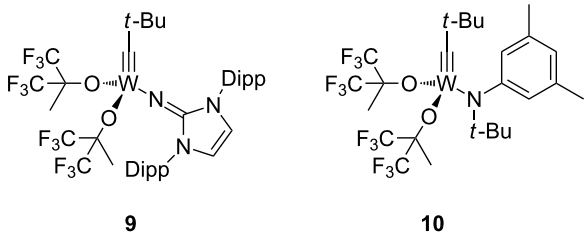

Figure 1: Alkylidyne complexes **9** and **10**.

ACM reactions with more complex substrates bearing different functional groups were studied in the presence of **6a** and **6b** as catalysts [70]. In the ACM of the 3-pentynyl ether **11**, tungsten and molybdenum benzylidyne complexes **6a** and **6b** were used as catalysts, both showing excellent activities under the same vacuum-driven reaction conditions (Table 2). In our hands, however, the tungsten system appeared to be a superior and

Table 2: ACM of **11** and **13** using **6a** and **6b** as catalysts.

substrate	product	catalyst		yield (%)[a]
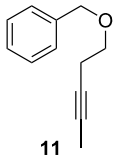 **11**	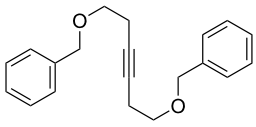 **12**	**6a**		98
		6b		97
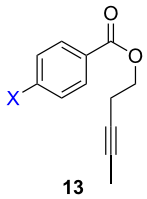 **13**	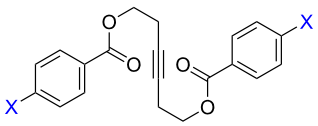 **14**	**6a**	**a** X = H	98
		6b	**a** X = H	97
		6a	**a** X = H	98
		6a	**b** X = Cl	98
		6a	**c** X = OMe	94
		6a	**d** X = NO_2	17
		6a	**e** X = NMe_2	90[b]

[a]1 mol % catalyst, toluene, rt, 1 h, 200 mbar. [b]5 mol % catalyst, toluene, rt, 2 h, 200 mbar, unpublished results.

more reliable catalyst system than its molybdenum congener, which was also supported by DFT calculations. Similar results were also found for the ACM of the 3-pentynyl benzoic esters **13** bearing a selection of functional groups in the 4-position of the phenyl ring (Table 2). With the tungsten catalyst **6a**, excellent yields were obtained for X = Cl, OMe and SMe, whereas only 17% of **14d** could be obtained for X = NO_2. Increasing the catalyst loading to 2 mol % gave a higher conversion (33%), and we have obtained similar results for other substrates. For instance, ACM of **13e** (X = NMe_2) was hardly successful in the presence of 2 mol % of the catalyst, whereas **14e** was isolated in 90% yield with a catalyst loading of 5 mol %. Further detailed studies are required to fully explain this ostensibly odd behavior.

Catalyst **5** was used in the RCAM of 6,15-dioxaeicosa-2,18-diyne (**15**) and *o*-, *m*- and *p*-bis(3-pentynyloxymethyl)benzenes **17** (Table 3). While the cyclic product **16** was obtained from **15** in high yield (95%), different selectivities toward the formation of monomeric [10]cyclophanes **18** and [10.10]cyclophanes **19** depending on the substitution pattern were observed [77]: The monomeric cycloalkyne **18b** and the dimeric cyclodiyne **19c** were exclusively formed from the *m*- and *p*-isomer **17b** and **17c**, respectively, whereas ring-closure of the *o*-isomer **17a** gave a mixture of both **18a** and **19a**. This observation is in agreement with DFT calculations suggesting that reversible ring-opening and ring-closing metathesis (RORCM) leads to an equilibrium between monomeric and dimeric products and their ratios are determined by their relative stabilities [77].

Table 3: RCAM of **15** and **17** using **5** as catalyst.

substrate	product		yield (%)[a]
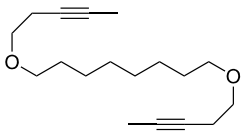 **15**	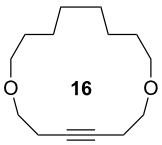 **16**		95
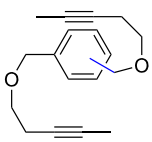 **17**	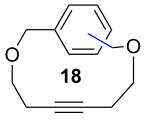 **18**	**a** *ortho*	24
		b *meta*	100
		c *para*	0
	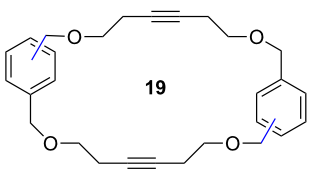 **19**	**a** *ortho*	76
		b *meta*	0
		c *para*	100

[a]2 mol % catalyst **5**, hexane, rt, 2 h, 350 mbar.

The catalytic performance of **6a** and **6b** in RCAM was demonstrated for the substrates *m*-bis(3-pentynyloxymethyl)benzene (**17b**) and bis(3-pentynyl)phthalate (**20**) (Table 4). The results showed that the tungsten benzylidyne complex can catalyze both reactions with high efficiency, whereas the molybdenum counterpart had a significantly lower activity, in agreement with a theoretically predicted higher activation barrier for the Mo system [70].

Table 4: RCAM of **17b** and **20** using **6a** and **6b** as catalysts.

substrate	product	catalyst	yield (%)[a]
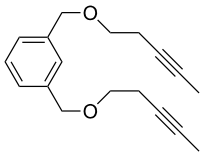	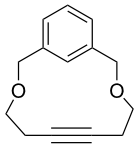	**6a** **6b**	86 47
17b	**18b**		
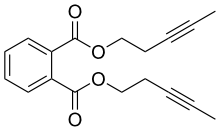	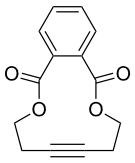	**6a** **6b**	98 20
20	**21**		

[a]2 mol % catalyst, 80 mL toluene, rt, 2 h, 300 mbar.

The ROAMP of cyclooctyne (**22**) was performed using **5** and **6a** as catalysts (Table 5) [78]. According to gel permeation chromatography (GPC) analysis, polymer parameters such as the molecular weight (M_n and M_w) and the polydispersity index (PDI) depend on the catalyst and substrate concentration, and the reaction medium. Besides polymer formation, cyclooligomers were also detected by GPC and mass spectrometry. As shown in Table 5, both catalysts **5** and **6a** catalyzed the ring-opening metathesis polymerization efficiently. It is also found that high yields of polymer were obtained when the reactions were performed on neat substrate, whereas lower substrate concentration increases the formation of cyclooligomers. This observation can be well explained by the Jacobson–Stockmayer theory of ring-chain equilibria [79].

Molybdenum nitride and alkylidyne complexes with silanolate ligands

Fürstner recently established a different design strategy for the development of novel alkyne metathesis catalysts. Inspired both by a report of Johnson and co-workers, who found that molybdenum and tungsten nitride complexes **24** with fluorinated alkoxide ligands react with alkynes to generate the corresponding metal alkylidynes **25** in situ (Scheme 6) [80,81], and by the work of Chiu et al. on the preparation of a silanolate-supported molybdenum-nitride complex [82], Fürstner's group introduced a novel user-friendly catalyst system for alkyne metathesis by employing triphenylsilanol (Ph_3SiOH) [83,84]. Two synthetic routes were developed, which are shown in Scheme 7. The one on the left-hand side starting from Na_2MoO_4 leads to molybdenum nitride pre-catalysts, while the one on the right-hand side starting from $[Mo(CO)_6]$ directly affords molybdenum alkylidyne complexes. This procedure resembles the low-oxidation-state route presented in Scheme 5.

Table 5: Ring-opening alkyne metathesis polymerization of cyclooctyne using **5** and **6a** as catalysts.

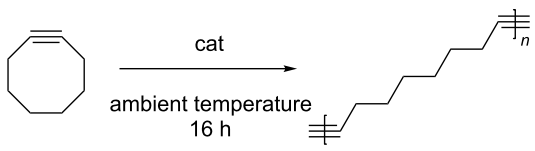

22 **23**

cat	mol %	solvent	c_{sub} (mol/L)	M_n (g/mol)	M_w (g/mol)	PDI	polymer yield (%)
5	1	-	neat	33000	46800	1.4	70
6a	1	-	neat	26400	41300	1.6	80
6a	5	-	neat	9960	23200	2.3	95
6a	5	toluene	0.03	82000	100000	1.2	7
6a	5	toluene	0.02	-[a]	-[a]	-[a]	0
6a	5	*n*-hexane	0.02	-[a]	-[a]	-[a]	0

[a]only cyclic oligomers were obtained.

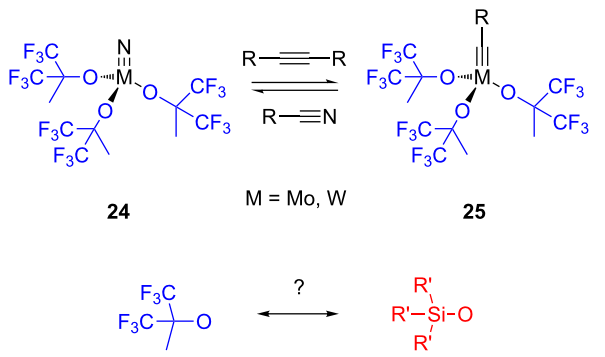

Scheme 6: Design strategy of Fürstner's new system.

The catalytic activities of the complexes **26**, **28**, **29**, **31**, **32** in ACM and RCAM were studied for a variety of substrates. In their initial publication [83], catalytic reactions were performed using **26**/Ph_3SiOH and **28** as catalysts. Although satisfactory to good yields were achieved, all reactions required elevated reaction temperatures (≥ 80 °C) and, in most cases, high catalyst loadings (up to 20%). However, the results were greatly improved for the 1,10-phenanthroline (phen) systems **29**/$MnCl_2$ and **32**/$MnCl_2$ – $MnCl_2$ is added to remove the phen-ligand by precipitation of $MnCl_2$•phen – and for the diethyl ether (Et_2O) complex **31** by addition of molecular sieves (MS 5 Å) to adsorb the 2-butyne formed during the metathesis reaction [84]. This method constitutes a significant advance, since it allows all reactions to be run in a closed system at ambient pressure.

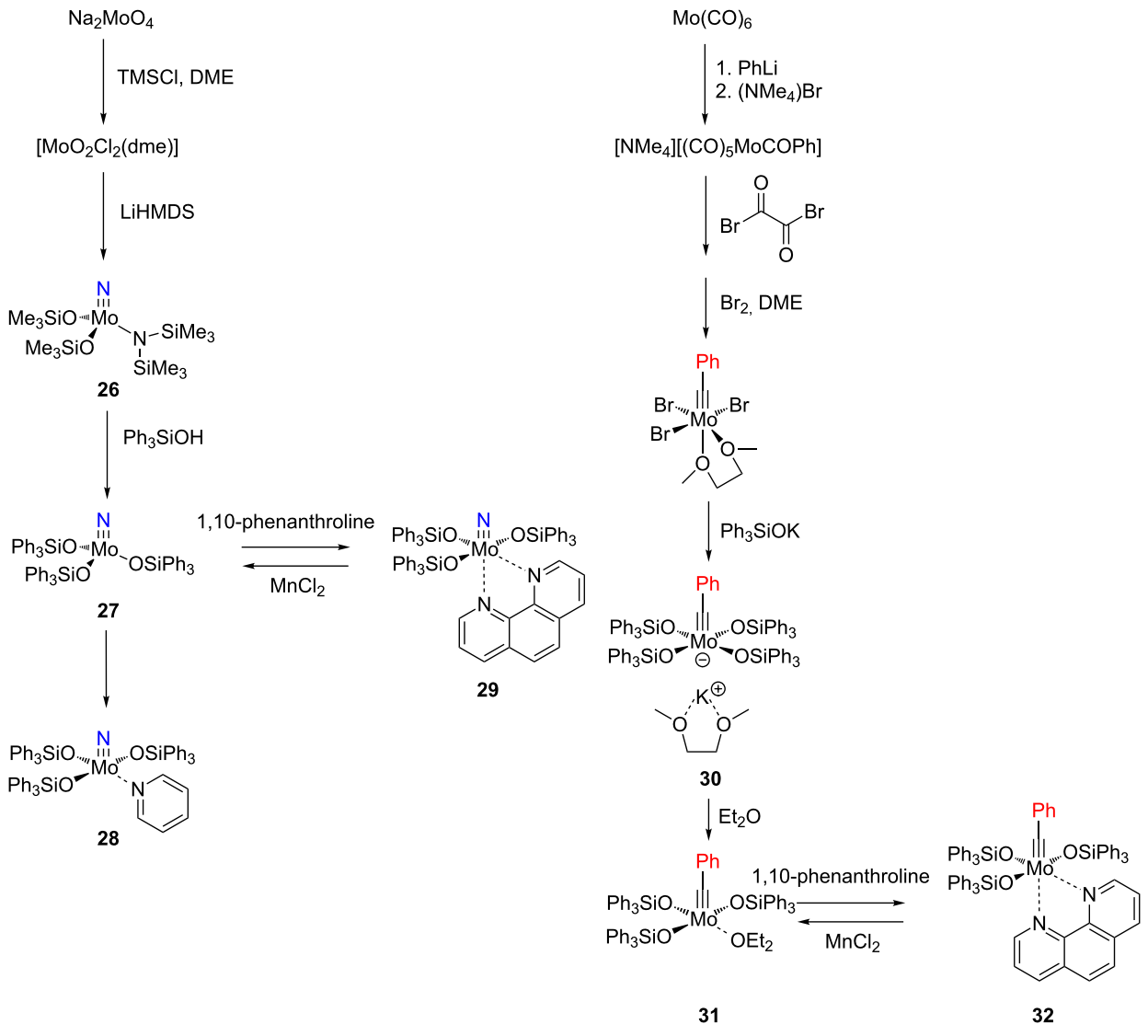

Scheme 7: Synthetic routes of Fürstner's new catalysts.

Accordingly, only the latter, improved results will be presented here, and Table 6 and Table 7 summarize the results for ACM and RCAM with the pre-catalysts **29**/$MnCl_2$, **31** and **32**/$MnCl_2$ [84].

The air-stable nitride complex **29** performs satisfactorily in the presence of $MnCl_2$ and MS 5 Å, however, its stability comes at the expense of higher catalyst loadings (10 mol %) and elevated reaction temperatures. In contrast, the phenanthroline–alkylidyne system **32** requires higher temperatures (80 °C) only for the activation with $MnCl_2$, whereas the metathesis reaction can be carried out at ambient temperature. Noteworthy, it is the Et_2O complex **31** that sets a new standard in alkyne metathesis, despite its reduced robustness in comparison with **32**. Like **29** and **32**, **31** – in combination with MS 5 Å – shows an excellent functional group tolerance together with a significantly enhanced catalytic performance even at lower catalyst concentrations and temperatures than indicated in Table 6 and Table 7 [84]. In addition, this catalyst was employed for the synthesis of various bioactive natural products and also for the total synthesis of natural occurring macrolactides [85,86], confirming and highlighting the strong potential of alkyne metathesis as a tool in organic synthetic methodology [9].

Table 6: ACM of **33** using **29**/$MnCl_2$, **31** and **32**/$MnCl_2$ as catalysts.

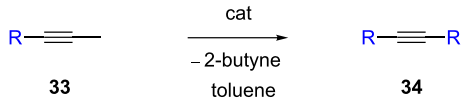

33 **34**

33	R-	catalyst and yield (%) **29**/$MnCl_2$[a]	**31**[b]	**32**/$MnCl_2$[c]
a[f]		99	99	99
b		96	97	97
c		87	98[d]	96[d]
d	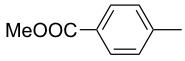	72[e]	95	97
e	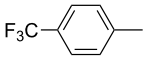	94	93	95
f	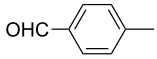	no reaction	no reaction	no reaction
g	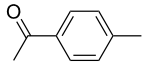	<40[e]	84	84
h		76[e]	90[d]	88[d]
i		86	88	87
j	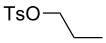	95	92	92
k	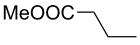	85	89	81
l	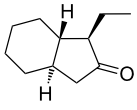		92	88
m	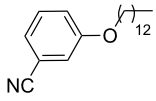	81	87	89

[a]**29** (10 mol %), activated by $MnCl_2$ (10 mol %) at 80 °C, molecular sieve, 80 °C. [b]**31** (2 mol %), molecular sieve, ambient temperature. [c]**32** (5 mol %), activated by $MnCl_2$ (5 mol %) at 80 °C, molecular sieve, ambient temperature. [d]50 °C. [e]100 °C. [f]**33a** and **34a** are the same as **7** and **8**, respectively.

Table 7: RCAM of **35** using **29**/$MnCl_2$, **31** and **32**/$MnCl_2$ as catalysts.

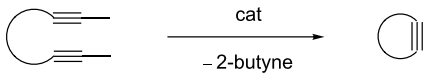

35 **36**

35	catalyst and yield (%) **29**/$MnCl_2$[a]	**31**[b]	**32**/$MnCl_2$[c]
a 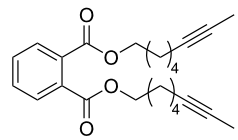	70	97	94
b 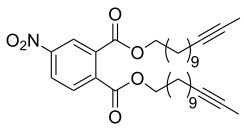		85	
c 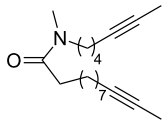	67	72	
d 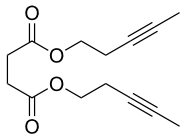	91	73	78
e 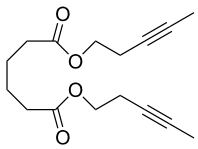	85	92	90

[a]**29** (10 mol %), activated by $MnCl_2$ (10 mol %) at 80 °C, without molecular sieve, 80 °C. [b]**31** (2 mol %), molecular sieve, ambient temperature. [c]**32** (5 mol %), activated by $MnCl_2$ (5 mol %) at 80 °C, molecular sieve, ambient temperature.

In a very recent report, Finke and Moore reported on the Lewis acid activation of the molybdenum nitrides **26** and **28**, which afforded the pre-catalysts **37** and **38** upon addition of one or two equivalents of $B(C_6F_5)_3$, respectively (Scheme 8) [87]. While the adduct **38** is found to be active in alkyne metathesis, the complex **37** requires additional activation by treatment with the electron-poor phenol 2-$(F_3C)C_6H_4OH$ to facilitate the formation of a catalytically active molybdenum alkylidyne species. The latter system was tested for the metathesis of several phenylalkynes, and yields up to 64% were obtained by application of relatively forcing reaction conditions (10 mol % nitride, 20 mol % borane, 30 mol % phenol, T = 90 °C). Nevertheless, the rate of metathesis is enhanced in comparison with the performance of the borane-free complexes, and these results might therefore pave the way for the development of alkyne metathesis catalysts based on transition metal nitrides.

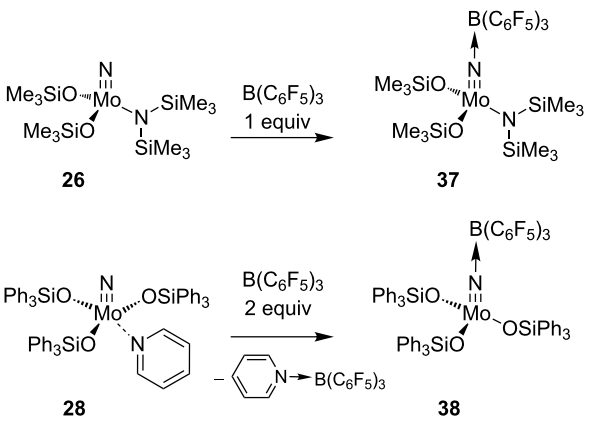

Scheme 8: Lewis acid addition of **26** and **28**.

Silanolate-supported tungsten alkylidyne complexes

The suitability of silanolates as suitable ancillary ligands for the development of alkyne metathesis catalysts is further confirmed by our independent synthesis of the tungsten benzylidyne complex **39** (Scheme 9), which can be isolated in high yield as a yellow crystalline solid from the reaction of the tribromide $[PhC{\equiv}WBr_3(dme)]$ (dme = 1,2-dimethoxyethane) with the lithium salt of the silanol $(t\text{-BuO})_3SiOH$ [88]. Since this silanol can be regarded as a mimic for silica surfaces [89-94], **39** might be regarded as a homogeneous model for silica-supported alkylidyne complexes [45,46,91-94]. Compound **39** exhibits excellent catalytic behavior in a number of ACM and RCAM reactions [88] (Table 8 and Table 9), and in analogy to Fürstner's report [84], our studies also indicate that the addition of MS 5 Å does further improve the activity and the ease of applicability of this catalyst system.

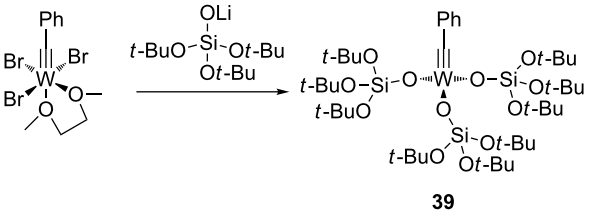

Scheme 9: Preparation of the silanolate–alkylidyne tungsten complex **39**.

Table 8: ACM using **39** as catalyst.

substrate	product	yield (%)[a]	yield (%)[b]
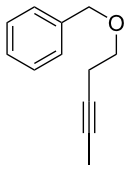 **11**	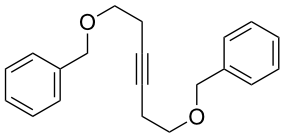 **12**	85	95
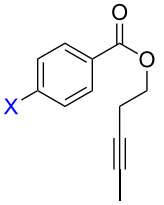 **13**	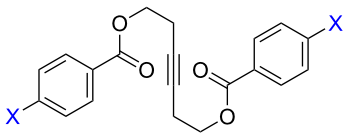 **14**	**a** X = H 97 **b** X = Cl 92 **c** X = OMe 96 **d** X = SMe 94[c]	**a** X = H 99 **b** X = Cl 97 **c** X = OMe 97 **d** X = SMe 99

[a]0.5 mmol substrate, 2 mol % catalyst **39**, 8 mL toluene, rt, 1 h, 200 mbar. [b]0.5 mmol substrate, 1 mol % catalyst **39**, 2 mL toluene, rt, 1 h, 500 mg, molecular sieve. [c]0.5 mmol, substrate, 5 mol % catalyst **39**, 8 mL toluene, rt, 1 h, 200 mbar.

Table 9: RCAM using **39** as catalyst.

substrate	product	yield (%)[a]	yield (%)[b]
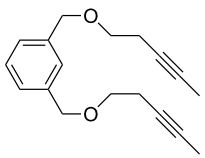 **17b**	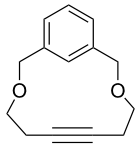 **18b**	80	95
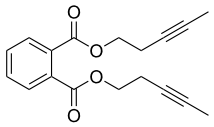 **20**	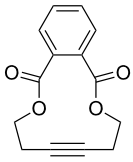 **21**	92	97
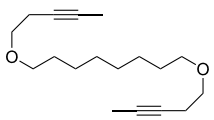 **15**	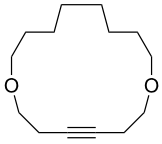 **16**	72	95
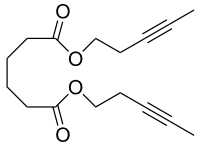 **35e**	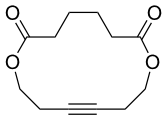 **36e**	73	99

[a]0.36 mmol substrate, 2 mol % catalyst **39**, 80 mL toluene, 80 °C, 2 h. [b]0.48 mmol substrate, 2 mol % catalyst **39**, 24 mL toluene, rt, 2 h, 1 g molecular sieve.

Conclusion

"Although alkyne metathesis may never reach the breadth of alkene metathesis because of a smaller substrate base" [84], the recent additions to the comparatively small family of alkyne metathesis catalysts – imidazolin-2-iminato- and silanolate-supported molybdenum and tungsten alkylidyne complexes – should certainly help to boost the recognition of alkyne metathesis and to overcome the prevalence of olefin metathesis. The synthetic protocols developed for the synthesis of these new (pre-) catalysts allow for fine-tuning of their steric and electronic properties in order to further optimize their stability and catalytic performance and to modulate their structure according to the requirements of specific applications and substrate classes. However, the development in alkyne metathesis has yet to overcome one major obstacle, and that is the impracticability of employing terminal alkynes as substrates, since these tend to form polymers [95] and were also shown to degrade Schrock alkylidynes by formation of deprotonated, inactive metallacyclobutadienes [96]. Hence, future efforts should also re-address this issue, e. g., by adjusting the properties of the metallacyclobutadiene key intermediates [97] in order to prevent their degeneration and therefore ineffectiveness in undergoing the Katz [2 + 2]cycloaddition/cycloreversion mechanism (Scheme 1).

Acknowledgements

Our work in this area was supported by the Deutsche Forschungsgemeinschaft (DFG) through grants TA 189/6-1, -2, and -3.

References

1. Diederich, F.; Stang, P. J.; Tykwinski, R. R., Eds. *Acetylene Chemistry: Chemistry, Biology and Material Science;* Wiley-VCH: Weinheim, Germany, 2005.
2. Zhang, W.; Moore, J. S. *Adv. Synth. Catal.* **2007,** *349,* 93–120. doi:10.1002/adsc.200600476
3. Schrock, R. R.; Czekelius, C. *Adv. Synth. Catal.* **2007,** *349,* 55–77. doi:10.1002/adsc.200600459
4. Van de Weghe, P.; Bisseret, P.; Blanchard, N.; Eustache, J. *J. Organomet. Chem.* **2006,** *691,* 5078–5108. doi:10.1016/j.jorganchem.2006.07.022
5. Mortreux, A.; Coutelier, O. *J. Mol. Catal. A: Chem.* **2006,** *254,* 96–104. doi:10.1016/j.molcata.2006.03.054
6. Schrock, R. R. *Chem. Commun.* **2005,** *22,* 2773–2777. doi:10.1039/b504541j
7. Bunz, U. H. F. *Science* **2005,** *308,* 216–217. doi:10.1126/science.1111098
8. Schrock, R. R. *Chem. Rev.* **2002,** *102,* 145–180. doi:10.1021/cr0103726
9. Fürstner, A.; Davis, P. W. *Chem. Commun.* **2005,** 2307–2320. doi:10.1039/b419143a
10. Schrock, R. R.; Hoveyda, A. H. *Angew. Chem., Int. Ed.* **2003,** *115,* 4740–4782. doi:10.1002/anie.200300576
11. Fürstner, A. Alkyne Metathesis. In *Handbook of Metathesis;* Grubbs, R., Ed.; Wiley-VCH: Weinheim, Germany, 2003; Vol. 2, pp 432–462. doi:10.1002/9783527619481.ch27
12. Katz, T. J.; McGinnis, J. *J. Am. Chem. Soc.* **1975,** *97,* 1592–1594. doi:10.1021/ja00839a063
13. Pennella, F.; Banks, R. L.; Bailey, G. C. *Chem. Commun. (London)* **1968,** 1548–1549. doi:10.1039/c19680001548
14. Mortreux, A.; Blanchard, M. *J. Chem. Soc., Chem. Commun.* **1974,** 786–787. doi:10.1039/C39740000786
15. Mortreux, A.; Dy, N.; Blanchard, M. *J. Mol. Catal.* **1975,** *76,* 101–109. doi:10.1016/0304-5102(76)80004-1
16. Mortreux, A.; Petit, F.; Blanchard, M. *Tetrahedron Lett.* **1978,** *19,* 4967–4968. doi:10.1016/S0040-4039(01)85783-X
17. Bencheick, A.; Petit, M.; Mortreux, A.; Petit, F. *J. Mol. Catal.* **1982,** *15,* 93–101. doi:10.1016/0304-5102(82)80008-4
18. Mortreux, A.; Delgrange, J. C.; Blanchard, M.; Lubochinsky, B. *J. Mol. Catal.* **1977,** *2,* 73–82. doi:10.1016/0304-5102(77)85018-9
19. Mortreux, A.; Petit, F.; Blanchard, M. *J. Mol. Catal.* **1980,** *8,* 97–106. doi:10.1016/0304-5102(80)87009-X
20. Kaneta, N.; Hikichi, K.; Asaka, S.-i.; Uemura, M.; Mori, M. *Chem. Lett.* **1995,** 1055–1066. doi:10.1246/cl.1995.1055

21. Zhang, W.; Moore, J. S. *Angew. Chem., Int. Ed.* **2006,** *118,* 4524–4548. doi:10.1002/anie.200503988
22. Zhao, D.; Moore, J. S. *Chem. Commun.* **2003,** 807–818. doi:10.1039/b207442g
23. Brizius, G.; Pschirer, N. G.; Steffen, W.; Stitzer, K.; zur Loye, H. C.; Bunz, U. H. F. *J. Am. Chem. Soc.* **2000,** *122,* 12435–12440. doi:10.1021/ja0010251
24. Ge, P. H.; Fu, W.; Herrmann, W. A.; Herdtweck, E.; Campana, C.; Adams, R. D.; Bunz, U. H. F. *Angew. Chem., Int. Ed.* **2000,** *112,* 3753–3756. doi:10.1002/1521-3773(20001016)39:20<3607::AID-ANIE3607>3.0.CO;2-S
25. Höger, S. *Angew. Chem., Int. Ed.* **2005,** *117,* 3872–3875. doi:10.1002/anie.200500681
26. Miljanic, O. S.; Vollhardt, K. P. C.; Whitener, G. D. *Synlett* **2003,** 29–34. doi:10.1055/s-2003-36233
27. Johnson, C. A., II; Lu, Y.; Haley, M. M. *Org. Lett.* **2007,** *9,* 3725–3728. doi:10.1021/ol7014253
28. Fürstner, A.; Guth, O.; Rumbo, A.; Seidel, G. *J. Am. Chem. Soc.* **1999,** *121,* 11108–11113. doi:10.1021/ja992074k
29. Sancho, J.; Schrock, R. R. *J. Mol. Catal.* **1982,** *15,* 75–79. doi:10.1016/0304-5102(82)80006-0
30. Schrock, R. R.; Clark, D. N.; Sancho, J.; Wengrovius, J. H.; Rocklage, S. M.; Pederson, S. F. *Organometallics* **1982,** *1,* 1645–1651. doi:10.1021/om00072a018
31. Wengrovius, J. H.; Sancho, J.; Schrock, R. R. *J. Am. Chem. Soc.* **1981,** *103,* 3932–3934. doi:10.1021/ja00403a058
32. Fürstner, A.; Seidel, G. *Angew. Chem., Int. Ed.* **1998,** *110,* 1758–1760. doi:10.1002/(SICI)1521-3773(19980703)37:12<1734::AID-ANIE1734>3.0.CO;2-6
33. Grela, K.; Ignatowska, J. *Org. Lett.* **2002,** *4,* 3747–3749. doi:10.1021/ol026690o
34. Song, D.; Blond, G.; Fürstner, A. *Tetrahedron* **2003,** *59,* 6899–6904. doi:10.1016/S0040-4020(03)00815-9
35. Fürstner, A.; Müller, G. *J. Organomet. Chem.* **2000,** *606,* 75–78. doi:10.1016/S0022-328X(00)00096-6
36. Laplaza, C. E.; Odom, A. L.; Davis, M. W.; Cummins, C. C.; Protasiewicz, J. D. *J. Am. Chem. Soc.* **1995,** *117,* 4999–5000. doi:10.1021/ja00122a033
37. Laplaza, C. E.; Cummins, C. C. *Science* **1995,** *268,* 861–863. doi:10.1126/science.268.5212.861
38. Laplaza, C. E.; Johnson, A. R.; Cummins, C. C. *J. Am. Chem. Soc.* **1996,** *118,* 709–710. doi:10.1021/ja953573y
39. Fürstner, A.; Mathes, C.; Lehmann, C. W. *J. Am. Chem. Soc.* **1999,** *121,* 9453–9454. doi:10.1021/ja991340r
40. Zhang, W.; Kraft, S.; Moore, J. S. *Chem. Commun.* **2003,** 832–833. doi:10.1039/b212405j
41. Zhang, W.; Kraft, S.; Moore, J. S. *J. Am. Chem. Soc.* **2004,** *126,* 329–335. doi:10.1021/ja0379868
42. Zhang, W.; Moore, J. S. *J. Am. Chem. Soc.* **2004,** *126,* 12796. doi:10.1021/ja046531v
43. Zhang, W.; Moore, J. S. *J. Am. Chem. Soc.* **2005,** *127,* 11863–11870. doi:10.1021/ja053466w
44. Zhang, W.; Brombosz, S. M.; Mendoza, J. L.; Moore, J. S. *J. Org. Chem.* **2005,** *70,* 10198–10201. doi:10.1021/jo0517803
45. Weissmann, H.; Plunkett, K. N.; Moore, J. S. *Angew. Chem., Int. Ed.* **2006,** *118,* 599–602. doi:10.1002/anie.200502840
46. Cho, H. M.; Weissmann, H.; Moore, J. S. *J. Org. Chem.* **2008,** *73,* 4256–4258. doi:10.1021/jo8003919
47. Blackwell, J. M.; Figueroa, J. S.; Stephens, F. H.; Cummins, C. C. *Organometallics* **2003,** *22,* 3351–3353. doi:10.1021/om0301482
48. Dehnicke, K.; Greiner, A. *Angew. Chem., Int. Ed.* **2003,** *115,* 1378–1392. doi:10.1002/anie.200390346
49. Dehnicke, K.; Krieger, M.; Massa, W. *Coord. Chem. Rev.* **1999,** *182,* 19–65. doi:10.1016/S0010-8545(98)00191-X
50. Dehnicke, K.; Weller, F. *Coord. Chem. Rev.* **1997,** *158,* 103–169. doi:10.1016/S0010-8545(97)90055-2
51. Dehnicke, K.; Strähle, J. *Polyhedron* **1989,** *8,* 707–726. doi:10.1016/S0277-5387(00)83838-3
52. Diefenbach, A.; Bickelhaupt, F. M. *Z. Anorg. Allg. Chem.* **1999,** *625,* 892–900. doi:10.1002/(SICI)1521-3749(199906)625:6<892::AID-ZAAC892>3.0.CO;2-7
53. Kuhn, N.; Göhner, M.; Grathwohl, M.; Wiethoff, J.; Frenking, G.; Chen, Y. *Z. Anorg. Allg. Chem.* **2003,** *629,* 793–802. doi:10.1002/zaac.200390141
54. Kuhn, N.; Fawzi, R.; Steinmann, M.; Wiethoff, J. *Z. Anorg. Allg. Chem.* **1997,** *623,* 769–774. doi:10.1002/zaac.199762301121
55. Kuhn, N.; Fawzi, R.; Steinmann, M.; Wiethoff, J.; Bläser, D.; Boese, R. *Z. Naturforsch.* **1995,** *50b,* 1779–1784.
56. Tamm, M.; Randoll, S.; Bannenberg, T.; Herdtweck, E. *Chem. Commun.* **2004,** 876–877. doi:10.1039/b401041h
57. Tamm, M.; Beer, S.; Herdtweck, E. *Z. Naturforsch.* **2004,** *59b,* 1497–1504.
58. Tamm, M.; Randoll, S.; Herdtweck, E.; Kleigrewe, N.; Kehr, G.; Erker, G.; Rieger, B. *Dalton Trans.* **2006,** 459–467. doi:10.1039/b511752f
59. Petrovic, D.; Tamm, M.; Herdtweck, E. *Acta Crystallogr.* **2006,** *C62,* 217–219. doi:10.1107/S0108270106008778
60. Tamm, M.; Petrovic, D.; Randoll, S.; Beer, S.; Bannenberg, T.; Jones, P. G.; Grunenberg, J. *Org. Biomol. Chem.* **2007,** *5,* 523–530. doi:10.1039/b615418b
61. Panda, T. K.; Randoll, S.; Hrib, C. G.; Jones, P. G.; Bannenberg, T.; Tamm, M. *Chem. Commun.* **2007,** 5007–5009. doi:10.1039/b711669a
62. Stelzig, S. H.; Tamm, M.; Waymouth, R. M. *J. Polym. Sci., Part A: Polym. Chem.* **2008,** *46,* 6064–6070. doi:10.1002/pola.22918
63. Panda, T. K.; Trambitas, A. G.; Bannenberg, T.; Hrib, C. G.; Randoll, S.; Jones, P. G.; Tamm, M. *Inorg. Chem.* **2009,** *48,* 5462–5472. doi:10.1021/ic900503q
64. Trambitas, A. G.; Panda, T. K.; Jenter, J.; Roesky, P. W.; Daniliuc, C.; Hrib, C. G.; Jones, P. G.; Tamm, M. *Inorg. Chem.* **2010,** *49,* 2435–2446. doi:10.1021/ic9024052
65. Tamm, M.; Trambitas, A. G.; Hrib, C. G.; Jones, P. G. *Terrae Rarae* **2010,** *7,* 1–4.
66. Panda, T. K.; Hrib, C. G.; Jones, P. G.; Tamm, M. *J. Organomet. Chem.* **2010,** *695,* 2768–2773. doi:10.1016/j.jorganchem.2010.06.028
67. Trambitas, A. G.; Panda, T. K.; Tamm, M. *Z. Anorg. Allg. Chem.* **2010,** *636,* 2156–2171. doi:10.1002/zaac.201000224
68. Mayr, A.; McDermott, G. A. *J. Am. Chem. Soc.* **1986,** *108,* 548–549. doi:10.1021/ja00263a054
69. McDermott, G. A.; Dorries, A. M.; Mayr, A. *Organometallics* **1987,** *6,* 925–931. doi:10.1021/om00148a005
70. Haberlag, B.; Wu, X.; Brandhorst, K.; Grunenberg, J.; Daniliuc, C. G.; Jones, P. G.; Tamm, M. *Chem.–Eur. J.* **2010,** *16,* 8868–8877. doi:10.1002/chem.201000597
71. Schrock, R. R.; Sancho, J.; Pederson, S. F. *Inorg. Synth.* **1989,** *26,* 44–51. doi:10.1002/9780470132579.ch10

72. Freudenberger, J. H.; Schrock, R. R.; Churchill, M. R.; Rheingold, A. L.; Ziller, J. W. *Organometallics* **1984,** *3,* 1563–1573. doi:10.1021/om00088a019
73. Beer, S.; Hrib, C. G.; Jones, P. G.; Brandhorst, K.; Grunenberg, J.; Tamm, M. *Angew. Chem., Int. Ed.* **2007,** *119,* 9047–9051. doi:10.1002/anie.200703184
74. Beer, S.; Brandhorst, K.; Hrib, C. G.; Wu, X.; Haberlag, B.; Grunenberg, J.; Jones, P. G.; Tamm, M. *Organometallics* **2009,** *28,* 1534–1545. doi:10.1021/om801119t
75. Schrock, R. R.; Weinstock, I. A.; Horton, A. D.; Liu, A. H.; Schofield, M. H. *J. Am. Chem. Soc.* **1988,** *110,* 2686–2687. doi:10.1021/ja00216a071
76. Tonzetich, Z. J.; Schrock, R. R.; Müller, P. *Organometallics* **2006,** *25,* 4301–4306. doi:10.1021/om060501e
77. Beer, S.; Brandhorst, K.; Grunenberg, J.; Hrib, C. G.; Jones, P. G.; Tamm, M. *Org. Lett.* **2008,** *10,* 981–984. doi:10.1021/ol800154y
78. Lysenko, S.; Haberlag, B.; Wu, X.; Tamm, M. *Macromol. Symp.* **2010,** *293,* 20–23. doi:10.1002/masy.200900046
79. Monfette, S.; Fogg, D. E. *Chem. Rev.* **2009,** *109,* 3783–3816. doi:10.1021/cr800541y
80. Gdula, R. L.; Johnson, M. J. A. *J. Am. Chem. Soc.* **2006,** *128,* 9614–9615. doi:10.1021/ja058036k
81. Geyer, A. M.; Wiedner, E. S.; Gary, J. B.; Gdula, R. L.; Kuhlmann, N. C.; Johnson, M. J. A.; Dunietz, B. D.; Kampf, J. W. *J. Am. Chem. Soc.* **2008,** *130,* 8984–8999. doi:10.1021/ja800020w
82. Chiu, H.-T.; Chen, Y.-P.; Chuang, S.-H.; Jen, J.-S.; Lee, G.-H.; Peng, S.-M. *Chem. Commun.* **1996,** 139–140. doi:10.1039/cc9960000139
83. Bindl, M.; Stade, R.; Heilmann, E. K.; Picot, A.; Goddard, R.; Fürstner, A. *J. Am. Chem. Soc.* **2009,** *131,* 9468–9470. doi:10.1021/ja903259g
84. Heppekausen, J.; Stade, R.; Goddard, R.; Fürstner, A. *J. Am. Chem. Soc.* **2010,** *132,* 11045–11057. doi:10.1021/ja104800w
85. Hickmann, V.; Alcarazo, M.; Fürstner, A. *J. Am. Chem. Soc.* **2010,** *132,* 11042–11044. doi:10.1021/ja104796a
86. Micoine, K.; Fürstner, A. *J. Am. Chem. Soc.* **2010,** *132,* 14064–14066. doi:10.1021/ja107141p
87. Finke, A. D.; Moore, J. S. *Chem. Commun.* **2010,** *46,* 7939–7941. doi:10.1039/c0cc03113e
88. Lysenko, S.; Haberlag, B.; Daniliuc, C. G.; Jones, P. G.; Tamm, M. *ChemCatChem* **2011,** *3,* 115–118. doi:10.1002/cctc.201000355
89. Fischbach, A.; Klimpel, M. G.; Widenmeyer, M.; Herdtweck, E.; Scherer, W.; Anwander, R. *Angew. Chem., Int. Ed.* **2004,** *116,* 2284–2289. doi:10.1002/anie.200352730
90. Duchateau, R. *Chem. Rev.* **2002,** *102,* 3525–3542. doi:10.1021/cr010386b
91. Chandrasekhar, V.; Boomishankar, R.; Nagendran, S. *Chem. Rev.* **2004,** *104,* 5847–5910. doi:10.1021/cr0306135
92. Cho, H. M.; Weissman, H.; Wilson, S. R.; Moore, J. S. *J. Am. Chem. Soc.* **2006,** *128,* 14742–14743. doi:10.1021/ja065101x
93. Chabanas, M.; Baudouin, A.; Copéret, C.; Basset, J. M. *J. Am. Chem. Soc.* **2001,** *123,* 2062–2063. doi:10.1021/ja000900f
94. Merle, N.; Taoufik, M.; Nayer, M.; Baudouin, A.; Le Boux, E.; Gauvin, R. M.; Lefebvre, F.; Thivolle-Gazat, J.; Basset, J. M. *J. Organomet. Chem.* **2008,** *693,* 1733–1737. doi:10.1016/j.jorganchem.2008.02.020
95. Bray, A.; Mortreux, A.; Petit, F.; Petit, M.; Szymanska-Buzar, T. *J. Chem. Soc., Chem. Commun.* **1993,** 197–199. doi:10.1039/C39930000197
96. McCullough, L. G.; Listemann, M. L.; Schrock, R. R.; Churchill, M. R.; Ziller, J. W. *J. Am. Chem. Soc.* **1983,** *105,* 6729–6730. doi:10.1021/ja00360a040
97. Suresh, C. H.; Frenking, G. *Organometallics* **2010,** *29,* 4766–4769. doi:10.1021/om100260p

License and Terms

Beilstein Journal of Organic Chemistry

Olefin metathesis in nano-sized systems

Didier Astruc*, Abdou K. Diallo, Sylvain Gatard, Liyuan Liang, Cátia Ornelas, Victor Martinez, Denise Méry and Jaime Ruiz

Review

Open Access

Address:
Institut des Sciences Moléculaires, UMR CNRS No 5255, Université Bordeaux 1, 351 Cours de la Libération, 33405 Talence Cedex, France

Email:
Didier Astruc* - d.astruc@ism.u-bordeaux1.fr

* Corresponding author

Keywords:
dendrimer; green chemistry; metathesis; nano-system; water

Beilstein J. Org. Chem. **2011,** *7,* 94–103.
doi:10.3762/bjoc.7.13

Received: 31 August 2010
Accepted: 09 November 2010
Published: 19 January 2011

Guest Editor: K. Grela

Abstract

The interplay between olefin metathesis and dendrimers and other nano systems is addressed in this mini review mostly based on the authors' own contributions over the last decade. Two subjects are presented and discussed: (i) The catalysis of olefin metathesis by dendritic nano-catalysts via either covalent attachment (ROMP) or, more usefully, dendrimer encapsulation – ring closing metathesis (RCM), cross metathesis (CM), enyne metathesis reactions (EYM) – for reactions in water without a co-solvent and (ii) construction and functionalization of dendrimers by CM reactions.

Introduction

Olefin metathesis reactions [1-7] have been successfully catalyzed under standard conditions, including reactions at room temperature and sometimes even in air, with commercial Grubbs-type catalysts [8,9]. These are now largely developed for industry with functional substrates for the synthesis of highly sophisticated pharmaceutical products and polymers. There is continuing research in the olefin metathesis field, however, because of the economical and ecological constraints of modern society. This requires that the catalyst amounts be as low as possible and that polluting classic organic solvents be replaced by "greener" solvents such as water or super-critical carbon dioxide. Therefore during the last decade, we have attempted to make progress in this field with dendrimers using nano-organometallic chemistry [10]. There are several ways in which dendrimer chemistry can be useful in this direction, and this short review article will indicate the various connections between metathesis reactions and dendrimer chemistry.

Review

Covalent attachment of the olefin metathesis catalyst to the tethers of the dendrimer periphery

The attachment of catalysts to dendrimers was mostly focused on the recovery of the catalyst. Only a few metallodendritic carbene complexes with covalent binding of the olefin metathesis catalyst are known. Prior to our involvement only compounds with four branches were known [11-14] but good

recyclability still remained a challenge. The difficulty resided in the need to sustain both metathesis activity and stability of the metallodendrimer. Thus, we selected the ruthenium family of catalysts and designed metallodendrimers containing ruthenium-benzylidene fragments located at the dendrimer periphery and chelating phosphine ligands on the branch termini. The choice of chelating phosphines may seem counter-intuitive, because the activity of Grubbs catalysts involves the decoordination of a phosphine from these *trans*-bis-phosphine complexes [15]. However, studies by the groups of Hofmann [16-18], Fog [19,20] and Leitner [20] had demonstrated the metathesis activity of *cis*-bis-phosphine ruthenium benzylidene catalysts. We therefore used Reetz's bis-phosphines derived from the commercial polyamine DSM dendrimers [21]. These dendritic bis-phosphines are useful and versatile in metallodendritic catalysis and provided the first recyclable metallodendritic catalysts [21]. Moreover, dendritic bis-phosphines with two phenyl groups on each phosphorus atom very cleanly yielded the first dendrimers decorated with clusters at the periphery via an efficient electron-transfer-chain reaction using $[Ru_3(CO)_{12}]$ catalyzed by $[Fe^{I}Cp(\eta^6\text{-}C_6Me_6)]$ leading to the substitution of a carbonyl of the $[Ru_3(CO)_{12}]$ by a dendritic phosphine on each tether [22]. Related dendritic bis-phosphines with two cyclohexyl groups on each phosphorus were decorated with ruthenium benzylidene metathesis functions using Hoveyda's ruthenium benzylidene metathesis catalyst, **1** [23], as the starting point. These reactions provided four generations of new, stable metallodendrimers **2** containing ruthenium-benzylidene fragments at the periphery (Scheme 1) [24,25]. The fourth-generation metallodendrimer containing 32 ruthenium-benzylidene fragments, however, was found to have a rather low solubility in common organic solvents, unlike the three first-generation complexes that contained 4, 8 and 16 ruthenium-benzylidene moieties, respectively. The weak solubility of the 32-Ru dendrimer is presumably due to steric congestion at its periphery. Such steric congestion is also responsible for the decrease of the catalytic activity of Ru and Pd high-generation dendritic catalysts, even when these metallodendritic catalysts are soluble. The X-ray crystal structure of the model mononuclear complex in which the dendritic branch was replaced by a benzyl group showed distorted square pyramidal geometry and the classic geometric features of a Ru=C double bond. The oxygen atom of the isopropyl aryl ether group is not coordinated unlike in Hoveyda's complex **1**. The fundamental organometallic chemistry of this monomeric model complex was also original [24,25].

The three first generations of metallodendrimers **2** and the model complex do not catalyze RCM reactions, but they were efficient catalysts for the ROMP of norbornene under ambient conditions, giving dendrimer-cored stars (Scheme 1 and Scheme 2) [24,25]. Analysis of the molecular weights by size exclusion chromatography gave data that were close to the theoretical values, which indicated that all the branches were efficiently polymerized. Dendritic-cored stars with an average of about 100 norbornene units on each dendritic branch were synthesized from the three first generations of ruthenium-carbene dendrimers containing 4, 8 and 16 Ru=C bonds, respectively.

Two kinds of dendritic effect were found on analysis of the kinetic data. First, the dendrimers were more efficient catalysts

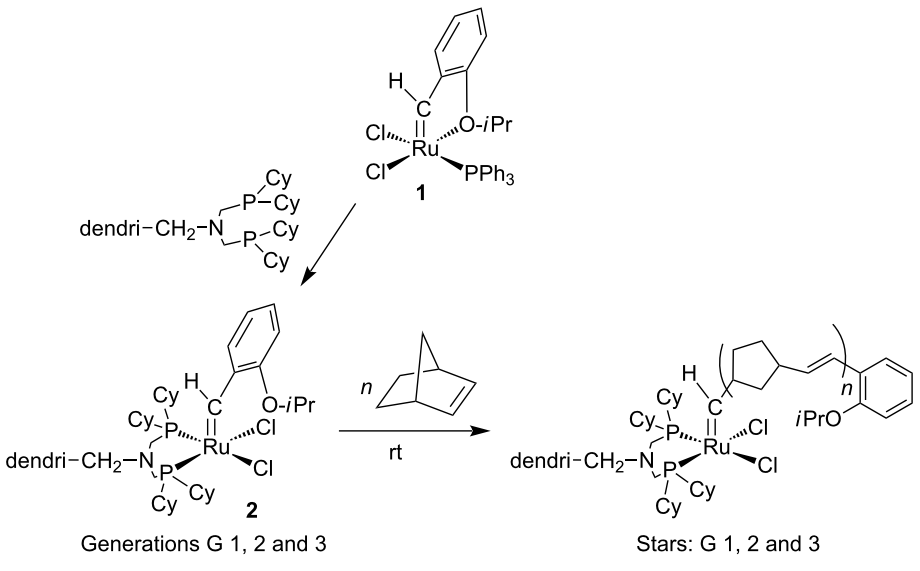

Scheme 1: Strategy for the ROMP of norbornene by Ru-benzylidene dendrimers to form dendrimer-cored stars.

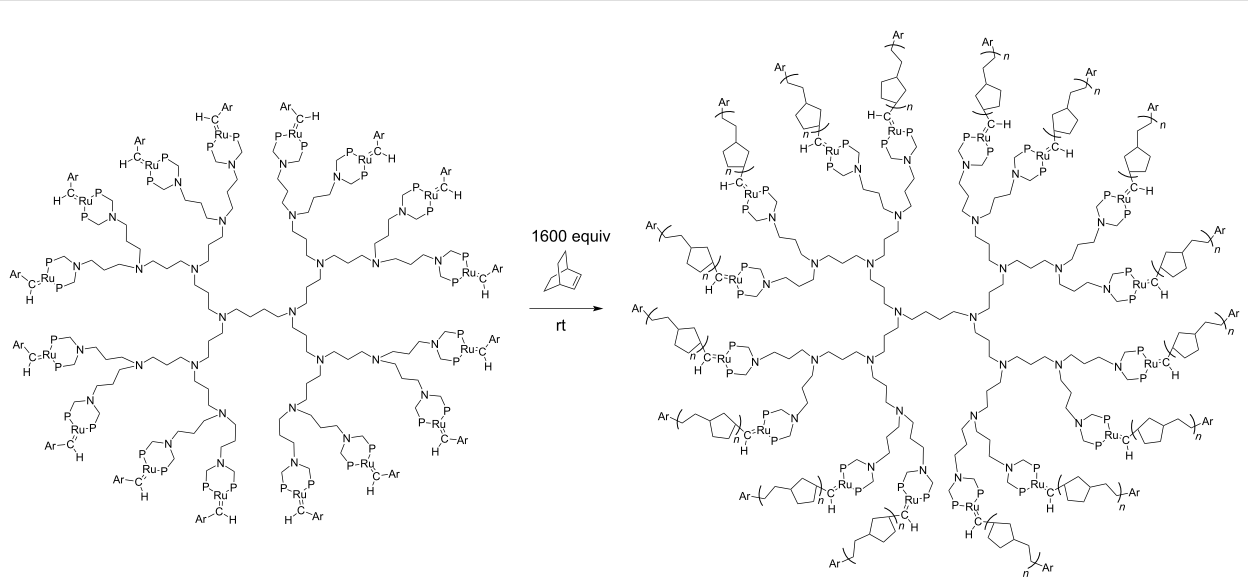

Scheme 2: Third-generation (16 Ru atoms) ruthenium-benzylidene dendrimer that catalyzes the ROMP of norbornene at 25 °C to form dendrimer-cored stars.

than the monomeric model complex. This could possibly be due to labilization of metal-phosphine bonds that is facilitated in dendrimers as compared to the monomer for entropic reasons. Indeed, DFT calculation showed that the catalytic process must involve decoordination of a phosphorus atom, since the interaction of the olefin with the diphosphine complex is non-bonding. The dendritic ruthenium-benzylidene dendrimers were air-sensitive in contrast to the monomer model complex, consistent with more rapid dissociation of the alkyl phosphine in the dendrimers than in the monomer. Secondly, the efficiency of catalysis decreased upon increasing the dendrimer generation. This second dendritic effect is thus a negative one, and it is probably related to the more difficult access to the metal center due to the increasing steric effect at the dendrimer periphery when the generation increases.

Analogous ruthenium benzylidene dendrimers were very recently synthesized with two *tert*-butyl groups on each phosphorus atom, and these were slightly more reactive ROMP catalysts for the polymerization of norbornene than those carrying cyclohexyl substituents [25]. These new dendritic ligands, in particular those of low generation (with up to 8 branches), also proved very efficient in palladium catalysis [26-31].

Construction and decoration of dendrimers using olefin metathesis reactions

Star-shaped and dendrimer compounds that are terminated by carbon–carbon double bonds can undergo CM reactions with olefins. To begin with, we examined cross olefin metathesis reactions with rather small aromatic molecules bearing a few double bonds, then continued the study with larger analogues. Temporary coordination of arenes to the strongly electron-withdrawing cationic 12-electron group $CpFe^+$ greatly increases the acidity of its benzylic protons (the pK_a values of the arenes in DMSO are lowered upon complexation with $CpFe^+$ by approximately 15 units, for instance from 43 to 28 in the case of C_6Me_6) [32,33]. Therefore, deprotonation of the $CpFe(arene)^+$ complexes is feasible under mild conditions with KOH. Deprotonated $CpFe(arene)^+$ complexes are good nucleophiles, and reactions with electrophiles such as the alkyl halides lead to the formation of new C–C bonds. Coupling the deprotonation and the nucleophilic reactions in situ in the presence of excess substrates leads to perfunctionalization in cascade multi-step reactions [34,35]. When the electrophile is allyl bromide, polyolefin compounds are produced after decomplexation by visible-light photolysis which removes the temporary activating $CpFe^+$ group [36-38]. These compounds are then ideal substrates for RCM and CM. New structures were obtained using this strategy with durene, *p*-xylene, mesitylene, and pentamethylcobalticinium [39-41]. The latter was perallylated to yield a deca-allylated cobalticinium, and then RCM of the organometallic complex proceeded to afford a pentacyclopentylcyclopentadienyl Co sandwich complex using the first-generation Grubbs catalyst $[Ru(PCy_3)_2Cl_2(=CHPh)]$, **3**. Activation of mesitylene by the $CpFe^+$ moiety in **4**, followed by a one-pot perallylation yielded $[CpFe(nonaallylmesitylene)^+]$-$[PF_6^-]$, **5,** from which the free arene derivative **6** was obtained on visible-light photolytic decomplexation [34,35,42]. First, a triple RCM reaction catalyzed by **3** proceeded in ten minutes under ambient condition, to afford an intermediate tetracyclic

iron arene complex. Furthermore and interestingly, when the metathesis reaction was carried out in refluxing dichloroethane with the addition of the second-generation Grubbs catalyst [$RuCl_2$(=CHPh)(bis-*N*-mesityl-NHC)], **7**, (Scheme 3, NHC = N-heterocyclic carbene), the di-iron cage compound **8** was formed. Similarly, the iron-free nonaallylated compound **6** gave, by metathesis catalyzed by **7**, the organic cage **9**. After hydrogenation with H_2/Pd/C in CH_2Cl_2 of the tripled-bridged cage **9**, a single hydrogenated product was isolated. Another very useful feature is that the organic cage formation can be totally inhibited in the presence of acrylic acid to produce the triacid **10** by a more rapid stereoselective CM (Scheme 3) [43,44].

Since successful CM with acrylic acid gave water-soluble compounds, this reaction was exploited to synthesize water-soluble dendrimers with carboxylate termini. Dendritic precursors were prepared with long tethers containing olefin termini so that no competitive RCM occurred unlike in the preceding example. Indeed, CM of these long-chain polyolefin dendrimers catalyzed by the 2nd generation Grubbs metathesis catalyst **7** proceeded selectively to produce dendrimers whose tethers were terminated by carboxylic acid groups (Scheme 4 and Scheme 5). The corresponding carboxylates are water-soluble. Higher-generation dendrimers with carboxylic acid termini have been synthesized similarly [43,44].

Other attempts have been reported in the literature for the metathesis of polyolefin dendrimers or star compounds from which ring-closing metathesis products were formed. For instance, a third generation Fréchet-type dendrimer containing 24 allyl ether end groups was synthesized by the Zimmerman group, cross-linked using the RCM reaction, and the core removed hydrolytically without any significant fragmentation [45-47]. The results are analogous to those previously reported for homoallyl ether dendrimers suggesting that the less readily

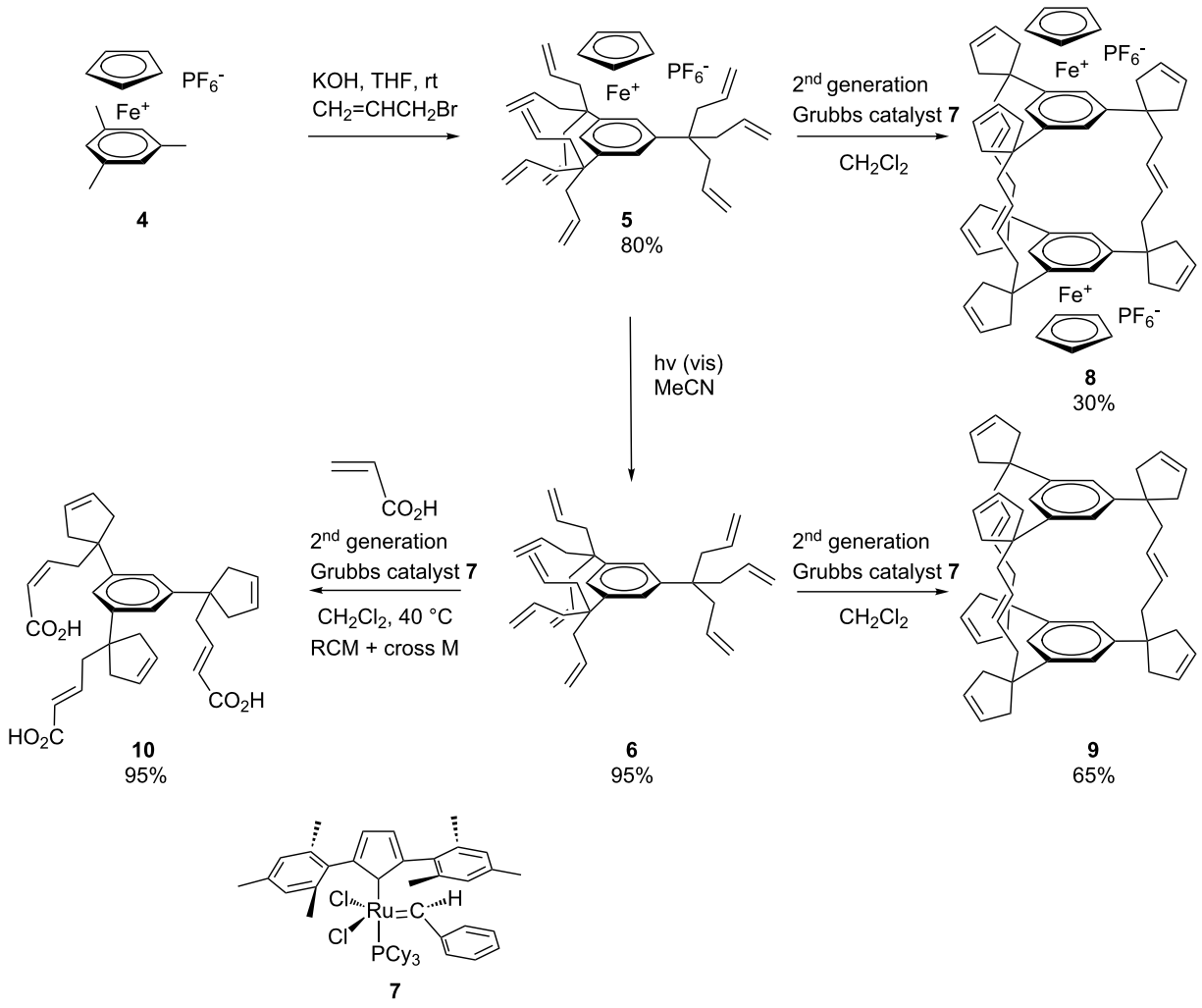

Scheme 3: Multiple carbon–carbon bond formation upon RCM and CM, and the complete switch of selectivity in the presence of acrylic acid.

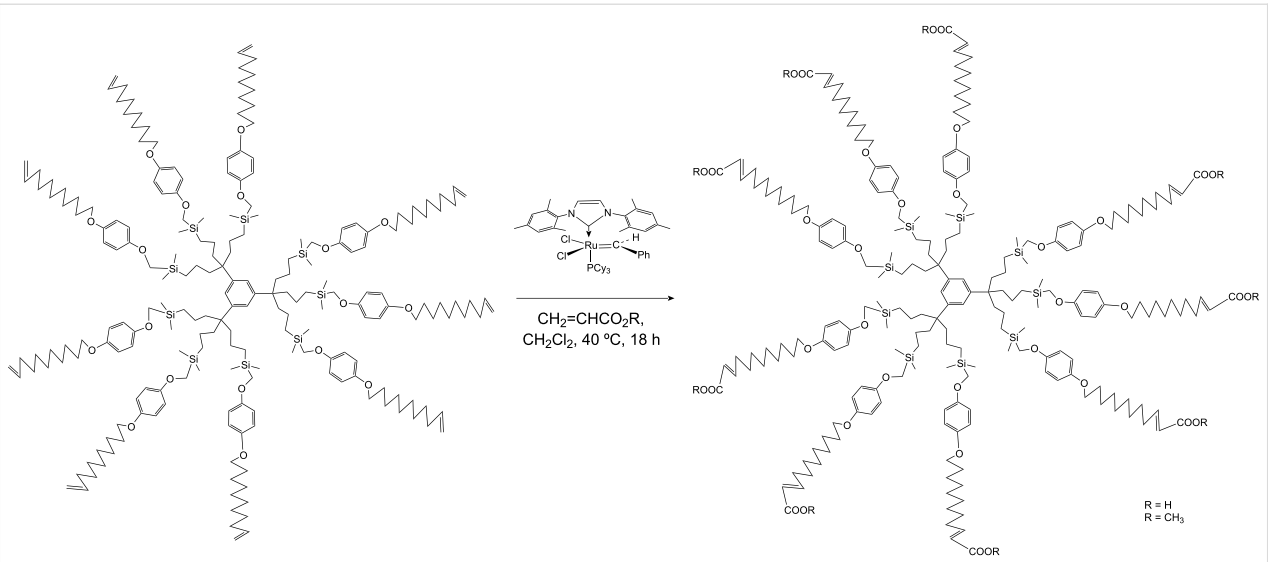

Scheme 4: Example of chemo-, regio- and stereoselective CM of polyolefin dendrimers catalyzed by the 2nd generation Grubbs metathesis catalyst to produce water-soluble dendrimers (R = H or CH_3).

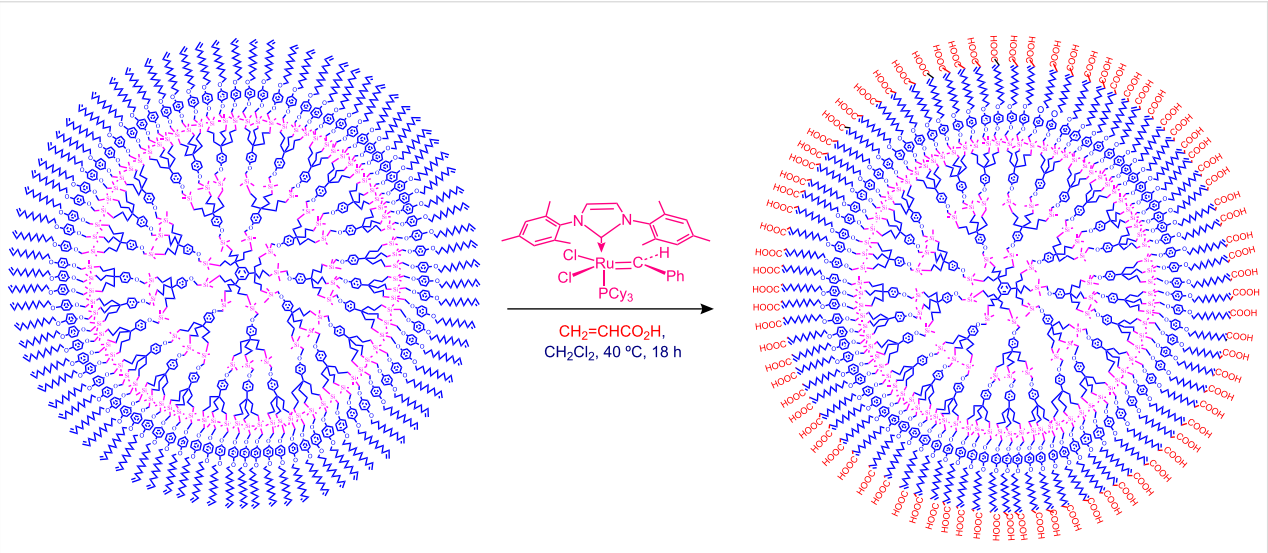

Scheme 5: Example of chemo-, regio- and stereoselective CM of polyolefin dendrimers catalyzed by the 2nd generation Grubbs metathesis catalyst: 81-tethered dendrimers.

available homoallyl ether dendrimers can be replaced by their allyl ether analogues. The strategy consisting of performing RCM of branches and then to remove the core has also been applied by the Peng group to produce nanoparticle-cored dendrimers [48-51].

Dendrimers have been synthesized by reaction sequences involving hydrosilylation of olefin-terminated dendrimer cores followed by Williamson reactions with the phenol triallyl dendron *p*-$HOC_6H_4C(CH_2CH{=}CH_2)_3$ and iterations [42,52,53]. This allowed the building of large dendrimers and the extension of their tethers with alkenyl termini. CM of these large olefin-terminated dendrimers with acrylic acid was carried out in order to synthesize dendrimers terminated by carboxy groups (Scheme 5). These CM reactions were also extended to acrylates that contained a dendronic group. This strategy allowed constructing dendrimers from one generation to the next. Thus, iteration allows synthesizing a dendrimer of second generation with 81 olefin termini from a dendritic core containing 9 allyl termini after two iterative metathesis-hydrosilylation reactions (Scheme 6). This principle has also been extended to polymers and gold nanoparticles [54].

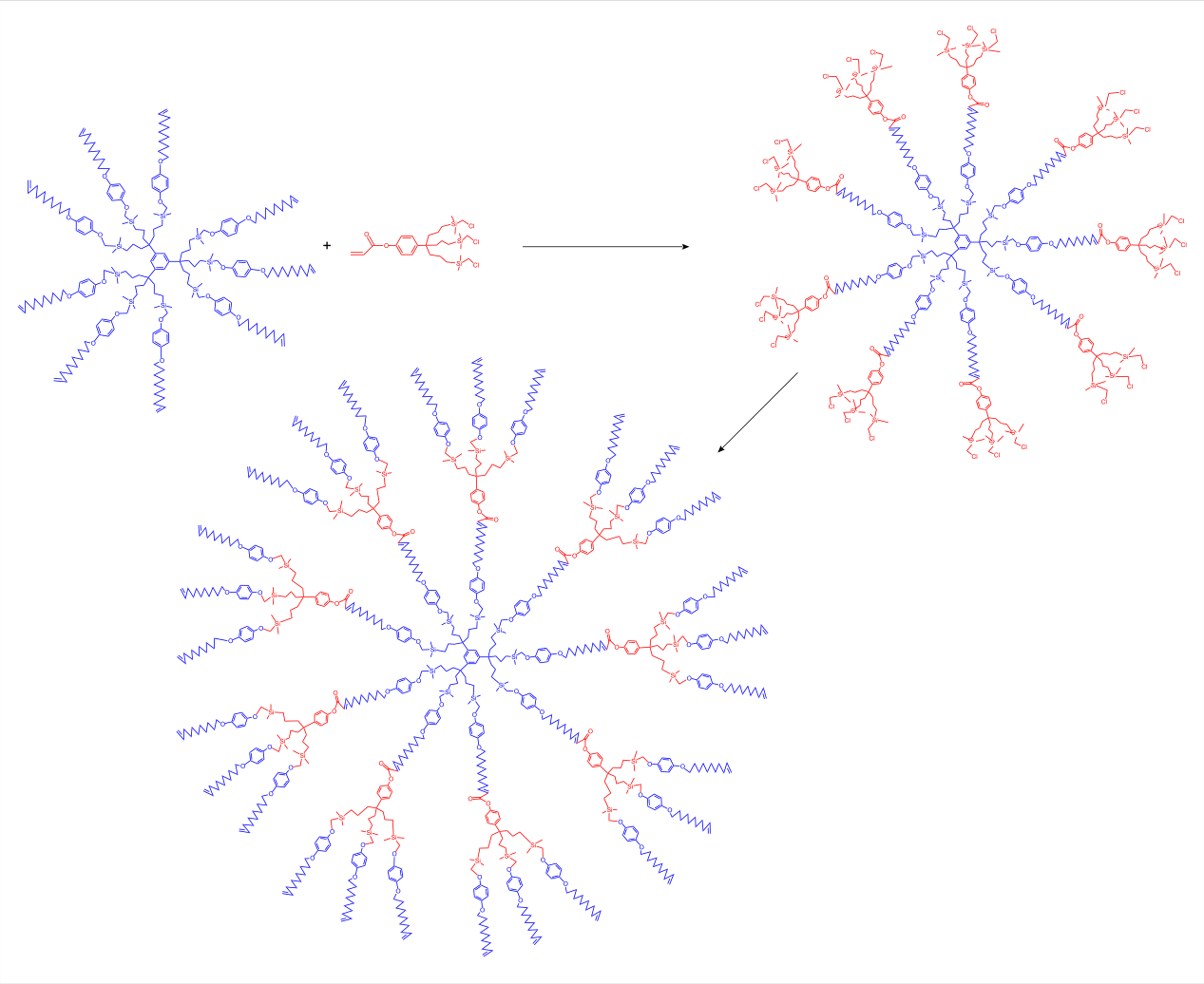

Scheme 6: Dendrimer construction scheme from a 9-olefinic dendrimer to a 27-olefinic dendrimer by regio-and stereoselective CM using Grubbs second generation catalyst in CH_2Cl_2 at 40 °C, followed by a Wiliamson reaction with *p*-HOC_6H_4-$O(CH_2)_8CH{=}CH_2$ in DMF at 80 °C. The next iteration of identical reaction sequence yields the 81-olefinic dendrimer.

Dendrimer-induced olefin metathesis in water

Olefin metathesis of hydrophobic substrates, which are the large majority, in water instead of organic solvents is an obvious challenge that has been actively pursued [54-57] with water-soluble ruthenium catalysts [54], surfactants [58] and sonochemistry [59-62]. Using a low amount (0.083 mol %) of dendrimer, we have induced efficient olefin metathesis catalysis in water and with down to 0.04 % of the second-generation Grubbs catalyst **7** for RCM, (Table 1) [63]. The dendrimer **11** contains triethylene glycol termini that solubilize it in water. In this way, the dendrimer serves as a molecular micelle [64,65] to solubilize the hydrophobic catalysts and substrate in the hydrophobic interior of the nanoreactor. Its "click" synthesis is shown in Scheme 7.

CM and EYM are also much favored by the presence of 0.083% mol of the dendrimer **11**, although these reactions still need 2% of Grubbs catalyst **7** [63], which is much more than the amount used for RCM.

RCM reactions can proceed in the presence of water even without surfactant, but the amount of 1st- or 2nd-generation Grubbs catalyst required then reaches 4 to 5% for good to high-yield reactions [66,67], which is of the order of 100 times more ruthenium catalyst than under our reaction conditions [63]. We have verified that these literature results [64,65] are reproducible with **7**.

Another key feature of the system is that the aqueous solution of the water-soluble dendrimer **11** can be recycled because **11** is insoluble in ether. Re-use of the aqueous solution of **11** is possible after subsequent filtration of the water-insoluble catalyst **7** after the reaction and removal of the organic reaction product by decantation or by extraction with ether. We have been

Table 1: Compared RCM and EYM catalyzed by **7** in water without co-solvent, in the presence and absence of dendrimer **11**.

	Substrate	Product	Mol % Cat. **7**[a]	Conv. (%) with 0% den. **11**	Conv. (%) with 0.083% den. **11**
A	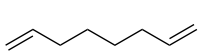		0.1	0	86[b]
B	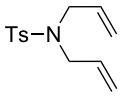	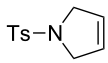	0.1 0.06 0.04	0 0 0	90[c] 66[c] 62[c]
C	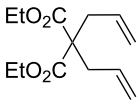	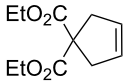	0.1	6[b]	89[b]
D	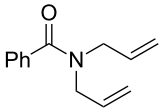	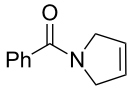	0.1	0	90[c]
E	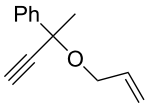	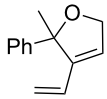	2	27[c]	97[c]
F	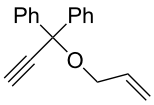	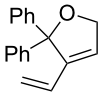	2	30[c]	99[c]

[a]The mol % catalyst **7** are pseudo-concentrations (rather than actual concentrations because **2** is insoluble in water; for instance, 4 mg of **7** dispersed in 47 mg of water, which corresponds to 0.1 mol % **7**). The dendrimer amount of 0.083 mol % corresponds to 28 mg. [b]The reaction mixture without the catalyst was analyzed by ^{1}H NMR in $CDCl_3$, following filtration of the Ru catalyst or resulting residual species and subsequent extraction with ether. [c]The reaction mixture without the catalyst was analyzed by GC (injection of the ether extract).

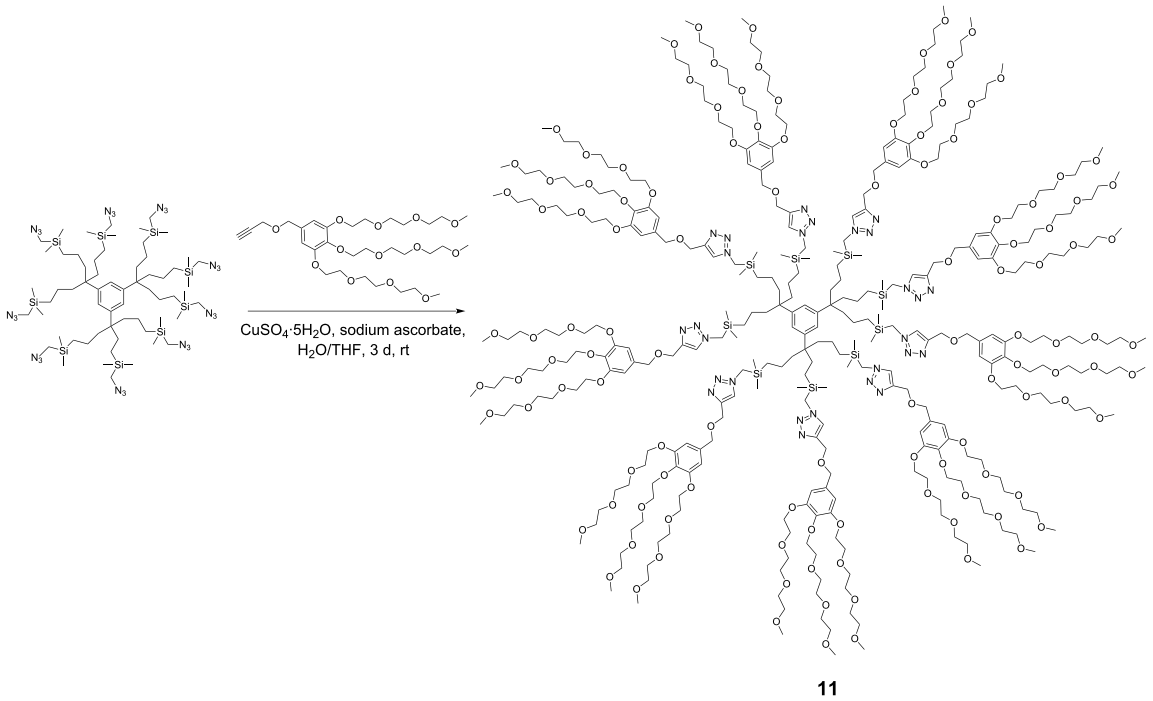

Scheme 7: Synthesis of the water-soluble dendritic nanoreactor **7** for olefin metathesis in water without co-solvent.

able to recycle this aqueous dendrimer solution at least ten times without any significant decrease in yield. We have tested the stability of the Grubbs-II catalyst **7** in the presence of water at ambient temperature for 24 h, and found that it is stable in the absence of an olefin substrate. For example, after stirring a suspension of **7 (**0.1 mol %) in water for one day at 25 °C in air, the substrate and the dendrimer **11** were added and, after an additional day, the results of the RCM reaction were not significantly changed (80% conversion) compared to the result indicated in Table 1, entry B (90% conversion) under the same conditions. This means that the pre-catalyst **7** itself is stable and that the relative instability of **7** during metathesis in the presence of water (but in the absence of dendrimer **11**) is due to the slow decomposition of the catalytically active species formed during the RCM catalytic cycle. In particular, it has been shown that the methylene species [Ru(=CH_2)Cl_2{1,3-bis(mesityl)-NHC}(PCy_3)], generated in the catalytic cycle of RCM reactions involving terminal olefins, is usually highly susceptible to dimerization and decomposition in CH_2Cl_2 or C_6H_6 [1]. Whatever the decomposition path of this species in the presence of water might be, it appears that the decomposition is considerably reduced when the dendrimer **11** is used for the RCM reactions. This strongly argues in favor of dendritic protection (probably by encapsulation) of the reactive species. RCM reactions need less catalyst **7** in organic solvents [1] than in the presence of water, especially in the absence of the dendrimer **11**. Thus the hydrophobic dendrimer interior should indeed favor the protection this intermediate ruthenium-methylene species from side reactions occurring in the presence of water.

Conclusion

Olefin metathesis reactions are powerful methods that can be used for the construction of dendrimers and their functionalization with water-solubilizing carboxylate groups and other termini. In turn, water-soluble dendrimers can be used as molecular micelles as exemplified here. The implication of dendrimers in olefin metathesis reactions has mainly been focused on recovering the catalyst by loading the dendrimer with a functionalized catalyst. This strategy has been of very little success, because the % of catalyst used in metathesis reactions was rather high. This is due to the reactivity of methylene-metal intermediates that leads to side reactions. Consequently, another strategy involves protecting the catalytic intermediate in nanoreactors. Dendrimers are shown here to be excellent reactors achieving the goal of decreasing the catalytic amount when water is used as solvent. The success of using water as a reaction medium, even without co-solvent, is important in avoiding polluting organic solvents. Moreover, a very low Ru catalyst loading is possible in RCM with the fully recyclable water solution of the dendritic nanoreactor.

Acknowledgements

Financial support from the Institut Universitaire de France (IUF), the Université Bordeaux I, the Centre National de la Recherche Scientifique (CNRS) and the Agence Nationale de la Recherche (ANR-07-CP2D-05-01) are gratefully acknowledged.

References

1. Grubbs, R. H., Ed. *Handbook of Metathesis;* Wiley-VCH: Weinheim, 2002; Vol. 1-3.
2. Chauvin, Y. *Angew. Chem., Int. Ed.* **2006,** *45,* 3740–3747. doi:10.1002/anie.200601234
3. Schrock, R. R. *Angew. Chem., Int. Ed.* **2006,** *45,* 3748–3759. doi:10.1002/anie.200600085
4. Grubbs, R. H. *Angew. Chem., Int. Ed.* **2006,** *45,* 3760–3765. doi:10.1002/anie.200600680
5. Fürstner, A. *Angew. Chem., Int. Ed.* **2000,** *39,* 3012–3043. doi:10.1002/1521-3773(20000901)39:17<3012::AID-ANIE3012>3.0.CO;2-G
6. Buchmeiser, M. R. *Chem. Rev.* **2000,** *100,* 1565–1604. doi:10.1021/cr990248a
7. Astruc, D. *New J. Chem.* **2005,** *29,* 42–56. doi:10.1039/b412198h
8. Trnka, T. M.; Grubbs, R. H. *Acc. Chem. Res.* **2001,** *34,* 18–29. doi:10.1021/ar000114f
9. Vougioukalakis, G. C.; Grubbs, R. H. *Chem. Rev.* **2010,** *110,* 1746–1787. doi:10.1021/cr9002424
10. Astruc, D. *Organometallic Chemistry and Catalysis;* Springer: Berlin, 2007; Chapters 9, 15 and 21.
11. Wijkens, P.; Jastrzebski, J. T. B. H.; van der Schaaf, P. A.; Kolly, R.; Hafner, A.; van Koten, G. *Org. Lett.* **2000,** *2,* 1621–1624. doi:10.1021/ol0059100
12. Garber, S. B.; Kingsbury, J. S.; Gray, B. L.; Hoveyda, A. H. *J. Am. Chem. Soc.* **2000,** *122,* 8168–8179. doi:10.1021/ja001179g
13. Beerens, H.; Verpoort, F.; Verdonck, L. *J. Mol. Catal. A: Chem.* **2000,** *151,* 279–282. doi:10.1016/S1381-1169(99)00362-3
14. Beerens, H.; Verpoort, F.; Verdonck, L. *J. Mol. Catal. A: Chem.* **2000,** *159,* 197–201. doi:10.1016/S1381-1169(00)00158-8
15. Sanford, M. S.; Ulman, M.; Grubbs, R. H. *J. Am. Chem. Soc.* **2001,** *123,* 749–750. doi:10.1021/ja003582t
16. Hansen, S. M.; Volland, M. A. O.; Rominger, F.; Eisenträger, F.; Hofmann, P. *Angew. Chem., Int. Ed.* **1999,** *38,* 1273–1276. doi:10.1002/(SICI)1521-3773(19990503)38:9<1273::AID-ANIE1273>3.0.CO;2-0
17. Hansen, S.; Rominger, F.; Metz, M.; Hofmann, P. *Chem.–Eur. J.* **1999,** *5,* 557–566. doi:10.1002/(SICI)1521-3765(19990201)5:2<557::AID-CHEM557>3.0.CO;2-A
18. Adlhart, C.; Volland, M. A. O.; Hofmann, P.; Chen, P. *Helv. Chim. Acta* **2000,** *83,* 3306–3311. doi:10.1002/1522-2675(20001220)83:12<3306::AID-HLCA3306>3.0.CO;2-7
19. Amoroso, D.; Fogg, D. E. *Macromolecules* **2000,** *33,* 2815–2818. doi:10.1021/ma9918856
20. Six, C.; Beck, K.; Wegner, A.; Leitner, W. *Organometallics* **2000,** *19,* 4639–4642. doi:10.1021/om000200j
21. Reetz, M. T.; Lohmer, G.; Schwickardi, R. *Angew. Chem., Int. Ed. Engl.* **1997,** *36,* 1526–1529. doi:10.1002/anie.199715261

22. Alonso, E.; Astruc, D. *J. Am. Chem. Soc.* **2000,** *122,* 3222–3223. doi:10.1021/ja994332j
23. Kingsbury, J.; Harrity, J. P. A.; Bonitatebus, P. J.; Hoveyda, A. H. *J. Am. Chem. Soc.* **1999,** *121,* 791–799. doi:10.1021/ja983222u
24. Gatard, S.; Nlate, S.; Cloutet, E.; Bravic, G.; Blais, J.-C.; Astruc, D. *Angew. Chem., Int. Ed.* **2003,** *42,* 452–456. doi:10.1002/anie.200390137
25. Gatard, S.; Kahlal, S.; Méry, D.; Nlate, S.; Cloutet, E.; Saillard, J.-Y.; Astruc, D. *Organometallics* **2004,** *23,* 1313–1324. doi:10.1021/om030608r
26. Méry, D.; Astruc, D. *J. Mol. Catal. A: Chem.* **2005,** *227,* 1–5. doi:10.1016/j.molcata.2004.08.050
27. Lemo, J.; Heuzé, K.; Astruc, D. *Org. Lett.* **2005,** *7,* 2253–2256. doi:10.1021/ol050645+
28. Astruc, D.; Heuzé, K.; Gatard, S.; Méry, D.; Nlate, S.; Plault, L. *Adv. Synth. Catal.* **2005,** *347,* 329–338. doi:10.1002/adsc.200404247
29. Heuze, K.; Méry, D.; Gauss, D.; Astruc, D. *Chem. Commun.* **2003,** 2274–2275. doi:10.1039/b307116m
30. Heuzé, K.; Méry, D.; Gauss, D.; Blais, J.-C.; Astruc, D. *Chem.–Eur. J.* **2004,** *10,* 3936–3944. doi:10.1002/chem.200400150
31. Lemo, J.; Heuzé, K.; Astruc, D. *Chem. Commun.* **2007,** 4351–4353. doi:10.1039/b710289e
32. Trujillo, H. A.; Casado, C. M.; Astruc, D. *J. Chem. Soc., Chem. Commun.* **1995,** 7–8. doi:10.1039/C39950000007
33. Trujillo, H. A.; Casado, C. M.; Ruiz, J.; Astruc, D. *J. Am. Chem. Soc.* **1999,** *121,* 5674–5686. doi:10.1021/ja984101x
34. Moulines, F.; Astruc, D. *Angew. Chem., Int. Ed. Engl.* **1988,** *27,* 1347–1349. doi:10.1002/anie.198813471
35. Moulines, F.; Djakovitch, L.; Boese, R.; Gloaguen, B.; Thiel, W.; Fillaut, J.-L.; Delville, M.-H.; Astruc, D. *Angew. Chem., Int. Ed. Engl.* **1993,** *32,* 1075–1077. doi:10.1002/anie.199310751
36. Catheline, D.; Astruc, D. *J. Organomet. Chem.* **1983,** *248,* C9–C12. doi:10.1016/0022-328X(83)85030-X
37. Catheline, D.; Astruc, D. *J. Organomet. Chem.* **1984,** *272,* 417–426. doi:10.1016/0022-328X(84)80485-4
38. Lacoste, M.; Rabaa, H.; Astruc, D.; Le Beuze, A.; Saillard, J.-Y.; Précigoux, G.; Courseille, C.; Ardoin, N.; Bowyer, W. *Organometallics* **1989,** *8,* 2233–2242. doi:10.1021/om00111a021
39. Martinez, V.; Blais, J.-C.; Astruc, D. *Org. Lett.* **2002,** *4,* 651–653. doi:10.1021/ol0172875
40. Martinez, V.; Blais, J.-C. *Angew. Chem., Int. Ed.* **2003,** *42,* 4366–4369. doi:10.1002/anie.200351795
41. Martinez, V.; Blais, J.-C.; Bravic, G.; Astruc, D. *Organometallics* **2004,** *23,* 861–874. doi:10.1021/om030623w
42. Astruc, D.; Ruiz, J. *Tetrahedron* **2010,** *66,* 1769–1785. doi:10.1016/j.tet.2009.11.116
43. Ornelas, C.; Méry, D.; Ruiz Aranzaes, J.; Blais, J.-C.; Cloutet, E.; Astruc, D. *Angew. Chem., Int. Ed.* **2005,** *44,* 7399–7404. doi:10.1002/anie.200502848
44. Ornelas, C.; Méry, D.; Cloutet, E.; Ruiz Aranzaes, J.; Astruc, D. *J. Am. Chem. Soc.* **2008,** *130,* 1495–1506. doi:10.1021/ja077392v
45. Beil, J. B.; Lemcoff, N. G.; Zimmerman, S. C. *J. Am. Chem. Soc.* **2004,** *126,* 13576–13577. doi:10.1021/ja045885j
46. Lemcoff, N. G.; Spurlin, T. A.; Gewirth, A. A.; Zimmerman, S. C.; Beil, J. B.; Elmer, S. L.; Vandeveer, H. G. *J. Am. Chem. Soc.* **2004,** *126,* 11420–11421. doi:10.1021/ja047055b
47. Wendland, M. S.; Zimmerman, S. C. *J. Am. Chem. Soc.* **1999,** *121,* 1389–1390. doi:10.1021/ja983097m
48. Aldama, J.; Wang, Y.; Peng, X. *J. Am. Chem. Soc.* **2001,** *123,* 8844–8850. doi:10.1021/ja016424q
49. Wang, Y. A.; Li, J. J.; Chen, H.; Peng, X. *J. Am. Chem. Soc.* **2002,** *124,* 2293–2298. doi:10.1021/ja016711u
50. Guo, W.; Li, J. J.; Wang, Y. A.; Peng, X. *J. Am. Chem. Soc.* **2003,** *125,* 3901–3909. doi:10.1021/ja028469c
51. Guo, W.; Peng, X. In *Dendrimers and Nanosciences, C. R. Chimie;* Astruc, D., Ed.; Elsevier: Paris, 2003; 8–10, p. 989.
52. Sartor, V.; Djakovitch, L.; Fillaut, J.-L.; Moulines, F.; Neveu, F.; Marvaud, V.; Guittard, J.; Blais, J.-C.; Astruc, D. *J. Am. Chem. Soc.* **1999,** *121,* 2929–2930. doi:10.1021/ja983868m
53. Ruiz, J.; Lafuente, G.; Marcen, S.; Ornelas, C.; Lazare, S.; Blais, J.-C.; Cloutet, E.; Astruc, D. *J. Am. Chem. Soc.* **2003,** *125,* 7250–7257. doi:10.1021/ja021147o
54. Burtscher, D.; Grela, K. *Angew. Chem., Int. Ed.* **2009,** *48,* 442–454. doi:10.1002/anie.200801451
    Review on olefin metathesis in water and aqueous solvents.
55. Connon, S. J.; Rivard, M.; Zaja, M.; Blechert, S. *Adv. Synth. Catal.* **2003,** *345,* 572–575. doi:10.1002/adsc.200202201
56. Michrowska, A.; Gulajski, L.; Kaczmarska, Z.; Mennecke, K.; Kirschning, A.; Grela, K. *Green Chem.* **2006,** *8,* 685–688. doi:10.1039/b605138c
57. Binder, J. B.; Blank, J. J.; Raines, R. T. *Org. Lett.* **2007,** *9,* 4885–4888. doi:10.1021/ol7022505
58. Gulajski, L.; Sledz, P.; Grela, K. *Green Chem.* **2008,** *10,* 271–274. doi:10.1039/b719493e
    For utrasonification-facilitated metathesis in water.
59. Mingotaud, A. F.; Krämer, M.; Mingotaud, C. *J. Mol. Cat. A: Chem.* **2007,** *263,* 39–47. doi:10.1016/j.molcata.2006.08.015
    For Surfactant-facilitated metathesis in water (see also [60-62]).
60. Lipschulz, B. H.; Aguinaldo, G. T.; Ghorai, S.; Voigtritter, K. *Org. Lett.* **2008,** *10,* 1325–1328. doi:10.1021/ol800028x
61. Lipschutz, B. H.; Ghorai, S.; Aguinaldo, G. T. *Adv. Synth. Catal.* **2008,** *350,* 953–956. doi:10.1002/adsc.200800114
62. Brendgen, T.; Fahlbusch, T.; Frank, M.; Schühle, D. T.; Sessler, M.; Schatz, J. *Adv. Synth. Catal.* **2009,** *351,* 303–307. doi:10.1002/adsc.200800637
63. Diallo, A. K.; Boisselier, E.; Liang, L.; Ruiz, J.; Astruc, D. *Chem.–Eur. J.* **2010,** *16,* 11832–11835. doi:10.1002/chem.201002014
64. Newkome, G. R.; Yao, Z.; Baker, G. R.; Gupta, V. K. *J. Org. Chem.* **1985,** *50,* 2003–2004. doi:10.1021/jo00211a052
65. Newkome, G. R.; Moorefield, C. N.; Baker, G. R.; Johnson, A. L.; Behera, R. K. *Angew. Chem., Int. Ed. Engl.* **1991,** *30,* 1176–1178. doi:10.1002/anie.199111761
66. Davis, K. J.; Sinou, D. *J. Mol. Catal. A: Chem.* **2002,** *177,* 173–178. doi:10.1016/S1381-1169(01)00239-4
67. Polshettiwar, V.; Varma, R. S. *J. Org. Chem.* **2008,** *73,* 7417–7419. doi:10.1021/jo801330c

Beilstein Journal of Organic Chemistry

Synthesis of Ru alkylidene complexes

Renat Kadyrov*[1] and Anna Rosiak[1,2]

Full Research Paper

Open Access

Address:
[1]Evonik Degussa GmbH, Rodenbacher Chaussee 4, 63457 Hanau-Wolfgang, Germany and [2]present address: ASM Research Chemicals, Feodor-Lynen-Str. 31, 30625 Hannover, Germany

Email:
Renat Kadyrov* - renat.kadyrov@evonik.com

* Corresponding author

Keywords:
alkylidene complexes; metathesis; rotation barrier; ruthenium

Beilstein J. Org. Chem. **2011,** *7,* 104–110.
doi:10.3762/bjoc.7.14

Received: 31 August 2010
Accepted: 16 November 2010
Published: 21 January 2011

Guest Editor: K. Grela

Abstract

The present work describes the robust synthesis of Ru alkylidene complexes $(PCy_3)_2Cl_2Ru{=}CHR$ – precursors for metathesis catalysts. Moreover, the dynamic behavior of complexes where R = 2-naphthyl and 2-thienyl was studied. ^{1}H NMR techniques were employed to establish the preferred conformations in solution for both complexes and the energy barrier for rotation around single (Ru=)CH–C(thienyl) bond was estimated ($\Delta G^{\neq}_{303K}$ = 12.6 kcal/mol).

Introduction

The key to active ruthenium metathesis initiators is the accessibility of the ruthenium precursor containing the alkylidene moiety. The most commonly used precursors for the "second generation" catalysts bearing NHC ligands are the alkylidene ruthenium complexes coordinated with two phosphines [1]. For recent reviews see [2-4]. There are several routes for accessing five-coordinated ruthenium(II) alkylidene complexes such as diazo-transfer [5] and the reaction of vinyl or propargyl halides with hydrido(dihydrogen)-Ru-complexes generated from $[Ru(COD)Cl_2]$ and PCy_3 under hydrogen pressure [6]. It should also be noted that the method for the generation of such highly reactive hydrido(dihydrogen)-Ru-complexes was first described by Werner and co-workers who employed two equivalents of iPr$_3$P in 2-butanol and hydrogen [7]. This last attractive one-pot procedure without the use of hydrogen was improved by the Ciba-group [8,9]. Werner and co-workers also published a one-pot synthesis of the complex $(PCy_3)_2Cl_2Ru{=}CHMe$ (**1a**) by direct reduction of $RuCl_3$ with $Mg/ClCH_2CH_2Cl$ in THF in the presence of excess PCy_3 and hydrogen followed by subsequent reaction with acetylene [10].

We report herein on an improved protocol for the synthesis of the ethylidene complex $(PCy_3)_2Cl_2Ru{=}CHMe$ (**1a**) under mild conditions which is an efficient precursor for the preparation of wide variety of other alkylidene complexes.

Results and Discussion

Van der Schaaf and co-workers published in 2000 a simple one-pot procedure for the synthesis of the ruthenium benzylidene complex $(i\text{Pr}_3\text{P})_2Cl_2Ru{=}CHPh$ [8]. It was mentioned that also $(PCy_3)_2Cl_2Ru{=}CHPh$ could be similarly prepared. To our surprise, by following exactly the given protocol using DBU as

base, a mixture of the desired benzylidene complex $(PCy_3)_2Cl_2Ru{=}CHPh$ together with the vinylidene complex $(PCy_3)_2Cl_2Ru{=}C{=}CHPh$ was obtained. Obviously, the last complex originated from reaction of an intermediate hydride species with phenyl acetylene along with formation of the benzylmethylidene complex $(PCy_3)_2Cl_2Ru{=}CHCH_2Ph$ as described previously by Werner [7]. We have found that the use of trimethylsilylacetylene afforded the ethylidene complex **1a** as the sole product in very good isolated yield (see Scheme 1).

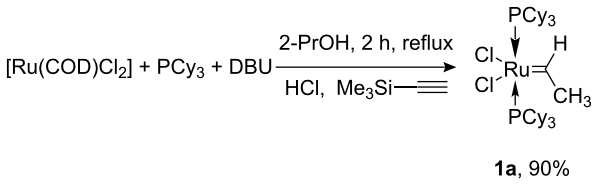

Scheme 1: Synthesis of complex **1a**.

In sharp contrast, the use of 1-phenyl-2-trimethylsilylacetylene or 1-trimethylsilyl-1-hexyne gave the vinylidene complexes **2** and **3** in only moderate isolated yields (see Scheme 2).

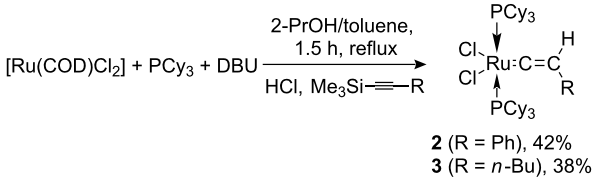

Scheme 2: Synthesis of complexes **2** and **3**.

Compound **1a** is remarkably stable below room temperature and readily exchanges the ethylidene moiety with other alkenes. Thus, compound **1a** is an ideal precursor for a variety of other ruthenium alkylidene complexes. Compounds **1b**–**i** (Scheme 3) were readily isolated and characterized spectroscopically. It is noteworthy, that with the exception of **1e** and **1g**, all isolated complexes decompose slowly in chlorinated organic solvents. Therefore, cross metatheses in toluene in general led to alkylidene complexes with higher isolated yields.

The NMR spectra of compounds **1b,c,e**–**i** displayed more or less broad signals at ambient temperature. In particular, lowering the temperature of solutions of **1e** and **1g** in CD_2Cl_2 caused further broadening of the NMR resonances which only become properly resolved for the aromatic and methylidene signals at −80 °C. The slow exchange resonances of compound **1g** are better resolved due to the lower concentration of the minor isomer. A $^1H,^1H$-COSY experiment at −80 °C enabled the identification of the aromatic resonances in the low temperature spectrum (Figure 1). The singlet at 8.49 ppm is assigned to H1 and the doublet at 9.01 ppm to H3 on the basis of the observed weak coupling ^4J(H1H3). The strong coupling of ^3J(H3H4) = 8.2 Hz with doublet at 9.01 ppm allows the assignment of H4 (7.78 ppm). Other coupling patterns are consistent with the resonances of the residual protons H5 (8.12, d, J = 8.2 Hz), H6 (7.50, t, J = 7.0 Hz) and H7/H8 (7.67-7.75, m).

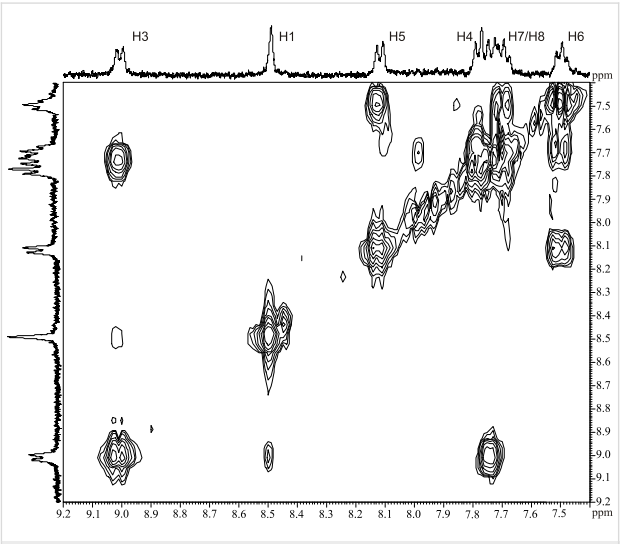

Figure 1: Naphthyl-group region of $^1H,^1H$-COSY NMR for **1g** in CD_2Cl_2 at −80 °C.

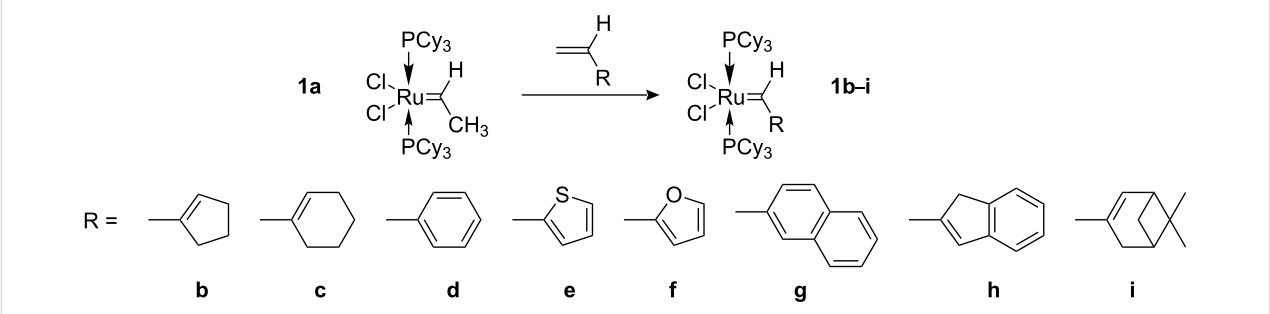

Scheme 3: Synthesis of complexes **1b**–**i**.

Strong NOE enhancement of H1 upon saturation of the carbene proton at 19.75 ppm (see Figure 2) is consistent with preferred conformer **1g** in which the naphthyl moiety is directed away from the phosphine ligand (see Scheme 4).

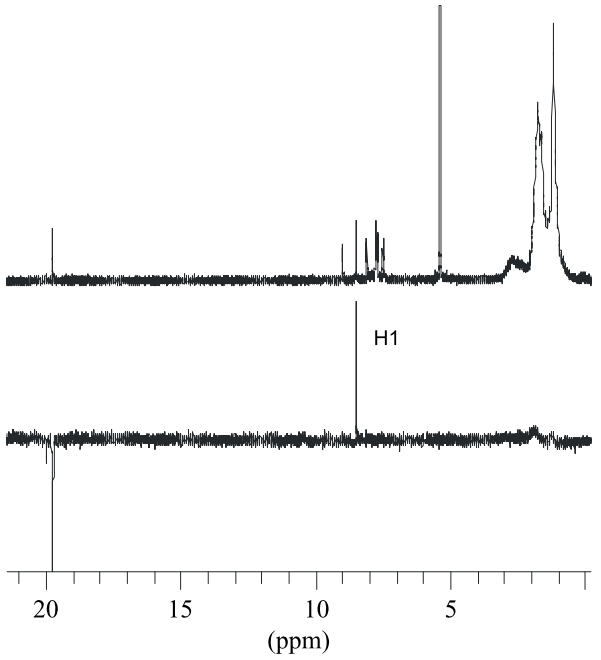

Figure 2: ^{1}H NMR (top) and NOE difference spectrum (bottom) of **1g** in CD_2Cl_2 at −80 °C, saturating the methylidene H signal at δ = 19.75 ppm.

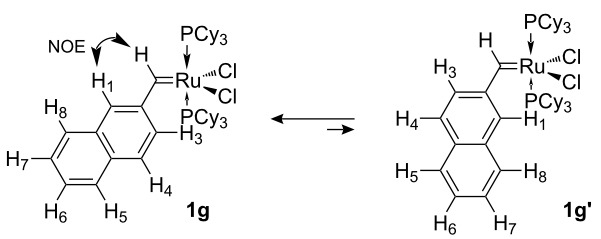

Scheme 4: Conformational isomerism in complex **1g**.

At low temperature both isomers of **1e** are visible in the NMR spectrum due to comparable concentrations (obtained enthalpy difference ΔH = 1.3 kcal/mol, see Supporting Information File 1). A number of NOE experiments at −40 °C allowed the assignment of the resonances of both isomers **1e** and **1e'**. Saturation of the carbene proton at 18.9 ppm led to strong NOE enhancement of the singlet at 7.68 ppm (Figure 3) and allowed the assignment of this signal to the H3 proton of the thienyl moiety and was consistent with the *s-trans* isomer **1e** being the preferred conformer (see Scheme 5). The EXSY effect made it possible to assign the signal at 8.80 ppm to H3' of the minor *s-cis* conformer. Enhancement of the signal at 6.99 ppm (Figure 4) by saturation of the signal at 8.07 ppm and EXSY inversion of the resonance at 7.79 ppm allowed the assignment of the signals for H5 (8.07 ppm), H4 (6.99 ppm), H5' (7.79 ppm) and H4' (7.03 ppm).

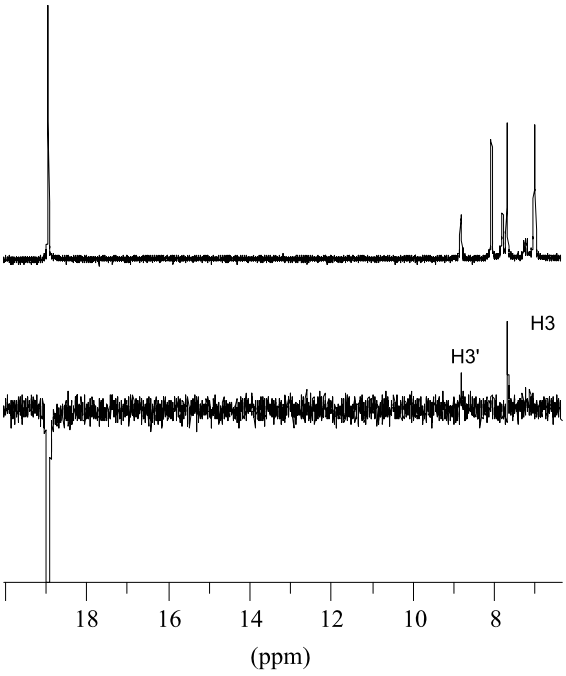

Figure 3: Olefin and alkylidene-proton region of the ^{1}H NMR (top) and NOE difference spectrum (bottom) of **1e** in CD_2Cl_2 at −40 °C, saturating the methylidene H signal at δ = 18.9 ppm.

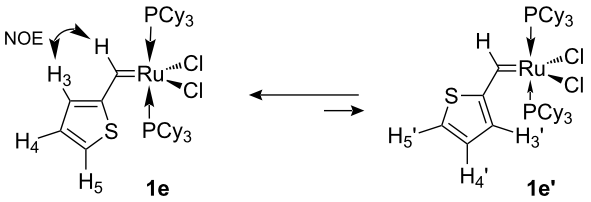

Scheme 5: Conformational isomerism in complex **1e**.

The thiophene region of the ^{1}H NMR spectrum of **1e** was simulated and iteratively fitted to the experimental spectra in order to evaluate the rate constants at various temperatures (Supporting Information File 1). Linear regression analysis of these data gave activation enthalpy $\Delta H^{\neq}$= 13.7 kcal/mol. From the rate constant at 303 K the value of free energy of activation ($\Delta G^{\neq}_{303K}$ = 12.6 kcal/mol) was also calculated. This is substantially higher than several calculated (E_a = 4.4 kcal/mol) [11,12] and experimentally estimated (E_a = 5.7 kcal/mol) [13] internal rotation barriers of styrene, 2-vinylthiophene (E_a =

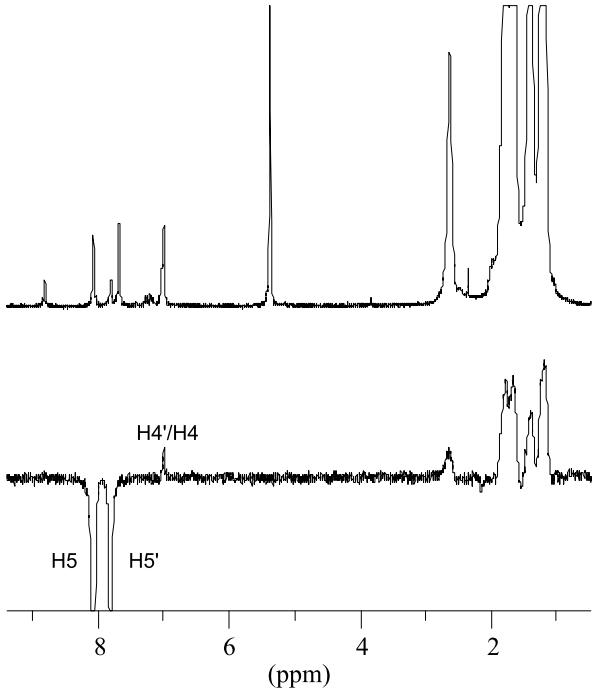

Figure 4: Olefin and alkyl group region of the ^{1}H NMR (top) and NOE difference spectrum (bottom) of **1e** in CD_2Cl_2 at −40 °C, saturating the thienyl-H5 signal at δ = 8.07 ppm.

4.8 kcal/mol) [14] and is comparable with rotation barrier of the aryl ring in chromium carbene complexes ($\Delta G^{\neq}_{298K}$ = 13.0–16.2 kcal/mol) [15].

Experimental

Routine, 2D-correlation spectra (^{1}H,^{1}H-COSY) and SELNOE experiments were recorded on a Bruker Avance-400 (BPFO-Plus with Z gradient) spectrometers. ^{1}H NMR chemical shifts are reported in ppm relative to TMS at 0 ppm. IR spectra were recorded on a Tensor 27 FT-IR Spectrometer (Bruker) with MKII Golden Gate Single Reflection Diamond ATR System. For ESI-MS spectra, a Q-TOF Premier (Waters) was used. All solvents used were anhydrous grade purchased from Aldrich. Commercially available compounds were used without further purification. 2-Vinylthiophene [16], 2-vinylfuran [17], 1-vinylcyclohexene [18], 1-vinylcyclopentene [18] and nopadiene [19] were prepared according to known procedures.

2-Vinylindene was prepared by a slightly modified literature procedure [18]**:** A solution of 2-indanone (5 g, 38 mmol) in dry THF (10 mL) was added over 10 min to a cooled (ice bath) and stirred solution of vinylmagnesium chloride (1.6 M in THF, 36 mL, 57 mmol). The mixture was stirred at 60 °C for a further 30 min and then cooled, quenched with saturated NH_4Cl solution, and finally extracted thoroughly with ether. The combined organic extracts were washed with brine, dried, and concentrated at reduced pressure. The residue was dissolved in pyridine (30 mL). $POCl_3$ (4.5 mL, 45 mmol) was slowly added to this solution at 4 °C under an argon atmosphere. The resulting mixture was stirred for further 10 h in an ice bath and then slowly allowed to warm to ambient temperature overnight. The resulting dark brown mixture was poured into ice water and the product extracted with ether. The extracts were washed successively with 2N HCl and then brine. After drying and filtration through a short pad of silica gel, the crude product was purified by distillation to yield 2-vinylindene (2.59 g, 18.2 mmol, 48%) as a colorless liquid, bp 93–94 °C/200 mbar. ^{1}H NMR ($CDCl_3$): δ = 7.38 (d, *J* = 7.1 Hz, 1H), 7.30 (d, *J* = 7.4 Hz, 1H), 7.21 (dd, *J* = 8.0 Hz, *J* = 7.5 Hz, 1H), 7.21 (dt, *J* = 1.1 Hz, *J* = 7.4 Hz, 1H), 6.74 (dd, *J* = 17.5 Hz, *J* = 10.6 Hz, 1H), 6.71 (s, 1H), 5.41 (d, *J* = 17.4 Hz, 1H), 7.30 (d, *J* = 10.6 Hz, 1H), 3.52 (s, 2H) ppm.

Dichlorobis(tricyclohexylphosphine)(ethylidene)ruthenium(II) (1a): 1,8-Diazabicyclo[5.4.0]undec-7-ene (3.3 mL, 22 mmol) and tricyclohexylphosphine (6.17 g, 22 mmol) were added under an argon atmosphere to a suspension of dichloro(1,5-cyclooctadiene)ruthenium(II) (2.8 g, 10 mmol) in isopropanol (100 mL). The resulting mixture was heated at reflux for 2 h. THF (150 mL) was added to the resulting brick-red suspension which was allowed to cool to 15 °C prior to the addition of 2M HCl in ether (12 mL). After stirring for 5 min, trimethylsilylacetylene (4.2 mL, 30 mmol) was added and the resulting purple colored mixture stirred in an ice bath for 3 h. THF was then evaporated at 4 °C in order to complete the precipitation. The solid product was filtered by suction, washed thoroughly with chilled methanol and vacuum dried at 0–5 °C to give 6.85 g (90%) of purple crystals. ^{31}P NMR ($CDCl_3$): δ = 35.8 ppm; ^{1}H NMR ($CDCl_3$): δ = 19.30 (q, *J* = 5.6 Hz, 1H), 2.60 (d, *J* = 5.5 Hz, 3H), 2.60–2.52 (m, 6H), 1.88–1.22 (m, 60H) ppm.

General procedure A for the synthesis of alkylidene complexes: (PCy_3)Cl_2Ru=CHMe (**1a**) (1 mmol) was added to a stirred and cooled (ice bath) solution containing a four-fold excess of the respective olefin in degassed CH_2Cl_2 (25 mL). Argon was bubbled through the resulting dark violet solution for 2 h at 4 °C and then for a further 30 min at room temperature. The reaction mixture was again chilled in ice bath. Degassed methanol (20 mL) was added and the CH_2Cl_2 removed in vacuo at 0–5 °C. To complete the precipitation another portion of degassed chilled methanol (10 mL) was added and the precipitated product was filtered by suction. The resulting solid was washed thoroughly with chilled methanol, sucked as dry as possible, washed with hexane and dried under vacuum.

General procedure B for the synthesis of alkylidene complexes: $(PCy_3)Cl_2Ru{=}CHMe$ (**1a**) (1 mmol) was added to a stirred and cooled (ice bath) solution containing a four-fold excess of the respective olefin in degassed toluene (25 mL). Argon was bubbled through the resulting dark violet solution for 2 h at 4 °C and then for a further 30 min at room temperature. Toluene was removed in vacuum at 20 °C and the residue triturated with chilled methanol (20 mL). The precipitated product was filtered by suction, washed thoroughly with chilled methanol and dried under vacuum.

Dichlorobis(tricyclohexylphosphine)(cyclopenten-1-ylmethylidene)ruthenium(II) (**1b**): The product (violet solid) was prepared according to general procedure B in 80% yield. ^{31}P NMR ($CDCl_3$): δ = 37.26 ppm; ^{1}H NMR ($CDCl_3$): δ = 19.30 (s, 1H), 6.97 (s, 1H), 3.14 (m, 2H), 2.60 (m, 6H), 1.95–1.11 (m, 64H) ppm. ^{13}C NMR: δ = 285.83, 164.61, 139.83, 36.97, 34.80; 31.95 (t, *J* = 9.1), 29.63, 27.91 (t, *J* = 5.0), 26.64, 25.15.

Dichlorobis(tricyclohexylphosphine)(cyclohexen-1-ylmethylidene)ruthenium(II) (**1c**): The product as a toluene adduct (intensive violet solid) was prepared according to general procedure B in 46% yield. ^{31}P NMR (C_6D_6): δ = 36.53 ppm; ^{1}H NMR (C_6D_6): δ =19.08 (s, 1H), 7.21 (s, 1H), 2.87 (m, 2H), 2.60 (m, 6H), 1.95–1.11 (m, 66H) ppm. ^{13}C NMR: δ = 296.40 (d, *J* = 113.4), 157.46, 140.27, 32.08 (t, *J* = 9.1); 30.28, 29.99, 29.70; 27.93 (t, *J* = 5.0), 27.93, 26.67, 22.97, 21.45. Toluene 137.82, 129.05, 128.24, 125.31, 21.41.

Dichlorobis(tricyclohexylphosphine)(benzylidene)ruthenium(II) (**1d**): The product (violet solid) was prepared according to general procedure A in 81% yield. The NMR spectra were in agreement with the spectra reported in the literature [5].

Dichlorobis(tricyclohexylphosphine)(thien-2-yl-methylidene)ruthenium(II) (**1e**): The product (dark violet solid) was prepared according to general procedure A in 71% yield. ^{31}P NMR ($CDCl_3$): δ = 35.96 ppm; ^{1}H NMR (CD_2Cl_2): δ = 19.05 (s, 1H), 8.09 (s, br., 1H), 7.84 (d, *J* = 4.1 Hz, 1H), 6.90 (t, *J* = 4.3 Hz, 1H), 2.55 (m, 6H), 1.75–1.60 (m, 30H), 1.39–1.35 (m, 12H), 1.20–1.12 (m, 18H) ppm. ^{13}C NMR ($CDCl_3$): δ = 269.11, 163.84 (br.), 133.09 (br.), 129.22, 32.26 (t, *J* 0 9.1), 29.68, 27.85 (t, *J* = 5.0), 26.55. IR (ATR): λ^{-1} = 2919 (vs), 2848 (s), 2169 (w), 2051 (w), 1936 (w), 1901 (w), 1443 (m), 1403 (m), 1353 (m), 1263 (m), 1005 (m), 734 (vs) cm^{-1}. MS(ESI): m/z (%) = 828 (21) [M^+], 793 (9), 281 (100).

Dichlorobis(tricyclohexylphosphine)(fur-2-ylmethylidene)-ruthenium(II) (**1f**): The product (dark violet solid) was prepared according to general procedure A in 56% yield. ^{31}P NMR ($CDCl_3$): δ = 37.04 ppm; ^{1}H NMR ($CDCl_3$): δ = 18.79 (s, 1H), 8.12 (s, br., 1H), 7.74 (s, br., 1H), 6.43 (dd, *J* = 3.6 Hz, *J* = 1.7, 1H), 2.64 (m, 6H), 1.81–1.67 (m, 30H), 1.48–1.41 (m, 12H), 1.27–1.14 (m, 18H) ppm. ^{13}C NMR: δ = 259.90 (d, *J* = 105.1), 172.34 (br.), 141.71 (br.), 121.54 (br.), 115,44, 32,11 (t, *J* = 9.0), 29.62, 27.85 (t, *J* = 5.1), 26.56.

Dichlorobis(tricyclohexylphosphine)(naphth-2-ylmethylidene)ruthenium(II) (**1g**): The product (dark violet solid) was prepared according to general procedure A in 56% yield. ^{31}P NMR ($CDCl_3$): δ = 37.43 ppm; ^{1}H NMR ($CDCl_3$): δ = 20.12 (s, 1H), 8.82 (s, br., 1H), 8.77 (d, *J* = 8.5 Hz, 1H), 8.06 (d, *J* = 8.1 Hz, 1H), 7.74 (d, *J* = 8.1 Hz, 1H), 7.71 (d, *J* = 8.4 Hz, 1H), 7.67–7.63 (m, 1H), 7.46–7.42 (m, 1H), 2.63 (m, 6H), 1.90–1.60 (m, 30H), 1.46–1.37 (m, 12H), 1.30–1.10 (m, 18H) ppm. ^{13}C NMR: δ = 292.71, 150.48, 133.98, 133.11, 130.56, 129.77, 129.04, 128.35, 128.05, 127.23, 126.86, 32.19 (t, *J* = 9.1), 29.70, 27.85 (t, *J* = 5.1), 26.54. IR (ATR): λ^{-1} = 2922 (vs), 2848 (s), 2358 (w), 2003 (w), 1443 (m), 1265 (m), 1004 (m), 733 (vs) cm^{-1}. MS (ESI): m/z (%) = 872 (2) [M^+], 333 (100).

Dichlorobis(tricyclohexylphosphine)(inden-2-ylmethylidene)ruthenium(II) (**1h**): The product (brick-red solid) was prepared according to general procedure A in 37% yield. ^{31}P NMR ($CDCl_3$): δ = 36.93 ppm; ^{1}H NMR ($CDCl_3$): δ = 19.64 (s, 1H), 7.94 (s, br., 1H), 7.73 (d, *J* = 7.7 Hz, 1H), 7.45 (m, 3H), 4.23 (s, 2H), 2.63 (m, 6H), 1.81 (d, *J* = 12.0 Hz, 18H), 1.70 (dd, *J* = 23.7, *J* = 11.9, 12H), 1.47 (dd, *J* = 23.7 Hz, *J* = 11.9 Hz, 12H), 1.28–1.17 (m, 18H) ppm.

Dichlorobis(tricyclohexylphosphine)(norpinanylmethylidene)ruthenium(II) (**1i**): The product (violet solid) was prepared according to general procedure B in 43 % yield. ^{31}P NMR ($CDCl_3$): δ = 36.54 ppm; ^{1}H NMR ($CDCl_3$): δ = 19.12 (s, 1H), 7.65 (s, 1H), 3.02 (m, 1H), 2.48 (m, 6H), 2.30 (m, 1H), 2.09–1.12 (m, 67H), 0.70 (s, 3H) ppm. ^{13}C NMR: δ = 291.46, 163.88, 134.87, 49.14, 39.66, 38.84, 34.77, 31.98 (t, *J* = 9.0), 31.84, 29.72 (d, *J* = 11.0), 27.93 (t, *J* = 4.7), 26.60, 26.45, 20.77 ppm.

Dichlorobis(tricyclohexylphosphine)(2-phenylvinylylidene)-ruthenium(II) (**2**): 1,8-Diazabicyclo[5.4.0]undec-7-ene (0.75 mL, 5.2 mmol) and a 20% solution of tricyclohexylphosphine in toluene (7.7 mL, 5.9 mmol) were added under an argon atmosphere to a suspension of dichloro(1,5-cyclooctadiene)ruthenium(II) (660 mg, 2.35 mmol) in isopropanol (20 mL). The mixture was heated at reflux under an argon atmosphere for 1 h. Toluene (24 mL) was added to the resulting brick-red suspension and the mixture heated for further 30 min at reflux and then allowed to cool to 5–10 °C. 1-Phenyl-2-trimethylsilylacetylene

(1.4 ml, 7 mmol) was added followed 10 min later by HCl in ether (2M, 2.4 mL, 4.8 mmol). The resulting purple colored mixture was stirred at ambient temperature for 2h and then concentrated. The residue was treated with 40 mL of chilled methanol and the precipitated product was filtered by suction. The solid was washed thoroughly with chilled methanol and dried under vacuum at 0–5 °C to yield 826 mg (42%) of a violet solid. ^{31}P NMR ($CDCl_3$): δ = 22.54 ppm; ^{1}H NMR ($CDCl_3$): δ = 7.13 (t, *J* = 7.6 Hz, 2H), 6.89 (d, *J* = 7.5 Hz, 2H), 6.84 (t, *J* = 7.2 Hz, 1H), 4.35 (t, *J* = 3.3 Hz, 1H), 2.62 (m, 6H), 2.06 (d, *J* = 12.3 Hz, 12H), 1.66–1.73 (m, 18H), 1.59 (dd, *J* = 23.6 Hz, *J* = 11.9 Hz, 12H), 1.16–1.26 (m, 18H) ppm. These data are in agreement with the literature [20].

Dichlorobis(tricyclohexylphosphine)(2-butylvinylidene)ruthenium(II) (**3**): 1,8-Diazabicyclo[5.4.0]undec-7-ene (0.75 mL, 52 mmol) and 20% solution of tricyclohexylphosphine in toluene (7.7 mL, 5.9 mmol) were added under an argon atmosphere to a suspension of dichloro(1,5-cyclooctadiene)ruthenium(II) (660 mg, 2.35 mmol) in isopropanol (20 mL). The mixture was then heated at reflux under an argon atmosphere for 1 h. Toluene (24 mL) was added to the resulting brick-red suspension and the mixture heated for further 30 min at reflux and then allowed to cool to 5–10 °C. 1-Trimethylsilyl-1-hexyne (1.4 mL, 7 mmol) was added followed 10 min later by HCl in ether (2M, 2.4 mL, 4.8 mmol) and the resulting purple colored mixture stirred at ambient temperature for 2 h and then concentrated. The residue was treated with 40 mL of chilled methanol and the precipitated product was filtered by suction. The solid was washed thoroughly with chilled methanol and dried under vacuum to give 720 mg (38%) of a red-brown solid. ^{31}P NMR ($CDCl_3$): δ = 25.34 ppm; ^{1}H NMR ($CDCl_3$): δ = 3.41 (tt, *J* = 7.3 Hz, *J* = 1.7 Hz, 1H), 2.59 (m, 6H), 2.36 (dd, *J* = 14.0 Hz, *J* = 7.1 Hz, 2H), 2.06 (d, *J* = 12.1 Hz, 12H), 1.72–1.81 (m, 20H), 1.59 (dd, *J* = 22.7 Hz, *J* = 11.5 Hz, 12H), 1.16–1.26 (m, 22H), 0.87 (t, *J* = 6.8 Hz, 3H) ppm.

Supporting Information

Features variable-temperature and simulated ^{1}H NMR spectra of various compounds, Arrhenius plot of the equilibrium constants for **1e** and Eyring plot of the rate constants for **1e** interconversion.

Supporting Information File 1

Detailed experimental data.
[http://www.beilstein-journals.org/bjoc/content/supplementary/1860-5397-7-14-S1.pdf]

References

1. Weskamp, T.; Schattenmann, W. C.; Spiegler, M.; Herrmann, W. A. *Angew. Chem.* **1998,** *110,* 2631–2633. doi:10.1002/(SICI)1521-3757(19980918)110:18<2631::AID-ANGE2631>3.0.CO;2-J
Angew. Chem. Int. Ed. **1998,** *37,* 2490–2493.
2. Diesendruck, C. E.; Tzur, E.; Lemcoff, N. G. *Eur. J. Inorg. Chem.* **2009,** 4185–4203. doi:10.1002/ejic.200900526
3. Samojłowicz, C.; Bieniek, M.; Grela, K. *Chem. Rev.* **2009,** *109,* 3708–3742. doi:10.1021/cr800524f
4. Vougioukalakis, G. C.; Grubbs, R. H. *Chem. Rev.* **2010,** *110,* 1746–1787. doi:10.1021/cr9002424
5. Schwab, P.; Grubbs, R. H.; Ziller, J. W. *J. Am. Chem. Soc.* **1996,** *118,* 100–110. doi:10.1021/ja952676d
6. Wilhelm, T. E.; Belderrain, T. R.; Brown, S. N.; Grubbs, R. H. *Organometallics* **1997,** *16,* 3867–3869. doi:10.1021/om9705259
7. Grünwald, C.; Gevert, O.; Wolf, J.; González-Herrero, P.; Werner, H. *Organometallics* **1996,** *15,* 1960–1962. doi:10.1021/om9509554
8. van der Schaaf, P. A.; Kolly, R.; Hafner, A. *Chem. Commun.* **2000,** 1045–1046. doi:10.1039/b002298p
9. van der Schaaf, P. A.; Kolly, R.; Kirner, H.-J.; Rime, F.; Mühlebach, A.; Hafner, A. *J. Organomet. Chem.* **2000,** *606,* 65–74. doi:10.1016/S0022-328X(00)00289-8
10. Wolf, J.; Stüer, W.; Grünwald, C.; Werner, H.; Schwab, P.; Schulz, M. *Angew. Chem., Int. Ed.* **1998,** *37,* 1124–1126. doi:10.1002/(SICI)1521-3773(19980504)37:8<1124::AID-ANIE1124>3.0.CO;2-C
Angew. Chem. **1998,** *110,* 1165–1167.
11. Sebbar, N.; Bockhorn, H.; Bozzelli, J. W. *J. Phys. Chem. A* **2005,** *109,* 2233–2253. doi:10.1021/jp046285+
12. Head-Gordon, M.; Pople, J. A. *J. Phys. Chem.* **1993,** *97,* 1147–1151. doi:10.1021/j100108a008
13. Grajcar, L.; Baudet, J. *J. Mol. Struct.* **1977,** *38,* 121–134. doi:10.1016/0022-2860(77)87084-1
14. Parr, W. J. E.; Wasylishen, R. E.; Schaefer, T. *Can. J. Chem.* **1976,** *54,* 3216–3223. doi:10.1139/v76-459
15. Tobrman, T.; Meca, L.; Dvořáková, H.; Černý, J.; Dvořák, D. *Organometallics* **2006,** *25,* 5540–5548. doi:10.1021/om0605837
16. Emerson, W. S.; Patrick, T. M., Jr. *Org. Synth.* **1963,** Coll. Vol. 4, 980–983.
17. Schmidt, U.; Werner, J. *Synthesis* **1986,** *1986,* 986–992. doi:10.1055/s-1986-31846
18. Herz, W.; Juo, R.-R. *J. Org. Chem.* **1985,** *50,* 618–627. doi:10.1021/jo00205a013
19. Paquette, L. A.; Gugelchuk, M.; McLaughlin, M. L. *J. Org. Chem.* **1987,** *52,* 4732–4740. doi:10.1021/jo00230a015
20. Katayama, H.; Ozawa, F. *Organometallics* **1998,** *17,* 5190–5196. doi:10.1021/om980582h

Beilstein Journal of Organic Chemistry

Ene–yne cross-metathesis with ruthenium carbene catalysts

Cédric Fischmeister and Christian Bruneau*§

Review

Open Access

Address:
UMR 6226-CNRS-Université de Rennes 1, Sciences Chimiques de Rennes, Catalyse et Organométalliques, Campus de Beaulieu, 263 avenue du général Leclerc, 35042 Rennes cedex, France

Email:
Christian Bruneau* - christian.bruneau@univ-rennes1.fr

* Corresponding author
§ Fax: + 33(0)23236939; Tel: + 33(0)23236283

Keywords:
catalysis; cross-metathesis; enyne; fatty acid esters; ruthenium

Beilstein J. Org. Chem. **2011,** *7,* 156–166.
doi:10.3762/bjoc.7.22

Received: 27 August 2010
Accepted: 30 December 2010
Published: 04 February 2011

Guest Editor: K. Grela

Abstract

Conjugated 1,3-dienes are important building blocks in organic and polymer chemistry. Enyne metathesis is a powerful catalytic reaction to access such structural domains. Recent advances and developments in ene–yne cross-metathesis (EYCM) leading to various compounds of interest and their intermediates, that can directly be transformed in tandem procedures, are reviewed in this article. In addition, the use of bio-resourced olefinic substrates is presented.

Introduction

The interaction of alkyne triple bonds with metal carbenes or metal vinylidene species was already known before the discovery of the very efficient molybdenum and ruthenium metathesis catalysts. In 1980, the polymerization of alkynes initiated by tungsten carbene was demonstrated by Katz [1,2] who proposed metallacyclobutenes as key intermediates in this polymerization. At the same period of time, Geoffroy [3] demonstrated that alkyne polymerization could be initiated directly from terminal alkynes without previous preparation of a metal carbene but via the formation of a reactive vinylidene tungsten species. Later on, the efficiency of ruthenium vinylidene precursors was also shown in olefin metathesis [4-10]. It is noteworthy that polymerization of terminal alkynes [11-13] and cyclotrimerization of triynes [14-20] with ruthenium carbene precursors is still a topic of current interest. Then, Fischer tungsten carbene complexes were used by Katz [21], and later Mori [22,23] utilized chromium alkoxycarbene to develop the first cyclizations via catalytic intramolecular enyne metathesis transformation. These initial works gave reason to postulate the interaction of metal carbene with alkyne to form a metallacyclobutene that rearranges to give a metal vinylcarbene (Scheme 1). This is the mechanistic basis of intramolecular enyne metathesis and EYCM reactions.

In this review, we will focus on recent developments in EYCM transformations with ruthenium carbene catalysts [24-32]. This will include some general features on EYCM. Examples involve ethylene, terminal olefins, cyclic olefins, diene metathesis with alkynes and finally applications in unsaturated fatty acid ester transformations.

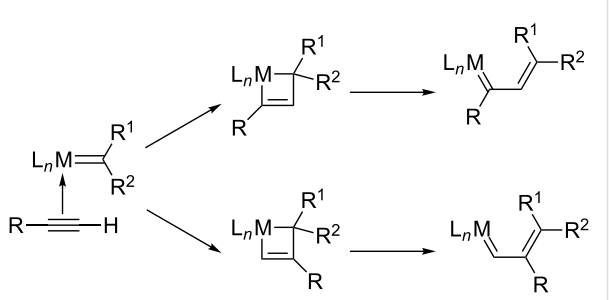

Scheme 1: Interaction of triple bonds with a metal carbene.

Review

General considerations on EYCM

The EYCM is an attractive bimolecular transformation as it is an atom economical reaction which results in formal cleavage of a double bond and introduction of the two generated alkylidene fragments to the triple bond with formation of a conjugated 1,3-diene. However, this metathesis reaction is associated with some difficulties due to possible formation of several regio- and stereoisomers, as well as possible olefin self-metathesis (SM) and even secondary EYCM (Scheme 2). Though, at the moment the latter problems do not seriously appear to the best of our knowledge since the EYCM involving internal olefins has not been reported yet, except in the case of cyclic olefins.

To date, most of the EYCM were performed using the first and second generation Grubbs (**I**, **II**) and Hoveyda (**III**, **IV**) catalysts (Figure 1).

Concerning the catalytic cycles, several pathways have been proposed. Mechanistic studies based on kinetic measurements assisted or not with calculations have been carried out for both the intra- and intermolecular ene–yne metathesis versions [33-38]. For EYCM the two pathways involve either an alkyne interaction with a methylidene metal species (Scheme 3) or an alkylidene metal intermediate (Scheme 4). In both cases, the ancillary ligands tricyclohexylphosphine or *N*-heterocyclic carbene have a crucial influence on the reaction, and the approach of the alkyne to the ruthenium center has to be controlled to obtain high regioselectivity. This corresponds to the exo/endo approaches reported in intramolecular ene–yne metathesis, which lead to cyclic products with different ring sizes.

EYCM with ruthenium catalysts was initiated in 1997 when Mori [39] and Blechert [40] reported the first examples with ethylene and higher olefins, respectively.

EYCM with ethylene

The EYCM with ethylene is one of the simplest methods to generate conjugated dienes with two terminal methylene groups from alkynes (Scheme 5). In this special case there is no problem of regioselectivity and no risk of polluting the olefin formation as the self-metathesis of ethylene is non-productive. For these reasons, the reaction is highly selective.

The EYCM was initially performed with catalyst **I** under an atmosphere of ethylene at room temperature [39,41,42]. When the substrates were not reactive under these mild conditions,

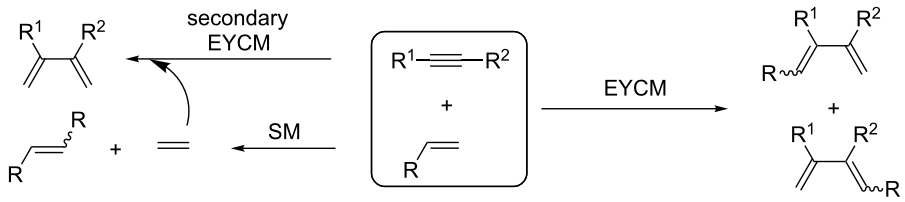

Scheme 2: General scheme for EYCM and side reactions.

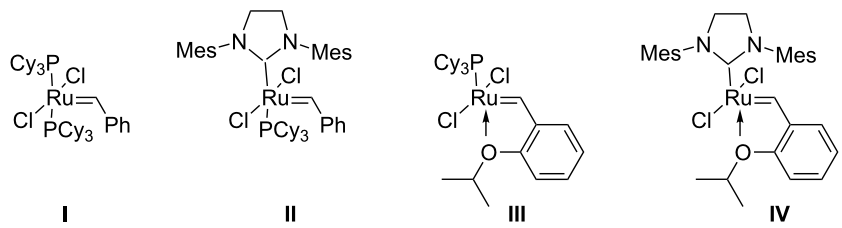

Figure 1: Selected ruthenium catalysts able to perform EYCM.

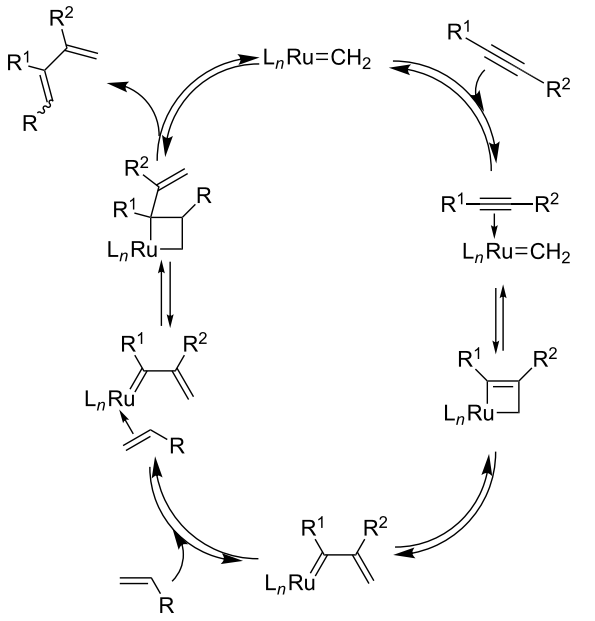

Scheme 3: Catalytic cycle with initial interaction of a metal methylidene with the triple bond.

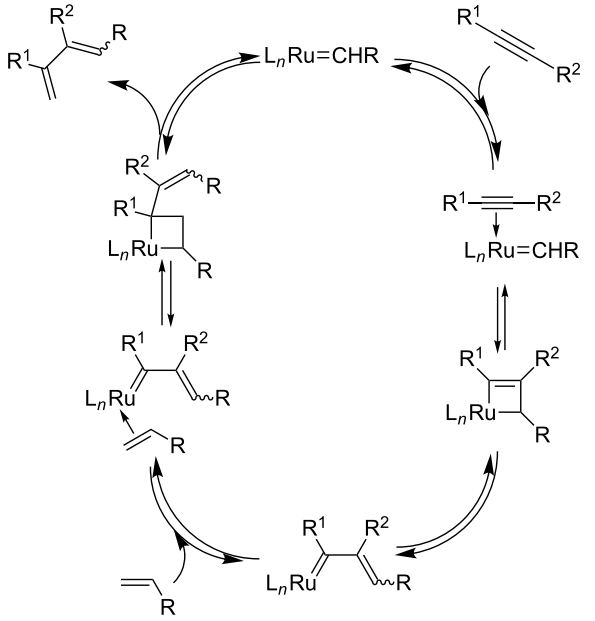

Scheme 4: Catalytic cycle with initial interaction of a metal alkylidene with the triple bond.

cross-metathesis efficiency was improved by using higher ethylene pressure [43] or changing the ruthenium precursor to the second generation Grubbs catalyst **II** and adjusting temperature and ethylene pressure [44-47]. Most of these studies were performed with model substrates, especially propargylic derivatives such as ethers, esters, thioethers, and included both terminal and internal alkynes. When catalyst **I** was used, a beneficial effect of a heteroatom in propargylic position (especially from an ester or carbonate) in terms of reactivity has been shown, whereas a reverse effect was obtained, when the heteroatom was located in homopropargylic position [41,48]. In the presence of second generation catalysts, unprotected functional groups such as hydroxyl [44] or fluoride [49] were tolerated in propargylic position. EYCM with ethylene has been used in several types of applications in organic synthesis, either

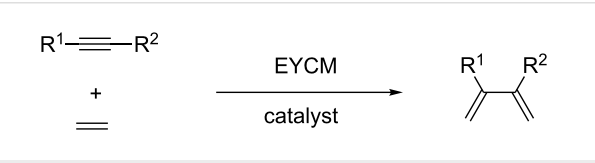

Scheme 5: Formation of 2,3-disubstituted dienes via cross-metathesis of alkynes with ethylene.

to prepare compounds with the final 1,3-diene motive in their structure, or to use them as the first step of a sequential synthesis. The first case is illustrated by the synthesis of Anolignans [48] and another closely related example is shown in the preparation of Amphidinolide E [50,51] where the diene system is extended by further cross-metathesis with 2-methylpenta-1,4-diene (Figure 2).

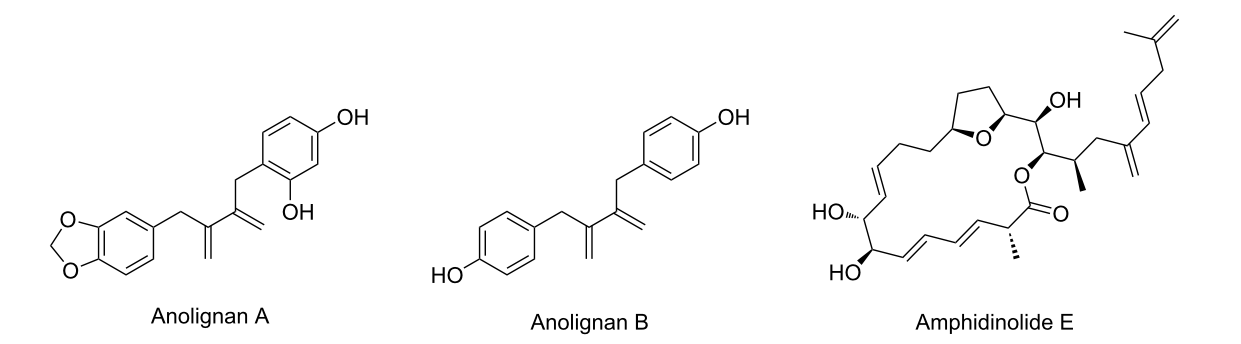

Figure 2: Applications of EYCM with ethylene in natural product synthesis.

The Diels–Alder reaction is one of the most popular transformations of 1,3-dienes. This procedure has been successfully used to prepare *C*-aryl glycoside from *C*-alkynyl glycoside and ethylene according to an EYCM/Diels–Alder/oxidation sequence (Scheme 6) [52,53].

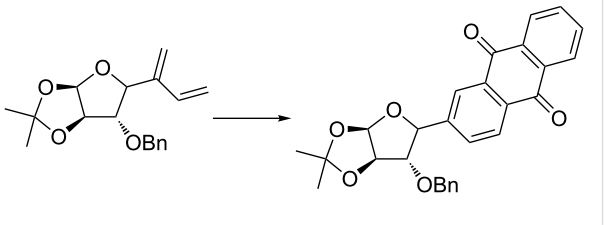

Scheme 6: Application of EYCM in sugar chemistry.

The selective cyclopropanation of the most electron deficient double bond of the unsymmetrical dienic system has been performed to reach 24,25-ethanovitamine D3 lactones (Scheme 7) [54].

Recently, conjugated dienes resulting from EYCM of terminal and symmetrical propargylic carbonates with ethylene have been prepared in the presence of Grubbs second generation catalyst **II**. They have been used in sequential catalytic transformations in the presence of ruthenium catalysts, which are able to perform regioselective allylic substitution by O-, N- and C-nucleophiles (Scheme 8a) [55] and elimination to provide a new access to dendralenes (Scheme 8b) [56].

Higher olefin–alkyne cross-metathesis

This cross-metathesis reaction was introduced in 1997 with the first generation Grubbs catalyst **II** [40] and the initial results indicated that propargylic alcohol derivatives and terminal olefins with oxygen-containing functional groups were well tolerated [57]. As emphasized in the introduction, self-metathesis of the terminal olefin in the presence of a metathesis catalyst competes with EYCM. Essentially for this reason, an excess of olefin with respect to the alkyne (usually from 2 to 9 equiv) was always used to favor complete conversion of the latter. Following the first results and to avoid the competing metathetic reactions, it was shown by Blechert that EYCM reactions could be performed starting from either the olefin or the alkyne substrate bound to a support [58-60]. An improvement of the EYCM was achieved with the second generation Grubbs catalyst **II** starting from terminal alkynes, especially sterically hindered ones. More interestingly, internal alkynes, which were non-reactive with the first generation catalyst, could participate in cross-metathesis with terminal allylic olefins with the second generation Grubbs catalyst [61]. Alkynes substituted by a silylated group have received special attention in EYCM with terminal alkenes in the presence of Grubbs second generation catalyst. It was found that depending on the nature of the alkyne (terminal or internal), the regioselectivity of the cross-coupling

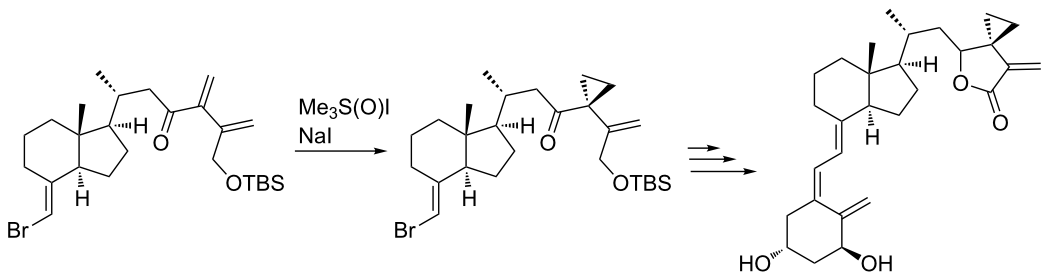

Scheme 7: EYCM as determining step to form vinylcyclopropane derivatives.

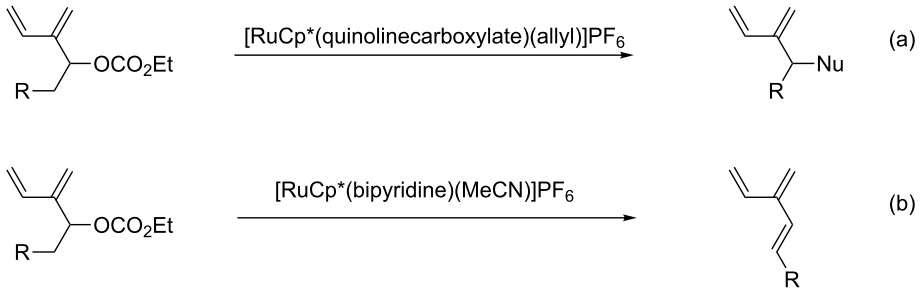

Scheme 8: Sequential EYCM with ethylene/nucleophilic substitution or elimination.

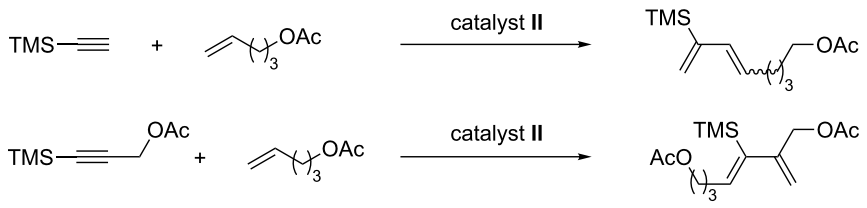

Scheme 9: Various regioselectivities in EYCM of silylated alkynes.

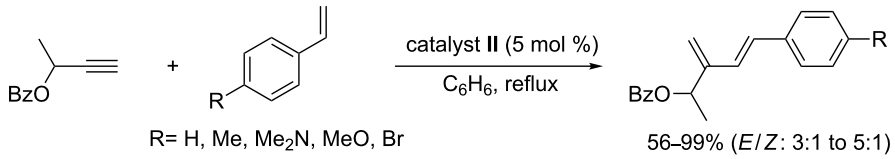

Scheme 10: High regio- and stereoselectivities obtained for EYCM with styrenes.

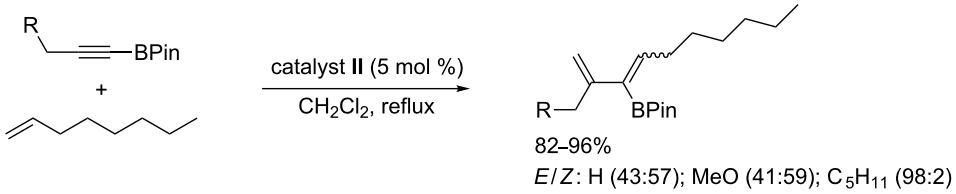

Scheme 11: EYCM of terminal olefins with internal borylated alkynes.

changed. Terminal alkynes gave 1,3-dienes with a 1,3-relationship between the alkenyl substituent and the silyl group, whereas a 1,2-relationship was observed starting from internal alkynes (Scheme 9) [62,63]. In addition, the stereoselectivity was low in the first case (3:1) and a single regio- and stereoisomer was obtained from internal alkynes. The regioselectivity was proposed to originate from the steric and stereoelectronic biasing effect of the silyl group during the propagation at the metal alkylidene species. Minimization of steric interactions might be effective during the cycloreversion of the ruthenacyclobutene which is the reason for the observed stereoselectivity. It is noteworthy that internal conjugated diynes protected by a silyl group are also reactive with high regioselectivity [64].

Cross-metathesis of *p*-substituted styrenes with a propargylic benzoate catalyzed by catalyst **II** in refluxing benzene has been performed in almost quantitative yields with perfect regioselectivity leading to 1,3-disubstituted 1,3-dienes and high stereoselectivity in favor of the (*E*)-isomers [65]. The kinetic study of this catalytic system suggests that the formation of an arylidene ruthenium species takes place first; thus, initial interaction of the olefin with the catalyst is preferred (Scheme 10).

Regioselective cross-metathesis was also observed when internal borylated alkynes and terminal alkenes were used as substrates in the presence of catalyst **II** in refluxing CH_2Cl_2. The stereoselectivity was found to be very dependent on the substituent both on the alkyne and the alkene (Scheme 11) [66].

2,2-Disubstituted terminal olefins have scarcely been involved in EYCM. The recent utilization of methylenecyclobutane revealed that second generation catalysts were able to perform the cross-metathesis with a variety of terminal alkynes. The formation of 1,1,3-trisubstituted 1,3-dienes was regioselective and the products were obtained in excellent yields at low temperature (Scheme 12) [67].

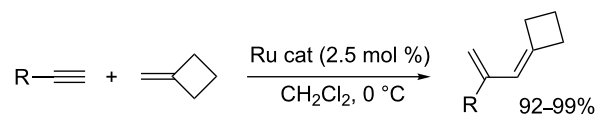

Scheme 12: Synthesis of propenylidene cyclobutane via EYCM.

The cross-metathesis of terminal enol ethers with terminal and internal alkynes in the presence of catalyst **II** has led to the

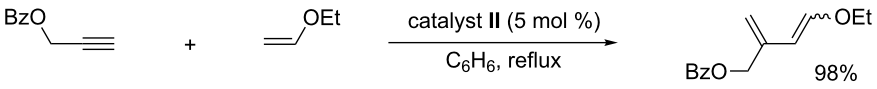

Scheme 13: Efficient EYCM with vinyl ethers.

regioselective formation of electron rich dienes, precursors of choice for Diels–Alder reactions (Scheme 13) [68]. This is surprising as enol ethers are known to be moderately reactive in olefin metathesis [69] and ethyl vinyl ether is often used to stop ring opening metathesis polymerizations. Vinyl acetate is also a good partner for EYCM under similar conditions.

In the presence of 10 mol % of Grubbs **II** catalyst and 2 equiv of $CuSO_4$, the cross-metathesis of terminal alkynes with ethyl vinyl ether led to the expected dienyl ether at 80 °C under microwave heating in toluene, whereas in H_2O/*t*-BuOH conjugated enals were formed [70].

As already mentioned with dienes resulting from EYCM with ethylene, Diels–Alder reactions have been attempted starting from the more substituted dienes arising from metathesis of alkynes with higher olefins. It must be noted that the regioselectivity of these EYCM always leads to 1,3-dienes with a terminal and a substituted methylene group. It has been shown that the disubstituted double bond possessing a (*Z*)-configuration does not participate in Diels–Alder reactions [61]. Using the EYCM/Diels–Alder sequence, tetrahydropyridines [57], substituted phenylalanines [71,72], modified porphyrins [73], carbocycle-linked oligosaccharides [74] and heterocycles [75,76] were prepared. One-pot EYCM followed by Brønsted acid catalyzed cyclization enabled the formation of monounsaturated cyclic amines [77]. The EYCM of homopropargylic tosylate with allylic alcohol derivatives has been used as a key step for the construction of the side chain of mycothiazole [78].

Cyclic olefin–alkyne cross-metathesis

As already mentioned, EYCM involving internal linear olefins has not been reported. On the other hand, the cross-metathesis of terminal alkynes with the internal carbon–carbon double bond of cyclopentene has been performed in the presence of catalyst **II** under mild conditions to stereoselectively form expanded 7-membered cycloheptadiene products [79]. To avoid ring opening metathesis polymerization of the cyclic olefin, a special procedure involving high dilution and slow syringe pump addition of the olefin had to be used (Scheme 14). The success of this metathesis reaction demonstrated that ruthenium alkylidene was the active catalytic species (methylidene free conditions).

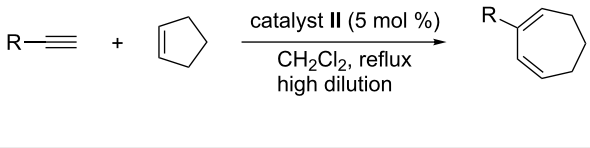

Scheme 14: From cyclopentene to cyclohepta-1,3-dienes via cyclic olefin-alkyne cross-metathesis.

This ring expansion could be extended to fused cycloalkene substrates such as tetrahydroindene and bicyclo[3.2.0]heptenone, both of them featuring a cyclopentene unit to form functionalized cycloheptadienes (Scheme 15) [80].

Starting from 1,5-cyclooctadiene, EYCM also took place with terminal alkynes and the same catalyst, but with this substrate a ring contraction was observed. Conjugated cyclohexa-1,3-dienes were formed in good yields with propargylic and homopropargylic alkynes via methylene-free ene–yne metathesis (Scheme 16) [81]. In these two examples, the driving force seems to be the initial ring opening, which triggers the interaction with the alkyne.

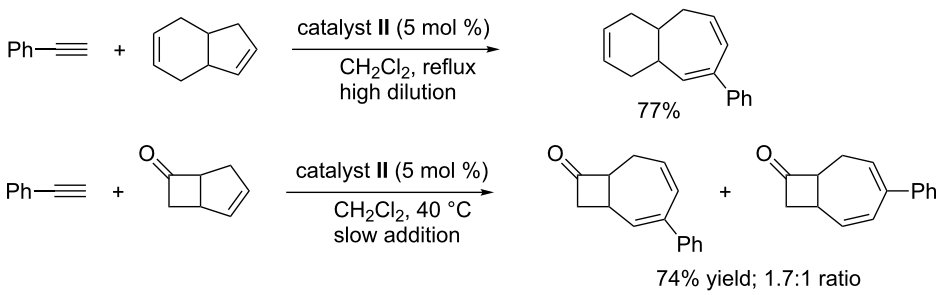

Scheme 15: Ring expansion via EYCM from bicyclic olefins.

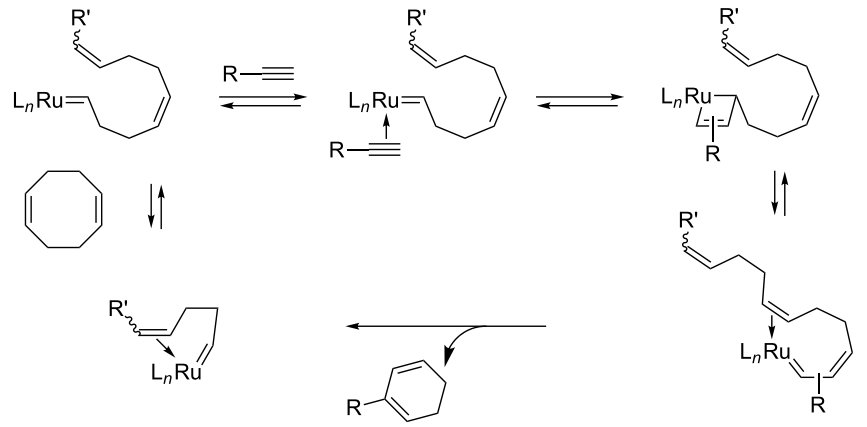

Scheme 16: Ring contraction resulting from EYCM of cyclooctadiene.

Diene–alkyne cross-metathesis

Very few examples of EYCM of alkynes with non-symmetrical α,ω-dienes have been reported. To perform this type of reaction in a selective manner it is required that the two double bonds have different reactivities with respect to EYCM and that the intramolecular olefin ring closing metathesis is not efficient. Such a reaction has been performed from dienes containing a non-activated double bond and an electron-deficient double bond. Only the non-activated double bond participated in the EYCM. Depending on the chain length in-between the diene functionality and the electron-deficient double bond, the resulting triene could either be isolated or directly cyclized (Scheme 17) [82].

Ethylene-promoted EYCM

The positive influence of ethylene in metathesis in the presence of ruthenium catalysts was first evidenced by Mori during the intramolecular ring closing metathesis of enynes [83]. The excess of ethylene would favor the formation of ruthenium methylidene intermediates, and thus prevent catalyst decomposition and maintain catalytic activity. It has also been shown that the presence of ethylene had a beneficial effect either on reactivity or on stereoselectivity in EYCM. The EYCM of vinyl ether, which was successful with some selected alkynes [68], failed when propargylic thiobenzoates were used as alkynes. However, under moderate ethylene pressure (5 psig), the cross-metathesis reaction took place at room temperature (Scheme 18) [84]. The reactivity of various electron rich olefins such as (*tert*-butyldimethylsilyloxy)ethylene and *tert*-butyl vinyl ether was also increased in the presence of ethylene. On the other hand, no improvement of stereoselectivity was obtained under these experimental conditions. It was shown that ethylene increased the lifetime of the Fischer carbene intermediate. Moreover, its role might consist in supporting the methylene transfer, thereby enhancing catalyst turnover.

In this process, ethylene was not directly involved in competing ethylene–alkyne cross-metathesis. This was not the case when it was used to perform the cross-metathesis of some homopropargylic alkynes with alkenes that are not functionalized in allylic position. It was assumed that the ethylene–alkyne cross-metathesis producing a conjugated diene was the first catalytic event followed by olefin cross-metathesis of the less substituted double bond of the resulting diene with the alkene partner

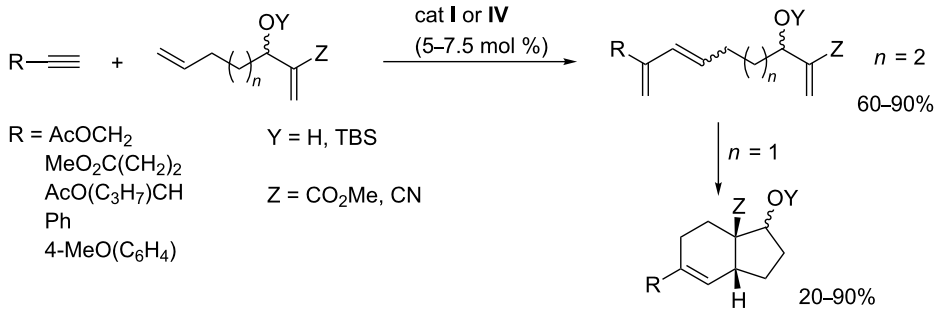

Scheme 17: Preparation of bicyclic products via diene-alkyne cross-metathesis.

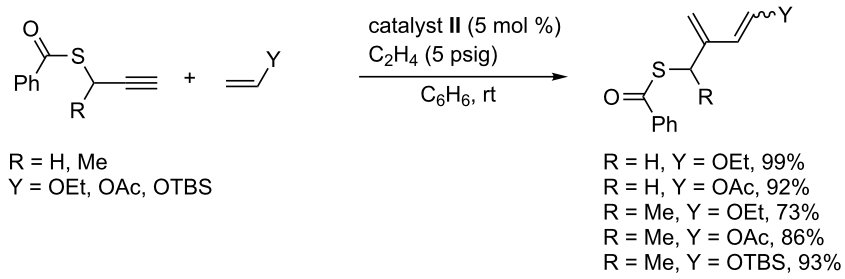

Scheme 18: Ethylene helping effect in EYCM.

[85]. The presence of ethylene not only simplified the reaction but also led to a stereoselective cross-metathesis with formation of the (*E*)-isomer as major product (*E*:*Z* ratio > 20:1 and sometimes the (*Z*)-isomer was not detected) (Scheme 19). Unfortunately, such high stereoselectivity was not observed when starting from the same alkynes with olefins substituted in allylic position such as 3-(trimethylsilyl)prop-1-ene, 3-*n*-butoxyprop-1-ene and allyl acetate.

Applications in fatty acid ester derivative transformations

The direct transformation of unsaturated fatty acid esters by EYCM has never been performed. This is not surprising as no catalyst has been able to perform the cross-metathesis of alkynes with acyclic internal olefins up to now. This would allow the introduction of a conjugated diene system into an aliphatic hydrocarbon chain. However, the production of terminal olefins upon ethenolysis of unsaturated fatty acid esters followed by cross-metathesis with an alkyne in one pot has recently been carried out in our group using dimethyl carbonate (DMC) as solvent (Scheme 20) [86].

The ethenolysis cleavage was performed in the presence of catalyst **III**, which led to 93% conversion of the starting oleate and selective production of dec-1-ene and methyl undec-9-enoate with trace amounts of octadec-9-ene and dimethyl octadec-9-enedioate resulting from secondary self metathesis of the generated terminal olefins. The cross-metathesis with a

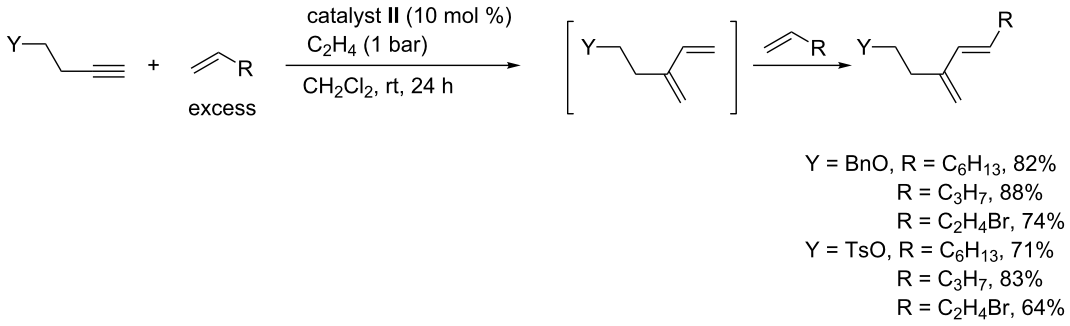

Scheme 19: Stereoselective EYCM in the presence of ethylene.

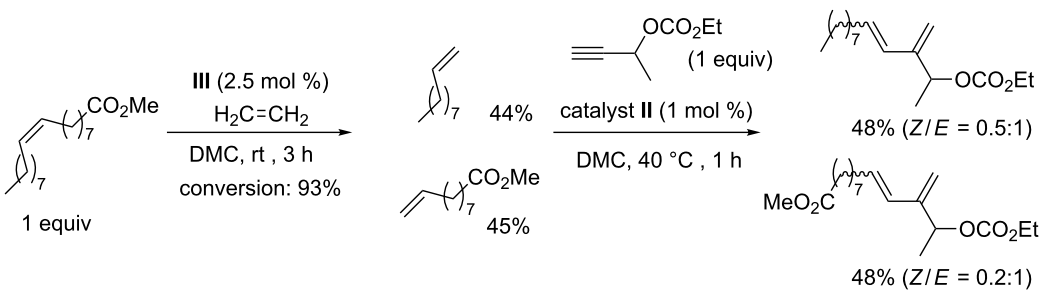

Scheme 20: Sequential ethenolysis/EYCM applied to unsaturated fatty acid esters.

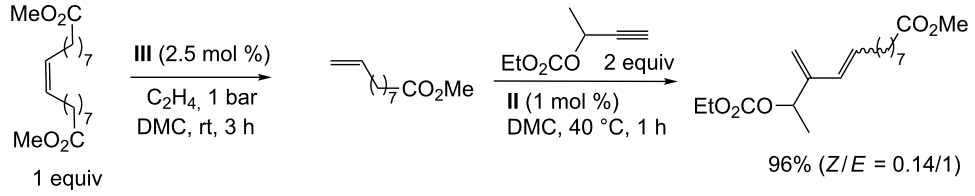

Scheme 21: Sequential ethenolysis/EYCM applied to symmetrical unsaturated fatty acid derivatives for the production of a sole product.

terminal propargylic carbonate was then carried out in the same pot with catalyst **II** and led to the formation of dienes. It was not detected that the hindered diene with the carbonate group and the aliphatic chain connected to the same double bond gave a trisubstituted olefin, which indicated a regioselective cross-coupling reaction. On the other hand, the stereoselectivity of the 1,2-disubstituted double bond was not controlled. Under the conditions for the second catalytic step mentioned above, a two-fold excess of olefin was used in a way that only half of the olefin could be transformed by EYCM.

The utilization of a symmetrical fatty acid diester arising from self metathesis or selective oxidation of oleate leads to improved experimental conditions as only one terminal olefin was produced upon ethenolysis, and the subsequent EYCM also yielded only one diene (Scheme 21). We have recently shown that a protocol based on syringe pump addition of the alkyne into the reaction medium already containing the olefin and the catalyst precursor, allows to perform the EYCM with stoichiometric amounts of olefin and alkyne. This represents an economical and technical advantage compared to the classical strategy using an excess of olefin [87].

Conclusion

The EYCM is a very efficient transformation which creates conjugated diene structures with atom economy. It has not been developed as rapidly as the olefin cross-metathesis because it suffers from some reactivity and selectivity issues that have not yet been solved. Regioselectivity of the cross-coupling reaction is usually good as no problem is encountered starting from symmetrical alkynes; and in the case of unsymmetrical alkynes, the products featuring less steric hindrance are formed. The stereoselectivity of the newly formed trisubstituted double bonds is still not controlled. It must be noted that no EYCM starting from acetylene has been described. On the contrary, polymerization of acetylene in the presence of ruthenium carbene complexes has been reported [11]. A challenge that has still to be faced is the EYCM starting from acyclic internal olefins.

References

1. Katz, T. J.; Lee, S. J. *J. Am. Chem. Soc.* **1980,** *102,* 422–424. doi:10.1021/ja00521a094
2. Katz, T. J.; Ho, T. H.; Shih, N.-Y.; Ying, Y.-C.; Stuart, V. I. W. *J. Am. Chem. Soc.* **1984,** *106,* 2659–2668. doi:10.1021/ja00321a029
3. Landon, S. J.; Shulman, P. M.; Geoffroy, G. L. *J. Am. Chem. Soc.* **1985,** *107,* 6739–6740. doi:10.1021/ja00309a069
4. Katayama, H.; Ozawa, F. *Chem. Lett.* **1998,** *27,* 67–68. doi:10.1246/cl.1998.67
5. Katayama, H.; Yoshida, T.; Ozawa, F. *J. Organomet. Chem.* **1998,** *562,* 203–206. doi:10.1016/S0022-328X(98)00566-X
6. del Rio, I.; van Koten, G. *Tetrahedron Lett.* **1999,** *40,* 1401–1404. doi:10.1016/S0040-4039(98)02619-7
7. Louie, J.; Grubbs, R. H. *Angew. Chem., Int. Ed.* **2001,** *40,* 247–249. doi:10.1002/1521-3773(20010105)40:1<247::AID-ANIE247>3.0.CO;2-4
8. Katayama, H.; Ozawa, F. *Coord. Chem. Rev.* **2004,** *248,* 1703–1715. doi:10.1016/j.ccr.2004.05.031
9. Dragutan, V.; Dragutan, I. *Platinum Metal Rev.* **2004,** *48,* 148–153. doi:10.1595/147106704X4835
10. Bruneau, C.; Dixneuf, P. H. *Angew. Chem., Int. Ed.* **2006,** *45,* 2176–2203. doi:10.1002/anie.200501391
11. Schuehler, D. E.; Williams, J. E.; Sponsler, M. B. *Macromolecules* **2004,** *37,* 6255–6257. doi:10.1021/ma048694+
12. Katsumata, T.; Shiotsuki, M.; Sanda, F.; Sauvage, X.; Delaude, L.; Masuda, T. *Macromol. Chem. Phys.* **2009,** *210,* 1891–1902. doi:10.1002/macp.200900245
13. Santhosh Kumar, P.; Wurst, K.; Buchmeiser, M. R. *J. Am. Chem. Soc.* **2009,** *131,* 387–395. doi:10.1021/ja804563t
14. Peters, J.-U.; Blechert, S. *Chem. Commun.* **1997,** 1983–1984. doi:10.1039/a705718k
15. Das, S. K.; Roy, R. *Tetrahedron Lett.* **1999,** *40,* 4015–4018. doi:10.1016/S0040-4039(99)00674-7
16. Witulski, B.; Stengel, T.; Fernández-Hernández, J. M. *Chem. Commun.* **2000,** 1965–1966. doi:10.1039/b005636g
17. Hoven, G. B.; Efskind, J.; Rømming, C.; Undheim, K. *J. Org. Chem.* **2002,** *67,* 2459–2463. doi:10.1021/jo010888p
18. Efskind, J.; Undheim, K. *Tetrahedron Lett.* **2003,** *44,* 2837–2839. doi:10.1016/S0040-4039(03)00452-0
19. Torrent, A.; González, I.; Pla-Quintana, A.; Roglans, A.; Moreno-Mañas, M.; Parella, T.; Benet-Buchholz, J. *J. Org. Chem.* **2005,** *70,* 2033–2041. doi:10.1021/jo048056p
20. Novák, P.; Čihalová, S.; Otmar, M.; Hocek, M.; Kotora, M. *Tetrahedron* **2008,** *64,* 5200–5207. doi:10.1016/j.tet.2008.03.046
21. Katz, T. J.; Sivavec, T. M. *J. Am. Chem. Soc.* **1985,** *107,* 737–738. doi:10.1021/ja00289a054

22. Watanuki, S.; Ochifuji, N.; Mori, M. *Organometallics* **1994,** *13,* 4129–4130. doi:10.1021/om00023a002
23. Watanuki, S.; Ochifuji, N.; Mori, M. *Organometallics* **1995,** *14,* 5062–5067. doi:10.1021/om00011a027
24. Mori, M. *Top. Organomet. Chem.* **1999,** *1,* 133–154. doi:10.1007/3-540-69708-X_5
25. Mori, M. In *Handbook of Metathesis;* Grubbs, R. H., Ed.; Wiley: Weinheim, 2008; Vol. 2, pp 176–204. doi:10.1002/9783527619481.ch17
26. Mori, M. *J. Mol. Catal. A: Chem.* **2004,** *213,* 73–79. doi:10.1016/j.molcata.2003.10.051
27. Mori, M. *Materials* **2010,** *3,* 2087–2140. doi:10.3390/ma3032087
28. Mulzer, J.; Öhler, E. *Top. Organomet. Chem.* **2004,** *13,* 269–366. doi:10.1007/b98768
29. Diver, S. T.; Giessert, A. J. *Chem. Rev.* **2004,** *104,* 1317–1382. doi:10.1021/cr020009e
30. Poulsen, C. S.; Madsen, R. *Synthesis* **2003,** 1–18. doi:10.1055/s-2003-36243
31. Villar, H.; Frings, M.; Bolm, C. *Chem. Soc. Rev.* **2007,** *36,* 55–66. doi:10.1039/b508899m
32. van de Weghe, P.; Bisseret, P.; Blanchard, N.; Eustache, J. *J. Organomet. Chem.* **2006,** *691,* 5078–5108. doi:10.1016/j.jorganchem.2006.07.022
33. Galan, B. R.; Giessert, A. J.; Keister, J. B.; Diver, S. T. *J. Am. Chem. Soc.* **2005,** *127,* 5762–5763. doi:10.1021/ja050174m
34. Lippstreu, J. J.; Straub, B. F. *J. Am. Chem. Soc.* **2005,** *127,* 7444–7457. doi:10.1021/ja042622g
35. Lloyd-Jones, G. C.; Margue, R. G.; de Vries, J. G. *Angew. Chem., Int. Ed.* **2005,** *44,* 7442–7447. doi:10.1002/anie.200502243
36. Hansen, E. C.; Lee, D. *Acc. Chem. Res.* **2006,** *39,* 509–519. doi:10.1021/ar050024g
37. Hoye, T. R.; Donaldson, S. M.; Vos, T. J. *Org. Lett.* **1999,** *1,* 277–280. doi:10.1021/ol9905912
38. Schramm, M. P.; Reddy, D. S.; Kozmin, S. A. *Angew. Chem., Int. Ed.* **2001,** *40,* 4274–4277. doi:10.1002/1521-3773(20011119)40:22<4274::AID-ANIE4274>3.0.CO;2-#
39. Kinoshita, A.; Sakakibara, N.; Mori, M. *J. Am. Chem. Soc.* **1997,** *119,* 12388–12389. doi:10.1021/ja973134u
40. Stragies, R.; Schuster, M.; Blechert, S. *Angew. Chem., Int. Ed.* **1997,** *36,* 2518–2520. doi:10.1002/anie.199725181
41. Kinoshita, A.; Sakakibara, N.; Mori, M. *Tetrahedron* **1999,** *55,* 8155–8167. doi:10.1016/S0040-4020(99)00297-5
42. Zheng, G.; Dougherty, T. J.; Pandey, R. K. *Chem. Commun.* **1999,** 2469–2470. doi:10.1039/a906889i
43. Smulik, J. A.; Diver, S. T. *J. Org. Chem.* **2000,** *65,* 1788–1792. doi:10.1021/jo9916941
44. Smulik, J. A.; Diver, S. T. *Org. Lett.* **2000,** *2,* 2271–2274. doi:10.1021/ol006035l
45. Tonogaki, K.; Mori, M. *Tetrahedron Lett.* **2002,** *43,* 2235–2238. doi:10.1016/S0040-4039(02)00215-0
46. Smulik, J. A.; Giessert, A. J.; Diver, S. T. *Tetrahedron Lett.* **2002,** *43,* 209–211. doi:10.1016/S0040-4039(01)02098-6
47. Mori, M.; Tonogaki, K.; Kinoshita, A. *Org. Synth.* **2005,** *81,* 1–13.
48. Mori, M.; Tonogaki, K.; Nishiguchi, N. *J. Org. Chem.* **2002,** *67,* 224–226. doi:10.1021/jo0107913
49. Pujari, S. A.; Kaliappan, K. P.; Valleix, A.; Grée, D.; Grée, R. *Synlett* **2008,** 2503–2507. doi:10.1055/s-2008-1078179
50. Kim, C. H.; An, H. J.; Shin, W. K.; Yu, W.; Woo, S. K.; Jung, S. K.; Lee, E. *Chem.–Asian J.* **2008,** *3,* 1523–1534. doi:10.1002/asia.200800062
51. Kim, C. H.; An, H. J.; Shin, W. K.; Yu, W.; Woo, S. K.; Jung, S. K.; Lee, E. *Angew. Chem., Int. Ed.* **2006,** *45,* 8019–8021. doi:10.1002/anie.200603363
52. Kaliappan, K. P.; Subrahmanyam, A. V. *Org. Lett.* **2007,** *9,* 1121–1124. doi:10.1021/ol0701159
53. Kotha, S.; Meshram, M.; Tiwari, A. *Chem. Soc. Rev.* **2009,** *38,* 2065–2092. doi:10.1039/B810094M
54. Saito, N.; Masuda, M.; Saito, H.; Takenouchi, K.; Ishizuka, S.; Namekawa, J.; Takimoto-Kamimura, M.; Kittaka, A. *Synthesis* **2005,** 2533–2543. doi:10.1055/s-2005-872075
55. Achard, M.; Derrien, N.; Zhang, H.-J.; Demerseman, B.; Bruneau, C. *Org. Lett.* **2009,** *11,* 185–188. doi:10.1021/ol8023488
56. Beydoun, K.; Zhang, H.-J.; Sundararaju, B.; Demerseman, B.; Achard, M.; Xi, Z.; Bruneau, C. *Chem. Commun.* **2009,** 6580–6582. doi:10.1039/b913595b
57. Schürer, S. C.; Blechert, S. *Tetrahedron Lett.* **1999,** *40,* 1877–1880. doi:10.1016/S0040-4039(99)00091-X
58. Schuster, M.; Blechert, S. *Tetrahedron Lett.* **1998,** *39,* 2295–2298. doi:10.1016/S0040-4039(98)00245-7
59. Schürer, S. C.; Blechert, S. *Synlett* **1999,** 1879–1882. doi:10.1055/s-1999-2961
60. Schürer, S. C.; Blechert, S. *Synlett* **1998,** 166–168. doi:10.1055/s-1998-1591
61. Stragies, R.; Voigtmann, U.; Blechert, S. *Tetrahedron Lett.* **2000,** *41,* 5465–5468. doi:10.1016/S0040-4039(00)00858-3
62. Kim, M.; Park, S.; Maifeld, S. V.; Lee, D. *J. Am. Chem. Soc.* **2004,** *126,* 10242–10243. doi:10.1021/ja0465909
63. Park, S.; Kim, M.; Lee, D. *J. Am. Chem. Soc.* **2005,** *127,* 9410–9415. doi:10.1021/ja0520159
64. Kim, M.; Miller, R. L.; Lee, D. *J. Am. Chem. Soc.* **2005,** *127,* 12818–12819. doi:10.1021/ja054875v
65. Giessert, A. J.; Diver, S. T. *Org. Lett.* **2005,** *7,* 351–354. doi:10.1021/ol047533n
66. Kim, M.; Lee, D. *Org. Lett.* **2005,** *7,* 1865–1868. doi:10.1021/ol050542r
67. Clark, D. A.; Basile, B. S.; Karnofel, W. S.; Diver, S. T. *Org. Lett.* **2008,** *10,* 4927–4929. doi:10.1021/ol802007q
68. Giessert, A. J.; Snyder, L.; Markham, J.; Diver, S. T. *Org. Lett.* **2003,** *5,* 1793–1796. doi:10.1021/ol034459k
69. Louie, J.; Grubbs, R. H. *Organometallics* **2002,** *21,* 2153–2164. doi:10.1021/om011037a
70. Castagnolo, D.; Botta, L.; Botta, M. *J. Org. Chem.* **2009,** *74,* 3172–3174. doi:10.1021/jo900205x
71. Kotha, S.; Halder, S.; Brahmachary, E. *Tetrahedron* **2002,** *58,* 9203–9208. doi:10.1016/S0040-4020(02)01178-X
72. Kotha, S.; Halder, S.; Brahmachary, E.; Ganesh, T. *Synlett* **2000,** 853–855. doi:10.1055/s-2000-6706
73. Zheng, G.; Graham, A.; Shibata, M.; Missert, J. R.; Oseroff, A. R.; Dougherty, T. J.; Pandey, R. K. *J. Org. Chem.* **2001,** *66,* 8709–8716. doi:10.1021/jo0105080
74. Schürer, S. C.; Blechert, S. *Chem. Commun.* **1999,** 1203–1204. doi:10.1039/a903208h
75. Castagnolo, D.; Botta, L.; Botta, M. *Tetrahedron Lett.* **2009,** *50,* 1526–1528. doi:10.1016/j.tetlet.2009.01.047
76. Castagnolo, D.; Botta, L.; Botta, M. *Carbohydr. Res.* **2009,** *344,* 1285–1288. doi:10.1016/j.carres.2009.05.007
77. Kalbarczyk, K. P.; Diver, S. T. *J. Org. Chem.* **2009,** *74,* 2193–2196. doi:10.1021/jo802582k

78. Rodríguez-Conesa, S.; Candal, P.; Jiménez, C.; Rodríguez, J. *Tetrahedron Lett.* **2001,** *42,* 6699–6702. doi:10.1016/S0040-4039(01)01380-6
79. Kulkarni, A. A.; Diver, S. T. *Org. Lett.* **2003,** *5,* 3463–3466. doi:10.1021/ol035246y
80. Diver, S. T.; Clark, D. A.; Kulkarni, A. A. *Tetrahedron* **2008,** *64,* 6909–6919. doi:10.1016/j.tet.2008.03.027
81. Kulkarni, A. A.; Diver, S. T. *J. Am. Chem. Soc.* **2004,** *126,* 8110–8111. doi:10.1021/ja0476922
82. Mix, S.; Blechert, S. *Org. Lett.* **2005,** *7,* 2015–2018. doi:10.1021/ol050508c
83. Mori, M.; Sakakibara, N.; Kinoshita, A. *J. Org. Chem.* **1998,** *63,* 6082–6083. doi:10.1021/jo980896e
84. Giessert, A. J.; Brazis, N. J.; Diver, S. T. *Org. Lett.* **2003,** *5,* 3819–3822. doi:10.1021/ol035270b
85. Lee, H.-Y.; Kim, B. G.; Snapper, M. L. *Org. Lett.* **2003,** *5,* 1855–1858. doi:10.1021/ol034408n
86. Le Ravalec, V.; Fischmeister, C.; Bruneau, C. *Adv. Synth. Catal.* **2009,** *351,* 1115–1122. doi:10.1002/adsc.200800726
87. Le Ravalec, V.; Dupé, A.; Fischmeister, C.; Bruneau, C. *ChemSusChem* **2010,** *3,* 1291–1297. doi:10.1002/cssc.201000212

License and Terms

Beilstein Journal of Organic Chemistry

Metathesis access to monocyclic iminocyclitol-based therapeutic agents

Ileana Dragutan*[1], Valerian Dragutan*[1], Carmen Mitan[1], Hermanus C.M. Vosloo[2], Lionel Delaude[3] and Albert Demonceau[3]

Review

Open Access

Address:
[1]Institute of Organic Chemistry, Romanian Academy, 202B Spl. Independentei, P.O. Box 35-108, Bucharest 060023, Romania, [2]School of Physical and Chemical Sciences, North-West University, Hoffman Street, Potchefstroom 2520, South Africa and [3]Macromolecular Chemistry and Organic Catalysis, Institute of Chemistry (B6a), University of Liège, Sart Tilman, Liège 4000, Belgium

Email:
Ileana Dragutan* - idragutan@yahoo.com; Valerian Dragutan* - vdragutan@yahoo.com

* Corresponding author

Keywords:
azasugars; iminocyclitols; natural products; olefin metathesis; Ru-alkylidene catalysts

Beilstein J. Org. Chem. **2011,** *7,* 699–716.
doi:10.3762/bjoc.7.81

Received: 05 February 2011
Accepted: 05 May 2011
Published: 27 May 2011

This article is part of the Thematic Series "Progress in metathesis chemistry".

Guest Editor: K. Grela

Abstract

By focusing on recent developments on natural and non-natural azasugars (iminocyclitols), this review bolsters the case for the role of olefin metathesis reactions (RCM, CM) as key transformations in the multistep syntheses of pyrrolidine-, piperidine- and azepane-based iminocyclitols, as important therapeutic agents against a range of common diseases and as tools for studying metabolic disorders. Considerable improvements brought about by introduction of one or more metathesis steps are outlined, with emphasis on the exquisite steric control and atom-economical outcome of the overall process. The comparative performance of several established metathesis catalysts is also highlighted.

Review

Introduction

Synthetic and natural polyhydroxylated N-heterocyclic compounds (pyrrolidines, piperidines, piperazines, indolizines, etc., and higher homologues), commonly referred to as azasugars, iminosugars or iminocyclitols, can be considered as carbohydrate mimics in which the endocyclic oxygen atom of sugars has been replaced by an imino group. This vast and highly diversified class has attracted considerable interest due to the remarkable biological profile shown by many of its members which has been detailed in a number of excellent books and reviews [1-12]. Natural iminosugars (i.e., alkaloids mimicking

the structures of sugars, widespread in many plants or microorganisms) [12-15], as well as non-natural counterparts, are becoming important leads for drug development in a variety of therapeutic areas, e.g., treatment of cancer [16-20], glycosphingolipid storage disorders [21,22], Gaucher's disease [23], type-II diabetes [24-26], other metabolic disorders [10], and viral diseases [27,28] such as HIV [29,30] and hepatitis B [31,32] and C [27,33]. Some such products have been already marketed, such as *N*-hydroxyethyl-1-deoxynojirimycin (Miglitol) and *N*-butyl-1-deoxynojirimycin (Miglustat) which are active against type-II diabetes and Gaucher's disease, respectively.

The broad biological activity of iminocyclitols has attracted growing interest in the synthesis of naturally occurring iminocyclitols and in their structural modification. Consequently, efficient and stereoselective synthetic routes have been developed, often starting from an inexpensive chiral-pool of precursors, in particular carbohydrates that share structural features with iminocyclitols. The main hurdles in this approach are the singling out of only one of the hydroxy groups in the open carbohydrate-derived intermediate, converting this hydroxy group into an amino group, and intramolecularly closing this intermediate [8,34-36]. Because of the high density of functional groups, proper protection throughout the overall synthesis scheme is an important feature that must be considered carefully, with full deprotection occurring in the final step.

With the advent of well-defined Mo- and Ru-alkylidene metathesis catalysts (e.g., **1**–**10**; Scheme 1) [37-47] the RCM strategy was immediately recognized as central to success in the flexible construction of N-heterocyclic compounds, including azasugars. Moreover, the metathesis approach to azasugars has greatly benefited from the vast synthetic experience acquired in RCM preparation of a host of heterocycles. Any RCM-based protocol to iminocyclitols implies three crucial stages: (i) discovery of a route to obtain stereoselectively, starting from an ordinary substrate, the N-containing prerequisite diene precursor; (ii) RCM cyclization of this diene, with an active catalyst, to access the core cyclic olefin; and (iii) dihydroxylation of the endocyclic double bond in a highly diastereoselective manner to form the target product.

In comparison to the traditional, lengthier syntheses of iminocyclitols, the metathesis approach has emerged as a highly advantageous method in terms of atom economy. However, before carrying out the RCM reaction, the basic amino group (incompatible with most metathesis catalysts because of chelation to the metal center) [48] must either be protected (as *N*–Boc, *N*–Cbz, etc.), masked by incorporation into a cleavable heteroatom-containing cycle (oxazolidine, cyclic ketal, etc.), or deactivated by conversion into amide or carbamate functions. Due to these protective groups even metathesis catalysts sensitive to functionalities can act efficiently under reaction conditions where an adequate balance between activity/stability factors has been met. In addition, the reaction conditions (temperature, solvents) currently employed in olefin metathesis reactions can be productively transferred to the metathesis steps of iminocyclitols synthesis.

By surveying the field of recent azasugar developments, this review focuses on metathesis reactions (mainly RCM, CM) as essential transformations in the multistep synthesis of mono-

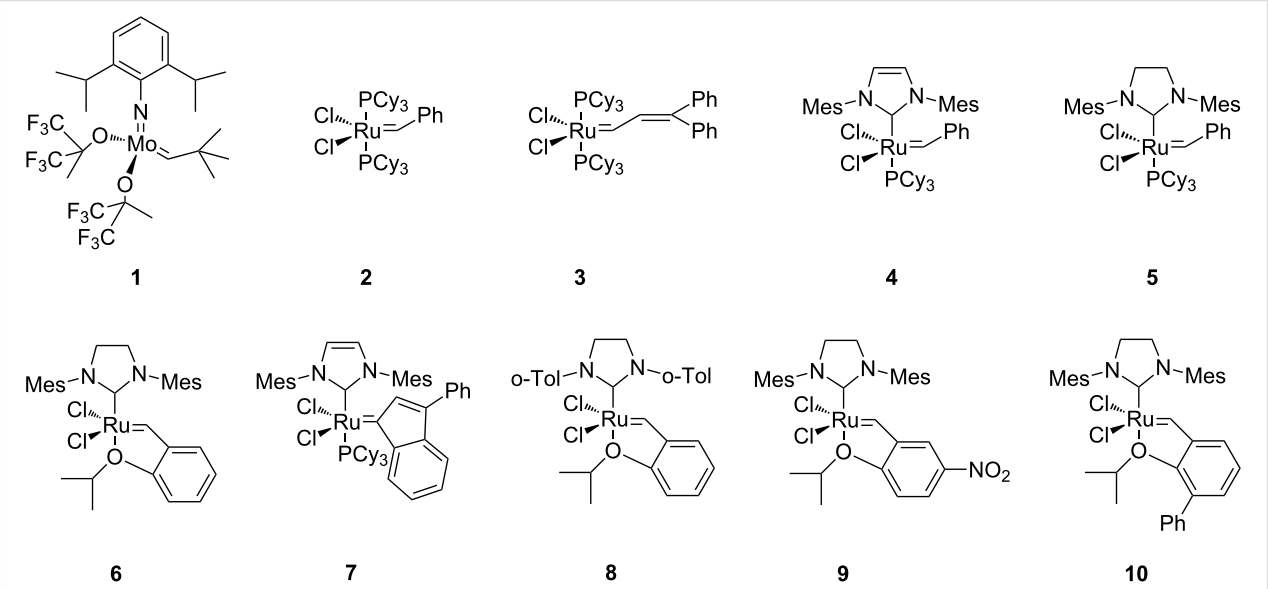

Scheme 1: Well-defined Mo- and Ru-alkylidene metathesis catalysts.

cyclic iminocyclitols, while also discussing the successes and failures in effecting the above mentioned three critical stages. New perspectives may open up for practitioners of both glyco- and metathesis chemistry involved in the synthesis and development of iminocyclitols.

Pyrrolidine-based iminocyclitols

Recently, pyrrolidine-based iminocyclitols have assumed increasing importance and some of them have achieved even higher biological significance than the established six-membered piperidine deoxynojirimycin (DNJ) and deoxygalactonojirimycin (DGJ). Five-membered iminocyclitols possessing N-alkyl and C_1-alkyl substituents form a class of potent antiviral compounds active, e.g., against hepatitis B virus (HBV), hepatitis C virus (HCV), and human immunodeficiency virus (HIV) [49-52].

Biological activity of this family of iminocyclitols is dictated by the stereochemistry at all carbon atoms of the pyrrolidine ring system which can adopt either a manno or a galacto conformation, therefore inhibiting either α-mannosidases (e.g., **11**–**13**) or α-galactosidases (e.g., **14**) (Scheme 2). A characteristic feature in **11**–**14** is the presence of a 1,2-dihydroxyethyl side chain.

Following the RCM-based strategy (vide supra), an elegant and quite flexible synthesis of five-membered iminocyclitols was achieved by Huwe and Blechert as early as 1997 [53]. Starting from (±)-vinylglycine methyl ester **15** and going successively via amino protection (Cbz) and ester group reduction ($LiBH_4$), a protected racemic diene **16** was obtained; RCM cyclization of the latter using the Grubbs catalyst $Cl_2(PCy_3)_2Ru{=}CH{-}CH{=}CPh_2$ (**3**) led to the racemic dehydroprolinol derivative **17** in high yield. Subsequent O-protection with trityl chloride and dihydroxylation (with OsO_4 or stereoselective epoxidation followed by regioselective epoxide opening) produced the racemic iminocyclitols (**18**–**20**) in good overall yields (Scheme 3).

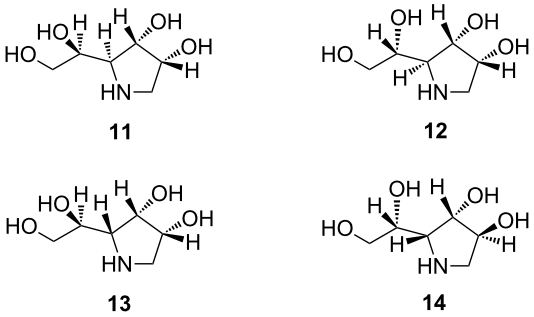

Scheme 2: Representative pyrrolidine-based iminocyclitols.

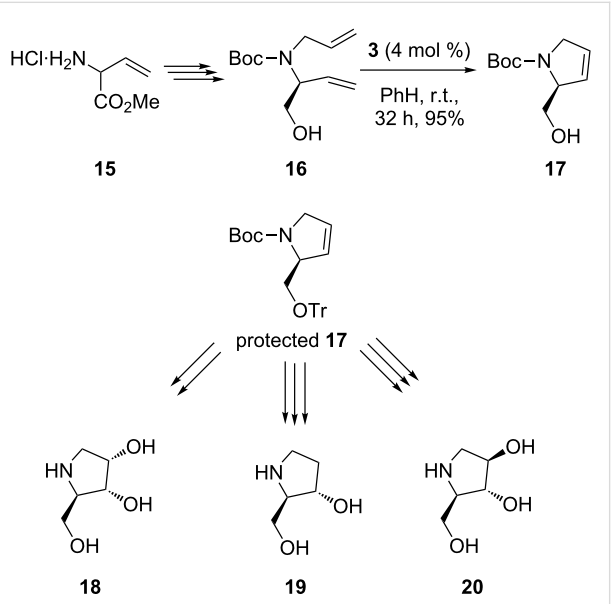

Scheme 3: Synthesis of (±)-(2*R**,3*R**,4*S**)-2-hydroxymethylpyrrolidin-3,4-diol (**18**), (±)-2-hydroxymethylpyrrolidin-3-ol (**19**) and (±)-(2*R**,3*R**,4*R**)-2-hydroxymethylpyrrolidin-3,4-diol (**20**).

In addition, Blechert showed that this method was more adaptable as it could also yield enantiopure **18**–**20**, provided that racemization was avoided both during ester group reduction and the subsequent steps. By a similar approach (Scheme 4), these authors also obtained the enantiopure homoiminocyclitol (−)-(2*S*,3*R*,4*S*,5*S*)-2,5-dihydroxymethylpyrrolidin-3,4-diol (**23**).

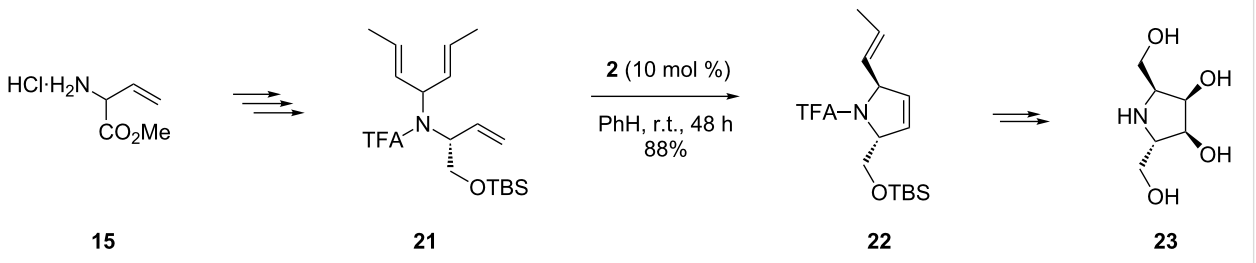

Scheme 4: Synthesis of enantiopure iminocyclitol (−)-(2*S*,3*R*,4*S*,5*S*)-2,5-dihydroxymethylpyrrolidin-3,4-diol (**23**).

Starting from the same racemic vinyl glycine methyl ester and introducing enzymatic resolution in the ester reduction step, enantiopure (+)-**21** was obtained. 1st-generation Grubbs catalyst was used for the RCM of (+)-**21**. It should be noted that the yield of (+)-**22** in RCM (10 mol % **2**, in benzene) was temperature dependent (88% at room temperature and 98% at 80 °C). Further stereocontrolled dihydroxylation with simultaneous deprotection of (+)-**22** gave the final product (−)-**23** in good yield.

In an interesting work by Rao and co-workers [54] a Grignard reaction was employed to design the diene with desired stereochemistry for the synthesis of 1,4-dideoxy-1,4-imino-D-allitol (**29**) and the formal synthesis of (2*S*,3*R*,4*S*)-3,4-dihydroxyproline (**30**) (Scheme 5). According to their methodology, (*R*)-2,3-*O*-isopropylidene-D-glyceraldehyde (**24**) was treated in a one-pot reaction with benzylamine and then subjected to Grignard addition with vinylmagnesium bromide to provide the alkene **25** as a single diastereomer. The nitrogen atom in **25** was then Boc-protected, debenzylated, and allylated to give the diene **26**. RCM of the latter with 1st-generation Grubbs catalyst (10 mol % **2**, in dichloromethane, at room temperature) provided the pyrrole scaffold **27**. Subsequent stereoselective dihydroxylation (OsO_4 and 4-methylmorpholine *N*-oxide (NMO) in acetone) to yield **28** and final deprotection (MeOH–HCl) gave the imino-D-allitol **29** as the HCl salt. Formal synthesis of (2*S*,3*R*,4*S*)-3,4-dihydroxyproline (**30**) starting from **24** was carried identically by RCM to afford **27** and subsequent conversion of **28** to **30** was achieved in several steps via the Fleet protocol [55].

The tandem RCM/dihydroxylation sequence was also applied by Davis et al. in the synthesis of (−)-2,3-*trans*-3,4-*cis*-dihydroxyproline. In this case, an α-amino aldehyde, prepared by addition of a 1,3-dithiane to a chiral *N*-sulfinyl imine, was used as the chiral starting material [56]. Syntheses of 1,4-dideoxy-1,4-imino derivatives of L-allitol and D-talitol were also accomplished following a similar RCM methodology by Rao and co-workers [57].

1,4-Dideoxy-1,4-imino-D-ribitol (**35**), known as (+)-DRB, is a potent inhibitor of glucosidases and of eukaryotic DNA polymerases. Its synthesis, as well as that of its dihydroxylated homologue **36**, features as the key step five-membered ring formation via RCM induced by the 2nd-generation Grubbs catalyst **5** (Scheme 6) [58].

A further contribution to new pyrrolidine-based azasugars, characteristically having 1,2-dihydroxyethyl side chains and a quaternary C-atom possessing a hydroxy and a hydroxymethyl group, was made by Vankar et al. [59] (Scheme 7). By ingeniously combining a Baylis–Hillman addition with RCM as the

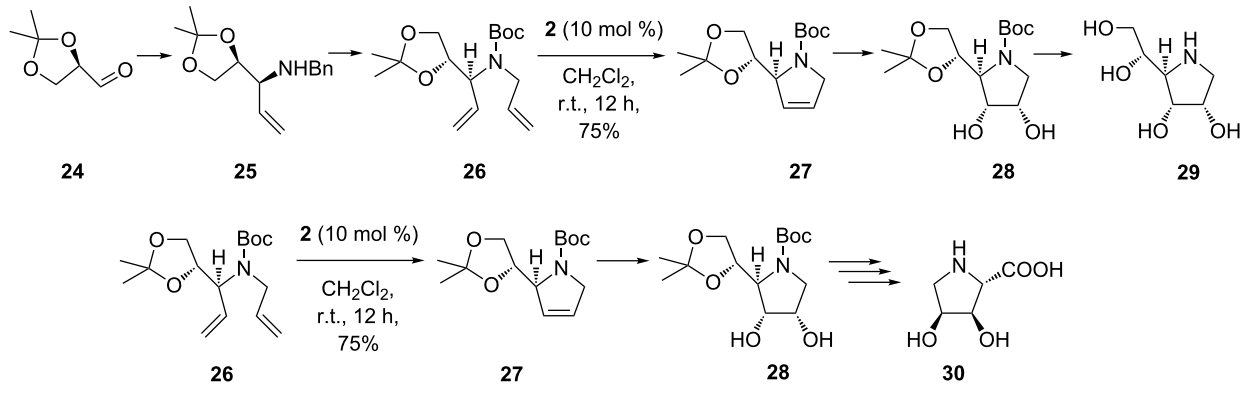

Scheme 5: Synthesis of 1,4-dideoxy-1,4-imino-D-allitol (**29**) and formal synthesis of (2*S*,3*R*,4*S*)-3,4-dihydroxyproline (**30**).

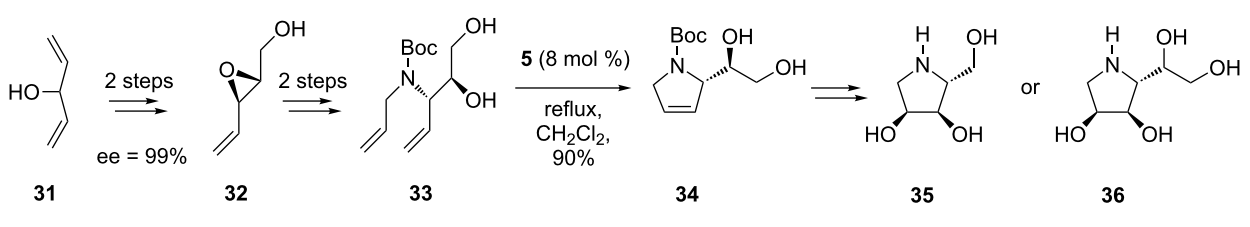

Scheme 6: Synthesis of iminocyclitols **35** and **36**.

key steps, they obtained, stereoselectively and in high yields, 1,4-dideoxy-1,4-iminohexitols **40** and **44** which showed moderate inhibition of β-galactosidase, and α-galacto- and α-mannosidases, respectively. It should be noted that diene **38** did not cyclize in the presence of 1st-generation Grubbs catalyst, even in refluxing toluene, whereas 2nd-generation Grubbs catalyst afforded (in toluene, at 60 °C) the cyclic products **39** and **43** in 89% and 86% yields, respectively. Interestingly, Upjohn dihydroxylation of **39** or **43** (OsO_4, NMO, acetone/H_2O/*t*-BuOH; HCl, MeOH; Ac_2O, Et_3N, DMAP) gave only one diastereomeric diol, because the bulky acetonide group blocks the β-face of the trisubstituted double bond of the pyrrolidine ring and is thus responsible for the high diastereoselectivity.

A metathesis approach has elegantly been used by Trost et al. for the total synthesis of 2,5-dideoxy-2,5-imino-D-mannitol [(+)-DMDP], **49**, (−)-bulgecinine, **50**, and (+)-broussonetine G, **53** [60,61]. The crucial intermediate, the protected annulated oxazolone **48**, resulted from RCM (2nd-generation Grubbs catalyst) of the imino diene **47** (previously produced by a Pd-catalyzed asymmetric transformation). The following three or five steps, respectively, including the enantioselective dihydroxylation of the RCM product **48**, occurred smoothly to produce the (+)-DMDP (**49**) and (−)-bulgecinine (**50**) (Scheme 8).

The starting point in the synthesis of (+)-broussonetine G, **53**, was the same annulated oxazolone **48** which, after conversion into the Weinreb amide **51**, was coupled with the alkyl bromide substituted spiro compound **52** (Scheme 9).

In fact, the case of broussonetines is much more complicated. This subgroup is currently represented by 30 reported examples, all isolated from plant species and used in folk medicine in China and Japan. Most broussonetines display marked inhibitory activities on various glycosidase types, with selectivities differing from that of other standard iminosugars such as DNJ. In the majority of the broussonetines (**54**, Scheme 10), a

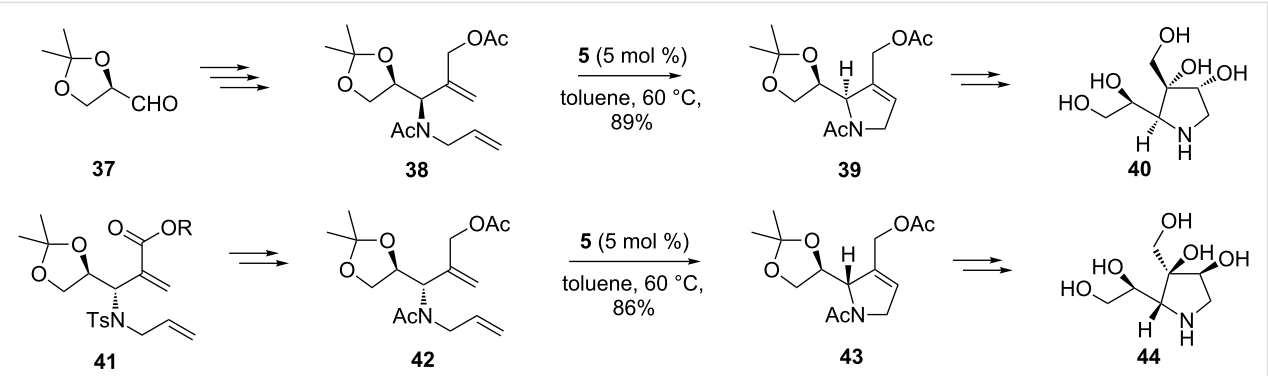

Scheme 7: Total synthesis of iminocyclitols **40** and **44**.

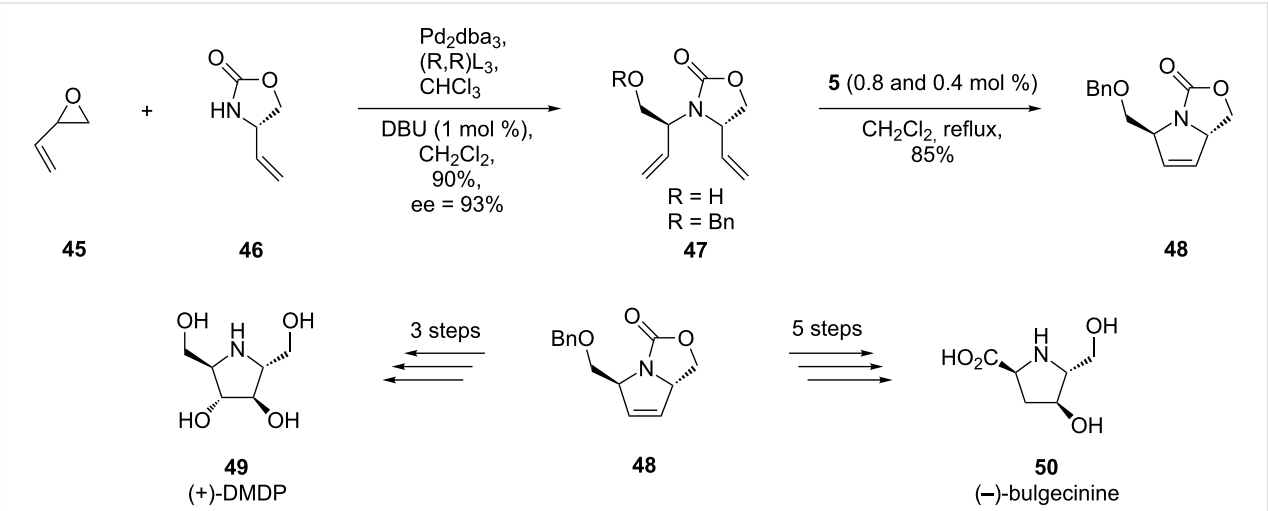

Scheme 8: Synthesis of 2,5-dideoxy-2,5-imino-D-mannitol [(+)-DMDP] (**49**) and (−)-bulgecinine **(50)**.

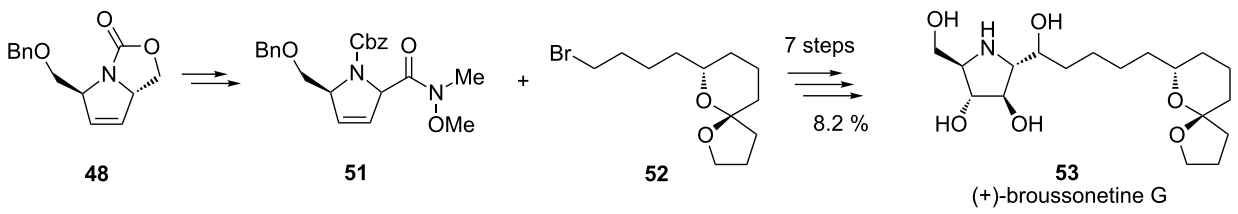

Scheme 9: Synthesis of (+)-broussonetine G (**53**).

common polyhydroxylated pyrrolidine building block (possibly prepared via protocols including RCM) is bound to a side chain fragment of 13 C-atoms, diversely functionalized. For the introduction of the appropriate side chain, cross-metathesis appeared to be the most versatile method, permitting access to many members of this family, both naturally occurring and analogues. Two types of metathesis processes, RCM and CM, can be thus advantageously intertwined in the synthesis of broussonetines.

For instance, the syntheses of broussonetines C, D, M, O and P were completed by Falomir, Marco et al. [62,63] in a convergent, stereocontrolled way starting from commercial D-serine (**55**) as the chiral precursor and by applying the critical step of cross-metathesis (the first-ever synthesis of broussonetines O and P) (Scheme 11).

The cross-metathesis reaction was promoted by the 2nd-generation Grubbs catalyst (**5**, in CH_2Cl_2, by heating under reflux in a N_2 atmosphere for 24 h or by heating for 1 h at 100 °C under microwave irradiation). As expected in a cross-metathesis process, a mixture of three products (CM product plus the two homo-metathesis products, all in both stereoisomeric forms) was obtained. Homo-metathesis products from either **56** or the alkene were recycled in the cross-metathesis stage to provide an additional amount of the useful product **57**, thus enhancing the overall yield.

Piperidine-based iminocyclitols

During the last decade, polyhydroxylated piperidines have been the target of much cutting-edge synthesis work [8]. Such com-

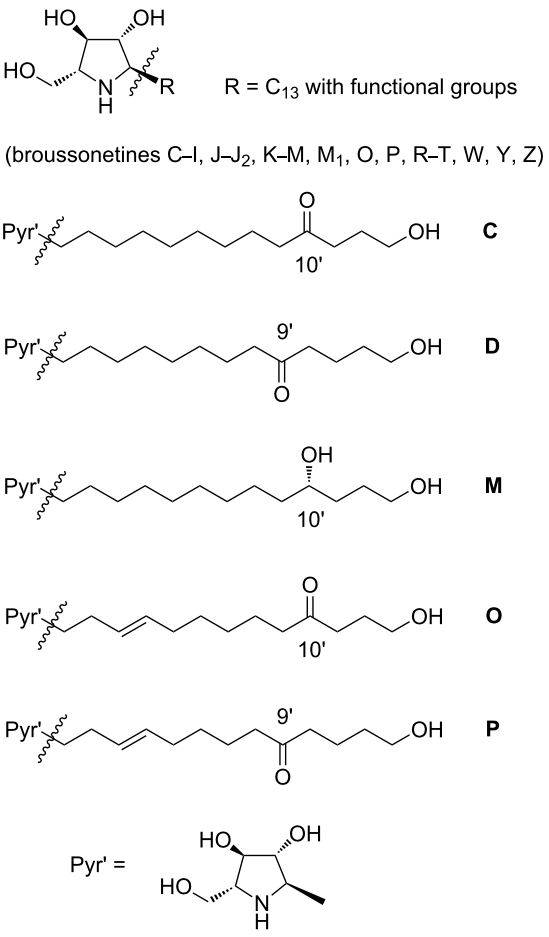

Scheme 10: Structural features of broussonetines **54**.

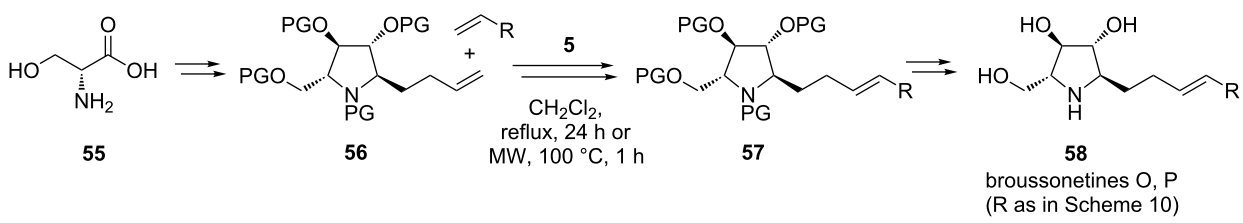

Scheme 11: Synthesis of broussonetines by cross-metathesis.

pounds are of special interest as therapeutic agents and as tools for the study of cellular mechanisms and metabolic diseases. From this class, nojirimycin (NJ, trivial name for 5-amino-5-deoxy-D-glucopyranose) (**59**), the first alkaloid discovered that mimicks a sugar (originally isolated from *Streptomyces* filtrate but also found in other bacterial cultures and plant sources), is a potent glycosidase inhibitor. In aqueous solution nojirimycin exists in both the α- and β-forms, each of which is responsible for inhibition of α- or β-glucosidase, respectively. Similar to its other congeners, mannonojirimycin (**60**; MJ or nojirimycin B) and galactonojirimycin (**61**; GJ or galactostatin), nojirimycin is unstable because hemiacetal structures can be adopted [8]. 1-Deoxynojirimycin (**62**; DNJ), the more stable 1-deoxy analogue of nojirimycin, represents the main motif of a large family of iminocyclitols (e.g., **63**–**66**). Although numerous other piperidine iminocyclitols have shown encouraging results against HIV and in cancer therapy, the deoxynojirimycin family is certainly the most interesting. Two deoxynojirimycin derivatives have already found clinical applications: *N*-butyl-1-deoxynojirimycin (Miglustat, **67**), in the treatment of type-II diabetes, and *N*-hydroxyethyl-1-deoxynojirimycin (Miglitol, **68**; FDA approved) in the treatment of Gaucher's disease (Scheme 12) [8].

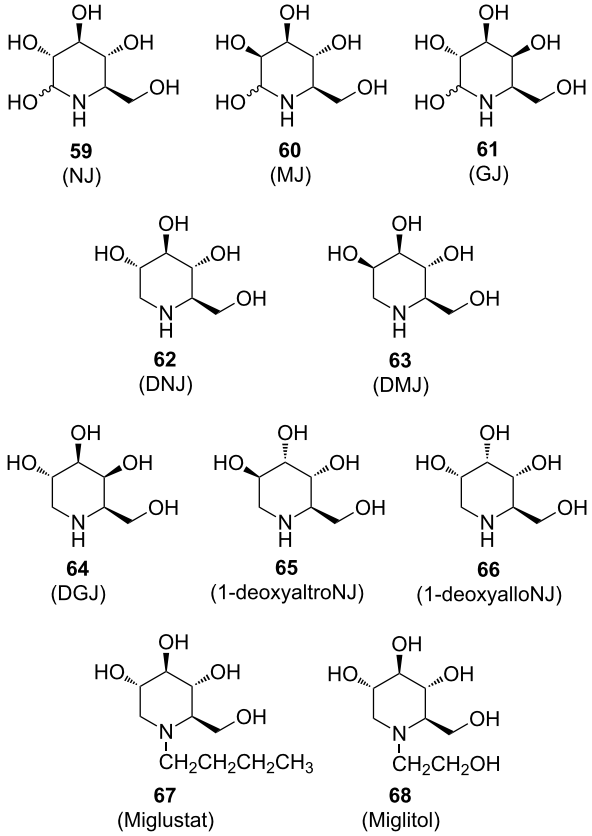

Scheme 12: Representative piperidine-based iminocyclitols.

Takahata et al. [64] exploited RCM for the contruction of the piperidine ring of 1-deoxynojirimycin (**62**) and its congeners (1-deoxymannonojirimycin (**63**), 1-deoxyaltronojirimycin (**65**), and 1-deoxyallonojirimycin (**66**), Scheme 13). In their methodology, the D-serine-derived Garner aldehyde **69** provides an attractive starting point since it reacts with organometallic

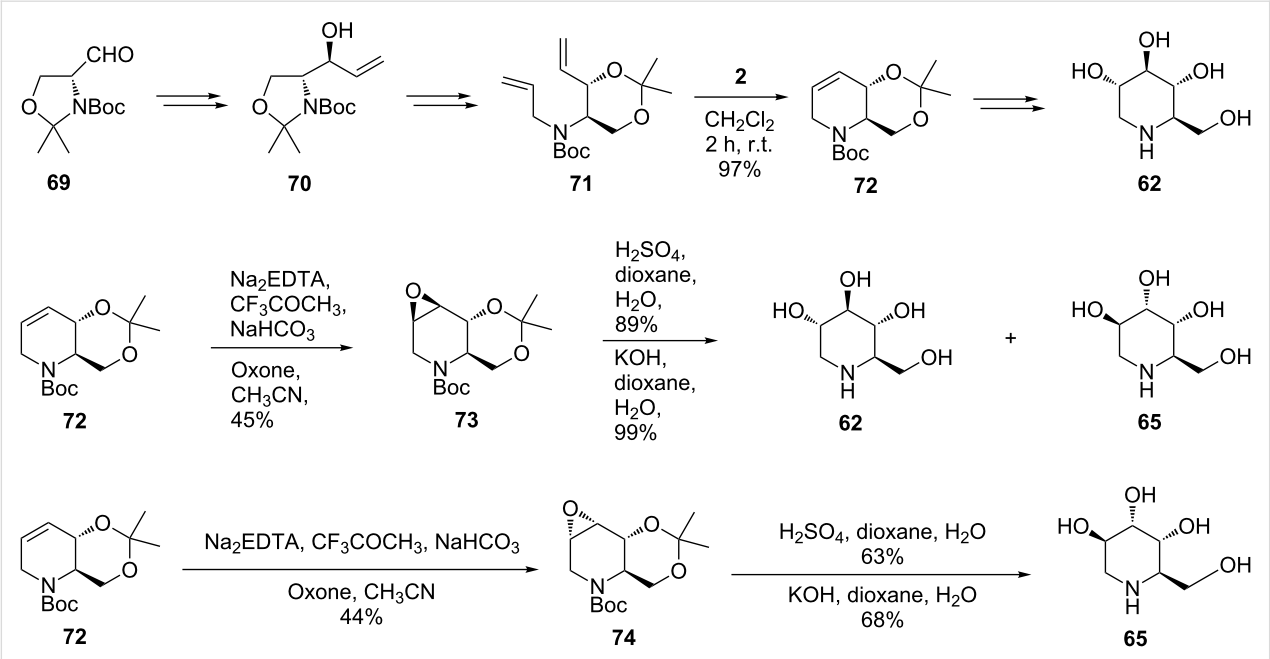

Scheme 13: Total synthesis of 1-deoxynojirimycin (**62**) and 1-deoxyaltronojirimycin (**65**).

reagents with a high degree of diastereoselectivity and minimal racemization. N-allylation (allyl iodide/NaH; 95% yield) of an intermediate derived from **70** gave the diolefin product **71,** which was then subjected to RCM (dichloromethane, 20 °C) in the presence of the 1st-generation Grubbs catalyst [($Cl_2(Cy_3P)_2Ru$=CHPh)] (**2**) to form the chiral tetrahydropyridine building block **72** in 97% yield. The stereochemistry of **72** was unambiguously confirmed by transformation into the known *trans*-3-hydroxy-2-hydroxy-methylpiperidine. The tetrahydropyridine scaffold **72** allowed an efficient synthesis of 1-deoxynojirimycin **62**, and its stereoisomers **65** and **66**. Thus, acid hydrolysis of the epoxy ring in the *anti* isomer **73** (H_2SO_4/dioxane/H_2O, 0.2:3:2) gave 1-deoxynojirimycin (**62**) and 1-deoxyaltronojirimycin (**65**) in a 1:1 ratio and in 89% yield. Conversely, basic cleavage of the epoxide **73** (KOH/dioxane/H_2O) led preferentially to **65** (1:1.5 ratio **62**/**65**; 99% yield). It should be noted that in the case of the *syn* epoxide **74** both acidic and basic hydrolysis afforded only 1-deoxyaltronojirimycin (**65**), in 63 and 68% yields, respectively.

Further manipulations based mainly on stereoselective dihydroxylation ($K_2OsO_4{\cdot}2H_2O$; NMO as co-oxidant) of the useful building block **72** are at the core of the synthesis of 1-deoxymannonojirimycin (**63**) and 1-deoxyallonojirimycin (**66**) (Scheme 14). Although 1-deoxynojirimycin (**62**) and 1-deoxyaltronojirimycin (**65**) were obtained in a rather selective manner, a similar route to deoxymannojirimycin **(63**) and 1-deoxyallonojirimycin (**66**) did not achieve the same degree of selectivity, presumably due to difficulties in transforming the endocyclic double bond of the RCM product **72** into the targeted *trans* diols. Clean epoxide opening is frequently troublesome, being governed by a number of factors.

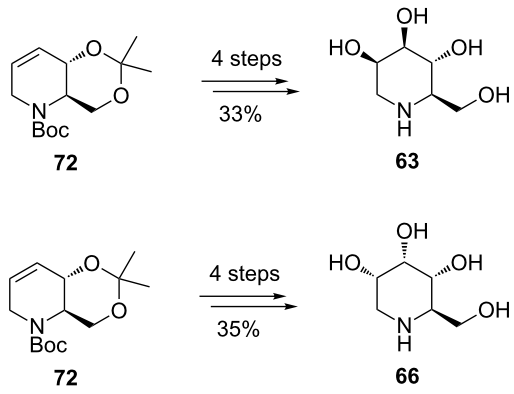

Scheme 14: Synthesis by RCM of 1-deoxymannonojirimycin (**63**) and 1-deoxyallonojirimycin (**66**).

An improvement in the selectivity and efficiency of the total synthesis of (+)-1-deoxynojirimycin (**62**) (24% overall yield) was made by Poisson et al. [65], who developed a one-pot tandem protocol involving enol ether RCM/hydroboration/oxidation, which gave the best results when the Hoveyda–Grubbs catalyst **6** was used in the RCM (Scheme 15).

Interestingly, in this case the asymmetric synthesis of the protected RCM precursor **78** started from a non-chiral source, the alcohol **75**, and proceeded with complete stereocontrol over the 11 steps involved. All attempts to achieve metathesis on another diene precursor having an endocyclic N-atom (the result of N-alkylation of **77** with 3-iodo-2-(methoxymethyloxy)prop-1-ene) led to either recovery of the starting material or olefin isomerization, even in the presence of a number of ruthenium

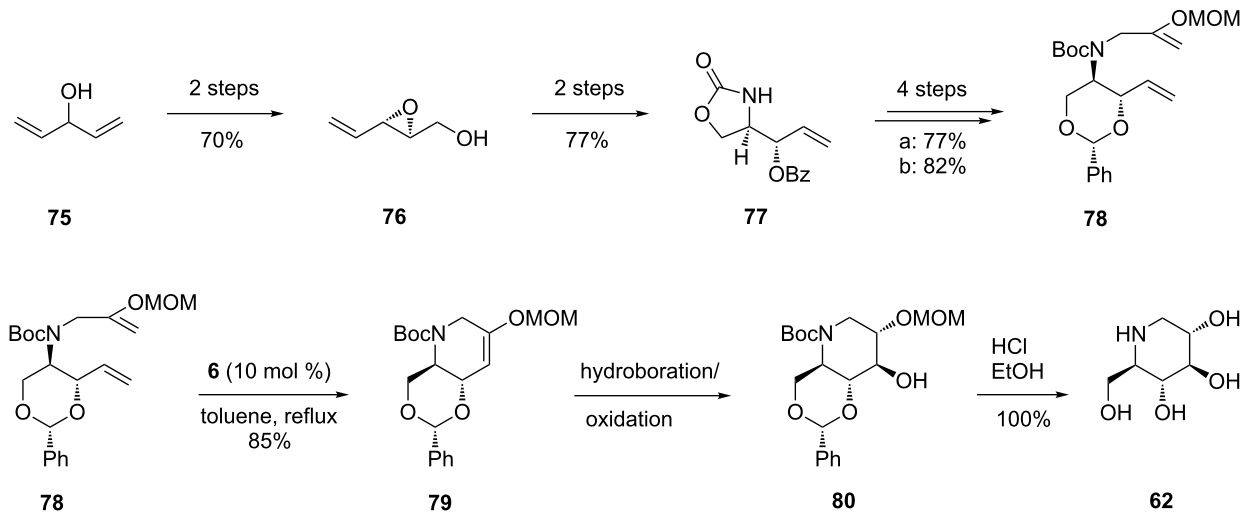

Scheme 15: Total synthesis of (+)-1-deoxynojirimycin (**62**).

hydride traps. Satisfactory results in RCM were, however, obtained from **78**: in the presence of the 2nd-generation Grubbs catalyst **5** and benzoquinone in refluxing toluene, **78** was converted into the cyclized enol ether **79** in 70% yield, while with the Hoveyda–Grubbs catalyst (**6**, 10 mol %; benzoquinone 10 mol %; in refluxing toluene) **79** was obtained in 85% yield. The three reaction steps leading from **78** to **80**, i.e., RCM/hydroboration/oxidation, could be accomplished in one-pot to afford the product as a single isomer (all-*trans* triol). The prepared (+)-1-deoxynojirimycin (**62**) displayed spectroscopic data which perfectly matched those of the natural product.

An important precursor for the synthesis of polyhydroxylated piperidines, (3*R*,4*S*)-3-hydroxy-4-*N*-allyl-*N*-Boc-amino-1-pentene (**81**), could be obtained as a single diastereomer via the addition of vinyl Grignard to the *N*-Boc-*N*-allyl aminoaldehyde, which was derived from the methyl ester of natural, enantiopure L-alanine. Having built the tetrahydropyridine scaffold **82** by RCM of **81** using the 2nd-generation Grubbs catalyst (**5**; 85% yield), Park et al. [66] were able to effect its stereodivergent dihydroxylation, via a common epoxide intermediate, to yield a range of interesting hydroxylated piperidines. This included *ent*-1,6-dideoxynojirimycin (*ent*-1,6-dDNJ, **83**) (28% overall yield from *N*-Boc-L-alanine methyl ester) and 5-amino-1,5,6-trideoxyaltrose (**84**) (29% overall yield from *N*-Boc-L-alanine methyl ester), which were produced with excellent diastereoselectivity (>99:1 dr, Scheme 16). It appears that this total synthesis of *ent*-1,6-dDNJ (**83**) is the most expeditious to date.

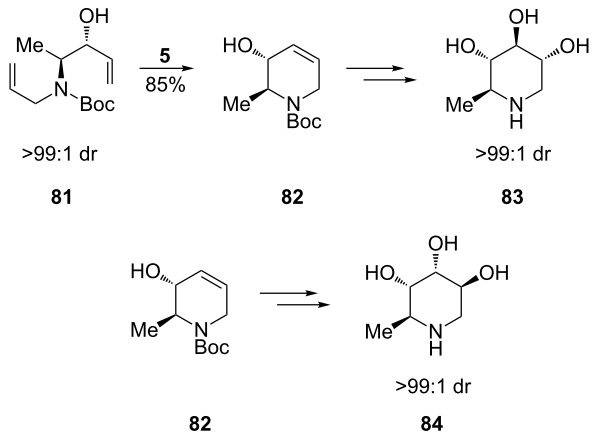

Scheme 16: Synthesis of *ent*-1,6-dideoxynojirimycin (**83**) and 5-amino-1,5,6-trideoxyaltrose (**84**).

It was again Takahata et al. [67] who successfully tackled the synthesis of 1-deoxygalactonojirimycin (**64**, DGJ) and its congeners, 1-deoxygulonojirimycin (**91**) and 1-deoxyidonojirimycin (**93**) (Scheme 17), relying in the first step on the diastereoselective addition of a vinyl organometallic reagent to D-Garner aldehyde. Once more, for construction of the piperidine ring in **86**, RCM (1st-generation Grubbs catalyst, **2**) was applied to the prerequisite diene **85** bearing a cyclic conformation constraint. The stereochemistry of the chiral building block **86** was confirmed by conversion into the known compound, *cis*-2-hydroxymethyl-3-hydroxypiperidine (**87**), (step a). For 1-deoxygulonojirimycin (**91**) a highly selective dihydroxylation (step f) was performed on **86**, under Upjohn conditions. For 1-deoxygalactonojirimycin (**64**) and 1-deoxyidonojirimycin (**93**), transformation of **86** proceeded via *syn* (step c) and *anti* (step h) epoxidation of the internal double bond in **86**, respectively, and subsequent hydrolysis.

Quite recently, an interesting synthesis of three 1-deoxynojirimycin-related iminosugars, L-1-deoxyaltronojirimycin (**96**), D-1-deoxyallonojirimycin (**66**), and D-1-deoxygalactonojirimycin (**64**), was reported by Overkleeft et al. to occur from a single chiral cyanohydrin **94**, made available via a chemoenzymatic approach with almond hydroxynitrile lyase (*pa*HNL) [68]. The key steps in the synthetic scheme comprise the cascade Dibal reduction/transimination/$NaBH_4$ reduction of the enantiomerically pure **94**, followed by the RCM step (CH_2Cl_2, 3.5 mol % 1st-generation Grubbs catalyst, reflux under Ar for 48 h) and Upjohn dihydroxylation to afford the target compounds (Scheme 18 for **96**).

RCM promoted by the 1st-generation Grubbs catalyst **2** is starring again in the divergent, flexible methodology disclosed by Singh and Han [69] for the asymmetric synthesis of several deoxyiminocyclitols (1-deoxymannonojirimycin (**63**), 1-deoxyaltronojirimycin (**65**), 1-deoxygulonojirimycin (**91**), 1-deoxyidonojirimycin (**93**), Scheme 19). Ingeniously selecting as starting material the achiral olefin **97**, suitable for electronic and aryl–aryl stacking interactions with the regioselective osmium catalyst, they conducted asymmetric aminohydroxylation (regioselectivity >20:1; enantioselectivity >99% ee) in good yield (70%) to get the RCM precursor diene **98**, appropriately protected. Under common RCM conditions (10 mol % 1st-generation Grubbs catalyst **2**, toluene, 90 °C, 2 h) **98** was then converted to the key cyclo-olefin intermediate **99** (80% yield). From the latter, the targeted iminocyclitols **63** and **91** have been obtained after artful manipulation of routine protocols (diastereoselective dihydroxylation and protection/deprotection). To access 1-deoxyaltronojirimycin (**65**) and 1-deoxyidonojirimycin (**93**), introduction of an additional step involving a cyclic sulfate was necessary.

A similar methodology was used by Han [70] to prepare 5-des(hydroxymethyl)-1-deoxynojirimycin (**114**) and its mannose analogue **111** (as HCl salts) in a highly stereoselective

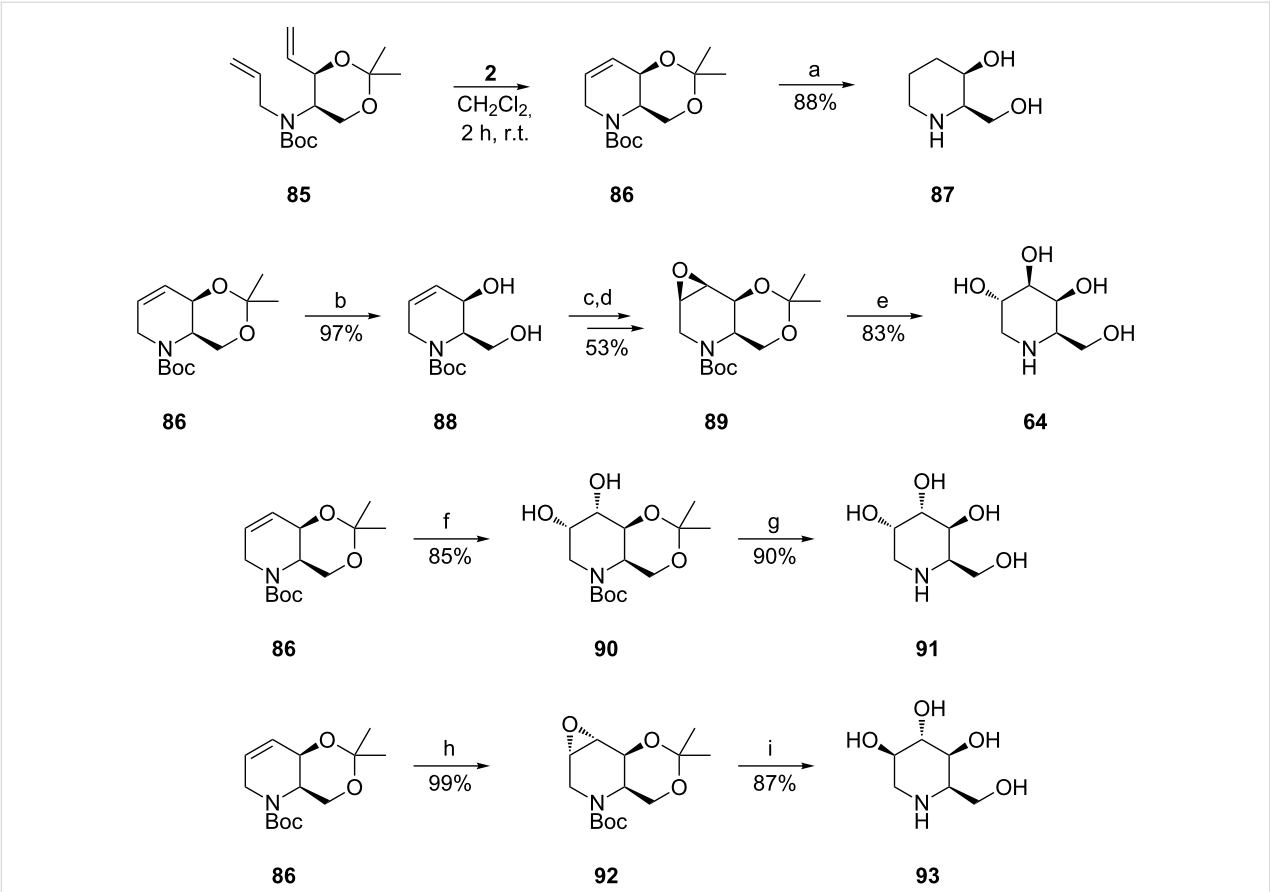

Scheme 17: Synthesis of 1-deoxygalactonojirimycin (**64**), 1-deoxygulonojirimycin (**91**) and 1-deoxyidonojirimycin (**93**) [Step c: *m*-CPBA, NaH_2PO_4, CH_2Cl_2, 0 °C to r.t. Step d: 2,2-dimethoxypropane, PPTS, acetone, r.t. Step e: H_2SO_4, 1,4-dioxane, H_2O, reflux. Step f: $K_2OsO_4{\cdot}2H_2O$, NMO, acetone, H_2O, r.t. Step g: HCl, MeOH. Step h: Oxone, CF_3COCH_3, $NaHCO_3$, aqueous $Na_2{\cdot}EDTA$, CH_3CN, 0 °C. Step i: 0.3 M KOH, 1,4-dioxane, H_2O, reflux].

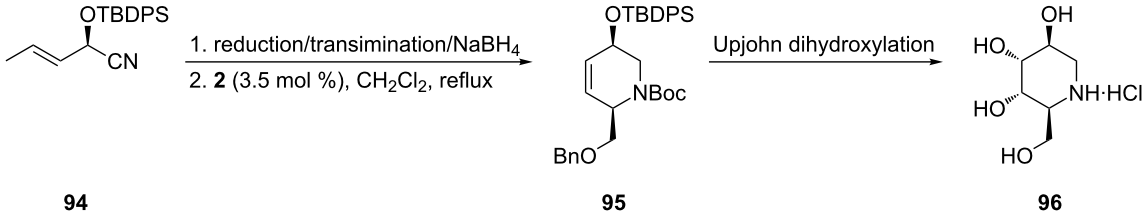

Scheme 18: Synthesis of L-1-deoxyaltronojirimycin (**96**).

mode starting from a different common olefin, **107** (Scheme 20). In this case, RCM was promoted by the 2nd-generation Grubbs catalyst **5** which ensured a high yield of the ring closure (89%) under milder conditions (CH_2Cl_2): all attempts to employ the 1st-generation Grubbs catalyst **2** in RCM failed, supposedly because of an unfavourable steric environment during generation of the Ru–carbene species from **109,** as compared to **98** (distinct N-protective groups). Cyclic sulfate chemistry was again invoked for effectively performing the synthesis of **114**.

Introducing a genereal strategy for synthesis of deoxyazasugars based on cheap D-glucose, Ghosh et al. also laid groundwork for the preparation of D-1-deoxygulonojirimycin (**91**) (previously communicated by Takahata [67]; Scheme 17) and L-1-deoxyallonojirimycin (**122**) (Scheme 21) starting from protected diacetone glucose **115** [71]. Different pathways were devised for **91** and **122** via the epimeric RCM precursors **117** and **120**, respectively. High yielding cyclization of these dienes, in the presence of the 1st-generation Grubbs catalyst **2** (10 mol %, in CH_2Cl_2, under argon, 24 h at 50 °C), led to **118** and **121** with

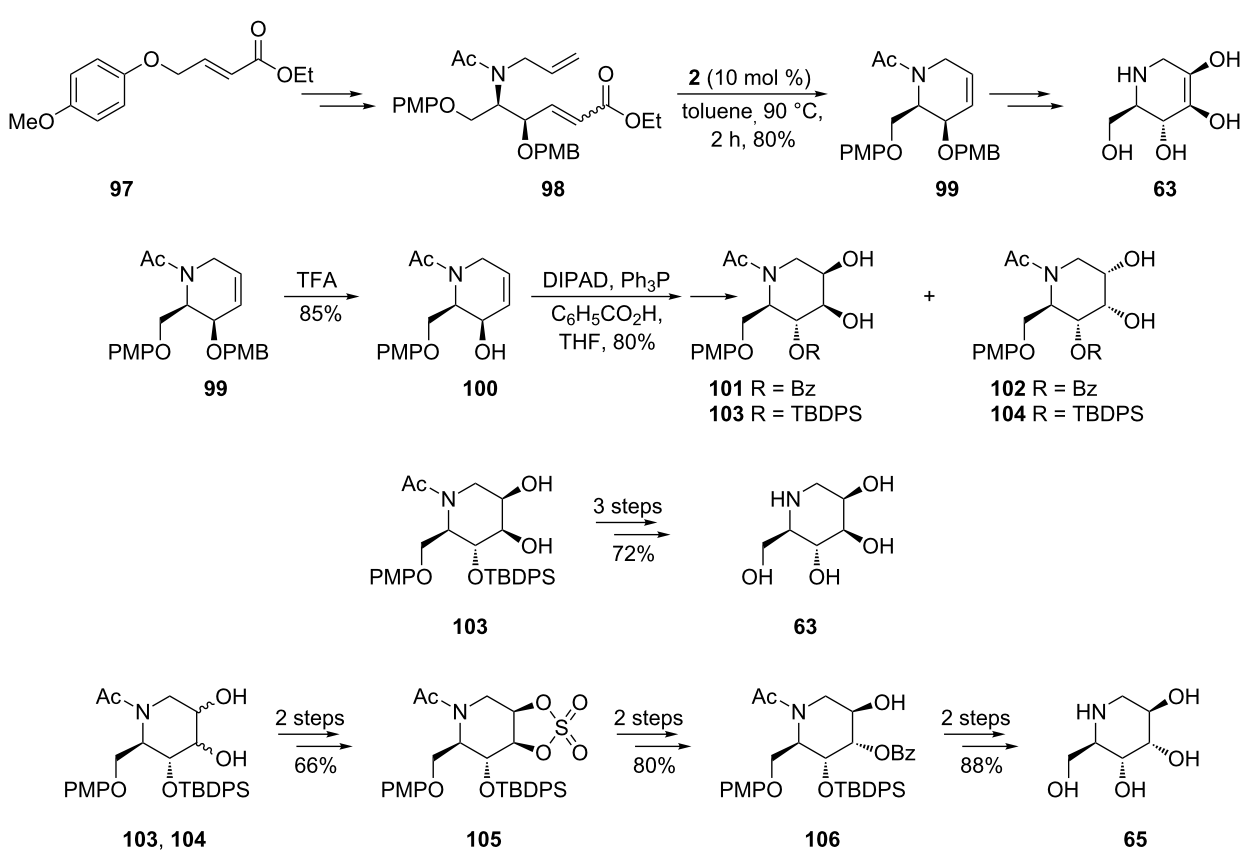

Scheme 19: Synthesis of 1-deoxymannonojirimycin (**63**) and 1-deoxyaltronojirimycin (**65**).

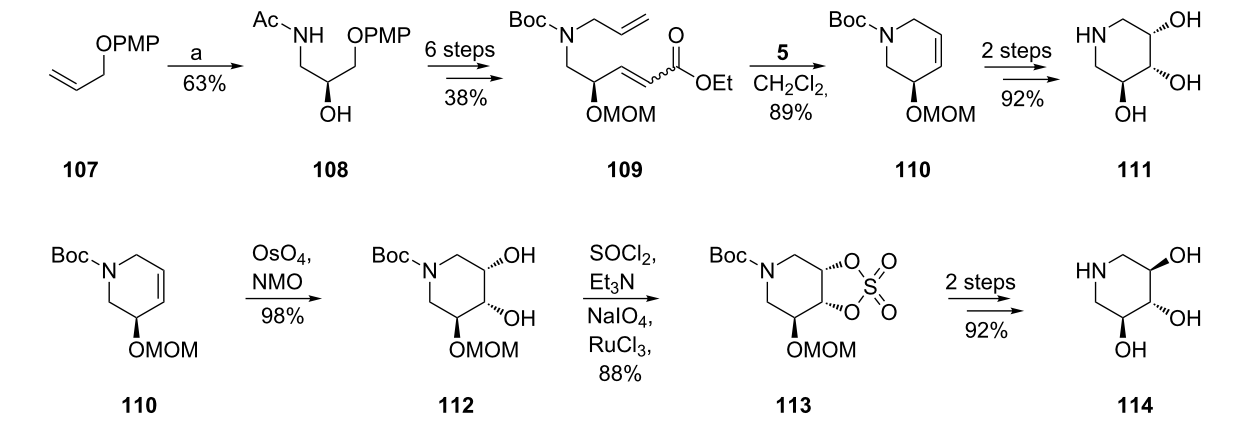

Scheme 20: Synthesis of 5-des(hydroxymethyl)-1-deoxymannonojirimycin (**111**) and 5-des(hydroxymethyl)-1-deoxynojirimycin (**114**).

preserved configurations at the stereogenic centre, which therefore allowed the desired stereochemistry in the isomeric final products **91** and **122**.

D-Fagomine (1,2,5-trideoxy-1,5-imino-D-arabinitol or 1,2-dideoxynojirimycin) (**129**) a natural iminosugar present in buckwheat (widely used in traditional recipes) is an efficient agent for preventing sharp blood glucose peaks after the intake of refined carbohydrates and for positively influencing intestinal microbiota by favouring adhesion of probiotics. It is supposed that fagomine enhances glucose-induced insulin secretion by accelerating the processes which follow glyceraldehyde 3-phosphate formation in the glycolytic pathway.

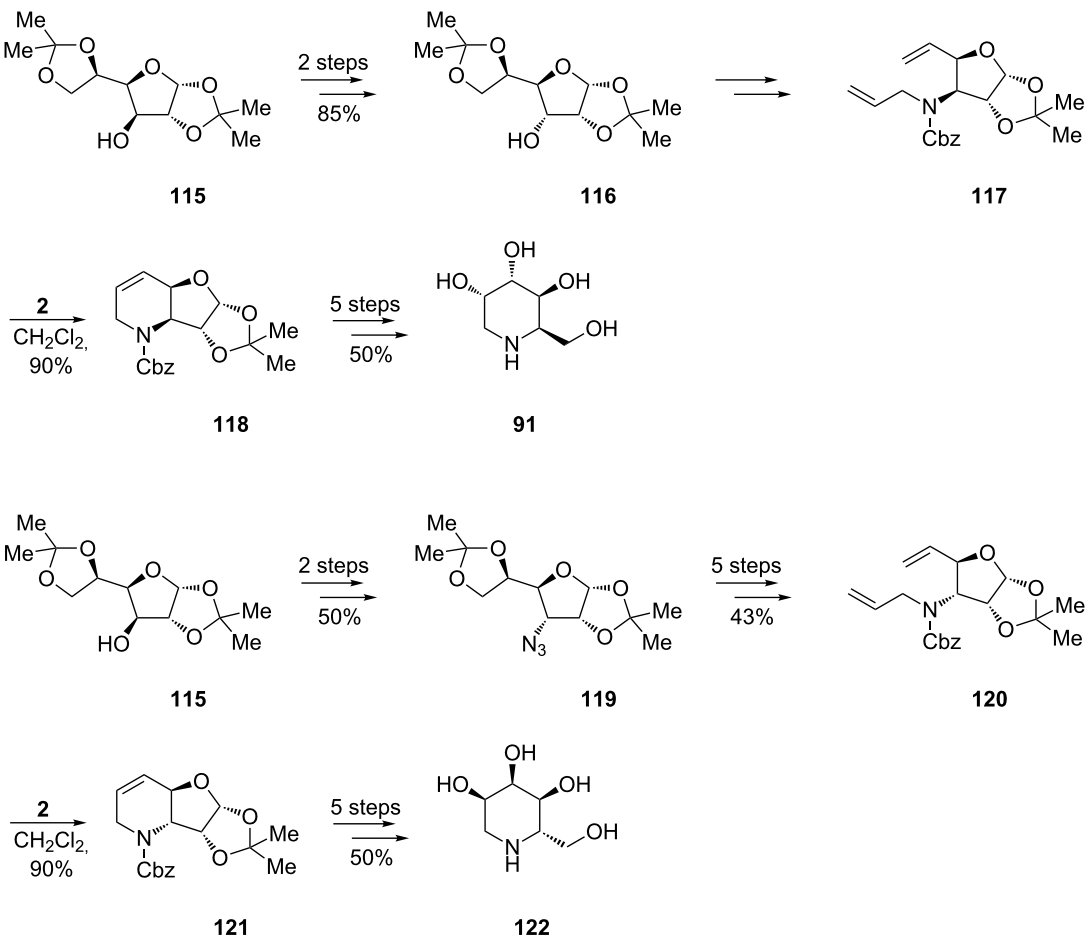

Scheme 21: Synthesis of D-1-deoxygulonojirimycin (**91**) and L-1-deoxyallonojirimycin (**122**).

The total synthesis, involving RCM, of fagomine (**129**) and its congeners 3-*epi*-fagomine (**126**) and 3,4-di-*epi*-fagomine (**130**) was achieved by Takahata et al. [72] based again on the Garner aldehyde **69** derived from D-serine. To construct the chiral 1,2,5,6-tetrahydropyridine core **125**, the authors resorted to catalytic ring-closing metathesis induced by the 1st-generation Grubbs catalyst **2**, with subsequent stereoselective dihydroxylation (under modified Upjohn conditions, Scheme 22). For iminocyclitols containing *trans* diols at the 3- and 4-positions an epoxy functionality at the double bond in **125** was introduced. While the *syn* epoxide **128** led to a mixture of fagomine (**129)** and 3,4-di-*epi*-fagomine (**130**), the *anti* epoxide **127** gave **129** selectively. The 3-*epi*-fagomine (**126**) could also be obtained from the RCM product **125** (by conventional dihydroxylation/deprotection; 10 steps from Garner's aldehyde **69**).

Adenophorine (α-1-deoxy-1-*C*-methylhomonojirimycin) is a further important iminocyclitol in whose synthesis RCM proved helpful. (+)-Adenophorine (**135)**, a naturally occurring iminocyclitol with a lipophilic substituent at the anomeric position, is active on α-glucosidase which is a valid proof that α-alkylation at C1 does not supress the glycosidase inhibitory effect. Its lack of activity on β-galactosidase once again indicates that the relative position of hydroxy substituents is critical for selectivity. In the seminal work by Lebreton and coworkers [73], the first asymmetric total synthesis of (+)-adenophorine was achieved in 14 steps (3.5% overall yield, Scheme 23), starting from the Garner's aldehyde **69**. RCM is essential for construction of the 6-membered N-heterocycle in **133.** Protection of the amino alcohols *trans*-**132** and *cis*-**132**, as the corresponding *trans* and *cis* oxazolidinones, afforded a mixture of diastereomers that were not separable on silica gel. After effecting RCM (2nd-generation Grubbs catalyst **5,** 5 mol %) on this mixture, separation of the diastereomers by flash chromatography was possible, affording the pure tetrahydropyridine derivative *trans*-**133** in 74% yield. Successive epoxidations on enantiopure *trans*-**133** and then **134**, followed each time by regioselective epoxide opening (with a selenium–boron complex and water, respectively), gave finally **135** with good stereoselectivity. This

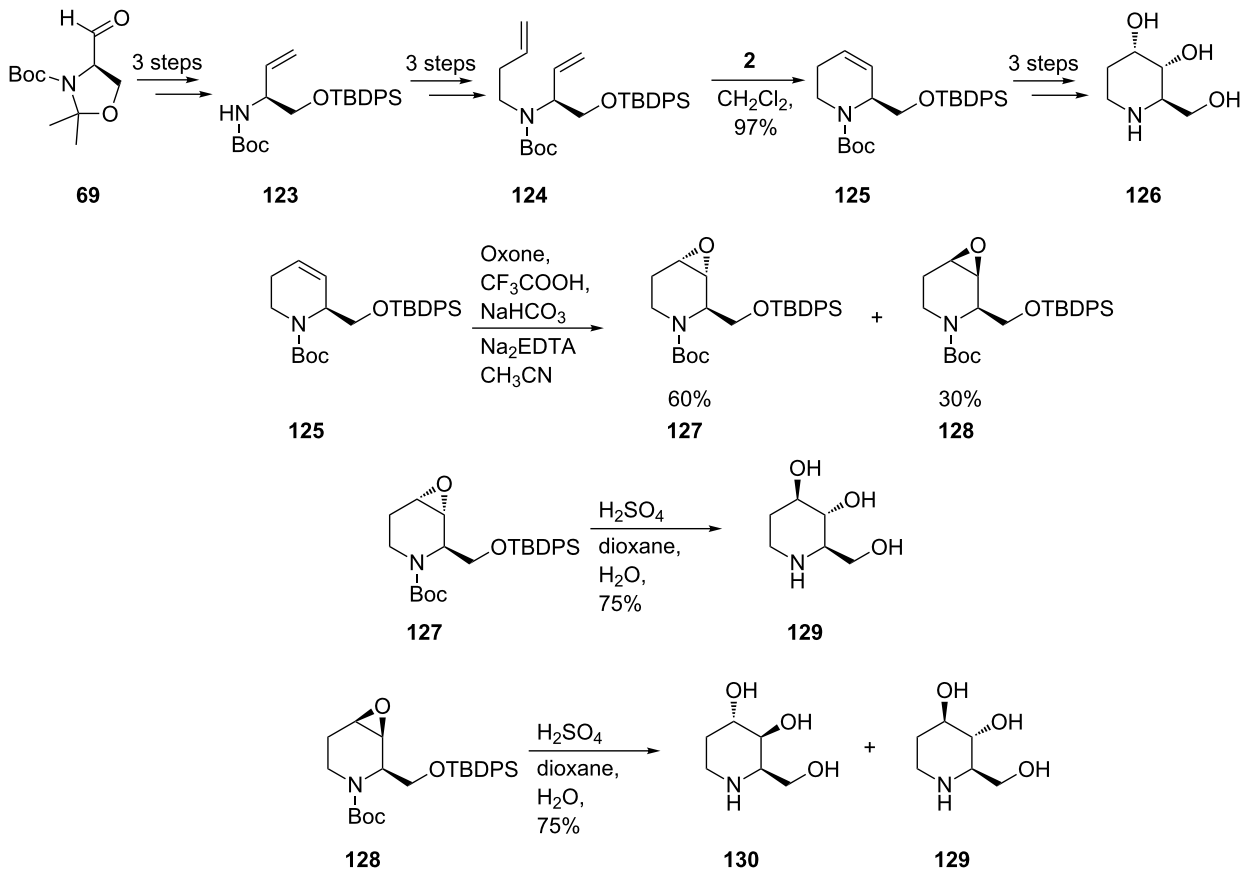

Scheme 22: Total synthesis of fagomine (**129**), 3-*epi*-fagomine (**126**) and 3,4-di-*epi*-fagomine (**130**).

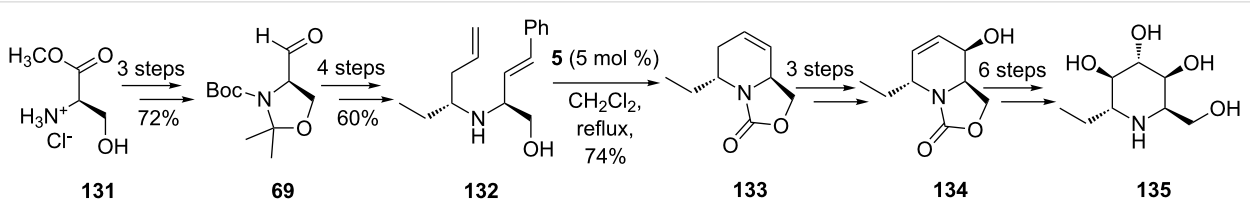

Scheme 23: Total synthesis of (+)-adenophorine (**135**).

overall synthesis demonstrates rigorous control at every stage of both the steric configuration of the starting materials and the steric effects induced by substituents attached to the piperidine moiety.

Related studies by Lebreton et al. [74-76] explored the synthesis of a panel of 6-alkyl substituted piperidine iminocyclitols that had been previously isolated by Asano and coworkers [77] from *Adenophora* spp. These natural products display an unusual structure in that they possess a hydrophobic substituent such as a undecyl, heptyl, butyl or ethyl group at the α position of 1-C. The strategy for (+)-5-deoxyadenophorine (**138**) and analogues **142**–**145** began again from D-Garner aldehyde **69** and also used the powerful RCM as the key step (catalyst **5**, 5 mol %; CH_2Cl_2, reflux 1 h) for building the chiral *trans*-2,6-disubstituted-1,2,5,6-tetrahydropyridine scaffold (72–88% yield, Scheme 24).

Azepane-based iminocyclitols

Iminocyclitols incorporating the azepane ring system are more flexible than the parent pyrrolidine and piperidine iminosugars, and they adopt quasi-flattened, low-energy conformations which can potentially lead to a more favourable binding with the active site of enzymes. The unusual spatial distribution of the hydroxy groups in these compounds should generate new inhibitory profiles. According to in vitro assays, seven-

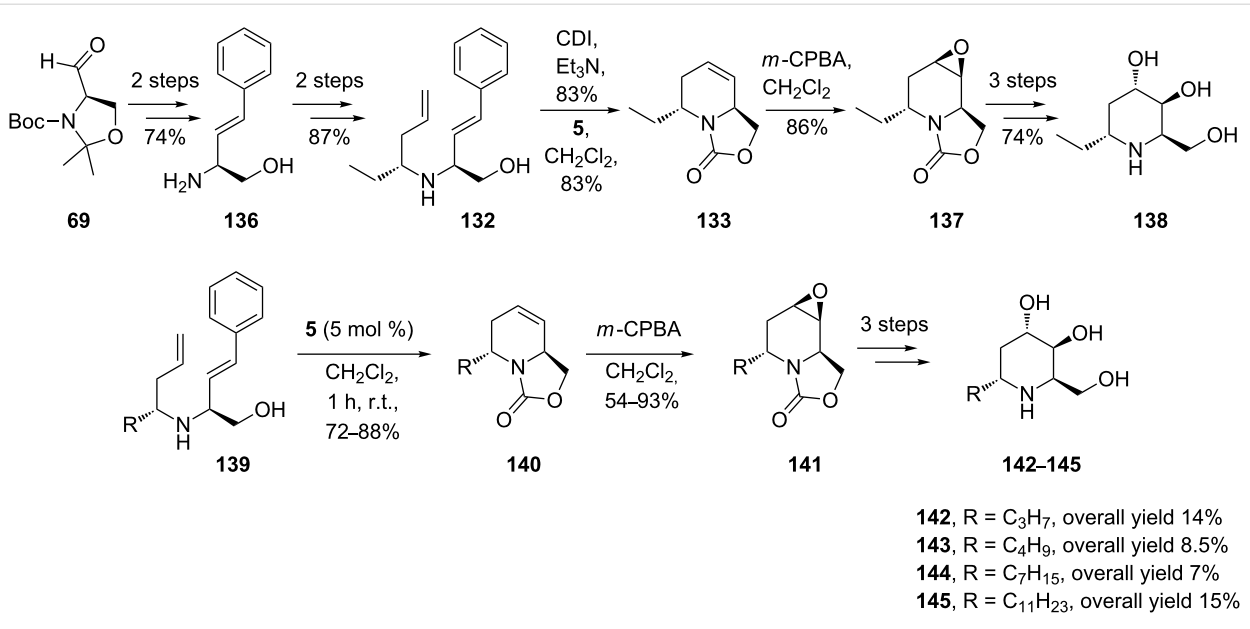

Scheme 24: Total synthesis of (+)-5-deoxyadenophorine (**138**) and analogues **142**–**145**.

membered ring iminocyclitols are noted inhibitors of α-mannosidase, an enzyme that plays important roles in glycoprotein biosynthesis. Derivatives of this class bearing hydroxymethyl groups at C-6 have been shown to inhibit powerfully lysosomal α-mannosidase while displaying varying potencies toward α-1,6-mannosidase. On the other hand, N-alkylated polyhydroxylated azepanes with the D-glucose or L-idose configuration proved to be potent β-glucosidase inhibitors that showed only weak activity towards α-glucosidase and α-mannosidase [78-80]. Malto-oligosaccharides and analogues of di- and trisaccharides containing polyhydroxylated azepane moieties are glucosidase or HIV/FIV-protease blockers, or both.

As for the previous classes, in the synthesis of seven-membered iminocyclitols RCM provides a focal point in ring closure being responsible for constructing the azepane framework. For example, 1,6-dideoxy-1,6-iminoheptitols **148** and **149**, that can be viewed as higher homologues of fagomine and nojirimycin, respectively, are easily accessed from the protected diene **146**. RCM of this diene with 1st-generation Grubbs catalyst (**2**, CH_2Cl_2, 45 °C) gives the common N-heterocyclic intermediate **147** (91% yield, Scheme 25). Hydrogenation of the latter gives the iminocyclitol **148** whereas its *cis*-selective dihydroxylation affords the pentahydroxy derivative **149**.

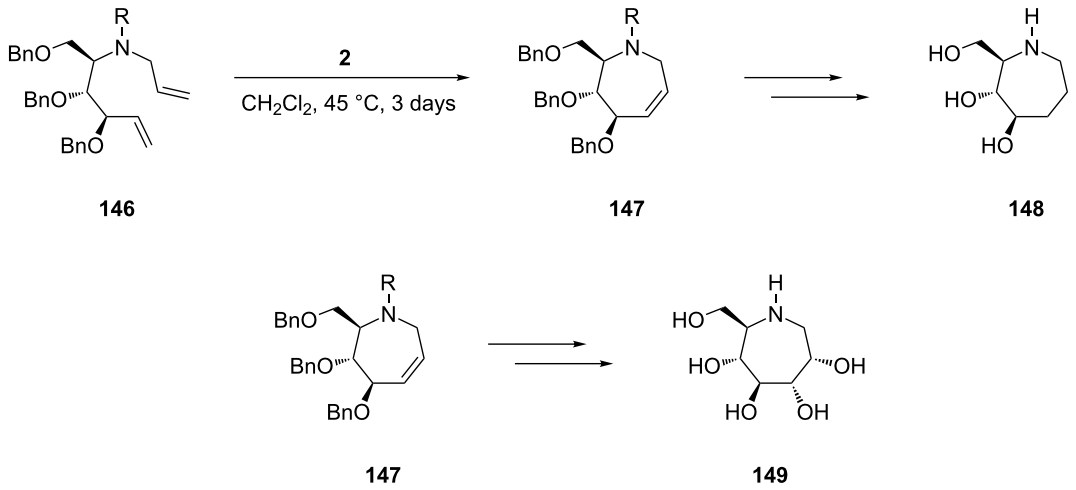

Scheme 25: Synthesis by RCM of 1,6-dideoxy-1,6-iminoheptitols **148** and **149**.

Starting from L-serine **150**, Lin et al. [81] devised a refined method for the synthesis of structurally diverse stereoisomers of polyhydroxyazepanes. In their complex strategy, RCM (1st-generation Grubbs catalyst, 10 mol %, CH_2Cl_2, reflux, 12 h) plays a significant role by leading to a panel of oxazolidinyl azacyclic products (e.g., **152** and **154**). Remarkably, the authors expertly arranged the positions of the double bonds involved in RCM on the one hand by addition of alkenyl nucleophiles (with different lengths) on aldehyde intermediates, and on the other hand by placing the second double bond at a different distance relative to the nitrogen atom (Scheme 26).

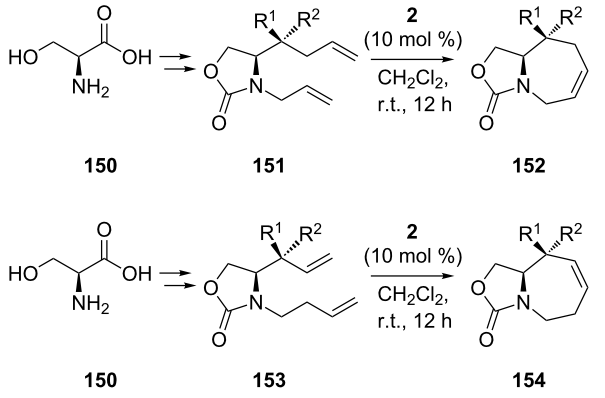

Scheme 26: Synthesis by RCM of oxazolidinyl azacycles **152** and **154**.

There are two advantageous follow-ups: (i) a desired location of the double bond in the azacyclic RCM product, and therefore of the hydroxyls in the final iminocyclitol products, and (ii) possible extension of the methodology to the construction of other ring sizes (5- to 8-membered). This versatile approach, featuring the basic sequence metathesis/dihydroxylation, led in good yields to a number of stereoisomers of seven-membered iminocyclitols exhibiting glycosidase inhibitory properties (Scheme 27). Of the compounds shown in Scheme 27, compound **161** with L-configuration at C-6 exhibited the highest inhibition.

As illustrated in Scheme 28, the 2nd-generation Grubbs catalyst **5** found further application in the recent synthesis of seven-membered ring iminocyclitols, e.g., of 7-hydroxymethyl-1-(4-methylphenylsulfonyl)azepane-3,4,5-triol (**169**). This compound shares a common configuration of the hydroxy groups with its lower cyclic homologue, 1-deoxymannojirimycin (DMJ, **63**), a selective inhibitor of α-mannosidase I [82].

Lee et al. [83] also used RCM induced by the 1st-generation Grubbs catalyst **2** or the 2nd-generation Grubbs catalyst **5** (10 mol %, reflux in toluene; 90–91% yield) in an efficient approach to targeted enantiomerically pure, stereochemically defined, six- and seven-membered heterocyclic scaffolds, i.e., the tetrahydropyridin-3-ol **171** and tetrahydroazepin-3-ol **173** (Scheme 29).

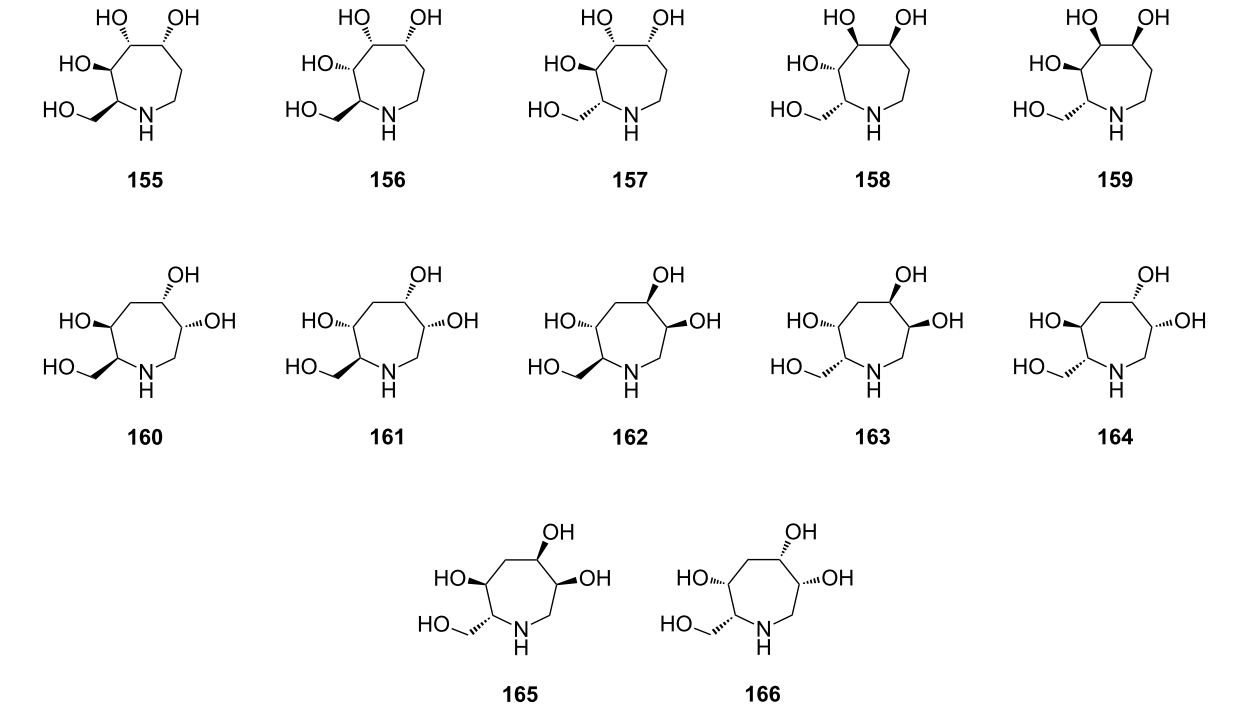

Scheme 27: Representative azepane-based iminocyclitols.

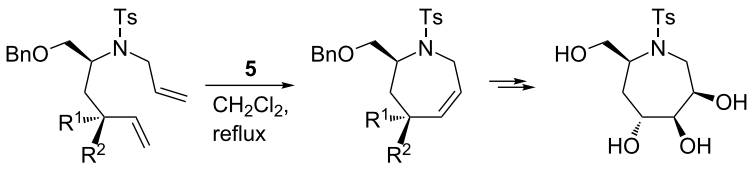

167 168 169

Scheme 28: Synthesis of hydroxymethyl-1-(4-methylphenylsulfonyl)-azepane 3,4,5-triol (**169**).

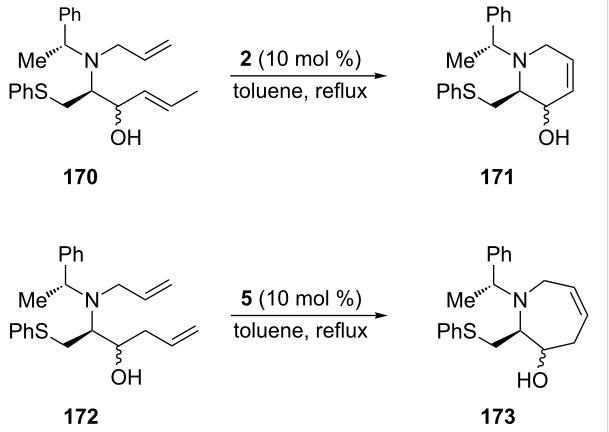

170 171 172 173

Scheme 29: Synthesis by RCM of tetrahydropyridin-3-ol **171** and tetrahydroazepin-3-ol **173**.

These diversely substituted N-heterocyclic compounds, endowed with an internal double bond, are versatile precursors suitable for further functionalization. Asymmetric syntheses employing such intermediates could lead to disclosure of further biologically relevant piperidine/azepane alkaloids and iminosugars.

Conclusion

The paper introduces the broad scope of olefin metathesis as a key reaction in synthetic strategies for the preparation of monocyclic iminocyclitols. In comparison with earlier well-established protocols, olefin metathesis (RCM, CM) offers shorter, simpler and atom-economical routes, and preserving at the same time the carefully designed and worked for stereochemistry of the precursors. Whereas RCM is the method of choice for constructing the pyrrolidine, piperidine or azepane cores of monocyclic iminocyclitols, CM rewardingly permits access to a collection of new iminocyclitols simply by using one heterocyclic intermediate endowed with an olefinic side-chain and changing only its olefin partner. The reaction conditions applied in these crucial steps are rather conventional for metathesis processes, with the choice of the temperature and solvent (refluxing CH_2Cl_2 or toluene) being dictated by steric demands, and hence energetics, for ring-closing or cross-coupling. While the 1st- and 2nd-generation Grubbs catalysts (5–10 mol %) are the catalysts most frequently employed, the 2nd-generation Grubbs and Hoveyda–Grubbs catalysts perform better when harsher conditions are required. Despite the various functionalities existing on the metathesis precursors and products, sensitive metathesis catalysts are quite productive due to inventive protection/deprotection at the O- and N-heteroatoms. Such delicate operations are skillfully conceived so as to either maintain or reverse the geometry at stereogenic centres, as required. In the ensemble of stereocontrolled reactions concentrating on the economical achievement of the targeted number and relative positions of hydroxy, hydroxyalkyl or other substituents, i.e., the overall structure that hinges on the biological activity, metathesis is surely a fine addition which is bound to succeed in creating novel azasugars with a larger therapeutic window. The metathesis approach may ultimately yield benefits for patients suffering from metabolic disorders, cancer and viral diseases.

References

1. Compain, P.; Martin, O. R., Eds. *Iminosugars: From Synthesis to Therapeutic Applications;* Wiley-VCH: Weinheim, Germany, 2007.
2. Stütz, A. E. *Iminosugars as Glycosidase Inhibitors: Nojirimycin and Beyond;* Wiley-VCH: Weinheim, Germany, 1999.
3. Martin, O. R.; Compain, P., Eds. Iminosugars: Recent Insights into Their Bioactivity Potential as Therapeutic Agents. *Curr. Top. Med. Chem.* **2003,** *3,* 471–591.
4. Winchester, B.; Fleet, G. W. J. *Glycobiology* **1992,** *2,* 199–210. doi:10.1093/glycob/2.3.199
5. Stocker, B. L.; Dangerfield, E. M.; Win-Mason, A. L.; Haslett, G. W.; Timmer, M. S. M. *Eur. J. Org. Chem.* **2010,** 1615–1637. doi:10.1002/ejoc.200901320
6. Davis, B. G. *Tetrahedron: Asymmetry* **2009,** *20,* 652–671. doi:10.1016/j.tetasy.2009.03.013
7. Compain, P.; Chagnault, V.; Martin, O. R. *Tetrahedron: Asymmetry* **2009,** *20,* 672–711. doi:10.1016/j.tetasy.2009.03.031
8. Pearson, M. S. M.; Mathé-Allainmat, M.; Fargeas, V.; Lebreton, J. *Eur. J. Org. Chem.* **2005,** 2159–2191. doi:10.1002/ejoc.200400823
9. Compain, P.; Martin, O. R. *Curr. Top. Med. Chem.* **2003,** *3,* 541–560. doi:10.2174/1568026033452474
10. Lillelund, V. H.; Jensen, H. H.; Liang, X.; Bols, M. *Chem. Rev.* **2002,** *102,* 515–554. doi:10.1021/cr000433k
11. Moreno-Clavijo, E.; Carmona, A. T.; Moreno-Vargas, A. J.; Molina, L.; Robina, I. *Curr. Org. Synth.* **2011,** *8,* 102–133.

12. Asano, N.; Nash, R. J.; Molyneux, R. J.; Fleet, G. W. J. *Tetrahedron: Asymmetry* **2000,** *11,* 1645–1680. doi:10.1016/S0957-4166(00)00113-0
13. Asano, N. Naturally Occurring Iminosugars and Related Alkaloids: Structure, Activity and Applications. In *Iminosugars: From Synthesis to Therapeutic Applications;* Compain, P.; Martin, O. R., Eds.; Wiley-VCH: Weinheim, Germany , 2007; pp 7–24. doi:10.1002/9780470517437.ch2
14. Asano, N. *Curr. Top. Med. Chem.* **2003,** *3,* 471–484. doi:10.2174/1568026033452438
15. Watson, A. A.; Fleet, G. W. J.; Asano, N.; Molyneux, R. J.; Nash, R. J. *Phytochemistry* **2001,** *56,* 265–295. doi:10.1016/S0031-9422(00)00451-9
16. Goss, P. E.; Baptiste, J.; Fernandes, B.; Baker, M. A.; Dennis, J. W. *Cancer Res.* **1994,** *54,* 1450–1457.
17. Goss, P. E.; Baker, M. A.; Carver, J. P.; Dennis, J. W. *Clin. Cancer Res.* **1995,** *1,* 935–944.
18. Asano, N. *Glycobiology* **2003,** *13,* 93R–104R. doi:10.1093/glycob/cwg090
19. Nishimura, Y. *Curr. Top. Med. Chem.* **2003,** *3,* 575–591. doi:10.2174/1568026033452492
20. Nishimura, Y. Iminosugar-based antitumoural agents. In *Iminosugars: From Synthesis to Therapeutic Applications;* Compain, P.; Martin, O. R., Eds.; Wiley-VCH: Weinheim, Germany, 2007; pp 269–294. doi:10.1002/9780470517437.ch12
21. Butters, T. D.; Dwek, R. A.; Platt, F. M. *Chem. Rev.* **2000,** *100,* 4683–4696. doi:10.1021/cr990292q
22. Fan, J. Q. *Trends Pharmacol. Sci.* **2003,** *24,* 355–360. doi:10.1016/S0165-6147(03)00158-5
23. Yu, Z.; Sawkar, A. R.; Whalen, L. J.; Wong, C.; Kelly, J. W. *J. Med. Chem.* **2007,** *50,* 94–100. doi:10.1021/jm060677i
24. Mitrakou, A.; Tountas, N.; Raptis, A. E.; Bauer, R. J.; Schulz, H.; Raptis, S. A. *Diabetic Med.* **1998,** *15,* 657–660. doi:10.1002/(SICI)1096-9136(199808)15:8<657::AID-DIA652>3.0.CO;2-7
25. Andersen, B.; Rassov, A.; Westergaard, N.; Lundgren, K. *Biochem. J.* **1999,** *342,* 545–550.
26. Somsak, L.; Nagy, V.; Hadazy, Z.; Docsa, T.; Gergely, P. *Curr. Pharm. Des.* **2003,** *9,* 1177–1189.
27. Durantel, D.; Branza-Nichita, N.; Carrouee-Durantel, S.; Butters, T. D.; Dwek, R. A.; Zitzmann, N. *J. Virol.* **2001,** *75,* 8987–8998. doi:10.1128/JVI.75.19.8987-8998.2001
28. Greimel, P.; Spreitz, J.; Stütz, A. E.; Wrodnigg, T. M. *Curr. Top. Med. Chem.* **2003,** *3,* 513–523. doi:10.2174/1568026033452456
29. Gruters, R. A.; Neefjes, J. J.; Tersmette, M.; de Goede, R. E.; Tulp, A.; Huisman, H. G.; Miedema, F.; Ploegh, H. L. *Nature* **1987,** *330,* 74–77. doi:10.1038/330074a0
30. Walker, B. D.; Kowalski, M.; Goh, W. C.; Kozarsky, K.; Krieger, M.; Rosen, C.; Rohrschneider, L.; Haseltine, W. A.; Sodroski, J. *Proc. Natl. Acad. Sci. U. S. A.* **1987,** *84,* 8120–8124.
31. Block, T. M.; Lu, X.; Platt, F. M.; Foster, G. R.; Gerlich, W. H.; Blumberg, B. S.; Dwek, R. A. *Proc. Natl. Acad. Sci. U. S. A.* **1994,** *91,* 2235–2239.
32. Mehta, A.; Carrouee, S.; Conyers, B.; Jordan, R.; Butters, T. D.; Dwek, R. A.; Block, T. M. *Hepatology (Hoboken, NJ, U. S.)* **2001,** *33,* 1488–1495. doi:10.1053/jhep.2001.25103
33. Durantel, D.; Carrouée-Durantel, S.; Branza-Nichita, N.; Dwek, R. A.; Zitzmann, N. *Antimicrob. Agents Chemother.* **2004,** *48,* 497–504. doi:10.1128/AAC.48.2.497-504.2004
34. Ye, X.-S.; Sun, F.; Liu, M.; Li, Q.; Wang, Y.; Zhang, G.; Zhang, L.-H.; Zhang, X. L. *J. Med. Chem.* **2005,** *48,* 3688–3691. doi:10.1021/jm050169t
35. Désiré, J.; Dransfield, P. J.; Gore, P. M.; Shipman, M. *Synlett* **2001,** 1329–1331. doi:10.1055/s-2001-16039
36. Kumar, V.; Ramesh, N. G. *Tetrahedron* **2006,** *62,* 1877–1885. doi:10.1016/j.tet.2005.11.037
37. Schrock, R. R.; Hoveyda, A. H. *Angew. Chem., Int. Ed.* **2003,** *42,* 4592–4633. doi:10.1002/anie.200300576
38. Grubbs, R. H., Ed. *Handbook of Metathesis;* Wiley-VCH: Weinheim, Germany, 2003; Vol. 1.
39. Vougioukalakis, G. C.; Grubbs, R. H. *Chem. Rev.* **2010,** *110,* 1746–1787. doi:10.1021/cr9002424
40. Dunne, A. M.; Mix, S.; Blechert, S. *Tetrahedron Lett.* **2003,** *44,* 2733–2736. doi:10.1016/S0040-4039(03)00346-0
41. Bieniek, M.; Michrowska, A.; Usanov, D. L.; Grela, K. *Chem.–Eur. J.* **2008,** *14,* 806–818. doi:10.1002/chem.200701340
42. Sauvage, X.; Borguet, Y.; Zaragoza, G.; Demonceau, A.; Delaude, L. *Adv. Synth. Catal.* **2009,** *351,* 441–455. doi:10.1002/adsc.200800664
43. Nolan, S. P.; Clavier, H. *Chem. Soc. Rev.* **2010,** *39,* 3305–3316. doi:10.1039/b912410c
44. Ding, F.; Sun, Y. G.; Monsaert, S.; Dragutan, I.; Dragutan, V.; Verpoort, F. *Curr. Org. Synth.* **2008,** *5,* 291–304.
45. Krehl, S.; Geissler, D.; Hauke, S.; Kunz, O.; Staude, L.; Schmidt, B. *Beilstein J. Org. Chem.* **2010,** *6,* 1188–1198. doi:10.3762/bjoc.6.136
46. Dragutan, V.; Dragutan, I.; Balaban, A. T. *Platinum Met. Rev.* **2000,** *44,* 112–118.
47. Dragutan, I.; Dragutan, V.; Delaude, L.; Demonceau, A.; Noels, A. F. *Rev. Roum. Chim.* **2007,** *52,* 1013–1025.
48. Felpin, F.-X.; Lebreton, J. *Eur. J. Org. Chem.* **2003,** 3693–3712. doi:10.1002/ejoc.200300193
49. Saotome, C.; Wong, C.-H.; Kanie, O. *Chem. Biol.* **2001,** *8,* 1061–1070. doi:10.1016/S1074-5521(01)00074-6
50. Behling, J. R.; Campbell, A. L.; Babiak, K. A.; Ng, J. S.; Medic, J.; Farid, P.; Fleet, G. W. J. *Tetrahedron* **1993,** *49,* 3359–3366. doi:10.1016/S0040-4020(01)90163-2
51. Moriarty, R. M.; Mitan, C. I.; Branza-Nichita, N.; Phares, K. R.; Parrish, D. *Org. Lett.* **2006,** *8,* 3465–3467. doi:10.1021/ol061071r
52. Cren, S.; Wilson, C.; Thomas, N. R. *Org. Lett.* **2005,** *7,* 3521–3523. doi:10.1021/ol051232b
53. Huwe, C. M.; Blechert, S. *Synthesis* **1997,** 61–67. doi:10.1055/s-1997-1497
54. Madhan, A.; Rao, B. V. *Tetrahedron Lett.* **2003,** *44,* 5641–5643. doi:10.1016/S0040-4039(03)01366-2
55. Fleet, G. W. J.; Son, J. C. *Tetrahedron* **1988,** *44,* 2637–2647. doi:10.1016/S0040-4020(01)81716-6
56. Davis, F. A.; Ramachandar, T.; Chai, J.; Skucas, E. *Tetrahedron Lett.* **2006,** *47,* 2743–2746. doi:10.1016/j.tetlet.2006.02.092
57. Chandrasekhar, B.; Madhan, A.; Rao, B. V. *Tetrahedron* **2007,** *63,* 8746–8751. doi:10.1016/j.tet.2007.06.044
58. Murruzzu, C.; Riera, A. *Tetrahedron: Asymmetry* **2007,** *18,* 149–154. doi:10.1016/j.tetasy.2006.12.023
59. Doddi, V. R.; Vankar, Y. D. *Eur. J. Org. Chem.* **2007,** 5583–5589. doi:10.1002/ejoc.200700719
60. Trost, B. M.; Horne, D. B.; Woltering, M. J. *Chem.–Eur. J.* **2006,** *12,* 6607–6620. doi:10.1002/chem.200600202
61. Trost, B. M.; Horne, D. B.; Woltering, M. J. *Angew. Chem., Int. Ed.* **2003,** *42,* 5987–5990. doi:10.1002/anie.200352857
62. Ribes, C.; Falomir, E.; Murga, J.; Carda, M.; Marco, J. A. *Org. Biomol. Chem.* **2009,** *7,* 1355–1360. doi:10.1039/B821431J

63. Ribes, C.; Falomir, E.; Murga, J.; Carda, M.; Marco, J. A. *Tetrahedron* **2009,** *65,* 10612–10616. doi:10.1016/j.tet.2009.10.066
64. Takahata, H.; Banba, Y.; Sasatani, M.; Nemoto, H.; Kato, A.; Adachi, I. *Tetrahedron* **2004,** *60,* 8199–8205. doi:10.1016/j.tet.2004.06.112
65. Danoun, G.; Ceccon, J.; Greene, A. E.; Poisson, J.-F. *Eur. J. Org. Chem.* **2009,** 4221–4224. doi:10.1002/ejoc.200900595
66. Rengasamy, R.; Curtis-Long, M. J.; Seo, W. D.; Jeong, S. H.; Jeong, I.-Y.; Park, K. H. *J. Org. Chem.* **2008,** *73,* 2898–2901. doi:10.1021/jo702480y
67. Takahata, H.; Banba, Y.; Ouchi, H.; Nemoto, H. *Org. Lett.* **2003,** *5,* 2527–2529. doi:10.1021/ol034886y
68. van den Nieuwendijk, A. M. C. H.; Ruben, M.; Engelsma, S. E.; Risseeuw, M. D. P.; van den Berg, R. J. B. H. N.; Boot, R. G.; Aerts, J. M.; Brussee, J.; van der Marel, G. A.; Overkleeft, H. S. *Org. Lett.* **2010,** *12,* 3957–3959. doi:10.1021/ol101556k
69. Singh, O. V.; Han, H. *Tetrahedron Lett.* **2003,** *44,* 2387–2391. doi:10.1016/S0040-4039(03)00218-1
70. Han, H. *Tetrahedron Lett.* **2003,** *44,* 1567–1569. doi:10.1016/S0040-4039(03)00014-5
71. Ghosh, S.; Shashidhar, J.; Dutta, S. K. *Tetrahedron Lett.* **2006,** *47,* 6041–6044. doi:10.1016/j.tetlet.2006.06.110
72. Banba, Y.; Abe, C.; Nemoto, H.; Kato, A.; Adachi, I.; Takahata, H. *Tetrahedron: Asymmetry* **2001,** *12,* 817–819. doi:10.1016/S0957-4166(01)00136-7
73. Pearson, M. S. M.; Evain, M.; Mathé-Allainmat, M.; Lebreton, J. *Eur. J. Org. Chem.* **2007,** 4888–4894. doi:10.1002/ejoc.200700459
74. Felpin, F.-X.; Boubekeur, K.; Lebreton, J. *J. Org. Chem.* **2004,** *69,* 1497–1503. doi:10.1021/jo035522m
75. Felpin, F.-X.; Lebreton, J. *Tetrahedron Lett.* **2003,** *44,* 527–530. doi:10.1016/S0040-4039(02)02586-8
76. Felpin, F.-X.; Boubekeur, K.; Lebreton, J. *Eur. J. Org. Chem.* **2003,** 4518–4527. doi:10.1002/ejoc.200300423
77. Ikeda, K.; Takahashi, M.; Nishida, M.; Miyauchi, M.; Kizu, H.; Kameda, Y.; Arisawa, M.; Watson, A. A.; Nash, R. J.; Fleet, G. W. J.; Asano, N. *Carbohydr. Res.* **1999,** *323,* 73–80. doi:10.1016/S0008-6215(99)00246-3
78. Butters, T. D.; Alonzi, D. S.; Kukushkin, N. V.; Ren, Y.; Blériot, Y. *Glycoconjugate J.* **2009,** *26,* 1109–1116. doi:10.1007/s10719-009-9231-3
79. Li, H.; Liu, T.; Zhang, Y.; Favre, S.; Bello, C.; Vogel, P.; Butters, T. D.; Oikonomakos, N. G.; Marrot, J.; Blériot, Y. *ChemBioChem* **2008,** *9,* 253–260. doi:10.1002/cbic.200700496
80. Li, H.; Blériot, Y.; Chantereau, C.; Mallet, J.-M.; Sollogoub, M.; Zhang, Y.; Rodriquez-García, E.; Vogel, P.; Jiménez-Barbero, J.; Sinaÿ, P. *Org. Biomol. Chem.* **2004,** *2,* 1492–1499. doi:10.1039/b402542c
81. Lin, C.-C.; Pan, Y.-s.; Patkar, L. N.; Lin, H.-M.; Tzou, D.-L. M.; Subramanian, T.; Lin, C.-C. *Bioorg. Med. Chem.* **2004,** *12,* 3259–3267. doi:10.1016/j.bmc.2004.03.064
82. Chang, M.-Y.; Kung, Y.-H.; Ma, C.-C.; Chen, S.-T. *Tetrahedron* **2007,** *63,* 1339–1344. doi:10.1016/j.tet.2006.12.002
83. Lee, H. K.; Im, J. H.; Jung, S. H. *Tetrahedron* **2007,** *63,* 3321–3327. doi:10.1016/j.tet.2007.02.045

License and Terms